

独立行政法人国立病院機構
水戸医療センター

研 究 業 績 集

令和4年度



巻頭言

病院長 米野琢哉

水戸医療センターの基本方針として、「臨床研究を積極的に推進します」を掲げています。令和4年度は、COVID-19 に継続的に対応しながらも、日常診療を黙々とこなし、臨床研究にも真摯に取り組んでいただきました。職員の皆様のご努力に敬意をはらいたいと思います。

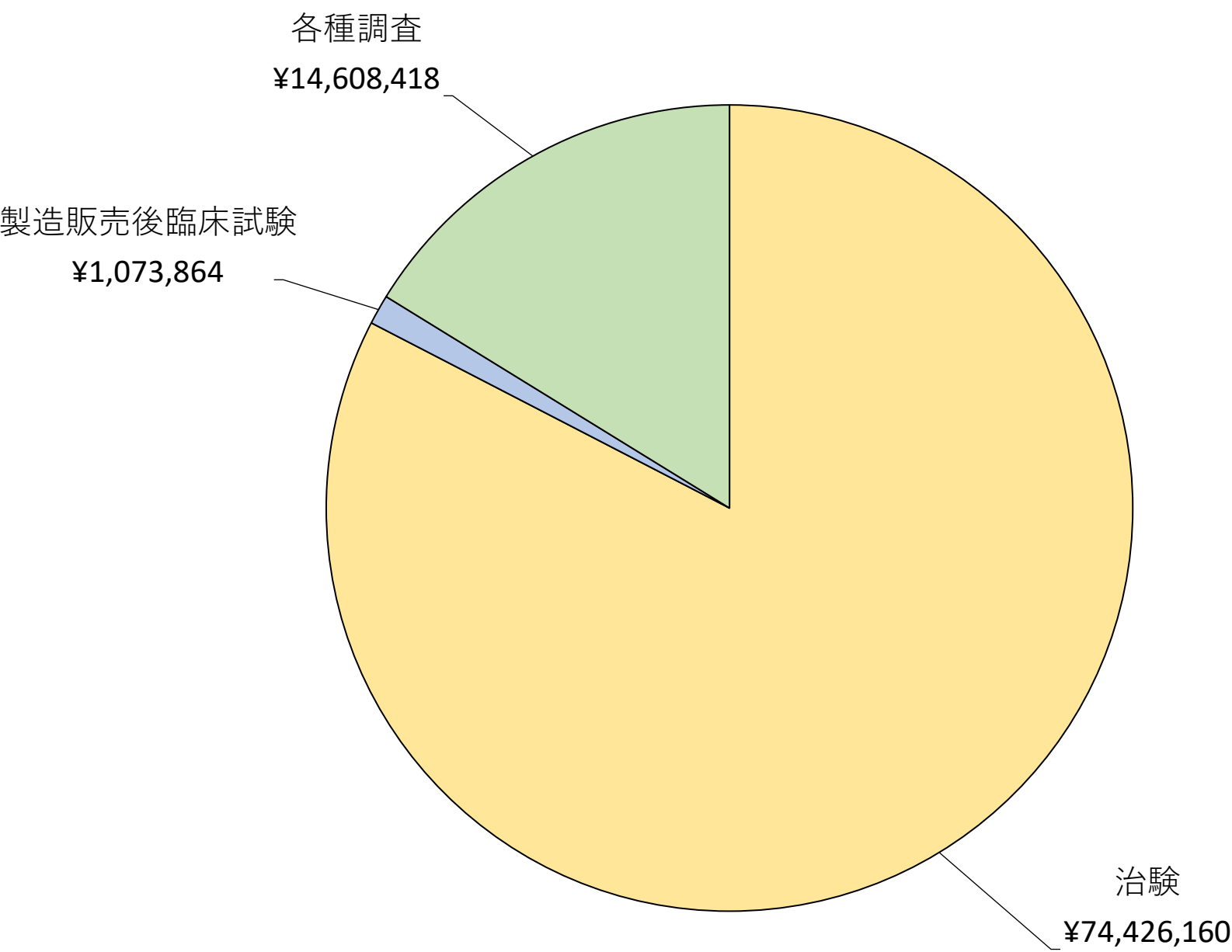
臨床研究の推進は、診療の質向上のためにも必須です。様々な職種の方々が研究に取り組むことによって、診療の活性化にもつながると期待しております。病院としても、臨床研究部を中心に、資金提供、研究に必要な文書作成のアドバイスなど研究実施のサポートを継続していきます。今後も是非臨床研究にチャレンジしてみてください。

2022年度

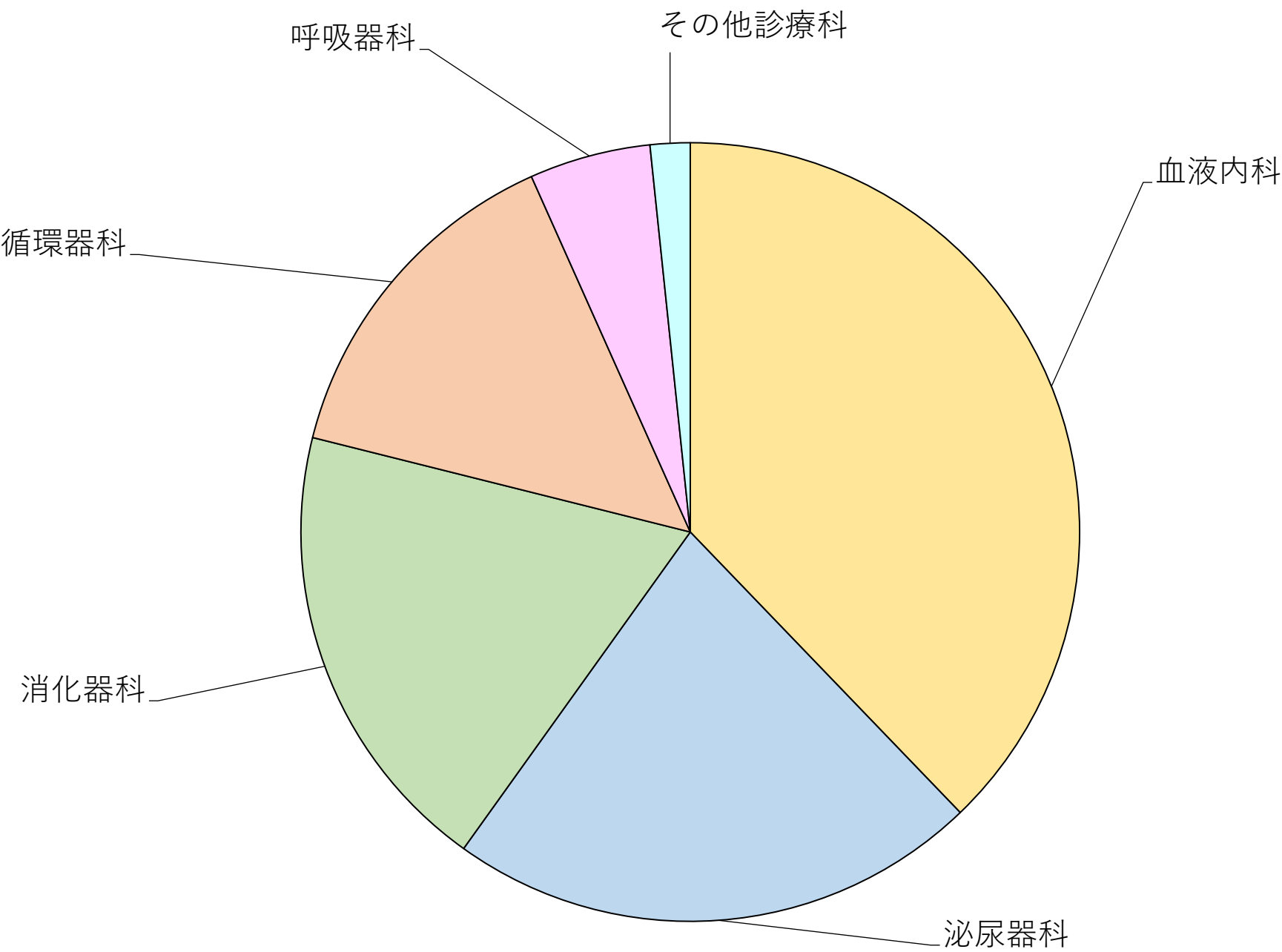
受託研究実績金額

9,010万円

契約種類別グラフ

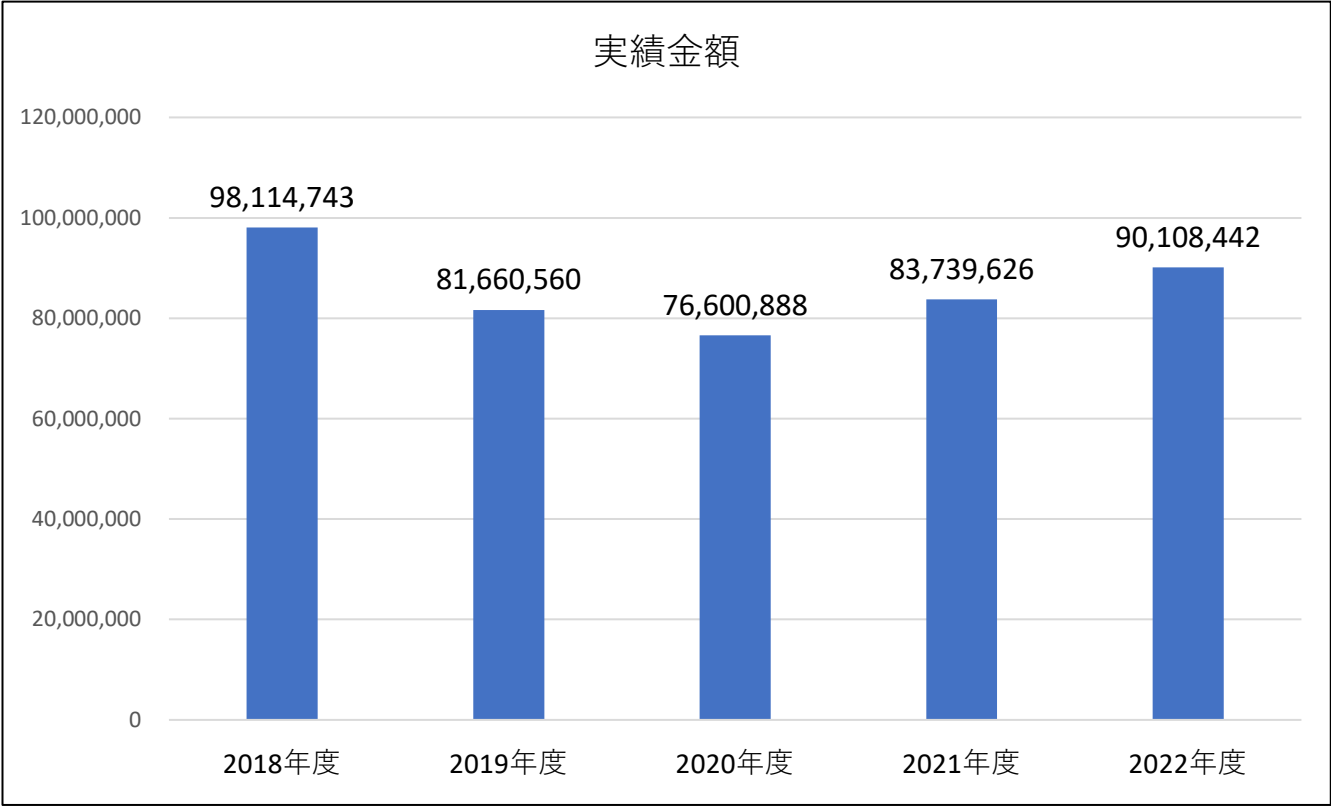


診療科別グラフ

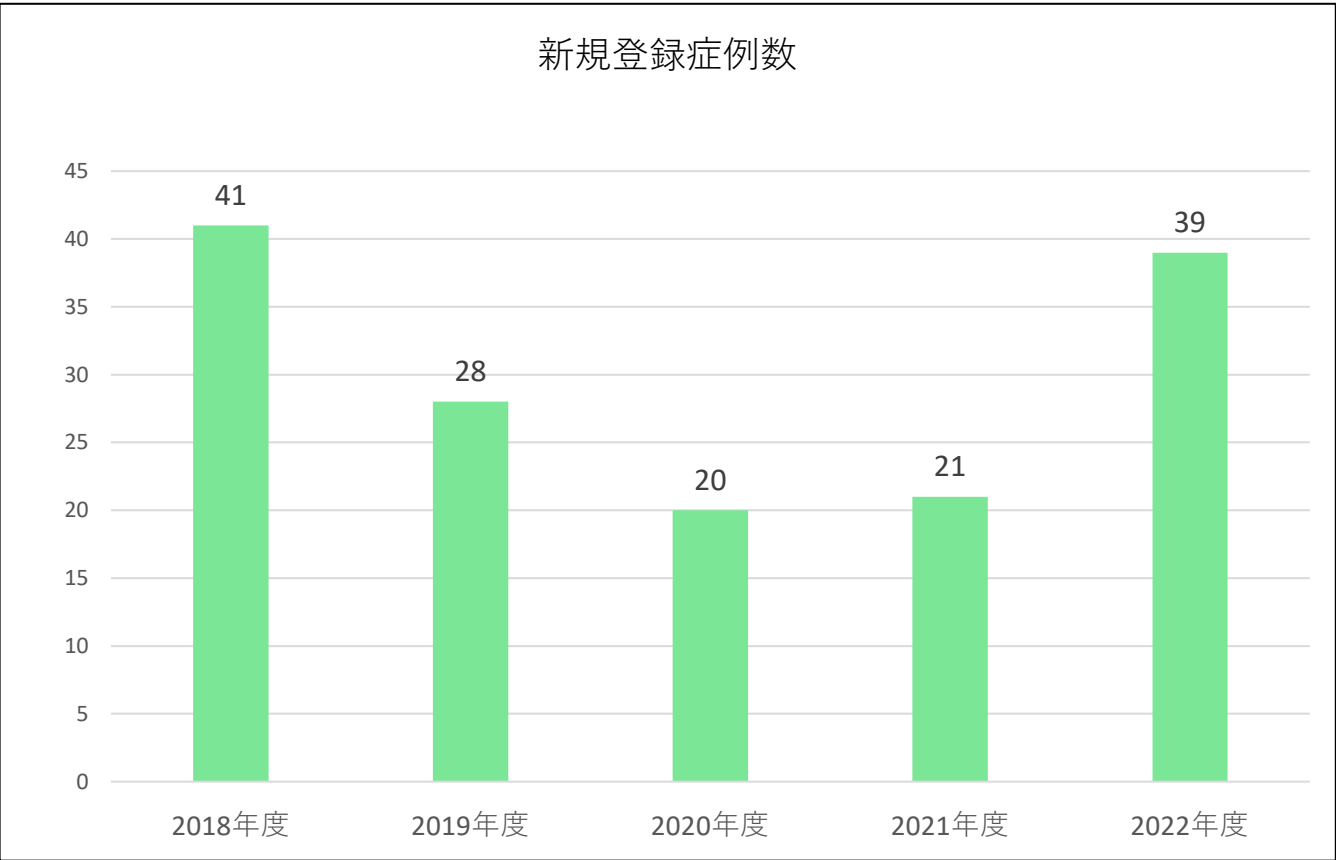


受託研究実績報告

① 受託研究実績金額（治験・製造販売後臨床試験・製造販売後調査）



② 治験・製造販売後臨床試験 新規登録症例数



NHOネットワーク共同研究 新規症例登録数

研究責任者	研究課題名(採択番号)	研究代表者(施設名)	文書同意 有・無	当該施設 新規症例 登録数
堤 育代	未治療濾胞性リンパ腫における Obinutuzumabの治療成績、 QOL、費用対効果、予後に関する 多施設前向きコホート研究（採択 番号：H31-NHO(血液)-01）	堤育代 （水戸医療センター）	有	4
稲毛 芳永	膵癌における腹腔洗浄細胞診を補 完する新規バイオマーカーの確立に関 する研究	末永 雅也 （名古屋医療センター）	有	8

競争的研究費

項目	研究課題名	研究者名	研究事業名 (依頼者名)	主任 分担	研究費 受領日	研究費 (単位：円)
科学研究費助成事業（学術研究助成基金助成金）	医師の病院前診察における網羅的文献データベース構築とエビデンス診療ギャップの解明 (21K10386)	堤 悠介	水戸医療センター (堤 悠介)	主任	R4.4.8	1,885,000
厚生労働科学研究費	心停止後臓器提供数の減少への効果的な対策に資する研究 (21FF2001)	湯沢賢治	水戸医療センター (湯沢賢治)	主任	R4.6.30	3,000,000
厚生労働科学研究費	新型インフルエンザ等の感染症発症時のリスクマネジメントに資する感染症のリスク評価及び公衆衛生的対策の強化のための研究 (20HA1005)	安田 貢	国立病院機構三重病院 (谷口清洲)	分担	R4.8.3	500,000
科学研究費助成事業（科学研究費補助金）	臓器移植法制・法政策の包括的再検証—改正法施行10年目の現況を踏まえた提言 (20H01430)	湯沢賢治	北海道大学 大学院法学研究科(城下祐二)	分担	R4.8.4	520,000
科学研究費助成事業（学術研究助成基金助成金）	包括的外傷長期予後データベースを用いたテラーメイド型社会復帰支援システムの確立(22K10476)	堤 悠介	東海大学 (土谷飛鳥)	分担	R4.8.5	65,000
厚生労働科学研究費	HAMならびに類縁疾患の患者レジストリによる相談機能の強化と診療ガイドラインの改訂(22FC1013)	湯沢賢治	聖マリアンナ医科大学医学研究科(山野嘉久)	分担	R4.8.16	200,000
日本医療研究開発機構研究費	HAM・HTLV-1陽性難治性疾患の患者レジストリ活用によるエビデンス創出 (22ek0109529h0002)	湯沢賢治	聖マリアンナ医科大学医学研究科(山野嘉久)	分担	R4.8.16	325,000
日本医療研究開発機構研究費	新規HTLV-1感染モデルを用いたHAMの発症予防法・治療法の開発 (22ek0109441h0003)	湯沢賢治	聖マリアンナ医科大学医学研究科(山野嘉久)	分担	R4.8.16	910,000
科学研究費助成事業（学術研究助成基金助成金）	文献レジストリ構築とリアルワールドデータによる膠原病予後因子の網羅的負荷推計 (22K10423)	堤 悠介	昭和大学 (辻本 康)	分担	R4.8.17	65,000
民間セクターからの寄附金	腹水濾過濃縮再静注法の臨床応用への適応拡大	矢田部芳治	中外製薬株式会社	主任	R4.11.21	200,000

英文論文

No	タイトル	著者	ポイント
1	Real-world treatment patterns and clinical outcomes in patients with AML in Japan who were ineligible for first-line intensive chemotherapy	吉田近思	12.200
2	Methodological Quality of Physical Therapy-Related Trials Published in Open Access and Subscription Journal A Cross-sectional Meta-Epidemiological Study	堤 悠介	6.000
3	Analyzing Chronological Change in Postoperative Magnetic Resonance Imaging Results in Patients With Kienbock's Disease by Using an Original Grading System	小川健	10.400
4	Prognostic Implication of PD-L1 Expression on Osimertinib Treatment for EGFR-mutated Non-small Cell Lung Cancer	沼田岳士	5.000
5	Macrophage behaviour 72 hours after implantation of biodegradable polymer-based sirolimus-eluting stent in a case of ST elevation myocardial infarction	小泉智三	1.450
6	Impact of COVID-19 on living donor liver and kidney transplantation programs in Japan in 2020	湯沢賢治	5.600
7	Prospective analysis of the expression status of FGFR2 and HER2 in colorectal and gastric cancer populations: DS-Screen Study	石田博保	5.800
8	Effect of Postoperative Muscle Loss After Resection of Non-small Cell Lung Cancer on Surgical Outcomes	中村亮太	12.000
9	Impact of chronological age on efficacy and safety of fluoropyrimidine plus bevacizumab in older non-frail patients with metastatic colorectal cancer: a combined analysis of individual data from two phase II studies of patients aged > 75 years	石田博保	5.400
10	Proportion attributable to contextual effects in general medicine: a meta-epidemiological study based on Cochrane reviews	堤 悠介	19.600
11	Individual Evaluation of the Common Extensor Tendon and Lateral Collateral Ligament Improves the Severity Diagnostic Accuracy of Magnetic Resonance Imaging for Lateral Epicondylitis	小川健	6.600
12	Novel translocation of POGZ/STK11 in de novo mast cell leukemia with KIT D816H mutation	稲留征典	2.300
13	The effectiveness of exercise with behavior change techniques in people with knee osteoarthritis: A systematic review with meta-analysis	堤 悠介	2.050

No	タイトル	著者	ポイント
14	'Hook' Shape Lister Tubercle Is Associated with a Greater Incidence of Extensor Pollicis Longus Tendon Rupture after Distal Radius Fracture	小川健	3.000
15	Use of a Small Car-Mounted Magnetic Resonance Imaging System for On-Field Screening for Osteochondritis Dissecans of the Humeral Capitellum	小川健	6.600
16	First manifestation of AQP4-IgG-positive neuromyelitis optica spectrum disorder following the COVID-19 mRNA vaccine BNT162b2	田代裕一	2.650
17	Prediction of early graft function after living donor kidney transplantation by quantifying the "nephron mass" using CT-volumetric software	湯沢賢治	6.900
18	Clinical Relevance of Ultrasonographic and Electrophysiological Findings of the Median Nerve in Unilateral Carpal Tunnel Syndrome Patients	小川健	6.600
19	Clinical Significance of Maximum Intensity Projection Method for Diagnostic Imaging of Thoracic Outlet Syndrome	小川健	15.200
20	Importance of TKI treatment duration in treatment-free remission of chronic myeloid leukemia: results of the D-FREE study	吉田近思	12.200
21	Sustained Lumen Area by Paclitaxel-Coated Balloon Following Rotational Atherectomy for Napkin-Ring Left Main Trunk Ostial Lesion	小泉智三	1.450
22	Classifications of moderate to severe asthma phenotypes in Japan and analysis of serum biomarkers: A Nationwide Cohort Study in Japan (NHOM Asthma Study)	遠藤健夫	9.800
23	Prognostic factors for recurrence in patients with surgically resected non-small cell lung cancer	中村亮太	1.000
24	Surgical treatment of pulmonary bullous diseases	中村亮太	1.800
25	Flexor Pollicis Longus Tendon Rupture and Carpal Tunnel Syndrome due to Scaphoid Nonunion Advanced Collapse: A Case Report.	小川健	1.000
26	Potential Relationships between the Median Nerve Cross-Sectional Area and Physical Characteristics in Unilateral Symptomatic Carpal Tunnel Syndrome Patients.	小川健	6.900
27	Abdominal compartment syndrome after endoscopic combined intrarenal surgery	岡田脩平	2.000

No	タイトル	著者	ポイント
28	Elevation of C-reactive protein during concurrent chemoradiotherapy is a poor predictive factor for head and neck cancer	瀬成田雅光	4.700

和文論文

No	論文名	著者	ポイント
1	NUP98::DDX10融合遺伝子を有した急性骨髄性白血病	吉田近思	1.000
2	急性骨髄性白血病に対するベネトクラクス治療マネジメント	吉田近思	1.000
3	茨城県における新型コロナウイルス感染症医療体制の構築	安田 貢	1.500
4	茨城県における新型コロナウイルス感染症医療体制と連携機能強化-行政と医療の連携、県調整本部活動と統括医療連携システム (I-HOPE) -	安田 貢	1.500
5	二次医療機関での時間外の外傷用CT撮像プロトコル作成	山名英俊	1.500
6	食道再建術における縫合不全回避のための工夫	福富俊明	1.500
7	組織オキシメータを用いた腸管血流評価法についての検討	加藤丈人	1.500
8	当院のBRCA1/2遺伝子検査の現状と課題について	森 千子	1.500
9	パンデミックは移植医療にどんな影響を与えていますか？	湯沢賢治	1.500
10	ドナー②術前検査 1)生体腎移植	湯沢賢治	1.500
11	ドナー②術前検査 2)死体(献)腎移植	湯沢賢治	1.500
12	新型コロナウイルス感染症 (COVID-19) の腎移植への影響	湯沢賢治	1.500
13	心停止後臓器提供	湯沢賢治	1.500
14	移植医からみた子宮移植の論点	湯沢賢治	1.500
15	COVID-19感染流行期における摘出医の負担軽減を目指した臓器摘出機材貸出シミュレーション	湯沢賢治	1.000
16	日本移植学会2021年症例登録 統計報告	湯沢賢治	1.500
17	わが国における臓器移植のための臓器摘出の現状と実績 (2022)	湯沢賢治	1.500
18	腎移植臨床登録集計報告 (2022) 2021年実施症例の集計報告と追跡調査結果	湯沢賢治	1.000
19	本邦における腎移植後管理の現状調査と今後の課題	湯沢賢治	1.000

No	論文名	著者	ポイント
20	腎移植登録事業の現況ードナーのフォローの必要性ー	湯沢賢治	1.000
21	固形臓器移植患者におけるSARS-CoV-2ワクチン接種後抗体獲得率に関する実態調査	湯沢賢治	1.000
22	CT-volumetricソフトウェアを用いたnephron mass定量による生体腎移植後早期グラフト機能の予測	湯沢賢治	1.000
23	三次救命救急センターにおけるびまん性特発性骨増殖症の有病率と骨折椎体高位の関係	森田純一郎	1.000
24	胸郭出口症候群の診断におけるMRIの有用性の検討	小川 健	1.500
25	手根管症候群で片側に症状を呈した症例における正中神経の電気生理学的特徴	小川 健	1.000
26	肘関節terrible triad injuryの治療戦略 前方要素の修復は必須か？	小川 健	1.500
27	【四肢骨折プレート固定術の創意工夫】鎖骨骨幹部骨折(1)(解説)	小川 健	1.500
28	創外固定で加療した小児上腕骨顆上骨折の治療成績(原著論文)	小川 健	1.000
29	【上肢の麻痺と痛み】複合性局所疼痛症候群(CRPS)に伴う上肢麻痺と痛み(解説).	小川 健	1.500
30	救急CT画像活用法-診断・治療・予後-	田中善啓	1.500

国際学会

学会名	演題名	演者名	発表年月日
American Heart Association Scientific Session 2022	Different Distribution of CD 163 Positive Macrophages in Thrombus Retrieved from infarct-related Artery :Atherothrombosis vs.Cardiogenic Thrombosis,Pathlolgical Analyses From MITO study	Tomomi Koizumi , Noriyuki Inamoto, Koji Nakano, Yu Yamada, Yuto Abe, Fumimasa tabata, Tomosato Yamazaki, Masao Ono	2022/11/5-7
European Congress of Radiology 2023, Vienna, Austria	Ecessity of remote 3D imaging creation in Emergency Radiology: An optimal way to enhance patient satisfaction for quality of emergency care delivery by improving availability.	田中善啓	2023/3/1

国内学会

学会名	演題名	演者名	発表年月日
第62回日本リンパ網内系学会 学術集会・総会	A case of cardiac tamponade diagnosed as recurrence of AITL by detection of the p.Gly17ValRHOA mutation in pericardial effusions	坪井宥璃	2022/6/24
第41回茨城造血器疾患研究会	骨髄異形成症候群に合併した TRALI type Ⅰ	橋川 諒	2022/6/5
第83回日本血液学会学術集 会	A real-world multicenter prospective cohort study in localized diffuse large B-cell lymphoma	堤 育代	2022/10/14
日本内科学会第684回関東地 方会	輸血製剤中の抗HLA抗体に起因する輸 血関連急性肺 傷害(TRALI)type 1	橋川 諒	2023/2/12
第44回日本造血・免疫細胞療 法学会総会	骨髄腫に対するVRD 療法と低用量シクロ フォスファミド＋ボルテゾミブによる幹細胞動 員・自家移植の有効性	堤 育代	2022/5/13
第87回 日本循環器学会学術 集会 JCS2023 FUKUOKA	【ポスターセッションA】(PE04-1) Impact of Onset-to-balIn Time on In hospital Mortality in Nonagenarian with ST-elevation My-ocardial infarction(Report fromMie ACS Reg- istry)	Tomomi Koizumi (FJCS)	2023/3/10
第87回 日本循環器学会学術 集会 JCS2023 FUKUOKA	Oral Presentation26 PCI Imaging / Physiology	(OE26-8) Yoshinobu Murasato,Hitoshi Nakashima,Hiroshi Suigino,Masaya Arakawa,Fumuaki Mori,Yasunori Ueda,Kerisuke Matumura,Mitsuura Abe, Tomomi Koizumi,Mitsuhiro Shimomura,Kazuteru Fuji- moto,Takahiro Saeki,shogo ImagawaTakashi Takenaka,Yukiko Morita,Katsuro Kashima,Akira Takami,Yujiro Ono,Atsuki	2023/3/10
第87回 日本循環器学会学術 集会 JCS2023 FUKUOKA	Heart Failure Diagnosis	(OJ24-3) 小泉智三	2023/3/11
第87回 日本循環器学会学術 集会 JCS2023 FUKUOKA	CROJ12-5 Ivabradine Effective Inappropriate Sinus Tachycar-dia Induced Cardiomyopathy	川邊 優希、小泉 智三、田畑 文昌、丸田 俊介、宇佐美 恭 平、貝塚 奈穂	2023/3/11

学会名	演題名	演者名	発表年月日
第62回日本呼吸器学会学術講演会	典型的な画像所見を呈さず経食道的気管支鏡下穿刺吸引生検法により診断した播種性クリプトコッカス症の一例	羽鳥貴士	2022/4/24
第37回日本環境感染学会	急性期病院での抗菌薬適正支援チーム（AST）活動の効果	箭内英俊	2022/6/17
第251回日本呼吸器学会関東地方会	肺小細胞癌に対してデュルバルマブ投与後に irAE による自己免疫性脳炎を呈した一例	山崎健斗	2022/9/10
第253回日本呼吸器学会関東地方会	肺扁平上皮癌に対する免疫チェックポイント阻害薬（ICI）使用後に肺結核を発症した一例	武石 岳大（退職）	2023/2/25
第684回日本内科学会関東地方会	尿中抗原が陰性であったが、気管支肺胞洗浄液のPCR・培養検査で診断に至ったレジオネラ肺炎の1例	山崎健斗	2023/2/12
第220回茨城内科学会	十二指腸転移を認めた小細胞肺がんの1例	米野友一朗	2022/6/18
第221回茨城内科学会	両肺に多発する浸潤影、左胸水を呈した肺原発T細胞性リンパ腫の1例	和田亮一郎	2022/10/16
第222回茨城内科学会	非典型的な画像を呈した肺腺癌・癌性リンパ管症の1例	寺門正尊	2023/3/18
第53回抗酸菌症治療研究会	忘れ去られたインフルエンザ～今冬、捲土重来なるか～	遠藤健夫	2022/12/4
茨城県Respiratory Conference	気管支喘息治療－現状と課題－	遠藤健夫	2022/10/5
第7回桜の郷チェストカンファレンス	呼吸器領域における興味深い症例の提示	太田恭子	2022/11/16
茨城県中央保健所感染症対策研修会	忘れ去られたインフルエンザ～今冬、復活なるか～	遠藤健夫	2022/11/18
Lung Cancer Webinar For Pharmacist	肺癌の薬物療法について Part1～薬物療法を知る～	遠藤健夫	2022/5/18
Lung Cancer Webinar For Pharmacist	肺癌の薬物療法における副作用について Part2～副作用を知る～	太田恭子	2022/5/18
水戸エリア 肺扁平上皮癌WEBセミナー	ネツツムマブによる副作用への対応について	箭内英俊	2022/6/8
北関東 NTM誌上座談会	茨城県内における肺NTM症への取り組みと今後の展望	遠藤健夫	2022/6/11
Lung Cancer Online Meeting	完全切除後の非小細胞肺癌（NSCLC）治療におけるアンメットメディカ	遠藤健夫	2022/12/12
令和4年度肺がん検診従事者講演会	令和4年度肺がん検診従事者講演会	遠藤健夫	2023/1/25
呼吸器DICフォーラムin 水戸	呼吸器疾患とDIC	遠藤健夫	2023/1/26
日本消化器病学会関東支部 第372回例会	合併症のない40代男性が出血性胆嚢炎を来した一例	辻実季	2022/12/10
日本内科学会第685回関東地方会	胃癌に対するニボルマブ投与後に発症した irAE腸炎の1例	藤川健太郎	2023/3/11
日本内科学会 第677回関東地方会	小細胞肺癌に対してデュルバルマブ投与後に発症した抗NMDA受容体抗体陽性自己免疫性脳炎のirAE例	相澤哲史	2022/5/8
日本内科学会 第680回関東地方会	骨転移による背部痛で発症した胃悪性黒色腫の1例	李 礼真	2022/9/4

学会名	演題名	演者名	発表年月日
第24回 茨城県脊髄・脊椎研究会	背部痛で発症し原発巣検索に難渋した転移性椎体腫瘍の1例	相澤哲史	2022/12/5
第242回日本神経学会関東甲信越地方会	関節症状を認めず発症した抗MOG抗体陽性のリウマチ性髄膜炎の一例	井岡桂	2022/9/5
第25回日本臨床救急医学会総会・学術集会	茨城県におけるCOVID-19臨時医療施設体制整備と運用	安田 貢	2022/5/26
第46回茨城県救急医学会	新型コロナウイルス感染症・茨城県における有事医療体制構築の実際と課題	安田 貢	2022/9/10
第46回茨城県救急医学会	県内における新型コロナウイルス感染疑い傷病者に対する救急車搬送困難対策の早期立案と効果	安田 貢	2022/9/10
第76回国立病院総合医学会	茨城県における新型コロナウイルス感染症医療体制構築-行政と医療の連携、県庁調整本部活動と医療連携システム（i-HOPE）	安田貢、石上耕司、塚田紀明	2022/10/7
第50回日本集中治療医学会	集中治療領域におけるランダム化比較試験と系統的レビューの出版数の傾向：メタ疫学研究	堤 悠介	2023/3/2
第75回日本胸部外科学会定期学術集会	術前体組成計を用いて筋量を評価した肺癌手術症例の検討	飛田理香	2022/10/8
第84回 日本臨床外科学会総会	腹部主要3動脈の慢性狭窄を背景に生じた右側結腸虚血に対し血管内治療が奏功した1例	小林仁存	2022/11/25
第59回 日本腹部救急医学会総会	適切に診断・治療し重篤化重篤化を回避できた胆嚢出血の1例	和田亮一郎	2023/3/10
第250回 茨城外科学会	上部消化管造影検査後にバリウム塊によるS状結腸穿孔を来たし治療に難渋した肥満男性の1例	山本恭彰	2022/5/21
第11回 茨城消化器鏡視下治療研究会（IDES文科会）	LAR ～助手との協調～	山本恭彰	2023/3/23
第59回 日本腹部救急医学会総会	腹腔鏡手術を施行した結腸脾彎曲部捻転の1例	成田保和	2023/3/9
第37回 日本環境感染学会総会・学術集会	当院のサイトメガロウイルス(CMV)抗体陽性 ドナーから抗体陰性レシピエント腎移植の対策	小崎浩一	2022/6/16
第30回 日本乳癌学会学術総会	乳癌患者の難治性大量腹水に対する腹水濾過濃縮再静注法（CART）	小崎浩一	2022/6/30
第67回 日本透析医学会学術集会・総会	腎移植患者の自己腎腎癌の検討	小崎浩一	2022/7/1
第77回 日本消化器外科学会総会	Result of 10 years of surveillance for surgical site infection in lower gastrointestinal surgery	小崎浩一	2022/7/20
第46回 茨城県救急医学会	同一ドナーから提供された 同日2腎献腎移植の経験	小崎浩一	2022/9/10
第58回 日本移植学会総会	わが県の腎移植に現状からみた地域の移植医療の未来 ～働き方改革で問題は解決するのか？～	小崎浩一	2022/10/13
第30回 日本消化器関連学会週間（JDDW 2022）	消化器悪性腫瘍難治性腹水に対する低温保存腹水濾過濃縮再静注法	小崎浩一	2022/10/28

学会名	演題名	演者名	発表年月日
第35回 日本外科感染症学会総会学術集会	ワークショップ：「移植関連（移植患者の外科感染症対策）」 腎移植患者における尿路感染症発症のrisk factorの検討	小崎浩一	2022/11/8
第43回 日本アフェシス学会学術大会	S状結腸癌腹膜播種による難治性腹水に対し繰り返し腹水濾過濃縮再静注法を行った高齢者患者の一例	小崎浩一	2022/11/10
第56回 茨城人工透析談話会	抗ドナー抗体陽性腎移植の3例	小崎浩一	2022/11/13
第19回 CART研究会学術集会	ワークショップ：低温保存腹水CART（腹水濾過濃縮再静注法）の安全性に関する検討～CART研究会・多施設共同研究～	小崎浩一	2022/12/3
第56回 日本臨床腎移植学会	ABO血液型不適合・抗ドナー抗体陽性腎再移植の2例	小崎浩一	2022/2/11
第39回日本呼吸器外科学会学術集会	当院における病理病期Ⅰ期肺腺癌症例の検討	栗原秀輔	2022/5/20
第59回 日本腹部救急医学会総会	診断に苦慮した膿瘍形成下行結腸粘液癌の1例	栗原秀輔	2023/3/10
第30回 日本乳癌学会学術総会	進行・再発乳癌の腫瘍マーカーの推移についての検討	森 千子	2022/6/30
第18回 日本乳癌学会関東地方会	腎細胞癌術後乳腺転移の1例	森 千子	2022/12/3
第日本外科代謝栄養学会 第59回学術集会	胃切除術後再建方法と骨格筋量減少の関連	米山 智	2022/7/7
第77回 日本消化器外科学会総会	異なるアプローチ法を行った腰ヘルニアの2例	米山 智	2022/7/21
第35回 日本内視鏡外科学会総会	右側肝円索に伴う左側胆嚢に対して腹腔鏡下胆嚢摘出術を行った1例	米山 智	2022/12/9
第59回 日本腹部救急医学会総会	当院における閉鎖孔ヘルニアの治療成績	米山 智	2023/3/10
我が街脳卒中を考える会	県央地区の脳卒中急性期治療に対する取り組みについて	山崎友郷	2022/4/19
茨城県央県北ブレインアタックフォーラム	水戸・ひたちなか医療圏の脳卒中連携について再考する	加藤徳之	2022/6/4
第81回 日本脳神経外科学会学術総会	脳出血に対する磁場式ナビゲーション下血腫吸引術+ウロキナーゼ注入療法の安全性と効果の検討	山崎友郷	2022/9/28
第81回 日本脳神経外科学会学術総会	血流改変 (Flow diverter stent)ステント留置術後に広範白質浮腫を呈した1例	加藤徳之	2022/9/28
第107回茨城脳神経外科集談会	血流改変 (Flow diverter stent)ステント留置術後に広範白質浮腫を呈した1例	加藤徳之	2022/10/16
PIPELINE STEP UP SEMINAR	当院でのFD使用経験	加藤徳之	2022/10/21
茨城脊椎・脊髄カンファレンス	嚥下障害で発症したびまん性特発性骨増殖症(DISH)の1例	加藤徳之	2022/12/5
第5回関東HLA研究会学術集会	臓器移植とHLA	湯沢賢治	2022/6/4
第67回日本透析医学会学術集会 ・総会	腎移植up to date, 腎移植登録事業の現況,	湯沢賢治	2022/7/1

学会名	演題名	演者名	発表年月日
第48回日本臓器保存生物医学学会学術集会	臓器移植患者のCOVID-19－日本移植学会COVID-19対策委員会の活動－	湯沢賢治	2022/11/4
第48回日本骨折治療学会学術集会	上方アプローチによる人工骨頭置換術は第一助手の経験が重要である	森田純一郎	2022/6/25
第48回日本骨折治療学会学術集会	2方向透視法による経皮的椎弓根スクリュー固定の逸脱率と関連因子の検討	森田純一郎	2022/6/25
第45回日本骨・関節感染症学会学術集会	BCG膀胱内注入療法後に感染性大動脈瘤を経て結核性脊椎炎を発症した1例	小林賢司	2022/7/8
第37回日本整形外科学会基礎学術集会	Transiliac-transsacral screw挿入のための術中透視仙骨側面像の検討	森田純一郎	2022/10/14
第37回日本整形外科学会基礎学術集会	ゲームエンジンをういた骨折手術VRプレート術前計画の試み 模擬骨を使用した基礎実験	森田純一郎	2022/10/13
第36回東日本手外科研究会	キーンバック病に対する骨髄血移植・創外固定・低出力超音波併用治療	小川 健	2022/3/5
第65回日本手外科学会学術集会	キーンバック病の病態に迫る	小川 健	2022/4/23
第95回日本整形外科学会学術総会	Chronological change in postoperative magnetic resonance imaging results in patients with Kienböck's disease using an original grading system	小川 健	2022/5/21
第35回日本肘関節学会学術集会	スポーツ選手における特発性肘部管症候群手術例の特徴	小川 健	2023/2/4
第35回日本肘関節学会学術集会	スポーツ選手の特発性肘部管症候群手術例における神経伝導速度検査の有用性	小川 健	2023/2/4
第35回日本肘関節学会学術集会	上腕骨遠位端骨折に対するA.L.P.S.Elbow Plating Systemの治療成績	小川 健	2023/2/4
第35回日本肘関節学会学術集会	思春期前のリトルリーガーにおける肘関節内側障害に関する高分解能MRI	小川 健	2023/2/3
第95回日本整形外科学会学術総会	母指CM関節症患者における牽引MRIによる関節軟骨評価	小川 健	2022/5/21
第95回日本整形外科学会学術総会	野球選手における超音波検査での肘関節外反弛緩性評価時の至適肢位	小川 健	2022/5/21
第95回日本整形外科学会学術総会	大学野球選手における肩関節外転外旋位での回旋筋力の特徴	小川 健	2022/5/21
第95回日本整形外科学会学術総会	車載型ポータブルMRIによる上腕骨離断性骨軟骨炎検診の有用性	小川 健	2022/5/21
第33回日本臨床スポーツ医学会学術集会	野球選手の尺骨神経脱臼は投球側で多いか？	小川 健	2022/11/12
第95回日本整形外科学会学術総会	胸郭出口症候群の補助診断としてMRI最大値投射法は有効か	小川 健	2022/5/21
第95回日本整形外科学会学術総会	上腕骨外側上顆炎に対するMRI検査治療指標としての有用性の検討	小川 健	2022/5/20

学会名	演題名	演者名	発表年月日
第19回茨城形成外科研究会	遊離DIEP皮弁による再建乳房・採取部に低温熱傷を生じた1例	手口円花	2022/6/10
栃木・茨城（第6回形成外科）Peer Review Meeting	左脛腓骨開放骨折Gastilo3Bの1例	笠井丈博	2022/8/14
第20回茨城形成外科研究会	Local flapとcomposite graftを併用した鼻翼再建の2例	笠井丈博	2022/11/12
第16回筑波大学形成外科同門会	汚染が疑われる眼窩部複合組織損傷に対して、一期的に再建した1例	手口円花	2023/3/11
第36回日本泌尿器内視鏡・ロボティクス学会総会	悪性を否定しえない前立腺間質腫瘍に対しロボット支援腹腔鏡下前立腺全摘術を施行した1例	岡田脩平	2022/11/11
第26回秋田腎不全研究会	腸管利用膀胱拡大術後30年目に腎後性腎不全のため透析導入に至った1例	岡田脩平	2022/12/4
第36回日本泌尿器内視鏡・ロボティクス学会総会	当院におけるロボット支援下体外尿路変更膀胱全摘術の初期経験	飯沼昌宏	2022/11/11
第87回日本泌尿器科学会東部総会	腎癌術後12年目に乳腺転移をきたした1例	飯沼昌宏	2022/10/29
第19回泌尿器再建再生研究会	右腎尿管膀胱全摘回腸導管術後の骨盤再発による左水腎症に対して腹腔鏡下尿管皮膚瘻作成術を行った1例	飯沼昌宏	2022/6/4
第123回茨城地方会	同一腎に腎血管金脂肪腫と腎細胞癌が同時発生した1例	齋藤拓郎	2022/6/18
第124回茨城地方会	後腹膜に発生した骨髄脂肪腫の1例	齋藤拓郎	2022/10/16
第125回茨城地方会	新型コロナウイルス感染症に関連した虚血性持続勃起症の1例	齋藤拓郎	2023/2/18
日本サイコネフロジー学会	移植腎廃絶後の透析回避	仲宮優子	2022/7/23
第46回茨城県救急医学会	COVID-19禍の献腎移植	仲宮優子	2022/9/10
第76回国立病院総合医学会	当院におけるOICに対する治療の現状 ナルデメジントシル塩酸錠の使用状況と効果	木村梨奈	2022/10/8
日本移植学会	RTCが考える腎代替療法選択におけるSDM	仲宮優子	2022/10/15
日本臨床腎移植学会	RTCの育成 ～私がRTCを目指し、継続できた理由～	仲宮優子	2023/2/12
第76回国立病院総合医学会	カルバペネム系抗菌薬の使用実態と薬剤師の関わり方	田所あき穂	2022/10/7
第78回日本放射線技術学会総会学術大会	CT撮影における標準化改訂 救急領域	田中善啓	2022/4/16
第25回日本臨床救急医学会総会・学術集会	COVID-19における放射線部門の感染対策：ハイブリットチーム化の有用性	田中善啓	2022/5/26
第36回日本外傷学会総会・学術集会	外傷における潜伏性股関節骨折の早期診断MRIとCTスキャンの比較	田中善啓	2022/7/1
第76回国立病院総合医学会	腎細胞癌術後13年で発見された転移性乳腺腫瘍の1例	新井杏奈	2022/10/8
第28回日本心臓リハビリテーション学会学術集会	高齢心不全患者における退院時身体機能と再入院までの期間の検討(県内2施設前向き観察研究)	幡谷夏海	2022/6/12

学会名	演題名	演者名	発表年月日
第 7 6 回国立病院総合医学会	橋損傷患者における前頭葉由来の高次脳機能障害の調査	中津川泰生	2022/10/8
第 7 6回国立病院総合医学会	運動恐怖症がTKA術後患者の身体機能に及ぼす影響について	村島昂瑛	2022/10/7
第76回国立病院総合医学会	高齢HFpEF患者における入院中の心臓リハビリテーションが身体機能に与える効果の検討	柳澤宏昭	2022/10/8
第76回国立病院総合医学会	サルコペニアを有する周術期肺がん患者のリハビリテーションの必要性	木村匠吾	2022/10/7
第22回　CRCと臨床試験のあり方を考える会議	感染管理体制下における、治験実施体制整備の取り組みについて ～COVID-19対象患者の治験からCRCの役割について考える～	小野直美	2022/9/17

令和4年度院内臨床研究課題

研究代表者	課題名	配分額
相澤哲史	免疫チェックポイント阻害薬を使用した担癌患者における免疫関連有害事象（irAE）発現に影響を与える因子を探索する後ろ向き症例集積研究	690,000
小川 健	手関節周辺疾患に対する造影ダイナミックMRIの有用性に関する研究	800,000
佐藤真剛	亜急性期大動脈解離に対するステントグラフト治療の中期成績	450,000
田中善啓	放射線診断における遠隔3D画像作成運用の可能性と検証	1,000,000
堤 悠介	外傷診療中のCTにおける偶発的所見の発見率：系統的レビュー・メタアナリシス	630,000
中村亮太	肺癌術前の筋量・筋力が術後に与える影響について明らかにする	600,000
森田純一郎	寛骨臼骨折に対する骨盤模型を用いたプレート成形の有効性を検討する観察研究	500,000
山崎友郷	茨城県のELVOスクリーンによる主幹動脈閉塞症例搬送システム導入による臨床転帰に与える影響について	500,000
山本恭彰	横行結腸癌の発生部位の差における至適術式についての後ろ向き観察研究	500,000
米山 智	胃切除術後の再建形成と骨格筋量・体脂肪量変化の関連および臨床経過との関連についての研究	600,000

水戸医療センター

令和4年度 代表的論文





Real-world treatment patterns and clinical outcomes in patients with AML in Japan who were ineligible for first-line intensive chemotherapy

Chikashi Yoshida¹ · Takeshi Kondo² · Tomoki Ito³ · Masahiro Kizaki⁴ · Kazuhiko Yamamoto⁵ · Toshihiro Miyamoto⁶ · Yasuyoshi Morita⁷ · Tetsuya Eto⁸ · Yuna Katsuoka⁹ · Naoki Takezako¹⁰ · Nobuhiko Uoshima¹¹ · Kazunori Imada¹² · Jun Ando¹³ · Takuya Komeno¹ · Akio Mori² · Yuichi Ishikawa¹⁴ · Atsushi Satake³ · Junichi Watanabe⁴ · Yoshiko Kawakami¹⁵ · Tetsuo Morita¹⁵ · Ikue Taneike¹⁵ · Masahiko Nakayama¹⁵ · Yinghui Duan¹⁶ · Belen Garbayo Guijarro¹⁷ · Alexander Delgado¹⁸ · Cynthia Llamas¹⁶ · Hitoshi Kiyoi¹⁴

Received: 16 November 2021 / Revised: 15 March 2022 / Accepted: 15 March 2022
© Japanese Society of Hematology 2022

Abstract

Acute myeloid leukemia (AML) predominantly affects elderly adults, and its prognosis worsens with age. Treatment options for patients in Japan ineligible for intensive chemotherapy include cytarabine/aclarubicin ± granulocyte colony-stimulating factor (CA ± G), azacitidine (AZA), low-dose cytarabine (LDAC), targeted therapy, and best supportive care (BSC). The country's aging population and the evolving treatment landscape are contributing to a need to understand treatment pathways and associated outcomes. This retrospective chart review evaluated outcomes in patients across Japan with primary/secondary AML who were ineligible for intensive chemotherapy and began first-line treatment or BSC between 01/01/2015 and 12/31/2018. The primary endpoint was overall survival (OS); secondary endpoints included progression-free survival (PFS) and healthcare resource utilization (HRU). Of 199 patients (58% > 75 years), 121 received systemic therapy (38 CA ± G, 37 AZA, 7 LDAC, 39 other) and 78 received BSC. Median OS was 5.4, 9.2, 2.2, 3.8, and 2.2 months for CA ± G, AZA, LDAC, other systemic therapy, and BSC, respectively; median PFS was 3.4, 7.7, 1.6, 2.3, and 2.1 months, respectively. HRU rates were uniformly high, with > 80% patients hospitalized in each cohort. The poor clinical outcomes and high HRU among Japanese AML patients who are ineligible for intensive chemotherapy highlight an unmet need for novel therapies.

Keywords Acute myeloid leukemia · Azacitidine · Aclarubicin ± granulocyte colony-stimulating factor · Low-dose cytarabine

Department and institution in which the work was done: **Kyushu University Hospital**, Department of Hematology, Oncology & Cardiovascular Medicine. **Hamanomachi Hospital**, Department of Hematology. **Okayama City General Medical Center**, Department of Hematology. **Osaka Red Cross Hospital**, Department of Hematology. **Kindai University Hospital**, Department of Hematology and Rheumatology. **Kansai Medical University Hospital**, Department of Hematology-Oncology. **Japanese Red Cross Kyoto Daini Hospital**, Department of Hematology. **Nagoya University Hospital**, Department of Hematology. **Juntendo University Hospital**, Department of Hematology. **National Hospital Organization Disaster Medical Center**, Department of Hematology. **Saitama Medical Center, Saitama Medical University**, Department of Hematology. **National Hospital Organization Mito Medical Center**, Department of Hematology. **Sendai Medical Center**, Department of Hematology. **Aiiku Hospital**, Department of Hematology and Blood Disorders Center.

Extended author information available on the last page of the article

Introduction

Acute myeloid leukemia (AML) is a clonal hematopoietic malignancy characterized by high molecular and pathogenic heterogeneity [1, 2]. Although AML accounts for only about 1% of cancers, it is the most common form of acute leukemia in adults (approximately a quarter of total leukemia cases) and is the leading cause of leukemia-related death [1, 3]. AML primarily affects older adults, and the median age at diagnosis is 68 years [3]. In Japan, approximately 40–50% of patients with leukemia are diagnosed at the age of 75 years or older [4]. The global incidence of AML is rising with an aging population, almost doubling between 1990 and 2017 [5, 6]. In Japan, the annual incidence of AML is 5.6/100,000 and this rises to 10–17/100,000 for those older than age 69 years [7].

Patients with AML have a poor prognosis, particularly those with advanced age [8]. Older patients have a long-term survival rate of < 10%, compared with 30–50% for patients younger than age 60 years [1]. For patients aged 75 years or older, the estimated 5-year survival rate is as low as 1.5% [6].

Historically, the standard of care for AML has been induction therapy with 7 days of standard-dose cytarabine and 3 days of an anthracycline ('7 + 3' regimen) followed by consolidation therapy, with hematopoietic stem cell transplantation an option for eligible patients [1, 2, 9, 10]. However, older patients and those with comorbidities or a poor performance status are often unable to tolerate such intensive therapy [9, 10]. For patients considered ineligible for intensive treatment, low-dose cytarabine (LDAC) and best supportive care (BSC) are among the few options recommended by Japanese guidelines [11, 12]. In Japan, cytarabine, aclarubicin \pm granulocyte colony-stimulating factor (CA \pm G) [11, 13–15], and the recently approved hypomethylating agent, azacitidine (AZA) [16], have also been practical treatment options for patients with AML ineligible for intensive treatment.

Despite complete remission (CR) rates of up to 58% reported following treatment with CA \pm G [13], outcomes in patients with AML deemed ineligible for intensive chemotherapy typically remain poor [17–21], and overall survival (OS) estimates range from 7.5–12.1 months for CA \pm G, 7.7–10.4 months for hypomethylating agents, 4.1–6.4 months for LDAC, and 3.6–3.7 months for BSC [15, 17, 18, 22–27].

Increased understanding of the heterogeneity of AML has led to the development of targeted, chemotherapy-free therapies including B-cell lymphoma-2 (BCL-2), FMS-like tyrosine kinase-3 (FLT3), and hedgehog inhibitors [1, 2, 8, 9]. Although the use of targeted therapies as first-line therapy for AML is currently limited in Japan, the recent approval of venetoclax, a BCL-2 inhibitor, has expanded the available options for patients with AML ineligible for intensive chemotherapy [28].

As novel agents and management strategies become increasingly, but not uniformly, available, there is an unmet need to understand current treatment pathways and their associated clinical outcomes. Furthermore, patients with AML place a high burden on healthcare systems, with hospitalizations more frequent among older patients than their younger counterparts [29]. There is also a need to understand the healthcare resource utilization (HRU) affiliated with different treatment pathways.

CURRENT (Real-World Treatment Patterns and Clinical Outcomes in Unfit AML Patients Receiving First Line Systemic Treatment or Best Supportive Care) was a retrospective chart review designed to examine real-world treatment patterns and HRU in patients who were ineligible for

intensive chemotherapy and received first-line systemic therapy or BSC [30]. Here, we report a subanalysis of the CURRENT study population that evaluated the clinical outcomes, patient characteristics, treatment patterns, and HRU of patients with AML in Japan. This study collated data from patients who initiated treatment between 2015 and 2018, therefore, prior to the approval of venetoclax and AZA for AML in Japan.

Methods

Study design

This noninterventional retrospective chart review was carried out in patients diagnosed with AML who were considered ineligible for intensive induction chemotherapy and who initiated first-line treatment or BSC between January 1, 2015 and December 31, 2018. Sites with eligible patients that exceeded the site enrolment limit (10–27 patients depending on the site) used a random sampling method to select patients for inclusion; the total number of eligible patients was divided by the maximum number allowed to enrol to determine the selection factor (i.e., every 3rd or 4th patient). The study was carried out in accordance with the guidelines for good pharmacoepidemiology practices in non-interventional studies and the ethical guidelines for medical and health research involving human subjects. Treatment was determined by each treating investigator. Data collection was carried out anonymously following ethics committee approval. CURRENT was conducted across 112 centers in 22 countries. This subanalysis focused on the patients who received treatment at 14 centers across Japan.

Patient selection and data collection

Patients were ≥ 18 years old, diagnosed with primary or secondary AML, and were deemed ineligible for intensive chemotherapy. Ineligibility for intensive induction therapy was defined on the basis of treating physician's assessment of age, Eastern Cooperative Oncology Group (ECOG) performance status, comorbidities, regional guidelines, and institutional practice [31]. Patients with unconfirmed AML diagnosis, acute promyelocytic leukemia, and those who received first-line treatment within a clinical trial were excluded. Patients had to have received first-line systemic treatment with CA \pm G, AZA, LDAC, targeted therapy, or BSC, and had ≥ 2 practice visits during the treatment period, in addition to the initial treatment visit (defined as start of systemic treatment or BSC). Patients were followed until the last recorded contact or death, whichever was applicable at the time of data collection. Anonymized patient data were extracted from patient charts and/or site documentation and

recorded via electronic case report forms (CRFs) completed by each center.

Endpoints

The primary endpoint was overall survival (OS), measured from diagnosis of AML. Secondary clinical endpoints included progression-free survival (PFS, measured from diagnosis of AML to physician-assessed disease progression or death), time to treatment failure (TTF; defined as the time from start of first-line systemic therapy or BSC until treatment discontinuation for any reason), and response rates (complete remission [CR] + CR with incomplete hematologic recovery [CRi]) according to the treating physician's assessment. Additional secondary endpoints were minimal residual disease (MRD) testing rates, and HRU determined by hospitalizations, outpatient consultations, transfusions (red blood cell [RBC] and/or platelet), supportive care (including growth factors) and other medications (including antibiotics, antivirals, and antifungals) from the initiation of first-line systemic therapy or BSC until treatment discontinuation.

Statistical analysis

Formal statistical power considerations are not provided due to the descriptive nature of the study. The final data cutoff was March 31, 2020. Continuous variables are described with mean, standard deviation, median, and ranges. Categorical variables are reported as counts and proportions. Time-to-event data were estimated using the Kaplan–Meier method, with median time and 95% confidence intervals (CIs) reported.

Results

Baseline demographics and patient disposition

In total, the CURRENT study enrolled 1,762 patients across 22 countries. The highest recruitment was from the Japan and Asia–Pacific region ($n=610$; 35%), including 199 patients who were enrolled from Japan. The majority of patients treated in Japan were male ($n=125$; 63%) and older than age 75 years at diagnosis ($n=116$; 58%). Most patients had intermediate ($n=88$; 44%) or poor ($n=76$; 38%) cytogenetic risk and 42% ($n=27$) of those with available data carried a mutation.

Of the 199 patients enrolled from Japan, 121 (61%) received first-line systemic therapy: 38 (31%) received CA \pm G; 37 (31%) received AZA; 7 (6%) received LDAC; and 39 (32%) received other systemic therapy which included cytarabine, aclarubicin, FLT3 inhibitors,

gemtuzumab ozogamicin, enocitabine, venetoclax, and therapy combinations which included CA \pm G, AZA, and LDAC. The remaining 78 patients (39%) received BSC, which included transfusions as needed ($n=63$; 81%), infection management ($n=47$; 60%), pain relief ($n=27$; 35%), nutritional support ($n=19$; 24%), and other supportive measures ($n=6$; 8%).

Baseline characteristics were generally similar between the systemic therapy and BSC cohorts, although the LDAC group had a higher proportion of patients older than age 75 years at diagnosis (86 vs 59% of all patients who received first-line systemic therapy) and the majority of patients in this group had secondary AML (71%) versus 32–46% in the other treatment groups. The AZA group and CA \pm G groups had a higher proportion of patients with ECOG performance status 0–1 (70 and 58%, respectively, vs 31–49% in the other treatment groups), and the AZA and other systemic therapy groups had a higher proportion of patients with poor cytogenetic risk (43 and 59%, respectively, vs 28–34% in the other treatment groups; Table 1). Overall, there were no consistent imbalances of comorbidities across groups.

For patients with available data, the median proportion of blast cells in bone marrow aspirate at baseline was 46% (range 2.0–96.0%) for patients who received CA \pm G, 30% (10.0–88.0%) for AZA, 42% (22.0–99.0%) for LDAC, 65% (22.8–98.5%) for other systemic therapy, and 41% (0.8–97.4%) for BSC, respectively.

At the time of the data cutoff, first-line treatment had been discontinued by 95% of patients in the CA \pm G group, 95% of the AZA group, 100% of the LDAC group, 97% of the other systemic therapy group, and 90% of the BSC group (Fig. 1). The most common reasons for discontinuation across the systemic treatment groups were disease progression ($n=49$; 42%), treatment completion ($n=28$; 24%), and death ($n=20$; 17%). The most common reasons for discontinuation of BSC were death ($n=47$; 67%) and patient preference ($n=11$; 16%).

Second-line systemic therapy was received by 49 (25%) patients, the majority of whom received CA \pm G ($n=13$; 27%) or AZA ($n=12$; 24%) (Fig. 2A). The majority of patients who went on to receive BSC had initially received first-line AZA. Most patients who initially received BSC did not receive any subsequent therapy (Fig. 2B).

Primary endpoint

There were 166 (85%) deaths by the final data cutoff on March 31, 2020, which included 84% ($n=32$), 81% ($n=30$), 86% ($n=6$), 92% ($n=35$), and 83% ($n=63$) of patients who received CA \pm G, AZA, LDAC, other systemic therapy and BSC, respectively. Median OS from diagnosis was 4.0 months (95% CI 3.1–5.1) for the overall population. Median (95% CI) OS from diagnosis was 5.4 (2.7–14.6)

Table 1 Baseline demographics and disease characteristics

	First-line systemic therapy (<i>n</i> = 121)				BSC <i>n</i> = 78
	CA ± G <i>n</i> = 38	AZA <i>n</i> = 37	LDAC <i>n</i> = 7	Other ^a <i>n</i> = 39	
Gender					
Male	21 (55)	22 (60)	4 (57)	21 (54)	57 (73)
Age at diagnosis					
Age, median (range), years	77 (52–89)	78 (64–88)	80 (70–85)	76 (57–89)	77 (49–89)
> 75 years	22 (58)	22 (59)	6 (86)	21 (54)	45 (58)
Secondary AML					
Yes	12 (32)	17 (46)	5 (71)	13 (33)	35 (45)
No	25 (66)	19 (51)	2 (29)	25 (64)	38 (49)
Unknown	1 (3)	1 (3)	0	1 (3)	5 (6)
ECOG performance status					
0–1	22 (58)	26 (70)	3 (43)	19 (49)	24 (31)
≥ 2	11 (29)	8 (22)	3 (43)	19 (49)	38 (49)
Unknown	5 (13)	3 (8)	1 (14)	1 (3)	16 (21)
AML classification (WHO)					
AML with recurrent genetic abnormalities	4 (11)	0	0	4 (10)	7 (9)
AML with MDS-related changes	17 (45)	27 (73)	3 (43)	13 (33)	33 (42)
Therapy-related myeloid neoplasms	2 (5)	1 (3)	0	1 (3)	2 (3)
AML not otherwise specified	9 (24)	6 (16)	2 (29)	12 (31)	17 (22)
Myeloid sarcoma	1 (3)	0	0	1 (3)	0
Unknown	5 (13)	3 (8)	2 (29)	9 (23)	19 (24)
Molecular features identified ^b					
Any mutation ^c	2 (5)	2 (5)	0	11 (28)	12 (15)
TP53 mutation	0	1 (50)	0	1 (9)	3 (25)
FLT3 mutation ^d	0	0	0	1 (9)	1 (8)
FLT3 ^{ITD} mutation	0	0	0	4 (36)	2 (17)
No mutation	6 (16)	12 (32)	2 (29)	8 (21)	10 (13)
Unknown molecular profile	30 (79)	23 (62)	5 (71)	20 (51)	56 (72)
Cytogenetic risk					
Favorable	4 (11)	0	0	1 (3)	4 (5)
Intermediate	20 (53)	19 (51)	4 (57)	12 (31)	33 (42)
Poor	13 (34)	16 (43)	2 (29)	23 (59)	22 (28)
Unknown	1 (3)	2 (5)	1 (14)	3 (8)	19 (24)
Comorbidities ^b					
Any	30 (79)	26 (70)	5 (71)	32 (82)	67 (86)
Myocardial infarction	1 (3)	1 (3)	0	3 (8)	4 (5)
Angina/coronary artery disease	0	5 (14)	1 (14)	5 (13)	3 (4)
Congestive heart failure	6 (16)	2 (5)	0	1 (3)	2 (3)
Arrhythmias	2 (5)	1 (3)	1 (14)	2 (5)	5 (6)
Restrictive lung disease or COPD	0	5 (14)	0	2 (5)	5 (6)
Liver cirrhosis (Child Pugh A, B, or C)	2 (5)	0	0	1 (3)	2 (3)
Elevated transaminases (elevation not related to liver cirrhosis)	2 (5)	2 (5)	0	0	1 (1)
Renal failure or CKD stage 3, 4 or 5	1 (3)	2 (5)	0	2 (5)	8 (10)
Other	22 (58)	20 (54)	4 (57)	23 (59)	56 (72)
None	8 (21)	10 (27)	2 (29)	7 (18)	10 (13)
Unknown	0	1 (3)	0	0	1 (1)
Elevated transaminases (elevation not related to liver cirrhosis) OR Renal failure or CKD stage 3, 4	4 (11)	2 (5)	0	2 (5)	8 (10)

Table 1 (continued)Data are *n* (%) unless otherwise stated

AML acute myeloid leukemia, *ASXL1* additional sex comb-like 1, AZA azacitidine, BSC best supportive care, CA±G cytarabine aclarubicin±granulocyte colony-stimulating factor, CKD chronic kidney disease, COPD chronic obstructive pulmonary disease, C-P Child Pugh, ECOG Eastern Cooperative Oncology Group, *FLT3* FMS-like tyrosine kinase-3, *FLT3*^{ITD} *FLT3* mutation with the internal tandem duplication, *FLT3*^{TKD} *FLT3* mutation in the tyrosine kinase domain, G-CSF granulocyte colony-stimulating factor, *JAK2* Janus kinase 2, LDAC low-dose cytarabine, MDS myelodysplastic syndrome, *TET2* Ten-Eleven-Translocation-2, *TP53* tumor protein p53, WHO World Health Organization

^aOther includes cytarabine, aclarubicin, *FLT3* inhibitors, gemtuzumab ozogamicin, enocitabine, venetoclax, and therapy combinations which included AZA, LDAC, and CA±G

^bPercentages may sum up to > 100% as multi-selection was permitted

^cUsed as a denominator for the following subcategories

^dNot specified as *FLT3*^{ITD} or *FLT3*^{TKD} mutation

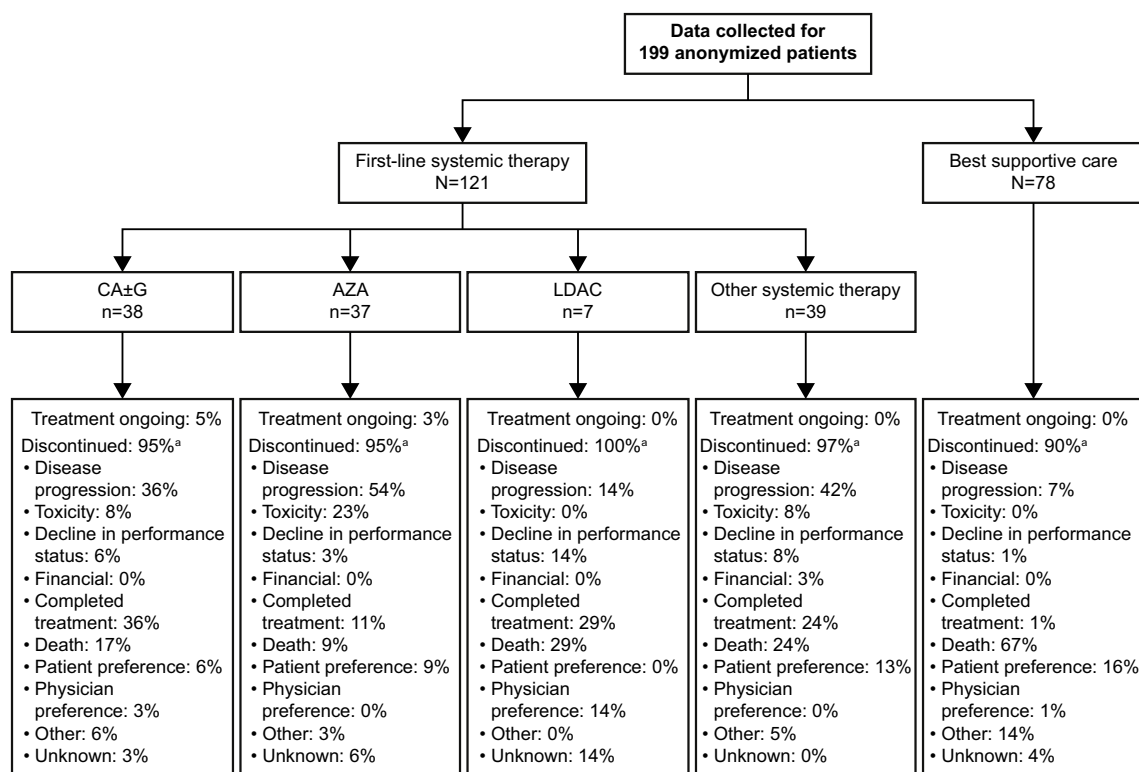


Fig. 1 Patient disposition. ^aPercentages may sum up to > 100% as multi-selection was permitted. AZA azacitidine, CA±G cytarabine, aclarubicin±granulocyte colony-stimulating factor, LDAC low-dose cytarabine

months for patients who received CA±G, 9.2 (5.0–13.1) months for patients who received AZA, 2.2 (0.1–16.6) months for patients who received LDAC, 3.8 (1.4–9.1) months for patients who received other systemic therapy, and 2.2 (1.7–3.6) months for patients who received BSC (Fig. 3).

Secondary efficacy endpoints

The median PFS was 3.0 months (95% CI 2.2–3.8) for the overall population. The median (95% CI) PFS was 3.4 (1.7–5.7), 7.7 (3.4–10.1), 1.6 (0.1–2.3), 2.3 (0.9–4.4), and

2.1 (1.6–3.1) months for patients who received CA±G, AZA, LDAC, other systemic therapy, and BSC, respectively (Fig. 4). The median (95% CI) TTF was 1.5 (0.5–23.3), 5.8 (2.1–10.5), 0.3 (0.1–not estimable), 1.3 (0.3–8.0), and 1.5 (0.7–1.9) months, respectively (Fig. 5).

Of the 121 patients who received first-line systemic therapy, CR/CRi was achieved by 19 (16%) patients, including 12 (32%) who received CA±G, 1 (3%) who received AZA, none who received LDAC, and 6 (15%) who received other systemic therapy (Table 2). The median time to best response was 34, 64, 38, and 29 days for patients who received CA±G, AZA, LDAC, and

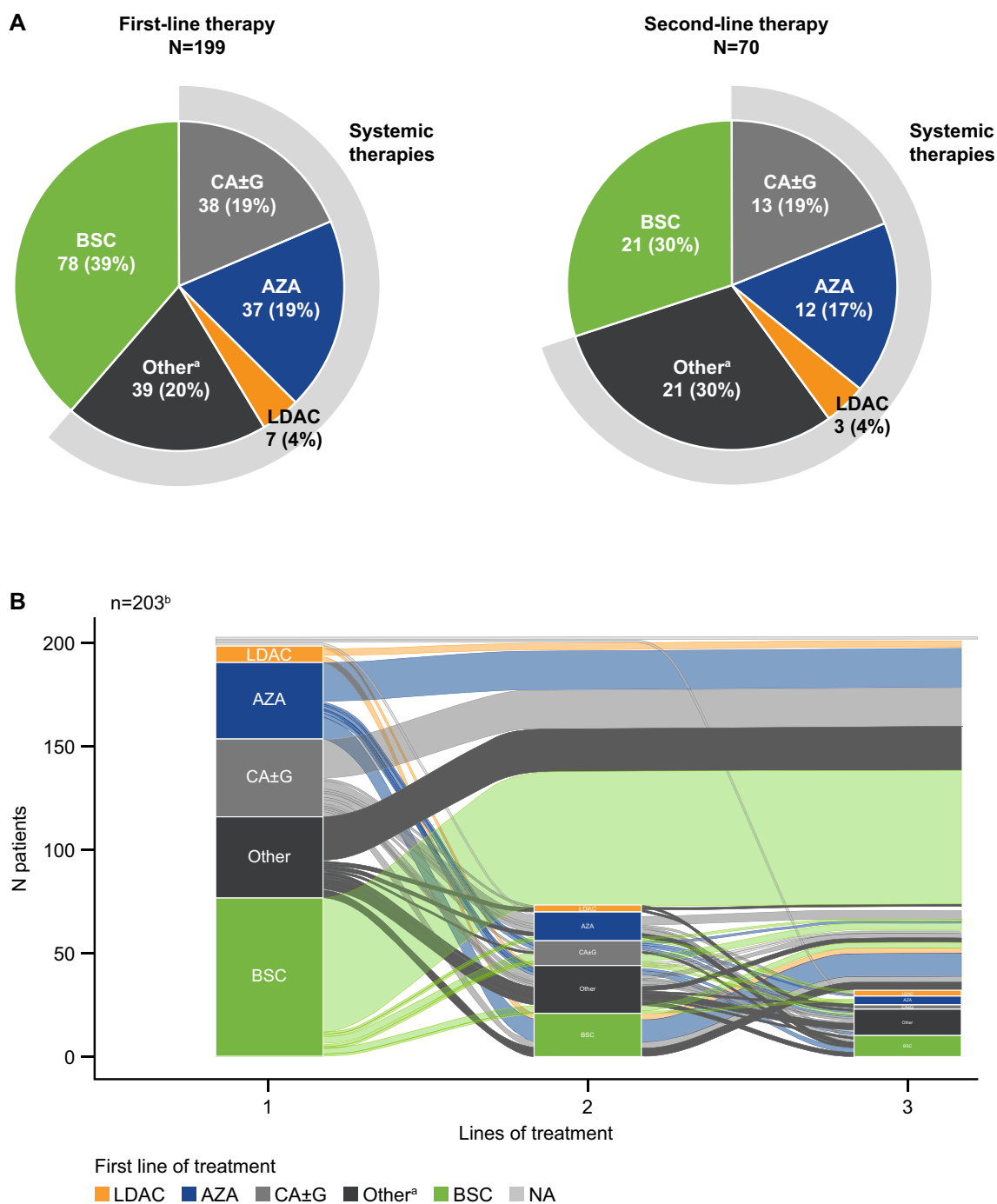


Fig. 2 Overview of first-and second-lines of treatment received (**A**) and an alluvial plot detailing treatment patterns over four lines of treatments (**B**). ^aOther includes cytarabine, aclarubicin, FLT3 inhibitors, gemtuzumab ozogamicin, enocitabine, venetoclax, and therapy combinations which included AZA, LDAC, and CA±G. ^bFour patients are included who did not have first-line therapy data; these

patients were not included in the main analysis but are shown here because they had recorded data for subsequent lines of therapy. AZA azacitidine, BSC best supportive care, CA±G cytarabine, aclarubicin±granulocyte colony-stimulating factor, LDAC low-dose cytarabine

other systemic therapy, respectively. The median duration of CR/CRi for patients who received first-line systemic therapy was 189 days (range 47–648), including 191, 80,

Fig. 3 KM curves for OS in patients who received CA ± G, AZA, LDAC, other systemic therapy and BSC. ^aOther includes cytarabine, aclarubicin, FLT3 inhibitors, gemtuzumab ozogamicin, enocitabine, venetoclax, and therapy combinations which included AZA, LDAC, and CA ± G. AZA azacitidine, BSC best supportive care, CA ± G cytarabine, aclarubicin ± granulocyte colony-stimulating factor, CI confidence interval, KM Kaplan–Meier, LDAC low-dose cytarabine, OS overall survival

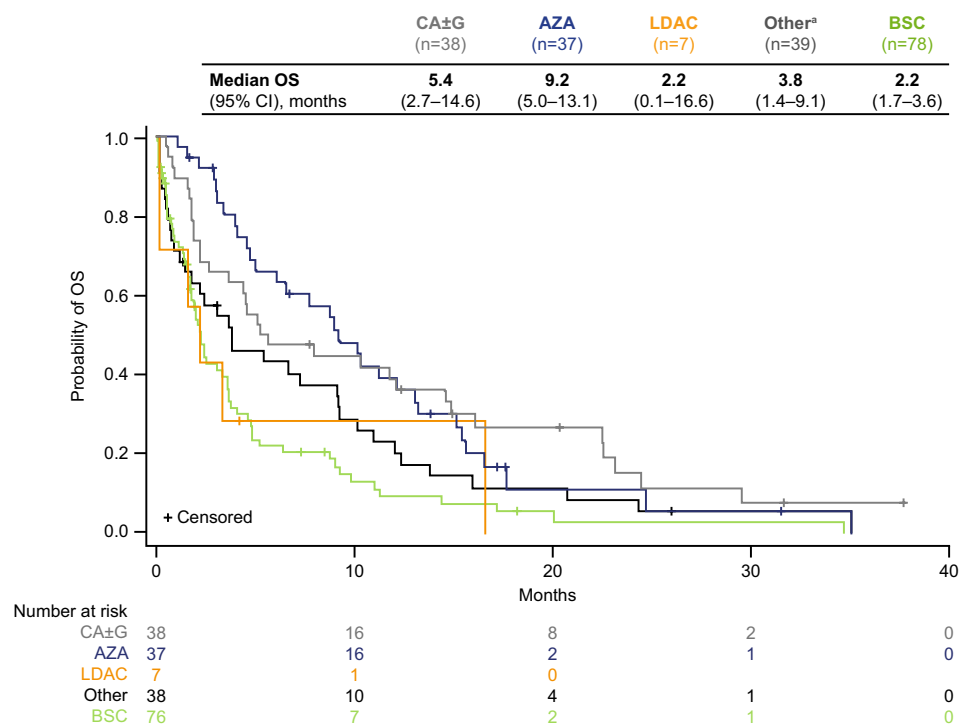
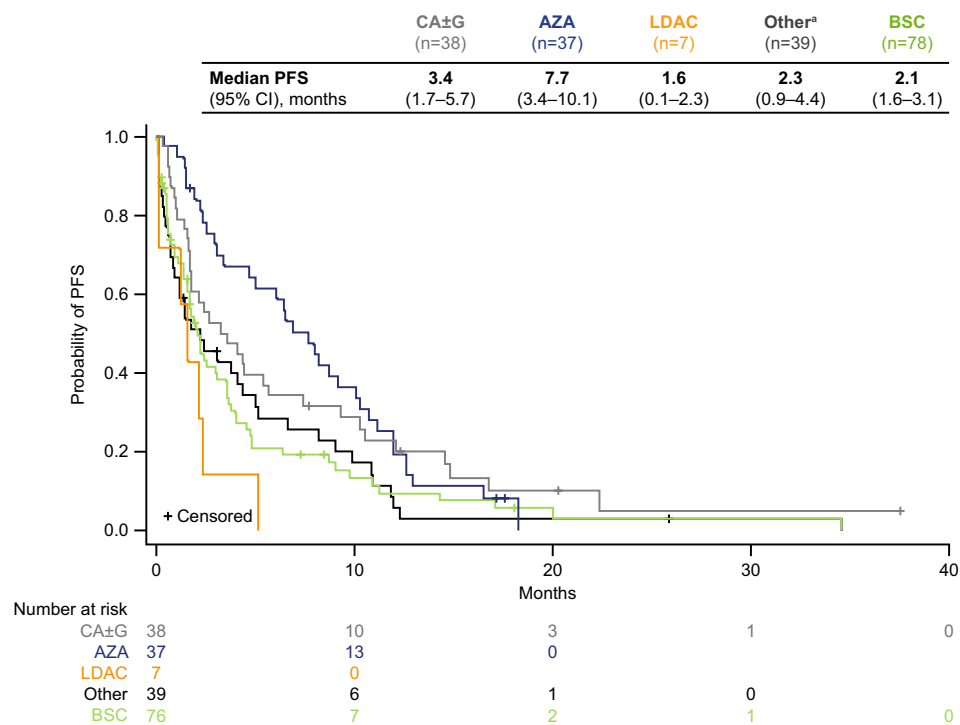


Fig. 4 KM curves for PFS in patients who received CA ± G, AZA, LDAC, other systemic therapy and BSC. ^aOther includes cytarabine, aclarubicin, FLT3 inhibitors, gemtuzumab ozogamicin, enocitabine, venetoclax, and therapy combinations which included AZA, LDAC, and CA ± G. AZA azacitidine, BSC best supportive care, CA ± G cytarabine, aclarubicin ± granulocyte colony-stimulating factor, CI confidence interval, KM Kaplan–Meier, LDAC low-dose cytarabine, PFS progression-free survival



and 214 days for patients who received CA ± G, AZA, and other systemic therapy, respectively.

MRD assessments were carried out for 7 (6%) patients who received first-line systemic treatment. All 7 patients received just one assessment which was evaluated by

real-time quantitative polymerase chain reaction. Peripheral blood was used for analysis in 5 (71%) patients and bone marrow was used for 2 (29%) patients. One patient had undetectable MRD, 5 had detectable MRD, and MRD status was unknown for one.

Fig. 5 KM curves for TTF in patients who received CA ± G, AZA, LDAC, other systemic therapy and BSC. ^aOther includes cytarabine, aclarubicin, FLT3 inhibitors, gemtuzumab ozogamicin, enocitabine, venetoclax, and therapy combinations which included AZA, LDAC, and CA ± G. AZA azacitidine, BSC best supportive care, CA ± G cytarabine, aclarubicin ± granulocyte colony-stimulating factor, CI confidence interval, KM Kaplan–Meier, LDAC low-dose cytarabine, TTF time to treatment failure

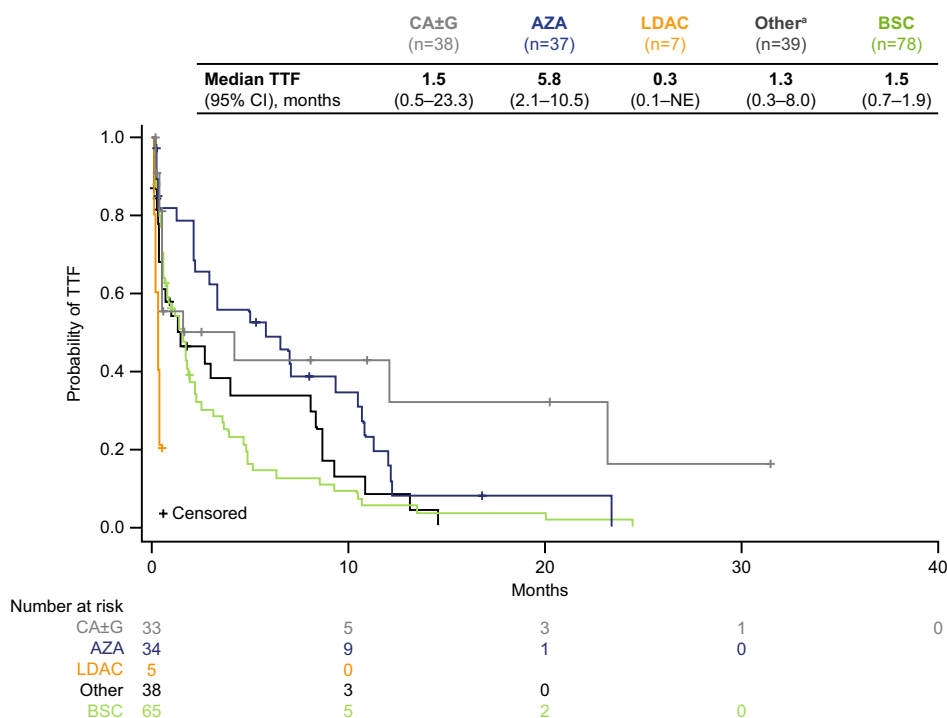


Table 2 Response outcomes of first-line systemic treatment

	First-line systemic therapy (n = 121)			
	CA ± G n = 38	AZA n = 37	LDAC n = 7	Other ^a n = 39
Best response, n (%)				
CR	10 (26)	1 (3)	0	6 (15)
CRi	2 (5)	0	0	0
PR	4 (11)	10 (27)	1 (14)	4 (10)
SD	9 (24)	11 (30)	1 (14)	8 (21)
PD	7 (18)	7 (19)	0	8 (21)
Unknown	6 (16)	8 (22)	5 (71)	13 (33)
Median time from start of treatment to best response, days (range)	34 (6–126)	64 (3–477)	38 (22–54)	29 (0–81)
Median duration of CR/CRi, days (range)	191 (47–648)	80 (80–80)	–	214 (132–362)
Median time from start of treatment to disease progression, days (range)	69 (9–676)	203 (8–553)	51 (2–150)	119 (0–356)

AZA azacitidine, CA ± G cytarabine aclarubicin ± granulocyte colony-stimulating factor, CR complete response, CRi CR with incomplete hematologic recovery, FLT3 FMS-like tyrosine kinase-3, LDAC low-dose cytarabine, PD disease progression, PR partial response, SD stable disease

^aOther includes cytarabine, aclarubicin, FLT3 inhibitors, gemtuzumab ozogamicin, enocitabine, venetoclax, and therapy combinations which included AZA, LDAC, and CA ± G

Healthcare resource utilization

Hospitalization rates were high in all treatment groups, with 84% of patients who received CA ± G, 92% of patients who received AZA, 86% of patients who received LDAC, 90% of patients who received other systemic therapy, and 90% of patients who received BSC admitted to hospital during first-line treatment (Table 3). The median number

of days hospitalized was 21 for patients who received first-line systemic therapy and 14 for patients who received BSC. The most common reasons for hospitalization during first-line systemic therapy were treatment administration (79%) and infection (26%). Among patients who received BSC, the most common reasons for hospitalization were infection (43%) and transfusion (36%).

Table 3 Healthcare resource utilization during first-line systemic treatment or BSC

	First-line systemic therapy <i>n</i> = 121	BSC <i>n</i> = 78
Hospitalized, <i>n</i> (%)	107 (88)	70 (90)
Median days hospitalized (range)	21 (1–933)	14 (1–99)
Outpatient consultations, <i>n</i> (%)	64 (53)	37 (47)
Median number of visits (range)	8 (1–296)	9 (1–250)
RBC/platelet transfusions, <i>n</i> (%)	51 (42)	39 (50)
Median number of RBC transfusions (range)	5 (0–71)	5 (0–42)
Median number of platelet transfusions (range)	4 (0–129)	2 (0–42)
Antibiotic or antiviral use, <i>n</i> (%)	104 (86)	56 (72)
Prophylactic use ^a , <i>n</i> (%)	54 (52)	25 (45)
Curative use ^a , <i>n</i> (%)	74 (71)	45 (80)
Unknown ^a , <i>n</i> (%)	6 (6)	7 (13)
Median days on treatment (range)	25 (1–370)	20 (3–740)
Antifungal use, <i>n</i> (%)	84 (69)	30 (39)
Prophylactic use ^a , <i>n</i> (%)	59 (70)	17 (57)
Curative use ^a , <i>n</i> (%)	31 (37)	15 (50)
Unknown ^a , <i>n</i> (%)	5 (6)	7 (23)
Median days on treatment (range)	33 (1–548)	29 (8–724)
Growth factor use, <i>n</i> (%)	28 (23)	3 (4)
Prophylactic use ^a , <i>n</i> (%)	2 (7)	0
Curative use ^a , <i>n</i> (%)	25 (89)	3 (100)
Unknown ^a , <i>n</i> (%)	1 (4)	0
Median days on treatment (range)	14 (2–56)	–

AZA azacitidine, BSC best supportive care, CA ± G cytarabine, aclarubicin ± granulocyte colony-stimulating factor, *FLT3* FMS-like tyrosine kinase-3, LDAC low-dose cytarabine, RBC red blood cell

^aPercentages may sum up to more than 100% as multi-selection is allowed

The majority of patients received antibiotics or antivirals during first-line treatment (86% of patients in the first-line systemic therapy groups and 72% of patients in the BSC group). Antibiotics and antivirals were most often used in response to infection rather than prophylactically in the first-line systemic therapy (71 and 52%) and BSC groups (80 and 45%). Patients received antibiotics and antivirals for a median of 25 days (range 1–370) across the first-line systemic therapy groups and 20 days (range 3–740) in the BSC group. Antifungals were received by 69% of patients in the first-line systemic therapy groups and 38% of patients

who received BSC. Antifungals were more frequently used prophylactically than in response to infection (70 and 37% in the first-line systemic therapy groups, and 57% and 50% in the BSC group). Patients received antifungals for a median of 33 days (range 1–548) across the first-line systemic therapy groups and 29 days (range 8–724) in the BSC group. A minority of patients received growth factors (23% of patients who received first-line systemic therapy and 4% of patients who received BSC), which were most often used in response to infection rather than prophylactically in the first-line systemic therapy (89 and 7%) and BSC groups (100 and 0%). Growth factors were received for a median of 14 days (range 2–56) across the first-line systemic therapy groups (unknown duration for the patients who received BSC; Table 3).

Discussion

This noninterventional, retrospective chart review assessed the clinical outcomes and treatment patterns of patients with AML who were ineligible for intensive therapy and who instead received treatment with CA ± G, AZA, LDAC, other systemic therapy, or BSC in Japan. The cohort of 199 patients recruited from Japan was generally older than the overall CURRENT cohort, with 58 versus 47% older than age 75 years at diagnosis [30]. Patients treated in Japan also had a higher rate of intermediate (44 vs 32%) and poor (38 vs 25%) cytogenetics than those in the overall cohort, which may reflect the increased likelihood of unfavorable cytogenetics observed in older patients [12, 30].

The majority of patients treated in Japan received first-line systemic treatment (61%), with approximately equal proportions (~20% each) receiving CA ± G, AZA, and other systemic therapy. LDAC was not commonly selected, despite being recommended by Japanese guidelines [32], and BSC was received by 39% of patients. Contrary to guideline recommendations, use of AZA and CA ± G was common and use of LDAC was infrequent, showing the gap between these guidelines and real-world practice. In the overall CURRENT cohort a higher proportion (74%) received first-line systemic therapy and 26% received BSC. Furthermore, of those patients who received first-line systemic therapy in the overall cohort, the majority (62%) received hypomethylating agents, and CA ± G was not a common choice. The differences in treatment patterns between cohorts may be partly reflective of the older age and more unfavorable cytogenetics of patients treated in Japan.

The median OS of the Japan cohort ranged from 2.2 months (LDAC and BSC groups) to 9.2 months (AZA group). Patients who received CA ± G had a numerically shorter median OS than those who received AZA (5.4 months vs 9.2 months) despite a numerically higher rate of CR/CRi (32 vs 3%). Although baseline characteristics

were broadly comparable between these groups, it is noteworthy that the AZA group had a higher proportion of patients with secondary AML and poor cytogenetic risk than the CA \pm G group.

Of patients who received first-line systemic therapy, the LDAC group had particularly poor outcomes. The percentage of patients older than age 75 years at diagnosis was higher in the LDAC group (86 vs 59% of all patients who received first-line systemic therapy) and most patients who received LDAC had secondary AML (71%), whereas the majority of patients in other therapy groups had primary AML. However, it is worth noting that just 7 patients received LDAC therapy in Japan so these data should be interpreted with particular caution.

Median OS was numerically lower in this cohort from Japan compared with the overall CURRENT cohort (4.0 vs 6.2 months), which, again, may reflect the older age and more unfavorable cytogenetics of patients treated in Japan. However, median OS was consistent between the Japan and overall cohorts for patients who received hypomethylating agents (9.2 and 9.9 months, respectively) and BSC (2.2 and 2.5 months), but lower for those who received LDAC (2.2 and 7.9 months) or other systemic therapy (3.8 and 5.4 months) in Japan [30]. Although meaningful comparison with previous studies is limited by inter-study variability and small patient numbers, survival outcomes in this cohort from Japan were broadly comparable with previous reports for those who received AZA, but lower for the CA \pm G, LDAC, and BSC groups [15, 17, 18, 22–27].

Rates of CR/CRi were also consistently lower across the groups for patients treated in Japan compared with the overall cohort (16 vs 21% for all patients who received first-line systemic therapy); however, the CR/CRi rate was notably higher for the CA \pm G group versus the other groups in Japan, a treatment group not stratified in the overall cohort due to low utilization [30]. This is consistent with previous reports of complete remission rates for CA \pm G of 20–58% [13–15, 26].

This subanalysis highlights the rationale for use of CA \pm G and AZA in Japan for patients who are considered ineligible for standard intensive chemotherapy. Although AZA use in this study may have been limited as it was not approved for the treatment of AML in Japan during the follow-up period, these data support its use as a practical option for this patient population in the real-world scenario. It is also notable that almost 40% of patients received BSC. In this subanalysis, there was no substantial difference in age, ECOG performance status, and comorbidities between the patient groups receiving BSC and first-line systemic therapies. It is possible that the attending physicians factored in all these biometrics when making treatment decisions in selecting BSC or first-line systemic therapy. In addition, the intentions of the patients and their families might have had

impacted treatment decisions. Therefore, how these factors have influenced the treatment outcome is not clear and is beyond the scope of this retrospective chart review.

HRU was consistently high between this analysis and the overall CURRENT cohort, with consistently high rates of hospitalization across the treatment groups. The highest rates of outpatient consultations and RBC/platelet transfusions were reported for the AZA group (65% for both, vs 29–53% and 29–50% for the other treatment groups). A lower proportion of patients in the Japan cohort had outpatient consultations or transfusions compared with the real-world cohort across all treatment groups [33]. These data are consistent with previous reports of high HRU by patients with AML [29, 34] and reflects a need to alleviate the burden on healthcare systems.

The treatment landscape has evolved since the inception of this study, with increased understanding of the molecular heterogeneity of AML driving the emergence of novel, targeted therapies [1, 2, 9]. Notably, 67% of patients in this subanalysis did not have molecular profiling, compared with 47% in the overall CURRENT cohort, which may be reflective of insurance coverage and limited access to molecular profiling in clinical practice in Japan. Subsequently, only 20% of patients received other systemic therapies. Consensus guidelines are needed to guide treatment selection and optimize outcomes, alongside a greater understanding of how to best utilize novel therapies.

The results of this chart review are limited by several factors which should be considered when interpreting these data. The design is uncontrolled and nonrandomized, increasing the potential for patient selection bias. Small group sizes, particularly for those who received LDAC ($n = 7$), limit meaningful conclusions. The findings are also limited by missing data (26% of patients were missing response data). The extensive number of treatment combinations utilized within the “other systemic therapy” group confound interpretation of these data. The limited use of some targeted agents reflects their approval status in Japan during the study period.

This subanalysis of CURRENT, a large real-world study, provides insight into treatment patterns and their associated outcomes for patients with AML in Japan at a time of landscape evolution. Overall, the clinical outcomes for patients with AML in Japan who are ineligible for intensive chemotherapy remain poor and HRU by this population is high. There is an unmet need to develop novel therapies and newer combination regimens for this patient population to improve outcomes and alleviate the burden on healthcare systems.

Acknowledgements Medical writing support was provided by Hayley Ellis, PhD, of Fishawack Communications Ltd, and funded by AbbVie.

Author contributions Study conception and design: Yoshiko Kawakami, Tetsuo Morita, Ikue Taneike, Masahiko Nakayama, Yinghui Duan, Belen Garbayo Guijarro, Alexander Delgado, and Cynthia Llamas. Collection and assembly of data: All authors. Analysis and interpretation of data: All authors. Manuscript writing, editing, and approval: All authors.

Funding AbbVie funded this study and participated in the study design, research, analysis, data collection, interpretation of data, reviewing, and approval of the publication. All authors had access to relevant data and participated in the drafting, review, and approval of this publication. No honoraria or payments were made for authorship.

Data sharing statement AbbVie is committed to responsible data sharing regarding the clinical trials we sponsor. This includes access to anonymized, individual, and trial-level data (analysis data sets), as well as other information (e.g., protocols and Clinical Study Reports), as long as the trials are not part of an ongoing or planned regulatory submission. This includes requests for clinical trial data for unlicensed products and indications. This clinical trial data can be requested by any qualified researchers who engage in rigorous, independent scientific research, and will be provided following review and approval of a research proposal and Statistical Analysis Plan (SAP) and execution of a Data Sharing Agreement (DSA). Data requests can be submitted at any time and the data will be accessible for 12 months, with possible extensions considered. For more information on the process, or to submit a request, visit the following link: <https://www.abbvie.com/our-science/clinical-trials/clinical-trials-data-and-information-sharing/data-and-information-sharing-with-qualified-researchers.html>.

Declarations

Conflict of interest C. Yoshida: Investigator on AbbVie-funded clinical study. Honoraria from Bristol Myers Squibb, Novartis Pharma KK, Pfizer Japan Inc., Otsuka Pharmaceutical, AbbVie, Janssen Pharmaceutical KK, Nippon Shinyaku Co., Ltd., Chugai Pharmaceutical Co., Ltd. Research funding from Bristol Myers Squibb. T. Kondo: Advisory role for Astellas Pharma, Otsuka Pharmaceutical. Honoraria from Astellas Pharma, Bristol Myers Squibb, Otsuka Pharmaceutical, Novartis, and Sumitomo Dainippon Pharma. T. Ito: Research funding from AbbVie and Bristol Myers Squibb. Honoraria from AbbVie, Bristol Myers Squibb, Takeda Pharmaceutical Sanofi, CSL Behring, and Novartis. M. Kizaki, Y. Morita, T. Eto, Y. Katsuoka, N. Takezako, N. Uoshima, J. Ando, A. Mori, A. Satake, J. Watanabe: No potential conflicts of interest are reported. K. Yamamoto, T. Komeno: Investigator on AbbVie-funded clinical study. T. Miyamoto: Honoraria from AbbVie, Astellas Pharmaceutical, Astellas Amgen Pharmaceutical, Bristol Myers Squibb, Celgene, Merck Sharp & Dohme, Otsuka Pharmaceutical, and Takeda Pharmaceutical. K. Imada: Honoraria from Astellas Pharma, Bristol Myers Squibb, Celgene, Chugai Pharmaceutical, Kyowa Hakko Kirin, Nippon Shinyaku, Novartis, Otsuka Pharmaceutical, and Takeda Pharmaceutical. Y. Ishikawa: Personal fees from AbbVie, Astellas Pharma, Chugai Pharmaceutical, Daiichi-Sankyo, FUJIFILM, Kyowa Hakko Kirin, Nippon Shinyaku, Novartis, and Pfizer. Y. Kawakami, T. Morita, I. Taneike, M. Nakayama, Y. Duan, B. Garbayo Guijarro, A. Delgado, C. Llamas: Employees of AbbVie and may hold stock or options. H. Kiyoi: Research funding from AbbVie, Astellas Pharma, Bristol Myers Squibb, Chugai Pharmaceutical, CURED Inc., Daiichi Sankyo, Eisai, FUJIFILM, Kyowa Hakko Kirin, Nippon Shinyaku, Novartis, Otsuka Pharmaceutical, Perseus Proteomics, Pfizer, Sanofi, Sumitomo Dainippon Pharma, Takeda Pharmaceutical, and Zenyaku Kogyo. Honoraria from Astellas Pharma, Bristol Myers Squibb, and Novartis.

References

- Hou HA, Tien HF. Genomic landscape in acute myeloid leukemia and its implications in risk classification and targeted therapies. *J Biomed Sci.* 2020;27:81.
- Kantarjian H, Kadia T, DiNardo C, Daver N, Borthakur G, Jabbour E, et al. Acute myeloid leukemia: current progress and future directions. *Blood Cancer J.* 2021;11:41.
- National Cancer Institute. Cancer stat facts: leukemia—acute myeloid leukemia (AML) 2020 [Available from: <https://seer.cancer.gov/statfacts/html/amyl.html>].
- Cancer Information Service NCC, Japan. Chronic lymphocytic leukemia/small lymphocytic lymphoma. 2016. Available from: <https://ganjoho.jp/public/cancer/CLL/>.
- Yi M, Li A, Zhou L, Chu Q, Song Y, Wu K. The global burden and attributable risk factor analysis of acute myeloid leukemia in 195 countries and territories from 1990 to 2017: estimates based on the global burden of disease study 2017. *J Hematol Oncol.* 2020;13:72.
- Thein MS, Ershler WB, Jemal A, Yates JW, Baer MR. Outcome of older patients with acute myeloid leukemia: an analysis of SEER data over 3 decades. *Cancer.* 2013;119:2720–7.
- Miyamoto K, Minami Y. Precision medicine and novel molecular target therapies in acute myeloid leukemia: the background of hematologic malignancies (HM)-SCREEN-Japan 01. *Int J Clin Oncol.* 2019;24:893–8.
- Palmieri R, Paterno G, De Bellis E, Mercante L, Buzzatti E, Esposito F, et al. Therapeutic choice in older patients with acute myeloid leukemia: a matter of fitness. *Cancers (Basel).* 2020. <https://doi.org/10.3390/cancers12010120>.
- National Comprehensive Cancer Network. Clinical practice guidelines in oncology. Acute Myeloid Leukemia. 2020;2:2021.
- Heuser M, Ofran Y, Boissel N, Brunet Mauri S, Craddock C, Janssen J, et al. Acute myeloid leukaemia in adult patients: ESMO clinical practice guidelines for diagnosis, treatment and follow-up. *Ann Oncol.* 2020;31:697–712.
- Kiyoi H, Yamaguchi H, Maeda Y, Yamauchi T. JSH practical guidelines for hematological malignancies, 2018: I. Leukemia-1. Acute myeloid leukemia (AML). *Int J Hematol.* 2020;111:595–613.
- Naoe T. Editors' choice how to improve outcomes of elderly patients with acute myeloid leukemia: era of excitement. *Nagoya J Med Sci.* 2020;82:151–60.
- Wei G, Ni W, Chiao JW, Cai Z, Huang H, Liu D. A meta-analysis of CAG (cytarabine, aclarubicin, G-CSF) regimen for the treatment of 1029 patients with acute myeloid leukemia and myelodysplastic syndrome. *J Hematol Oncol.* 2011;4:46.
- Minakata D, Fujiwara S, Ito S, Mashima K, Umino K, Nakano H, et al. A low-dose cytarabine, aclarubicin and granulocyte colony-stimulating factor priming regimen versus a daunorubicin plus cytarabine regimen as induction therapy for older patients with acute myeloid leukemia: a propensity score analysis. *Leuk Res.* 2016;42:82–7.
- Jin J, Chen J, Suo S, Qian W, Meng H, Mai W, et al. Low-dose cytarabine, aclarubicin and granulocyte colony-stimulating factor priming regimen versus idarubicin plus cytarabine regimen as induction therapy for older patients with acute myeloid leukemia. *Leuk Lymphoma.* 2015;56:1691–7.
- MHLW approval of Vidaza® (azacitidine) for the treatment of acute myeloid leukemia. [press release]. 2021.
- Dombret H, Seymour JF, Butrym A, Wierzbowska A, Selleslag D, Jang JH, et al. International phase 3 study of azacitidine vs conventional care regimens in older patients with newly diagnosed AML with >30% blasts. *Blood.* 2015;126:291–9.

18. Amadori S, Suciu S, Selleslag D, Aversa F, Gaidano G, Musso M, et al. Gemtuzumab ozogamicin versus best supportive care in older patients with newly diagnosed acute myeloid leukemia unsuitable for intensive chemotherapy: results of the randomized phase III EORTC-GIMEMA AML-19 trial. *J Clin Oncol*. 2016;34:972–9.
19. Ma E, Bonthapally V, Chawla A, Lefebvre P, Swords R, Lafeuille MH, et al. An evaluation of treatment patterns and outcomes in elderly patients newly diagnosed with acute myeloid leukemia: a retrospective analysis of electronic medical records from US community oncology practices. *Clin Lymphoma Myeloma Leuk*. 2016;16:625–36 e3.
20. Medeiros BC, Satram-Hoang S, Hurst D, Hoang KQ, Momin F, Reyes C. Big data analysis of treatment patterns and outcomes among elderly acute myeloid leukemia patients in the United States. *Ann Hematol*. 2015;94:1127–38.
21. DiNardo CD, Pratz K, Pullarkat V, Jonas BA, Arellano M, Becker PS, et al. Venetoclax combined with decitabine or azacitidine in treatment-naïve, elderly patients with acute myeloid leukemia. *Blood*. 2019;133:7–17.
22. Seymour JF, Dohner H, Butrym A, Wierzbowska A, Selleslag D, Jang JH, et al. Azacitidine improves clinical outcomes in older patients with acute myeloid leukaemia with myelodysplasia-related changes compared with conventional care regimens. *BMC Cancer*. 2017;17:852.
23. Kantarjian HM, Thomas XG, Dmoszynska A, Wierzbowska A, Mazur G, Mayer J, et al. Multicenter, randomized, open-label, phase III trial of decitabine versus patient choice, with physician advice, of either supportive care or low-dose cytarabine for the treatment of older patients with newly diagnosed acute myeloid leukemia. *J Clin Oncol*. 2012;30:2670–7.
24. Wei AH, Montesinos P, Ivanov V, DiNardo CD, Novak J, Laribi K, et al. Venetoclax plus LDAC for newly diagnosed AML ineligible for intensive chemotherapy: a phase 3 randomized placebo-controlled trial. *Blood*. 2020;135:2137–45.
25. DiNardo CD, Jonas BA, Pullarkat V, Thirman MJ, Garcia JS, Wei A, et al. Azacitidine and venetoclax in previously untreated acute myeloid leukemia. *N Engl J Med*. 2020;383(7):617–29.
26. Chen Y, Yang T, Zheng X, Yang X, Zheng Z, Zheng J, et al. The outcome and prognostic factors of 248 elderly patients with acute myeloid leukemia treated with standard-dose or low-intensity induction therapy. *Medicine (Baltimore)*. 2016;95:e4182.
27. Xu J, Lv TT, Zhou XF, Huang Y, Liu DD, Yuan GL. Efficacy of common salvage chemotherapy regimens in patients with refractory or relapsed acute myeloid leukemia: a retrospective cohort study. *Medicine (Baltimore)*. 2018;97:e12102.
28. Venclexta PI (Japanese label). 2021.
29. Griffin JD, Yang H, Song Y, Kinrich D, Shah MV, Bui CN. Treatment patterns and healthcare resource utilization in patients with FLT3-mutated and wild-type acute myeloid leukemia: a medical chart study. *Eur J Haematol*. 2019;102:341–50.
30. Miyamoto T, Sanford D, Tomuleasa C, Hsiao HH, Olivera LJE, Enjeti AK, et al. Real-world treatment patterns and clinical outcomes in patients with AML unfit for first-line intensive chemotherapy. *Leuk Lymphoma*. 2022. <https://doi.org/10.1080/10428194.2021.2002321>.
31. DiNardo CD, Pratz KW, Letai A, Jonas BA, Wei AH, Thirman M, et al. Safety and preliminary efficacy of venetoclax with decitabine or azacitidine in elderly patients with previously untreated acute myeloid leukaemia: a non-randomised, open-label, phase 1b study. *Lancet Oncol*. 2018;19:216–28.
32. Miyawaki S. JSH guideline for tumors of hematopoietic and lymphoid tissues: leukemia 1. Acute myeloid leukemia (AML). *Int J Hematol*. 2017;106:310–25.
33. Ito T, Sanford D, Tomuleasa C, Hsiao H-H, Enciso Olivera L, Enjeti A, et al. Patterns of healthcare resource utilization (HRU) in unfit patients with acute myeloid leukemia (AML) receiving first-line systemic treatment or best supportive care (BSC): a multicenter international study (CURRENT). Lawrenceville: ISPOR; 2021.
34. Stein EM, Bonifacio G, Latremouille-Viau D, Guerin A, Shi S, Gagnon-Sanschagrin P, et al. Treatment patterns, healthcare resource utilization, and costs in patients with acute myeloid leukemia in commercially insured and Medicare populations. *J Med Econ*. 2018;21:556–63.

Publisher's Note Springer Nature remains neutral with regard to jurisdictional claims in published maps and institutional affiliations.

Authors and Affiliations

Chikashi Yoshida¹ · Takeshi Kondo² · Tomoki Ito³ · Masahiro Kizaki⁴ · Kazuhiko Yamamoto⁵ · Toshihiro Miyamoto⁶ · Yasuyoshi Morita⁷ · Tetsuya Eto⁸ · Yuna Katsuoka⁹ · Naoki Takezako¹⁰ · Nobuhiko Uoshima¹¹ · Kazunori Imada¹² · Jun Ando¹³ · Takuya Komeno¹ · Akio Mori² · Yuichi Ishikawa¹⁴ · Atsushi Satake³ · Junichi Watanabe⁴ · Yoshiko Kawakami¹⁵ · Tetsuo Morita¹⁵ · Ikue Taneike¹⁵ · Masahiko Nakayama¹⁵ · Yinghui Duan¹⁶ · Belen Garbayo Guijarro¹⁷ · Alexander Delgado¹⁸ · Cynthia Llamas¹⁶ · Hitoshi Kiyoi¹⁴

✉ Chikashi Yoshida
c.yoshida@mitomedical.org

¹ Department of Hematology, National Hospital Organization Mito Medical Center, Ibaraki-machi, Japan

² Blood Disorders Center, Aiiiku Hospital, Sapporo, Japan

³ First Department of Internal Medicine, Kansai Medical University, Osaka, Japan

⁴ Department of Hematology, Saitama Medical Center, Saitama Medical University, Saitama, Japan

⁵ Department of Hematology, Okayama City Hospital, Okayama, Japan

⁶ Medicine and Biosystemic Science, Graduate School of Medical Sciences, Kyushu University, Fukuoka, Japan

⁷ Division of Hematology and Rheumatology, Department of Internal Medicine, Kindai University, Osaka, Japan

⁸ Department of Hematology, Hamanomachi Hospital, Fukuoka, Japan

⁹ Department of Hematology, Sendai Medical Center, National Hospital Organization, Sendai, Japan

¹⁰ Department of Hematology, Disaster Medical Center, Tokyo, Japan

¹¹ Department of Hematology, Kyoto Second Red Cross Hospital, Kyoto, Japan

¹² Department of Hematology, Japanese Red Cross Osaka Hospital, Osaka, Japan

¹³ Department of Hematology, Juntendo University School of Medicine, Tokyo, Japan

¹⁴ Department of Hematology and Oncology, Nagoya University Graduate School of Medicine, Nagoya, Japan

¹⁵ AbbVie GK, Tokyo, Japan

¹⁶ AbbVie, Inc., North Chicago, IL, USA

¹⁷ AbbVie, Inc., Madrid, Spain

¹⁸ AbbVie, Inc., Singapore, Singapore

Review began 03/22/2022
Review ended 04/13/2022
Published 04/16/2022

© Copyright 2022
Ogawa et al. This is an open access article
distributed under the terms of the Creative
Commons Attribution License CC-BY 4.0.,
which permits unrestricted use, distribution,
and reproduction in any medium, provided
the original author and source are credited.

Analyzing Chronological Change in Postoperative Magnetic Resonance Imaging Results in Patients With Kienböck's Disease by Using an Original Grading System

Takeshi Ogawa¹, Akira Ikumi², Sho Kohyama³, Yuki Hara⁴, Yuichi Yoshii⁵, Naoyuki Ochiai³, Masashi Yamazaki⁴

1. Department of Orthopedic Surgery, National Hospital Organization, Mito Medical Center, Ibaraki, JPN 2. Department of Orthopedic Surgery and Sports Medicine, Tsukuba University Hospital Mito Clinical Education and Training Center, Mito, JPN 3. Department of Orthopedic Surgery, Kikkoman General Hospital, Noda, JPN 4. Department of Orthopedic Surgery, Faculty of Medicine, University of Tsukuba, Tsukuba, JPN 5. Department of Orthopedic Surgery, Tokyo Medical University Ibaraki Medical Center, Ibaraki, JPN

Corresponding author: Takeshi Ogawa, ogawat@tsukuba-seikei.jp

Abstract

Background and objective

Signal changes in MRI for Kienböck's disease have only been qualitatively assessed so far. In light of this, we proposed a new grading system for quantitative analysis with an ordinal scale.

Methods

The study included 31 patients (17 men, 14 women) with Kienböck's disease. By referring to Nakamura's MRI grading system, we devised a grading system with five grades (Grades 1-5) using proton density-weighted (PDW) coronal images with respect to the signal intensity of the lunate. All cases were examined by using the MRI grading system by three hand surgeons, both preoperatively and postoperatively. We evaluated the inter-rater reliability of our grading system by using the interclass correlation coefficient. After surgery, we implemented annual MRI evaluation for as long as possible and quantitatively assessed changes in MRI grades. We also investigated the correlation between postoperative MRI grades, Mayo Wrist Scores (MWS), and age at the surgery by using Pearson's coefficient.

Results

The MRI evaluation was performed 2-15 years after surgery. The reliability of our grading system was high; inter-rater interclass correlation coefficients were 0.783 (examiners 1-2), 0.780 (examiners 1-3), and 0.825 (examiners 2-3), representing a substantial agreement. The correlation coefficient between the MRI grade and MWS was -0.31, suggesting a mild negative correlation; postoperative MRI grade also correlated with age at surgery (Pearson's coefficient: 0.447).

Conclusions

Our proposed MRI grading system has high reliability and could be used to assess the regeneration of a necrotic lunate for quantitative analysis on an ordinal scale. Improvements were observed one to four years postoperatively, demonstrating a mild correlation with the clinical results.

Categories: Radiology, Orthopedics

Keywords: ordinal scale, quantitative analysis, proton density weighted image, magnetic resonance imaging, necrotic lunate, kienböck's disease

Introduction

Kienböck's disease was first described in 1910 by radiologist Robert Kienböck, who described radiographic changes associated with lunate malacia [1]. The exact mechanism of Kienböck's disease is not yet fully understood. It is believed to be an interaction between altered vascular perfusion, repeated microtrauma, changes in lunate bone structure, changes in loading and movement, and potential systemic disease [2]. Signal changes during MRI evaluation for Kienböck's disease have been qualitatively assessed [3]. In order to properly diagnose Kienböck's disease and its progression, it is necessary to establish a standardized test based on MRI analysis. In this study, we developed a new evaluation method by using an ordinal scale that can be classified into five levels according to the degree of disease progression based on MRI signal intensity. MRI analysis by using this ordinal scale is expected to assess the effectiveness of the treatment and progress of necrosis. In patients with Kienböck's disease, we performed a combined therapy that included non-concentrated bone marrow transfusion, low-intensity pulsed ultrasound, and external fixation

How to cite this article

Ogawa T, Ikumi A, Kohyama S, et al. (April 16, 2022) Analyzing Chronological Change in Postoperative Magnetic Resonance Imaging Results in Patients With Kienböck's Disease by Using an Original Grading System. Cureus 14(4): e24178. DOI 10.7759/cureus.24178

[3,4]; however, this treatment did not result in better outcomes than other treatments [5-9]. There are some questions that remain unanswered regarding this method, such as when is the improvement of MRI signal after surgery observed, whether the improvement is continuous, and whether MRI signal improvement correlates with clinical results or patients' age. In this study, we, therefore, assessed the validity of the grading system, quantitatively evaluated postoperative MRI changes over time, and evaluated the correlation between MRI signal improvement and clinical results following our procedure for Kienböck's disease.

Materials And Methods

Our study involved 31 patients (17 men, 14 women) with Kienböck's disease by using Ogawa's procedure [3,4]. This retrospective study was approved by our hospital's ethical committee (R02-106), and written informed consent was obtained from all participants. Our indications for surgical intervention were diagnosis of Kienböck's disease at stages II, IIIa, and IIIb. Preoperative Lichtman stages observed were as follows: stage II in nine patients, stage IIIa in 16 patients, and stage IIIb in six patients; the mean age at the time of surgery was 43.6 (16-78) years. A 1.5- or 3-T magnetic resonance apparatus (Gyrosan NT Intera, Philips Medical Systems, Amsterdam, Netherlands), with a small-diameter surface coil (Philips Medical Systems), was used for MRI evaluation [10]. We referred to Nakamura's MRI grading system [11] to devise an individual grading system using proton density-weighted (PDW) coronal images. On this scale, with respect to the signal intensity of the lunate, Grade I was considered almost normal; Grade II indicated localized regions of slightly decreased signal intensity; Grade III indicated a slight, generalized decrease in signal intensity; Grade IV represented a low signal intensity with regions of high or isointense signals; and Grade V indicated a low, generalized signal intensity (Figure 1).

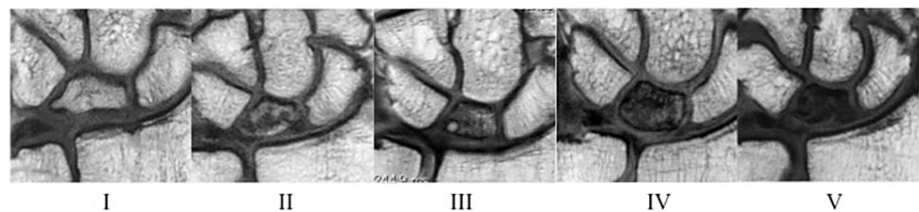


FIGURE 1: MRI grading system using the T1 or PDW coronal image

On this scale, with respect to the signal intensity of the lunate, Grade I was considered almost normal; Grade II indicated localized regions of slightly decreased signal intensity; Grade III indicated a slight, generalized decrease in signal intensity; Grade IV represented low signal intensity with regions of high or isointense signals, and Grade V indicated generalized low signal intensity

MRI: magnetic resonance imaging; PDW: proton density-weighted

Grades were determined by using the most severe coronal slice on MRI. Using the MRI grading system, all cases were both preoperatively and postoperatively examined by three hand surgeons. We then evaluated the inter-rater reliability of the grading system by using the interclass correlation coefficient. After surgery, we implemented an annual MRI evaluation and assessed the changes in MRI grade on an ordinal scale. We also investigated the correlation between MRI grade at the final follow-up, Mayo Wrist Score (MWS) [12], and age at the time of surgery, by using Pearson's coefficient.

Statistical analysis

We evaluated the inter-rater reliability of our MRI grading system by using the interclass correlation coefficient. We evaluated the correlation between the clinical results, MWS, and age using Pearson's correlation coefficient; the significance level was set at $p=0.05$. All statistical analyses were performed with Bellcurve for Excel version 3.20 (SSRI Co., Tokyo, Japan).

Results

MRI evaluation was performed for 2-15 years after surgery. The reliability of our MRI grading system was high, with inter-rater interclass correlation coefficients of 0.783 (examiners 1-2), 0.780 (examiners 1-3), and 0.825 (examiners 2-3), representing a substantial or near-perfect agreement. Improvements were observed one to four years postoperatively (Figure 2), from an average grade of 4.5 (range: 3-5) preoperatively to 2.75 (range: 1-5) at the final follow-up.

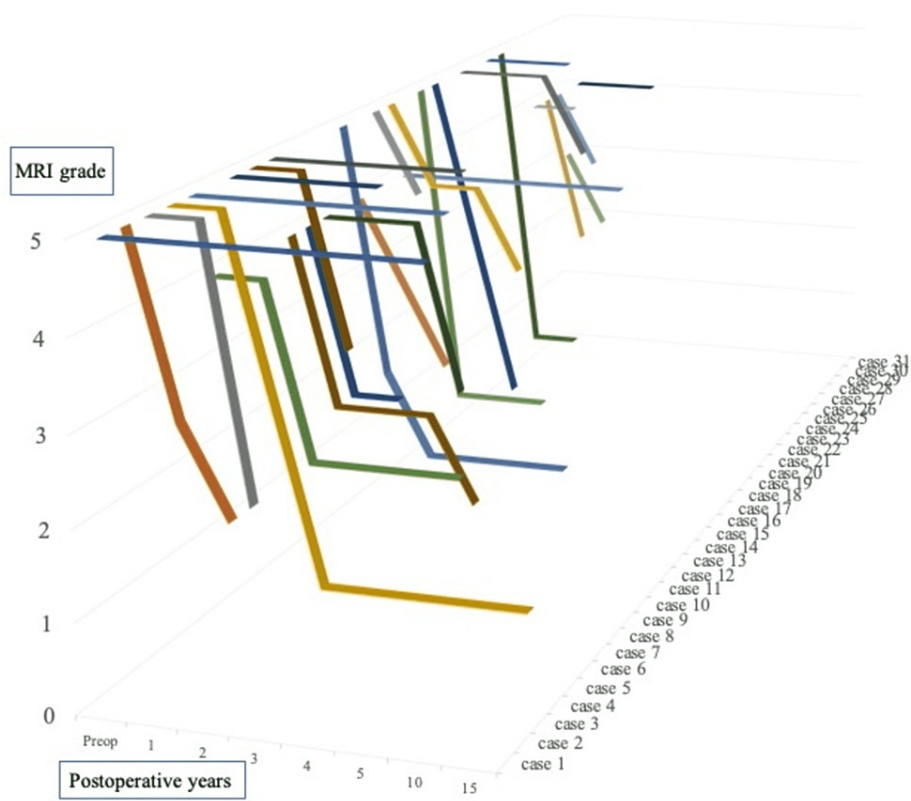


FIGURE 2: Chronological change in postoperative MRI grade for all patients

MRI: magnetic resonance imaging

Improved MRI signal intensity was observed in 23 patients (74%): 13 cases within one year, six patients after one to two years, and four patients after more than two years. To date, none of the improved patients have deteriorated since experiencing improvement. A satisfactory improvement in MRI Grade I or II was observed in 17 patients (74%); additionally, there were no cases in which the recovered intensity of the lunate worsened. The average MWS at the last follow-up was 83.4 (65-100), and the Pearson's coefficient was -0.315, which slightly correlated with the MRI grade at the last follow-up (Figure 3).

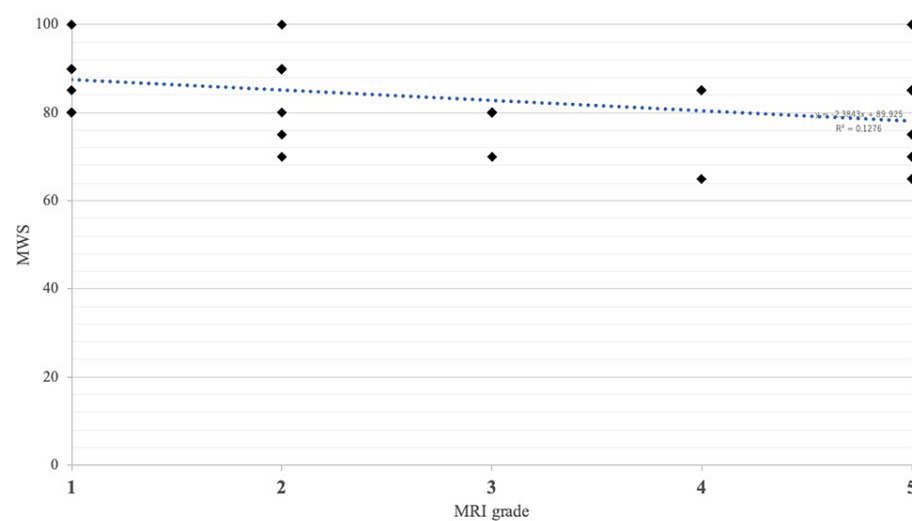


FIGURE 3: Pearson's coefficient between MWS and MRI grades

Pearson's coefficient was -0.315

MRI: magnetic resonance imaging; MWS: Mayo Wrist Score

The postoperative MRI grade also correlated with age at the time of surgery (Pearson's coefficient: 0.447) (Figure 4).

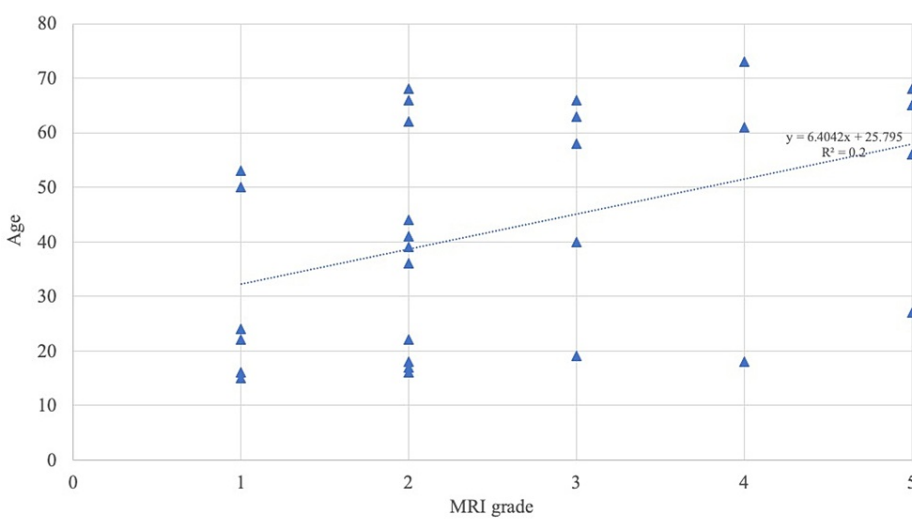


FIGURE 4: Pearson's coefficient between age at the surgery and MRI grade at the final follow-up

Pearson's coefficient was 0.447

MRI: magnetic resonance imaging

By contrast, there was no correlation between MWS and age (Pearson's coefficient: 0.068).

The representative case involved a 41-year-old man who underwent surgery. His preoperative MRI Grade was IV, which improved to Grade IV at one year, Grade IV at two years, and Grade II at five years postoperatively (Figures 5A-5D). He reported no pain at three months postoperatively, and his MWS was 90 points at one year postoperatively; therefore, MRI was not performed at three and four years postoperatively.

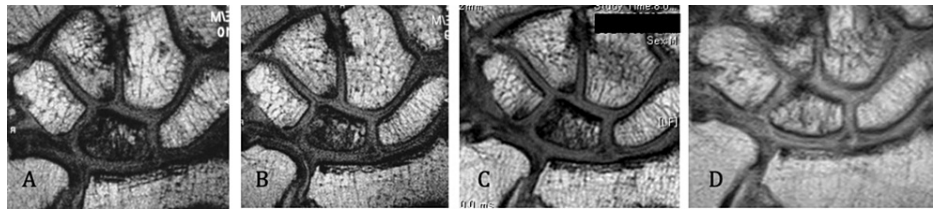


FIGURE 5: Chronological change in the postoperative MRI results of a 41-year-old man before and after surgery for Kienböck's disease

A. Preoperative magnetic resonance image (Grade IV). B. One year postoperatively (Grade IV). C. Two years postoperatively (Grade IV). D. Three years postoperatively (Grade II)

MRI: magnetic resonance imaging

Discussion

We investigated the chronological change in postoperative MRI results in 31 patients with Kienböck's disease by using a novel grading system. The validity of the grading system was assessed and changes in postoperative MRI over time were evaluated on an ordinal scale. Improved MRI signal intensity was observed in 23 patients, with changes appearing within one year in 13 patients. Furthermore, the MRI grade exhibited a slight correlation with the clinical results.

Very few reports have quantitatively evaluated the MRI findings in Kienböck's disease. Nakamura et al. [11] classified the appearance of the lunate; its signal intensity was graded on a scale of I to V, and they evaluated T1- and T2-weighted images both preoperatively and postoperatively. Imaeda et al. [13] also concluded that the intensity of the signal of the lunate on T2-weighted images indicates the severity of the disease, with a decreased signal containing a high spot or an increased signal suggesting revascularization. Conversely, Ogawa et al. [10] described that PDW (T1-weighted) MRI accurately reflects the vascular status of the lunate, as evidenced by comparison with histological analyses of lunate specimens. They also reported that in the fast-field echo (T2-weighted) images, there were no correlations with histopathological observations.

T2-weighted images reflect various changes, including bone marrow edema, blood vessels, and bleeding. We, therefore, attempted to quantitatively evaluate lunate regeneration using the PDW images. By contrast, Schmitt et al. [14] described gadolinium-enhanced MRI-based classification to delineate the pattern of osteonecrosis in different parts of the lunate bone; middle reparative zone; and distal, normal, viable lunate bone. Based on the signal intensity in different zones of the lunate on MRI, Schmitt et al. classified three stages of Kienböck's disease: stage A was "Marrow edema with viable and intact bony trabeculae", stage B was "Early marrow necrosis with fibrovascular reparative tissue", and stage C was "Necrotic bone marrow with collapse [14]". We also considered the best way to investigate the recovery from bone avascular necrosis using both gadolinium-enhanced MRI and PDW imaging. Gadolinium-enhanced MRI may reflect blood flow and may be useful in combination with PDW, which reflects bone regeneration, to assess treatment efficacy and stage. This is one of the limitations of the present study. Consequently, the reliability of our classification was high, demonstrating a slight correlation with the clinical results. Nakamura et al. [11] reported that there was no significant correlation between lunate signal intensity and clinical outcomes. Although there were good clinical outcomes in our case, some patients exhibited poor MRI recovery, which is another limitation of this study. Additionally, we believe that considering the correlation between MRI and clinical outcomes, it may be useful to employ gadolinium-enhanced MRI together with our MRI grading system.

Regarding the age of patients with Kienböck's disease, van Leeuwen et al. [15] described age as a risk factor for lunate collapse, while Koh et al. [16] reported that the younger generation had better radiological improvement, implying more revascularization of the lunate. The correlation between age and MRI improvement remains unclear, and there are no reports pertaining to age and MRI improvement in the literature. Matsui et al. [17] reported that younger patients had a tendency toward improvement in MRI findings; however, no significant differences in the clinical outcomes, regardless of whether MRI improvement was achieved, were observed. In our study, there was a significant difference between older and younger patients in terms of MRI improvement (Figure 4); however, our study included nine women in menopause. The conditions of Kienböck's disease may differ between younger and older individuals; hence, our data remain theoretical.

Conclusions

Our proposed MRI grading system demonstrated high reliability and could be used to assess the regeneration of the necrotic lunate on an ordinal scale. Using this MRI ordinal scale, the correlation between the clinical

outcomes after treatment for Kienböck's disease was recognized, and improvements in MRI grade were observed one to four years postoperatively. Furthermore, the recovered intensity of the lunate remained at the same level as the intensity.

Additional Information

Disclosures

Human subjects: Consent was obtained or waived by all participants in this study. The Ethical Committee at the University of Tsukuba Hospital issued approval R02-106. **Animal subjects:** All authors have confirmed that this study did not involve animal subjects or tissue. **Conflicts of interest:** In compliance with the ICMJE uniform disclosure form, all authors declare the following: **Payment/services info:** All authors have declared that no financial support was received from any organization for the submitted work. **Financial relationships:** All authors have declared that they have no financial relationships at present or within the previous three years with any organizations that might have an interest in the submitted work. **Other relationships:** All authors have declared that there are no other relationships or activities that could appear to have influenced the submitted work.

Acknowledgements

The authors would like to thank Dr. Yoshio Nakata, an associate professor at the Faculty of Medicine at the University of Tsukuba, for his advice regarding statistical analysis.

References

- Wagner JP, Chung KC: A historical report on Robert Kienböck (1871-1953) and Kienböck's disease. *J Hand Surg Am.* 2005, 30:1117-21. [10.1016/j.jhsa.2005.08.002](https://doi.org/10.1016/j.jhsa.2005.08.002)
- Lichtman DM, Lesley NE, Simmons SP: The classification and treatment of Kienböck's disease: the state of the art and a look at the future. *J Hand Surg Eur Vol.* 2010, 35:549-54. [10.1177/1753193410374690](https://doi.org/10.1177/1753193410374690)
- Ogawa T, Ochiai N, Nishiura Y, Tanaka T, Hara Y: A new treatment strategy for Kienböck's disease: combination of bone marrow transfusion, low-intensity pulsed ultrasound therapy, and external fixation. *J Orthop Sci.* 2013, 18:230-7. [10.1007/s00776-012-0332-7](https://doi.org/10.1007/s00776-012-0332-7)
- Ogawa T, Ochiai N, Hara Y: Bone marrow from the iliac crest versus from the distal radius for revitalizing the necrotic lunate for Kienböck disease. *J Hand Surg Eur Vol.* 2020, 45:299-301. [10.1177/1753193419886724](https://doi.org/10.1177/1753193419886724)
- Nakamura R, Tsuge S, Watanabe K, Tsunoda K: Radial wedge osteotomy for Kienböck disease. *J Bone Joint Surg Am.* 1991, 73:1391-6.
- Fujiwara H, Oda R, Morisaki S, Ikoma K, Kubo T: Long-term results of vascularized bone graft for stage III Kienböck disease. *J Hand Surg Am.* 2013, 38:904-8. [10.1016/j.jhsa.2013.02.010](https://doi.org/10.1016/j.jhsa.2013.02.010)
- Watanabe T, Takahara M, Tsuchida H, Yamahara S, Kikuchi N, Ogino T: Long-term follow-up of radial shortening osteotomy for Kienböck disease. *J Bone Joint Surg Am.* 2008, 90:1705-11. [10.2106/JBJS.G.00421](https://doi.org/10.2106/JBJS.G.00421)
- Arimitsu S, Shimada K, Moritomo H: Lunate fracture healing after partial capitate shortening in Kienböck disease. *J Orthop Sci.* 2020, 25:428-34. [10.1016/j.jos.2019.06.001](https://doi.org/10.1016/j.jos.2019.06.001)
- De Carli P, Zaidenberg EE, Alfie V, Donndorff A, Boretto JG, Gallucci GL: Radius core decompression for Kienböck disease stage IIIA: outcomes at 13 years follow-up. *J Hand Surg Am.* 2017, 42:752.e1-6. [10.1016/j.jhsa.2017.05.017](https://doi.org/10.1016/j.jhsa.2017.05.017)
- Ogawa T, Nishiura Y, Hara Y, Okamoto Y, Ochiai N: Correlation of histopathology with magnetic resonance imaging in Kienböck disease. *J Hand Surg Am.* 2012, 37:83-9. [10.1016/j.jhsa.2011.09.027](https://doi.org/10.1016/j.jhsa.2011.09.027)
- Nakamura R, Watanabe K, Tsunoda K, Miura T: Radial osteotomy for Kienböck's disease evaluated by magnetic resonance imaging. 24 cases followed for 1-3 years. *Acta Orthop Scand.* 1993, 64:207-11. [10.3109/17453679308994572](https://doi.org/10.3109/17453679308994572)
- Amadio PC, Berquist TH, Smith DK, Ilstrup DM, Cooney WP 3rd, Linscheid RL: Scaphoid malunion. *J Hand Surg Am.* 1989, 14:679-87. [10.1016/0363-5023\(89\)90191-3](https://doi.org/10.1016/0363-5023(89)90191-3)
- Imaeda T, Nakamura R, Miura T, Makino N: Magnetic resonance imaging in Kienböck's disease. *J Hand Surg Br.* 1992, 17:12-9. [10.1016/0266-7681\(92\)90006-n](https://doi.org/10.1016/0266-7681(92)90006-n)
- Schmitt R, Heinze A, Fellner F, Obletter N, Strühn R, Bautz W: Imaging and staging of avascular osteonecroses at the wrist and hand. *Eur J Radiol.* 1997, 25:92-103. [10.1016/s0720-048x\(97\)00065-x](https://doi.org/10.1016/s0720-048x(97)00065-x)
- van Leeuwen WF, Tarabochia MA, Schuurman AH, Chen N, Ring D: Risk factors of lunate collapse in Kienböck disease. *J Hand Surg Am.* 2017, 42:883-8. [10.1016/j.jhsa.2017.06.107](https://doi.org/10.1016/j.jhsa.2017.06.107)
- Koh S, Nakamura R, Horii E, Nakao E, Inagaki H, Yajima H: Surgical outcome of radial osteotomy for Kienböck's disease-minimum 10 years of follow-up. *J Hand Surg Am.* 2013, 28:910-6. [10.1016/s0363-5023\(03\)00490-8](https://doi.org/10.1016/s0363-5023(03)00490-8)
- Matsui Y, Funakoshi T, Motomiya M, Urita A, Minami M, Iwasaki N: Radial shortening osteotomy for Kienböck disease: minimum 10-year follow-up. *J Hand Surg Am.* 2014, 39:679-85. [10.1016/j.jhsa.2014.01.020](https://doi.org/10.1016/j.jhsa.2014.01.020)

Prognostic Implication of PD-L1 Expression on Osimertinib Treatment for *EGFR*-mutated Non-small Cell Lung Cancer

TOSHIHIRO SHIOZAWA^{1*}, TAKESHI NUMATA^{2*}, TOMOHIRO TAMURA³, TAKEO ENDO²,
TAKAYUKI KABURAGI³, YUSUKE YAMAMOTO⁴, HIDEYASU YAMADA⁵, NORIHIRO KIKUCHI⁶,
KAZUHITO SAITO⁷, MASAHARU INAGAKI⁷, KOICHI KURISHIMA⁸, YASUNORI FUNAYAMA⁹,
KUNIHICO MIYAZAKI¹⁰, NOBUYUKI KOYAMA¹¹, KINYA FURUKAWA¹²,
HIROYUKI NAKAMURA¹², SHINJI KIKUCHI¹³, HIDEO ICHIMURA¹³,
YUKIO SATO¹³, IKUO SEKINE¹⁴, HIROAKI SATOH¹⁵ and NOBUYUKI HIZAWA¹

¹Department of Respiratory Medicine, Faculty of Medicine, University of Tsukuba, Tsukuba, Japan;

²Division of Respiratory Medicine, Mito Medical Center, Mito, Japan;

³Respiratory Center, Ibaraki Prefectural Central Hospital, Kasama, Japan;

⁴Division of Respiratory Medicine, Hitachi General Hospital, Hitachi, Japan;

⁵Division of Respiratory Medicine, Hitachinaka Medical Center, University of Tsukuba, Hitachinaka, Japan;

⁶Division of Respiratory Medicine, Kasumigaura Medical Center, Tsuchiura, Japan;

⁷Divisions of Respiratory Medicine and Thoracic Surgery, Tsuchiura Kyodo General Hospital, Tsuchiura, Japan;

⁸Division of Respiratory Medicine, Tsukuba Medical Center Hospital, Tsukuba, Japan;

⁹Division of Respiratory Medicine, Tsukuba Gakuen Hospital, Tsukuba, Japan;

¹⁰Division of Respiratory Medicine, Ryugasaki Saiseikai Hospital, Ryugasaki, Japan;

¹¹Department of Respiratory Medicine, Saitama Medical Center, Saitama Medical University, Saitama, Japan;

¹²Divisions of Respiratory Medicine and Thoracic Surgery,

Tokyo Medical University, Ibaraki Medical Center, Ami, Japan;

¹³Department of Thoracic Surgery, Faculty of Medicine, University of Tsukuba, Tsukuba, Japan;

¹⁴Department of Medical Oncology, Faculty of Medicine, University of Tsukuba, Tsukuba, Japan;

¹⁵Division of Respiratory Medicine, Mito Kyodo General Hospital-Mito Medical Center,
University of Tsukuba, Mito, Japan

Abstract. *Background/Aim:* Real-world data on the clinical outcomes of first-line osimertinib treatment for non-small cell lung cancer (NSCLC) with epidermal growth factor receptor (EGFR) mutations is lacking. This study aimed to reveal the treatment outcomes and prognostic factors of osimertinib as first-line therapy in clinical practice settings. *Patients and Methods:* We retrospectively evaluated clinical

outcomes of patients with EGFR-mutated NSCLC treated with osimertinib as first-line therapy across 12 institutions in Japan between August 2018 and March 2020. *Results:* Among 158 enrolled patients, the objective response rate (ORR) was 68%, and the estimated median progression-free survival (PFS) was 17.1 months [95% confidence interval (CI)=14.5-19.7]. Subgroup analysis showed that PFS in the group with high programmed death-ligand 1 (PD-L1) expression was significantly shorter than that in groups with low or no PD-L1 expression (10.1 vs. 16.1 vs. 19.0 months; $p=0.03$). Univariate and multivariate analyses demonstrated that high PD-L1 expression was the only independent adverse prognostic factor of osimertinib outcome related to PFS (hazard ratio=2.71; 95%CI=1.26-5.84; $p=0.01$). In terms of anti-tumor response, there was no statistically significant correlation between PD-L1 expression and the ORR (67% vs. 76% vs. 65%; $p=0.51$). No significant correlation was also found between PD-L1 and the incidence of de novo resistance to osimertinib ($p=0.39$). *Conclusion:* Although PD-L1 expression was not associated with either

*These Authors contributed equally to the present study.

Correspondence to: Toshihiro Shiozawa, MD, Department of Respiratory Medicine, Faculty of Medicine, University of Tsukuba, 1-1-1 Tennoudai, Tsukuba, Ibaraki 305-8575, Japan. Tel: +81 298533144, Fax: +81 298533144, e-mail: t-shiozawa@md.tsukuba.ac.jp

Key Words: Lung cancer, EGFR mutation, osimertinib, PD-L1.



This article is an open access article distributed under the terms and conditions of the Creative Commons Attribution (CC BY-NC-ND) 4.0 international license (<https://creativecommons.org/licenses/by-nc-nd/4.0>).

the ORR or frequency of de novo resistance, high PD-L1 expression could be an independent adverse prognostic factor related to PFS in osimertinib treatment.

Molecularly targeted therapies have contributed to an improvement in the survival of patients with recurrent or advanced non-small cell lung cancer (NSCLC) harboring driver oncogenes. Mutations in the epidermal growth factor receptor (*EGFR*), which is a driver oncogene in NSCLC, lead to tumorigenesis and tumor growth via the activated *EGFR* signaling pathway (1). Previous phase III studies demonstrated that *EGFR* tyrosine kinase inhibitors (*EGFR*-TKIs) as first-line therapy for *EGFR*-mutated NSCLC had better outcomes than a platinum-based regimen in terms of both progression-free survival (PFS) and objective response rate (ORR) (2-4). *EGFR*-TKIs are thus the current standard first-line agents for treating patients with *EGFR*-mutated advanced NSCLC.

First- to third-generation *EGFR*-TKIs are available in clinical practice. Of these, osimertinib, categorized as a third-generation *EGFR*-TKI, has irreversible anti-tumor activity against both *EGFR*-sensitizing and *EGFR*-resistant T790M mutations. In the global phase III FLAURA trial involving patients with untreated *EGFR*-mutated recurrent or advanced NSCLC, osimertinib prolonged PFS and overall survival (OS) compared with the standard of care achieved by first-generation *EGFR*-TKIs (5, 6). Thus, osimertinib is regarded as the most recommended first-line agent in these patients (7).

In clinical practice, osimertinib is indicated for a heterogeneous population, including patients with decreased performance status, symptomatic brain or leptomeningeal metastases, and uncommon mutations. However, as per the criteria of FLAURA trials, these patient groups are ineligible for osimertinib treatment. This discrepancy in recommendations suggests that there is a data gap regarding treatment outcomes between the results of the FLAURA trial and those noted in current clinical practice. Therefore, in addition to pivotal clinical trial data, it is important to collect and analyze post-marketing clinical data. Although the use of osimertinib as a first-line agent has increased since its approval, data regarding outcomes and prognostic factors with this treatment in clinical practice are still lacking.

To bridge this knowledge gap, we conducted this multi-institutional, retrospective, observational study to evaluate the treatment outcomes and prognostic factors of first-line osimertinib for treatment of patients with recurrent or advanced *EGFR*-mutated NSCLC.

Patients and Methods

Data collection. Twelve institutions in Ibaraki Prefecture, Japan participated in this study. We enrolled patients with recurrent or advanced NSCLC with *EGFR* mutations who received osimertinib as a first-line agent between August 2018 and March 2020. The data cut-off was May 31, 2020.

The following clinical data were collected: age, sex, smoking status (current, former, or never), Eastern Cooperative Oncology Group performance status (PS), stage at diagnosis according to the TNM Classification of Malignant Tumors (eighth edition), histology, type of *EGFR* mutation, presence of central nervous system (CNS) metastasis, and programmed death-ligand 1 (PD-L1) expression status using immunohistochemistry. Based on previous studies, PD-L1 expression was classified as none, low, and high if the tumor percentage score (TPS) of PD-L1 was <1%, 1%-49%, and > 50%, respectively (8, 9).

Statistical analysis. The endpoints in this study were the efficacy outcomes. The radiological anti-tumor response was evaluated based on the Response Evaluation Criteria in Solid Tumors (version 1.0.10). The ORR was defined as the proportion of patients who achieved anti-tumor response with complete response (CR) or partial response (PR). The disease control rate (DCR) was defined as the ORR plus the proportion of patients achieving stable disease (SD).

The definition of *de novo* resistance was based on a previous report as those whose best overall response was PD or whose PFS was less than 6 months (10). PFS was defined as the duration from the initiation of osimertinib treatment to disease progression or death from any cause. OS was defined as the duration from the initiation of osimertinib treatment to death from any cause. If death did not occur at the cut-off date, patients were censored. If patients were lost during the observation period, they were censored on the last day of confirmed survival. Clinical evaluations of PFS and OS were conducted using the Kaplan–Meier method. The log-rank test was used to compare two different survival curves. A Cox regression model was applied to examine prognostic factors related to survival. Univariate and multivariate hazard ratios (HRs) were reported with 95% confidence intervals (CIs). Statistical analysis was performed using IBM SPSS Statistics for Windows (version 24.0; IBM Corp., Armonk, NY, USA). All tests were two-sided and judged statistically significant if the calculated *p*-values were <0.05.

Ethical approval. This study was initiated after the study protocol was approved by the institutional review board of all institutions (approval number in Tsukuba University Hospital: R01-385). This retrospective observational study was conducted in compliance with the Helsinki Declaration. Individual patient data were anonymized prior to enrollment.

Informed consent was waived because the present study was a retrospective, observational research. Opt-out was done on the website of each institution.

Results

Patient characteristics. Among 161 patients initially enrolled, three were excluded from the analysis owing to the lack of data, resulting in a total of 158 eligible patients for the current study. Table I shows the patient characteristics. The median age was 73 years (range=39-93 years). Females accounted for 58% of the sample population, and adenocarcinoma was present in 95% of all cases. The proportions of *EGFR* mutation subtypes were 52% exon19 deletion, 43% exon21 L858R point mutation, and 5% uncommon mutation. Forty-five patients (28%) had CNS metastases at the time of diagnosis. The TPS of PD-L1 was none, low, and high in 60

Table I. Patient characteristics.

	N=158
Age (years)	73 (39-93)
Sex	
Male	66
Female	92
Smoking status	
Never	83
Former or current	74
Unknown	1
PS	
0/1/2/3/4/unknown	50/79/18/7/2/2
Clinical stage	
3/4/recurrent/other	15/120/22/1
Histology	
Adenocarcinoma	150
Squamous cell carcinoma	5
Other	3
EGFR mutation	
Exon 19 del	82
L858R	68
Uncommon	8
CNS metastasis	
Yes	45
No	113
PD-L1 expression	
None	60
Low	41
High	27
Unknown	30

PS: Performance status; EGFR: epidermal growth factor receptor; CNS: central nervous system; PD-L1: programmed death-ligand 1.

(38%), 41 (26%), and 27 (17%) patients, respectively. The remaining 30 patients (19%) had unknown TPS.

Survival. The median follow-up period of the present study was 12.5 months. The estimated median PFS was 17.1 months (95%CI=14.5-19.7). OS did not reach the median.

We examined the outcomes of osimertinib therapy according to patient subgroups of age, sex, smoking status, PS, stage, mutation subtype, CNS metastases, and TPS. No significant difference in PFS was observed with respect to age (<70 vs. ≥70 years, Figure 1A), sex (male vs. female, Figure 1B), smoking status (never vs. current or former, Figure 1C), PS (0-1 vs. 2-4, Figure 1D), stage (III or recurrent vs. IV, Figure 1E), mutation subtype (Exon 19 del vs. L858R vs. uncommon, Figure 1F), and CNS metastasis (present vs. absent Figure 1G). However, the high TPS group had a significantly poorer PFS of 10.1 months compared with the low and no TPS groups that had a PFS of 16.1 and 19.0 months, respectively (log-rank $p=0.03$, Figure 1H).

Next, we performed univariate and multivariate analyses to evaluate prognostic factors associated with PFS. Among

collected patient characteristics, we selected the eight factors mentioned above. As shown in Table II, only high TPS was found to be a statistically significant adverse prognostic factor related to PFS (HR=2.71; 95%CI=1.26-5.84; $p=0.01$).

Anti-tumor response. At the cut-off date, a response assessment was obtained for 140 patients. The best overall responses to osimertinib in the overall population included a CR of 3% ($n=6$), PR of 65% ($n=102$), SD of 14% ($n=22$), and PD of 6% ($n=10$), with an ORR of 68% and a DCR of 82%. We further compared best overall responses to osimertinib focusing on PD-L1 expression (Figure 2). There was no statistically significant difference in the ORR among the high, low, and no TPS groups (67%, 76%, and 65%, respectively; $p=0.51$, Figure 2A). DCR was also similar among the high, low, and no TPS groups (81%, 88%, and 80%, respectively; $p=0.57$, Figure 2B).

De novo resistance to osimertinib. We further evaluated the relationship between PD-L1 expression and the incidence of *de novo* resistance. We excluded cases whose best overall response was not evaluable and whose information regarding PD-L1 expression was not obtained; as a result, 114 cases were included. As shown in Table III, there was no statistically significant correlation between PD-L1 expression and the incidence of *de novo* resistance to osimertinib ($p=0.39$).

Discussion

The present study investigated the clinical outcomes and prognostic factors of osimertinib as a first-line treatment for advanced or recurrent NSCLC harboring *EGFR* mutations in a clinical practice setting. The results showed that the efficacy of osimertinib in the overall population was favorable, similar to that in the FLAURA trial. Although there was no statistically significant difference in the ORR and the incidence of *de novo* resistance among the high, low, and no TPS groups, the PFS of osimertinib in the high TPS group was inferior to that in the low or no TPS groups. Furthermore, univariate and multivariate analyses showed that high PD-L1 expression was an independent adverse prognostic factor associated with PFS in osimertinib treatment.

Compared to the FLAURA study, there were several differences in baseline patient characteristics in the present study. Specifically, in our study, there were more elderly patients and a higher frequency of decreased PS and presence of CNS metastases, while there was a lower frequency of never smokers. Racial differences were also observed. Some clinical factors, such as decreased PS and the presence of CNS metastasis, are poor prognostic factors for advanced NSCLC. Therefore, we conducted a subgroup analysis to evaluate whether these clinical factors affected the efficacy of osimertinib. The results showed that factors

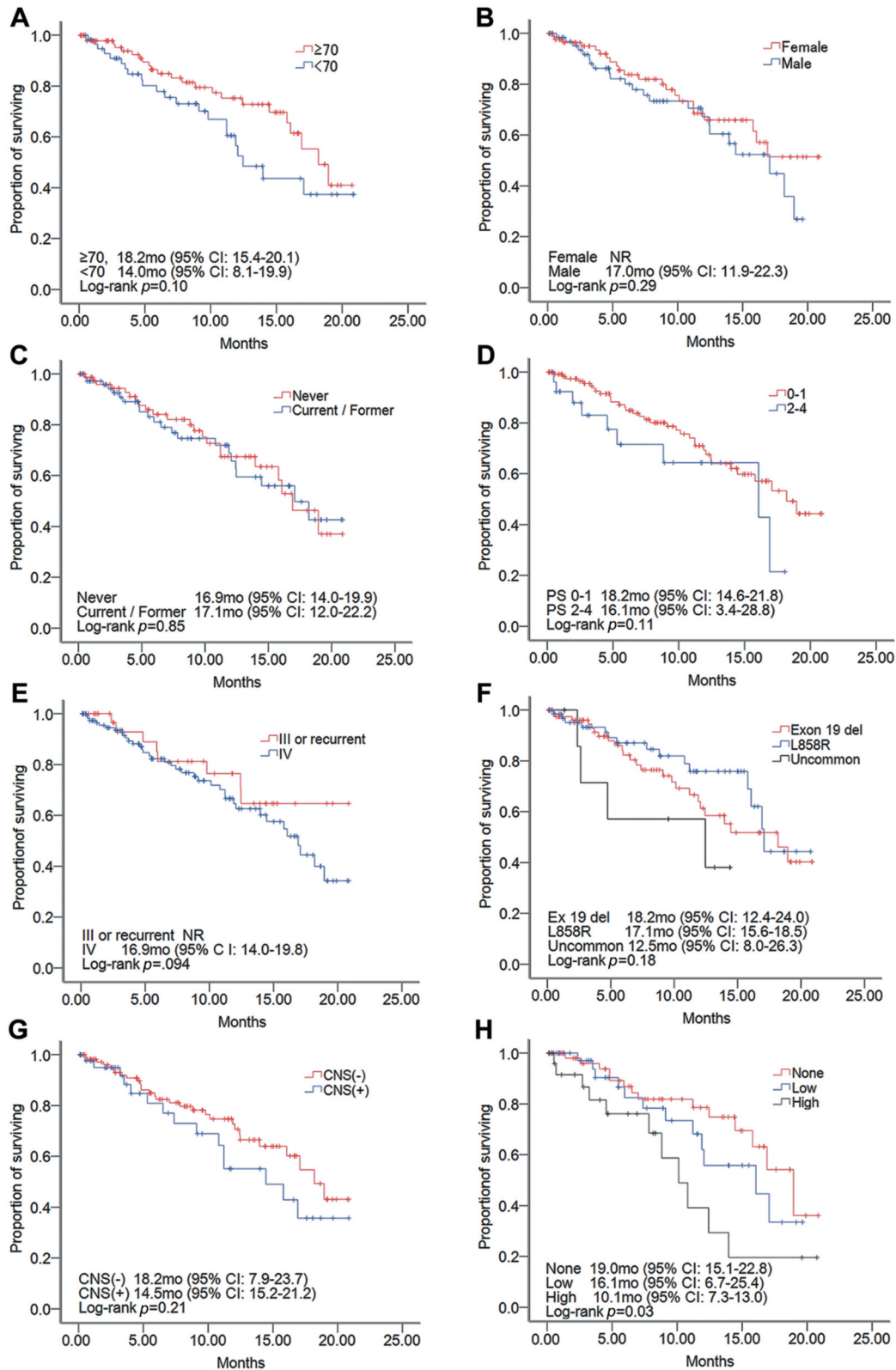


Figure 1. Progression-free survival according to age (A), sex (B), smoking status (C), PS (D), stage (E), mutation subtype (F), CNS metastasis (G), and PD-L1 expression levels (H). PS: Performance status; CNS: central nervous system; PD-L1: programmed death-ligand 1; CI: confidence interval; NR: not reached.

Table II. Univariate and multivariate analyses of factors related to PFS.

Variables	Univariate		Multivariate	
	HR 95%CI	p-Value	HR 95%CI	p-Value
Age				
<70 years	ref		ref	
≥70 years	0.73 (0.37-1.44)	0.36	1.00 (0.47-2.11)	0.99
Sex				
Male	ref		ref	
Female	1.56 (0.79-3.50)	0.20	1.58 (0.064-3.84)	0.32
Smoking				
Never	ref		ref	
Current/former	1.06 (0.54-2.07)	0.87	0.98 (0.39-2.45)	0.96
PS				
0-1	ref		ref	
2-4	1.48 (0.57-3.85)	0.41	1.67 (0.60-4.63)	0.32
Stage				
III or recurrent	ref		ref	
IV	0.66 (0.33-1.32)	0.24	0.40 (0.13-1.21)	0.10
Mutation type				
Exon 19 del	ref		ref	
L858r	1.41 (0.62-3.11)	0.42	1.97 (0.86-4.50)	0.10
CNS metastasis				
Absent	ref		ref	
Present	1.18 (0.57-2.43)	0.65	1.20 (0.53-2.68)	0.66
TPS				
None or low	ref		ref	
High	2.37 (1.16-4.83)	0.02	2.71 (1.26-5.84)	0.01

PFS: Progression-free survival; HR: hazard ratio; CI: confidence interval; PS: performance status; CNS: central nervous system TPS: tumor proportion score; ref: reference.

other than TPS did not affect the outcome (PFS) of osimertinib treatment. A previous phase II trial showed that osimertinib treatment provides a clinical benefit for patients with *EGFR* T790M-mutated NSCLC whose PS score has declined to 2-4 (11). In the FLAURA study, osimertinib resulted in significantly longer survival than the standard of care with first-generation *EGFR*-TKIs, even in patients who had CNS metastases at diagnosis (12). Together with these previous reports, the present study indicates that osimertinib could be administered to such patients in clinical practice.

In the present study, the estimated median PFS of osimertinib in the high TPS group was 10.1 months (95%CI=7.3-13.0), which was significantly shorter than that in the low or no TPS groups. Additionally, the present study showed that high TPS was an independent adverse factor associated with the PFS of osimertinib treatment. The subset analysis from the FLAURA trial examined the clinical outcomes of osimertinib, focusing on PD-L1 expression (13). Although the PFS of osimertinib was comparable in both PD-L1 positive and negative groups, the threshold for PD-L1 expression in the tumor cells (TCs) was set at 1%. Additionally, evaluation for TC≥50% of the population was lacking in a few cases (n=7). A recent study with 71 patients who received first-line osimertinib revealed that

patients with high PD-L1 expression had poorer PFS than those with low or negative PD-L1 (median PFS, 5.0 vs. 17.4 months, $p<0.001$) (14). The present study demonstrated results similar to that study in a larger sample size.

The present study suggested that the patients with high TPS had a higher risk of acquired resistance to osimertinib, because there was no statistically significant difference in the incidence of *de novo* resistance between the group with high TPS and the other two groups, despite of the inferior PFS in the group with high TPS. Accordingly, physicians should be aware of the acquired resistance to osimertinib for patients with high PD-L1 expression, even though they initially had favorable anti-tumor response. There was a discrepancy in the anti-tumor response and *de novo* resistance rate between the previous and present studies. Previous studies reported that patients with high PD-L1 expression had lower ORR and more frequent *de novo* resistance to *EGFR*-TKIs compared with the group with low or no PD-L1 expression (14, 15). It remains controversial whether increased PD-L1 expression contributed to primary or acquired resistance to osimertinib treatment. One speculation to the result of the present study is the association between Yes-associated protein (YAP) activity and PD-L1 expression on the *EGFR* signaling

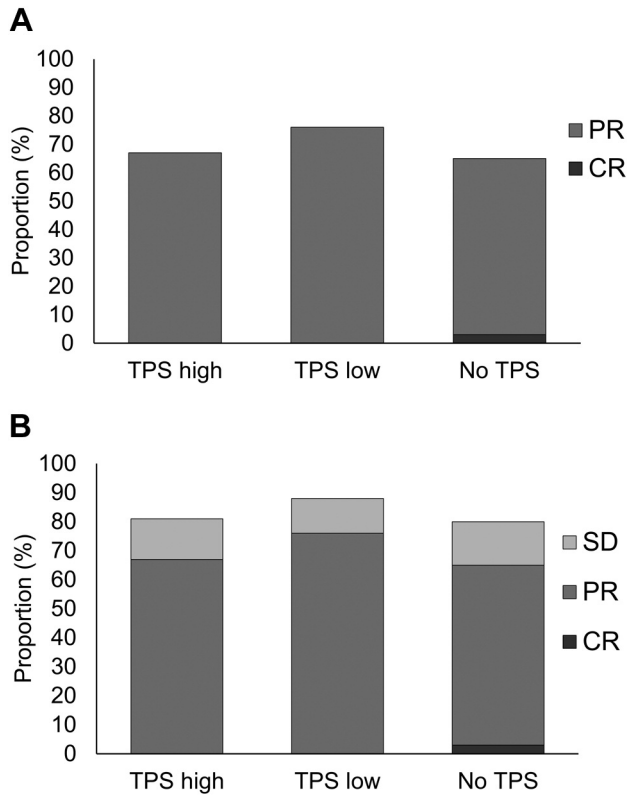


Figure 2. Best overall response according to tumor proportion score (TPS). Objective response rate stratified by TPS (A) and disease control rate stratified by TPS (B). CR: Complete response; PR: partial response; SD: stable disease.

pathway. Positive association was reported between EGFR pathway activation and PD-L1 expression in *EGFR*-mutated NSCLC (16). Specifically, the activated EGFR signaling pathway increased PD-L1 expression via IL-6/JAK/STAT3, or p-ERK1/2/p-c-JUN signaling pathway. Previous studies also reported that PD-L1 expression was decreased due to the blockade of the EGFR signaling pathway by EGFR-TKI administration (17-19). Recent studies reported that YAP, known to be associated with acquired resistance to EGFR-TKI therapy, had an important role as a regulator of PD-L1 expression (20-22). Accordingly, in patients with high PD-L1 expression, down-regulation of PD-L1 by osimertinib administration might lead to YAP-1 activation, resulting in the induction of acquired resistance to osimertinib treatment. Resistance to osimertinib is a current unmet need in *EGFR*-mutant NSCLC, and the development of novel therapeutic strategy to overcome it is under investigation (23). Further basic research to reveal the molecular mechanism of the correlation between response to osimertinib and PD-L1 expression and clinical validation with a large cohort are warranted.

Table III. Relationship between PD-L1 expression and de-novo resistance to osimertinib.

	N	TPS			p-value
		None	Low	High	
<i>De novo</i>	15	5 (33%)	5 (33%)	5 (33%)	0.39
<i>Non-de novo</i>	99	19 (19%)	33 (33%)	47 (48%)	

PD-L1: Programmed death-ligand 1; TPS: tumor proportion score.

This study had some limitations. First, there was a bias originating from the study's retrospective nature. Second, OS was not reached owing to the short observation period. Third, information regarding TPS was not obtained in approximately 20% of the participants. Finally, the current study included only Japanese patients; hence, ethnic differences may affect the results.

In conclusion, the present study provided clinically relevant data on the outcomes of first-line osimertinib for advanced or recurrent NSCLC with *EGFR* mutations. The favorable efficacy of osimertinib in this study was similar to that observed in the FLAURA trial. High TPS could be an independent adverse prognostic factor for PFS in osimertinib therapy, though the ORR and incidence of *de novo* resistance were similar regardless of PD-L1 expression. For patients with *EGFR*-mutated advanced NSCLC with high PD-L1 expression, physicians should be aware of the risk of acquired resistance to osimertinib, even though osimertinib initially showed favorable anti-tumor response.

Conflicts of Interest

There are no relevant conflicts of interest to be disclosed.

Authors' Contributions

Toshihiro Shiozawa, Hiroaki Satoh, and Nobuyuki Hizawa planned and designed this study. Toshihiro Shiozawa, Takeshi Numata, Tomohiro Tamura, Takeo Endo, Takayuki Kaburagi, Yusuke Yamamoto, Hideo Ichimura, Hideyasu Yamada, Norihiro Kikuchi, Kazuhito Saito, Masaharu Inagaki, Koichi Kurishima, Yasunori Funayama, Kunihiro Miyazaki, Nobuyuki Koyama, Kinya Furukawa, Hiroyuki Nakamura, Shinji Kikuchi, Yukio Sato, Ikuno Sekine, and Hiroaki Satoh collected the data. Toshihiro Shiozawa and Tomohiro Tamura analyzed the data. Toshihiro Shiozawa and Takeshi Numata wrote the original draft. Nobuyuki Hizawa supervised the manuscript preparation. All Authors discussed the results and agreed on the final draft.

Acknowledgements

The Authors would like to acknowledge Editage (<https://www.editage.jp>) for English language editing.

References

- Jorissen RN, Walker F, Pouliot N, Garrett TP, Ward CW and Burgess AW: Epidermal growth factor receptor: mechanisms of activation and signalling. *Exp Cell Res* 284(1): 31-53, 2003. PMID: 12648464. DOI: 10.1016/s0014-4827(02)00098-8
- Maemondo M, Inoue A, Kobayashi K, Sugawara S, Oizumi S, Isoobe H, Gemma A, Harada M, Yoshizawa H, Kinoshita I, Fujita Y, Okinaga S, Hirano H, Yoshimori K, Harada T, Ogura T, Ando M, Miyazawa H, Tanaka T, Saijo Y, Hagiwara K, Morita S, Nukiwa T and North-East Japan Study Group: Gefitinib or chemotherapy for non-small-cell lung cancer with mutated EGFR. *N Engl J Med* 362(25): 2380-2388, 2010. PMID: 20573926. DOI: 10.1056/NEJMoa0909530
- Zhou C, Wu YL, Chen G, Feng J, Liu XQ, Wang C, Zhang S, Wang J, Zhou S, Ren S, Lu S, Zhang L, Hu C, Hu C, Luo Y, Chen L, Ye M, Huang J, Zhi X, Zhang Y, Xiu Q, Ma J, Zhang L and You C: Erlotinib versus chemotherapy as first-line treatment for patients with advanced EGFR mutation-positive non-small-cell lung cancer (OPTIMAL, CTONG-0802): a multicentre, open-label, randomised, phase 3 study. *Lancet Oncol* 12(8): 735-742, 2011. PMID: 21783417. DOI: 10.1016/S1470-2045(11)70184-X
- Sequist LV, Yang JC, Yamamoto N, O'Byrne K, Hirsh V, Mok T, Geater SL, Orlov S, Tsai CM, Boyer M, Su WC, Bannouna J, Kato T, Gorbunova V, Lee KH, Shah R, Massey D, Zazulina V, Shahidi M and Schuler M: Phase III study of afatinib or cisplatin plus pemetrexed in patients with metastatic lung adenocarcinoma with EGFR mutations. *J Clin Oncol* 31(27): 3327-3334, 2013. PMID: 23816960. DOI: 10.1200/JCO.2012.44.2806
- Soria JC, Ohe Y, Vansteenkiste J, Reungwetwattana T, Chewaskulyong B, Lee KH, Dechaphunkul A, Imamura F, Nogami N, Kurata T, Okamoto I, Zhou C, Cho BC, Cheng Y, Cho EK, Voon PJ, Planchard D, Su WC, Gray JE, Lee SM, Hodge R, Marotti M, Rukazenzov Y, Ramalingam SS and FLAURA Investigators: Osimertinib in untreated EGFR-mutated advanced non-small-cell lung cancer. *N Engl J Med* 378(2): 113-125, 2018. PMID: 29151359. DOI: 10.1056/NEJMoa1713137
- Ramalingam SS, Vansteenkiste J, Planchard D, Cho BC, Gray JE, Ohe Y, Zhou C, Reungwetwattana T, Cheng Y, Chewaskulyong B, Shah R, Cobo M, Lee KH, Cheema P, Tiseo M, John T, Lin MC, Imamura F, Kurata T, Todd A, Hodge R, Saggese M, Rukazenzov Y, Soria JC and FLAURA Investigators: Overall survival with osimertinib in untreated, EGFR-mutated advanced NSCLC. *N Engl J Med* 382(1): 41-50, 2020. PMID: 31751012. DOI: 10.1056/NEJMoa1913662
- Hanna NH, Robinson AG, Temin S, Baker S Jr, Brahmer JR, Ellis PM, Gaspar LE, Haddad RY, Hesketh PJ, Jain D, Jaiyesimi I, Johnson DH, Leighl NB, Moffitt PR, Phillips T, Riely GJ, Rosell R, Schiller JH, Schneider BJ, Singh N, Spigel DR, Tashbar J and Masters G: Therapy for stage IV non-small-cell lung cancer with driver alterations: ASCO and OH (CCO) joint guideline update. *J Clin Oncol* 39(9): 1040-1091, 2021. PMID: 33591844. DOI: 10.1200/JCO.20.03570
- Herbst RS, Baas P, Kim DW, Felip E, Pérez-Gracia JL, Han JY, Molina J, Kim JH, Arvis CD, Ahn MJ, Majem M, Fidler MJ, de Castro G Jr, Garrido M, Lubiniecki GM, Shentu Y, Im E, Dolled-Filhart M and Garon EB: Pembrolizumab versus docetaxel for previously treated, PD-L1-positive, advanced non-small-cell lung cancer (KEYNOTE-010): a randomised controlled trial. *Lancet* 387(10027): 1540-1550, 2016. PMID: 26712084. DOI: 10.1016/S0140-6736(15)01281-7
- Reck M, Rodríguez-Abreu D, Robinson AG, Hui R, Csöszszi T, Fülöp A, Gottfried M, Peled N, Tafreshi A, Cuffe S, O'Brien M, Rao S, Hotta K, Leiby MA, Lubiniecki GM, Shentu Y, Rangwala R, Brahmer JR and KEYNOTE-024 Investigators: Pembrolizumab versus chemotherapy for PD-L1-positive non-small-cell lung cancer. *N Engl J Med* 375(19): 1823-1833, 2016. PMID: 27718847. DOI: 10.1056/NEJMoa1606774
- Jackman D, Pao W, Riely GJ, Engelman JA, Kris MG, Jänne PA, Lynch T, Johnson BE and Miller VA: Clinical definition of acquired resistance to epidermal growth factor receptor tyrosine kinase inhibitors in non-small-cell lung cancer. *J Clin Oncol* 28(2): 357-360, 2010. PMID: 19949011. DOI: 10.1200/JCO.2009.24.7049
- Nakashima K, Ozawa Y, Daga H, Imai H, Tamiya M, Tokito T, Kawamura T, Akamatsu H, Tsuboguchi Y, Takahashi T, Yamamoto N, Mori K and Murakami H: Osimertinib for patients with poor performance status and EGFR T790M mutation-positive advanced non-small cell lung cancer: a phase II clinical trial. *Invest New Drugs* 38(6): 1854-1861, 2020. PMID: 32424780. DOI: 10.1007/s10637-020-00943-0
- Reungwetwattana T, Nakagawa K, Cho BC, Cobo M, Cho EK, Bertolini A, Bohnet S, Zhou C, Lee KH, Nogami N, Okamoto I, Leighl N, Hodge R, McKeown A, Brown AP, Rukazenzov Y, Ramalingam SS and Vansteenkiste J: CNS response to osimertinib versus standard epidermal growth factor receptor tyrosine kinase inhibitors in patients with untreated EGFR-mutated advanced non-small-cell lung cancer. *J Clin Oncol*: JCO2018783118, 2018. PMID: 30153097. DOI: 10.1200/JCO.2018.78.3118
- Brown H, Vansteenkiste J, Nakagawa K, Cobo M, John T, Barker C, Kohlmann A, Todd A, Saggese M, Chmielecki J, Markovets A, Scott M and Ramalingam SS: Programmed cell death ligand 1 expression in untreated EGFR mutated advanced NSCLC and response to osimertinib versus comparator in FLAURA. *J Thorac Oncol* 15(1): 138-143, 2020. PMID: 31605792. DOI: 10.1016/j.jtho.2019.09.009
- Yoshimura A, Yamada T, Okuma Y, Fukuda A, Watanabe S, Nishioka N, Takeda T, Chihara Y, Takemoto S, Harada T, Hiranuma O, Shirai Y, Nishiyama A, Yano S, Goto Y, Shiotsu S, Kunimasa K, Morimoto Y, Iwasaku M, Kaneko Y, Uchino J, Kenmotsu H, Takahashi T and Takayama K: Impact of tumor programmed death ligand-1 expression on osimertinib efficacy in untreated EGFR-mutated advanced non-small cell lung cancer: a prospective observational study. *Transl Lung Cancer Res* 10(8): 3582-3593, 2021. PMID: 34584858. DOI: 10.21037/tlcr-21-461
- Su S, Dong ZY, Xie Z, Yan LX, Li YF, Su J, Liu SY, Yin K, Chen RL, Huang SM, Chen ZH, Yang JJ, Tu HY, Zhou Q, Zhong WZ, Zhang XC and Wu YL: Strong programmed death ligand 1 expression predicts poor response and de novo resistance to EGFR tyrosine kinase inhibitors among NSCLC patients with EGFR mutation. *J Thorac Oncol* 13(11): 1668-1675, 2018. PMID: 30056164. DOI: 10.1016/j.jtho.2018.07.016
- Bassanelli M, Sioletic S, Martini M, Giacinti S, Viterbo A, Staddon A, Liberati F and Ceribelli A: Heterogeneity of PD-L1 expression and relationship with biology of NSCLC. *Anticancer Res* 38(7): 3789-3796, 2018. PMID: 29970498. DOI: 10.21873/anticancer.12662
- Zhang N, Zeng Y, Du W, Zhu J, Shen D, Liu Z and Huang JA: The EGFR pathway is involved in the regulation of PD-L1 expression

- via the IL-6/JAK/STAT3 signaling pathway in EGFR-mutated non-small cell lung cancer. *Int J Oncol* 49(4): 1360-1368, 2016. PMID: 27499357. DOI: 10.3892/ijo.2016.3632
- 18 Chen N, Fang W, Zhan J, Hong S, Tang Y, Kang S, Zhang Y, He X, Zhou T, Qin T, Huang Y, Yi X and Zhang L: Upregulation of PD-L1 by EGFR activation mediates the immune escape in EGFR-driven NSCLC: Implication for optional immune targeted therapy for NSCLC patients with EGFR mutation. *J Thorac Oncol* 10(6): 910-923, 2015. PMID: 25658629. DOI: 10.1097/JTO.0000000000000500
- 19 Lin K, Cheng J, Yang T, Li Y and Zhu B: EGFR-TKI down-regulates PD-L1 in EGFR mutant NSCLC through inhibiting NF- κ B. *Biochem Biophys Res Commun* 463(1-2): 95-101, 2015. PMID: 25998384. DOI: 10.1016/j.bbrc.2015.05.030
- 20 McGowan M, Kleinberg L, Halvorsen AR, Helland Å and Brustugun OT: NSCLC depend upon YAP expression and nuclear localization after acquiring resistance to EGFR inhibitors. *Genes Cancer* 8(3-4): 497-504, 2017. PMID: 28680534. DOI: 10.18632/genesandcancer.136
- 21 Lee JE, Park HS, Lee D, Yoo G, Kim T, Jeon H, Yeo MK, Lee CS, Moon JY, Jung SS, Kim JO, Kim SY, Park DI, Park YH, Lee JC, Oh IJ, Lim DS and Chung C: Hippo pathway effector YAP inhibition restores the sensitivity of EGFR-TKI in lung adenocarcinoma having primary or acquired EGFR-TKI resistance. *Biochem Biophys Res Commun* 474(1): 154-160, 2016. PMID: 27105908. DOI: 10.1016/j.bbrc.2016.04.089
- 22 Tung JN, Lin PL, Wang YC, Wu DW, Chen CY and Lee H: PD-L1 confers resistance to EGFR mutation-independent tyrosine kinase inhibitors in non-small cell lung cancer *via* upregulation of YAP1 expression. *Oncotarget* 9(4): 4637-4646, 2017. PMID: 29435131. DOI: 10.18632/oncotarget.23161
- 23 Takano N, Seike M, Sugano T, Matsuda K, Hisakane K, Yoshikawa A, Nakamichi S, Noro R and Gemma A: A novel molecular target in *EGFR*-mutant lung cancer treated with the combination of osimertinib and pemetrexed. *Anticancer Res* 42(2): 709-722, 2022. PMID: 35093869. DOI: 10.21873/anticancer.15529

Received March 7, 2022

Revised March 27, 2022

Accepted March 28, 2022



OPEN ACCESS

Macrophage behaviour 72 hours after implantation of biodegradable polymer-based sirolimus-eluting stent in a case of ST elevation myocardial infarction

Koji Nakano,¹ Tomomi Koizumi ,¹ Yuto Abe,¹ Masao Ono²

¹Department of Cardiovascular Medicine, National Hospital Organization Mito Medical Center, Higashi-Ibarakigun, Japan

²Department of Laboratory Medicine, National Hospital Organization Mito Medical Center, Higashi-Ibarakigun, Japan

Correspondence to

Dr Tomomi Koizumi;
tomomikzm2014@gmail.com

Accepted 5 April 2022

SUMMARY

While the vascular healing process after drug-eluting stent implantation is not fully elucidated, it is generally accepted that macrophages play an important role in inflammation. It is also known that macrophages involved in the pathogenesis of atherosclerosis may stem from several origins, that is, monocyte-derived macrophages versus resident macrophages. However, little is known about the role of human macrophages on reperfusion of culprit coronary arteries in patients with atherosclerotic disease who have sustained acute coronary syndrome. In this present case report, we describe the presence of cluster of differentiation (CD) 163-positive macrophages in close proximity to the stent struts at the luminal site 72 hours after drug-eluting stent implantation in the culprit coronary lesion for ST elevation myocardial infarction by postmortem examination.

BACKGROUND

The healing process after coronary artery stent implantation is dependent on the resolution of the inflammatory reaction that drives atherogenesis. Macrophages are known to play an important role in the development of atherosclerotic lesions¹ with two macrophage phenotypes having been associated with different areas of the lesions: M1 (pro-inflammatory) macrophages that have been detected in the rupture-prone area of the intima, and M2 (anti-inflammatory) macrophages that have been localised in the adventitia underlying advanced plaques.^{2–5}

However, little is known about which type of macrophage is mobilised just after stent implantation on vulnerable plaques in a culprit coronary artery after ST elevation myocardial infarction (STEMI).⁶ Behaviour of human macrophages just after stent implantation in the infarct-related artery in STEMI patients is rarely investigated because the only definitive examination could occur post-mortem. As such, we describe a postmortem case with the presence of cluster of differentiation (CD) 163-positive macrophages in close proximity to the stent struts 72 hours after drug-eluting stent implantation in the culprit coronary lesion for STEMI.

CASE PRESENTATION

The patient was a man in his 80s transferred to our hospital with chief complaint of chest pain. Interval of symptom onset to hospital arrival was 110 min. The patient reported a medical history of

hypertension which was controlled by medication. On initial examination, his systolic blood pressure was 70 mm Hg, heart rate was 60 beats per minute and pulse oximetric oxygen saturation was 94% on room air.

INVESTIGATIONS

A 12-lead ECG revealed sinus rhythm and ST-segment elevation in leads II, III, aVF and ST-segment depression in leads I, aVL, V2–V5. Transthoracic echocardiogram illustrated hypokinesia in the infero-lateral wall and left ventricular ejection fraction of 40%. Initial coronary angiography showed total occlusion of the proximal left circumflex artery (LCX) (figure 1A).

TREATMENT

Primary percutaneous coronary intervention (PCI) to the proximal LCX was performed and a biodegradable polymer-based sirolimus-eluting stent (Orsiro 2.5×15 mm; Biotronik, Bülach, Switzerland) was implanted (figure 1B) in the culprit lesion. Although reperfusion therapy was successful with resultant thrombolysis in myocardial infarction flow grade 3 (door to balloon time was 81 min) (figure 1C), the patient's continued haemodynamic instability required both mechanical (intra-aortic balloon pumping and percutaneous cardiopulmonary support) and pharmacological circulatory support with catecholamines.

OUTCOME AND FOLLOW-UP

Unfortunately, the patient's blood pressure did not recover, and 72 hours after PCI, he passed away.

Postmortem examination was performed 3 hours 50 min after death. His autopsy revealed extensive lateral wall myocardial infarction with haemorrhage on macroscopic examination. The coronary arteries were extracted and the LCX (figure 1D) was incised to examine the stent (figure 1E). The dissected coronary artery with the stented segment was fixed with 5% formalin. After excision of the metal struts, the stented region (figure 2B), with reference segments (figure 2A,C) within 5 mm of both the proximal and distal ends, was processed for H&E staining or immunohistochemical staining. Immunohistochemical staining for CD68, CD80, CD163 and arginase 1 was performed.

Light microscopy of cross-sections of the artery, stained by H&E, revealed eccentric arteriosclerotic plaques in reference segments (figure 2 A# C#) and stented segment (figure 2 B#). On higher



© BMJ Publishing Group Limited 2022. Re-use permitted under CC BY-NC. No commercial re-use. See rights and permissions. Published by BMJ.

To cite: Nakano K, Koizumi T, Abe Y, et al. *BMJ Case Rep* 2022;**15**:e248539. doi:10.1136/bcr-2021-248539

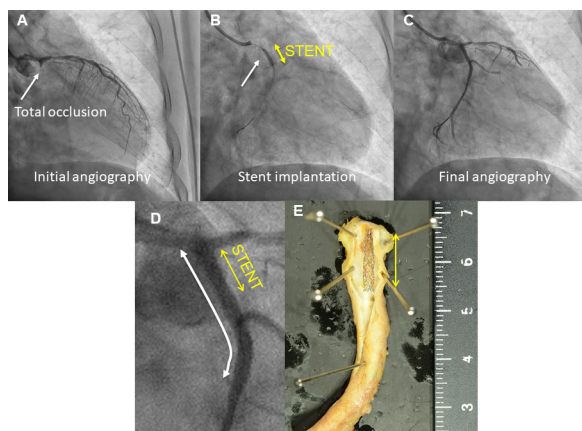


Figure 1 (A) The left coronary artery in initial coronary angiography in the RAO 30 and CAU 20 view. Total occlusion in the proximal circumflex artery is observed (white arrow). (B) RAO 24 and CAU 17 view, illustrating a balloon (yellow arrow) inflating stent in the occlusion lesion (white arrow). (C) Final angiography by RAO 24 and CAU 17 view, indicating TIMI flow grade 3 in the circumflex artery. (D) Magnification image of (C). White double-headed arrow represents the length of the extracted segment of the LCX. Yellow double-headed arrow represents the actual stent. (E) Autopsy specimen of the extracted segment of the LCX. Yellow double-headed arrow demonstrates the length of the implanted stent that is visible with the artery. CAU: caudal, LCX: left circumflex, RAO: right anterior oblique, TIMI: thrombolysis in myocardial infarction.

magnification, the stented segment appeared hypocellular, with scant inflammatory cells including lymphocytes or neutrophils observed around the stent struts (figure 2D,E). By immunohistochemical staining, CD80-positive cells were not observed in either the luminal site or the vessel wall, including around the stent struts and both the distal and proximal vessel ends. Both CD163-positive cells and arginase 1-positive cells were identified at the border of the vascular lumen (CD163 and arginase 1, figure 3A,C) and appeared to be in close proximity to the edge of each stent strut (* shows site of the stent strut, CD163 and arginase 1, figure 3B,D) in the culprit lesion. Moreover, both

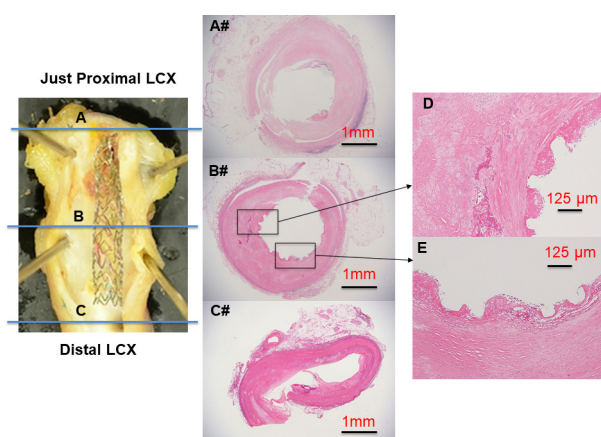


Figure 2 Left panel: The extracted proximal LCX segment with a stent. Blue lines A, B and C correspond to the sites of cross-sectioning of the artery. Middle panel: Cross-sectional images of the proximal LCX (A#), stented segment (B#) and distal LCX (C#) stained for H&E. Right panel: D, E represent high magnification H&E-stained images of the stented segment around the stent struts. LCX: left circumflex.

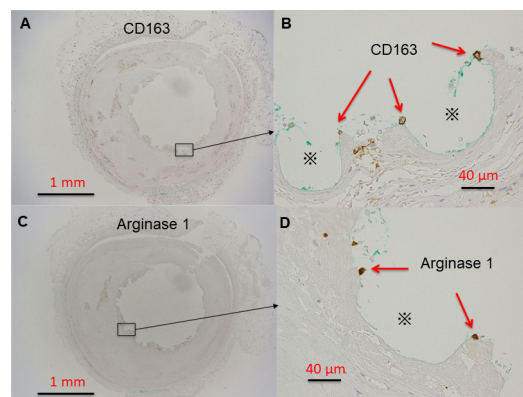


Figure 3 (A, B): CD163 stain, (C, D): arginase 1 stain of the culprit lesion after stent implantation. Black square frames in A and C are magnified in B and D. Note that both CD163-positive cells and arginase 1-positive cells (red arrows) are next to the stent struts (* shows site of the stent strut). CD: cluster of differentiation.

CD163-positive cells and arginase 1-positive cells were detected in the adventitia of the stented segment of the coronary artery.

DISCUSSION

To the best of our knowledge, this is the first report of both CD163-positive macrophages and arginase 1-positive macrophages detected close to the stent struts in the context of STEMI in humans. It has been reported that M2 macrophages play a reparative role.⁴ Indeed, the present images suggest that vascular injury repair by M2 macrophages may start 3 days after sirolimus-eluting stent implantation for STEMI.

M2 macrophages were also detected in the adventitia of the stented segment of the culprit coronary artery, which is consistent with a former report.⁵ There were almost no M2 macrophages either in the subintimal area or the intima 3 days after stent implantation. This leads us to deduce that the M2 macrophages in close proximity to the stent struts only at luminal site might not have migrated from the adventitia to the luminal site within 3 days, but may have originated from circulating monocytes.

However, the role of M2 macrophages in atherosclerosis progression remains controversial. Recent reports indicate that CD163 macrophages are associated with plaque progression⁷ and that CD163-expressing macrophages have a protective role during the progression of atherosclerosis.⁸ Moreover, the role of CD163 macrophages in adventitia has not been fully elucidated; therefore, further studies are warranted to understand the role of CD163 in culprit coronary artery in patients with STEMI.

Of note, scant number of inflammatory cells were detected in the stented segment of the culprit coronary artery and in both the proximal and distal segments of the artery shortly after STEMI, although, the culprit arterial wall was expected to be filled with abundant inflammatory cells.⁹ Taking into account that plaque morphology and cellular composition of coronary atherosclerosis leading to thrombosis is a heterogeneous process, and coronary erosion has less macrophages than plaque rupture, the formation of thrombosis is probably due to superficial erosion in the present case.⁹ Therefore, accumulation of pathological data including inflammatory cells will elucidate the mechanisms of coronary atherothrombosis at the very onset of STEMI.

CONCLUSION

CD163-positive macrophages and arginase 1-positive macrophages were detected in close proximity to drug-eluting stent

Learning points

- ▶ Acute coronary syndrome is a leading cause of death, provoked by acute coronary thrombosis, where inflammation has been reported as its main processes.
- ▶ Macrophages play an important role in inflammation, but behaviour of human macrophages just after coronary thrombosis and stent implantation in the infarct-related artery (IRA) is not fully elucidated.
- ▶ Present ST elevation myocardial infarction (STEMI) case shows that CD163-positive macrophages are neighbouring on stent struts 72 hours after stent implantation in IRA, indicating CD163-positive macrophages were recruited for healing process after stent implantation in IRA in patient with STEMI.
- ▶ The present results give us an opportunity to clarify a part of the process of healing vasculature after stent implantation in human coronary atherothrombosis.

struts deployed 3 days prior in the culprit coronary artery in patient with STEMI, giving us an opportunity to clarify a part of the process of healing vasculature after stent implantation in atherothrombosis.

Acknowledgements The authors thank Heidi N Bonneau, RN, MS, CCA for review of this report.

Contributors KN, TK helped in writing. KN, YA, TK contributed in collecting data. MO has done pathological assessment.

Funding The authors have not declared a specific grant for this research from any funding agency in the public, commercial or not-for-profit sectors.

Competing interests None declared.

Patient consent for publication Consent obtained from parent(s)/guardian(s).

Provenance and peer review Not commissioned; externally peer reviewed.

Open access This is an open access article distributed in accordance with the Creative Commons Attribution Non Commercial (CC BY-NC 4.0) license, which permits others to distribute, remix, adapt, build upon this work non-commercially, and license their derivative works on different terms, provided the original work is properly cited and the use is non-commercial. See: <http://creativecommons.org/licenses/by-nc/4.0/>.

Case reports provide a valuable learning resource for the scientific community and can indicate areas of interest for future research. They should not be used in isolation to guide treatment choices or public health policy.

ORCID iD

Tomomi Koizumi <http://orcid.org/0000-0001-7984-0755>

REFERENCES

- 1 Robbins CS, Hilgendorf I, Weber GF, *et al*. Local proliferation dominates lesional macrophage accumulation in atherosclerosis. *Nat Med* 2013;19:1166–72.
- 2 Colin S, Chinetti-Gbaguidi G, Staels B. Macrophage phenotypes in atherosclerosis. *Immunol Rev* 2014;262:153–66.
- 3 Gordon S. Alternative activation of macrophages. *Nat Rev Immunol* 2003;3:23–35.
- 4 Murray PJ, Wynn TA. Protective and pathogenic functions of macrophage subsets. *Nat Rev Immunol* 2011;11:723–37.
- 5 Stöger JL, Gijbels MJJ, van der Velden S, *et al*. Distribution of macrophage polarization markers in human atherosclerosis. *Atherosclerosis* 2012;225:461–8.
- 6 Honold L, Nahrendorf M. Resident and monocyte-derived macrophages in cardiovascular disease. *Circ Res* 2018;122:113–27.
- 7 Guo L, Akahori H, Harari E, *et al*. CD163+ macrophages promote angiogenesis and vascular permeability accompanied by inflammation in atherosclerosis. *J Clin Invest* 2018;128:1106–24.
- 8 Gutiérrez-Muñoz C, Méndez-Barbero N, Svendsen P, *et al*. CD163 deficiency increases foam cell formation and plaque progression in atherosclerotic mice. *Faseb J* 2020;34:14960–76.
- 9 van der Wal AC, Becker AE, van der Loos CM, *et al*. Site of intimal rupture or erosion of thrombotic coronary atherosclerotic plaques is characterized by an inflammatory process irrespective of the dominant plaque morphology. *Circulation* 1994;89:36–44.

Copyright 2022 BMJ Publishing Group. All rights reserved. For permission to reuse any of this content visit <https://www.bmj.com/company/products-services/rights-and-licensing/permissions/>. BMJ Case Report Fellows may re-use this article for personal use and teaching without any further permission.

Become a Fellow of BMJ Case Reports today and you can:

- ▶ Submit as many cases as you like
- ▶ Enjoy fast sympathetic peer review and rapid publication of accepted articles
- ▶ Access all the published articles
- ▶ Re-use any of the published material for personal use and teaching without further permission

Customer Service

If you have any further queries about your subscription, please contact our customer services team on +44 (0) 207111 1105 or via email at support@bmj.com.

Visit casereports.bmj.com for more articles like this and to become a Fellow



ORIGINAL ARTICLE

Impact of COVID-19 on living donor liver and kidney transplantation programs in Japan in 2020

Kaori Kuramitsu¹ | Shigeyoshi Yamanaga² | Ryosuke Osawa³ | Taizo Hibi⁴ | Mikiko Yoshikawa⁵ | Mariko Toyoda² | Keita Shimata⁴ | Ebisu Yosuke³ | Minoru Ono⁶ | Takashi Kenmochi⁷ | Hiroshi Sogawa⁸ | Yoichiro Natori⁹ | Harumi Yano¹⁰ | Toyofumi Chen-Yoshikawa¹¹ | Kazunari Yoshida¹² | Takumi Fukumoto¹ | Kenji Yuzawa¹³ | Hiroto Egawa¹⁴

¹Department of Surgery, Division of Hepato-Biliary and Pancreatic Surgery, Graduate School of Medicine, Kobe University, Hyogo, Japan

²Department of Surgery, Japanese Red Cross Kumamoto Hospital, Kumamoto, Japan

³Department of Infectious Disease, Kameda Medical Center, Chiba, Japan

⁴Department of Pediatric Surgery and Transplantation, Kumamoto University Hospital, Kumamoto, Japan

⁵Department of Transplant and Regenerative Surgery, Kyoto Prefectural University of Medicine, Kyoto, Japan

⁶Department of Cardiac Surgery, Tokyo University, Tokyo, Japan

⁷Department of Transplantation, Fujita Health University, Aichi, Japan

⁸Department of Surgery, Westchester Medical Center/New York Medical College, New York, USA

⁹Division of Infectious Disease, Department of Medicine, University of Miami, Florida, USA

¹⁰Department of Public Health, International University of Health and Welfare, Chiba, Japan

¹¹Department of Thoracic Surgery, Nagoya University, Aichi, Japan

¹²Department of Organ Transplant Medicine, Kitasato University, Kanagawa, Japan

¹³Department of Transplant Surgery, Mito Medical Center, Ibaraki, Japan

¹⁴Department of Surgery, Institute of Gastroenterology, Tokyo Women's Medical University, Tokyo, Japan

Correspondence

Kaori Kuramitsu, Department of Surgery, Division of Hepato-Biliary and Pancreatic Surgery, Kobe University Graduate School of Medicine, 7-5-2 Kusunoki-cho, Chuo-ku, Kobe City, Hyogo, Japan.
Email: kkuramit@med.kobe-u.ac.jp

Abstract

Background: Although many transplant programs have been forced to suspend living donor transplants due to the emergence of coronavirus disease (COVID-19), there are relatively few real-time databases to assess center-level transplant activities. We aimed to delineate the actual impact of COVID-19 on living donor transplant programs and the resumption process in Japan.

Methods: In a nationwide survey, questionnaires were sent to 32 liver transplant programs that had performed at least more than one case of living donor liver transplantation in 2019 and 132 kidney transplant programs that had performed more than one living donor kidney transplantation in 2018.

Results: Thirty-one (96.9%) and 125 (94.7%) liver and kidney transplant programs responded, respectively. In the early pandemic period, 67.7% (21/31) of liver programs



and 29.8% (37/125) of kidney programs were able to maintain transplant activities similar to those during the pre-pandemic period. After temporal suspension, 58.1% of kidney programs resumed their transplant activity after the number of local COVID-19 cases peaked. Establishing institutional COVID-19 screening, triage, and therapeutic management protocols was mandatory to resume transplant activity for 64.5% and 67.7% of liver and kidney programs, respectively. In the future wave of COVID-19, 67.7% of liver programs would be affected by institutional COVID-19 intensive care unit-bound patient numbers, and 55.7% of kidney programs would stop if hospital-acquired severe acute respiratory syndrome coronavirus-2 (SARS-CoV-2) infection spreads.

Conclusions: This nationwide survey revealed for the first time how living donor liver and kidney: transplant programs changed in response to the COVID-19 pandemic in a country where living donor transplantations are predominant.

KEYWORDS

COVID-19, living donor kidney transplantation, living donor liver transplantation

1 | INTRODUCTION

Severe acute respiratory syndrome coronavirus-2 (SARS-CoV-2) was identified in December 2019 and was subsequently determined to be the cause of coronavirus disease (COVID-19).^{1,2} The risk of death from COVID-19 is higher among immunosuppressed patients than in the general population.³ Accordingly, elective surgeries, including living donor transplant procedures, were paused in many countries.^{4,5} It is important to note that organ transplantation in Japan depends heavily on living donors due to a shortage of deceased donors. Responding to the inquiries from multiple transplant programs, the Japan Society for Transplantation (JST) published a set of guidelines on March 6, 2020 (version 1). In the guidelines, the JST recommended continuing transplants for immediate life-saving organs such as the heart, lung, and liver (for fulminant liver failure) after performing a risk–benefit assessment for each case. Nonurgent transplants of the kidney, pancreas, and bowel, as well as all nonlife-threatening living donor transplantations, were recommended to be postponed. For urgent living donor transplants, including living donor liver transplantation (LDLT), preventative measures such as 14 days of home or inpatient quarantine and a COVID-19 screening test for both donors and recipients were recommended. Many transplant programs have suspended their living donor transplants in response to the guidelines in Japan.

As the first wave of COVID-19 peaked, the JST announced the fourth edition of the guidelines on May 29, 2020 (version 4) and proposed a checklist to help determine the appropriate time to resume living donor kidney transplantation (LDKT) programs. These guidelines also recommended resuming living donor transplant activities based on the local community and institutional transmission risk. For living donor liver and kidney transplant donors and recipients, preventive measures, such as 14 days of home or inpatient quarantine and COVID-19 polymerase chain reaction (PCR) tests, were recommended.

Most recently, the JST announced the fifth edition of the guidelines on November 8, 2021 (version 5) and proposed a checklist to help determine de novo transplantation for both living donors and recipients who recovered from COVID-19.

Each transplant facility faced a difficult situation in which they had to make decisions individually to resume or postpone transplant surgeries. Since there are relatively few real-time databases to assess center-level transplant activities and no evidence-based guidelines for the management of transplant patients (especially from living donors in Japan), communication of knowledge is vital.⁶

This study aimed to understand the impact of COVID-19 on transplant activities across Japan and to explore center-level variations in activity, clinical practice, testing, and policies. Through this study, we examined how living donor transplant programs in Japan were previously suspended or continued; this information is critical for the maintenance of programs and for the future if COVID-19 re-spikes.

2 | MATERIALS AND METHODS

The survey was conducted from October 20, 2020, to November 30, 2020. Questionnaires were constituted only for this survey. The surveys were reviewed by the project members of the grant and adapted based on the feedback. Questionnaires were sent via e-mail to 32 liver transplant programs that had performed at least more than one case of LDLT in 2019 and 132 kidney transplant programs that had performed more than one LDKT in 2018. Data were collected from 96.9% (31/32) of the LDLT programs and 94.7% (125/132) of the LDKT programs. One answer from the two LDKT programs (Hirosaki University and Oyokyo Kidney Research Institute Hirosaki Hospital, run by the same team) was counted as one program for the analysis. The ques-

tionnaire consisted of four sections: (1) institutional transplant activities, (2) influence of COVID-19 on the institutional transplantation program, (3) institutional transplant outpatient practices, and (4) institutional COVID-19 treatment practices (Table S1).

Section 1 focused on the number of LDLT, LDKT, deceased donor liver transplantation (DDLTL), and deceased donor kidney transplantations (DDKT) performed in 2017, 2018, and 2019, as well as the number of LDLT, LDKT, DDLTL, and DDKT performed per month in 2020.

Section 2 focused on the present status of the institutional transplant program at the time of the survey (October 2020). The survey asked who approved the institutional transplant activities (institution, department, or government) during the pandemic, if there were any adverse effects on the recipients by resuming the transplant program, how to manage future transplant programs and the preoperative COVID-19 preventative measures for both donors and recipients.

Section 3 focused on outpatient management. Specifically, items about the recipient routine check-up list, number of donor/recipient outpatients, number of patients who delayed their routine visits, and institutional measures taken to reduce the risk of COVID-19 in outpatient clinics were included.

Section 4 focused on the hospital's experience in dealing with COVID-19. Items about center-level COVID-19 treatment systems were included.

An additional survey was performed to reveal the COVID-19 test status of the donors and the recipients who underwent transplantation during the survey period. Twenty-eight (85.7%) liver transplant programs and 111 (89.5%) kidney transplant programs responded to the additional survey.

On April 7, 2020, to prevent the spread of COVID-19, a state of emergency was declared in seven prefectures (Saitama, Chiba, Tokyo, Kanagawa, Osaka, Hyogo, and Fukuoka), which had an increasing number of new cases. On April 16, six prefectures (Hokkaido, Ibaraki, Ishikawa, Gifu, Aichi, and Kyoto) were added. These 13 prefectures either had a high population density and high levels of traffic or had clusters of COVID-19. In general, for living donor transplantation programs in Japan, recipients and donors are from the same or neighboring prefectures, except in pediatric cases. We categorized the transplantation programs into two groups based on their location: red zone—transplant programs located in the 13 prefectures where the state of emergency was declared (Figure 1A), and blue zone—the remaining 34 prefectures where a state of emergency was not issued. Based on this definition, 58.1% of the transplantation programs were categorized as the red zone group, and the remaining 41.9% were categorized as the blue zone group (Figure 1B).

3 | RESULTS

Answers from 31 LDLT and 124 LDKT programs were analyzed in the study.

3.1 | Institutional transplantation activities

3.1.1 | Transplantation numbers in the pre-pandemic era

The yearly number of cases of living donor liver and kidney transplantations was 334/1402 in 2017, 343/1555 in 2018, and 312/1701 in 2019. From deceased donors, the number of yearly liver/kidney transplant cases was 63/127 in 2017, 59/121 in 2018, and 88/176 in 2019. Categorized by zone, 219 (70.2%) LDLTs, 66 (75.0%) DDLTs, 1192 (70.1%) LDKTs, and 135 (76.7%) DDKTs were performed in 2019 in the red zone.

3.2 | Transplantation numbers in the pandemic era

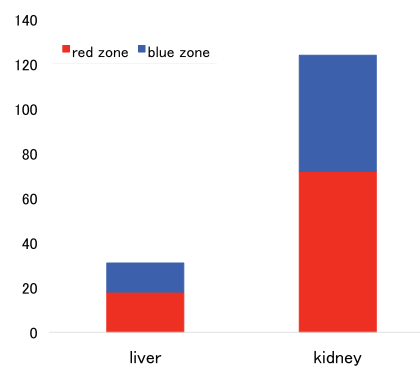
Figure 1C shows the total number of transplantations per month from January to September 2020. Although LDLTs were routinely performed at 25 cases per month on average, the number of LDKTs dropped to 55% (an average of 115 cases per month) from March to June; the rate increased gradually thereafter. In total, 229 LDLTs and 1034 LDKTs were performed. The number of deceased donor transplantations decreased slightly at an earlier stage. On average, six cases of DDLTs and 11 cases of DDKTs were performed per month from January to September 2020. In total, 52 DDLTs and 97 DDKTs were performed. To examine the regional impact of COVID-19, the total number of transplantations was sorted according to the red and blue zones. Figure 1D shows the total number of LDLT cases per month, which were routinely performed during the study period. Figure 1E shows the total number of DDLT cases per month. The total number decreased in March, April, and May, and a decrease was observed in both the red and blue zones. The number of DDLT cases increased in June. In total, 22 liver transplantations (18 LDLTs and four DDLTs) were performed per month in the red zone, whereas only nine (eight LDLTs and one DDLT) were performed in the blue zone. Throughout the pandemic era, 161 (70.3%) LDLTs and 39 (75.0%) DDLTs were performed in the red zone. Figure 1F,G shows the total number of kidney transplantation cases per month. The number of LDKT cases decreased drastically in April and May and that of DDKT cases decreased in March and April. A decrease was observed in both the red and blue zones. The number of LDKT started to increase in June and DDKT in May. In total, 89 kidney transplantations (81 LDKTs and eight DDKTs) were performed per month in the red zone, and 36 (33 LDKTs and three DDKTs) were performed per month in the blue zone. Throughout the pandemic era, 759 (73.4%) LDKTs and 71 (73.2%) DDKTs were performed in the red zone. In short, although the number of cases of LDLT did not change, DDLT and kidney transplantation decreased in the pandemic era.



(A) Location of 13 red zone transplant programs



(B) Liver/kidney transplant programs categorized by red/blue zones



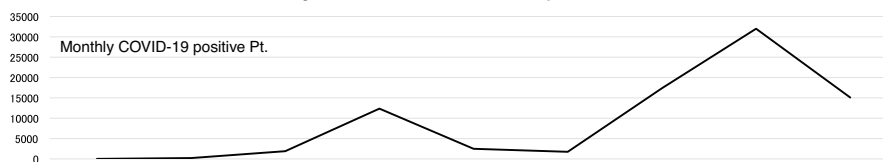
(C)

Government

Academic
(Japan Society for
Transplantation)

Guideline Ver.1

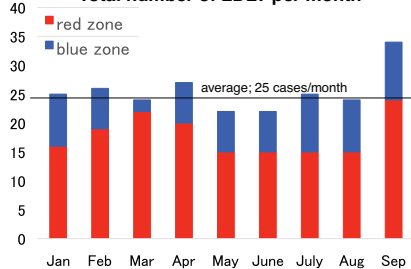
Guideline Ver.4

State of emergency
declared

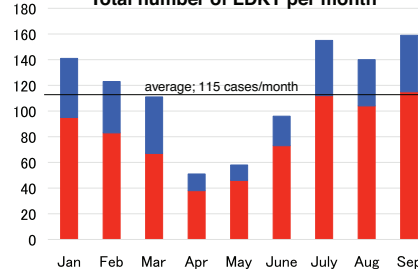
Total number of liver/kidney transplantations per month

	Jan	Feb	Mar	Apr	May	June	July	Aug	Sep
Living donor									
Liver	25	26	24	27	22	22	25	24	34
Kidney	141	122	112	51	58	96	155	140	159
Deceased donor									
Liver	7	7	4	3	3	5	6	8	9
Kidney	10	12	7	7	9	9	15	15	13

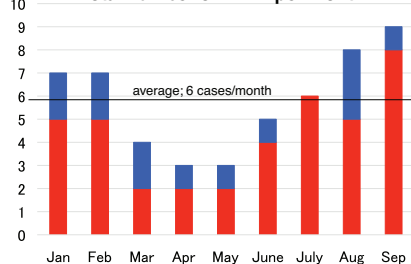
(D) Total number of LDLT per month



(E) Total number of LDKT per month



(F) Total number of DDLT per month



(G) Total number of DDKT per month

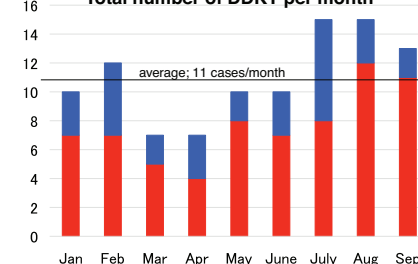


TABLE 1 Institutional transplantation activities

	Liver	Kidney
Institutional activity on October 2020		
Without any regulation	67.7%	29.8%
Only urgent/selected transplantation	19.4%	6.5%
Resume after local COVID-19 peak out	9.7%	58.1%
Pause	3.2%	5.6%
Institutional approval for transplantation activities		
Institutional board	61.3%	52.4%
Department board	67.7%	68.6%
Government guidelines	0%	1.6%

Abbreviation: COVID-19, coronavirus disease.

3.3 | Influence of COVID-19 on institutional transplantation programs

3.3.1 | Institutional transplantation activities

Twenty-seven (87.1%) LDLT and 117 (94.4%) LDKT programs followed the guidelines proposed by the JST on the management of COVID-19. In addition, 110 (88.7%) LDKT programs referred to the checklist in the JST guidelines. Table 1 shows the institutional transplantation activities at the end of October 2020. Although almost 70% of the LDLT programs could continue transplant activities without any regulations, almost 60% of the LDKT programs resumed after the number of local COVID-19 patients peaked. Most transplant programs were approved by either an institutional or departmental board. As an indicator of urgent LDLT, the Model for End-Stage Liver Disease score was used, ranging from 15 to 30 (average, 22). Acute liver failure ($n = 29$) and pediatric transplantation ($n = 14$) were also evaluated to determine the urgency of LDLT. For LDKT, difficulty in creating vascular access ($n = 48$), preemptive cases ($n = 53$), pediatric cases ($n = 36$), and marginal donors ($n = 26$) were considered factors for immediate transplantation. Although most of the transplant programs indicated that interruption of transplant programs did not impact the awaiting donors and recipients, death of the recipient during the waiting time

TABLE 2 Reasons to resume the institutional transplant program

	Liver	Kidney
Institutional		
Operation restriction was released	22.6%	26.6%
COVID-19 treatment system was constituted	64.5%	67.7%
COVID-19 infection status was improved	25.8%	25.0%
No COVID-19 spread	51.6%	42.7%
Regional		
COVID-19 infection status was improved	41.9%	46.0%

Abbreviation: COVID-19, coronavirus disease.

TABLE 3 Institutional liver transplantation activities categorized by zones

	Red zone	Blue zone
Institutional activity on October 2020		
Without any regulation	72.2%	61.5%
Only urgent/selected transplantation	16.7%	23.1%
Resume after local COVID-19 peak out	11.1%	7.7%
Pause	0%	7.7%

Abbreviation: COVID-19, coronavirus disease.

($n = 1$), and deterioration of patient condition beyond the indication ($n = 2$) were reported from LDLT programs, and patient death due to acute myocardial infarction ($n = 1$), deterioration of patient condition ($n = 3$), and unexpected temporal introduction of hemodialysis ($n = 16$) were reported from LDKT programs.

Table 2 indicates the reasons that led to institutional transplant resumption. Most of the transplant programs were resumed because institutional COVID-19-related treatment and the screening system were established. Additional analyses were performed to examine the regional impacts of COVID-19. Tables 3 and 5 show institutional liver/kidney transplantation activities, and Tables 4 and 6 indicate the reasons for resuming liver/kidney transplant programs categorized by red and blue zones. Although liver transplant programs could continue without any regulations regardless of the

FIGURE 1 (A) The 13 prefectures where the state of emergency was declared in Japan on April 7 and 16, 2020 to prevent the spread of coronavirus disease (COVID-19) (Saitama, Chiba, Tokyo, Kanagawa, Osaka, Hyogo, Fukuoka, Hokkaido, Ibaraki, Ishikawa, Gifu, Aichi, and Kyoto). (B) Red zone: transplant programs located in the 13 prefectures where the state of emergency was issued. Blue zone: the remaining 34 prefectures where the state of emergency was not issued. (C) The monthly case numbers of liver and kidney transplantations in 2020 along with the timing of when the state of emergency was declared; the first and fourth versions of the guidelines were published by the Japan Society for Transplantation (JST). In version 1, the JST recommended continuing transplants for life-saving organs such as the heart, lungs, and status 1 livers, requiring a risk-benefit assessment for each case. The JST recommended postponing any nonurgent transplants of the kidney, pancreas, and bowel, as well as all nonlife-threatening living donor transplantations. In version 4, the JST recommended resuming living donor transplant programs based on the local community and institutional transmission risk. They also proposed a checklist to help determine the restart of the living donor kidney transplantation (LDKT) programs. The JST guidelines are summarized in Table S2. (D)–(G) The monthly case numbers of liver and kidney transplantations in 2020 categorized by blue and red zone groups. The straight line indicates the average transplantation case number during the respective period. (D) Living donor liver transplantation (LDLT); (E) deceased donor liver transplantation (DDLTL); (F) LDKT; (G) deceased donor kidney transplantation (DDKT). Blue zones indicate prefectures where emergency measures were not implemented; red zones indicate prefectures where emergency measures were implemented

TABLE 4 Reasons to resume the institutional liver transplant program categorized by zones

	Red zone	Blue zone
Institutional		
Operation restriction was released	11.1%	23.1%
COVID-19 treatment system was constituted	66.7%	61.5%
COVID-19 infection status was improved	33.3%	30.8%
No COVID-19 spread	44.4%	46.2%
Regional		
COVID-19 infection status was improved	22.2%	69.2%

Abbreviation: COVID-19, coronavirus disease.

TABLE 5 Institutional kidney transplantation activities categorized by zones

	Red zone	Blue zone
Institutional activity on October 2020		
Without any regulation	29.2%	30.1%
Only urgent/selected transplantation	8.3%	3.8%
Resume after local COVID-19 peak out	58.3%	57.7%
Pause	4.2%	7.7%

Abbreviation: COVID-19, coronavirus disease.

TABLE 6 Reasons to resume the institutional kidney transplant program

	Red zone	Blue zone
Institutional		
Operation restriction was released	30.6%	21.2%
COVID-19 treatment system was constituted	70.8%	63.5%
COVID-19 infection status was improved	31.9%	26.9%
No COVID-19 spread	48.6%	25.0%
Regional		
COVID-19 infection status was improved	34.7%	59.6%

Abbreviation: COVID-19, coronavirus disease.

zones, kidney transplant programs in the red zone resumed once there was no institutional COVID-19 spread, and the blue zone groups resumed once the regional SARS-CoV-2 infection status improved.

Table 7 shows the items that would affect transplant activities if there were to be a future wave of COVID-19. Although most of the LDLT programs said that they would depend on the COVID-19 intensive care unit (ICU)-bound patient number, LDKT programs said that they would stop if institutional transmission of COVID-19 occurred. Tables 8 and 9 list the items that would affect transplant activities stratified by red and blue zones; these were not significantly different between the groups. In short, after the constitution of the COVID-

TABLE 7 Items that affect future transplant activities

	Liver	Kidney
Stop once institutional COVID-19 infection appears	29.0%	55.7%
Institutional COVID-19 patient number	35.5%	42.0%
Institutional COVID-19 ICU-bound patient number	67.7%	40.3%
Will not stop transplant program	22.6%	8.9%

Abbreviations: COVID-19, coronavirus disease; ICU, intensive care unit.

TABLE 8 Items that affect future liver transplant activities categorized by zones

	Red zone	Blue zone
Stop once institutional COVID-19 infection appears	22.2%	38.5%
Institutional COVID-19 patient number	33.3%	38.5%
Institutional COVID-19 ICU-bound patient number	55.6%	92.3%
Will not stop transplant program	27.8%	7.7%

Abbreviations: COVID-19, coronavirus disease; ICU, intensive care unit.

TABLE 9 Items that affect future kidney transplant activities categorized by zones

	Red zone	Blue zone
Stop once institutional COVID-19 infection appears	54.2%	51.9%
Institutional COVID-19 patient number	43.1%	44.2%
Institutional COVID-19 ICU-bound patient number	41.7%	38.5%
Will not stop transplant program	9.7%	7.7%

Abbreviations: COVID-19, coronavirus disease; ICU, intensive care unit.

19-related screening system, most of the LDLT programs could continue transplantation activities, and the number of transplantations that can be performed in the future would be affected by institutional COVID-19 ICU-bound patient numbers regardless of the facility location. Although LDKT programs in the red zone resumed as there was no institutional COVID-19 spread and blue zone groups resumed as the regional SARS-CoV-2 infection status improved, future transplant activity would be stopped once institutional COVID-19 infection appears.

3.3.2 | Preoperative check-up system for donors and recipients

Table 10 shows the preoperative check-up systems for the donors and recipients. A preoperative COVID-19 screening test was performed

TABLE 10 Preoperative check-up system for donors and recipients

	Liver	Kidney
COVID-19 preoperative screening test		
Recipient	93.6%	87.9%
Donor	90.3%	86.3%
COVID-19 test samples		
Nasopharyngeal swab	71.0%	56.5%
Nasal swab	25.8%	21.8%
Sputum	3.2%	3.2%
Saliva	19.4%	32.3%
COVID-19 screening test		
RT-PCR	96.8%	93.6%
Qualitative antigen test	3.2%	12.1%
Quantitative antigen test	3.2%	6.5%
Antibody test	0%	3.2%
Chest CT scan for the recipient		
Routinely performed	83.9%	65.3%
Performed initially but stopped	0%	12.1%
Not performed	16.1%	22.6%
Chest CT scan for the donor		
Routinely performed	54.8%	58.9%
Performed initially but stopped	0%	12.1%
Not performed	45.2%	29.0%
Preoperative self-quarantine period for the recipient		
28 days	3.2%	3.2%
14 days	67.7%	60.5%
7 days	0%	12.9%
Not fixed	29.0%	23.4%
Preoperative self-quarantine period for the donor		
28 days	0%	1.6%
14 days	48.4%	53.2%
7 days	19.4%	9.7%
Not fixed	32.3%	35.5%

Abbreviations: COVID-19, coronavirus disease; CT, computed tomography; RT-PCR, reverse transcription polymerase chain reaction.

in almost 90% of transplant programs for both recipients and donors. A nasopharyngeal swab was mainly used for test samples, and as a COVID-19 screening test, more than 90% of the transplant programs used reverse transcription polymerase chain reaction (RT-PCR). Computed tomography (CT) chest scans for the recipients were routinely performed in 83.9% of the LDLT and 65.3% of the LDKT programs, and for donors, the proportion decreased to 54.8% and 58.9%, respectively. More than 60% of the transplant programs set the preoperative self-quarantine period for the recipients as 14 days. In terms of the preoperative isolation period for donors, almost 50% of the transplant programs set the period as 14 days.

TABLE 11 Management of fever transplant patients

	Liver	Kidney
Management of the patient		
At fever clinic	61.3%	66.9%
At transplant clinic	58.1%	48.4%
COVID-19 screening test		
Routinely performed	19.4%	20.2%
Only suspicious cases	83.9%	66.1%
Chest CT		
Routinely performed	19.4%	30.7%
Only with cough cases	41.9%	30.7%

Abbreviations: COVID-19, coronavirus disease; CT, computed tomography.

3.4 | Institutional transplant outpatient practices

The usual check-up list for the recipients included patients' body weight, blood pressure, heart rate, body temperature, water intake, urinary volume (kidney transplant), adherence to medication, number of steps (liver transplant), and glucose level at outpatient clinics with modifications at each facility. In total, 5842 (average 195, 5–1000) liver transplant recipients and 3280 (average 106, 0–700) donors visited the outpatient clinic, whereas 20 451 (average 165, 10–2500) kidney transplant recipients and 10 365 (average 86, 0–700) donors visited the outpatient clinic. From January 1, 2020, to September 30, 2020, a total of 991 (average 32, 0–95) LDLT recipients and 5079 (average 41, 0–100) LDKT recipients postponed their consultation at the outpatient clinic. Most of the programs implemented several preventative measures to reduce COVID-19 transmission risk, such as reducing the frequency of outpatient clinic visits, extending the interval for refilling prescriptions, reducing the frequency of tests, shortening the length of hospital stay, and minimizing contact between other patients. To reduce the frequency of outpatient visits, 38.7% of LDLT and 21.8% of LDKT programs conducted telemedicine. Moreover, 87% of LDLT and 66.9% of LDKT facilities utilized an application system to support remote consultations.

3.5 | Institutional COVID-19 treatment practices

The facilities of 27 (87.1%) LDLT and 106 (85.5%) LDKT programs had experience accepting COVID-19 patients. The outpatient fever clinic was established in 27 (87.1%) LDLT and 99 (79.8%) LDKT programs. The general ward was used for COVID-19 patients in 27 (87.1%) LDLT and 102 (82.3%) LDKT programs, and COVID-19 patients were treated in the ICU in 29 (93.6%) LDLT and 84 (67.7%) LDKT programs. The routes for transplant and COVID-19 patients were separated into 26 (83.9%) LDLT and 108 (87.1%) LDKT programs, and 31 (100%) LDLT and 112 (90.3%) LDKT programs had already established a collaboration system between infectious disease specialists and intensivists to treat transplant recipients who had COVID-19. Table 11 shows the management of febrile transplant patients. More than half of the

patients were referred to fever clinics or managed at transplant outpatient clinics. COVID-19 testing was mainly performed if the disease was suspected after a medical history interview. Of the LDLT and LDKT programs, 40% and 30.7% performed chest CT if the recipients presented with cough, respectively.

3.6 | Impact of COVID-19 on transplantation

Twenty-eight (87.5%) liver transplant programs responded to the additional survey. Among the living donors and the recipients who underwent LDLT from January to September 2020, no patient was diagnosed with COVID-19 before transplantation. After transplantation, one donor (3.57%) and four recipients (10.71%) were diagnosed with COVID-19. Based on the national registry of the Japanese Liver Transplant Society, the 1-year patient survival after LDLT was 85.4% and after DDLT was 89.2% during the pre-COVID period (accessed at <http://jlts.umin.ac.jp/images/annual/JLTSRegistry2019.pdf> [in Japanese]). For the patients who underwent liver transplantation during the COVID-19 era from January to September 2020, the 1-year survival for LDLT was 90.2% and 88.1% for DDLT.

One hundred and eleven (89.5%) kidney transplant programs responded to the additional survey. There were no donors or recipients who were diagnosed with COVID-19 before transplantation. After transplantation, one donor (0.92%) and 15 recipients (11.82%) were diagnosed with COVID-19. Based on the national registry, the 1-year patient survival was 99.5%, and graft survival was 98.8% in the pre-COVID period. For the patients who underwent kidney transplantation during the COVID-19 era from January to September 2020, the 1-year patient survival was 99.8%, and the graft survival was 99.2%.

4 | DISCUSSION

To the best of our knowledge, this is the first national survey that has been conducted to examine the impact of COVID-19 on institutional living donor transplantation programs. We found that although most of the LDLT programs continued liver transplantation without any regulations, most of the LDKT programs were forced to pause; accordingly, the number of cases substantially decreased during this period. Most transplant programs resumed living donor transplant activities after constituting an institutional COVID-19 treatment system. Almost 70% of transplantations were performed before and during the era of the COVID-19 pandemic in areas where the state of emergency was declared. In areas where the state of emergency was not issued, the regional SARS-CoV-2 infection status had to be considered. In the case of a future COVID-19 wave, liver transplant activity would continue if the number of ICU-bound COVID-19 patients was not too high, while kidney transplant activity would stop if institutional SARS-CoV-2 spread appeared.

Several systematic reviews and meta-analyses have shown that transplant recipients have a higher risk of developing critical COVID-

19 illness due to chronic immunosuppression than the general population.^{7,8} International and national registries showed a mortality rate between 19% and 32% among solid organ transplant recipients with COVID-19.^{9–11} Regarding the clinical outcomes of liver transplant recipients with COVID-19, international registries reported a mortality rate of 18%–19%.^{12,13} In Japan, the Japanese registry by JST, accessed on February 8, 2021, reported that the case-fatality rate for organ transplant recipients was 7.1% (accessed at <http://square.umin.ac.jp/jst-covid-19> [in Japanese]). Based on the Johns Hopkins Coronavirus Resource Center accessed on February 11, 2021 (accessed at <https://coronavirus.jhu.edu/data/mortality>), the case-fatality rate for the general population was 2.9% in the United Kingdom, 1.7% in the United States, 2.1% in Spain, 2.3% in France, and 1.6% in Japan. To date, some studies have concluded that there is no difference in overall mortality between the general population and solid organ transplant recipients,^{14,15} and there is also an opinion that this conclusion needs further analysis because the study group was limited only to inpatients or ICU-bound patients.¹⁶ As LDLT and LDKT programs are performed in the presence of living donors, concrete policies to reduce the risk of COVID-19 infections should be thoroughly discussed at each transplant center.

The response rate for this study was as high as $\geq 90\%$, implying a strong national need to better understand the impact of COVID-19. In short, the results of the study can be summarized as follows: (1) although the LDKT program decreased drastically, the LDLT program was not affected by the emergence of COVID-19; (2) transplant programs stopped once and restarted based on either institutional or department policies; (3) almost 20% of the transplanted recipients postponed their routine check-up at the outpatient clinic; (4) more than 85% of transplant programs accepted COVID-19 patients, and (5) short-term patient/graft survival was not affected by the emergence of COVID-19. In the raw data, there were some differences between liver and kidney transplant programs. In general, LDKT programs implemented more rigorous restrictions than LDLT programs. While most liver patients require urgent transplantation, kidney transplantation is an alternative option for renal replacement therapy. As resources outlining safety measures for COVID-19 in the early phase of the pandemic were scarce, most kidney transplant programs were more cautious in avoiding potential harm to both recipients and donors. Moreover, the JST recommended postponing nonurgent kidney transplants. All these factors decreased the total number of kidney transplantations that were performed during the COVID-19 era. However, a recent report from Belgium found that the cumulative incidence of COVID-19 was 5.31% in hemodialysis patients, 1.82% in peritoneal dialysis patients, and 1.40% in kidney transplant patients,¹⁷ suggesting that transplant patients have a decreased chance of contracting COVID-19, possibly due to less frequent visits to the hospital compared to dialysis patients. Furthermore, delaying kidney transplantation by 1 year would decrease patient survival.¹⁸ A risk-benefit analysis should be carefully performed for each patient considering the availability of resources, the intensity of the pandemic in the patient's region, and their comorbidities.¹⁹ COVID-19 preoperative screening was performed in more than 90% of transplant

programs, as recommended in the JST guidelines (accessed at <https://square.umin.ac.jp/jst-covid-19/images/guidance4.1.pdf> [in Japanese]). The RT-PCR assay was used in most cases; however, since RT-PCR was not available in Japan during the early phases of the pandemic, less sensitive antigen assays were performed in two (6.4%) LDLT and 23 (18.6%) LDKT programs. Although RT-PCR is highly sensitive, a single negative result is insufficient to exclude the diagnosis of COVID-19 if the suspicion of COVID-19 remains high.²⁰ Thus, the JST guidelines emphasize the importance of practices that minimize the risk of COVID-19 exposure, including social distancing and self-quarantine for 14 days before donation and transplantation for both donors and recipients. Our survey found that approximately 20% of transplant programs did not encourage self-quarantine before donation or transplantation. Although the reasons why these measures were not implemented were unknown, pre-transplant self-quarantine may not be feasible for some donors and recipients, especially when they can still work before transplantation. In such cases, simple measures such as social distancing, universal masking, and frequent hand washing should be advised to minimize the risk of COVID-19 during the pre-transplant period. Importantly, there were no liver/kidney donors or recipients who were diagnosed with COVID-19 before transplantation, thus supporting the JST guidelines of preoperative self-quarantine.

A limitation of the study is that because this survey collected responses from transplant surgeons, the results may have been different if the survey answers were collected from referring physicians, as they evaluate transplant indication. Accordingly, the number of transplants is extensively influenced by the number of referred patients from physicians. Another limitation is that because the survey was conducted to clarify general practices and policies at each transplant program, patient-level data on COVID-19 treatments or changes in immunosuppressant regimens were not collected. In the study, more transplants occurred in the red zone than in the blue zone. Based on the Japan Statistical Yearbook 2022, the total population of 13 red zone prefectures was 77 million, which was almost 61.6% of the total Japanese population as of December 1, 2020 (accessed at <https://www.stat.go.jp/English/data/nenkan/71nenkan/index.html>). Transplant centers and universities were historically established in the area, which had a large population and convenient location. Judging from the fact that almost 70% of transplantations were already performed in the red zone before the era of the COVID-19 pandemic, the case number bias was caused by the definition of the red zone itself that these areas had a high population density and high levels of traffic or had clusters of COVID-19.

Based on the Japanese Ministry of Health, Labor, and Welfare data, the actual ICU utilization rate ranged from approximately 70% to 75% during the survey period (https://www.mhlw.go.jp/stf/seisakunitsuite/bunya/0000121431_00180.html). As the ICU utilization rate itself does not reflect the availability of ICUs for transplant patients, we focused on the monthly number of newly introduced respirators and extracorporeal membrane oxygenation (ECMO). Based on the cross-ICU searchable information system data, the monthly number of newly introduced respirators ranged from 20 (in June) to 393 (in April), and

the monthly number of newly introduced ECMO ranged from 6 (in June) to 110 (in April) (<https://www.ecmonet.jp/crisis>). These data suggest that although the actual ICU utilization rate did not drastically change, ICU-bound patient disease distribution shifted to COVID-19. Despite the negative surroundings, the total number of LDLTs was preserved, which was the result of an excellent team effort of all concerned with transplantation.

In conclusion, this nationwide survey in Japan revealed that transplant programs for LDKT decreased drastically at one point and recovered after institutional resumption policies were implemented. Most of the transplant programs complied with the JST guidelines, including performing preoperative COVID-19 tests and promoting self-quarantine for both donors and recipients, while also considering the regional COVID-19 infection status. Although vaccination and therapeutics were introduced after the survey era, how the living donor transplant program was modified in Japan at the early phase of the pandemic was elucidated through the study. There were no donors/recipients who were diagnosed with COVID-19 before transplantation, thus affirming self-quarantine. The maintained LDLT case numbers with shifted COVID-19 ICU surroundings suggested efforts by the transplant team with the ICU team to protect end-stage liver disease patients. Supported by preserved transplant patient survival during the era of COVID-19, this study provides valuable information to transplant facilities on how to prepare for future pandemics so that we can ensure that such living donor transplant programs continue unhindered.

ACKNOWLEDGMENTS

This study was supported by grants from the Ministry of Health, Labor, and Welfare in Japan. We are grateful to our colleagues at the transplant institutions who responded to the questionnaires and made this study possible. For the revised analysis, Dr. Koji Umeshita (Osaka University, Osaka) and Dr. Yuki Nakagawa (Juntendo University, Tokyo) performed the national data analysis. We are also grateful to Mrs. Mine Yamanaga, who helped edit the entire manuscript. This study was supported by grants from the Ministry of Health, Labor, and Welfare in Japan.

LDLT facilities: Okinawa Chubu Hospital (Dr. Murakami), Fujita Health University (Dr. Suzuki), Kanagawa Children's Medical Center (Dr. Shinkai), Kyoto University (Dr. Ito), Nagasaki University (Dr. Soyama), Kumamoto University (Dr. Shimata), Chiba University (Dr. Otsuka), Hiroshima University (Dr. Ohira), Tokyo Medical University (Dr. Kawachi), Okayama University (Dr. Yagi), Saitama Medical Center (Dr. Maki), Iwate Medical University (Dr. Takahara), Tokyo Women's Medical University (Dr. Egawa), Mie University (Dr. Tane-mura), Hokkaido University (Dr. Goto), Tokyo University (Dr. Akamatsu), Jichi Medical University (Dr. Sakuma), Nagoya University (Dr. Ogura), Osaka University (Dr. Goto), Asahikawa Medical University (Dr. Furukawa), Yamaguchi University (Dr. Nagano), Tohoku University (Dr. Miyagi), Kyushu University (Dr. Yoshizumi), National Center for Child Health and Development (Dr. Kasahara), Tokyo Jikei University School of Medicine (Dr. Ikegami), Shinshu University (Dr. Soejima), Saitama Children's Medical Center (Dr. Mizuta), Ehime University (Dr. Takada),



Fukushima Medical University (Dr. Maruhashi), Keio University (Dr. Hasegawa), and Kobe University.

LDKT facilities: Nagano Red Cross Hospital (Dr. Imao), Yokkaichi Municipal Hospital (Dr. Okumura), University Hospital Kyoto Prefectural University of Medicine (Dr. Ushigome), Tokyo Dental College Ichikawa General Hospital (Dr. Kohno), Nagoya University (Dr. Kato), Okayama Medical Center (Dr. Fujiwara), Kinki University (Dr. Nose), Kawashima Hospital (Dr. Minakuchi), Toyama Prefectural Central Hospital (Dr. Seto), Toyooka Public Hospital (Dr. Machida), Kanazawa Medical University Hospital (Dr. Tanaka), Kure Medical Center (Dr. Tashiro), Hidaka Hospital (Dr. Soeno), Juntendo University Urayasu Hospital (Dr. Nosaki), Kitano Hospital (Dr. Ikeuchi), Okinawa Chubu Hospital (Dr. Shimabukuro), Kagawa University (Dr. Taoka), Yamaguchi University (Dr. Isoyama), Edogawa Hospital (Dr. Koga), Miyazaki University (Dr. Uemura), Ehime Prefectural Central Hospital (Dr. Okamoto), Saga-ken Medical Center Koseikan (Dr. Tokuda), Iwate Medical University (Dr. Sugimura), Showa University (Dr. Yoshitake), Ota Memorial Hospital (Dr. Mizutani), Tokyo Women's Medical University (Dr. Unagami), Jikei University School of Medicine (Dr. Yamamoto), National Defense Medical College Hospital (Dr. Tasaki), Niigata University (Dr. Saito), Masuko Memorial Hospital (Dr. Uchida), Joban Hospital (Dr. Shinmura), Sumitomo Hospital (Dr. Ichimaru), Tokyo University (Dr. Yamada), Yuuai Medical Center (Dr. Ota), Akita University (Dr. Sato), Toranomon Hospital (Dr. Nakamura), Tokyo Medical University (Dr. Iwamoto), Kochi Health Sciences Center (Dr. Shibuya), Osaka Medical College Hospital (Dr. Hirano), Japan Community Health care Organization Sendai Hospital (Dr. Haga), Sapporo Hokuyu Hospital (Dr. Miura), Okayama University (Dr. Araki), Komaki City Hospital (Dr. Uehira), Osaka City General Hospital (Dr. Asai), Shizuoka Children's Hospital (Dr. Kitayama), Kansai Medical University Hospital (Dr. Yanishi), Gifu University (Dr. Tsuchiya), Japanese Red Cross Medical Center (Dr. Ishibashi), Toyohashi Municipal Hospital (Dr. Nagasaka), Osaka Women's and Children's Hospital (Dr. Yazawa), International University of Health and Welfare Mita Hospital (Dr. Tonsho), Osaka General Medical Center (Dr. Tsutahara), Nara Medical University Hospital (Dr. Yoneda), Ehime University (Dr. Miyauchi), Mito Medical Center (Dr. Yuzawa), Saku Central Hospital (Dr. Murakami), Dokkyo Medical University Saitama Medical Center (Dr. Tokumoto), Jichi Medical University Hospital (Dr. Iwami), Hokkaido University (Dr. Hotta), Kagoshima University (Dr. Yamada), Tokyo Women's Medical University (Dr. Hattori), Tokyo Metropolitan Children's Medical Center (Dr. Sato), Itabashi Chuo Medical Center (Dr. Koyama), Fujita Health University (Dr. Itoh), Yamanashi University (Dr. Kamiyama), Shonan Kamakura General Hospital (Dr. Igarashi), Fukui University (Dr. Fukiage), Keio University (Dr. Morita), Japanese Red Cross Fukuoka Hospital (Dr. Motoyama), University of Tsukuba Hospital (Dr. Takahashi), Japanese Red Cross Wakayama Medical Center (Dr. Itoh), Yonago Medical Center (Dr. Sugitani), Japanese Red Cross Nagoya Daini Hospital (Dr. Watarai), Nagasaki Medical Center (Dr. Onita), Chiba University (Dr. Maruyama), Miyazaki Prefectural Miyazaki Hospital (Dr. Terasaka), Tokai University (Dr. Nakamura), Sapporo City General Hospital (Dr. Sasaki), Saitama University (Dr. Okada), Toranomon Hospital (Dr. Ishii), Kyushu University (Dr. Okabe), International University of Health and Welfare Atami Hospital (Dr.

Tojinbara), Wakayama Medical University Hospital (Dr. Yoshikawa), Shizuoka General Hospital (Dr. Shiraishi), Yokohama City University Medical Center (Dr. Teranishi), Hospital of Hyogo College of Medicine (Dr. Yamada), Mie University (Dr. Nishikawa), Toda Chuo General Hospital (Dr. Shimizu), Tokushima University (Dr. Yamaguchi), Kobe University (Dr. Ishimura), Hyogo Prefectural Nishinomiya Hospital (Dr. Kishikawa), Osaka University (Dr. Imamura), Saitama Medical Center (Dr. Maki), Kameda Medical Center (Dr. Ochi), Shinshu University (Dr. Minagawa), St. Luke's International Hospital (Dr. Nagahama), Hamamatsu University (Dr. Isobe), Hiroshima Prefectural Hospital (Dr. Ishimoto), National Center for Child Health and Development (Dr. Sato), Ohkubo Hospital (Dr. Shirakawa), Hiroshima University (Dr. Ide), Japan Community Health Care Organization Osaka Hospital (Dr. Fujimoto), Kyoto University (Dr. Kobayashi), Osaka City University Hospital (Dr. Uchida), Kushiro City General Hospital (Dr. Morita), St. Marianna University (Dr. Marui), Toho University Omori Medical Center (Dr. Shinoda), Aichi Medical University (Dr. Kobayashi), Hirosaki University (Dr. Hatakeyama), Oyokyo Kidney Research Institute Hirosaki Hospital (Dr. Hatakeyama), St. Mary Hospital (Dr. Taniguchi), Tokyo Women's Medical University Yachiyo Medical Center (Dr. Inui), Kanazawa University (Dr. Kadono), Nagasaki University (Dr. Mochizuki), Kitasato University (Dr. Yoshida), Ryukyu University (Dr. Kimura), Saiseikai Yahata General Hospital (Dr. Yasunaga), Oita University (Dr. Ando), Yamagata University (Dr. Nishida), Fukuoka University (Dr. Nakamura), Iwate Prefectural Isawa Hospital (Dr. Yoneda), Tohoku University (Dr. Tokodai), Fukushima Medical University (Dr. Hata), Sapporo Medical University (Dr. Tanaka), and the Japanese Red Cross Kumamoto Hospital (Dr. Yamanaga).

CONFLICT OF INTEREST

The authors declare no conflicts of interest.

AUTHOR CONTRIBUTIONS

All authors contributed to the manuscript and fulfilled criteria as per the uniform requirements set forth by the International Committee of Medical Journal Editors (ICJME) guidelines. All authors have reviewed and approved the final version of the manuscript.

ORCID

Kaori Kuramitsu  <https://orcid.org/0000-0002-9843-6800>

Yoichiro Natori  <https://orcid.org/0000-0002-4938-125X>

REFERENCES

- Morens DM, Daszak P, Taubenberger JK. Escaping Pandora's box—another novel coronavirus. *N Engl J Med*. 2020;382(14):1293-1295. [10.1056/NEJMp2002106](https://doi.org/10.1056/NEJMp2002106).
- Morens DM, Fauci AS. Emerging pandemic diseases: how we got to COVID-19. *Cell*. 2020;182(5):1077-1092. [10.1016/j.cell.2020.08.021](https://doi.org/10.1016/j.cell.2020.08.021).
- Caillard S, Chavarot N, Francois H, et al. COVID-19 infection more severe in kidney transplant recipients? *Am J Transplant*. 2021;21(3):1295-1303. [10.1111/ajt.16424](https://doi.org/10.1111/ajt.16424).
- Ahn C, Amer H, Anglicheau D, et al. Global transplantation COVID report March 2020. *Transplantation*. 2020;104(10):1974-1983. [10.1097/TP.0000000000003258](https://doi.org/10.1097/TP.0000000000003258).

5. Kumar D, Manuel O, Natori Y, et al. COVID-19: a global transplant perspective on successfully navigating a pandemic. *Am J Transplant*. 2020;20(7):1773-1779. [10.1111/ajt.15876](https://doi.org/10.1111/ajt.15876).
6. Strauss AT, Boyarsky BJ, Garonzik-Wang JM, et al. Liver transplantation in the United States during the COVID-19 pandemic: national and center-level responses. *Am J Transplant*. 2021;21(5):1838-1847. [10.1111/ajt.16373](https://doi.org/10.1111/ajt.16373).
7. Azzi Y, Bartash R, Scalea J, Loarte-Campos P, Akalin E. COVID-19 and solid organ transplantation: a review article. *Transplantation*. 2021;105(1):37-55. [10.1097/TP.0000000000003523](https://doi.org/10.1097/TP.0000000000003523).
8. Raja MA, Mendoza MA, Villavicencio A, et al. COVID-19 in solid organ transplant recipients: a systematic review and meta-analysis of current literature. *Transplant Rev (Orlando)*. 2021;35(1):100588. [10.1016/j.trre.2020.100588](https://doi.org/10.1016/j.trre.2020.100588).
9. Cravedi P, Mothi SS, Azzi Y, et al. COVID-19 and kidney transplantation: results from the TANGO International Transplant Consortium. *Am J Transplant*. 2020;20(11):3140-3148. [10.1111/ajt.16185](https://doi.org/10.1111/ajt.16185).
10. Sánchez-Álvarez JE, Pérez Fontán M, Jiménez Martín C, et al. SARS-CoV-2 infection in patients on renal replacement therapy. Report of the COVID-19 Registry of the Spanish Society of Nephrology (SEN). *Nefrologia*. 2020;40(3):272-278. [10.1016/j.nefro.2020.04.002](https://doi.org/10.1016/j.nefro.2020.04.002).
11. Caillard S, Anglicheau D, Matignon M, et al. An initial report from the French SOT COVID Registry suggests high mortality due to COVID-19 in recipients of kidney transplants. *Kidney Int*. 2020;98(6):1549-1558. [10.1016/j.kint.2020.08.005](https://doi.org/10.1016/j.kint.2020.08.005).
12. Webb GJ, Marjot T, Cook JA, et al. Outcomes following SARS-CoV-2 infection in liver transplant recipients: an international registry study. *Lancet Gastroenterol Hepatol*. 2020;5(11):1008-1016. [10.1016/S2468-1253\(20\)30271-5](https://doi.org/10.1016/S2468-1253(20)30271-5).
13. Colmenero J, Rodríguez-Perálvarez M, Salcedo M, et al. Epidemiological pattern, incidence, and outcomes of COVID-19 in liver transplant patients. *J Hepatol*. 2021;74(1):148-155. [10.1016/j.jhep.2020.07.040](https://doi.org/10.1016/j.jhep.2020.07.040).
14. Molnar MZ, Bhalla A, Azhar A, et al. Outcomes of critically ill solid organ transplant patients with COVID-19 in the United States. *Am J Transplant*. 2020;20(11):3061-3071. [10.1111/ajt.16280](https://doi.org/10.1111/ajt.16280).
15. Chaudhry ZS, Williams JD, Vahia A, et al. Clinical characteristics and outcomes of COVID-19 in solid organ transplant recipients: a cohort study. *Am J Transplant*. 2020;20(11):3051-3060. [10.1111/ajt.16188](https://doi.org/10.1111/ajt.16188).
16. Mendoza MA, Raja M, Villavicencio A, Anjan S, Natori Y. Is the outcome of SARS-CoV-2 infection in solid organ transplant recipients really similar to that of the general population? *Am J Transplant*. 2021;21(4):1670-1671. [10.1111/ajt.16370](https://doi.org/10.1111/ajt.16370).
17. De Meester J, De Bacquer D, Naesens M, et al. Incidence, characteristics, and outcome of COVID-19 in adults on kidney replacement therapy: a nationwide registry study. *J Am Soc Nephrol*. 2021;32(2):385-396. [10.1681/ASN.2020060875](https://doi.org/10.1681/ASN.2020060875).
18. Massie AB, Boyarsky BJ, Werbel WA, et al. Identifying scenarios of benefit or harm from kidney transplantation during the COVID-19 pandemic: a stochastic simulation and machine learning study. *Am J Transplant*. 2020;20(11):2997-3007. [10.1111/ajt.16117](https://doi.org/10.1111/ajt.16117).
19. Thaumat O, Legeai C, Anglicheau D, et al. IMPact of the COVID-19 epidemic on the mORTAlity of kidney transplant recipients and candidates in a French Nationwide registry sTudy (IMPORTANT). *Kidney Int*. 2020;98(6):1568-1577. [10.1016/j.kint.2020.10.008](https://doi.org/10.1016/j.kint.2020.10.008).
20. Arevalo-Rodríguez I, Buitrago-García D, Simancas-Racines D, et al. False-negative results of initial RT-PCR assays for COVID-19: a systematic review. *PLoS One*. 2020;15(12):e0242958. [10.1371/journal.pone.0242958](https://doi.org/10.1371/journal.pone.0242958).

SUPPORTING INFORMATION

Additional supporting information can be found online in the Supporting Information section at the end of this article.

How to cite this article: Kuramitsu K, Yamanaga S, Osawa R, et al. Impact of COVID-19 on the living donor liver and kidney transplantation programs in Japan in 2020. *Transpl Infect Dis*. 2022;24:e13845. <https://doi.org/10.1111/tid.13845>



Prospective analysis of the expression status of FGFR2 and HER2 in colorectal and gastric cancer populations: DS-Screen Study

Hisateru Yasui¹ · Atsushi Takeno² · Hiroki Hara³ · Hiroshi Imamura⁴ · Hiroki Akamatsu⁵ · Kazumasa Fujitani⁶ · Minoru Nakane⁷ · Chihiro Nakayama Kondoh⁸ · Seigo Yukisawa⁹ · Junichiro Nasu¹⁰ · Yoshinori Miyata¹¹ · Akitaka Makiyama^{12,13} · Hiroyasu Ishida¹⁴ · Norimasa Yoshida¹⁵ · Eiji Matsumura¹⁶ · Masato Ishigami¹⁶ · Masahiro Sugihara¹⁶ · Atsushi Ochiai¹⁷ · Toshihiko Doi¹⁸

Accepted: 17 April 2022 / Published online: 19 May 2022
© The Author(s) 2022

Abstract

Purpose Fibroblast growth factor receptor 2 (FGFR2) and human epidermal growth factor receptor 2 (HER2) proteins are both molecular targets for cancer therapy. The objective of this study was to evaluate the expression status of FGFR2 and HER2 in patients with gastric cancer (GC) or colorectal cancer (CRC).

Methods Archived tumor tissue samples from patients with histologically-confirmed GC or CRC suitable for chemotherapy were analyzed for FGFR2 and HER2 expression using immunohistochemistry and fluorescence in situ hybridization (HER2 in CRC only).

Results A total of 176 GC patients and 389 CRC patients were enrolled. Among patients with GC, 25.6% were FGFR2-positive and 26.1% were HER2-positive. Among patients with CRC, 2.9% were FGFR2-positive and 16.2% were HER2-positive. No clear relationship was found between FGFR2 and HER2 status in either GC or CRC. In GC, FGFR2 and HER2 statuses did not differ between different primary cancer locations, whereas there were some differences between histological types. Based on FGFR2- and/or HER2-positive status, 117 patients were identified as potentially suitable for inclusion in clinical trials of therapeutic agents targeting the relevant protein (*GC* = 45, *CRC* = 72; *FGFR* = 56, *HER2* = 62), of whom 7 were eventually enrolled into such clinical trials.

Conclusions This study indicated the prevalence of FGFR2 and HER2 in GC and CRC in the Japanese population. The screening performed in this study could be useful for identifying eligible patients for future clinical trials of agents targeting these proteins.

Trial registration Clinical trial registration Japic CTI No.: JapicCTI-163380. <https://www.clinicaltrials.jp/cti-user/trial/ShowDirect.jsp?directLink=RNlzx1PPCuT.PrVNPxPRwA>.

Keywords Colorectal cancer · FGFR2 · Gastric cancer · HER2

✉ Toshihiko Doi
tdoi@east.ncc.go.jp

¹ Kobe City Medical Center General Hospital, Hyogo, Japan

² Kansai Rosai Hospital, Hyogo, Japan

³ Saitama Cancer Center, Saitama, Japan

⁴ Toyonaka Municipal Hospital, Osaka, Japan

⁵ Osaka Police Hospital, Osaka, Japan

⁶ Osaka General Medical Center, Osaka, Japan

⁷ Japanese Red Cross Musashino Hospital, Tokyo, Japan

⁸ Toranomon Hospital, Tokyo, Japan

⁹ Tochigi Cancer Center, Tochigi, Japan

¹⁰ Okayama Saiseikai General Hospital, Okayama, Japan

¹¹ Saku Central Hospital Advanced Care Center, Nagano, Japan

¹² Japan Community Healthcare Organization Kyushu Hospital, Fukuoka, Japan

¹³ Gifu University Hospital, Gifu, Japan

¹⁴ Mito Medical Center, Ibaraki, Japan

¹⁵ Japanese Red Cross Kyoto Daiichi Hospital, Kyoto, Japan

¹⁶ Daiichi Sankyo Co., Ltd, Tokyo, Japan

¹⁷ National Cancer Center Exploratory Oncology Research & Clinical Trial Center, Tokyo, Japan

¹⁸ National Cancer Center Hospital East, Chiba, Japan

Introduction

An increasing number of molecular-targeted therapies are available in the field of oncology. When using such treatments in the clinical setting, it is desirable to be able to identify those patients in whom the target molecule is expressed and who are therefore expected to benefit from the therapy.

Fibroblast growth factor receptor 2 (FGFR2) and human epidermal growth factor receptor 2 (HER2) proteins are well-known molecular targets for cancer therapy. FGFR2 consists of an extracellular ligand-binding region consisting of three Ig-like domains, a single transmembrane region, and an intracellular tyrosine kinase region [1]. Various cellular functions, including cell proliferation, migration, and differentiation, are regulated by the FGF signaling pathway [1, 2]. HER2, a receptor tyrosine kinase belonging to the epidermal growth factor receptor family, is involved in regulating the proliferation and differentiation of normal cells and also acts as an oncogene, driving gene amplification and mutation [3]. Novel agents targeting these proteins are emerging, including several next-generation antibodies with enhanced antibody-dependent cellular cytotoxicity (ADCC) activity [4] and antibody–drug conjugates [5, 6].

HER2 is overexpressed in 10–20% of gastric cancers (GCs), and assessment of HER2 status is necessary to identify patients eligible for treatment with drugs such as trastuzumab [7]. Less is known about the expression status of FGFR2 in GC or about HER2 and FGFR2 in other gastrointestinal cancers, such as colorectal cancer (CRC). Accurate characterization of HER2 and FGFR2 expression in specific types of cancer is important for determining the relevance of these proteins as markers for identifying potential candidates for treatment with relevant targeted therapies. Furthermore, to optimize the clinical development strategies of these emerging agents, it would be useful to investigate FGFR2 and HER2 expression patterns, such as whether they are co-expressed or expressed in a mutually-exclusive manner.

The primary objectives of this study were to investigate the expression status of FGFR2 and HER2 in tissue samples from patients with GC or CRC, and to evaluate the relationship between background factors and protein expression status. A secondary objective was to identify patients who were potentially eligible for clinical trials involving the therapeutic agents DS-1123 (a monoclonal antibody directed against FGFR2) or trastuzumab deruxtecan (DS-8201, T-DXd; an antibody–drug conjugate with a HER2 antibody, tetrapeptide-based cleavable linker, and a novel topoisomerase I inhibitor payload).

Patients and methods

This prospective, multicenter study, which was conducted in a routine clinical practice setting between November 2016 and June 2018, enrolled patients aged ≥ 20 years with histologically confirmed GC (including gastroesophageal junction [GEJ] cancer) or CRC for which chemotherapy was indicated. Enrollment of GC patients was stopped on April 2017 due to completion of a relevant clinical trial, DS1123-A-J101 (NCT02690337). To be eligible, patients were required to have archived tumor tissue samples that had been collected during surgery, endoscopy, or needle biopsy, and that were preserved as formalin-fixed paraffin-embedded blocks. Patients judged by the investigator to be inappropriate as study subjects were excluded.

The study was conducted in accordance with the principals of the Declaration of Helsinki. Ethical approval was obtained from the relevant ethical review board for each participating center, and patients provided written informed consent. Japic CTI No.: JapicCTI-163380.

Patient data

Patient details were collected using an electronic data capture system. This included demographics (age, sex); tumor characteristics (histopathological diagnosis and date of diagnosis, primary location, major histological type, stage, HER2 expression [for any patients with GC who had been tested for HER2 prior to the study], and presence/absence of *rat sarcoma viral oncogene homolog (RAS gene)* mutations [for any patients who had been confirmed as having a mutation prior to the study]); and tumor sampling information (date and location of sampling, primary or metastatic).

Tumor sample analysis

FGFR2 and HER2 expressions in GC and CRC samples were assessed using immunohistochemistry (IHC) at a central laboratory (SRL Medisearch Inc., Japan). For GC, the results of HER2 IHC performed at local laboratories were also collected, where available (HER2 IHC in GC patients is performed in routine clinical practice in Japan). In addition, samples from patients with CRC enrolled before December 2017 which were found to be HER2 IHC 2+ (in $\geq 10\%$ cells) were assessed for *HER2* gene amplification using fluorescence in situ hybridization (FISH) at a central laboratory,

if the patient had a suitable sample for testing and provided consent. Samples from patients with CRC enrolled after December 2017 were all assessed for HER2 FISH, regardless of HER2 IHC score.

IHC staining for FGFR2 was performed using a mouse chimeric anti-FGFR2 antibody produced in-house with Agilent DAKO EnVision™ FLEX + Mouse (LINKER) and Agilent DAKO Autostainer Link 48, which captures FGFR2 isoforms IIIb and IIIc. IHC staining for HER2 was performed using the Ventana I-VIEW pathway HER2 (4B5) kit. IHC scoring was evaluated based on three elements — IHC staining intensity, cellularity, and location — at the National Cancer Center Exploratory Oncology Research and Clinical Trial Center, Chiba, Japan (Online Resource). FISH was performed using Abbott PathVysion® HER2 DNA probe kit. *HER2* amplification was considered positive if the ratio of *HER2/CEP17* was ≥ 2.0 when counting total number of *HER2* and *CEP17* signals in at least 20 tumor cells.

FGFR2 positivity was defined as FGFR2 IHC 1+ to 3+ for both GC and CRC. HER2 positivity was defined as IHC 2+ or 3+ in GC, and HER2 IHC 2+ or 3+ in $\geq 10\%$ of cells in CRC (Online Resource).

Clinical trial participation

Patients who were found to be potentially eligible for participation in clinical trials of therapeutic agents targeting the relevant protein (i.e., GC patients with FGFR2 IHC 1+ to 3+ and CRC patients with FGFR2 IHC 1+ to 3+ or HER2

IHC 2+ or 3+ in $\geq 10\%$ of cells) were referred to ongoing clinical trials. Information on whether these patients went on to participate in the relevant clinical trial, including any reason for non-participation, was recorded.

Study outcomes

The primary endpoint was the percentage of patients with tumor samples in which FGFR2/HER2 protein expression was confirmed. In addition, the relationship between patient background factors and FGFR2/HER2 expression was also evaluated. Secondary endpoints included the proportion of patients with confirmed FGFR2 and HER2 expression who subsequently participated in clinical trials of therapeutic agents targeting the relevant protein.

Statistical analysis

FGFR2 and HER2 expression statuses were analyzed descriptively using central laboratory data. Summary statistics for patient characteristics and protein expression included mean and standard deviation, median (minimum–maximum), and number (percentage), as appropriate.

Results

A total of 565 patients (GC = 176, CRC = 389) were enrolled in the study between November 2016 and June 2018 from 15 sites across Japan. The full analysis set (FAS) included 560 patients (176 with GC, including 16 GEJ patients, and 384 with CRC); the majority of patients had stage III or IV

Table 1 Patient demographics

Parameter	Gastric cancer ^a (n = 176)	Colorectal cancer (n = 384)	Total (n = 560)
Age (years)			
Mean \pm SD	67.4 \pm 9.5	62.1 \pm 10.3	63.8 \pm 10.3
Median (range)	68.0 (34–93)	64.0 (29–83)	66.0 (29–93)
Female, n (%)	39 (22.2)	172 (44.8)	211 (37.7)
Stage, n (%)			
I	3 (1.7)	3 (0.8)	
II	12 (6.8)	38 (9.9)	
III	47 (26.7)	86 (22.4)	
IV	114 (64.8)	251 (65.4)	
Unknown	0 (0)	6 (1.6)	
Systemic chemotherapy prior to sampling, n (%)	27 (15.3)	55 (14.3)	82 (14.6)
History of radiation therapy to sampling location, n (%)	0 (0.0)	10 (2.6)	10 (1.8)

^aGastric cancer included 16 patients with gastroesophageal cancer

		HER2, n				Total (%)
FGFR2, n	0	0	1+	2+	3+	
	0	82	17	12	20	131 (74.4%)
	1+	13	5	4	5	27 (15.3%)
	2+	3	3	1	1	8 (4.5%)
	3+	7	0	2	1	10 (5.7%)
Total (%)		105 (59.7%)	25 (14.2%)	19 (10.8%)	27 (15.3%)	176 (100%)

FGFR2 positive (IHC 1+ to 3+) = 25.6% (45/176)*

HER2 positive (IHC 2+ and 3+) = 26.1% (46/176)*

FGFR2 positive / HER2 positive = 30.4% (14/46)

HER2 positive / FGFR2 positive = 31.1% (14/45)

* including 7/16 patients (43.8%) with GEJ

Fig. 1 Patient distribution by FGFR2 and HER2 IHC scores in gastric cancer

GC or CRC (Table 1). Five patients were excluded from the FAS because of discontinuation after informed consent due to disease worsening or no available tissue sample to submit.

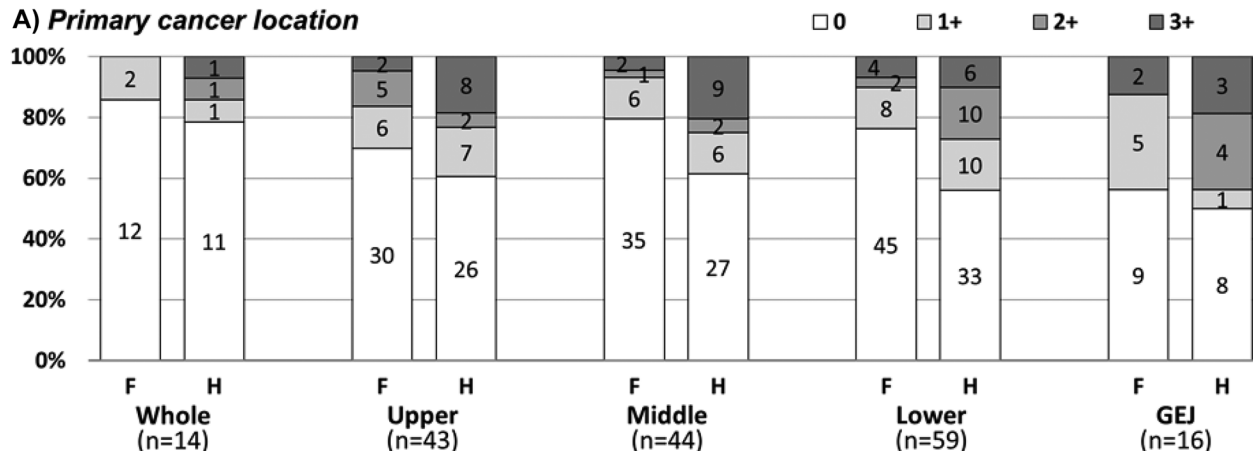
Gastric cancer

Among patients with GC, 25.6% (45/176) were FGFR2-positive and 26.1% (46/176) were HER2-positive. Among the subgroup

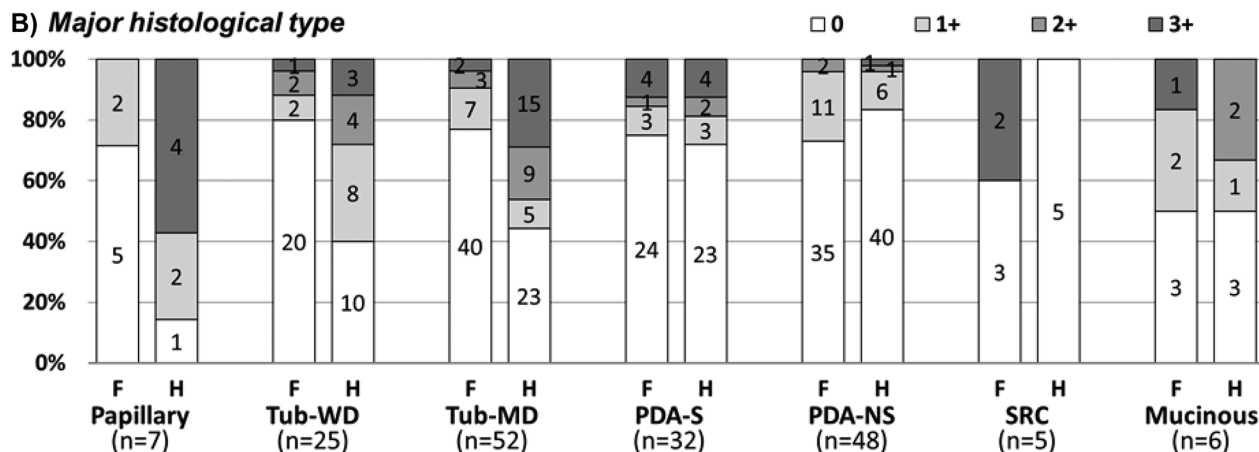
with GEJ, 43.8% (7/16) were positive for FGFR2 and 43.8% were positive for HER2.

There was no clear association between FGFR2 and HER2 status in patients with GC (Fig. 1). The proportion of FGFR2-positive patients among the whole population was 25.6% and among the HER2-positive population it was 30.4%. Similarly, the proportion of HER2-positive patients among the whole population was 26.1% and among the FGFR2-positive population it was 31.1%.

A) Primary cancer location



B) Major histological type



F = fibroblast growth factor receptor 2 (FGFR2), H = human epidermal growth factor receptor 2 (HER2), Whole = whole stomach, Upper = upper third of stomach, Middle = middle third of stomach, Lower = lower third of stomach, GEJ = gastroesophageal junction, Papillary = papillary adenocarcinoma, Tub-WD = tubular adenocarcinoma well-differentiated, Tub-MD = tubular adenocarcinoma moderately differentiated, PDA-S = poorly differentiated adenocarcinoma solid type, PDA-NS = poorly differentiated adenocarcinoma non-solid type, SRC = signet-ring cell carcinoma, Mucinous = mucinous adenocarcinoma.

Fig. 2 FGFR2 and HER2 IHC scores by primary location and major histology in gastric cancer

	HER2, n				Total (%)	
	0	1+	2+	3+		
FGFR2, n	0	218	93	46	15	372 (97.1%)
	1+	8	1	0	0	9 (2.3%)
	2+	1	0	0	0	1 (0.3%)
	3+	0	0	0	1	1 (0.3%)
Total (%)		227 (59.3%)	94 (24.5%)	46 (12.0%)	16 (4.2%)	383† (100%)

FGFR2 positive (IHC 1+ to 3+) = 2.9% (11/383)

HER2 positive (IHC 2+ and 3+) = 16.2% (62/383)

FGFR2 positive / HER2 positive = 1.6% (1/62)

HER2 positive / FGFR2 positive = 9.1% (1/11)

† One patient who didn't have FGFR2 IHC result was excluded.

Fig. 3 Patient distribution by FGFR2 and HER2 IHC scores in colorectal cancer

FGFR2 and HER2 statuses did not differ substantially between different primary cancer locations (Fig. 2A). With respect to major histological types, although sample numbers are low in these observations, the proportion of FGFR2-positive patients was numerically higher than that of HER2-positive patients for signet-ring carcinoma. On the other hand, for papillary adenocarcinoma and moderately differentiated tubular adenocarcinoma, the proportions of HER2-positive patients were numerically higher than those for FGFR2-positive patients (Fig. 2B).

Colorectal cancer

Among patients with CRC, 2.9% (11/383) were FGFR2-positive and 16.2% (62/383) were HER2-positive.

There was no clear association between FGFR2 and HER2 status in patients with CRC, although firm

conclusions could not be drawn because of the small number of FGFR2-positive patients (Fig. 3). The proportion of FGFR2-positive patients among the whole population was 2.9% and among the HER2-positive population it was 1.6%. Similarly, the proportion of HER2-positive patients among the whole population was 16.2% and among the FGFR2-positive population it was 9.1%.

No differences in FGFR2 or HER2 status according to primary cancer location or histological type could be identified because of the small number of FGFR2-positive patients (Fig. 4A, B). HER2 status appeared to be the same for right-side and left-side primary cancer locations (Fig. 4A).

Referral to clinical trials

Among the study population, 117 patients were identified as being potentially suitable for inclusion in clinical trials, based on FGFR2- and/or HER2-positive status ($GC = 45$, $CRC = 72$; $FGFR = 56$, $HER2 = 62$ [1 patient was FGFR2- and HER2-positive]). Ultimately, 7 of these patients ($GC = 4$, $CRC = 3$) were enrolled into clinical trials (Table 2).

Other findings

Among patients with CRC, the proportion with HER2 IHC 3+ tumors was higher in those who were *KRAS/NRAS* wild type positive (10/167) compared to those who were positive for *KRAS* or *NRAS* mutants (3/156), although the prevalence of HER2 IHC 3+ in these populations was low (Fig. 5).

Among patients with CRC, all those who were HER2 IHC 3+ were also HER2 amplified using FISH ($n = 3$). There were also some patients who were HER2 amplified using FISH in patients who were HER2 IHC 0, 1+, and 2+ (Table 3).

In an assessment of the concordance of IHC scores for GC samples tested at local and central laboratories, the rate

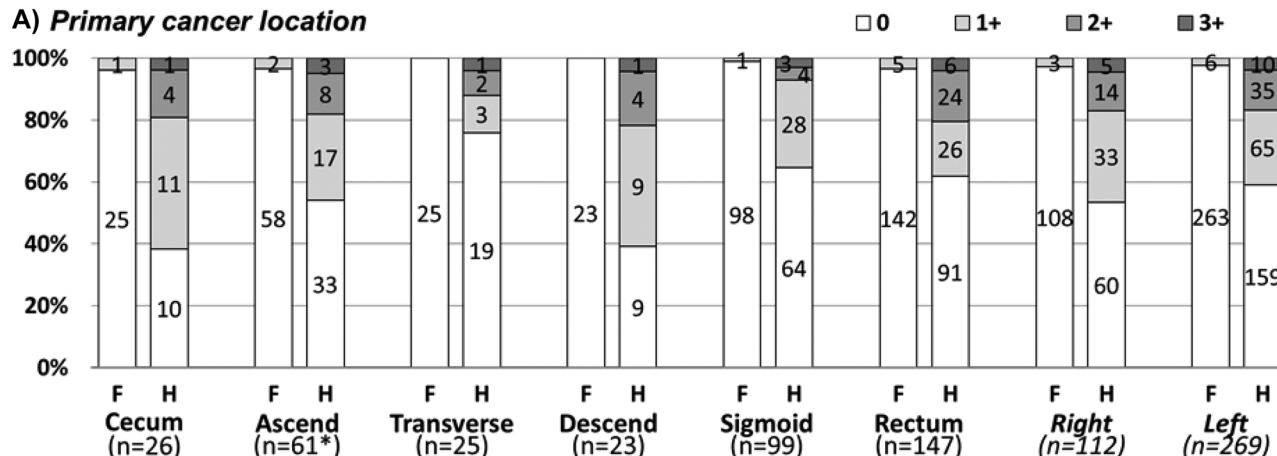
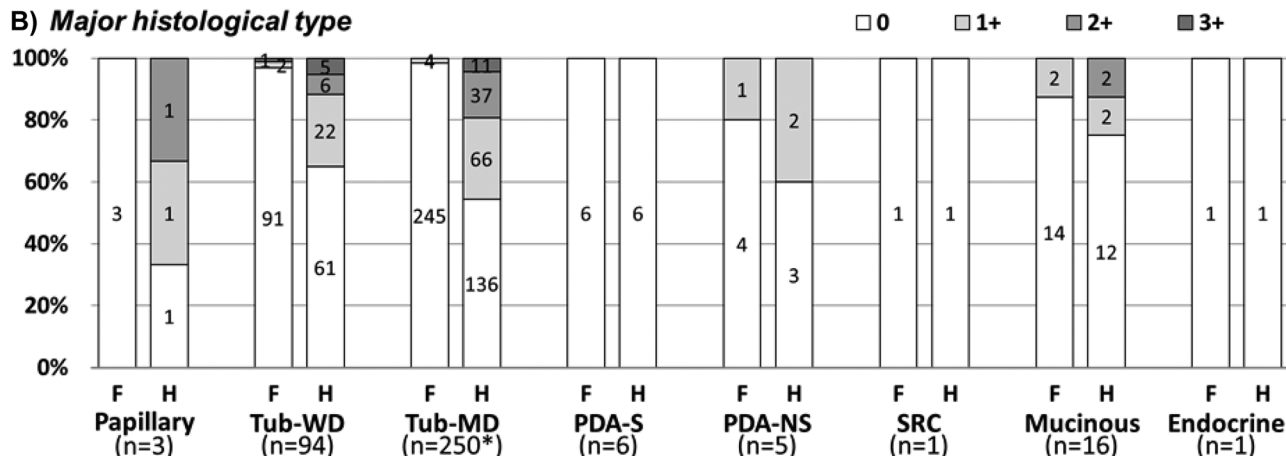
Table 2 Determination of eligibility and enrolment of FGFR2- or HER2-positive patients into clinical trials

Parameter, n (%)	Gastric cancer (n = 176)	Colorectal cancer (n = 384)	Total (n = 560)
FGFR2 IHC 1+ to 3+	45 (25.6)	11 (2.9)	56 (10.0)
HER2 IHC 2+ or 3+ in GC, or HER2 IHC 2+ or 3+ in $\geq 10\%$ of cells in CRC	46 (26.1)	62 (16.1)	108 (19.3)
Potentially suitable for clinical trials ^a	45 (25.6)	72 (18.8)	117 (20.9)
Referral to clinical trials ^b	5 (2.8)	4 (1.0)	9 (1.6)
Enrolled into clinical trials	4 (2.3)	3 (0.8)	7 (1.3)

CRC colorectal cancer, FGFR2 fibroblast growth factor receptor 2, GC gastric cancer, HER2 human epidermal growth factor receptor 2, IHC immunohistochemistry

^aFor gastric cancer, only FGFR2-positive patients were potentially eligible

^bThe major reasons that patients were not referred to clinical trials were as follows in descending order: the clinical trial recruitment period had ended, patients had been continuing prior therapy at the time of entry, or primary disease had worsened

A) Primary cancer location**B) Major histological type**

* Includes 1 patient who did not have an FGFR2 IHC result.

F = fibroblast growth factor receptor 2 (FGFR2), H = human epidermal growth factor receptor 2 (HER2),

Ascend = ascending colon, Transverse = transverse colon, Descend = descending colon, Sigmoid = sigmoid

colon, Papillary = papillary adenocarcinoma, Tub-WD = tubular adenocarcinoma well-differentiated, Tub-MD =

tubular adenocarcinoma moderately differentiated, PDA-S = poorly differentiated adenocarcinoma solid type,

PDA-NS = poorly differentiated adenocarcinoma non-solid type, SRC = signet-ring cell carcinoma, Mucinous =

mucinous adenocarcinoma, Endocrine = endocrine cell carcinoma.

Fig. 4 FGFR2 and HER2 IHC scores by primary location and major histology in colorectal cancer

of matched HER2 IHC scores (allowing 1 level difference) was 89.8% and the rate for completely matched cases was 59.9% (Fig. 6). The rate of concordance was not affected by a difference in the sample collection date between the laboratories or by the type of IHC testing kit used (Table 4).

Discussion

There is a need for additional information about the expression status of FGFR2 and HER2 in patients with gastrointestinal cancers. In our study, we evaluated patients with GC

Table 4 IHC scores concordance between local and central testing in gastric cancer

	Concordance between IHC scores from local and central testing, n (%)	
	Matched ^a	Completely matched
Difference between sample collection dates, days		
0 (n = 107)	94 (87.9)	63 (58.9)
>0 ^b (n = 50)	47 (94.0)	31 (62.0)
IHC kit for local laboratory testing ^c		
Ventana I-VIEW pathway HER2 (n = 98)	90 (91.8)	55 (56.1)
Daco HercepTest II (n = 32)	30 (93.8)	20 (62.5)
Histofine HER2 kit (poly) (n = 4)	4 (100.0)	3 (75.0)
Unknown (n = 6)	6 (100.0)	5 (83.3)
Others (n = 17)	11 (64.7)	11 (64.7)

HER2 human epidermal growth factor receptor 2, IHC immunohistochemistry

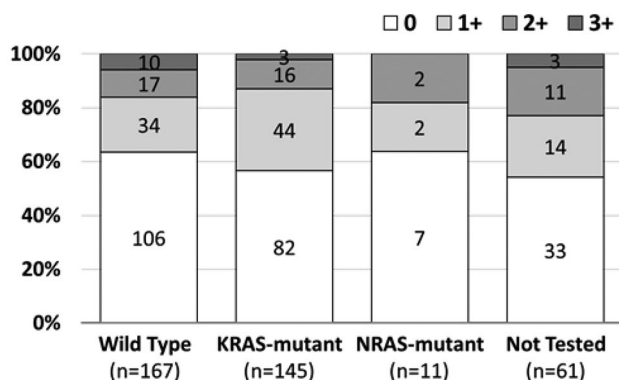
^a “Matched” allows 1 level difference

^b Mean 196.7 ± 258.7 days; median 51.5 days (min 1, max 842 days)

^c Central laboratory testing used Ventana I-VIEW pathway HER2

and CRC being managed in routine clinical practice. This is the first study to concurrently investigate the protein expression status of FGFR2 and HER2 in human tumor tissue from patients with CRC.

The HER2 positivity rate of 26.1% in GC found in the study is consistent with previous reports of HER2 overexpression of 10–23% [7–9]. HER2 expression is reported to be more common in GEJ cancer than in cancer located within the stomach [8, 9], and the rate in the GEJ subgroup in our study is consistent with this. With respect to FGFR2 positivity, the rate of 25.6% in GC in our study is within the range reported for previous studies (2.5–61%) [10].

**Fig. 5** HER2 IHC scores by RAS mutation status in colorectal cancer**Table 3** HER2 IHC scores and FISH status in colorectal cancer

	HER2 IHC scores, n (%)			
	0 (n = 44)	1+ (n = 21)	2+ (n = 15)	3+ (n = 3)
HER2 FISH status ^a				
Positive ^b	1 (2.3)	2 (9.5)	1 (6.6)	3 (100)
Negative	43 (97.7)	19 (90.5)	14 (93.3)	0 (0)

FISH fluorescence in situ hybridization, HER2 human epidermal growth factor receptor 2, IHC immunohistochemistry

^aHER2 FISH analysis was done for 83 CRC patients

^bIn the FISH analysis, HER2/CEP17 ratio ≥ 2 was defined as positive

Among patients with CRC, we found that 16.2% were positive for HER2, which lies within the range of rates reported in previous studies (0.5–54%) [3]. The most recent studies tend to suggest that HER2 overexpression accounts for 1–6% of CRCs, with HER2-positivity rates of around 5% reported in RAS wild-type tumors [3, 11]. Consistent with this, we found that among our CRC patients, the proportion of HER2 IHC 3+ cases was greater in RAS wild-type cancers compared with RAS-mutated cancers. There have been few reports of FGFR2 expression levels in patients with CRC, but our rate of 2.9% is consistent with the 1.4% reported in a previous study [12]. Although it was previously reported that HER2+ CRC tumors are usually left-sided [13], HER2 status appeared to be the same for right-side and left-side primary cancer locations in our study.

		HER2 IHC at Central Lab, n				Total (%)
		0	1+	2+	3+	
HER2 IHC at Local Lab, n	0	65	7	2	4	78 (49.7%)
	1+	20	6	9	0	35 (22.3%)
	2+	6	4	3	2	15 (9.6%)
	3+	3	1	5	20	29 (18.5%)
Total (%)		94 (59.9%)	18 (11.5%)	19 (12.1%)	26 (16.6%)	157* (100%)

Matched (allowing 1 level difference) = 89.8% (141/157)

Completely matched = 59.9% (94/157)

* Nineteen patients without an HER2 IHC result from the local laboratory were excluded.

Fig. 6 HER2 IHC scores from local and central laboratories for gastric cancer

Overall, we found no clear relationship between FGFR2 and HER2 status in either GC or CRC patients. Previous studies that focused specifically on amplifications found that HER2 and FGFR2 gene amplifications were usually mutually exclusive [14–16]. In our GC patients, neither FGFR2 nor HER2 expression status differed according to the primary cancer location; however, there were some differences between histological types. Previous reports have suggested that HER2 expression may vary between GC histological types, with higher rates reported for intestinal versus diffuse cancers [8, 9]. Although this study could not provide sufficient evidence to enable a clear conclusion to be reached, further investigation of the relationship between HER2 expression and GC histological type, with the molecular mechanism which defines the histological type, may provide insights to expand the indication for HER2 therapies. The limited number of FGFR2-positive CRC patients in our study meant that the relationship between FGFR2 and HER2 status in CRC could not be fully assessed with respect to differences between primary cancer locations and histological types. Despite this study not being able to reveal a relationship between FGFR2 and HER2 expression, it would be valuable to consider re-testing FGFR2 expression in tumor tissues of patients after HER2-targeted therapy to analyze the relationship between FGFR2 expression changes after HER2-targeted therapy and drug resistance, because studies have indicated the role of FGFR2 in HER2-targeted lapatinib resistance [17, 18].

Several studies have reported that gene amplification is generally present in CRC tumors that are strongly positive for HER2 overexpression on IHC [11, 19, 20]. Consistent with this, we found that CRC samples which were strongly positive for HER2 on IHC were also FISH positive.

More than 100 FGFR2- and/or HER2-positive patients were found in the current study, who were therefore potentially suitable for inclusion in clinical trials of targeted agents. Seven of these patients were successfully enrolled in other clinical trials, including DS1123-A-J101 (NCT02690337), DS8201-A-J101 (NCT02564900), and DS8201-A-J203 (NCT03384940). This suggests that the screening performed in the current study may be useful for identifying patients potentially eligible for clinical trials. This could be especially relevant for early phase trials targeting rare populations, such as patients with low biomarker prevalence. Moreover, this screening is a universal screening with IHC including pathological review by one pathologist to achieve standardized evaluation, with a cost of about US \$1700 per patient, which is almost comparable to that of next-generation sequencing (NGS). Therefore, this screening method may be useful for efficient acceleration of studies which require an eligibility check with IHC.

We used a central laboratory to perform IHC and FISH for the current study. IHC of GC tissue samples was also

performed at some local laboratories as part of routine clinical practice. This provided an opportunity to compare the results obtained in these different laboratory settings. We found that the results of HER2 IHC testing in GC matched between central and local laboratories in approximately 90% of cases (allowing for 1 level difference of IHC score). However, the rate of completely matched cases was only around 60%. The rate of matching was independent of whether or not the same sample was used for central and local testing (which could be assumed based on whether or not there was a difference in the sample collection dates) and was also independent of the type of IHC kit used. Overall, this suggests that improvements to, or standardization of, HER2 IHC laboratory methods may be desirable in the future.

In conclusion, this study determined the prevalence of FGFR2 and HER2 in Japanese patients with GC and CRC, and the values were concordant with previous reported prevalence rates. No clear relationship was found between FGFR2 and HER2 status in either the GC or CRC populations. FGFR2 and HER2 status did not differ according to the primary cancer location in GC, but there were some differences between GC histological types. These relationships could not be assessed properly in CRC, due to the limited number of FGFR2-positive patients. The screening performed in this study could be useful for identifying eligible patients for clinical trials of agents targeting these proteins.

Supplementary Information The online version contains supplementary material available at <https://doi.org/10.1007/s00384-022-04162-2>.

Acknowledgements We thank the patients who participated in this study, as well as their families and caregivers. We also thank Dr. Akiko Nagatsuma and Dr. Takeshi Kuwata of National Cancer Center Hospital East, and Yoshinobu Shiose, Tomoko Shibutani, Kokichi Honda, and Toshihiro Oguma of Daiichi Sankyo Co., Ltd. for their suggestions for our study. Medical writing assistance was provided by Content Ed Net, which was funded by Daiichi Sankyo Co., Ltd.

Author contribution TD, AO, EM, and MS were involved in study design and data interpretation. HY, AT, HH, HI, HA, KF, MN, CK, SY, JN, YM, AM, HI, and NY contributed to the acquisition of data. MS and EM were involved in the data analysis. AO was involved in the FGFR2 and HER2 scoring. HY, EM, MI, MS, and TD provided the idea to draft the manuscript. All authors reviewed and commented on drafts of the manuscript and approved the final manuscript.

Funding This study was sponsored by Daiichi Sankyo Co., Ltd.

Availability of data and materials There were no agreements from the participants for their data, so data sharing is not available.

Declarations

Ethics approval and consent to participate This study was conducted with the approval of the ethical review board at each study site. All patients provided written informed consent.

Consent for publication Not applicable.

Competing interests The first author (H. Yasui) declares the following conflict of interests: Research funding and honoraria for lectures from Daiichi Sankyo. H. Hara declares the following conflict of interests: Grants and personal fees from Daiichi Sankyo, Sumitomo Dainippon Pharma, Merck Biopharma, MSD, Taiho Pharma, Chugai Pharmaceutical, Boehringer Ingelheim, Ono Pharmaceutical, Bristol-Myers Squibb, and Bayer; Grants from AstraZeneca, Eisai, Elevar Therapeutics, Incyte, Pfizer, BeiGene, Astellas Pharm, and GSK; Personal fees from Eli Lilly Japan, Yakult Honsha, Sanofi, Takeda Pharmaceutical, and Kyowa Kirin. A. Makiyama declares the following conflict of interests: Honoraria from Eli Lilly Japan, Taiho Pharmaceutical, Ono Pharmaceutical, Bristol-Myers Squibb, and Daiichi Sankyo. T. Doi declares the following conflict of interests: Grants and personal fees from MSD, Daiichi Sankyo, Sumitomo Dainippon Pharma, Taiho Pharma, Novartis, Janssen Pharmaceutical, Boehringer Ingelheim, Bristol-Myers Squibb, and Abbvie; Grants from Lilly, Merck Serono Pharmaceutical, Pfizer, Quintiles (IQVIA), and Eisai; Personal fees from Amgen, Takeda Pharmaceutical, Chugai Pharmaceutical, Bayer, Rakuten Medical, Ono Pharmaceutical, Astellas Pharma, Oncolys BioPharma, and Otsuka Pharmaceutical. E. Matsumura, M. Ishigami and M. Sugihara are employees of Daiichi Sankyo. All other authors declare that they have no competing interests.

Open Access This article is licensed under a Creative Commons Attribution 4.0 International License, which permits use, sharing, adaptation, distribution and reproduction in any medium or format, as long as you give appropriate credit to the original author(s) and the source, provide a link to the Creative Commons licence, and indicate if changes were made. The images or other third party material in this article are included in the article's Creative Commons licence, unless indicated otherwise in a credit line to the material. If material is not included in the article's Creative Commons licence and your intended use is not permitted by statutory regulation or exceeds the permitted use, you will need to obtain permission directly from the copyright holder. To view a copy of this licence, visit <http://creativecommons.org/licenses/by/4.0/>.

References

- Brooks AN, Kilgour E, Smith PD (2012) Molecular pathways: fibroblast growth factor signaling: a new therapeutic opportunity in cancer. *Clin Cancer Res* 18:1855–1862. <https://doi.org/10.1158/1078-0432.CCR-11-0699>
- Eswarakumar VP, Lax I, Schlessinger J (2005) Cellular signaling by fibroblast growth factor receptors. *Cytokine Growth Factor Rev* 16:139–149. <https://doi.org/10.1016/j.cytogfr.2005.01.001>
- Siena S, Sartore-Bianchi A, Marsoni S, Hurwitz HI, McCall SJ, Penault-Llorca F, Srock S, Bardelli A, Trusolino L (2018) Targeting the human epidermal growth factor receptor 2 (HER2) oncogene in colorectal cancer. *Ann Oncol* 29:1108–1119. <https://doi.org/10.1093/annonc/mdy100>
- Gemo AT, Deshpande AM, Palencia S, Bellovin D, Brenna T, Patil N, Huang C, Los G, Pierce K (2014) FPA144: A therapeutic antibody for treating patients with gastric cancers bearing FGFR2 gene amplification. *Cancer Res* 74(Suppl):5446. <https://doi.org/10.1158/1538-7445.AM2014-5446>
- Sommer A, Kopitz C, Schatz CA, Nising CF, Mahler C, Lerchen HG, Stelte-Ludwig B, Hammer S, Greven S, Schuhmacher J, Braun M, Zierz R, Wittmer-Rump S, Harrenga A, Dittmer F, Reetz F, Apeler H, Jautelat R, Huynh H, Ziegelbauer K, Kreft B (2016) Preclinical efficacy of the auristatin-based antibody–drug conjugate BAY 1187982 for the treatment of FGFR2-positive solid tumors. *Cancer Res* 76:6331–6339. <https://doi.org/10.1158/0008-5472.CAN-16-0180>
- Black J, Menderes G, Bellone S, Schwab CL, Bonazzoli E, Ferrari F, Predolini F, De Haydu C, Cocco E, Buza N, Hui P, Wong S, Lopez S, Ratner E, Silasi DA, Azodi M, Litkouhi B, Schwartz PE, Goedings P, Beusker PH, van der Lee MM, Timmers CM, Dokter WH, Santin AD (2016) SYD985, a novel duocarmycin-based HER2-targeting antibody–drug conjugate, shows antitumor activity in uterine serous carcinoma with HER2/Neu expression. *Mol Cancer Ther* 15:1900–1909. <https://doi.org/10.1158/1535-7163.MCT-16-0163>
- Grillo F, Fassan M, Sarocchi F, Fiocca R, Mastracci L (2016) HER2 heterogeneity in gastric/gastroesophageal cancers: From benchside to practice. *World J Gastroenterol* 22:5879–5887. <https://doi.org/10.3748/wjg.v22.i26.5879>
- Gravalos C, Jimeno A (2008) HER2 in gastric cancer: a new prognostic factor and a novel therapeutic target. *Ann Oncol* 19:1523–1529. <https://doi.org/10.1093/annonc/mdn169>
- Van Cutsem E, Bang YJ, Feng-Yi F, Xu JM, Lee KW, Jiao SC, Chong JL, López-Sánchez RI, Price T, Gladkov O, Stoss O, Hill J, Ng V, Lehle M, Thomas M, Kiermaier A, Rüschhoff J (2015) HER2 screening data from ToGA: targeting HER2 in gastric and gastroesophageal junction cancer. *Gastric Cancer* 18:476–484. <https://doi.org/10.1007/s10120-014-0402-y>
- Kim HS, Kim JH, Jang HJ (2019) Pathological and prognostic impacts of *fgfr2* overexpression in gastric cancer: a meta-analysis. *J Cancer* 10:20–27. <https://doi.org/10.7150/jca.29184>
- Richman SD, Southward K, Chambers P, Cross D, Barrett J, Hemmings G, Taylor M, Wood H, Hutchins G, Foster JM, Oumie A, Spink KG, Brown SR, Jones M, Kerr D, Handley K, Gray R, Seymour M, Quirke P (2016) HER2 overexpression and amplification as a potential therapeutic target in colorectal cancer: analysis of 3256 patients enrolled in the QUASAR, FOCUS and PICCOLO colorectal cancer trials. *J Pathol* 238:562–570. <https://doi.org/10.1002/path.4679>
- Helsten T, Elkin S, Arthur E, Tomson BN, Carter J, Kurzrock R (2016) The FGFR landscape in cancer: analysis of 4,853 tumors by next-generation sequencing. *Clin Cancer Res* 22:259–267. <https://doi.org/10.1158/1078-0432.CCR-14-3212>
- Sartore-Bianchi A, Amatu A, Porcu L, Ghezzi S, Lonardi S, Leone F, Bergamo F, Fenocchio E, Martinelli E, Borelli B, Tosi F, Racca P, Valtorta E, Bonoldi E, Martino C, Vaghi C, Marrapese G, Ciardiello F, Zagonel V, Bardelli A, Trusolino L, Torri V, Marsoni S, Siena S (2019) HER2 positivity predicts unresponsiveness to EGFR-targeted treatment in metastatic colorectal cancer. *Oncologist* 24:1395–1402. <https://doi.org/10.1634/theoncologist.2018-0785>
- Su X, Zhan P, Gavine PR, Morgan S, Womack C, Ni X, Shen D, Bang YJ, Im SA, Ho Kim W, Jung EJ, Grabsch HI, Kilgour E (2014) FGFR2 amplification has prognostic significance in gastric cancer: results from a large international multicentre study. *Br J Cancer* 110:967–975. <https://doi.org/10.1038/bjc.2013.802>
- Deng N, Goh LK, Wang H, Das K, Tao J, Tan IB, Zhang S, Lee M, Wu J, Lim KH, Lei Z, Goh G, Lim QY, Tan AL, Sin Poh DY, Riahi S, Bell S, Shi MM, Linnartz R, Zhu F, Yeoh KG, Toh HC, Yong WP, Cheong HC, Rha SY, Boussioutas A, Grabsch H, Rozen S, Tan P (2012) A comprehensive survey of genomic alterations in gastric cancer reveals systematic patterns of molecular exclusivity and co-occurrence among distinct therapeutic targets. *Gut* 61:673–684. <https://doi.org/10.1136/gutjnl-2011-301839>
- Das K, Gunasegaran B, Tan IB, Deng N, Lim KH, Tan P (2014) Mutually exclusive FGFR2, HER2, and KRAS gene amplifications in gastric cancer revealed by multicolour FISH. *Cancer Lett* 353:167–175. <https://doi.org/10.1016/j.canlet.2014.07.021>
- Kim ST, Banks KC, Pectasides E, Kim SY, Kim K, Lanman RB, Talasz A, An J, Choi MG, Lee JH, Sohn TS, Bae JM, Kim S, Park SH, Park JO, Park YS, Lim HY, Kim NKD, Park W, Lee H, Bass AJ, Kim K, Kang WK, Lee J (2018) Impact of genomic

- alterations on lapatinib treatment outcome and cell-free genomic landscape during HER2 therapy in HER2+ gastric cancer patients. *Ann Oncol* 29:1037–1048. <https://doi.org/10.1093/annonc/mdy034>
18. Azuma K, Tsurutani J, Sakai K, Kaneda H, Fujisaka Y, Takeda M, Watatani M, Arai T, Satoh T, Okamoto I, Kurata T, Nishio K, Nakagawa K (2011) Switching addictions between HER2 and FGFR2 in HER2-positive breast tumor cells: FGFR2 as a potential target for salvage after lapatinib failure. *Biochem Biophys Res Commun* 407:219–224. <https://doi.org/10.1016/j.bbrc.2011.03.002>
 19. Nathanson DR, Culliford AT 4th, Shia J, Chen B, D'Alessio M, Zeng ZS, Nash GM, Gerald W, Barany F, Paty PB (2003) HER2/neu expression and gene amplification in colon cancer. *Int J Cancer* 105:796–802. <https://doi.org/10.1002/ijc.11137>
 20. Wang XY, Zheng ZX, Sun Y, Bai YH, Shi YF, Zhou LX, Yao YF, Wu AW, Cao DF (2019) Significance of HER2 protein expression and *HER2* gene amplification in colorectal adenocarcinomas. *World J Gastrointest Oncol* 11:335–347. <https://doi.org/10.4251/wjgo.v11.i4.335>

Publisher's Note Springer Nature remains neutral with regard to jurisdictional claims in published maps and institutional affiliations.

Effect of Postoperative Muscle Loss After Resection of Non-small Cell Lung Cancer on Surgical Outcomes

RYOTA NAKAMURA¹, SATOSHI YONEYAMA¹, RIKA TOBITA¹, SHUSUKE KURIHARA¹,
TAKASHI HATORI², TAKESHI NUMATA², KYOKO OTA², HIDETOSHI YANAI²,
TAKEO ENDO², YUKINORI INADOME³, HIROAKI SATOH⁴ and YOSHIIHISA INAGE¹

¹Department of Surgery, National Hospital Organization Mito Medical Center, Ibarakimachi, Japan;

²Department of Respiratory Medicine, National Hospital Organization Mito Medical Center, Ibarakimachi, Japan;

³Department of Pathology, National Hospital Organization Mito Medical Center, Ibarakimachi, Japan;

⁴Division of Respiratory Medicine, Mito Medical Center, University of Tsukuba, Mito, Japan

Abstract. *Background/Aim:* Preoperative depletion of psoas muscle mass index (PMI) in lung cancer patients is an unfavorable prognostic factor. The relationship between post-surgical changes in PMI and survival is not clear. Therefore, we conducted a retrospective study to clarify the prognostic significance of preoperative and postoperative PMI changes. *Patients and Methods:* We retrospectively reviewed lung cancer patients, who underwent curative surgical resection with lymph node dissection and computed tomography (CT) approximately six months post-surgery between 2010 and 2019. Pre- and postoperative PMI was measured from CT images at the third lumbar vertebra level. A sex-dependent PMI change ratio (postoperative PMI/preoperative PMI) was used to divide patients into two groups: high PMI loss (67 patients, $\leq 25^{\text{th}}$ lower quartile) and low PMI loss/PMI increase (204 patients, $> 25^{\text{th}}$ lower quartile), and clinicopathological features were compared. *Results:* Age ≥ 70 years, elevated preoperative carcinoembryonic antigen levels, advanced pathological stage, lymphatic permeation, vascular invasion, performance of adjuvant platinum-doublet chemotherapy, low body mass index, and postoperative recurrence were significantly higher in the high PMI loss group. Logistic regression analysis found that Charlson comorbidity index, low body mass index, advanced pathological stage, and postoperative recurrence were associated with high PMI loss. The five-year postoperative overall survival rate was 50% in the high PMI

loss group and 79% in the low PMI loss/PMI increase group ($p < 0.001$). High PMI loss was also an unfavorable factor in a multivariable Cox's proportional hazard model ($p = 0.002$). *Conclusion:* Postoperative muscle loss was an independent prognostic factor for poorer overall survival regardless of preoperative sarcopenia, in non-small cell lung cancer.

Non-small cell lung cancer (NSCLC) is one of the most common causes of cancer-related death worldwide (1) and surgery remains one of the most effective curative modalities for patients with early-stage NSCLC. Even with curative resection, however, tumor recurrence is common, and the prognosis in these patients is poor (2, 3). Therefore, there has been particular interest in factors that predict the prognosis of patients with resectable cancers. Currently, the most reliable factor associated to prognosis is widely recognized as the TNM stage (4). In many previous studies, other clinical factors associated with poor prognosis were reported to be tumor grade, older age, male sex, smoking status, performance status, and comorbidity (5-7).

Sarcopenia, which is defined as a loss of skeletal muscle mass and function, has recently been attracting attention in patients with various cancers. In early studies on sarcopenia, researchers focused on the absolute loss of skeletal muscle mass at one preoperative point, and they concluded that preoperative sarcopenia was correlated with postoperative complications and poor prognosis (8-11). Some recent studies, however, investigated postoperative changes in skeletal muscle mass in cancer patients, and highlighted the greater impact postoperative muscle loss had on prognosis in these patients (12-15). This might provide useful information in monitoring treatment intervention and in evaluating prognosis of individual patients. However, in patients with resectable lung cancer, the importance of postoperative changes in skeletal muscle mass remains unclear. Furthermore, the optimum computed tomography

Correspondence to: Ryota Nakamura, Department of Surgery, National Hospital Organization Mito Medical Center, 280 Sakuranosato Ibarakimachi, Higashiibarakigun, Ibaraki 311-3193, Japan. Tel: +81 292407711, Fax: +81 292407788, e-mail: ryo-naka@mail.goo.ne.jp

Key Words: Non-small cell lung cancer, surgery, sarcopenia, postoperative muscle loss.

(CT) measurement level for measuring skeletal muscle mass has not been determined.

One previous report showed that decreased paravertebral cross-sectional muscle area at the 12th thoracic vertebrae (Th12) level was associated with poorer postoperative outcomes (13). However, it is uncommon to evaluate whole-body muscle mass based on scans at the Th12 level. In contrast, psoas muscle mass index (PMI) at the third lumbar level on CT was correlated with entire body skeletal muscle mass (16).

Abdominal CT scans are a routine and commonly performed examination to investigate metastases to abdominal organs, both preoperatively and postoperatively. This study aimed to measure skeletal muscle mass using a simple, routine test that did not involve any additional cost. Therefore, we focused on the change in PMI based on skeletal muscle mass at the third lumbar level measured pre- and postoperatively with CT. The purpose of this study was to clarify whether changes in skeletal muscle could affect the long-term postoperative prognosis of lung cancer patients who underwent curative surgery. We also determined which clinicopathological factors predicted changes in PMI.

Patients and Methods

Patients. This retrospective study was approved by the Mito Medical Center Institutional Review Board (IRB number: 2021-78). We obtained comprehensive written consent from each patient for the use of clinical information obtained from the patient for academic research, such as conference presentations and the publication of articles, on the condition of anonymity. The study period was from April 2010 to December 2019. This study enrolled all consecutive patients at our institution with invasive NSCLC who underwent curative surgery by anatomical lung resections with systemic lymph node dissection, were disease-free for six months or longer, and were evaluated with abdominal CT scan performed within two months preoperatively and at approximately six months (range=4-8 months) postoperatively.

Patients with the following conditions were excluded from this study: 1) those that underwent wedge resection, 2) those with pathologically proven adenocarcinoma *in situ* and minimally invasive adenocarcinoma, 3) those with recurrence or any cause of death within six months after surgery, and 4) the pre- or postoperative CT was not available for assessment. The histologic classification of tumors was based on the WHO classification of lung cancer, and the pathologic stage was determined according to the 8th Edition of the TNM Classification of Malignant Tumors.

Image analysis and assessment of psoas muscle mass index. Preoperative and postoperative CT images were retrieved from picture archive and communication system (PACS), and the area of skeletal muscle was measured after manual tracing of the images. The cross-sectional areas of the right and left psoas muscles were calculated at the level of the caudal end of the third vertebra (Figure 1). The sums of psoas muscle areas were normalized for height as previously reported for PMI (10, 16). PMI is the cross-sectional area of the bilateral psoas muscle/height² (cm²/m²). The PMI cut-off

values for sarcopenia were defined as 6.36 cm²/m² for men, and 3.92 cm²/m² for women, as described in our previous study (10). The PMI change ratio was calculated as postoperative PMI/preoperative PMI. The study population was divided according to sex and interquartile range (IQR) of PMI change ratio as previously reported (17): high PMI loss group ($\leq 25^{\text{th}}$ lower quartile) and low PMI loss/PMI increase group ($> 25^{\text{th}}$ lower quartile).

Assessment of nutritional and immune status. We selected the prognostic nutritional index (PNI) as an indicator of nutritional and immunological status of patients with cancer. The PNI was calculated by combining the serum albumin concentration and total circulating lymphocyte count that was routinely performed before surgery. The PNI was calculated as follow: $10 \times \text{albumin (g/dl)} + 0.005 \times \text{lymphocyte count per (mm}^3\text{)}$. Recent reports have showed that pretreatment PNI was associated with prognosis in lung cancer (18), and we chose PNI <50 as the cut-off value for clinically significant malnutrition, as performed previously (18).

Postoperative follow-up surveillance. We classified the postoperative complications according to severity using the Clavien–Dindo classification system (19). We defined a major complication as a classification of grade 3 or higher.

The postoperative follow-up protocol was as follow: physical examination every 3 months for the first 3 years and after 3 years and then at 6-month intervals for 5 years. We performed chest and abdominal CT every 6 months for 5 years. If signs and symptoms of recurrence appeared, additional appropriate tests were performed. Recurrence was diagnosed based on the result of any imaging or pathological evidence of recurrence. Overall survival (OS) was considered as the time from the date of surgery until the date of death from any cause or last follow-up and disease-free survival (DFS) was defined as the time from the date of surgery until the date of recurrence or last follow-up.

Statistical analysis. The results are presented as the median and range. The Mann–Whitney *U*-test and Fisher's exact test were used to compare groups and categorical variables. The survival curves were plotted according to the Kaplan–Meier method, and the OS and DFS rates were compared using the log-rank test. Cox hazard models were used to analyze factors associated to OS. The PMI change ratio was assessed by a multivariable logistic regression model using clinicopathological factors. Any factors with $p < 0.10$ in univariable analysis using the above tests were examined by multivariable analysis. All analyses were performed using SPSS version 23 (IBM Corporation, Armonk, NY, USA). A p -value < 0.05 was considered to indicate statistical significance.

Results

Patient characteristics. There were 430 patients with confirmed NSCLC who underwent curative surgery during the study period. According to the inclusion and exclusion criteria, the current study enrolled 271 patients with invasive NSCLC who underwent anatomical lung resections with systemic lymph node dissection and were disease-free for six months or longer. The clinicopathological, operative and postoperative characteristics of the 271 patients in this study, comprising 172 men and 99 women, are summarized in Table I. The median

follow-up period for OS was 45.0 months (range=7-123 months). The median age of the study population was 70 years. As for surgery, 27 patients underwent segmentectomy, 234 patients underwent lobectomy, nine patients underwent bilobectomy, and one patient had pneumonectomy performed. The histological types that were pathologically proven invasive lung cancer included 177 cases of adenocarcinoma, 66 cases of squamous cell carcinoma, and 28 cases of other types of carcinomas.

Assessment of skeletal muscle mass and psoas muscle mass index change ratio. In male patients, the preoperative median PMI was 6.200 cm²/m² (range=2.910-10.458 cm²/m²) and the postoperative median PMI was 5.852 cm²/m² (range=2.570-9.166 cm²/m²), which was significantly different ($p<0.001$). In female patients, the preoperative median PMI was 4.756 cm²/m² (range=1.874-9.068 cm²/m²) and the postoperative median PMI was 4.668 cm²/m² (range=1.739-8.742 cm²/m²), also a significant difference ($p<0.001$; Figure 2A). As for the PMI ratios, the ratio in male patients (median: 0.942, range=0.707-1.235) was significantly less than that in female patients (median: 0.982, range=0.813-1.104) ($p=0.001$; Figure 2B). There have been several cut-off values used for postoperative loss of skeletal muscle mass, for example -10% (12, 13) and -19% (15). However, our data revealed that the PMI change ratio was significantly different between males and females. Therefore, different sex-specific cut-off values were deemed appropriate, and we divided the groups according to the IQR in Figure 2C and D as previously described (17). The cut-off value for the PMI change ratio was as follow: 0.8948 for male and 0.9503 for female.

Correlation with psoas muscle index change and clinicopathological, surgical, and postoperative findings. Characteristics of patients in the high PMI loss group and low PMI loss/PMI increase group are summarized in Table II. There were no significant differences regarding sex, smoking habit, respiratory function, PNI or having preoperative sarcopenia. The frequency of elevated serum carcinoembryonic antigen (CEA) level, having diabetes mellitus, and low BMI were significantly associated with the high PMI loss group than with the low PMI loss/PMI increase group ($p=0.026$, $p=0.017$ and $p=0.035$, respectively). Patients with high Charlson comorbidity index (CCI) tended to be more numerous in the high PMI loss group, but this was not statistically significant ($p=0.051$). There was no significant difference in surgical procedure. According to pathological findings, there were significant differences in pathological stage ($p<0.001$), lymphatic permeation ($p=0.022$), and vascular invasion ($p=0.021$), whereas there were no differences in histological type and pleural invasion. There was no difference in severe postoperative complications. There were significant

differences in whether postoperative adjuvant platinum-based doublet chemotherapy was performed and in postoperative recurrence ($p=0.003$ and $p<0.001$).

Association of psoas muscle index change with survival. Factors associated with OS prognosis by Cox proportional hazards analysis are shown in Table III, and Kaplan-Meier analysis showed that OS was 50% in the high PMI loss group and 79% in the low PMI loss/PMI increase group, which was significantly different ($p<0.001$) (Figure 3A). DFS was 32% in the high PMI loss group and 72% in the low PMI loss/PMI increase group, which was significantly different ($p<0.001$) (Figure 3B). Univariable analysis identified that, in the preoperative setting, age greater than 70 years, male sex, smoking habit, CCI, vital capacity less than 80%, elevation of serum CEA levels, having diabetes mellitus, PNI less than 50, and having preoperative sarcopenia were unfavorable factors for OS. With regard to postoperative findings, non-adenocarcinoma, advanced pathological stage, presence of blood vessel invasion, and high PMI loss were independent factors associated with worse OS. Multivariable analysis showed that age greater than 70 years, smoking habit, elevation of serum CEA levels, high PMI loss, having preoperative sarcopenia, and advanced pathological stage were factors associated with poorer outcomes. Regardless of the status of preoperative sarcopenia, the group that lost skeletal muscle postoperatively had worse outcomes than the group that did not (Figure 3C and D).

Risk factors for developing high PMI loss. We performed a multivariable logistic regression analysis to clarify the risk factors for high PMI loss (Table IV). This showed that CCI, low BMI, advanced pathological stage, and postoperative recurrence were associated with high PMI loss.

Discussion

In the present study, the degree of depletion in PMI calculated from pre- and postoperative CT scans was significantly associated with poor long-term outcome, as well as TNM stage, in invasive NSCLC patients who underwent surgical curative resection. In addition, the factors correlated with postoperative PMI depletion were higher CCI, lower BMI, advanced pathological stage, and postoperative recurrence.

There have been several modalities to assess muscle mass and function to diagnose sarcopenia (9). Among these, a recent focus has been on the association between "preoperative sarcopenia" and "postoperative prognosis and serious postoperative complications" (10). However, although very recent studies have been conducted on the prognostic impact of "postoperative skeletal muscle loss" in patients with various cancers (12-15), few studies have been conducted on patients with resectable lung cancer (13). In

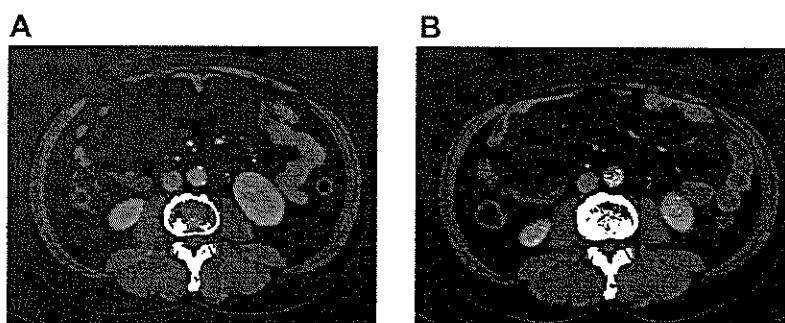


Figure 1. Measurement of bilateral psoas muscle areas. Bilateral psoas muscle areas were measured by manual tracing computed tomography (CT) images (area delineated) at the third lumbar vertebrae level on preoperative and postoperative scans. (A) preoperative CT; (B) postoperative CT.

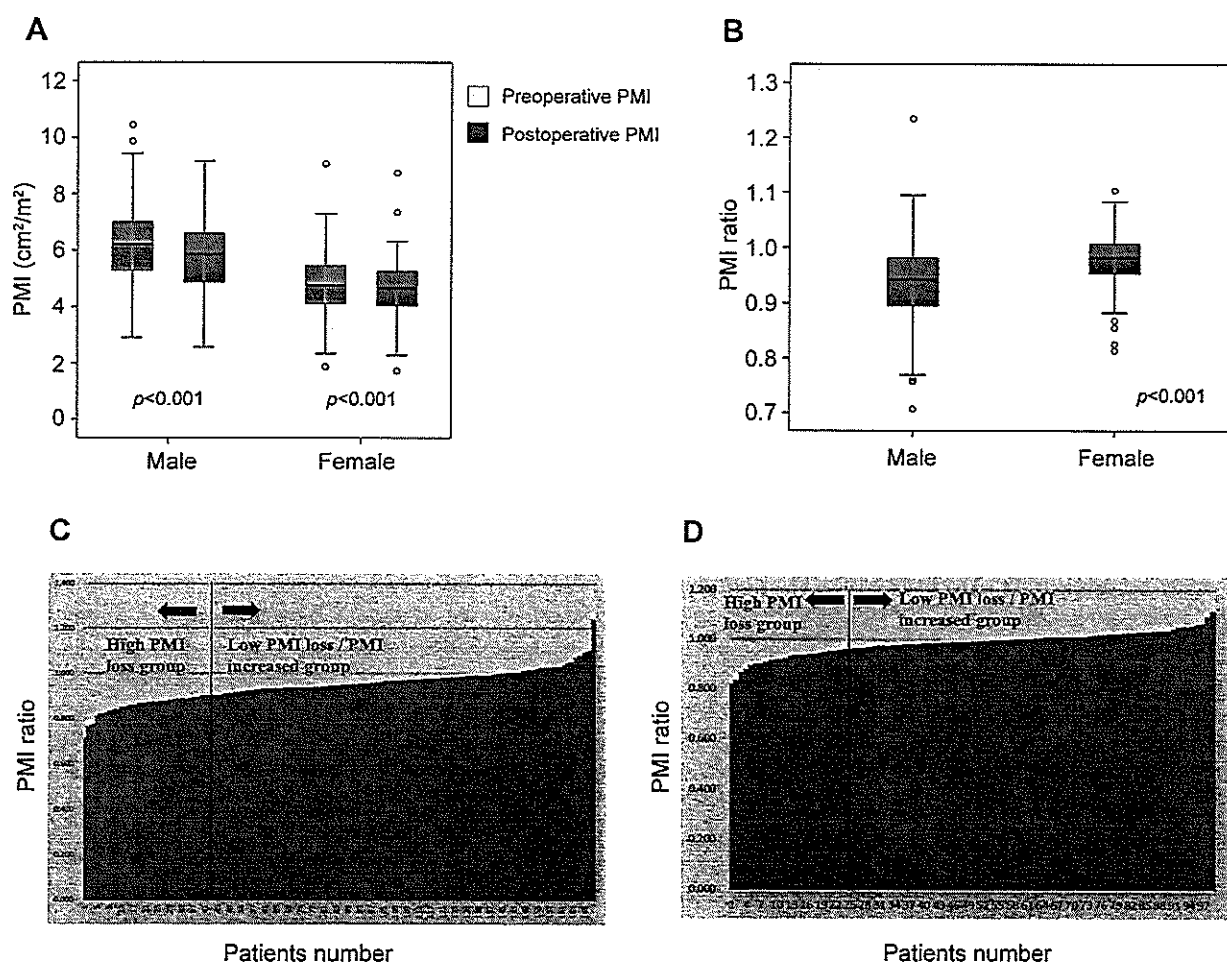


Figure 2. Psoas muscle mass index (PMI). (A) Box whisker plot comparing male and female PMI values. Each box plot shows the 25th and 75th percentiles, with the median values indicated by lines within the boxes. The bars extending above and below the box indicate the 90th and 10th percentiles, respectively. (B) Box whisker plot comparing male and female PMI ratio. Each box plot shows the 25th and 75th percentiles, with the median values indicated by lines within the boxes. The bars extending above and below the box indicate the 90th and 10th percentiles, respectively. (C) Histogram showing the postoperative/preoperative PMI ratio in male patients. (D) Histogram showing the postoperative/preoperative PMI ratio in female patients.

Table I. Characteristics of the patients' population.

Variable	No. or median value (range)
Age, y	70.0 (38-87)
Sex, male/female	172/99
Smoking habit (absent/present)	87/184
VC $\geq 80\%$ / $<80\%$	252/19
FEV ₁ $\geq 70\%$ / $<70\%$	199/72
CEA (ng/ml) >5.0 / ≤ 5.0	80/191
Diabetes Mellitus (absent/present)	214/57
CCI 0/1-2/ ≥ 3	95/133/43
PNI ≥ 50 / <50	175/96
Body mass index (kg/m ²)	22.9 (15.6-39.7)
Preoperative psoas muscle index (cm ² /m ²)	
Male	6.200 (2.910-10.458)
Female	4.756 (1.874-9.068)
Postoperative psoas muscle index (cm ² /m ²)	
Male	0.942 (0.707-1.235)
Female	0.982 (0.813-1.104)
Preoperative sarcopenia (absent/present)	156/115
Type of surgery, segmentectomy/ lobectomy or more	27/244
Adenocarcinoma/non adenocarcinoma	177/94
Pathological stage I/II/III	178/53/40
Pleural invasion (negative/positive)	202/69
Lymphatic permeation (negative/positive)	213/58
Vascular invasion (negative/positive)	162/109
Postoperative major complications (Clavien Dindo grade ≥ 3 / <3 , no complication)	15/256
Adjuvant platinum-doublet chemotherapy (yes/no)	75/196
Postoperative recurrence (yesc/no)	62/209

VC, Vital capacity; FEV₁, forced expiratory volume in 1 second; CEA, carcinoembryonic antigen; CCI, Charlson comorbidity index; PNI, prognostic nutritional index.

particular, no studies have investigated the relationship between skeletal muscle mass changes and prognosis using PMI at the third lumbar vertebra level by CT before and after lung resection. In lung cancer practice, chest and abdominal CT is usually performed for preoperative diagnosis and postoperative follow up as part of evaluation of distant metastasis. Furthermore, muscle mass can be properly assessed with routine CT scans in cancer practice. Therefore, it is not difficult to assess skeletal muscle changes using CT images, and no additional special equipment is needed.

Although few, some reports have focused on postoperative muscle change and survival in various cancers (12-15). For example, the median reduction in postoperative psoas muscle area in patients with urothelial cancer of the bladder was 10%, and those with 10% or more reduction in psoas muscle area had worse overall survival in multivariable analysis (12). Nakashima *et al.* reported that a decrease in skeletal muscle (approximately 19% loss) at six months after surgery was associated with a poorer OS in patients who underwent

surgical resection for esophageal carcinoma (14). In our study, postoperative skeletal muscle loss occurred in approximately 75% of patients following lung resection. There was a significant decrease in PMI after surgery (compared to before surgery) in both male and female patients, and the decrease in PMI ratio was greater in males than in females ($p < 0.001$). Therefore, we consider that it is essential to set specific cut-off values for each sex. A previous report showed the importance of sex differences in the correlation between prognosis and postoperative weight loss in patients with surgically resected NSCLC (20). According to that report, male NSCLC patients who lost more than 5% of their body weight within one year of surgery had a significantly worse outcome than the corresponding female patients (20). The results were similar to those of our study where males had a greater decrease in body composition than females.

There are several cut-off values for postoperative muscle loss. For example, Kudou *et al.* used a decrease of 19% as a cut-off value in patients with upper stomach and esophagogastric junction cancer, which was obtained using receiver operating characteristic (15), and 10% depletion was selected in urothelial carcinoma (12) and lung cancer (21). However, these reports did not consider sex differences. In our data, there was a significant difference in sex according to PMI ratio, with males having a greater decrease in postoperative PMI than women. Therefore, it is necessary to set appropriate cut-off values for each sex, and the quartile was used as the threshold value as previously described (17). Further optimization of cut-off values for postoperative muscle loss could be accomplished with data from additional studies.

With regard to the duration of skeletal muscle wasted from surgical invasion, Miyake *et al.* reported that psoas muscle area at L3 decreased more than 10% from one to three months after surgery (12). They found a transient reduction one to three months after surgery in psoas muscle area, and a postoperative reduction in psoas muscle compared to that preoperatively. However, the patient slowly recovered by 6 months postoperatively, and there was no significant loss of muscle mass compared to preoperatively (12). To investigate the relationship between long-term prognosis and muscle reduction, it is important to evaluate muscle mass six months after surgery rather than examining transient changes in muscle mass one to three months after surgery because the effects associated with surgical invasion could not be eliminated.

In the present study, postoperative skeletal muscle loss was an independent factor associated to prognosis, as well as having preoperative sarcopenia. Moreover, the high PMI loss group had a poorer prognosis with or without preoperative sarcopenia. It is important to assess sarcopenia preoperatively, but it is equally important to assess postoperative skeletal muscle loss. Having preoperative sarcopenia was not a predicting factor for postoperative

Table II. Relationships according to clinicopathological characteristics depend on psoas muscle change.

Variables	High PMI loss group	Low PMI loss/PMI increased group	p-Value
Age, y			
≥70/<70, n (%)	44 (66)/23 (34)	105 (51)/99 (49)	0.043
Sex			
Male/Female, n (%)	43 (64)/24 (36)	129 (63)/75 (37)	0.889
Smoking habit			
Absent/Present, n (%)	19 (28)/43 (72)	68 (33)/136 (67)	0.449
VC, %			
≥80/<80, n (%)	62 (93)/5 (7)	190 (93)/14 (7)	0.790
FEV ₁ , %			
≥70/<70, n (%)	53 (79)/14 (21)	146 (72)/58 (28)	0.226
CEA, ng/ml			
>5.0/≤5.0, n (%)	27 (40)/40 (80)	53 (26)/151 (74)	0.026
Diabetes Mellitus			
Absent/Present, n (%)	46 (69)/21 (31)	168 (82)/36 (18)	0.017
CCI			
0/1-2/≥3, n (%)	16 (24)/36 (54)/15 (22)	79(39)/97(46)/28 (15)	0.051
Body mass index, kg/m ²			
≥20/<20, n (%)	50 (75)/17 (25)	175 (86)/29 (14)	0.035
Preoperative sarcopenia			
Absent/present, n (%)	36 (54)/31 (46)	120 (59)/84 (41)	0.464
Type of surgery			
Segmentectomy/Lobectomy or more, n (%)	6 (9)/61 (91)	21 (10)/183 (90)	0.751
Histological type			
AD/Non-AD, n (%)	39 (58)/28 (42)	138 (68)/66 (32)	0.159
Pathological stage			
I/II+III, n (%)	29 (43)/38 (57)	149 (73)/55 (27)	<0.001
Pleural invasion			
Negative/Positive, n (%)	47 (70)/20 (30)	155 (76)/49 (24)	0.342
Lymphatic permeation			
Negative/Positive, n (%)	46 (69)/21 (31)	167 (82)/37 (18)	0.022
Vascular invasion			
Negative/Positive, n (%)	32 (48)/35 (52)	130 (64)/74 (36)	0.021
Postoperative complications, n (%)			
(Clavien Dindo grade ≥3/<3, no complication)	4 (6)/63 (94)	11 (5)/193 (95)	0.768
Adjuvant platinum-doublet chemotherapy			
Yes/No, n (%)	28 (42)/39 (58)	47 (24)/157 (76)	0.003
Postoperative recurrence			
Yes/No, n (%)	28 (42)/39 (58)	34 (17)/170 (77)	<0.001

VC, Vital capacity; FEV₁, forced expiratory volume in 1 second; CEA, carcinoembryonic antigen; CCI, Charlson comorbidity index; PNI, prognostic nutritional index.

muscle depletion. Rather, high CCI and low BMI were more associated with the high PMI loss group. These findings suggest that striving to control comorbidities and paying attention to postoperative loss of skeletal muscle mass are important for early postoperative patient management, especially for those with preoperative sarcopenia. This study also showed a relationship between high PMI loss and postoperative recurrence. Interestingly, the high PMI loss can be a predictor of subsequent cancer recurrence, and high PMI loss was observed prior to recurrence.

There have been areas of interest in basic and clinical medicine related to sarcopenia. First, in basic medicine, the relationship between the mechanism of distant metastasis and

sarcopenia. During the process of micro-metastasis, the tumor tissue produces a variety of pro-inflammatory cytokines that activate systemic inflammation and metabolic disorders that affect host immunity and are one of the physical findings of cachexia (22). It has also been suggested that it leads to sarcopenia (23). In addition, skeletal muscle loss can easily transform the state of the microenvironment into micro-metastases by stimulating epithelial-mesenchymal transition. The tumor micro-metastasis environment can induce skeletal muscle depletion, which in turn can promote tumor micro-infiltration (24, 25). Therefore, it is speculated that tumor micro-infiltration and skeletal muscle loss are mutually enhanced. In this study, significant differences were

Table III. Univariate and multivariate analysis of clinicopathological factors and overall survival after pulmonary resection of lung cancer.

Variables	Univariate			Multivariate		
	HR	95% CI	p-Value	HR	95% CI	p-Value
Age ≥ 70 y	1.865	1.113-3.075	0.015	2.429	1.429-4.127	0.001
Male sex	2.463	1.406-4.314	0.002			
Smoking habit	2.963	1.589-5.526	0.001	2.022	1.053-3.880	0.034
CCI						
0	Reference					
1-2	1.894	1.085-3.308	0.025			
≥ 3	2.572	1.223-5.412	0.013			
BMI < 20.0 kg/m ²	1.498	0.844-2.657	0.167			
VC $< 80\%$	3.112	1.587-6.102	0.001			
FEV 1.0 $< 70\%$	1.611	0.982-2.641	0.059			
CEA > 5.0 ng/ml	2.664	1.663-4.268	< 0.001	2.171	1.332-3.539	0.002
Diabetes Mellitus	2.057	1.237-3.420	0.005			
PNI < 50	1.692	1.048-2.733	0.031			
High PMI loss group	3.272	2.011-5.323	< 0.001	2.233	1.342-3.714	0.002
Preoperative sarcopenia	2.993	1.832-4.889	< 0.001	2.412	1.452-4.006	0.001
Segmentectomy	1.251	0.599-2.616	0.551			
Non-adenocarcinoma	1.793	1.118-2.876	0.015			
Pathological stage II+III	2.574	1.608-4.122	< 0.001	1.660	1.006-2.738	0.047
Visceral pleural invasion	1.166	0.681-1.997	0.575			
Lymphatic permeation	1.567	0.887-2.767	0.122			
Blood vessel invasion	1.761	1.099-2.822	0.019			
Postoperative complications						
(Clavien-Dindo grade ≥ 3)	0.624	0.153-2.554	0.624			
Adjuvant platinum-doublet chemotherapy	1.680	1.029-2.743	0.038			

HR, Hazard ratio; CI, confidence interval; VC, vital capacity; FEV1, forced expiratory volume in 1 second; BMI, body mass index; CEA, carcinoembryonic antigen; CCI, Charlson comorbidity index; PNI, prognostic nutritional index.

observed between the high PMI loss group and the low PMI loss/PMI increase group for lymphatic permeation and vascular invasion on resected specimens. Some researchers speculated that the association between lymphovascular invasion, the first step in metastasis, and PMI reduction supports the concept that the tumor micro-metastatic environment is closely associated with skeletal muscle depletion (24, 26). However, it is unclear whether microinvasion precedes skeletal muscle loss and whether skeletal muscle loss leads to an increased recurrence rate due to impaired immune function. Further studies are needed to clarify the association of postoperative muscle loss and cancer recurrence.

Preoperative rehabilitation is a widespread concept and has been adopted in ERAS (Enhanced Recovery After Surgery) protocols for various major surgical procedures. Guidelines for enhanced recovery after lung surgery, pulmonary rehabilitation, prehabilitation, and screening for preoperative nutritional status are strongly recommended (27). Preoperative physical conditioning, or prehabilitation, is the process of improving an individual's functional and physiological capacity and ability to tolerate surgical stress and assist in postoperative recovery (28), and prehabilitation

is more effective than postoperative rehabilitation for recovery of motor abilities above baseline in colorectal surgery (29). Recently, Gillis *et al.* reported that trimodal prehabilitation including exercise, nutrition, and anxiety-reduction elements was more effective in preventing postoperative lean body mass loss compared with rehabilitation only following colorectal surgery (30). In our study, the preoperative factors that contributed to postoperative skeletal muscle loss were CCI and low BMI. Since postoperative skeletal muscle loss occurs in patients with and without preoperative sarcopenia, it may be useful to detect CCI and low BMI in case selection. Appropriate prehabilitation and nutritional intervention could play a role in preservation of, or improve, muscle mass after surgery. Further studies would clarify the benefits of prehabilitation and nutritional intervention for surgical outcomes.

This study had several limitations. First, we did not elucidate the relationship between changes in postoperative PMI and the underlying biological mechanism. Second, it was a retrospective study that included patients with various baseline characteristics. Third, it involved a comparatively limited number of patients with a short follow-up period, and

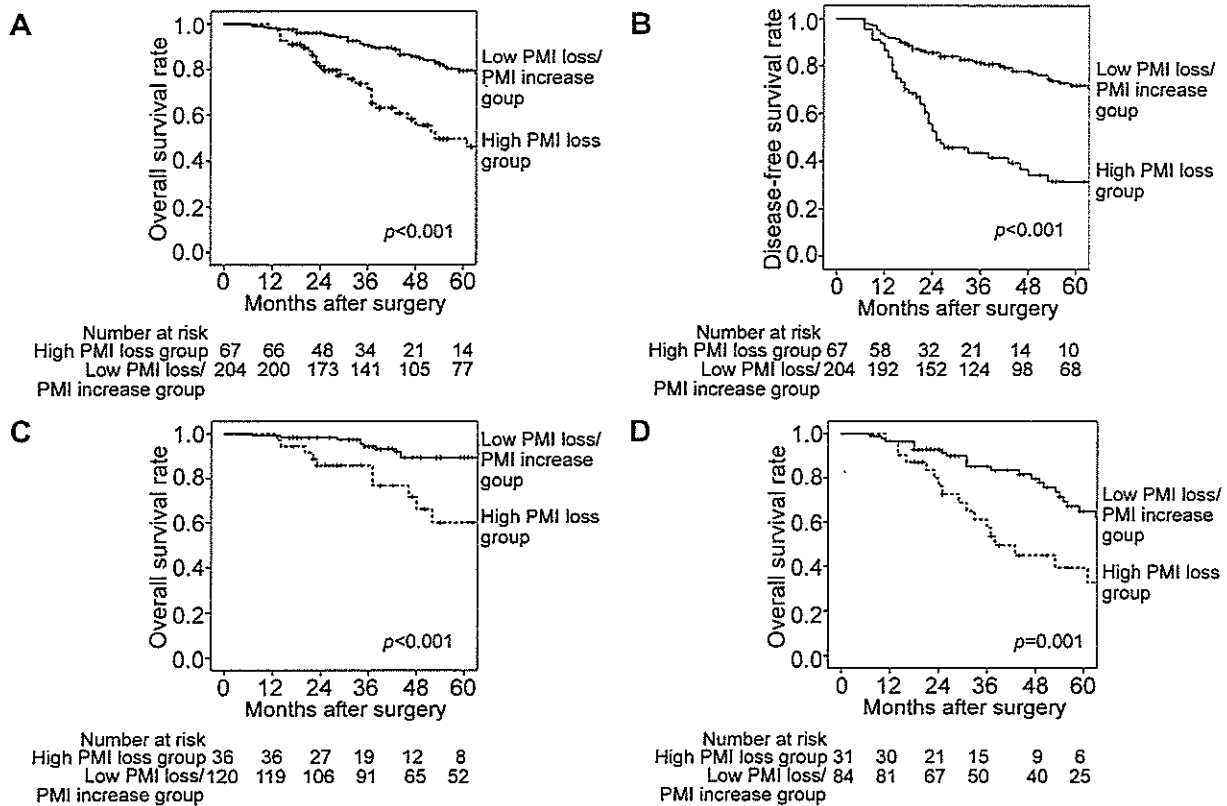


Figure 3. Survival relative to the postoperative/preoperative psoas muscle index ratio. The survival curves in patients according to the change in the postoperative/preoperative psoas muscle index ratio for (A) overall survival for all patients, (B) disease-free survival for all patients, (C) overall survival for patients without preoperative sarcopenia, and (D) overall survival patients with preoperative sarcopenia.

the number of patients required was not pre-set on a statistical basis. Fourth, it was unclear whether the patient grouping performed was optimal. In light of the results of this study, prospective studies are necessary.

Conclusion

The relationship between postoperative skeletal muscle depletion and postoperative prognosis, and the impact of skeletal muscle loss after surgery on postoperative outcomes, has been reported for various diseases. The present study showed that skeletal muscle loss was an independent factor associated to prognosis for poorer OS by multivariable analysis. Interestingly, in our study, having preoperative sarcopenia and postoperative skeletal muscle loss were independent factors associated to prognosis for OS. Moreover, having preoperative sarcopenia was not associated with postoperative skeletal muscle loss. Preoperative low BMI and CCI were identified as predictive risk factors for postoperative skeletal muscle loss. Preoperative sarcopenia is already known to be an important factor associated to

Table IV. Risk factors for developing massive postoperative skeletal muscle loss.

Variables	Multivariate analysis		
	OR	95% CI	p-Value
CCI			
0	Reference		
1-2	2.500	1.224-5.104	0.010
≥3	3.512	1.445-8.536	0.006
BMI <20	2.171	1.052-4.479	0.030
Pathological stage II+III	4.045	2.206-7.417	0.001
Recurrence	2.631	1.319-5.247	0.006

OR, Odds ratio; BMI, body mass index; CCI, Charlson comorbidity index.

prognosis. Furthermore, we emphasized that changes between pre- and postoperative muscle depletion could provide useful information for understanding the prognosis of curatively resected NSCLC patients.

Conflicts of Interest

The Authors declare that they have no known competing financial interests or personal relationships that could have appeared to influence the work reported in this paper.

Authors' Contributions

Ryota Nakamura: Conceptualization; Data curation; Formal analysis; Project administration; Writing-original draft. Satoshi Yoneyama: Data curation; Investigation. Rika Tobita: Data curation. Shusuke Kurihara: Data curation. Takashi Hatori: Data curation. Takeshi Numata: Data curation. Kyoko Ota: Data curation. Hidetoshi Yanai: Data curation. Takeo Endo: Data curation, Investigation. Yukinori Inadome: Data curation, investigation. Hiroaki Satoh: Investigation Writing-review&editing. Yoshihisa Inage: Data curation, Investigation.

References

- Siegel RL, Miller KD and Jemal A: Cancer statistics, 2017. *CA Cancer J Clin* 67(1): 7-30, 2017. PMID: 28055103. DOI: 10.3322/caac.21387
- Ettinger DS, Akerley W, Bepler G, Blum MG, Chang A, Cheney RT, Chirieac LR, D'Amico TA, Demmy TL, Ganti AK, Govindan R, Grannis FW Jr, Jahan T, Jahanzeb M, Johnson DH, Kessinger A, Komaki R, Kong FM, Kris MG, Krug LM, Le QT, Lennes IT, Martins R, O'Malley J, Osarogiagbon RU, Otterson GA, Patel JD, Pisters KM, Reckamp K, Riely GJ, Rohren E, Simon GR, Swanson SJ, Wood DE, Yang SC and NCCN Non-Small Cell Lung Cancer Panel Members: Non-small cell lung cancer. *J Natl Compr Canc Netw* 8(7): 740-801, 2010. PMID: 20679538. DOI: 10.6004/jnccn.2010.0056
- Uramoto H and Tanaka F: Recurrence after surgery in patients with NSCLC. *Transl Lung Cancer Res* 3(4): 242-249, 2014. PMID: 25806307. DOI: 10.3978/j.issn.2218-6751.2013.12.05
- Woodard GA, Jones KD and Jablons DM: Lung cancer staging and prognosis. *Cancer Treat Res* 170: 47-75, 2016. PMID: 27535389. DOI: 10.1007/978-3-319-40389-2_3
- Weichert W, Kossakowski C, Harms A, Schirmacher P, Muley T, Dienemann H and Warth A: Proposal of a prognostically relevant grading scheme for pulmonary squamous cell carcinoma. *Eur Respir J* 47(3): 938-946, 2016. PMID: 26541540. DOI: 10.1183/13993003.00937-2015
- Eguchi T, Bains S, Lee MC, Tan KS, Hristov B, Buitrago DH, Bains MS, Downey RJ, Huang J, Isbell JM, Park BJ, Rusch VW, Jones DR and Adusumilli PS: Impact of increasing age on cause-specific mortality and morbidity in patients with stage I non-small-cell lung cancer: a competing risks analysis. *J Clin Oncol* 35(3): 281-290, 2017. PMID: 28095268. DOI: 10.1200/JCO.2016.69.0834
- Sachs E, Sartipy U and Jackson V: Sex and survival after surgery for lung cancer: a Swedish nationwide cohort. *Chest* 159(5): 2029-2039, 2021. PMID: 33217414. DOI: 10.1016/j.chest.2020.11.010
- Rosenberg IH: Sarcopenia: origins and clinical relevance. *J Nutr* 127(5 Suppl): 990S-991S, 1997. PMID: 9164280. DOI: 10.1093/jn/127.5.990S
- Cruz-Jentoft AJ, Baeyens JP, Bauer JM, Boirie Y, Cederholm T, Landi F, Martin FC, Michel JP, Rolland Y, Schneider SM, Topinková E, Vandewoude M, Zamboni M and European Working Group on Sarcopenia in Older People: Sarcopenia: European consensus on definition and diagnosis: Report of the European Working Group on Sarcopenia in Older People. *Age Ageing* 39(4): 412-423, 2010. PMID: 20392703. DOI: 10.1093/ageing/afq034
- Nakamura R, Inage Y, Tobita R, Yoneyama S, Numata T, Ota K, Yanai H, Endo T, Inadome Y, Sakashita S, Satoh H, Yuzawa K and Terashima T: Sarcopenia in resected NSCLC: Effect on postoperative outcomes. *J Thorac Oncol* 13(7): 895-903, 2018. PMID: 29751134. DOI: 10.1016/j.jtho.2018.04.035
- Prado CM, Lieffers JR, McCargar LJ, Reiman T, Sawyer MB, Martin L and Baracos VE: Prevalence and clinical implications of sarcopenic obesity in patients with solid tumours of the respiratory and gastrointestinal tracts: a population-based study. *Lancet Oncol* 9(7): 629-635, 2008. PMID: 18539529. DOI: 10.1016/S1470-2045(08)70153-0
- Miyake M, Morizawa Y, Hori S, Marugami N, Shimada K, Gotoh D, Tatsumi Y, Nakai Y, Inoue T, Anai S, Torimoto K, Aoki K, Tanaka N and Fujimoto K: Clinical impact of postoperative loss in psoas major muscle and nutrition index after radical cystectomy for patients with urothelial carcinoma of the bladder. *BMC Cancer* 17(1): 237, 2017. PMID: 28359307. DOI: 10.1186/s12885-017-3231-7
- Takamori S, Toyokawa G, Okamoto T, Shimokawa M, Kinoshita F, Kozuma Y, Matsubara T, Haratake N, Akamine T, Takada K, Katsura M, Hirai F, Shoji F, Tagawa T, Oda Y, Honda H and Maehara Y: Clinical impact and risk factors for skeletal muscle loss after complete resection of early non-small cell lung cancer. *Ann Surg Oncol* 25(5): 1229-1236, 2018. PMID: 29327178. DOI: 10.1245/s10434-017-6328-y
- Nakashima Y, Saeki H, Hu Q, Tsuda Y, Zaito Y, Hisamatsu Y, Ando K, Kimura Y, Oki E and Mori M: Skeletal muscle loss after esophagectomy is an independent risk factor for patients with esophageal cancer. *Ann Surg Oncol* 27(2): 492-498, 2020. PMID: 31549319. DOI: 10.1245/s10434-019-07850-6
- Kudou K, Saeki H, Nakashima Y, Kimura K, Ando K, Oki E, Ikeda T and Maehara Y: Postoperative skeletal muscle loss predicts poor prognosis of adenocarcinoma of upper stomach and esophagogastric junction. *World J Surg* 43(4): 1068-1075, 2019. PMID: 30478682. DOI: 10.1007/s00268-018-4873-6
- Hamaguchi Y, Kaido T, Okumura S, Kobayashi A, Hammad A, Tamai Y, Inagaki N and Uemoto S: Proposal for new diagnostic criteria for low skeletal muscle mass based on computed tomography imaging in Asian adults. *Nutrition* 32(11-12): 1200-1205, 2016. PMID: 27292773. DOI: 10.1016/j.nut.2016.04.003
- Chae MS, Moon KU, Jung JY, Choi HJ, Chung HS, Park CS, Lee J, Choi JH and Hong SH: Perioperative loss of psoas muscle is associated with patient survival in living donor liver transplantation. *Liver Transpl* 24(5): 623-633, 2018. PMID: 29365358. DOI: 10.1002/lt.25022
- Shimizu K, Okita R, Saisho S, Maeda A, Nojima Y and Nakata M: Preoperative neutrophil/lymphocyte ratio and prognostic nutritional index predict survival in patients with non-small cell lung cancer. *World J Surg Oncol* 13: 291, 2015. PMID: 26424708. DOI: 10.1186/s12957-015-0710-7
- Clavien PA, Barkun J, de Oliveira ML, Vauthey JN, Dindo D, Schulick RD, de Santibañes E, Pekolj J, Slankamenac K, Bassi C, Graf R, Vonlanthen R, Padbury R, Cameron JL and Makuuchi M: The Clavien-Dindo classification of surgical complications:

- five-year experience. *Ann Surg* 250(2): 187-196, 2009. PMID: 19638912. DOI: 10.1097/SLA.0b013e3181b13ca2
- 20 Kawai H, Saito Y and Suzuki Y: Gender differences in the correlation between prognosis and postoperative weight loss in patients with non-small cell lung cancer. *Interact Cardiovasc Thorac Surg* 25(2): 272-277, 2017. PMID: 28444319. DOI: 10.1093/icvts/ivx092
- 21 Takamori S, Tagawa T, Toyokawa G, Shimokawa M, Kinoshita F, Kozuma Y, Matsubara T, Haratake N, Akamine T, Hirai F, Honda H and Maehara Y: Prognostic impact of postoperative skeletal muscle decrease in non-small cell lung cancer. *Ann Thorac Surg* 109(3): 914-920, 2020. PMID: 31655044. DOI: 10.1016/j.athoracsur.2019.09.035
- 22 Miyamoto Y, Hanna DL, Zhang W, Baba H and Lenz HJ: Molecular pathways: Cachexia signaling-a targeted approach to cancer treatment. *Clin Cancer Res* 22(16): 3999-4004, 2016. PMID: 27340276. DOI: 10.1158/1078-0432.CCR-16-0495
- 23 Muscaritoli M, Anker SD, Argilés J, Aversa Z, Bauer JM, Biolo G, Boirie Y, Bosaeus I, Cederholm T, Costelli P, Fearon KC, Laviano A, Maggio M, Rossi Fanelli F, Schneider SM, Schols A and Sieber CC: Consensus definition of sarcopenia, cachexia and pre-cachexia: joint document elaborated by Special Interest Groups (SIG) "cachexia-anorexia in chronic wasting diseases" and "nutrition in geriatrics". *Clin Nutr* 29(2): 154-159, 2010. PMID: 20060626. DOI: 10.1016/j.clnu.2009.12.004
- 24 Prado CM, Baracos VE, McCargar LJ, Reiman T, Mourtzakis M, Tonkin K, Mackey JR, Koski S, Pituskin E and Sawyer MB: Sarcopenia as a determinant of chemotherapy toxicity and time to tumor progression in metastatic breast cancer patients receiving capecitabine treatment. *Clin Cancer Res* 15(8): 2920-2926, 2009. PMID: 19351764. DOI: 10.1158/1078-0432.CCR-08-2242
- 25 Martinez-Outschoorn U, Sotgia F and Lisanti MP: Tumor microenvironment and metabolic synergy in breast cancers: critical importance of mitochondrial fuels and function. *Semin Oncol* 41(2): 195-216, 2014. PMID: 24787293. DOI: 10.1053/j.seminoncol.2014.03.002
- 26 Weidner N, Semple JP, Welch WR and Folkman J: Tumor angiogenesis and metastasis – correlation in invasive breast carcinoma. *N Engl J Med* 324(1): 1-8, 1991. PMID: 1701519. DOI: 10.1056/NEJM199101033240101
- 27 Batchelor TJP, Rasburn NJ, Abdelnour-Berchtold E, Brunelli A, Cerfolio RJ, Gonzalez M, Ljungqvist O, Petersen RH, Popescu WM, Slinger PD and Naidu B: Guidelines for enhanced recovery after lung surgery: recommendations of the Enhanced Recovery After Surgery (ERAS®) Society and the European Society of Thoracic Surgeons (ESTS). *Eur J Cardiothorac Surg* 55(1): 91-115, 2019. PMID: 30304509. DOI: 10.1093/ejcts/ezy301
- 28 Pouwels S, Hageman D, Gommans LN, Willigendael EM, Nienhuijs SW, Scheltinga MR and Teijink JA: Preoperative exercise therapy in surgical care: a scoping review. *J Clin Anesth* 33: 476-490, 2016. PMID: 27555213. DOI: 10.1016/j.jclinane.2016.06.032
- 29 Gillis C, Li C, Lee L, Awasthi R, Augustin B, Gamsa A, Liberman AS, Stein B, Charlebois P, Feldman LS and Carli F: Prehabilitation versus rehabilitation: a randomized control trial in patients undergoing colorectal resection for cancer. *Anesthesiology* 121(5): 937-947, 2014. PMID: 25076007. DOI: 10.1097/ALN.0000000000000393
- 30 Gillis C, Fenton TR, Sajobi TT, Minnella EM, Awasthi R, Loiselle SE, Liberman AS, Stein B, Charlebois P and Carli F: Trimodal prehabilitation for colorectal surgery attenuates post-surgical losses in lean body mass: A pooled analysis of randomized controlled trials. *Clin Nutr* 38(3): 1053-1060, 2019. PMID: 30025745. DOI: 10.1016/j.clnu.2018.06.982

Received March 23, 2022

Revised April 17, 2022

Accepted April 20, 2022

Original Article

Impact of chronological age on efficacy and safety of fluoropyrimidine plus bevacizumab in older non-frail patients with metastatic colorectal cancer: a combined analysis of individual data from two phase II studies of patients aged >75 years

Toshikazu Moriwaki^{1,*}, Tomohiro Nishina², Yoshinori Sakai³, Yoshiyuki Yamamoto¹, Mitsuo Shimada⁴, Hiroyasu Ishida⁵, Kenji Amagai⁶, Mikio Sato⁷, Shinji Endo⁸, Yuji Negro⁹, Hidekazu Kuramochi¹⁰, Tadamichi Denda¹¹, Yukimasa Hatachi^{12,†}, Kazuto Ikezawa¹³, Go Nakajima¹⁴, Yoshiaki Bando¹⁵, Akihito Tsuji¹⁶, Yuji Yamamoto^{17,‡}, Masamitsu Morimoto¹⁸, Kazuma Kobayashi¹⁹, and Ichinosuke Hyodo²

¹Department of Gastroenterology, Faculty of Medicine, University of Tsukuba, Tsukuba City, Japan, ²Department of Gastrointestinal Medical Oncology, National Hospital Organization Shikoku Cancer Center, Matsuyama City, Japan, ³Department of Gastroenterology, Tsuchiura Kyodo General Hospital, Tsuchiura City, Japan, ⁴Department of Surgery, Tokushima University, Tokushima City, Japan, ⁵Department of Gastroenterology, National Hospital Organization Mito Medical Center, Higashi Ibaraki gun, Japan, ⁶Division of Gastroenterology, Ibaraki Prefectural Central Hospital and Cancer Center, Kasama City, Japan, ⁷Department of Gastroenterology and Hepatology, Ryugasaki Saiseikai Hospital, Ryugasaki City, Japan, ⁸Department of Gastroenterology and Hepatology, Shinmatsudo Central General Hospital, Matsudo City, Japan, ⁹Department of Oncological Medicine, Kochi Health Sciences Center, Kochi City, Kochi, Japan, ¹⁰Department of Chemotherapy and Palliative Care, Tokyo Women's Medical University, Shinjuku-ku, Japan, ¹¹Division of Gastroenterology, Chiba Cancer Center, Chiba City, Japan, ¹²Department of Medical Oncology, Kobe City Medical Center General Hospital, Kobe City, Japan, ¹³Division of Gastroenterology, Tsukuba Memorial Hospital, Tsukuba City, Japan, ¹⁴Department of Chemotherapy and Palliative Care, Tokyo Women's Medical University, Shinjuku-ku, Japan, ¹⁵Department of Surgery, Tokushima Prefecture Naruto Hospital, Naruto City, Japan, ¹⁶Department of Clinical Oncology, Kagawa University Faculty of Medicine, Kita-gun, Japan, ¹⁷Department of Gastrointestinal Surgery and Surgical Oncology, Ehime University Graduate School of Medicine, Toon City, Japan, ¹⁸Department of Surgery, National Hospital Organization Ehime Medical Center, Toon City, Japan and ¹⁹Department of Surgery, Nagasaki University Graduate School of Biomedical Sciences, Nagasaki City, Japan

*For reprints and all correspondence: Toshikazu Moriwaki, Faculty of Medicine, Department of Gastroenterology, University of Tsukuba, 1-1-1 Tennodai, Tsukuba City 305-8575, Japan. E-mail: tmoriwak@md.tsukuba.ac.jp

†Present address: Department of Clinical Oncology, Kansai Rosai Hospital, Amagasaki City, Hyogo, Japan.

‡Present address: Division of Surgery, Minami Matsuyama Hospital, Matsuyama City, Ehime, Japan.

Received 29 November 2021; Editorial Decision 22 March 2022; Accepted 13 April 2022

Abstract

Objective: Many clinical trials for older patients with metastatic colorectal cancer have been conducted, and fluoropyrimidine and bevacizumab are standard treatments. However, the relationship

between age and the efficacy and safety of this treatment is unclear in older metastatic colorectal cancer patients.

Methods: Individual data from two phase II studies on older (≥ 75 years), non-frail patients with metastatic colorectal cancer treated with uracil-tegafur/leucovorin or S-1 combined with bevacizumab were collected. Patient characteristics were evaluated with multiple regression analyses for survival outcomes, using the Cox proportional hazard model and linear regression analyses for the worst grade of adverse events.

Results: We enrolled 102 patients with a median age of 80 years (range, 75–88 years). Of the 70 patients who died, seven (10%) died of causes unrelated to disease or treatment. The study treatment was discontinued due to adverse events in 19 patients (18.6%), with 63% aged ≥ 85 years. The adverse event that most commonly resulted in treatment discontinuation was grade 2 fatigue (21%). Chronological age was not associated with progression-free survival (Hazard ratio, 1.03; $P = 0.40$) or overall survival (Hazard ratio, 1.02; $P = 0.65$). Age was weakly associated with non-hematologic adverse events (regression coefficient [R], 0.27; $P = 0.007$), especially fatigue (R, 0.23; $P = 0.02$) and nausea (R, 0.19; $P = 0.06$), but not with hematologic (R, 0.05; $P = 0.43$) or bevacizumab-related (R, -0.06 ; $P = 0.56$) adverse events.

Conclusions: The efficacy of fluoropyrimidine plus bevacizumab was age-independent in patients with metastatic colorectal cancer aged ≥ 75 years, and attention should be paid to non-hematologic adverse events as age increases.

Key words: adverse event, age, bevacizumab, chemotherapy, colon cancer, older patients, fluoropyrimidine, rectal cancer, toxicity, vulnerability

Introduction

As the average life span increases, the number of elderly patients with cancer has also increased globally. Colorectal cancer (CRC) is the third most common cancer worldwide and the most common type of cancer in Japan (1,2). CRC is common in populations over 75 years of age, and mortality is known to increase with age (2). Older patients with CRC are less likely to be diagnosed at a metastatic stage than younger patients; however, older patients have the lowest survival rates because of age-related disadvantages, such as comorbidities (3). Although older patients do not commonly receive aggressive treatments, systemic chemotherapy can improve the overall survival (OS) of older patients with metastatic CRC (mCRC), similar to younger patients (4).

Fluoropyrimidine plus oxaliplatin, or irinotecan combined with a molecularly targeted agent, such as bevacizumab, cetuximab or panitumumab, is recommended as the standard chemotherapy for mCRC (5). These treatments are also offered to older patients to prolong their OS and maintain their general condition. However, the efficacy of doublet chemotherapy with/without a molecular-targeted agent is controversial because of the higher incidence of adverse events (AEs) compared with fluoropyrimidine with or without a molecularly targeted agent (6–8), despite the patients being eligible for doublet chemotherapy, defined as fit patients. Recently, capecitabine, an oral fluoropyrimidine, plus bevacizumab has been reported to improve progression-free survival (PFS) compared with capecitabine alone in older patients with mCRC who were incompatible for oxaliplatin- or irinotecan-containing chemotherapy, defined as vulnerable patients (9). Thus, fluoropyrimidine plus bevacizumab is recommended as an optional treatment for fit or vulnerable older patients in the National Comprehensive Cancer Network, European Society of Medical Oncology and Pan-Asian practice guidelines (10–12). In previous clinical studies on fluoropyrimidine plus bevacizumab for older patients with mCRC, the median PFS and OS were 8.1–9.9 and 20.7–25.0 months, respectively (9,13–15). However,

grade 3 or higher AEs were observed in 29–40% of the older patients, and 11–32% terminated treatment due to AEs. It remains unclear that age of non-frail older patients is associated with the outcomes of fluoropyrimidine plus bevacizumab, which is recognized as mild chemotherapy. Due to the diversity of older patients, various comprehensive geriatric assessments have been actively studied, but no standard evaluation methods have been established (16–18). Thus, it is difficult to determine whether patients can tolerate chemotherapy. Even in patients with mCRC with no vulnerabilities except for chronological age, there are still concerns regarding the impact of age on outcomes.

This study therefore aimed to investigate the association between chronological age and the efficacy and safety of fluoropyrimidine plus bevacizumab using individual data from two phase II trials for older non-frail patients with mCRC.

Materials and methods

Patients

The individual data of patients participating in either phase II studies of uracil-tegafur and oral leucovorin combined with bevacizumab (J-BLUE study) or S-1 on alternate days combined with bevacizumab (J-SAVER study), for non-frail patients with mCRC aged ≥ 75 years were collected (13,19). These studies were multicenter, single-arm phase II studies conducted by the non-profit organization Tsukuba Cancer Clinical Trial Group and the Shikoku Gastrointestinal Oncology Study Group in Japan. The study protocols were approved by the ethics committee of each participating institution and registered at the University Hospital Medical Information Network, UMIN000003515 and UMIN000010402. Both studies showed similar results. Briefly, the J-BLUE study, comprising 52 patients, showed a median PFS of 8.2 months and OS of 23.0 months. The most common grade 3 and grade 4 AEs were hypertension (12%), fatigue (8%),

anaemia (8%), nausea (6%) and diarrhoea (6%). Treatment-related deaths occurred in two patients. The J-SAVER study, comprising 50 patients, showed a median PFS of 8.1 months and OS of 23.1 months. The most common grade 3 and grade 4 AEs were hypertension (11%), fatigue (6%), anaemia (6%), nausea (6%) and proteinuria (6%). Treatment-related death occurred in one patient.

Data collection

The following individual pre-treatment clinical data and baseline laboratory values were collected and used in the analysis: age, sex, body mass index, Eastern Cooperative Oncology Group performance status (ECOG-PS), metastasis at diagnosis, resection of the primary tumour, site of the primary tumour, pathological type, number of metastatic organs, metastatic organs, RAS gene mutation status, white blood cell counts, neutrophil counts, platelet counts, and levels of haemoglobin, aspartate transaminase (AST), total bilirubin, creatinine clearance, serum carcinoembryonic antigen (CEA) and cancer antigen (CA)19-9.

Statistical analysis

PFS was defined as the time from enrollment to disease progression or death from any cause. OS was defined as the time from enrollment to death from any cause. Tumour assessments were performed every 8 weeks according to the Response Evaluation Criteria in Solid Tumors. AEs were assessed according to the Common Terminology Criteria for Adverse Events, version 3.0, in the J-BLUE study and version 4.0, in the J-SAVER study. In addition to hematologic and non-hematologic AEs, bevacizumab-related AEs, including hypertension, proteinuria, haemorrhage, thromboembolic events and gastrointestinal perforation, were defined and evaluated.

Survival outcomes were estimated using the Kaplan–Meier method and analysed by regression analysis using the Cox proportional hazard model. Associations between continuous clinical data and the worst grade of AEs were evaluated using regression analysis. Factors with $P < 0.2$ were used in the multivariate analysis. Differences in PFS and OS between the groups were evaluated using the log-rank test. For all statistical analyses, SPSS software package, version 27.0 (SPSS Inc., Tokyo, Japan) was used, and a value of $P < 0.05$ was considered significant.

Results

Patients

A total of 102 patients were enrolled, including 52 from the J-BLUE study and 50 from the J-SAVER study (Table 1). The median age was 80 (range: 75–88) years, and 65% had an ECOG-PS of 0. The patient's body mass index was normal. The median number of metastatic organs was two (range: 1–5), and the prevalence of RAS gene mutations was 35%. Creatinine clearance was <60 ml/min in 38% of patients.

Efficacy

The median follow-up was 33.7 months (95% CI: 22.3–45.1). The protocol treatment was terminated in 98 patients (96.1%), including 19 (19.4%) patients due to AEs. Of the 70 patients (71.4%) who died, seven died of causes other than disease progression or treatment-related death. The median PFS was 8.2 months (95% CI:

7.1–9.3), and the median OS was 23.0 months (95% CI: 18.2–27.8) (Supplementary Fig. 1).

Safety

Among treatment-related AEs (Supplementary Table 1), the most common hematologic AEs were anaemia of any grade (52.0%) and grade 3 (6.9%). The most common non-hematologic AEs were fatigue of any grade (41.2%) and grade 3 (6.9%). The most common bevacizumab-related AEs were proteinuria of any grade (39.2%) and hypertension of grade 3 or higher (11.8%). Treatment-related death was observed in three patients ($n = 1$; diarrhoea, $n = 1$; cerebral infarction, $n = 1$; sudden death due to myocardial infarction). The AEs that resulted in treatment discontinuation were grade 2 fatigue ($n = 4$), liver disorders ($n = 2$), skin disorders ($n = 1$), diarrhoea ($n = 1$) and edema ($n = 1$); grade 3 nausea ($n = 1$), hypertension with proteinuria ($n = 1$) and neutropenia ($n = 1$); grade 4 thromboembolic events ($n = 1$); and treatment-related death ($n = 3$).

The incidences of grade 2 non-hematologic and grade 3 or higher non-hematologic AEs were significantly higher in the AE discontinuation group than in the non-AE discontinuation group (57.9% vs. 31.6%, $P = 0.03$; 26.3% vs. 8.9%, $P = 0.04$, respectively) (Table 2). In the AE discontinuation group, grade 2 or higher fatigue was observed in eight patients (42.1%), followed by nausea or stomatitis in seven patients (36.8%).

Efficacy outcomes and reasons for treatment discontinuation

The individual PFS, status of disease progression or death and reasons for treatment discontinuation by age are shown in Fig. 1A. Patients with PFS over the median PFS were widely distributed among the ages, while patients who discontinued treatment due to AEs were older than 85 years ($n = 5/8$). No consistency was observed in the relationship between the OS duration and age (Fig. 1B). Deaths due to treatment-related toxicities and causes other than cancer progression were also widely distributed over the ages.

Associations of efficacy and patients' background factors

The association between PFS and age was not significant in the univariate analysis (HR, 1.03; 95% CI: 0.96–1.10, $P = 0.40$) (Table 3). In the multivariate analysis for PFS, metastasis at diagnosis, number of metastatic organs, CEA level and AST level were significant independent factors. The association between OS and age was also not significant in the univariate analysis (HR, 1.02; 95% CI: 0.95–1.09; $P = 0.65$) (Table 3). Resection of the primary tumour and AST level were significant independent factors for OS.

Efficacy parameters were compared between the three groups divided according to age groups: 75–79 years, 80–84 years and ≥ 85 years. Median PFS was 8.8 months (95% CI: 7.2–10.4) in the 75–79 years group, 7.8 months (95% CI: 7.2–8.4) in the 80–84 years group and 11.1 months (95% CI: 4.6–17.6) in the ≥ 85 years group ($P = 0.88$) (Fig. 2A). PFS, which was adjusted by independent factors, was not statistically significant between three groups (Supplementary Table 2). Median OS was 23.8 months (95% CI: 16.1–31.5) in the 75–79 years group, 18.9 months (95% CI: 9.8–28.0) in the 80–84 years group and 25.9 months (95% CI: 0.0–52.1) in the ≥ 85 years group ($P = 0.53$) (Fig. 2B). OS, which was adjusted

Table 1. Patient characteristics

		n	%
Trial	J-BLUE	52	51.0
	J-SAVER	50	49.0
Age	Median (range), years	80 (75–88)	
	75–79	50	49.0
	80–84	44	43.1
	≥85	8	7.8
Sex	Male	57	55.9
	Female	45	44.1
Body mass index	Median (range)	21.4 (15.2–34.0)	
ECOG-PS	0	66	64.7
	1	36	35.3
Metastasis at diagnosis	Synchronous	69	67.6
	Metachronous	33	32.4
Resection of primary tumour	Yes	81	79.4
	No	21	20.6
Site of primary tumour*	Right	26	25.5
	Left	76	74.5
Pathological type	Well and moderate differentiated	90	88.2
	Poorly differentiated and signet-ring cell	11	10.8
	Others	1	1.0
Number of metastatic organs	Median (range)	2 (1–5)	
	≥3	14	13.7
Metastatic organ	Liver	61	59.8
	Lung	42	41.2
	Lymph node	31	30.4
	Peritoneum	20	19.6
	Others	16	15.7
KRAS/RAS gene status	Wild	41	40.2
	Mutant	36	35.3
	Unknown	25	24.5
WBC counts	Median (range), mg/dl	5965 (3300–10 750)	
Neutrophil counts	Median (range), mg/dl	3840 (1587–83,00)	
Haemoglobin level	Median (range), g/dl	11.5 (9.0–15.3)	
Platelet counts	Median (range), $\times 10^4$ mg/dl	21.8 (10.8–55.8)	
AST level	Median (range), IU/L	15 (5–84)	
Total bilirubin level	Median (range), mg/dl	0.6 (0.1–4.3)	
Creatinine clearance	Median (range), ml/min	66.3 (25.3–203.0)	
	≥80	19	18.6
	<80, ≥60	44	43.1
	<60, ≥30	38	37.3
	<30	1	1.0
CEA level	Median (range), IU/L	19.8 (1.0–12854.0)	
	Abnormally	79	77.5
	Missing	1	1.0
CA 19–9 level	Median (range), IU/L	58.4 (0.0–37660.6)	
	Abnormally	54	52.9
	Missing	2	2.0
Reason for discontinuation of protocol treatment	Progressive disease	74	72.5
	Adverse event	19 [†]	18.6
	Others	6	5.9
	Ongoing	3	2.9

AST: aspartate transaminase, CA 19–9: cancer antigen 19–9, CEA: carcinoembryonic antigen, ECOG-PS: Eastern Cooperative Oncology Group performance status, WBC: white blood cell.

*Right included cecum, ascending colon and transverse colon, Left included descending colon, sigmoid colon and rectum. [†]Three patients had treatment-related deaths.

Table 2. The comparison of experienced maximum toxicity grade according to AE discontinuation

Category	AE discontinuation		Non-AE discontinuation		P value
	(n = 19)		(n = 79)		
	n	(%)	n	(%)	
Hematologic AEs					
Grade 1	4	(21.1)	35	(44.3)	0.06
Grade 2	6	(31.6)	13	(16.5)	0.13
Grade ≥3	2	(10.5)	6	(7.6)	0.68
Non-hematologic AEs					
Grade 1	2	(10.5)	23	(29.1)	0.10
Grade 2	11	(57.9)	25	(31.6)	0.03
Grade ≥3	5	(26.3)	7	(8.9)	0.04
Bevacizumab-related AEs					
Grade 1	3	(15.8)	19	(24.1)	0.44
Grade 2	5	(26.3)	22	(27.8)	0.89
Grade ≥3	5	(26.3)	13	(16.5)	0.33

AE, adverse event.

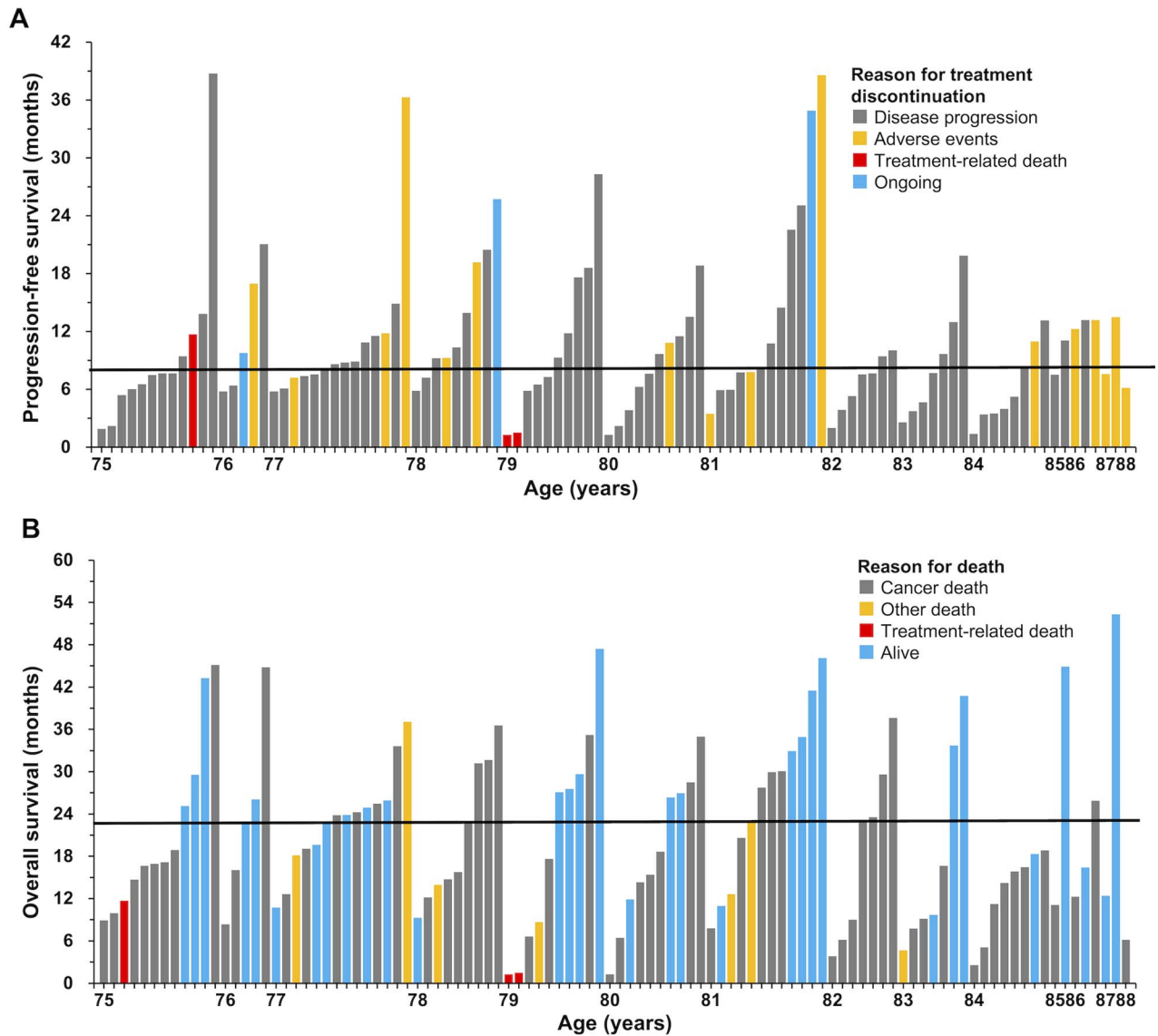
**Figure 1.** Progression-free survival or overall survival and the reasons for the event in individual patients. A: progression-free survival; B: overall survival. Solid horizontal line denotes median time.

Table 3. Regression analyses with Cox proportional hazard model for progression-free survival and overall survival

Variable	Unit or Group	Progression-free survival				Overall survival			
		Univariate		Multivariate		Univariate		Multivariate	
		HR	P value	HR (95% CI)	P value	HR	P value	HR (95% CI)	P value
Age	Year	1.03	0.40			1.02	0.65		
Body mass index	kg/m ²	0.93	0.041			0.96	0.30		
Tumour location*	Left vs Right	1.10	0.70			0.99	0.97		
Sex	Female vs Male	1.37	0.14			1.03	0.92		
ECOG-PS	1 vs 0	1.38	0.15			1.54	0.08		
Metastasis at diagnosis	Metachronous vs Synchronous	0.53	0.01	0.51 (0.31–0.84)	0.008	0.66	0.12		
Resection of primary tumour	Yes vs No	1.51	0.11			2.44	0.002	2.68 (1.53–4.70)	<0.001
Pathological type	Other vs Por vs Tub	1.42	0.28			2.50	0.009		
Liver metastasis	No vs Yes	0.70	0.11			0.64	0.085		
Peritoneal dissemination	No vs Yes	1.09	0.75			0.78	0.40		
No. of metastatic organs	Organ	1.36	0.008	1.36 (1.06–1.74)	0.015	1.51	0.001		
RAS gene status	Unknown vs Wild vs Mutant	0.91	0.47			1.13	0.44		
CEA level	IU/ml	0.50	0.008	0.98 (0.97–1.00)	0.044	0.47	0.019		
CA19–9 level	IU/ml	0.76	0.21			0.87	0.56		
Haemoglobin level	g/ml	0.87	0.027			0.92	0.26		
Platelet counts	/ml	1.02	0.27			1.01	0.59		
WBC counts	/ml	1.13	0.06			1.13	0.087		
Neutrophil counts	/ml	1.17	0.033			1.14	0.11		
AST level	IU/ml	1.17	0.013	1.21 (1.05–1.38)	0.009	1.25	0.002	1.26 (1.09–1.46)	0.001
Total bilirubin level	mg/dl	1.02	0.90			0.83	0.43		
Creatinine clearance	ml/min	1.00	0.85			1.00	0.85		

CI: confidence interval, HR: hazard ratio, WBC: white blood cell.

*Right included cecum, ascending colon and transverse colon, Left included descending colon, sigmoid colon and rectum.

by independent factors, was not statistically significant between three groups (Supplementary Table 2).

Associations of subsequent chemotherapy and age

Among 98 patients who discontinued protocol treatment, 65 patients (66.3%) received any subsequent chemotherapy (Table 4). In the 75–79 years group, oxaliplatin plus fluoropyrimidine combined with a molecular targeted agent, irinotecan combined with a molecular targeted agent and irinotecan alone were used in 22 (45.8%), 11 (22.9%) and 10 (20.8%) patients, respectively. In the 80–84 years group, oxaliplatin plus fluoropyrimidine combined with a molecular targeted agent, irinotecan combined with a molecular targeted agent and fluoropyrimidine combined with bevacizumab were used in 5 (11.9%), 4 (9.5%) and 4 (9.5%) patients, respectively. In the ≥85 years group, fluoropyrimidine alone and irinotecan alone were used in three (37.5%) and two (25.0%) patients, respectively.

Association of safety and patients' background factors

The regression analyses between the continuous variables of patients' background factors and the worst grades of AEs are shown in Fig. 3

and Supplementary Table 3. The association between age and hematologic AEs was not significant in the univariate analysis (regression coefficient [R], 0.05; $P = 0.43$). Hematologic AEs were weakly associated with resection of the primary tumour (partial R [pR], 0.20; $P = 0.034$) and creatinine clearance (pR, -0.25 ; $P = 0.009$) in the multivariate analysis. Non-hematologic AEs were weakly associated with age (pR, 0.25; $P = 0.009$), sex (pR, 0.19; $P = 0.046$) and platelet count (pR, -0.23 ; $P = 0.019$) in the multivariate analysis. The association of age with bevacizumab-related AEs was not significant in the univariate analysis (R, -0.06 ; $P = 0.56$). Bevacizumab-related AEs were weakly associated with the pathologic type (pR, 0.20; $P = 0.046$), neutrophil counts (pR, 0.30; $P = 0.003$) and AST level (pR, -0.25 ; $P = 0.014$). Among non-hematologic AEs, fatigue (R, 0.23; $P = 0.02$) and nausea (R, 0.19; $P = 0.06$) were weakly associated with age (Table 5). The four patients who discontinued treatment due to grade 2 fatigue were aged 77, 81, 86 and 86 years, and one of them also developed grade 3 nausea.

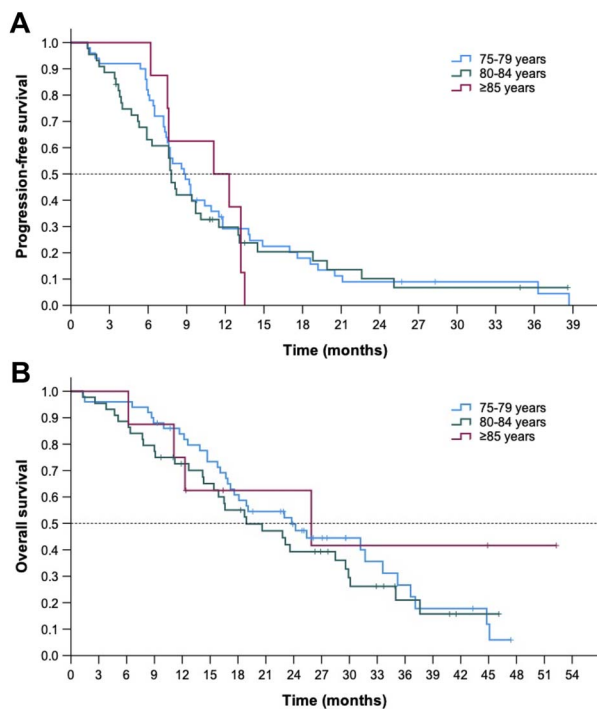
Discussion

This study showed that age was weakly associated with non-hematologic AEs, but not PFS and OS in non-frail patients with

Table 4. Subsequent chemotherapy according to age

	75–79 years		80–84 years		≥85 years	
	<i>n</i> = 48		<i>n</i> = 42		<i>n</i> = 8	
	<i>n</i>	(%)	<i>n</i>	(%)	<i>n</i>	(%)
No subsequent chemotherapy	12	(25.0)	18	(42.9)	3	(37.5)
FOLFOX/CapeOX/SOX+bevacizumab/panitumumab	22	(45.8)	5	(11.9)	1	(12.5)
FOLFOX/CapeOX/SOX	5	(10.4)	2	(4.8)	1	(12.5)
FOLFIRI/CapeIRI+bevacizumab	2	(4.2)	0	(0)	0	(0)
Irinotecan+bevacizumab/cetuximab/panitumumab	11	(22.9)	4	(9.5)	0	(0)
Irinotecan	10	(20.8)	2	(4.8)	2	(25.0)
FL/S-1/Capecitabine/UFT-LV + bevacizumab	6	(12.5)	4	(9.5)	1	(12.5)
S-1/UFT-LV	3	(6.3)	2	(4.8)	3	(37.5)
Panitumumab/cetuximab	2	(4.2)	3	(7.1)	1	(12.5)
Trifluridine-tipiracil	5	(10.4)	1	(2.4)	0	(0)
Regorafenib	2	(4.2)	0	(0)	0	(0)

CapeIRI, capecitabine+irinotecan; CapeOX, capecitabine+oxaliplatin; FOLFOX, infusional fluorouracil+leucovorin+oxaliplatin; FL, bolus fluorouracil+leucovorin; UFT-LV, uracil-tegafur+leucovorin.

**Figure 2.** Kaplan–Meier curves for each of the age groups: 75–79 years, 80–84 years and ≥85 years. A: progression-free survival; B: overall survival.

mCRC >75 years of age who received fluoropyrimidine plus bevacizumab.

Before these analyses, we hypothesized that age probably affected OS because chronological age in some of the patients was around the Japanese average life span (male: 81 years and female: 87 years, in 2018). Although OS in patients over 80 years of age showed a shorter trend than the others, there was no statistically significant difference. The proportion of patients aged ≥80 years who received any subsequent chemotherapy was lower than that of the 75–79 years

group. In particular, oxaliplatin- or irinotecan-containing therapy was less common in patients aged ≥80 years. Although the patient's condition after failure of first-line treatment affected the selection of subsequent treatment, age may be a factor for the decision. The PFS did not differ between these patients. These results suggest that a therapeutic effect could be expected regardless of age in older patients eligible for fluoropyrimidine plus bevacizumab treatment. The prognostic factors for PFS and OS obtained in this study have been reported in many previous reports, including younger patients (20–23). It is noteworthy that patients older than 85 years were more likely to discontinue treatment due to AEs, although the PFS was not necessarily short. This may indicate poor long-term tolerability in older patients.

The Cancer and Aging Research Group chemotherapy toxicity tool questionnaire was developed to predict chemotherapy-related severe toxicity in older cancer patients in Western countries (24–26). Geriatric assessment tools such as the G8 screening tool to separate older patients with cancer who are eligible to receive standard doublet treatment have also been developed (18). Although these tools were developed focusing on the onset of severe toxicity, our results suggest that the prediction of toxicity, including those with lower severity, is important. In this study, only non-hematologic AEs, particularly fatigue and nausea, were significantly associated with age, and these were generally mild or moderate (grade 3 of 5–7%). However, these mild or moderate AEs had a negative impact on treatment continuity, resulting in the discontinuation of treatment in 19 (19%) patients, and the AE that was most associated with treatment discontinuation was grade 2 fatigue. In addition, these patients experienced grade 2 or higher non-hematologic AEs more frequently than patients with non-AE discontinuation, and fatigue was the most common. Five of eight patients over 85 years of age discontinued treatment due to AEs. Two of these five patients had grade 2 fatigue (data not shown). In this patient population, earlier rest or dose reduction of fluoropyrimidine administration should be considered, despite not having severe toxicities. In one study using patient-reported data of the incidence of symptoms with new treatment regimens in older adults receiving chemotherapy for advanced cancer, ~60% experienced mild-to-moderate fatigue (18). The effective management of chemotherapy-related fatigue should

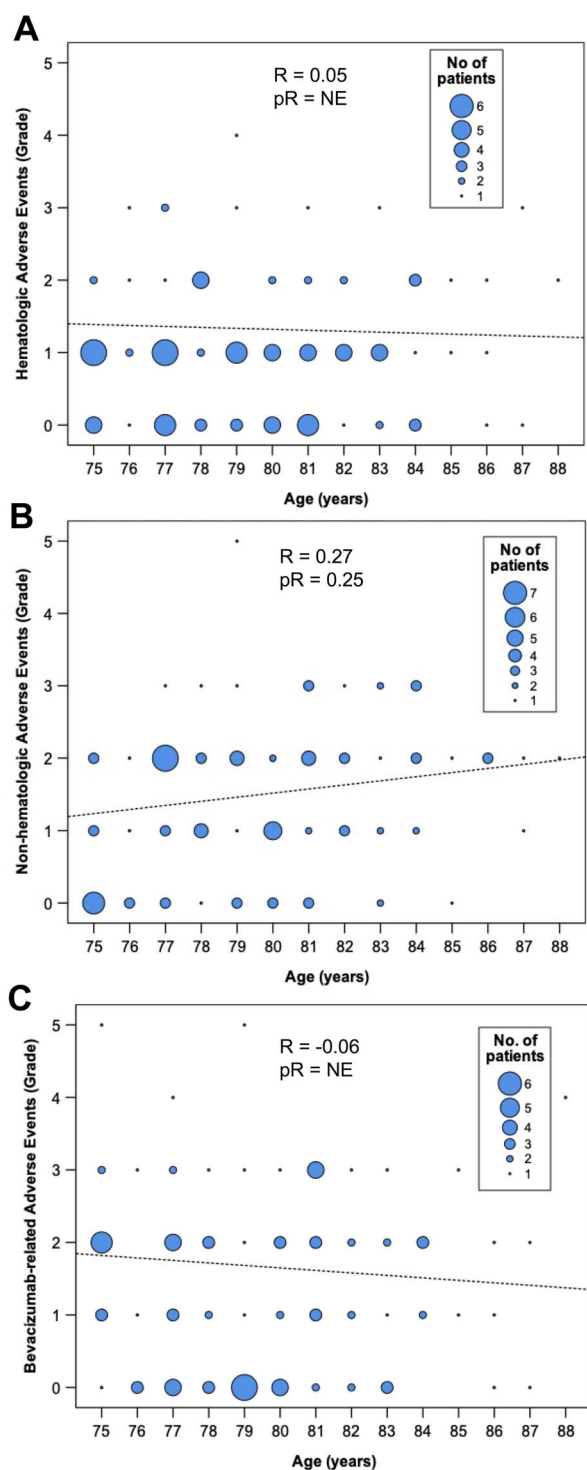


Figure 3. Scatterplots of age and worst grade of adverse events. A: hematologic adverse events; B: non-hematologic adverse events; C: bevacizumab-related adverse events. Circle size denotes the number of patients. NE, not evaluated; pR, partial regression coefficient; R, regression coefficient.

thus be considered an important issue for chemotherapy continuation in older patients. Hematologic AEs were not associated with age. The incidence of hematologic AEs of any grade was 67.6%, but most patients had grade 1 hematologic AEs. Hematologic AE grades

Table 5. Regression analysis for age and worst grade of non-hematologic adverse events

Adverse events	Regression coefficient	P value
Any	0.27	<0.01
Febrile neutropenia	–	–
Infection	0.07	0.47
Liver dysfunction	–0.01	0.87
Stomatitis	0.04	0.40
Nausea	0.19	0.06
Vomiting	0.11	0.26
Diarrhoea	0.08	0.81
Fatigue	0.23	0.02
Watering eyes	–0.10	0.33
Skin disorder	–0.10	0.34
Anorexia	–0.11	0.29

–Unanalysable.

with these regimens were too mild to investigate their relevance with age. However, creatinine clearance was significantly associated with hematologic AEs, because decreased creatinine clearance could lead to increased fluoropyrimidine concentration in the blood (27–29). Although this occurs regardless of age, it should be carefully monitored as decreased renal function is common in older patients. Bevacizumab-related AEs were weakly associated with pathologic type, neutrophil counts and AST levels. These relationships cannot be explained and further validation studies are required.

Recently, a randomized phase III trial (JCOG 1018) of fluoropyrimidine plus bevacizumab vs. oxaliplatin-containing therapy plus bevacizumab in older patients eligible for intensive chemotherapy was reported in ASCO-GI 2022 (30). PFS and OS in the oxaliplatin-added group did not improve survival compared with the fluoropyrimidine plus bevacizumab group. Moreover, grade 2 or higher nausea, diarrhoea and fatigue were common in the oxaliplatin-added group. As a result, 46% of patients terminated oxaliplatin-containing therapy plus bevacizumab treatment due to AEs. The association of age with clinical outcomes in this study is expected to be evaluated.

This study has some limitations. First, no comprehensive geriatric assessment was conducted. Although it was previously reported as a predictor of survival and AEs in various cancers, including mCRC, a strong relationship between the comprehensive geriatric assessment and chronological age has not been found in older patients with cancer (31,32). Second, our results did not reflect the clinical outcomes of fluoropyrimidine plus bevacizumab in the real world as the patients enrolled in this study were limited to those eligible for the phase II trials. Third, the number of patients was small, and the robustness of the results was weak. Therefore, a validation study with a large-scale sample or real-world setting is needed. Fourth, the data of patients who received different regimens were analysed in this study. However, the PFS and OS were similar between the two treatment groups, as well as the incidence of AEs except for the slightly higher incidence of any grade of thrombocytopenia, anorexia and proteinuria in the J-SAVR trial (13,19). Finally, the AEs were evaluated using different versions of the CTC-AE between the two studies. The corresponding AEs were vomiting, fatigue, hypertension, proteinuria, thromboembolic events and gastrointestinal perforation, but, except for vomiting and hypertension, these AEs did not affect grading.

In conclusion, this study suggested that the efficacy of fluoropyrimidine combined with bevacizumab was age-independent in

patients ≥ 75 years of age with mCRC who were not considered frail, and attention should be paid to non-hematologic AEs for patients as age increases.

Author Contributions

Study concepts: T. Moriwaki; Study design: T. Moriwaki and I. Hyodo; data acquisition: all authors; quality control of data and algorithms: T. Moriwaki and T. Nishina; Data analysis and interpretation: T. Moriwaki, T. Nishina, I. Hyodo; statistical analysis: T. Moriwaki; manuscript preparation: T. Moriwaki; manuscript editing: T. Nishina, I. Hyodo; Manuscript review: All authors; Approval of Final Article: All authors.

Funding

The authors received no specific funding for this work.

Declaration of Completing Interest

Toshikazu Moriwaki reports grants and personal fees from Taiho, grants and personal fees from Chugai, personal fees from Sanofi, personal fees from Bayer, grants and personal fees from Yakult and personal fees from Eli Lilly, outside the scope of the submitted work. Tomohiro Nishina reports grants and personal fees from Taiho, grants and personal fees from Chugai, grants from MSD, grants and personal fees from Ono, grants and personal fees from Bristol Myers Squibb, grants and personal fees from Lilly, grants from Dainippon Sumitomo and grants from AstraZeneca, outside the submitted work. Mitsuo Shimada reports grants from Taiho, grants from Takeda, grants from Ono, grants from Chugai and grants from AbbVie GK, outside the submitted work. Kenji Amagai reports grants from MSD, grants from Taiho, grants from Daiichi-Sankyo, grants from Nippon Zoki and grants from Hisamitsu, outside the submitted work. Hidekazu Kuramochi reports personal fees from Takeda, personal fees from Chugai, personal fees from Taiho, personal fees from Eli Lilly, personal fees from Yakult, personal fees from Bayer, personal fees from Ono, personal fees from Daiichi Sankyo, outside the submitted work; and scholarship donation to the clinical department: Chugai and Taiho. Tadamichi Denda reports personal fees from Sysmex, personal fees from Ono and personal fees from Sawai outside the submitted work. Kazuto Ikezawa reports personal fees from Takeda, personal fees from Olympus, personal fees from MOCHIDA, personal fees from Otsuka, personal fees from DAIICHI SANKYO, personal fees from Mitsubishi Tanabe, personal fees from Janssen, personal fees from EA Pharma, personal fees from TSUMURA, personal fees from AstraZeneca, personal fees from Astellas, personal fees from Eisai, personal fees from Gilead Sciences, outside the submitted work. Akihito Tsuji reports grants and personal fees from Chugai, grants and personal fees from Taiho, personal fees from Ono, personal fees from Eli Lilly Japan, personal fees from Sanofi, personal fees from Pfizer Japan, personal fees from Kyowa Hakko Kirin, personal fees from Eisai, personal fees from MSD, personal fees from Toray Medical, personal fees from Daiichi Sankyo, personal fees from Bristol-Myers Squibb, outside the submitted work. Ichinosuke Hyodo reports personal fees from Ono, personal fees from Chugai, personal fees from Daiichi-Sankyo, personal fees from Taiho, personal fees from Merck Serono, and personal fees from Asahi-Kasei, outside the submitted work. The remaining authors declare that they have no conflict of interest.

Acknowledgments

We would like to thank Editage (www.editage.jp) for English language editing.

References

1. Ferlay J, Colombet M, Soerjomataram I, Mathers C, Parkin DM, Pineros M, et al. Estimating the global cancer incidence and mortality in 2018: GLOBOCAN sources and methods. *Int J Cancer* 2019;144:1941–53.
2. Cancer Statistics. [cited 1 September 2021]. Available from: https://ganjoho.jp/reg_stat/statistics/stat/cancer/67_colorectal.html.
3. Siegel RL, Miller KD, Goding Sauer A, Fedewa SA, Butterly LF, Anderson JC, et al. Colorectal cancer statistics, 2020. *CA Cancer J Clin* 2020;70:145–64.
4. Grande R, Natoli C, Ciancola F, Gemma D, Pellegrino A, Pavese I, et al. Treatment of metastatic colorectal cancer patients ≥ 75 years old in clinical practice: a Multicenter analysis. *PLoS One* 2016;11:e0157751.
5. Biller LH, Schrag D. Diagnosis and treatment of metastatic colorectal cancer: a review. *JAMA* 2021;325:669–85.
6. Aparicio T, Lavau-Denes S, Philip JM, Maillard E, Jouve JL, Gargot D, et al. Randomized phase III trial in elderly patients comparing LV5FU2 with or without irinotecan for first-line treatment of metastatic colorectal cancer (FFCD 2001-02). *Ann Oncol* 2016;27:121–7.
7. Landre T, Uzzan B, Nicolas P, Aparicio T, Zelek L, Mary F, et al. Doublet chemotherapy vs. single-agent therapy with 5FU in elderly patients with metastatic colorectal cancer. A meta-analysis. *Int J Colorectal Dis* 2015;30:1305–10.
8. Landre T, Maillard E, Taleb C, Ghebriou D, Guetz GD, Zelek L, et al. Impact of the addition of bevacizumab, oxaliplatin, or irinotecan to fluoropyrimidin in the first-line treatment of metastatic colorectal cancer in elderly patients. *Int J Colorectal Dis* 2018;33:1125–30.
9. Cunningham D, Lang I, Marcuello E, Lorusso V, Ocvirk J, Shin DB, et al. Bevacizumab plus capecitabine versus capecitabine alone in elderly patients with previously untreated metastatic colorectal cancer (AVEX): an open-label, randomised phase 3 trial. *Lancet Oncol* 2013;14:1077–85.
10. Benson AB, Venook AP, Al-Hawary MM, Arain MA, Chen YJ, Ciombor KK, et al. Colon cancer, version 2.2021, NCCN clinical practice guidelines in oncology. *J Natl Compr Canc Netw* 2021;19:329–59.
11. Van Cutsem E, Cervantes A, Adam R, Sobrero A, Van Krieken JH, Aderka D, et al. ESMO consensus guidelines for the management of patients with metastatic colorectal cancer. *Ann Oncol* 2016;27:1386–422.
12. Yoshino T, Arnold D, Taniguchi H, Pentheroudakis G, Yamazaki K, Xu RH, et al. Pan-Asian adapted ESMO consensus guidelines for the management of patients with metastatic colorectal cancer: a JSMO-ESMO initiative endorsed by CSCO, KACO, MOS, SSO and TOS. *Ann Oncol* 2018;29:44–70.
13. Nishina T, Moriwaki T, Shimada M, Higashijima J, Sakai Y, Masuishi T, et al. Uracil-Tegafur and oral Leucovorin combined with bevacizumab in elderly patients (aged ≥ 75 years) with metastatic colorectal cancer: a Multicenter, phase II trial (joint study of bevacizumab, oral Leucovorin, and uracil-Tegafur in elderly patients [J-BLUE] study). *Clin Colorectal Cancer* 2016;15:236–42.
14. Mizushima T, Tamagawa H, Matsuda C, Murata K, Fukunaga M, Ota H, et al. Phase II study of oral Tegafur/uracil and Leucovorin plus bevacizumab as a first-line therapy for elderly patients with advanced or metastatic colorectal cancer. *Oncology* 2015;89:152–8.
15. Yoshida M, Muro K, Tsuji A, Hamamoto Y, Yoshino T, Yoshida K, et al. Combination chemotherapy with bevacizumab and S-1 for elderly patients with metastatic colorectal cancer (BASIC trial). *Eur J Cancer* 2015;51:935–41.
16. Rostoft S, O'Donovan A, Soubeyran P, Alibhai SMH, Hamaker ME. Geriatric assessment and Management in Cancer. *J Clin Oncol* 2021;39:2058–67.
17. Soto-Perez-de-Celis E, Li D, Yuan Y, Lau YM, Hurria A. Functional versus chronological age: geriatric assessments to guide decision making in older patients with cancer. *Lancet Oncol* 2018;19:e305–e16.

18. Flannery MA, Culakova E, Canin BE, Peppone L, Ramsdale E, Mohile SG. Understanding treatment tolerability in older adults with cancer. *J Clin Oncol* 2021;39:2150–63.
19. Moriwaki T, Sakai Y, Ishida H, Yamamoto Y, Endo S, Kuramochi H, et al. Phase II study of S-1 on alternate days plus bevacizumab in patients aged ≥ 75 years with metastatic colorectal cancer (J-SAVER). *Int J Clin Oncol* 2019;24:1214–22.
20. Kohne CH, Cunningham D, Di Costanzo F, Glimelius B, Blijham G, Aranda E, et al. Clinical determinants of survival in patients with 5-fluorouracil-based treatment for metastatic colorectal cancer: results of a multivariate analysis of 3825 patients. *Ann Oncol* 2002;13:308–17.
21. Chibaudel B, Bonnetain F, Tournigand C, Bengrine-Lefevre L, Teixeira L, Artru P, et al. Simplified prognostic model in patients with oxaliplatin-based or irinotecan-based first-line chemotherapy for metastatic colorectal cancer: a GERCOR study. *Oncologist* 2011;16:1228–38.
22. Song A, Eo W, Lee S. Comparison of selected inflammation-based prognostic markers in relapsed or refractory metastatic colorectal cancer patients. *World J Gastroenterol* 2015;21:12410–20.
23. Liu Z, Xu Y, Xu G, Baklaushev VP, Chekhonin VP, Peltzer K, et al. Nomogram for predicting overall survival in colorectal cancer with distant metastasis. *BMC Gastroenterol* 2021;21:103.
24. Ostwal V, Ramaswamy A, Bhargava P, Hatkhambkar T, Swami R, Rastogi S, et al. Cancer aging research group (CARG) score in older adults undergoing curative intent chemotherapy: a prospective cohort study. *BMJ Open* 2021;11:e047376.
25. Hurria A, Mohile S, Gajra A, Klepin H, Muss H, Chapman A, et al. Validation of a prediction tool for chemotherapy toxicity in older adults with cancer. *J Clin Oncol* 2016;34:2366–71.
26. Hurria A, Togawa K, Mohile SG, Owusu C, Klepin HD, Gross CP, et al. Predicting chemotherapy toxicity in older adults with cancer: a prospective multicenter study. *J Clin Oncol* 2011;29:3457–65.
27. Yamanaka T, Matsumoto S, Teramukai S, Ishiwata R, Nagai Y, Fukushima M. Safety evaluation of oral fluoropyrimidine S-1 for short- and long-term delivery in advanced gastric cancer: analysis of 3,758 patients. *Cancer Chemother Pharmacol* 2008;61:335–43.
28. Walko CM, Lindley C. Capecitabine: a review. *Clin Ther* 2005;27:23–44.
29. Gieschke R, Reigner B, Blesch KS, Steimer JL. Population pharmacokinetic analysis of the major metabolites of capecitabine. *J Pharmacokinet Pharmacodyn* 2002;29:25–47.
30. Hamaguchi T, Takashima A, Mizusawa J, Shimada Y, Nagashima F, Ando M, et al. A randomized phase III trial of mFOLFOX7 or CapeOX plus bevacizumab versus 5-FU/LV or capecitabine plus bevacizumab as initial therapy in elderly patients with metastatic colorectal cancer: JCOG1018 study (RESPECT). *J Clin Oncol* 2022;40:10.
31. Garcia MV, Agar MR, Soo WK, To T, Phillips JL. Screening tools for identifying older adults with cancer who may benefit from a geriatric assessment: a systematic review. *JAMA Oncol* 2021;7:616–27.
32. Decoster L, Van Puyvelde K, Mohile S, Wedding U, Basso U, Colloca G, et al. Screening tools for multidimensional health problems warranting a geriatric assessment in older cancer patients: an update on SIOG recommendations. *Ann Oncol* 2015;26:288–300.



Proportion attributable to contextual effects in general medicine: a meta-epidemiological study based on Cochrane reviews

Yusuke Tsutsumi ,^{1,2} Yasushi Tsujimoto,^{3,4} Aran Tajika,⁵ Kenji Omae,^{3,6} Tomoko Fujii,^{7,8} Akira Onishi,⁹ Yuki Kataoka,^{3,10} Morihiro Katsura,¹¹ Hisashi Noma,¹² Ethan Sahker,^{7,13} Edoardo Giuseppe Ostinelli,¹⁴ Toshi A Furukawa⁷

10.1136/bmjebm-2021-111861

► Additional supplemental material is published online only. To view, please visit the journal online (<http://dx.doi.org/10.1136/bmjebm-2021-111861>).

For numbered affiliations see end of article.

Correspondence to:

Dr Yusuke Tsutsumi, Kyoto University, Kyoto, Japan; tsutsumi.yusuke.84x@st.kyoto-u.ac.jp



© Author(s) (or their employer(s)) 2023. Re-use permitted under CC BY-NC. No commercial re-use. See rights and permissions. Published by BMJ.

To cite: Tsutsumi Y, Tsujimoto Y, Tajika A, et al. *BMJ Evidence-Based Medicine* 2023;**28**:40–47.

Abstract

Objectives Our objectives were to examine the magnitude of the proportion attributable to contextual effects (PCE), which shows what proportion of the treatment arm response can be achieved by the placebo arm across various interventions, and to examine PCE variability by outcome type and condition.

Design We conducted a meta-epidemiological study.

Setting We searched the Cochrane Database of Systematic Reviews with the keyword 'placebo' in titles, abstracts and keywords on 1 January 2020.

Participants We included reviews that showed statistically significant beneficial effects of the intervention over placebo for the first primary outcome.

Main outcome measures We performed a random-effects meta-analysis to calculate PCEs based on the pooled result of each included review, grouped by outcome type and condition. The PCE quantifies how much of the observed treatment response can be achieved by the contextual effects.

Public and patient involvement statement No patient or member of the public was involved in conducting this research.

Results We included 328 out of 3175 Cochrane systematic reviews. The results of meta-analyses showed that PCEs varied greatly depending on outcome type ($I^2=98\%$) or condition ($I^2=98\%$), but mostly lie between 0.40 and 0.95. Overall, the PCEs were 0.65 (95% CI 0.59 to 0.72) on average. Subjective outcomes were 0.50 (95% CI 0.41 to 0.59), which was significantly smaller than those of semiobjective (PCE 0.78; 95% CI 0.72 to 0.85) or objective outcomes (PCE 0.94; 95% CI 0.91 to 0.97).

Conclusions The results suggest that much of the observed benefit is not just due to the specific effect of the interventions. The specific effects of interventions may be larger for subjective outcomes than for objective or semiobjective outcomes. However, PCEs were exceptionally variable. When we evaluate the magnitude of PCEs, we should consider each PCE individually, for each condition, intervention and outcome in its context, to assess the importance of an intervention for each specific clinical setting.

WHAT IS ALREADY KNOWN ON THIS TOPIC

⇒ Although the proportion attributable to contextual effects (PCE) is highly important to interpreting the results of clinical trials and selecting the appropriate treatment in the clinical setting, a comprehensive review of PCEs among several outcome types and conditions was not yet available.

WHAT THIS STUDY ADDS

⇒ This study showed that the overall PCE was 0.65 (95% CI 0.59 to 0.72).
⇒ The PCE of subjective outcomes was 0.50 (95% CI 0.41 to 0.59), while that of semiobjective and objective outcomes were 0.78 (95% CI 0.72 to 0.85) and 0.94 (95% CI, 0.91 to 0.97), respectively.

HOW THIS STUDY MIGHT AFFECT RESEARCH, PRACTICE AND/OR POLICY

⇒ The results suggest that much of the observed benefits in clinical trials are actually due to factors other than specific intervention effects. A smaller PCE may indicate that the effect of interventions on subjective outcomes is larger than on different types of outcomes.
⇒ We should consider each PCE individually, for each condition, intervention and outcome in its context, to assess the importance of an intervention for each specific clinical setting.

Introduction

Placebo has long been used as a dummy treatment in control groups of randomised controlled trials (RCTs) to control for non-specific factors.^{1 2} Improvement seen in the intervention group (treatment response) can often be seen in the placebo group and is understood to be due to three contextual effects: the placebo effect, the natural course of the disease or regression to the mean.³ While the

nature and degree of the placebo effect itself have been controversial,^{4–6} assessing the amount of response due to contextual effects helps to explain the benefits specific to an intervention.

The proportion attributable to contextual effects (PCE) is a metric indicating what proportion of the treatment arm response can be achieved by the placebo arm. Response may be beneficial for a dichotomous outcome (eg, survival, remission) or a beneficial change for a continuous outcome (eg, reduction in pain, increase in quality of life (QoL)). Therefore, the PCE corresponds with the contextual effects (placebo effect +natural course +regression to the mean) divided by the intervention arm response (specific effect +placebo effect +natural course +regression to the mean). The PCE ranges from 0 to 1. A score of 0 means that none of the treatment response is due to the contextual effects. Conversely, a PCE score of 1 means that all of the treatment response is due to the contextual effects. A larger PCE reflects a larger contextual effect, or a smaller specific effect of the intervention.^{7–9}

An RCT usually focuses on the specific treatment effect, which is the difference in the outcome between the treatment arm and the placebo arm. However, in clinical practice, the overall treatment effect includes not only the specific treatment effect, but also the contextual effects. As a result, a treatment that did not show a large specific effect in an RCT, can still show a larger response in clinical practice than a treatment with large beneficial contextual effects. This phenomenon is called the Efficacy Paradox.¹⁰ Therefore, clinicians and patients should consider both the overall treatment effect and the PCE to interpret clinical trials properly and select appropriate treatments. A large PCE means that a large amount of response seen in patients receiving the treatment can also be seen in patients without receiving the active intervention. Some studies have shown that the PCE might reach 0.65–0.75.^{11, 12} However, there has been no systematic attempt to review PCEs across various current healthcare interventions.

In this study, we examine the magnitude of PCEs. This will inform how much of an intervention's beneficial effect can be achieved by the contextual effects. In addition, we evaluate PCE variability by outcome type and condition when contextual effects also show a beneficial effect. To achieve this, we systematically surveyed all relevant Cochrane reviews, calculated the PCEs in all fields of medicine, and compared them by the outcome, condition and degree of the certainty of evidence from existing reviews.

Methods

We followed the published reporting guideline for a meta-epidemiological study.¹³

Eligibility criteria

We included all systematic reviews (SRs) of randomised placebo-controlled trials published in the Cochrane Database of Systematic Reviews that showed statistically significant beneficial effects of the intervention over placebo in the first primary outcome. We regarded a two-tailed $p < 0.05$ as statistically significant. We excluded interventions whose efficacy is not established because it would be meaningless to examine PCEs for non-beneficial interventions. When there were multiple comparisons for the first primary outcome due to multiple intervention arms in a review, we selected the first comparison. We included reviews that reported a risk ratio (RR) or an OR for dichotomous outcomes. We excluded reviews reporting other effect sizes, such as HRs in survival analyses. For continuous outcomes, we were able to calculate PCE only when: (1) the meta-analysis reported change scores, (2) the weighted mean of both intervention and control arm showed the same direction of change and (3) larger changes

in the outcome equated to more beneficial changes. We excluded initial reviews that had been updated (ie, we included only the most recent version), reviews of studies other than placebo-controlled trials (eg, sham-controlled trials, non-RCTs, diagnostic test accuracy studies or prognostic studies), overviews of reviews and methodological reviews. We extracted the numerical data from the forest plot of the first meta-analysis. Therefore, we were obliged to exclude reviews that did not show the forest plot of their primary outcome.

Search strategy and study selection

We searched the Cochrane Database of Systematic Reviews with the keyword 'placebo' in titles, abstracts and keywords on 1 January 2020 and selected all the available reviews, regardless of the publication date. Two authors independently performed the initial screening of the titles and abstracts of all studies identified by the search and examined the potential eligibility for inclusion. After initial screening, the same authors assessed the eligibility based on a full-text review. Disagreements were resolved by discussion between the authors, with another author acting as an arbiter when necessary.

Data extraction

Two authors independently used a structured data extraction form to collect data from the included studies. Differences were resolved by consensus. We extracted the pooled RR, SE, and 95% CI when the review reported RR. We extracted the pooled OR, SE, 95% CI and the average control event rate (CER) when the review reported OR. When the review reported a mean difference (MD) of change scores, we extracted the change score and the number of participants for the intervention and placebo arms separately. When the review reported the standardised MD, we extracted the change score of the outcome, SE and the number of participants for the intervention and placebo arms separately.

In addition, we extracted the following information: the number of participants and trials in the meta-analysis of the first primary outcome, the sample size of intervention and placebo arms, outcome data type (dichotomous or continuous), outcome type, condition, intervention type (pharmacological or non-pharmacological), Cochrane review group and the Grading of Recommendations Assessment, Development and Evaluation (GRADE) category of the outcome.

We categorised outcome types and conditions following the categories used in previous studies.^{13–15} We modified the category of outcome types, in which we translated harmful outcomes into equivalent beneficial outcomes (eg, from mortality to survival).

We categorised outcome types as follows, following typologies used in the literature.^{14–16}

Objective outcome

Survival.

Semiobjective outcomes

No major morbidity events, improved obstetric outcomes, less resource use/shorter hospital stay, improved internal structure (structural outcome within the internal body such as radiograph outcomes), improved external structure (structural outcomes which can be externally observed such as eczema), improved biological markers, no unpleasant composite endpoint, no composite mortality/morbidity events, less drop-out from the treatment, no adverse events and others

Subjective outcomes

Pain relief, QoL improvement, mental health improvement, less consumption/satisfaction with care, cure of condition, no new signs of infection/disease and others

We categorised conditions as follows^{14–16}: cardiovascular, central nervous system/musculoskeletal, digestive system, infectious disease, mental health and behavioural conditions, obstetrics and gynaecology, respiratory disease, urogenital and others.

Statistical analyses

The definition of beneficial and harmful outcome measures

Some reviews used an outcome measure in which the higher number of events is better (eg, survival), while others examined the same outcome but used the opposite measure in which the lower number of events is better (eg, death). We defined the outcome measure in which the higher number of events is better as a beneficial outcome and the outcome measure in which the lower number of events is better as a harmful outcome.

Calculation of the CE for each intervention over placebo

We defined and calculated the PCE to designate how much of the beneficial outcome observed in the intervention group is realised in the placebo group. We assumed the independence between the specific treatment effect and the contextual effects.

Beneficial dichotomous outcomes

When the meta-analysis reported an RR for a beneficial outcome (RR > 1 expected), we defined the PCE as follows:

$$PCE = \frac{\text{Control event rate (CER)}}{\text{Experimental event rate (EER)}} \quad (1)$$

where the CER refers to the proportion of outcome events in the placebo group, and the experimental event rate (EER) refers to the proportion of outcome events in the intervention group. We calculated PCE as the inverse of the pooled RR.

When the meta-analysis reported an OR, we first converted the OR to an RR using the average CER obtained in the meta-analysis:

$$RR = \frac{OR}{1 - CER \times (1 - OR)} \quad (2)$$

PCE was then calculated using the RR according to the formula (1).

Harmful dichotomous outcomes

When the meta-analysis reported an RR for a harmful outcome, we converted the RR to an OR using the CER:

$$OR = \frac{RR \times (CER - 1)}{RR \times CER - 1} \quad (3)$$

Then we converted the OR of harmful outcomes to that of beneficial outcomes. For example, ORs for mortality were converted to ORs for survival, taking the inverse of the OR. Finally, we calculated the PCE using formulae (2) and (1).

When the meta-analysis reported an OR, we took the inverse of the OR to represent the OR for a beneficial outcome. Then we calculated the PCE using formulae (2) and (1).

For RRs and ORs, we calculated the 95% CI and SEs of the PCE using a formula for the variance estimators of log(RR) and log(OR), respectively. For dichotomous outcomes, the PCE means that the probability, given an individual had a positive outcome after treatment, would also have had a positive outcome after placebo.

Continuous outcomes

We define the PCE for the continuous outcome as follows in accordance with a previous study.⁷

$$PCE = \frac{\text{the mean change score of the placebo arm}}{\text{the mean change score of the intervention arm}} \quad (4)$$

In this study, we calculated the mean change score of each arm based on multiple studies rather than a single study. Therefore, we first calculated the standardised weighted change score means for both the intervention and placebo arms by meta-analysis, using the DerSimonian-Laird method for continuous outcomes.¹⁷

The PCE was then calculated as:

$$PCE = \frac{\text{weighted standardized mean change score of the placebo arm}}{\text{weighted standardized mean change score of the intervention arm}} \quad (5)$$

The conditions to calculate PCEs by formula (5) were that both groups showed the same direction of change (same positive or negative direction), and the change in the treatment group was greater than the change in the placebo group. Therefore, we excluded Cochrane reviews when the weighted mean of the intervention and control arms did not show the same direction of change or when the weighted standardised mean change score of the placebo arm was greater than that of the intervention arm.

To construct the CI of PCE, the ordinary Wald-type CI is unsuitable for the original scale because PCE is a ratio measure and usually has an asymmetric sample distribution. Thus, we adopted the approximate CI for log-transformed PCE. Using the Delta method, we obtained the SE estimator of the log(PCE) as follows¹⁸:

$$SE [\log (PCE)] = \sqrt{\frac{SE_{\text{intervention}}^2}{WSM_{\text{intervention}}^2} + \frac{SE_{\text{placebo}}^2}{WSM_{\text{placebo}}^2}} \quad (6)$$

where SE [log(PCE)] was the SE of log(PCE), SE_{intervention} and SE_{placebo} represent the SE of the weighted change score means of the intervention and placebo arms, respectively. WSM_{intervention} and WSM_{placebo} were the weighted standardised change score means of the intervention and placebo arms, respectively. The weighted standardised means were defined as pooled summaries of standardised mean change scores from the intervention and placebo arms of individual studies. The weights were defined by the corresponding meta-analysis methods. We could then obtain the Wald-type 95% CI for log(PCE) by the conventional normal approximation.¹⁹ The 95% CI of PCE can be calculated by back-transformation (exponential transformation) of the confidence limits.

Meta-analyses of PCEs

We pooled the logarithm-transformed PCEs for each outcome type, condition and GRADE category, using the DerSimonian-Laird method.¹⁷ We performed all analyses using meta (V.4.15–1) package of R V.4.0.0.^{20 21}

Changes from the protocol

The study protocol was uploaded to the Department of Health Promotion and Human Behaviour website, Kyoto University Graduate School of Medicine/School of Public Health (<http://ebmh.med.kyoto-u.ac.jp/r-meta.html>), attached as online supplemental file 1) on 4 September 2018. Changes to the protocol are listed in online supplemental file 2, and all were minor.

Patient and public involvement

No patient or member of the public was involved in conducting this research.

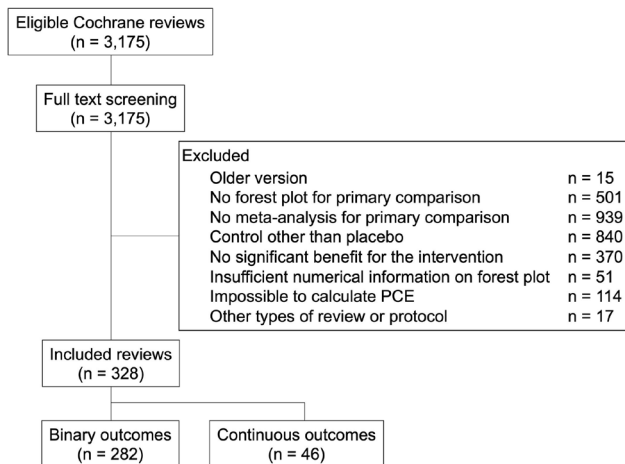


Figure 1 The flow chart for study selection. PCE, proportion attributable to contextual effect.

Results

Selected studies

Figure 1 shows the flowchart for study selection. The initial search identified 3175 Cochrane reviews, from which we excluded 2847 for reasons seen in figure 1. The final selection included 328 reviews. Of these, 282 reviews represent 1755 trials, with 2 625 184 participants reporting dichotomous outcomes. The remaining 46 reviews represent 259 trials, with 42 156 participants reporting continuous outcomes.

Over half of the reviews were published within the past 10 years. Approximately 70% of the included reviews reported subjective outcomes. Mental health and behaviour conditions was the most popular condition (table 1). Online supplemental file 3 shows all included SRs and their outcomes, conditions and PCEs calculated from the results of the meta-analysis from each review. For example, Bennett *et al*²² examined the effect of tranexamic acid on mortality for upper gastrointestinal bleeding. They reported an RR of 0.6. The CER for mortality was 8.4% and converted to a positive outcome CER for survival at 91.6%. The EER of survival was 95.0%. Dividing the CER of survival by the EER of survival gives a PCE of 0.96. By contrast, Derry *et al*²³ examined the effect of ibuprofen plus codeine for acute postoperative pain and showed an RR of 4.1. Their CER for a 50% reduction of maximum pain was 18.0%, and the EER was 64.0%. Thus, the calculated PCE was 0.24.

PCEs by outcome types, conditions and GRADE categories

Outcome types

We first pooled PCEs across all outcome types, including both dichotomous and continuous outcomes (figure 2, table 2). The pooled PCE across all outcomes was 0.65 (95% CI 0.59 to 0.72). When the outcome types were divided into subgroups, objective outcomes showed a PCE of 0.94 (95% CI 0.91 to 0.97), which was higher than that of semiobjective outcomes (PCE 0.78; 95% CI 0.72 to 0.85, $I^2=90\%$) and subjective outcomes (PCE 0.50; 95% CI 0.41 to 0.59, $I^2=99\%$). The PCE of typical patient-reported outcomes such as pain, QoL, and mental health outcomes ranged between 0.44 and 0.74.

We next pooled PCEs across all outcome types when the outcomes were dichotomous (online supplemental figure S1) or continuous (online supplemental figure S2).

Conditions

Figure 3 shows the PCE by condition. PCEs ranged widely from 0.40 in 'anaesthesia' to 0.89 in 'cardiovascular disease' ($I^2=98\%$). Online supplemental figure S3 and S4 present the results for dichotomous and continuous outcomes separately.

Grade categories

Among 156 Cochrane reviews that had reported a GRADE in the summary of findings table, the PCEs did not appear to be appreciably influenced by the certainty of evidence (online supplemental figure S5, $I^2=54\%$). Online supplemental figures S6 and S7 present these results for dichotomous and continuous outcomes separately.

Discussion

Key findings

Based on 328 Cochrane reviews representing 2014 trials and 2 667 340 participants, the overall PCE for various interventions in contemporary medicine was 0.65 (0.59 to 0.72). PCEs ranged from 0.28 to 0.94. The subjective outcomes showed lower PCEs than objective or semiobjective outcomes. They also varied depending on the condition. GRADE ratings did not appear to influence PCEs. These results suggest that PCEs should be considered according to the outcome type and condition when interpreting study results and determining the importance of interventions.

Comparisons with the previous literature

As previously stated, there is no study examining the PCE of several semiobjective outcomes. In our study, PCEs of the objective and semisubjective outcomes were mostly larger than 0.70. Several studies have reported PCEs for patient-reported outcomes in the literature. One study revealed a PCE of 0.72 for pain among burning mouth syndrome patients,²⁴ while another showed a PCE of 0.82 for antidepressant trials for depression.²⁵ When we examined PCEs for various patient-reported outcomes and conditions, the average PCE seemed to lie in the medium range between 0.40 and 0.75, which was lower than those reported in previous studies. The effects of the intervention on the subjective outcomes may be larger than those for the other types of outcomes. Previous studies suggest larger placebo effects for subjective outcomes than for objective outcomes.^{6 26} These findings are in line with the current findings of contextual effects. This is because, regardless of the magnitude of the placebo effect, PCEs represent the proportion of the contextual effects of the improvements observed in the active intervention arm.

Clinical interpretations

The contextual effects have been known to contribute to the treatment response.^{10 27} However, the magnitude of PCEs had not been examined in detail or quantified in the literature until this study. Our study presented the average PCEs across outcome types and conditions.

We found that subjective outcomes, including typical patient-reported outcomes such as pain, QoL, and mental health outcomes, showed PCEs of 0.44–0.74. This may reflect the fact that the specific intervention effect seen in subjective outcomes are likely to be of moderate magnitude and clinically important. On the other hand, 'hard' outcomes, including survival or morbidity events, showed PCEs above 0.80 or even 0.90. We assume PCEs seen in objective and semiobjective outcomes may reflect the fact that the natural disorder course plays a strong role in those outcomes. It would

Table 1 Characteristics of included studies

		Dichotomous outcome (n=282)	Continuous outcome (n=46)
No of included primary studies per meta-analysis, median (IQR)		4 (2–7)	4 (3–7)
No of included participants per meta-analysis, median (IQR)		557 (283–1490)	511 (229–1094.5)
Years of publication (%)	1998–2000	14 (5.0)	0 (0)
	2001–2005	27 (9.6)	10 (21.7)
	2006–2010	57 (20.2)	7 (15.2)
	2011–2015	101 (35.8)	12 (26.1)
	2016–2019	83 (29.4)	17 (37.0)
Outcome type (%)			
Objective outcome			
	Survival	7 (2.5)	0 (0)
Semiobjective outcomes			
	No major morbidity event	14 (5.0)	0 (0)
	Less drop-outs from the treatment	11 (3.9)	0 (0)
	Improved obstetric outcomes	9 (3.2)	0 (0)
	Less resource use/shorter hospital stay	9 (3.2)	0 (0)
	Improved internal structure	5 (1.8)	2 (4.3)
	Improved biological markers	4 (1.4)	6 (13.0)
	Improved external structure	4 (1.4)	1 (2.2)
	No unpleasant composite endpoint	4 (1.4)	0 (0)
	No adverse events	3 (1.1)	0 (0)
	No composite mortality/morbidity events	0 (0)	0 (0)
	Others (semiobjective)	1 (0.4)	6 (13.0)
Subjective outcomes			
	Pain relief	72 (25.5)	9 (19.6)
	Cure of condition	71 (25.2)	4 (8.7)
	Mental health outcomes improvement	35 (12.4)	12 (26.1)
	No new signs of infection/disease	17 (6.0)	0 (0.0)
	Quality of life	13 (4.6)	6 (13.0)
	Less consumption, satisfaction with care	1 (0.4)	0 (0.0)
	Others (Subjective)	2 (0.7)	0 (0.0)
Conditions (%)			
	Mental health and behavioural conditions	56 (19.9)	12 (26.1)
	Anaesthesia	48 (17.0)	3 (6.5)
	Central nervous system/ musculoskeletal	47 (16.7)	7 (15.2)
	Digestive system	29 (10.3)	0 (0)
	Infectious disease	26 (9.2)	1 (2.2)
	Respiratory disease	19 (6.7)	3 (6.5)
	Obstetrics and gynaecology	16 (5.7)	2 (4.3)
	Cardiovascular	12 (4.3)	7 (15.2)
	Urogenital	7 (2.5)	4 (8.7)
	Others	22 (7.8)	7 (15.2)
GRADE category (%)*	High	35 (25.9)	2 (9.5)
	Moderate	53 (39.3)	5 (23.8)
	Low	36 (26.7)	13 (61.9)
	Very low	11 (8.1)	1 (4.8)

*A total of 147 dichotomous outcomes and 25 continuous outcomes did not report the GRADE category in their summary of findings table.
GRADE, Grading of Recommendations Assessment, Development and Evaluation.

be relatively difficult for an intervention to show large effects in these ‘hard’ outcomes.

The pooled estimates are approximate indicators of how much PCE we can expect for each subgroup. However, the average PCEs are only a rough guide, and a starting point for clinical evaluation of an intervention effect. Generally, the higher the PCE, the greater the contextual effects. Therefore, watchful waiting or careful observation with follow-ups may be a reasonable choice,

rather than an active intervention, because much of the benefit can be expected from the placebo intervention. However, this general judgement should be tempered by the gravity of the outcome (eg, a small decrease in death may be as valuable as or even more valuable than a large decrease in some non-life-threatening consequences) and the burdens (side-effects and costs) of the alternative treatments. Moreover, our study revealed that PCEs were highly heterogeneous. We must consider the individual

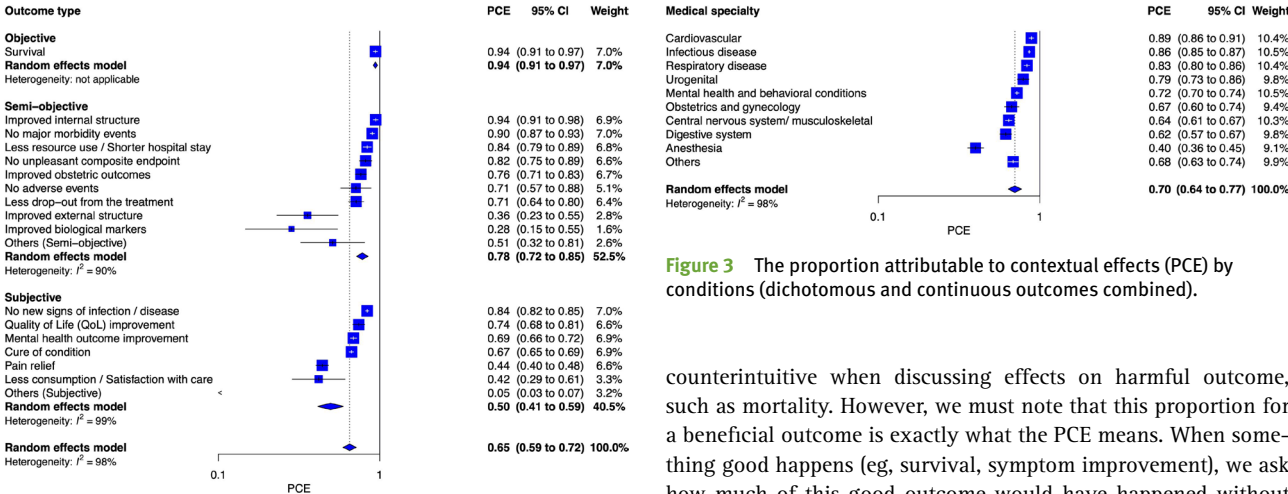


Figure 3 The proportion attributable to contextual effects (PCE) by conditions (dichotomous and continuous outcomes combined).

counterintuitive when discussing effects on harmful outcome, such as mortality. However, we must note that this proportion for a beneficial outcome is exactly what the PCE means. When something good happens (eg, survival, symptom improvement), we ask how much of this good outcome would have happened without the intervention (ie, it can be explained by the contextual effects). Second, we were unable to calculate PCE when the intervention showed improvement from baseline while the placebo group showed deterioration, or when the intervention showed deterioration while the placebo group showed greater deterioration. This may have led to overestimation or underestimation of PCE. This was inevitable, given the definition of PCE above. We wanted to quantify when something good happens following treatment and how much of that good could happen without the intervention. Third, there is intrinsic heterogeneity among outcomes belonging to the same type (eg, morbidity event) or used in the same condition (eg, respiratory disease). Each outcome may have different clinical importance depending on the context. Because PCE is a relative measure, the CER may also influence the absolute benefit. In other words, the absolute benefit is larger for events with large CERs, and smaller for events with smaller CERs for a given PCE. Therefore, each PCE of an intervention must be interpreted in its specific context and, ultimately, under each patient's preferences and values. However, it is scientifically meaningful to know the overall averages even when the apparent heterogeneity may be high. Fourth, measurement errors (random errors) are larger for subjective outcomes than semiobjective or objective outcomes. How such measurement errors may have contributed to the estimates of PCEs is not straightforward. However, by pooling across SRs, the overall averages would be less affected by such random errors. Fifth, our study calculated PCEs by outcome types and conditions independently. PCE is highly dependent on both the condition and outcome. For example, the PCE for pain in 'cardiovascular' may be larger than that in 'mental health and behavioural conditions' because the pain in cardiovascular is more likely

condition, intervention and outcome when we evaluate the clinical significance of the PCE.

We also found that PCEs were diverse over several conditions, partly reflecting outcome types commonly used in each condition. For example, the PCEs of cardiovascular disease, infectious disease, and respiratory disease were over 0.80. Trials examining these conditions usually select objective or semiobjective outcomes such as survival, major morbidity, composite endpoints or severity of symptoms as the primary outcome. In fact, 30 of 68 included reviews among these conditions reported objective or semiobjective outcomes. On the other hand, conditions with subjective main outcomes, such as pain, mental health or behaviour conditions, showed moderate PCEs.

Additionally, we found no remarkable diversity of PCEs depending on the GRADE category. However, over half of the included reviews did not report the GRADE category with a summary of findings table of their first primary outcome, which led to the loss of power in this analysis. We also found that out of 328 Cochrane reviews, 282 reported a dichotomous outcome, such as mortality, as their first primary outcome, and we were only able to identify 46 Cochrane reviews with a primary continuous outcome reported first.

Strengths and limitations

There are some weaknesses to our study. First, we calculated a PCE as the proportion of the contextual effects over the intervention response for a beneficial outcome. This might appear

Table 2 The proportion attributable to contextual effects by outcome type

		Outcome category		All
		Dichotomous	Continuous	
Outcome type	Objective	0.94 (0.91 to 0.97) (NA)	NA	0.94 (0.91 to 0.97) (NA)
	Semiobjective	0.81 (0.75 to 0.87) (0.64 to 1.00)	0.54 (0.38 to 0.77) (0.15 to 1.00)	0.78 (0.72 to 0.85) (0.60 to 1.00)
	Subjective	0.49 (0.41 to 0.59) (0.26 to 0.94)	0.60 (0.54 to 0.66) (0.46 to 0.79)	0.50 (0.41 to 0.59) (0.26 to 0.94)
All		0.67 (0.61 to 0.74) (0.45 to 0.99)	0.59 (0.53 to 0.66) (0.47 to 0.75)	0.65 (0.59 to 0.72) (0.44 to 0.97)
(Parentheses) show 95% CIs, and (brackets) show 95% prediction intervals.				
NA, not applicable.				

due to an organic cause. Finer subgroup analyses examining their interactions were impossible in the current study, as we had too many subgroups, but this would be desirable for future research. Finally, the specific and contextual effects are not independent of each other but may interact with each other when, for example, the side effects of the intervention may enhance the non-specific effects.²⁸ Thus, the same outcome for the same disease may show different PCEs depending on the intervention. We did not have enough variability in the interventions in our dataset to appreciate such interactions. Further research would be warranted to clarify the nature and degree of the relationships between specific effects and contextual effects.

Our study also has several strengths. First, to the best of our knowledge, this is the first study to examine PCEs comprehensively across outcome types and conditions. Second, our study is based on Cochrane reviews which are considered the best resources of evidence. We searched all the Cochrane reviews that had reported the results of head-to-head meta-analyses of interventions against placebo. We pooled these meta-analyses to calculate the PCEs by outcome type, condition and GRADE category.

Conclusions

In conclusion, our study showed that the overall PCE was 0.65 (95% CI 0.59 to 0.72). PCEs were smaller for subjective outcomes than for objective or semiobjective outcomes. The results suggest that much of the observed benefit is actually due to factors including the placebo effect, the natural course of the disease, and regression to the mean, rather than just the specific effect of the interventions. Specific effects of interventions may be larger for subjective than for objective or semiobjective outcomes. However, PCEs were exceptionally variable. When we evaluate the magnitude of PCEs, we should consider each PCE individually, for each condition, intervention and outcome in its context, to assess the importance of an intervention for each specific clinical setting.

Author affiliations

- ¹Human Health Sciences, Kyoto University Graduate School of Medicine, Kyoto, Japan
- ²Department of Emergency Medicine, National Hospital Organization Mito Medical Center, Ibaraki, Japan
- ³Department of Healthcare Epidemiology, Kyoto University Graduate School of Medicine/ School of Public Health, Kyoto, Japan
- ⁴Department of Nephrology and Dialysis, Kyoritsu Hospital, Kawanishi, Japan
- ⁵Department of Psychiatry, Kyoto University Hospital, Kyoto, Japan
- ⁶Department of Innovative Research and Education for Clinicians and Trainees (DiRECT), Fukushima Medical University Hospital, Fukushima, Japan
- ⁷Department of Health Promotion and Human Behavior, Kyoto University Graduate School of Medicine / School of Public Health, Kyoto, Japan
- ⁸Intensive Care Unit, Jikei University Hospital, Tokyo, Japan
- ⁹Department of Rheumatology and Clinical Immunology, Kobe University Graduate School of Medicine, Hyogo, Japan
- ¹⁰Hospital Care Research Unit/ Department of Respiratory Medicine, Hyogo Prefectural Amagasaki General Medical Center, Hyogo, Japan
- ¹¹Department of Surgery, Okinawa Chubu Hospital, Okinawa, Japan
- ¹²Department of Data Science, The Institute of Statistical Mathematics, Tokyo, Japan
- ¹³Population Health and Policy Research Unit, Medical Education Center, Kyoto University Graduate School of Medicine, Kyoto, Japan
- ¹⁴Oxford Health NHS Foundation Trust, Warneford Hospital /Department of Psychiatry, University of Oxford, Oxford, UK

Contributors YTsut, YTsuj, AT and TAF developed the conception and design of the research. YTsut and TAF are fully

responsible for writing the protocol. YTsut, YTsuj, AT, KO, TF, AO, YK, MK, ES, EGO extracted the data. YTsut analysed the data. HN supervised the statistical analyses. TAF supervised the research. All authors contributed to draft the manuscript and gave final approval of the manuscript before submission. TAF is the guarantor of the study.

Funding The authors have not declared a specific grant for this research from any funding agency in the public, commercial or not-for-profit sectors.

Competing interests None declared.

Patient and public involvement Patients and/or the public were not involved in the design, or conduct, or reporting, or dissemination plans of this research.

Patient consent for publication Not applicable.

Provenance and peer review Not commissioned; externally peer reviewed.

Data availability statement All data relevant to the study are included in the article or uploaded as online supplemental information.

Supplemental material This content has been supplied by the author(s). It has not been vetted by BMJ Publishing Group Limited (BMJ) and may not have been peer-reviewed. Any opinions or recommendations discussed are solely those of the author(s) and are not endorsed by BMJ. BMJ disclaims all liability and responsibility arising from any reliance placed on the content. Where the content includes any translated material, BMJ does not warrant the accuracy and reliability of the translations (including but not limited to local regulations, clinical guidelines, terminology, drug names and drug dosages), and is not responsible for any error and/or omissions arising from translation and adaptation or otherwise.

Open access This is an open access article distributed in accordance with the Creative Commons Attribution Non Commercial (CC BY-NC 4.0) license, which permits others to distribute, remix, adapt, build upon this work non-commercially, and license their derivative works on different terms, provided the original work is properly cited, appropriate credit is given, any changes made indicated, and the use is non-commercial. See: <http://creativecommons.org/licenses/by-nc/4.0/>.

ORCID iD

Yusuke Tsutsumi <http://orcid.org/0000-0002-9160-0241>

References

- 1 Beecher HK. The powerful placebo. *J Am Med Assoc* 1955;159:1602–6.
- 2 Blease CR, Bishop FL, Kaptschuk TJ. Informed consent and clinical trials: where is the placebo effect? *BMJ* 2017;356:j463.
- 3 Kirsch I. The placebo effect revisited: lessons learned to date. *Complement Ther Med* 2013;21:102–4.
- 4 Espay AJ, Norris MM, Eliassen JC, *et al*. Placebo effect of medication cost in Parkinson disease: a randomized double-blind study. *Neurology* 2015;84:794–802.
- 5 Kaptschuk TJ, Kelley JM, Conboy LA, *et al*. Components of placebo effect: randomised controlled trial in patients with irritable bowel syndrome. *BMJ* 2008;336:999–1003.
- 6 Hróbjartsson A, Gøtzsche PC. Placebo interventions for all clinical conditions. *Cochrane Database Syst Rev* 2010;1:CD003974.
- 7 Zou K, Wong J, Abdullah N, *et al*. Examination of overall treatment effect and the proportion attributable to contextual effect in osteoarthritis: meta-analysis of randomised controlled trials. *Ann Rheum Dis* 2016;75:1964–70.
- 8 Zhang W, Doherty M. Efficacy paradox and proportional contextual effect (PCE). *Clin Immunol* 2018;186:82–6.

- 9 Zhang W, Zou K, Doherty M. Placebos for Knee Osteoarthritis: Reaffirmation of "Needle Is Better Than Pill". *Ann Intern Med* 2015;163:392–3.
- 10 Walach H. Placebo Effects in Complementary and Alternative Medicine: The Self-Healing Response. In: Colloca L, Arve MA, Meissner K, eds. *Placebo and pain*. academic press. Elsevier, 2013: 189–202.
- 11 Kirsch I, Sapirstein G. Listening to Prozac but hearing placebo: a meta-analysis of antidepressant medication. *Prev Treat* 1998;1:2a.
- 12 Jonas WB, Crawford C, Colloca L, et al. To what extent are surgery and invasive procedures effective beyond a placebo response? A systematic review with meta-analysis of randomised, sham controlled trials. *BMJ Open* 2015;5:e009655.
- 13 Murad MH, Wang Z. Guidelines for reporting meta-epidemiological methodology research. *Evid Based Med* 2017;22:139–42.
- 14 Davey J, Turner RM, Clarke MJ, et al. Characteristics of meta-analyses and their component studies in the Cochrane database of systematic reviews: a cross-sectional, descriptive analysis. *BMC Med Res Methodol* 2011;11:160.
- 15 Rhodes KM, Turner RM, Higgins JPT. Predictive distributions were developed for the extent of heterogeneity in meta-analyses of continuous outcome data. *J Clin Epidemiol* 2015;68:52–60.
- 16 Turner RM, Davey J, Clarke MJ, et al. Predicting the extent of heterogeneity in meta-analysis, using empirical data from the Cochrane database of systematic reviews. *Int J Epidemiol* 2012;41:818–27.
- 17 DerSimonian R, Laird N. Chapter 10: meta-analysis in clinical trials. *Controlled Clinical Trials* 1986;7:177–88.
- 18 Oehlert GW. A note on the delta method. *Am Stat* 1992;46:27–9.
- 19 Cox DR, Hinkley DV, Statistics T. 1st ED. *London. Chapman and Hall* 1974.
- 20 Balduzzi S, Rücker G, Schwarzer G. How to perform a meta-analysis with R: a practical tutorial. *Evid Based Ment Health* 2019;22:153–60.
- 21 R Core Team. *R: a language and environment for statistical computing*. Vienna, Austria: R Foundation for Statistical Computing, 2020.
- 22 Bennett C, Klingenberg SL, Langholz E, et al. Tranexamic acid for upper gastrointestinal bleeding. *Cochrane Database Syst Rev* 2014;CD006640.
- 23 Derry S, Karlin SM, Moore RA. Single dose oral ibuprofen plus codeine for acute postoperative pain in adults. *Cochrane Database Syst Rev* 2015;2:CD010107.
- 24 Kuten-Shorrer M, Kelley JM, Sonis ST, et al. Placebo effect in burning mouth syndrome: a systematic review. *Oral Dis* 2014;20:e1–6.
- 25 Kirsch I, Deacon BJ, Huedo-Medina TB, et al. Initial severity and antidepressant benefits: a meta-analysis of data submitted to the food and drug administration. *PLoS Med* 2008;5:e45.
- 26 Hróbjartsson A, Gøtzsche PC. Is the placebo powerless? an analysis of clinical trials comparing placebo with no treatment. *N Engl J Med* 2001;344:1594–602.
- 27 Shaibani A, Frisaldi E, Benedetti F. Placebo response in pain, fatigue, and performance: possible implications for neuromuscular disorders. *Muscle Nerve* 2017;56:358–67.
- 28 Flaten MA, Simonsen T, Olsen H. Drug-Related information generates placebo and nocebo responses that modify the drug response. *Psychosom Med* 1999;61:250–5.

Article

Individual Evaluation of the Common Extensor Tendon and Lateral Collateral Ligament Improves the Severity Diagnostic Accuracy of Magnetic Resonance Imaging for Lateral Epicondylitis

Kazuhiro Ikeda ^{1,2,*}, Takeshi Ogawa ³, Akira Ikumi ², Yuichi Yoshii ⁴, Sho Kohyama ¹, Reimi Ikeda ⁵ and Masashi Yamazaki ²

¹ Department of Orthopedic Surgery, Kikkoman General Hospital, Noda 278-0005, Chiba, Japan; sho_kohyama_1025@tsukuba-seikei.jp

² Department of Orthopedic Surgery, Faculty of Medicine, University of Tsukuba, Tsukuba 305-8577, Ibaraki, Japan; ikumi@tsukuba-seikei.jp (A.I.); masashiy@tsukuba-seikei.jp (M.Y.)

³ Department of Orthopedic Surgery, Mito Medical Center, Mito 311-3193, Ibaraki, Japan; ogawat@tsukuba-seikei.jp

⁴ Department of Orthopedic Surgery, Tokyo Medical University Ibaraki Medical Center, Ami 300-0395, Ibaraki, Japan; yyoshii@tsukuba-seikei.jp

⁵ Department of Orthopedic Surgery, Moriya Daiichi General Hospital, Moriya 302-0102, Ibaraki, Japan; r.ikeda0418@tsukuba-seikei.jp

* Correspondence: ikdkzhr1129.med@gmail.com; Tel.: +81-09074199769



Citation: Ikeda, K.; Ogawa, T.; Ikumi, A.; Yoshii, Y.; Kohyama, S.; Ikeda, R.; Yamazaki, M. Individual Evaluation of the Common Extensor Tendon and Lateral Collateral Ligament Improves the Severity Diagnostic Accuracy of Magnetic Resonance Imaging for Lateral Epicondylitis. *Diagnostics* **2022**, *12*, 1871. <https://doi.org/10.3390/diagnostics12081871>

Academic Editor: Antonio Barile

Received: 1 July 2022

Accepted: 29 July 2022

Published: 2 August 2022

Publisher's Note: MDPI stays neutral with regard to jurisdictional claims in published maps and institutional affiliations.



Copyright: © 2022 by the authors. Licensee MDPI, Basel, Switzerland. This article is an open access article distributed under the terms and conditions of the Creative Commons Attribution (CC BY) license (<https://creativecommons.org/licenses/by/4.0/>).

Abstract: The effectiveness of magnetic resonance imaging for diagnosing lateral epicondylitis severity is controversial. We aimed to verify whether individual evaluations of the common extensor tendon and lateral collateral ligament would improve the severity diagnostic accuracy of magnetic resonance imaging for lateral epicondylitis. We obtained coronal images of the lateral elbow in three groups: healthy, clinically mild, and clinically severe. We used our scoring system for evaluation using combined and individual methods. We developed the receiver operating characteristic curve for diagnosis using the scores of the healthy and mild groups and that for severity diagnosis using the scores of the mild and severe groups. The scores, in decreasing value, were those of the severe, mild, and healthy groups, with a significant difference in both methods. The curve for diagnosis showed an area under the curve of 0.85 for the combined evaluation and 0.89 for the individual evaluation, without a significant difference between the methods ($p = 0.23$). The curve for severity diagnosis showed an area under the curve of 0.69 for combined and 0.81 for individual evaluation, with a significant difference between the methods ($p = 0.046$). Individual evaluation of the common extensor tendon and lateral collateral ligament improved the severity diagnostic accuracy of lateral epicondylitis.

Keywords: lateral epicondylitis; magnetic resonance imaging; severity diagnosis; diagnostic accuracy; MRI; high-resolution MRI

1. Introduction

Lateral epicondylitis (LE) is tendinopathy of the common extensor tendon (CET) of the forearm [1,2], with an estimated prevalence of 1.1–4.9% in the general population [3–6]. Recent studies reported that the lateral collateral ligament (LCL) of the elbow was also injured along with the CET in LE [7–9].

Imaging studies can detect this degeneration and damage to the CET/LCL complex; ultrasonography and magnetic resonance imaging (MRI) are used in daily examinations. Ultrasonography depicts edematous changes and degeneration at the CET/LCL complex as hypointense changes or thickening, with a sensitivity rate of 64% and specificity rate of

82% [10]. However, the accuracy of ultrasonography depends on the examiner's experience, resulting in low inter-examiner reliability [11]. The true value of ultrasonography lies in its simultaneous use in diagnosis and treatment, rather than its diagnostic ability alone. Ultrasonography is used as an essential tool for LE in accurate injection therapy and percutaneous needling [12–14].

Meanwhile, the validity of MRI for LE has been controversial. MRI of patients with LE shows high-signal changes in the CET/LCL complex reflecting degeneration or rupture [7,15,16]. Due to its excellent imaging quality, the inter-observer reliability is high [7,15]. However, the diagnosis of LE was based solely on physical examination findings [17,18]. MRI was only a supplemental examination for patients who had not responded to conservative treatment [1,17,19]. Although MRI is performed to diagnose pathogenesis and severity, in addition, MRI reflects asymptomatic structural abnormalities and degeneration [20,21]. Because of this low specificity, some studies have reported a negative relationship between MRI findings and clinical severity [22,23]. Conversely, more recent studies have reported positively, as MRI resolution has improved [7,15]. Despite such conflicting results, comparing the literature has proven difficult because there is no method for standard quantitative evaluation. For example, some papers evaluate the CET and the LCL together [23], while others evaluate them individually [7,15]. Furthermore, no studies have demonstrated the clinical validity for their MRI scoring. As a clinical indicator for LE, the validity of MRI remained unknown.

Based on these findings, we felt the need to demonstrate the clinical validity of MRI in the diagnosis of LE. We hypothesized that individual evaluation of the CET and the LCL would contribute to the accuracy of the assessment of severity. This study aimed to verify this hypothesis using high-resolution MRI.

2. Materials and Methods

2.1. Study Design and Participants

The study protocol conforms to the principles outlined in the 1964 Declaration of Helsinki. The study was approved by the institutional review boards of the institutions involved in this study: Mito Kyodo General Hospital (Study Number: 16–25, approved 7 September 2016) and Takahagi Kyodo General Hospital (Study Number: 10, approved 3 March 2021). We obtained written informed consent from all participating patients.

This was a case–control study. The inclusion criteria were LE patients with high-resolution MRI in our hospital and healthy adults without any history of elbow disorder. Exclusion criteria were a history of elbow trauma, elbow osteoarthritis (Kellgren–Lawrence classification 2 or higher), osteochondritis dissecans of the humeral capitellum, and rheumatoid arthritis. Our medical database identified 366 LE patients diagnosed from January 2013 to December 2020. We excluded 258 patients who did not undergo MRI, 7 patients with inappropriate MRI, and 1 patient with rheumatoid arthritis. We reviewed the electronic medical records of the remaining 100 candidates and classified them according to their clinical severity at the time of MRI; patients with a Nirschl phase rating scale of III or IV [18] were assigned to the clinically mild group (M group), and those with a score of V to VII were assigned to the clinically severe group (S group). We included 100 LE patients, of whom 41 constituted the M group and 59 the S group. Moreover, we included 30 volunteers for the healthy group (H group). The volunteers were medical coworkers in our hospital, and we selected them to match the LE patients in gender and age. The subjects comprised a total of 130 cases (median age, 49 years; age range, 23–78; 64 males, 66 females) (Figure 1).

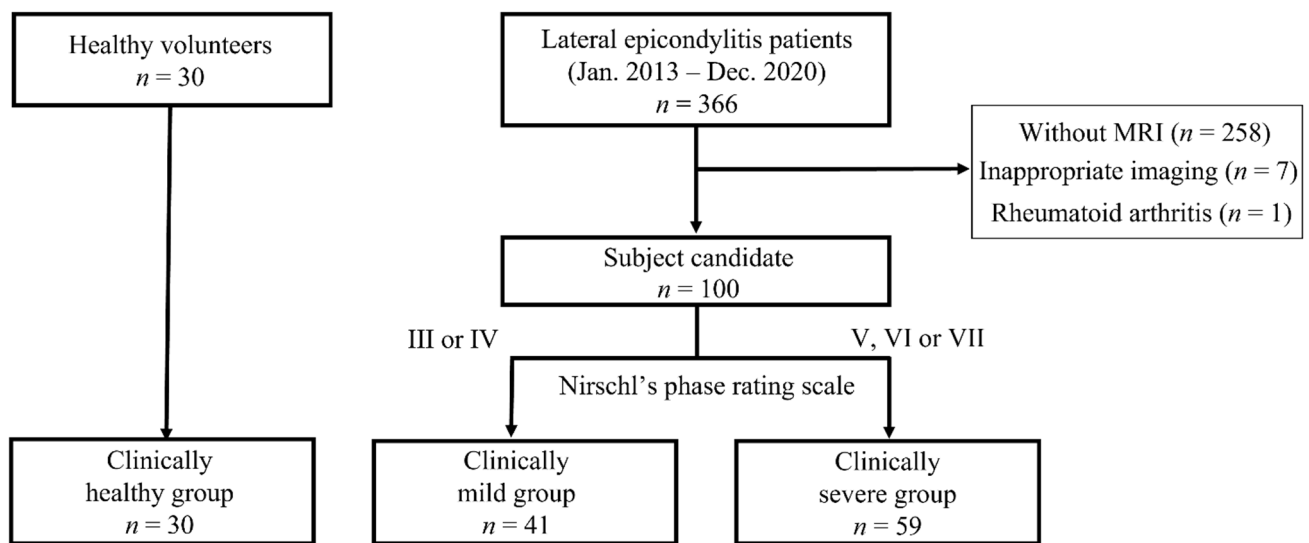


Figure 1. Flow diagram of patients included in the study.

Two upper-extremity orthopedic surgeons with 23 and 28 years of experience, respectively, made all clinical decisions for patients with LE. The diagnosis of LE was based on physical findings, positive Thomsen tests or middle finger tests, and tenderness at the lateral epicondyle [17,18,24]. Initially, we provided conservative treatment for all patients. We prescribed occupational therapy and elbow bands for all patients. Steroid injections were administered to patients, once extra-articularly and once intra-articularly, who did not respond to occupational therapy or orthotics. Some patients had received multiple steroid injections at their previous medical institutions. MRI was performed for patients who were refractory to the aforementioned conservative treatment for at least one month and had severe activity limitation due to pain, (i.e., Nirschl phase rating scale III or higher) [18].

2.2. MRI Protocol and Definition of the Structures

We used a clinical 3.0-Tesla imager (Magnetom Symphony, SIEMENS, Munchen, Germany) with a small-diameter surface coil (Loop Flex Coil, SIEMENS) above the lateral epicondyle of the humerus. We placed the patients' elbows in the center of the MRI scanner, with the elbow extended beside the trunk, and the forearm supinated. We obtained a coronal section of the lateral aspect of the elbow under the following three sequences: T2*-weighted images (T2*WI) using the gradient echo to evaluate synovial folds, proton-density-weighted images (PDWI) using the high-speed spin echo to recognize the morphology of the CET/LCL complex attachment, and T2 fat-saturated weighted images (T2FSWI) to evaluate the severity of LE (Table 1).

Table 1. Imaging parameters.

Sequence	T2*WI	PDWI	T2FSWI
Voxel size	$0.2 \times 0.2 \times 1.5$	$0.2 \times 0.2 \times 1.5$	$0.2 \times 0.2 \times 1.5$
Matrix	160×320	240×320	256×256
FOV	60 mm	60 mm	60 mm
Base resolution	320	320	256
Phase resolution	50%	50%	50%
Slice thickness	1.5 mm	1.5 mm	1.5 mm
TR	553.0 ms	553.0 ms	3000.0 ms
TE	24 ms	24 ms	94 ms
Bandwidth	180 Hz/Px	180 Hz/Px	145 Hz/Px
Flip angle	30	170	122

FOV: field-of-view, TR: repetition time, TE, echo time, T2*WI, T2*-weighted imaging; PDWI, proton-density-weighted imaging; T2FSWI, T2 fat-saturated weighted imaging.

Our protocol provided a clear and enlarged view of the lateral aspect of the elbow; we could recognize the CET and the LCL as rather isolated structures. Furthermore, we used bony landmarks to define the CET and the LCL independently (Figure 2) [25,26]. In the coronal MRI images, we defined the CET as the structure attached to the superior tubercle or the epicondylar ridge and the LCL as the structure attached to the intertubercular sulcus or the inferior surface of the posterior tubercle.

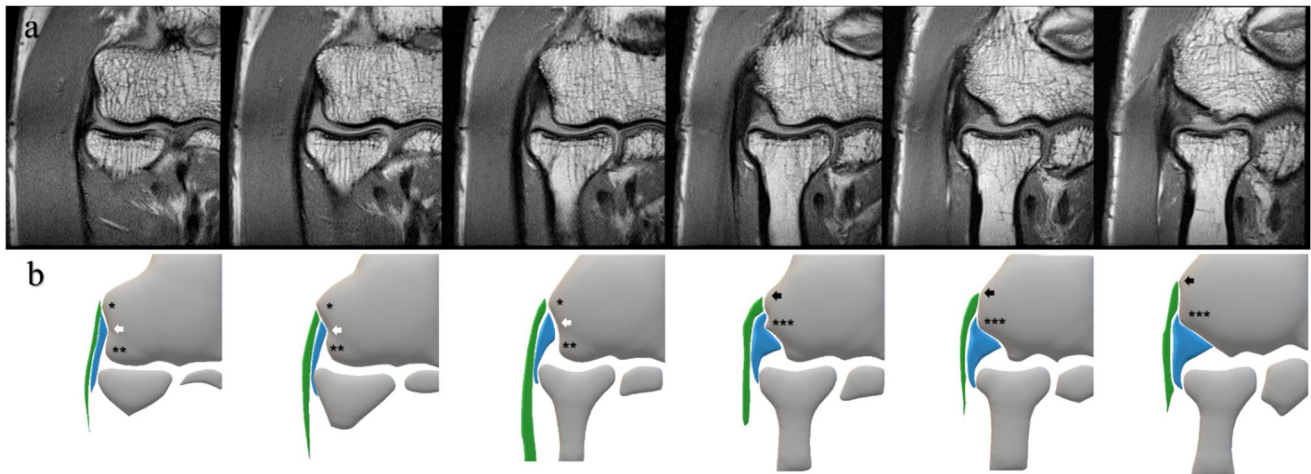


Figure 2. Consecutive MRI slices under PDWI of the unaffected lateral elbow (a) and corresponding schemas (b). These schemas represent bony landmarks and the CET and the LCL in this study. * superior tubercle; ** anterior tubercle; *** posterior tubercle; white arrow, intertubercular sulcus; black arrow, epicondylar ridge; green area, CET; blue area, LCL; MRI, magnetic resonance imaging; PDWI, proton-density-weighted imaging; CET, common extensor tendon; LCL, lateral collateral ligament.

2.3. MRI Scoring and Evaluation

We chose T2FSWI for MRI scoring because PDWI and T2*WI had short echo times and may have overestimated the findings due to the magic-angle phenomenon (Figure 3) [27–29].

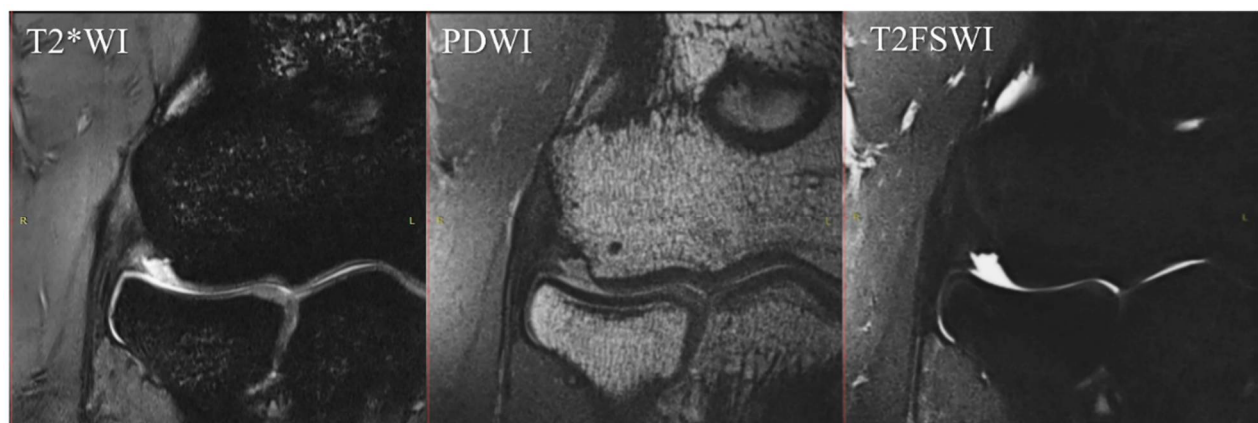


Figure 3. Differences in signal intensity of the CET/LCL complex by sequence. The unaffected elbow of a 32-year-old male. These images are same-level slices of the MRI coronal section in each sequence. In this case, T2*WI shows a high signal at the CET/LCL complex despite a complete low signal in the sequence of PDWI and T2FSWI. MRI, magnetic resonance imaging; T2*WI, T2*-weighted images; PDWI, proton-density-weighted images; T2FSWI, T2 fat-saturated weighted images; CET, common extensor tendon; LCL, lateral collateral ligament.

With reference to the previous literature [30,31], we created an MRI scoring scale which evaluated the strength and extent of signal changes within a coronal section on

a scale of 0 to 4. The region of interest for our MRI scoring was the CET and the LCL between the articular surface of the radial head and lateral epicondyle of the humerus. Using this MRI scoring, we performed two patterns of MRI evaluation. The combined evaluation method evaluated the CET and the LCL together on a scale of 0–4. In contrast, the individual evaluation method evaluated the CET and the LCL individually on a scale of 0–4 and subsequently added the individual scores for a total score of 0–8 (Figure 4).

Two examiners independently assessed the images: an orthopedic surgeon (examiner 1) and a hand surgeon (examiner 2) with 9 and 23 years of experience, respectively. The examiners repeated the image analysis twice, with the second analysis being performed one month after the initial analysis. In the MRI evaluation, a third person blinded any clinical data and randomized the MR images.

2.4. Statistical Analysis

We adopted the values measured by examiner 1 for further analysis. We performed the Shapiro–Wilk test for each evaluation item as a normality test, and none of them followed a normal distribution.

We compared all of the groups' collected variables, including clinical characteristics and MRI scores. We used the chi-squared test for categorical variables, the Mann–Whitney *U* test for continuous variables between two groups, and the Kruskal–Wallis test for comparison among three groups. When the Kruskal–Wallis test showed a significant difference, we performed Scheffe's multiple comparison procedure. In cases of missing data for clinical characteristics, we replaced the data with the median scores of the other patients in the same group.

We created the receiver operating characteristic curve (ROC curve) for the diagnosis of LE from the MRI scoring of the H and M groups, and the ROC curve for the diagnosis of severity from the M and S groups.

We used Fleiss' kappa analysis to evaluate intra-observer and inter-observer reliability for the entire MRI scoring process. The interpretation of the kappa coefficient was defined as follows: 0.81–1.00 = excellent, 0.61–0.80 = good, and 0.41–0.60 = fair.

In principle, we set the level of statistical significance as $p < 0.05$. In performing the chi-square test among three groups, we corrected the significance level with Bonferroni's method (i.e., $p < 0.016$).

We performed all statistical analyses using Bellcurve for Excel version 3.20 (SSRI Co., Tokyo, Japan).

2.5. Sample Size

Based on the previous studies [20,32], we predicted the area under curve (AUC) of ROC curves for diagnosis to be 0.65 to 0.85. Subsequently, we calculated that with a sample of 30 patients per group, the study would have an 80% power to create an ROC curve with an AUC of 0.68 and a type I error of 5%. For the diagnosis of severity, we predicted the AUC of ROC curves for severity diagnosis to be 0.6 to 0.8 [15]. We calculated that with a sample of 98 patients, with 49 patients per group, the study would have 80% power to create an ROC curve with an AUC of 0.6 and a type I error of 5%. From these results, we collected 30 cases for the H group and a total of 100 cases for the M and S groups.

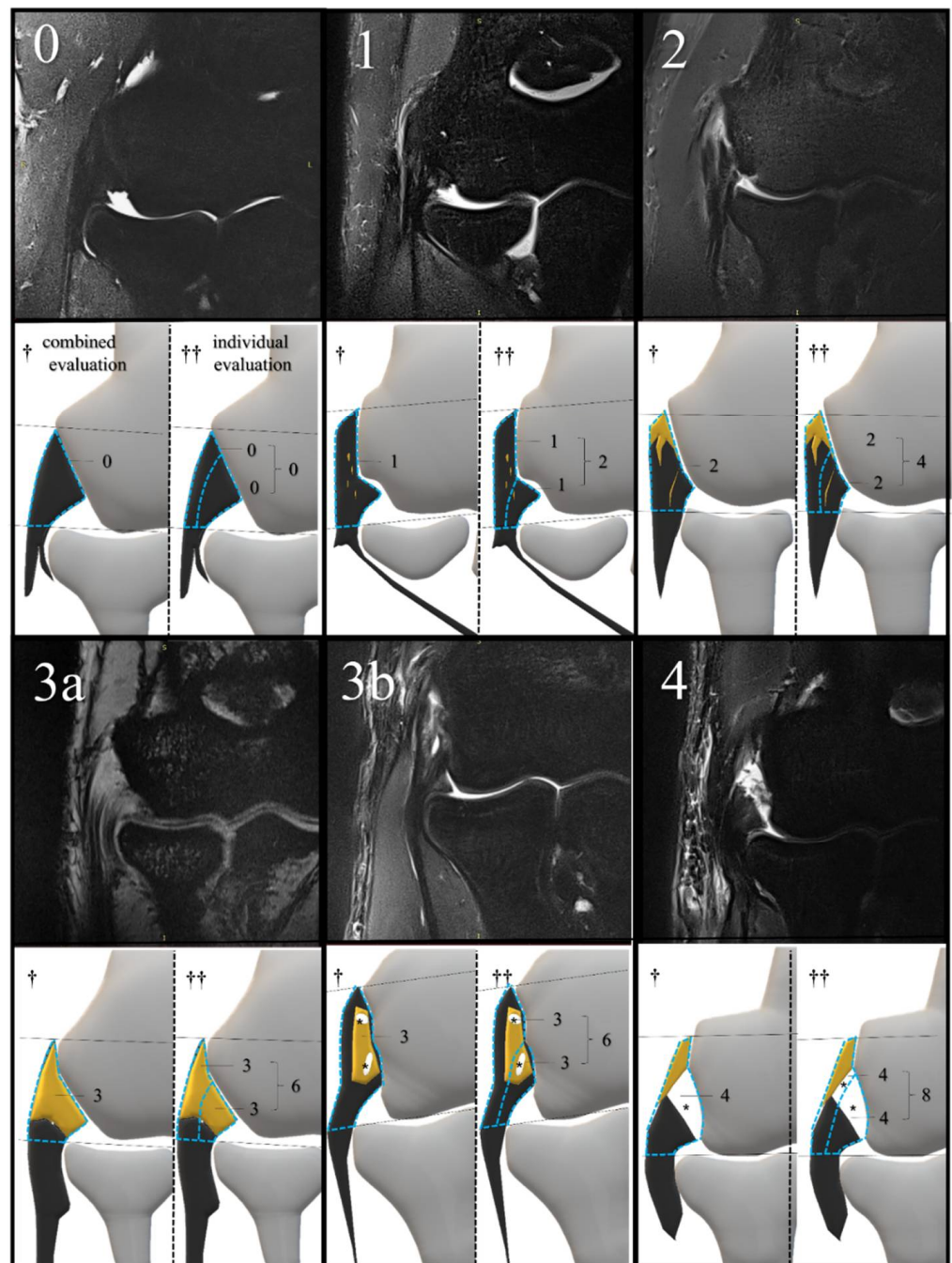


Figure 4. MRI examples of each score and its corresponding schema. The scoring criteria are as follows: (0) (normal), dark, linear low-signal structure without changes in signal intensity; (1) (mild degeneration), thickening or mild signal change below the signal intensity of the muscle; (2) (localized degeneration), high signal change above the signal intensity of the muscle, localized below 50% of the evaluation range; (3a) (extensive degeneration), high signal change above the signal intensity of the muscle, beyond 50% of the evaluation range; (3b) (partial tear), high signal change equivalent to joint fluid, within 75% of the tendon or ligament width; (4) (extensive tear), high signal change equivalent to joint fluid, more than 75% of the tendon or ligament's width. The yellow area indicates degeneration; * tear; MRI, magnetic resonance imaging. The blue dotted line surrounds the region of interest for MRI scoring in each evaluation method. Black lines are auxiliary lines to determine the evaluation area, which runs parallel to the articular surface of the radial head. † combined evaluation; †† individual evaluation; yellow area, degeneration.

3. Results

3.1. Demographic and Clinical Characteristics

Table 2 summarizes the demographic and clinical data of each group. There was no significant difference in gender or age between the H, M, and S groups. As for comparisons between the two groups, the S group received more frequent injection therapy and was affected for a longer period than the M group. Fifty patients of the S group did not respond to conservative treatment and received surgical treatment; no patients of the M group required surgery.

Table 2. Demographic and clinical data of each group.

	Healthy Group	Mild Group	Severe Group	<i>p</i> -Value
Sex Male	12	21	31	$p = 0.51$
Female	18	20	28	
Age (y) †	49 (27–69)	49 (34–77)	49 (23–78)	$p = 0.27$
Injection therapy	-			$p < 0.001$
0		21	6	
1–2		17	29	
3≤		3	24	
unidentified		0	0	
Duration of pain (months) †	-	6.4 (2.1–81.0)	12.5 (1.4–133.1)	$p = 0.032$
0–1 month		0	0	
1–3 months		6	4	
3–6 months		12	12	
6–12 months		12	12	
>12 months		9	31	
Unidentified		2	0	
Required surgery ††	-	0/41	50/59	$p < 0.001$

† Data are presented as median (minimum–maximum); †† The surgical indication was for the patients with Nirschl's clinical scale score of V or higher, who were resistant to the conservative treatment for at least 6 months.

3.2. MRI Scoring

In the combined evaluation, the median MRI score and 25–75 percentile were 1 (1–2), 3 (2–3), and 4 (3–4) in the H, M, and S groups, respectively. There was a significant difference among all groups: $p < 0.001$ for the H and M groups, $p < 0.001$ for the H and S groups, and $p = 0.001$ for the M and S groups (Figure 5). In the individual evaluation, the median MRI score and 25–75 percentile were 2 (1–2), 4 (3–5) and 6 (5–6) in the H, M, and S groups, respectively. There was a significant difference among all groups: $p < 0.001$ for the H and M groups, H and S groups, and for the M and S groups (Figure 6). Additionally, we described the distribution of the CET and LCL scores in each group in the supplementary materials (Table S1).

3.3. ROC Curve

In the ROC curve for diagnosis, shown in Figure 7, the AUC was 0.84 for combined evaluation ($p < 0.001$) and 0.86 for individual evaluation ($p < 0.001$). In the comparison of the evaluation methods, there was no significant difference in the AUC ($p = 0.63$).

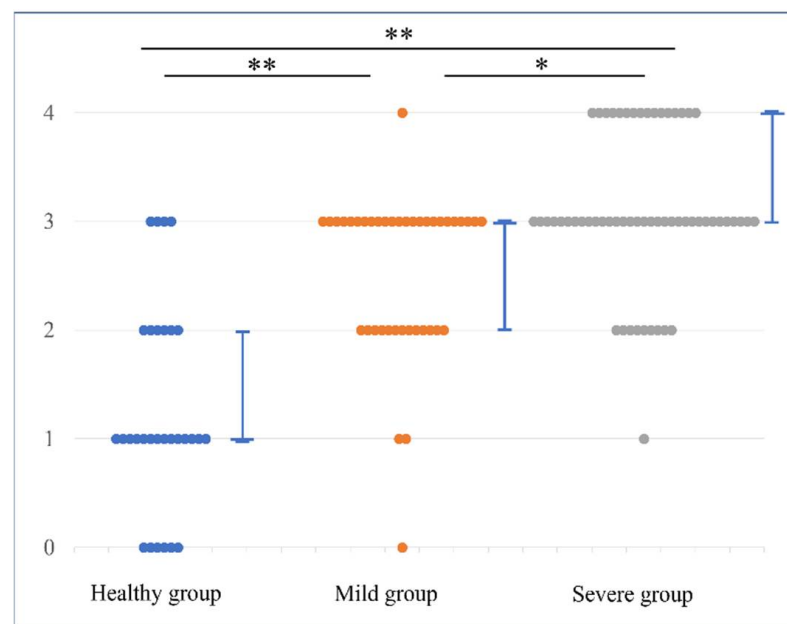


Figure 5. MRI scores in combined evaluation method. Dot plots show the differences in the distribution of MRI scores for each group. The MRI scores were valued as follows: healthy group < mild group < severe group, with significant differences. The line graph represents the median value and 25–75 percentile. * $p < 0.05$, ** $p < 0.01$.

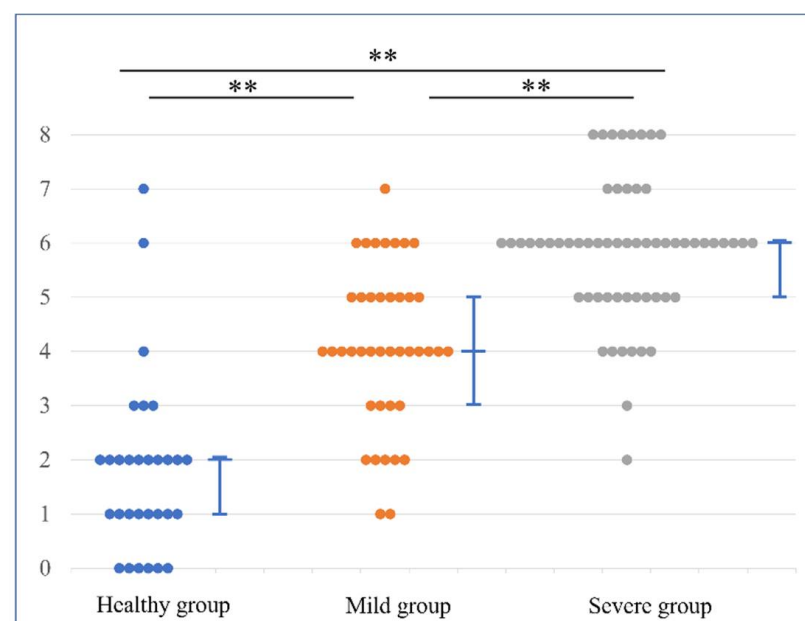
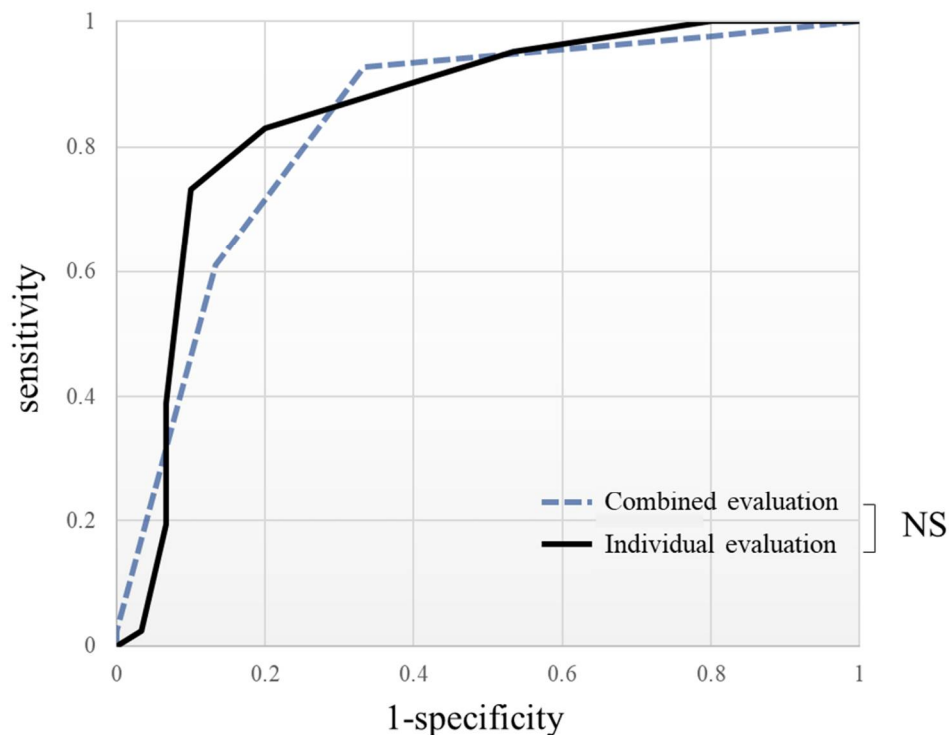


Figure 6. MRI scores in the individual evaluation method. Dot plots show the differences in the distribution of MRI scores for each group. The MRI scores were valued as follows: healthy group < mild group < severe group, with significant differences. The line graph represents the median value and 25–75 percentile. ** $p < 0.01$.



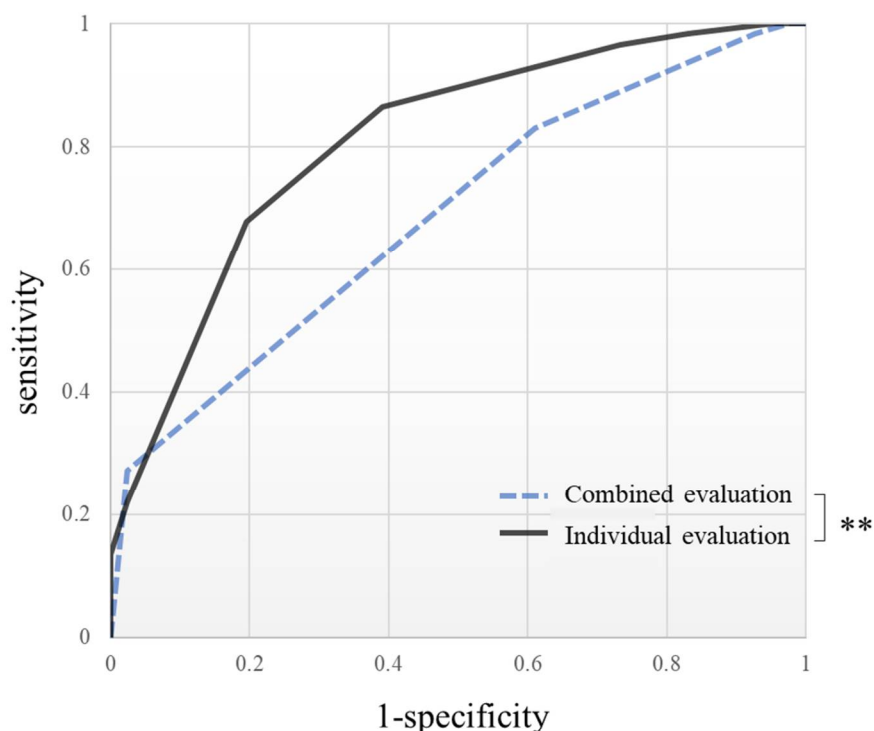
ROC curve of	Variable	AUC				Cut-off value				
		AUC	95% confidence interval	Standard error	P-value	Cut-off value	Sensitivity	specificity	PPV	NPV
Combined evaluation	MRI score	0.84	0.74–0.93	0.048	< 0.001	2	0.93	0.66	0.79	0.86
Individual evaluation	MRI score	0.86	0.76–0.95	0.050	< 0.001	3	0.80	0.83	0.85	0.77

Figure 7. The ROC curve shows the capability of MRI to diagnose lateral epicondylitis for each evaluation method. In a comparison of AUC, there was no significant difference between the evaluation methods ($p = 0.23$). ROC curve, receiver operating characteristic curve; PPV, positive predictive value; NPV, negative predictive value; NS, not significant.

In the ROC curve for the diagnosis of clinical severity, shown in Figure 8, the AUC was 0.69 for the combined evaluation ($p < 0.001$) and 0.81 for the individual evaluation ($p < 0.001$). In the comparison of the evaluation methods, the AUC of the individual evaluation was significantly larger than that of the combined evaluation ($p = 0.003$).

3.4. Repeatability of MRI Scoring in This Study

The kappa values and their 95% confidence intervals for intra-observer agreement were 0.87 (0.85–0.90: $p < 0.001$) for examiner 1 and 0.86 (0.84–0.89: $p < 0.001$) for examiner 2. For inter-observer agreement between examiners 1 and 2, the kappa value was 0.84 (0.82–0.86: $p < 0.001$). The repeatability of MRI scoring was excellent.



ROC curve of	Variable	AUC				Cut-off value				
		AUC	95% confidence interval	Standard error	P-value	Cut-off value	Sensitivity	specificity	PPV	NPV
Combined evaluation	MRI score	0.69	0.60–0.78	0.046	< 0.001	3	0.83	0.40	0.66	0.62
Individual evaluation	MRI score	0.81	0.73–0.89	0.043	< 0.001	6	0.68	0.80	0.83	0.63

Figure 8. The ROC curve shows the capability of MRI to diagnose the clinical severity for each evaluation method. In a comparison of AUCs, individual evaluation was significantly superior to combined evaluation ($p = 0.046$). ** $p < 0.05$, ROC curve, receiver operating characteristic curve; PPV, positive predictive value; NPV, negative predictive value.

4. Discussion

The most significant finding of this study was that individual MRI evaluations of the CET and the LCL improved the accuracy of the severity diagnosis of LE. Since MRI images reflect pathological change, we can accurately quantify pathological severity with detailed MRI scoring. Some of the studies investigating the relationship between clinical and MRI severity are commensurate with the results of this study. The literature with quantitative, individual evaluations of the CET and the LCL reported a positive association between clinical and MRI severity [7,15]; the studies without quantitative evaluation did not show this association [22]. Studies with quantitative, combined evaluations of the CET and the LCL reported conflicting conclusions [23,33]. This study suggests that the CET and the LCL should be individually evaluated using MRI to indicate the severity diagnosis.

Furthermore, we demonstrated the accuracy of MRI for the diagnosis of LE. According to the ROC curve for the diagnosis of LE, MRI had a high diagnostic capability, as reported in other tendinopathies [32]. Nevertheless, MRI is not always necessary for diagnosis since most patients with LE can be diagnosed based on physical findings. We should perform MRI only for patients who are refractory to conservative treatment. Differential diagnosis should be considered when MRI shows an absence or slight change in the signal on CET/LCL, e.g., the entrapment of the posterior antebrachial cutaneous nerve [34,35], radial tunnel syndrome, synovial fold disorder, posterolateral elbow instability, inflammatory disorders, cervical radiculopathy, and so on [36].

Meanwhile, further study is necessary to demonstrate the validity of MRI-positive findings for the severity diagnosis. Although MRI scores were higher in the group with higher clinical severity, there was some variation among cases. As Nirschl et al. showed, there is interindividual variation in symptoms and pathologic severity of LE [18,37]. Furthermore, some studies reported that psychological factors play a role in the intensity of the clinical symptoms in LE [38,39]. These findings indicate that the symptoms of LE are multifactorial, though based on pathological abnormalities. Thus, the cross-sectional study of the correlation between MRI scoring and clinical severity is necessarily limited. A longitudinal study should be conducted in the future to reveal the validity of positive MRI findings in LE. Since the literature suggests surgery in cases with severe pathology [18,37,40], MRI severity may predict the prognosis of conservative treatment. In particular, since posterolateral instability is reported to be associated with clinical severity [41,42], individual evaluation of LCL is significant. Overall, the findings of this study will be a basis for future research.

Our study had several strengths. Firstly, to our knowledge, this study used the highest-resolution MRI of any study to date; this allowed us to provide reliable data. The repeatability of MRI scoring was excellent. Secondly, we conducted a quantitative evaluation with a sufficient sample size, including the healthy group. Since previous reports have not quantitatively evaluated healthy subjects, we believe our data will serve as a basis for future MRI evaluations.

Although the study had many strengths, it also had some limitations. This study was retrospective, and we collected data on clinical symptoms from medical records. Although our treatment protocols and MRI indications are standardized at a single institution, there were some differences in the timing of MRI imaging in some cases. Additionally, our study included patients who received steroid injection therapy, which may have influenced the MRI findings or clinical assessment. Finally, we selected the subjects of the H group from a specific environment of medical coworkers in our hospital. Therefore, there is a possibility of selection bias that we could not predict.

In conclusion, MRI individual evaluation of the CET and the LCL improved the accuracy of diagnosing the severity of LE. The CET and LCL should be evaluated individually to reflect the relationship of clinical severity to MRI severity accurately.

Supplementary Materials: The following supporting information can be downloaded at: <https://www.mdpi.com/article/10.3390/diagnostics12081871/s1>. Table S1: distribution of the CET and LCL scores in each group.

Author Contributions: Conceptualization, K.I.; methodology, K.I. and T.O.; validation, K.I. and T.O.; formal analysis, K.I. and R.I.; investigation, K.I.; resources, T.O. and A.I.; data curation, K.I. and R.I.; writing—original draft preparation, K.I.; writing—review and editing, T.O., A.I., Y.Y. and S.K.; visualization, K.I.; supervision, T.O. and M.Y.; project administration, M.Y. All authors have read and agreed to the published version of the manuscript.

Funding: This research received no external funding.

Institutional Review Board Statement: The study was conducted according to the guidelines of the Declaration of Helsinki and approved by the Institutional Review Board of the Mito Kyodo General Hospital (Study Number: 16–25, approved 7 September 2016) and Takahagi Kyodo General Hospital (Study Number: 10, approved 3 March 2021).

Informed Consent Statement: Informed consent was obtained from all subjects involved in the study.

Data Availability Statement: Not applicable.

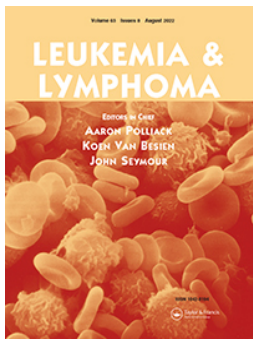
Acknowledgments: We would like to thank Atsushi Hirano and Yuki Hara for providing us with the opportunity to conduct this study. We would also like to thank the radiology groups of Mito Kyodo Hospital and Takahagi Kyodo Hospital for their cooperation in the MRI examinations.

Conflicts of Interest: The authors declare no conflict of interest.

References

1. Ahmad, Z.; Siddiqui, N.; Malik, S.S.; Abdus-Samee, M.; Tytherleigh-Strong, G.; Rushton, N. Lateral epicondylitis: A review of pathology and management. *Bone Jt. J.* **2013**, *95B*, 1158–1164. [\[CrossRef\]](#) [\[PubMed\]](#)
2. Runge, F. Zur Genese und Behandlung des schreibe Kranfes. *Bed. Klin. Worchenschr.* **1873**, *10*, 245–248.
3. Shiri, R.; Viikari-Juntura, E. Lateral and medial epicondylitis: Role of occupational factors. *Best. Pract. Res. Clin. Rheumatol.* **2011**, *25*, 43–57. [\[CrossRef\]](#) [\[PubMed\]](#)
4. Wolf, J.M.; Mountcastle, S.; Burks, R.; Sturdivant, R.X.; Owens, B.D. Epidemiology of lateral and medial epicondylitis in a military population. *Mil. Med.* **2010**, *175*, 336–339. [\[CrossRef\]](#)
5. Fan, Z.J.; Silverstein, B.A.; Bao, S.; Bonauto, D.K.; Howard, N.L.; Spielholz, P.O.; Smith, C.K.; Polissar, N.L.; Viikari-Juntura, E. Quantitative exposure-response relations between physical workload and prevalence of lateral epicondylitis in a working population. *Am. J. Ind. Med.* **2009**, *52*, 479–490. [\[CrossRef\]](#)
6. Shiri, R.; Viikari-Juntura, E.; Varonen, H.; Heliövaara, M. Prevalence and determinants of lateral and medial epicondylitis: A population study. *Am. J. Epidemiol.* **2006**, *164*, 1065–1074. [\[CrossRef\]](#)
7. Cha, Y.K.; Kim, S.J.; Park, N.H.; Kim, J.Y.; Kim, J.H.; Park, J.Y. Magnetic resonance imaging of patients with lateral epicondylitis: Relationship between pain and severity of imaging features in elbow joints. *Acta. Orthop. Traumatol. Turc.* **2019**, *53*, 366–371. [\[CrossRef\]](#)
8. Bredella, M.A.; Tirman, P.F.; Fritz, R.C.; Feller, J.F.; Wischer, T.K.; Genant, H.K. MR imaging findings of lateral ulnar collateral ligament abnormalities in patients with lateral epicondylitis. *AJR Am. J. Roentgenol.* **1999**, *173*, 1379–1382. [\[CrossRef\]](#)
9. Kalainov, D.M.; Cohen, M.S. Posterolateral rotatory instability of the elbow in association with lateral epicondylitis. A report of three cases. *J. Bone Joint Surg. Am.* **2005**, *87*, 1120–1125. [\[CrossRef\]](#)
10. Dones, V.C., 3rd; Grimmer, K.; Thoirs, K.; Suarez, C.G.; Luker, J. The diagnostic validity of musculoskeletal ultrasound in lateral epicondylalgia: A systematic review. *BMC Med. Imaging* **2014**, *14*, e10. [\[CrossRef\]](#)
11. Latham, S.K.; Smith, T.O. The diagnostic test accuracy of ultrasound for the detection of lateral epicondylitis: A systematic review and meta-analysis. *Orthop. Traumatol. Surg. Resarch* **2014**, *100*, 281–286. [\[CrossRef\]](#)
12. Khattab, E.M.; Abowarda, M.H. Role of Ultrasound Guided Platelet-Rich Plasma (PRP) Injection in Treatment of Lateral Epicondylitis. *Egypt. J. Radiol. Nucl. Med.* **2017**, *48*, 403–413. [\[CrossRef\]](#)
13. Ruiz, A.G.; Diaz, G.V.; Fernandez, B.R.; Vargas, C.E.R.D. Effects of Ultrasound-Guided Administration of Botulinum Toxin (IncobotulinumtoxinA) in Patients with Lateral Epicondylitis. *Toxins* **2019**, *46*, e11010046.
14. Casu, E.; Obradov-Rajic, M. Ultrasound Guided Standalone Percutaneous Needle Tenotomy for Chronic Lateral Epicondylitis: A Systematic Review. *Adv. Tech. Musculoskelet. Surg.* **2018**, *2*, 18–28.
15. Jeon, J.Y.; Lee, M.H.; Jeon, I.H.; Chung, H.W.; Lee, S.H.; Shin, M.J. Lateral epicondylitis: Associations of MR imaging and clinical assessments with treatment options in patients receiving conservative and arthroscopic management. *Eur. Radiol.* **2018**, *28*, 972–981. [\[CrossRef\]](#)
16. Lombardi, A.; Ashir, A.; Gorbachova, T.; Taljanovic, M.; Chang, E.Y. Magnetic resonance imaging of the elbow. *Pol. J. Radiol.* **2020**, *85*, e440–e460. [\[CrossRef\]](#)
17. Waseem, M.; Nuhmani, S.; Ram, C.S.; Sachin, Y. Lateral epicondylitis: A review of the literature. *J. Back Musculoskelet. Rehabil.* **2012**, *25*, 131–142. [\[CrossRef\]](#)
18. Nirschl, R.P.; Ashman, E.S. Elbow tendinopathy: Tennis elbow. *Clin. Sports Med.* **2003**, *22*, 813–836. [\[CrossRef\]](#)
19. Ma, K.L.; Wang, H.Q. Management of Lateral Epicondylitis: A Narrative Literature Review. *Pain Res. Manag.* **2020**, *2020*, e6965381. [\[CrossRef\]](#)
20. Pasternack, I.; Tuovinen, E.M.; Lohman, M.; Vehmas, T.; Malmivaara, A. MR findings in humeral epicondylitis. A systematic review. *Acta. Radiol.* **2001**, *42*, 434–440.
21. Regan, W.; Wold, L.E.; Coonrad, R.; Morrey, B.F. Microscopic histopathology of chronic refractory lateral epicondylitis. *Am. J. Sports Med.* **1992**, *20*, 746–749. [\[CrossRef\]](#)
22. Savnik, A.; Jensen, B.; Nørregaard, J.; Egund, N.; Danneskiold-Samsøe, B.; Bliddal, H. Magnetic resonance imaging in the evaluation of treatment response of lateral epicondylitis of the elbow. *Eur. Radiol.* **2004**, *14*, 964–969. [\[CrossRef\]](#)
23. Walton, M.J.; Mackie, K.; Fallon, M.; Butler, R.; Breidahl, W.; Zheng, M.H.; Wang, A. The reliability and validity of magnetic resonance imaging in the assessment of chronic lateral epicondylitis. *J. Hand Surg. Am.* **2011**, *36*, 475–479. [\[CrossRef\]](#)
24. Elisa, L.Z.; Matthijs, P.S.; Francois, M.; Jelle, H.; Denise, E.; Michel, P.B. Physical examination of the elbow, what is the evidence? A systematic literature review. *Br. J. Sports Med.* **2018**, *52*, 1253–1260.
25. Zoner, C.S.; Buck, F.M.; Cardoso, F.N.; Gheno, R.; Trudell, D.J.; Randall, T.D.; Resnick, D. Detailed MRI-anatomic study of the lateral epicondyle of the elbow and its tendinous and ligamentous attachments in cadavers. *Am. J. Roentgenol.* **2010**, *195*, 629–636. [\[CrossRef\]](#) [\[PubMed\]](#)
26. Nimura, A.; Fujishiro, H.; Wakabayashi, Y.; Imatani, J.; Sugaya, H.; Akita, K. Joint capsule attachment to the extensor carpi. *J. Hand Surg. Am.* **2014**, *39*, 219–225. [\[CrossRef\]](#) [\[PubMed\]](#)
27. Bydder, M.; Rahal, A.; Fullerton, G.D.; Bydder, G.M. The magic angle effect: A source of artifact, determinant of image contrast, and technique for imaging. *J. Magn. Reson. Imaging* **2007**, *25*, 290–300. [\[CrossRef\]](#) [\[PubMed\]](#)
28. Du, J.; Pak, B.C.; Znamirovski, R.; Statum, S.; Takahashi, A.; Chung, C.B.; Bydder, G.M. Magic angle effect in magnetic resonance imaging of the Achilles tendon and enthesis. *Magn. Reson. Imaging* **2009**, *27*, 557–564. [\[CrossRef\]](#)

29. Zurlo, J.V.; Blacksin, M.F.; Karimi, S. The influence of flip angle on the magic angle effect. *Skeletal Radiol.* **2000**, *29*, 593–596. [[CrossRef](#)]
30. Steinborn, M.; Heuck, A.; Jessel, C.; Bonel, H.; Reiser, M. Magnetic resonance imaging of lateral epicondylitis of the elbow with a 0.2-T dedicated system. *Eur. Radiol.* **1999**, *9*, 1376–1380. [[CrossRef](#)]
31. Qi, L.; Zhang, Y.-D.; Yu, R.-B.; Shi, H.-B. Magnetic resonance imaging of patients with chronic lateral epicondylitis: Is there a relationship between magnetic resonance imaging abnormalities of the common extensor tendon and the patient's clinical symptom? *Medicine* **2016**, *95*, e2681. [[CrossRef](#)]
32. Gatz, M.; Bode, D.; Betsch, M.; Quack, V.; Tingart, M.; Kuhl, C.; Schradang, S.; Dirrichs, T. Multimodal ultrasound Versus MRI for the diagnosis and monitoring of Achilles tendinopathy: A prospective longitudinal study. *Orthop. J. Sport Med.* **2021**, *9*, 23259671211006826. [[CrossRef](#)]
33. Qi, L.; Zhu, Z.-F.; Li, F.; Wang, R.-F. MR imaging of patients with lateral epicondylitis of the elbow: Is the common extensor tendon an isolated lesion? *PLoS ONE*. **2013**, *8*, e79498. [[CrossRef](#)]
34. Chang, K.V.; Mezan, K.; Nanka, O.; Wu, W.T.; Lou, Y.M.; Wang, J.C.; Martinoli, C.; Ozcakar, L. Ultrasound Imaging for the Cutaneous Nerves of the Extremities and Relevant Entrapment Syndromes: From Anatomy to Clinical Implications. *J. Clin. Med.* **2018**, *7*, e7110457. [[CrossRef](#)]
35. Wagle, S.; Glazebrook, K.; Moynagh, M.; Smith, J.; Sellon, J.; Skinner, J.; Morrey, M. Role of ultrasound-guided perineural injection of the posterior antebrachial cutaneous nerve for diagnosis and potential treatment of chronic lateral elbow pain. *Skeletal Radiol.* **2021**, *50*, 425–430. [[CrossRef](#)]
36. Ahmed, A.F.; Rayyan, R.; Zikria, B.; Salameh, M. Lateral epicondylitis of the elbow: An up-to-date review of management. *Eur. J. Orthop. Surg. Traumatol.* **2022**, *21*, e03181. [[CrossRef](#)]
37. Kraushaar, B.S.; Nirschl, R.P. Tendinosis of the elbow (Tennis elbow): Clinical features and findings of histological, immunohistochemical, and electron microscopy studies. *J. Bone Jt. Surg. Ser. A*. **1999**, *81*, 259–278. [[CrossRef](#)]
38. Aurelie, A.; Lieven, D.W.; Nadine, H.; Carlos, H.; Marc, V.; Koen, P.; Alexander, V.T. Tennis elbow: Associated psychological factors. *J. Shoulder Elb. Surg.* **2018**, *27*, 387–392.
39. Van, R.R.M.; Huisstede, B.M.; Koes, B.W.; Burdorf, A.B. Associations between work-related factors and specific disorders at the elbow: A systematic literature review. *Rheumatology* **2009**, *48*, 528–536.
40. Bhabra, G.; Wang, A.; Ebert, J.R.; Edwards, P.; Zheng, M.; Zheng, M.H. Lateral Elbow Tendinopathy: Development of a Pathophysiology-Based Treatment Algorithm. *Orthop. J. Sports Med.* **2016**, *4*, 2325967116670635. [[CrossRef](#)]
41. Kwak, S.H.; Lee, S.J.; Jeong, H.S.; Do, M.U.; Suh, K.T. Subtle elbow instability associated with lateral epicondylitis. *BMC Musculoskeletal Disord.* **2018**, *19*, 136. [[CrossRef](#)]
42. Noh, Y.M.; Kong, G.M.; Moon, S.W.; Jang, H.S.; Kim, S.; Bak, G.G.; Kim, Y. Lateral ulnar collateral ligament (LUCL) reconstruction for the treatment of recalcitrant lateral epicondylitis of the elbow: A comparison with open débridement of the extensor origin. *JSES Int.* **2021**, *16*, 578–587. [[CrossRef](#)]



Novel translocation of *POGZ/STK11* in *de novo* mast cell leukemia with *KIT* D816H mutation

Kantaro Ishitsuka, Yuki Yoshizawa, Hidekazu Nishikii, Manabu Kusakabe, Yufu Ito, Yukinori Inadome, Tatsuhiro Sakamoto, Takayasu Kato, Naoki Kurita, Yasuhisa Yokoyama, Naoshi Obara, Yuichi Hasegawa, Yasuhito Nannya, Seishi Ogawa, Mamiko Sakata-Yanagimoto & Shigeru Chiba

To cite this article: Kantaro Ishitsuka, Yuki Yoshizawa, Hidekazu Nishikii, Manabu Kusakabe, Yufu Ito, Yukinori Inadome, Tatsuhiro Sakamoto, Takayasu Kato, Naoki Kurita, Yasuhisa Yokoyama, Naoshi Obara, Yuichi Hasegawa, Yasuhito Nannya, Seishi Ogawa, Mamiko Sakata-Yanagimoto & Shigeru Chiba (2022): Novel translocation of *POGZ/STK11* in *de novo* mast cell leukemia with *KIT* D816H mutation, *Leukemia & Lymphoma*, DOI: [10.1080/10428194.2022.2123235](https://doi.org/10.1080/10428194.2022.2123235)

To link to this article: <https://doi.org/10.1080/10428194.2022.2123235>



Published online: 20 Sep 2022.



Submit your article to this journal [↗](#)





View related articles [↗](#)



View Crossmark data [↗](#)

Novel translocation of *POGZ/STK11* in *de novo* mast cell leukemia with *KIT* D816H mutation

Kantaro Ishitsuka^a, Yuki Yoshizawa^a, Hidekazu Nishikii^{a,b} , Manabu Kusakabe^{a,b} , Yufu Ito^c, Yukinori Inadome^d, Tatsuhiro Sakamoto^{a,b}, Takayasu Kato^{a,b}, Naoki Kurita^{a,b}, Yasuhisa Yokoyama^{a,b}, Naoshi Obara^{a,b}, Yuichi Hasegawa^{a,b}, Yasuhito Nannya^{e,f}, Seishi Ogawa^f, Mamiko Sakata-Yanagimoto^{a,b} and Shigeru Chiba^{a,b}

^aDepartment of Hematology, University of Tsukuba Hospital, Ibaraki, Japan; ^bDepartment of Hematology, Faculty of Medicine, University of Tsukuba, Ibaraki, Japan; ^cDepartment of Hematology, Tsuchiura Kyodo General Hospital, Ibaraki, Japan; ^dDepartment of Pathology, National Hospital Organization Mito Medical Center, Ibaraki, Japan; ^eDepartment of Hematology/Oncology, Institute of Medical Science, University of Tokyo, Tokyo, Japan; ^fDepartment of Pathology and Tumor Biology, Kyoto University, Kyoto, Japan

ARTICLE HISTORY Received 13 April 2022; Accepted 4 September 2022

Introduction

Systemic mastocytosis (SM) is defined as a new distinct disease category in the 2016 revision of the World Health Organization (WHO) classification [1]. It refers to symptoms resulting from the proliferation of abnormal mast cells (MCs) and their organ infiltration. It was reported that specific mutations of *KIT* can cause a ligand-independent activation of the c-Kit signaling pathway in a human mast cell leukemia cell line [2]. In fact, *KIT* D816V is a hotspot mutation and is associated with disease onset [3]. Mast cell leukemia (MCL) is the most aggressive and extremely rare subtype of SM. The prognosis of MCL is often very poor and there is no standard therapy available [4]. Moreover, a lack of knowledge regarding the molecular mechanisms of the disease, except for *KIT* mutation, limits the development of effective therapeutic strategies. In this report, we describe a novel translocation that is a potential driver of MCL in combination with *KIT* mutations. We present the first case of a patient with MCL who carried a *KIT* D816H mutation and a translocation between the pogo transposable element derived with ZNF domain (*POGZ*) and serine/threonine kinase 11 (*STK11*, also known as *LKB1*) loci. This novel combination of oncogenic events could explain the pathogenesis and treatment resistance of MCL in the present case.

A previously healthy 48-year-old woman presented with a chronic cough and was admitted to the local clinic. Her complete blood count results showed bicytopenia (hemoglobin 8.6 g/dL, platelet count 92 K/ μ L). Subsequently, symptoms of low-grade fever, night sweats, and systemic edema appeared. Eventually, blood tests revealed progressive bicytopenia and circulating atypical MCs (21% of white blood cells). Chest X-ray showed bilateral pleural effusion and the computed

tomography showed hepatosplenomegaly. Atypical MCs accounted for 92.4% of the nucleated cells in the bone marrow (BM) aspirate, and they were negative for myeloperoxidase (MPO) and nonspecific esterase staining (Figure 1(A)). No blastic cells were observed. Immunohistochemical staining revealed that the MCs were positive for c-KIT and tryptase (Figure 1(A)). Flow cytometric analysis revealed that the MCs were positive for CD45 (dim), CD13, and CD33 but negative for the other tested markers (CD3, cyCD3, CD10, CD19, CD34, CD38, CD56, MPO, and terminal deoxynucleotidyl transferase). Cytogenetic analysis showed the presence of a complex karyotype (Figure 1(B)). Serum tryptase (179 μ g/L, normal range < 11.5 μ g/L) and histamine (70.3 ng/ml, normal range 0.15–0.23 ng/ml) levels were markedly elevated. Molecular testing with targeted sequencing revealed a *KIT* D816H mutation and the fusion of *POGZ/STK11* (Figure 1(C–E)). The patient met the WHO 2016 criteria for MCL without comorbidities. Based on the above findings, a diagnosis of *de novo* MCL was made.

There is no standard treatment for MCL; therefore, the remission induction chemotherapy (idarubicin 12 mg/m² on days 1–3, cytarabine 100 mg/m² on days 1–7) used for acute myeloid leukemia (AML) [5] was selected as the initial treatment. From day 3, systemic erythema occurred, which may be due to allergic mediators released from the MCs. After the atypical MCs disappeared from the peripheral blood, her symptoms disappeared. Hematological remission was achieved after the chemotherapy, following which, serum tryptase and histamine levels were reduced to the normal range (Figure 2(A)). After one course of consolidation chemotherapy (mitoxantrone 7 mg/m² on days 1–3, cytarabine 100 mg/m² on days 1–5), the patient received a cord blood transplant (CBT) with a 5/8 HLA

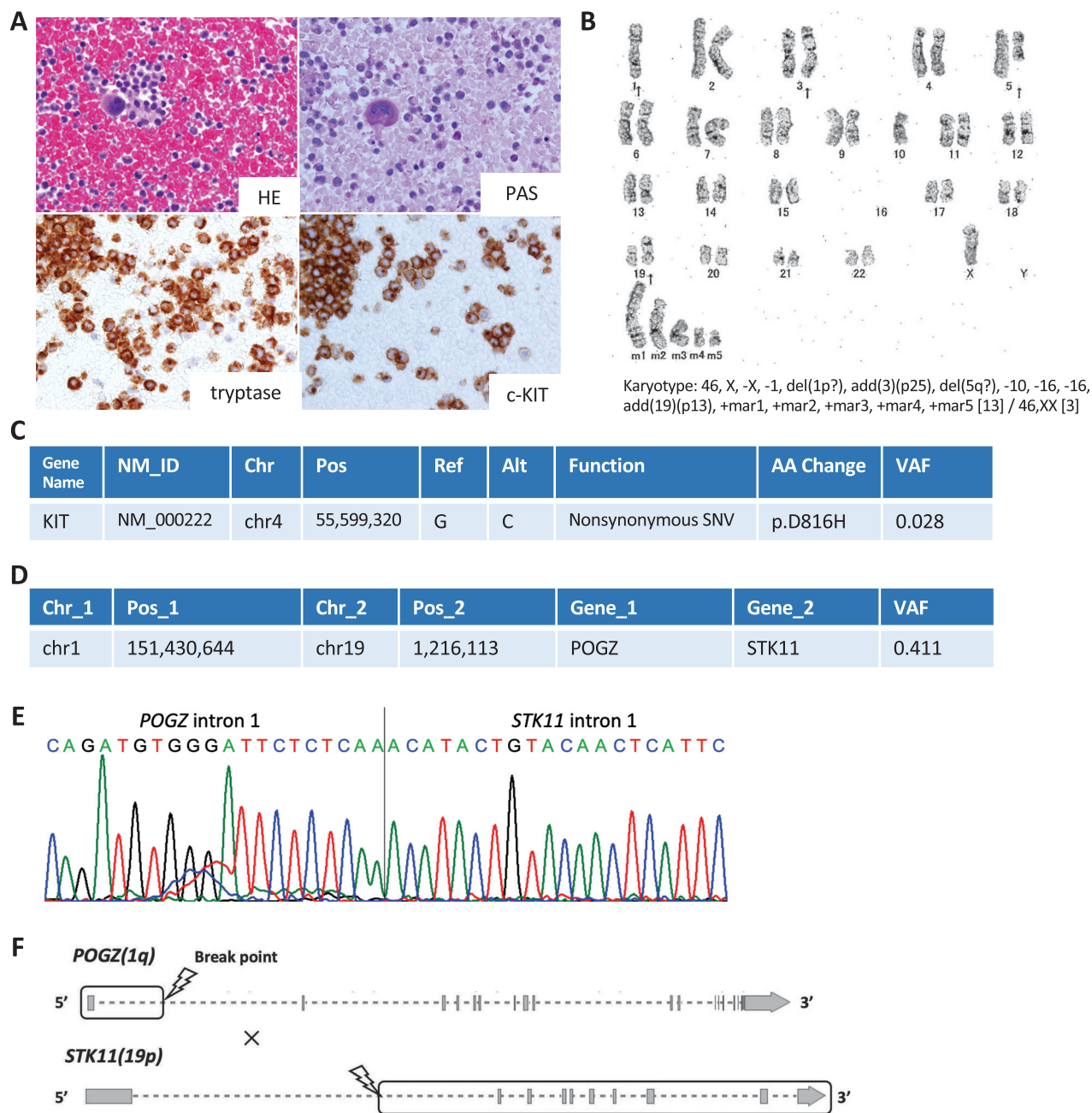


Figure 1. (A) Mast cells (MCs) in the bone marrow (BM) specimen. MCs infiltrate the BM and aggregate together (HE: hematoxylin and eosin staining ($\times 400$) and PAS: Periodic acid-Schiff staining ($\times 400$)). MCs are strongly positive for tryptase ($\times 400$) and c-KIT ($\times 400$). (B) G-banded karyotype of BM cells at the onset of disease. (C) The somatic mutation was detected with the BM specimen. NM_ID; Accession ID for transcript, Chr, chromosome; Pos, position; Ref, reference; Alt, alteration; AA amino acid; VAF, variant allele frequency; SNV, single nucleotide variant. (D) The translocation was detected with the BM specimen. Chr, chromosome; Pos, position; VAF, variant allele frequency. (E) Genomic breakpoint found in this case. Nucleotide sequencing analysis revealed a junction between POGZ intron 1 and STK11 intron 1. (F) Schematic representation of the POGZ/STK11 fusion. Boxes indicate exons and dotted lines indicate introns. Arrows indicate breakpoints for the fusion found in this case.

allele-matched donor graft (total number of nucleated cells: 3.48×10^7 cells/kg, CD34 positive cells: 1.10×10^5 cells/kg). The conditioning regimen comprised cyclophosphamide (50 mg/kg on days -5 and -4) and total body irradiation (TBI) (12 Gy/6 fr from day -1 to day -1). Tacrolimus and mycophenolate mofetil (2000 mg from day -1 to day 30) were administered as graft versus host disease (GVHD) prophylaxis. However, primary graft failure was diagnosed on day 25 after CBT. After a re-conditioning regimen [6] (fludarabine 30 mg/m² from day -4 to day -2 , cyclophosphamide 2 g/m² on day -2 , and TBI 2 Gy on day -1), a second CBT was performed on day 35 after the initial CBT. Neutrophil engraftment was recorded on day 14 after the second CBT. Hematological remission

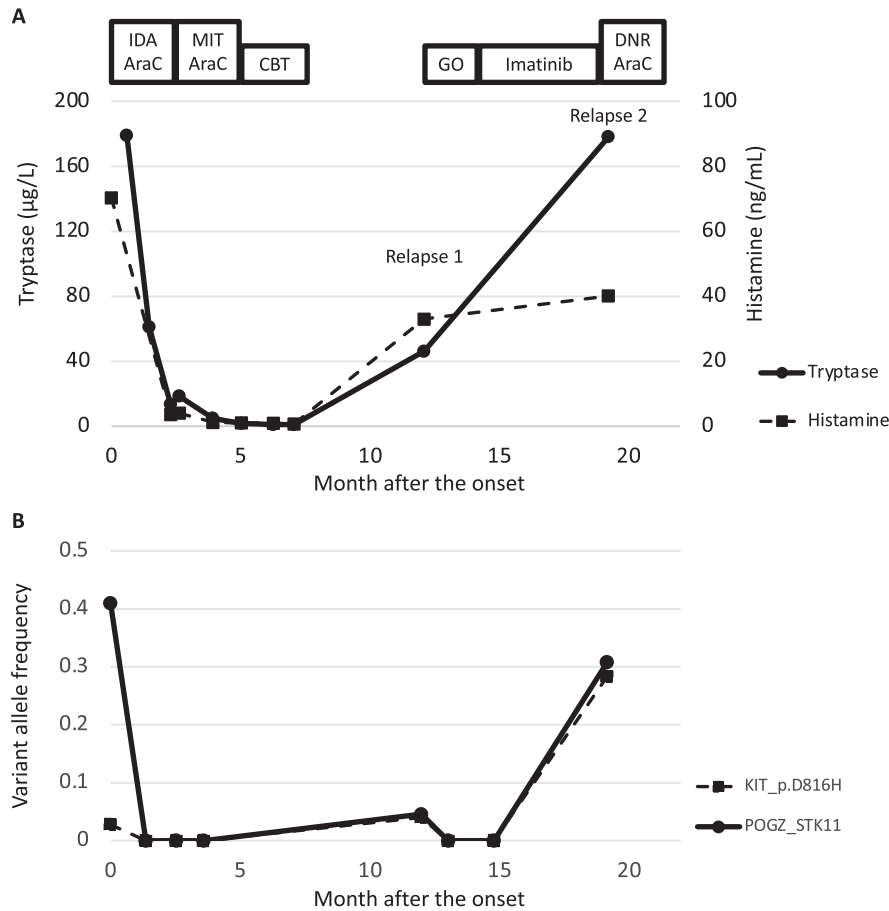


Figure 2. Clinical course. (A) tryptase and histamine levels during the treatment. IDA, idarubicin; AraC, cytarabine; MIT, mitoxantrone; CBT, cord blood transplant; GO, gemtuzumab ozogamicin; DNR, daunorubicin. (B) variant allele frequencies of *KIT* p.D816 and *POGZ/STK11* during the treatment.

was confirmed on day 28 and acute skin GVHD (stage 3, grade 2) appeared at the same time but responded to the topical steroid. She was discharged on day 93 after the second CBT and there were no signs of chronic GVHD. On day 240 after the second CBT, atypical MCs were observed in the BM aspirate, and fluorescence *in situ* hybridization of the sex chromosome showed the recipient-derived karyotype at a frequency of 6.4%, indicating disease relapse. We started salvage therapy with gemtuzumab ozogamicin (GO, 6 mg/m² on days 1 and 15). Following GO administration, hematological remission was achieved. We then repeated another course of GO and started imatinib (100 mg/day) as subsequent maintenance therapy. However, a secondary relapse occurred 8 months after the first relapse (Figure 2 (A)). Atypical MCs constituted almost all of the nucleated cells in the BM aspirate. The variant allele frequencies (VAFs) of *KIT* 816H and *POGZ/STK11* were also elevated (Figure 2 (B)). Severe anaphylactic shock (hypotension, systematic erythema, and airway obstruction) due to tumor lysis occurred on the day 1 after another salvage chemotherapy (daunorubicin 50 mg/m² on days 1–5, cytarabine 50 mg/m² on days 1–7). Despite intensive treatment, the patient died of pneumonia after 1 year and 9 months of MCL onset.

The prognosis of MCL is dismal, and the estimated overall survival (OS) is only a few months [4]. *De novo* MCL is resistant to many therapeutic agents, including tyrosine kinase inhibitors, 2-chlorodeoxyadenosine, interferon-alpha, and GO, which show some degree of efficacy against other subtypes of SM [7].

Considering that cytoreductive chemotherapy was needed in the case reported here, we opted to employ the standard remission induction therapy for AML. After achieving hematological remission, we performed allogeneic hematopoietic stem cell transplantation (HSCT). Recently, it was reported that allogeneic HSCT for MCL in 12 patients resulted in a 3-year OS in only 17% of the cases [8]. However, most of the patients undergoing transplantation had not achieved remission before the transplantation in this study. In this case, hematological remission without the detection of both *KIT* D816H mutation and *POGZ/STK11* translocation was achieved; therefore, we hypothesized that allogeneic HSCT would potentially improve the OS. However, the disease relapsed 8 months after CBT.

Several driver mutations in *KIT* have been detected in 80% of SM cases including those of MCL. However, 19% of *de novo* MCL patients do not exhibit *KIT* mutations [9].

Additional mutations in *SRSF2*, *ASXL1*, and *RUNX1*, together with those in *KIT*, are related to a poor prognosis. Approximately half of the patients with MCL (13 out of 24 patients) exhibited these mutations [9], suggesting that gene mutations other than *KIT* might be involved in the pathogenesis of MCL.

In this case, a *KIT* D816H mutation and the novel *POGZ/STK11* translocation were detected using targeted sequencing with a 390-gene panel for myeloid neoplasms. No other mutation was detected using this sequencing panel. We identified the *POGZ/STK11* translocation by sequencing *STK11* using genomic DNA from BM cells followed by validation through Sanger sequencing. The fusion occurs between the *POGZ* gene intron1 on chromosome 1q21.3 and the *STK11* gene intron1 on 19p13.3, which was previously undescribed. Of note, the VAF of *KIT* D816H was low compared to the observed number of atypical MCs in the BM at the onset of MCL, while the VAF of *POGZ/STK11* was proportional to the tumor burden. Considering these results and the VAFs of the two mutations during the entire disease course, it is suggested that clonal MCs with *POGZ/STK11* translocation expanded at the onset of MCL, and then a small subclone with a *KIT* D816H mutation dominantly expanded during disease relapse.

The role of the *POGZ/STK11* translocation in the pathogenesis of MCL is not elucidated yet because this translocation was not previously reported. However, the mutation in *STK11*, which induces the loss of function, was associated with tumorigenesis in diseases including myeloproliferative disease and AML [10,11]. Further, somatic mutations of *STK11* are associated with the inherited cancer predisposition disease, Peutz-Jeghers syndrome [12]. In addition, the deletion of *STK11* induces aberrant mast cell activation through the regulation of AMP-activating protein kinase signaling [13,14]. Therefore, dysfunction in *STK11* could be a possible mechanism underlying MCL induction in this case.

Several fusion genes associated with *STK11* were detected in cancer tissues [15]. Considering that *STK11* is a tumor suppressor gene, these fusions would induce dysfunction of *STK11*. In this case, the translocation induced the loss of the promoter region in intron 1 on *STK11*, possibly leading to the transcriptional deactivation of the kinase domains (exon 4–6) on *STK11*.

In summary, this is the first reported case of MCL with *POGZ/STK11* translocation and *KIT* D816H mutation. Although the patient achieved hematological remission once, the *KIT* D816H-mutated subclone of MCs dominantly expanded and became refractory to multiple treatments. This report contributes to understanding the molecular pathogenesis and clinical features of MCL. Further studies are needed to develop a better treatment strategy.

Acknowledgment

The authors thank the patient for providing valuable information.

Ethical statements

The study was approved by the institutional review board at University of Tsukuba Hospital. Written informed consent was obtained from the patient and her families.

Disclosure statement

The authors declare no conflict of interest.

Funding

This work was supported by Grants-in-Aid for Scientific Research (KAKENHI: 21J20378[K.I.], 18K16076[M.K.], 21H02945[M.S.-Y.], and 19H03684[S.C.]) from the Ministry of Education, Culture, Sports, and Science of Japan.

ORCID

Hidekazu Nishikii  <http://orcid.org/0000-0002-6277-4082>

Manabu Kusakabe  <http://orcid.org/0000-0003-2518-0776>

Data availability statement


All data and materials are available upon request.

References

- [1] Arber DA, Orazi A, Hasserjian R, et al. The 2016 revision to the world health organization classification of myeloid neoplasms and acute leukemia. *Blood*. 2016;127(20):2391–2405.
- [2] Furitsu T, Tsujimura T, Tono T, et al. Identification of mutations in the coding sequence of the proto-oncogene c-kit in a human mast cell leukemia cell line causing ligand-independent activation of c-kit product. *J Clin Invest*. 1993;92(4):1736–1744.
- [3] Piao X, Paulson R, van der Geer P, et al. Oncogenic mutation in the kit receptor tyrosine kinase alters substrate specificity and induces degradation of the protein tyrosine phosphatase SHP-1. *Proc Natl Acad Sci USA*. 1996;93(25):14665–14669.
- [4] Pardanani A. Systemic mastocytosis in adults: 2019 update on diagnosis, risk stratification and management. *Am J Hematol*. 2019;94(3):363–377.
- [5] Miyawaki S, Sakamaki H, Ohtake S, et al. A randomized, post-remission comparison of four courses of standard-dose consolidation therapy without maintenance therapy versus three courses of standard-dose consolidation with maintenance therapy in adults with acute myeloid leukemia: the Japan adult leukemia study group AML97 study. *Cancer*. 2005;104(12):2726–2734.
- [6] Suma S, Yokoyama Y, Momose H, et al. Salvage cord blood transplantation using a short-term reduced-intensity conditioning regimen for graft failure. *Intern Med*. 2022;61(11):1673–1679.
- [7] Georgin-Lavialle S, Lhermitte L, Dubreuil P, et al. Mast cell leukemia. *Blood*. 2013;121(8):1285–1295.
- [8] Ustun C, Reiter A, Scott BL, et al. Hematopoietic stem-cell transplantation for advanced systemic mastocytosis. *J Clin Oncol*. 2014;32(29):3264–3274.
- [9] Jawhar M, Schwaab J, Meggendorfer M, et al. The clinical and molecular diversity of mast cell leukemia with or without

- associated hematologic neoplasm. *Haematologica*. 2017; 102(6):1035–1043.
- [10] Marinaccio C, Suraneni P, Celik H, et al. LKB1/STK11 is a tumor suppressor in the progression of myeloproliferative neoplasms. *Cancer Discov*. 2021;11(6):1398–1410.
- [11] Green AS, Chapuis N, Maciel TT, et al. The LKB1/AMPK signaling pathway has tumor suppressor activity in acute myeloid leukemia through the repression of mTOR-dependent oncogenic mRNA translation. *Blood*. 2010;116(20):4262–4273.
- [12] Hezel AF, Bardeesy N. LKB1; linking cell structure and tumor suppression. *Oncogene*. 2008;27(55):6908–6919.
- [13] Jin F, Li X, Deng Y, et al. The orphan nuclear receptor NR4A1 promotes Fc ϵ RI – stimulated mast cell activation and anaphylaxis by counteracting the inhibitory LKB1/AMPK axis. *Allergy*. 2019;74(6):1145–1156.
- [14] Hwang SL, Li X, Lu Y, et al. AMP-activated protein kinase negatively regulates Fc ϵ RI-mediated mast cell signaling and anaphylaxis in mice. *J Allergy Clin Immunol*. 2013;132(3):729–736.e12.
- [15] Gao Q, Liang WW, Foltz SM, et al. Driver fusions and their implications in the development and treatment of human cancers. *Cell Rep*. 2018;23(1):227–238.e3.

The effectiveness of exercise with behavior change techniques in people with knee osteoarthritis: A systematic review with meta-analysis

Takashi Arie PhD, MSc^{1,2}  | Hiroshi Takasaki PhD³ | Ryota Okoba PhD¹ |
Hiroki Chiba BSc⁴ | Yusuke Handa BSc⁴ | Takahiro Miki MSc⁴ |
Shunsuke Taito PhD^{2,5} | Yusuke Tsutsumi DrPH^{2,6} | Masaharu Morita PhD⁷

¹Department of Physical Therapy, School of Health Sciences at Fukuoka, International University of Health and Welfare, Fukuoka, Japan

²Scientific Research WorkS Peer Support Group (SRWS-PSG), Osaka, Japan

³Department of Physical Therapy, Saitama Prefectural University, Saitama, Japan

⁴Graduate school of Rehabilitation Science, Saitama Prefectural University, Saitama, Japan

⁵Division of Rehabilitation, Department of Clinical Practice and Support, Hiroshima University Hospital, Hiroshima, Japan

⁶Department of Emergency Medicine, National Hospital Organization Mito Medical Center, Ibaraki, Japan

⁷Department of Physical Therapy, Health Sciences at Odawara, International University of Health and Welfare, Kanagawa, Japan

Correspondence

Takashi Arie, Department of Physical Therapy, School of Health Sciences at Fukuoka, International University of Health and Welfare, 137-1 Enokizu, Okawa-shi, Fukuoka, Japan.

Email: tarie@iuhw.ac.jp

Abstract

Objective: The purpose of this systematic review with meta-analysis was to examine the effectiveness of exercise with behavior change techniques (BCTs) on core outcome sets in people with knee osteoarthritis.

Literature Survey: We searched randomized controlled trials (RCTs) in eight databases (MEDLINE, Embase, CENTRAL, CINAHL, PsycINFO, PEDro, ICTRP, and ClinicalTrials.gov) up to November 4, 2021.

Methodology: Eligible participants were people with knee osteoarthritis. The intervention was exercise with BCTs. Primary outcomes included physical function, quality of life (QOL) 6 to 12 months after intervention, and adverse events. Secondary outcomes were knee pain, exercise adherence, mobility, and self-efficacy 3 months or more after intervention. The bias risk was assessed using the Risk of Bias 2 tool. The random-effects model was used for the meta-analysis.

Synthesis: We found 16 individual BCTs, and 37.7% of trials used a single BCT. For meta-analysis, we included 21 RCTs ($n = 1623$). Most outcomes had a very low certainty of evidence, and the risk of bias was the consistent reason for downgrading evidence levels. The standardized mean difference (SMD) with 95% confidence interval (95% CI) was 0.00 (−0.24, 0.24) in physical function, 0.33 (−0.51, 1.17) in exercise adherence, and 0.04 (−0.39, 0.47) in self-efficacy. The risk ratio (95% CI) of adverse events was 3.6 (0.79, 16.45). QOL was not pooled due to insufficient data (very low certainty of evidence). In contrast, the SMD (95% CI) for knee pain reduction and mobility improvement was −0.33 (−0.53, −0.13) and 0.21 (−0.05, 0.47) with moderate and low certainty of evidence, respectively.

Conclusion: The evidence is inconclusive regarding the effectiveness of BCTs with exercises on core outcome sets. Further research should explore the effectiveness of BCTs with valid design.

Protocol Registration: PROSPERO (CRD42020212904).

INTRODUCTION

Knee osteoarthritis is one of the leading causes of disability globally.¹ The social cost of osteoarthritis has been estimated to reach 0.50% of a country's gross domestic product.² Non-surgical management, especially exercise, is consistently recommended in clinical

practice guidelines as first-line treatment.³ However, exercise adherence is generally poor in people with knee osteoarthritis,⁴ limiting the short-term (2- to 6-month) benefits.⁵ Previous systematic reviews^{6,7} indicate that interventions with behavior change techniques (BCTs) may improve exercise adherence in people with musculoskeletal diseases, associated with

long-term improvement of pain and physical function in the knee osteoarthritis population.⁸

Behavior change techniques (BCTs) are “observable, replicable, and irreducible components of an intervention designed to alter or redirect causal processes that regulate behavior”⁹ that can be used to improve exercise adherence.¹⁰ BCTs can be incorporated into exercise programs. For instance, therapists can “ask the person to walk for 100 yards a day for the first week, then half a mile a day after they have successfully achieved 100 yards, then 2 miles a day after they have successfully achieved 1 mile” (graded tasks).⁹ In addition, BCTs can be provided separately from exercise. Therapists may “prompt the patient to identify barriers preventing them from starting a new exercise regimen” (problem solving).⁹

The European League Against Rheumatism recommends exercise intervention, incorporating BCTs to increase the amount of physical activity.¹¹ However, the effectiveness of exercise with BCTs on other core outcome sets, such as physical function, quality of life (QOL), or knee pain, has not been investigated.¹² The Outcome Measures in Rheumatology–Osteoarthritis Research Society International reported core outcome sets that clinical trials should assess and report, including physical function, QOL, and pain as mandatory domains in the hip and knee osteoarthritis population.¹³ The aim of this systematic review was to comprehensively examine the effectiveness of exercise with BCT on core outcome sets including physical function, QOL, or adverse events, compared to exercise without BCTs, usual care, or no active intervention in adults with knee osteoarthritis.

METHODOLOGY

The Preferred Reporting Items for Systematic Reviews and Meta-Analyses (PRISMA) guidelines were followed,¹⁴ and the checklist can be found in Table S1. This review protocol was registered with PROSPERO (CRD42020212904).¹⁵

Literature search

The following databases were searched on November 4, 2021: MEDLINE, Embase, Cochrane Central Register of Controlled Trials (CENTRAL), CINAHL, PsycINFO, and PEDro. Ongoing trials in the World Health Organization International Clinical Trials Registry Platform (<http://apps.who.int/trialsearch/>) and Clinical Trials.gov (ClinicalTrials.gov) were also searched on November 4, 2021. Table S2 outlines the search strategy. The references of relevant guidelines (the European League Against Rheumatism Recommendations^{11,12} and the Osteoarthritis Research Society International guidelines¹⁶) and all references

included in each article were also searched. When the available information was insufficient, we contacted the study authors via email. A second attempt was made if the first remained unanswered.

Inclusion and exclusion criteria

Randomized-controlled trials (RCTs), crossover RCTs, and cluster RCTs were eligible for this systematic review. Both published and unpublished trials were included. There were no restrictions on the intervention duration, follow-up period, language, or study location. Cluster RCTs were excluded if an intraclass correlation coefficient (ICC) to consider the variability of clusters for appropriate analyses was not available. Eligible participants included adults (≥ 18 years) with knee osteoarthritis with or without radiographic diagnosis, or who self-reported knee osteoarthritis based on chronic joint pain as defined by the study author. Participants who had a knee joint operation within 6 months of the study were excluded. Interventions containing exercise with BCTs were eligible. We included any exercise programs aimed at improving symptoms, regardless of intensity, duration, content, or frequency that can be provided in any form, such as by health care providers or booklets including physical activity interventions. If interventions included other conservative management that may influence the outcome, including electrotherapy, diet, or medication, participants were excluded. For BCTs, an appropriate taxonomy was used to identify the techniques and to categorize the technique type.⁹ International experts developed the taxonomy, and all 93 techniques were defined for coding. We followed the standardized BCT coding⁹: “(1) contain verbs that refer to the action(s) taken by the person/s delivering the technique and (2) contain the term behavior referring to a single action or sequence of actions that includes the performance of wanted behavior(s) and/or inhibition (non-performance) of unwanted behavior(s).” The taxonomy of BCT includes 93 techniques, such as “adding objects to the environment” (e.g., providing elastic bands to promote exercise, providing a pedometer to promote walking, or providing a yoga mat for home exercise), “self-monitoring of behavior” (e.g., asking patients to record the daily total number of steps in a diary), and “social support (unspecified)” (e.g., advising patients to call staff when they experience difficulty with exercise).⁹ Any BCTs defined in the taxonomy, such as “graded tasks,” which may be part of an exercise regimen, or “problem solving,” which may be provided separately from exercise, were accepted. Prescribing exercise interventions can potentially include some BCT components, such as “instruction on how to perform a behavior” or “action planning.” Therefore, if interventions did not explicitly describe BCT components in the articles

or protocols, they were not considered as appropriate BCTs (e.g., “instruction on how to perform a behavior” is defined as “advise or agree on how to perform the behavior.” If the study mentioned that “an intervention group conducted a walking exercise,” this intervention was coded as “instruction on how to perform a behavior.” If the study mentioned that “therapists advised participants on how to walk on a treadmill,” then this intervention was coded as “instruction on how to perform a behavior.”) In addition, if interventions including the definition of BCTs were a part of the research procedure (e.g., one of the BCTs, “self-monitoring of behavior,” should not be just a part of the data collection procedure), it was not considered an appropriate BCT. A control group was eligible if they received any exercise program described above. This comparison is ideal for examining the additional effect of BCTs on exercise. Therefore, studies were excluded if the control intervention contained BCTs. Usual care was also included as defined by the authors, and no active intervention, including a waitlist, as the control intervention.

Three primary outcomes and four secondary outcomes were selected as recommended by the Cochrane Handbook for Systematic Reviews of Interventions.¹⁷ The outcomes were selected based on the core outcome sets in clinical trials of knee osteoarthritis.¹³ In addition, we prioritized outcome domains in which the effectiveness was poorly reported in previous reviews.^{5,10,12,18} Primary outcomes were physical function, QOL 6 to 12 months after the end of the intervention, and the number of all adverse events at any time point. Physical function was defined as measures used in self-reported questionnaires, such as the Western Ontario and McMaster Universities Osteoarthritis Index (WOMAC). QOL included self-reported questionnaires, such as the Euro QOL 5 Dimensions Questionnaire or the 36-item Short-Form Survey. The number of all adverse events as defined by the author, such as falls, was included.

Secondary outcomes were knee pain as measured by a self-reported scale (e.g., visual analog scale, numerical rating scale, or a questionnaire, such as WOMAC); exercise adherence as measured by a self-rated scale, a logbook, or a questionnaire; mobility as measured by a walking test, like the Six-Minute Walk Test (6MWT); and self-efficacy related to symptoms or the ability to perform the exercise as measured by a self-rated scale or questionnaire 3 months or more after the end of the intervention. If studies reported multiple eligible outcomes, we prioritized measures that we used as examples in our pre-registered protocol. The latest follow-up time point was used if the included studies measured multiple time points.

Study selection

Pairs of review authors (H.T., R.O., H.C., Y.H., T.M., and T.A.) independently assessed records from the

titles and abstracts to identify eligible studies using Rayan software (available at <https://www.rayyan.ai/>). First, the six authors screened 50 records for calibration training to find and resolve ambiguity in the eligibility criteria. Then, pairs of review authors (H.T., R.O., H.C., Y.H., T.M., and T.A.) independently conducted full-text screening to assess whether the studies met the criteria. If two authors were conflicted in their decision to include a study, they discussed the matter to reach an agreement. If they could not do so, the third author (S.T.) mediated and helped reach a conclusion. After the full-text screening, eligibility of the intervention components of the included studies was assessed independently by the two authors (Y.H. and T.A.) who had completed an online BCT coding training (available at <https://www.bcttaxonomy.com/>). For studies excluded for having the “wrong intervention,” two authors (Y.H. and T.A.) assessed the intervention again to avoid dismissing relevant studies.

Methodological quality assessment

Pairs of review authors (R.O., H.C., and T.A.) independently assessed the risk of bias of studies included in the quantitative analysis using the Risk of Bias 2 tool.¹⁹ This tool assesses five domains (the randomization process, deviations from intended interventions, missing outcome data, outcome measurement, and the reported results). The randomization process domain assessed the method of randomization, allocation, and baseline characteristics. The deviations from intended interventions domain assessed the blinding of participants and therapists, drop out from the intervention, or the use of intention-to-treat analysis. The missing outcome data domain assessed missing variables and statistical methods. The outcome measurement domain assessed the validity of the measurement, assessor blind and outcome characteristics. The tool assessed these domains for each outcome in RCTs. Thus this tool could consider the difference of risk of bias for each outcome in a single RCT. Pairs of review authors assessed three included studies for calibration training to find, clarify, and resolve ambiguity between assessors. If two authors had a conflict, they discussed the matter until they reached an agreement. The third author (S.T.) resolved any remaining conflicts.

Data extraction

Pairs of review authors (H.T., R.O., H.C., Y.H., and T.A.) independently extracted data using data extraction forms that were pilot-tested in advance on 10 random studies. When the two authors were conflicted, they discussed the matter to reach an agreement. A third author (S.T.) resolved any remaining conflicts. The characteristics of the studies (the name of the first

author, publication year, and study location), participants (sample size, gender, disease condition, and age), interventions (contents, duration, and BCT), outcome measures, and results (post-intervention values) were extracted.

Statistical analysis

The data were analyzed using Review Manager software (RevMan 5.4). For the meta-analysis, the random-effects model was used. For dichotomous outcomes, we used the Mantel–Haenszel method. For continuous outcomes, we used the Inverse Variance Method to synthesize the data. All of the data were analyzed for discrete variables according to the intention-to-treat (ITT) concept. We did not perform imputation of missing values for continuous variables, per the Cochrane handbook recommendation.¹⁷ The standardized mean difference (SMD) with a 95% confidence interval (CI) for continuous outcome data were calculated if studies used the same outcomes but different measurement tools. A risk ratio with a 95% CI for dichotomous outcome data was calculated.

We performed the meta-analyses using the original data. When the included study used more than two eligible intervention groups, the statistical data (mean value, standard deviation, and sample size) of the two groups were combined following the Cochrane handbook guidelines to present as a single intervention group using the RevMan calculator.¹⁷

We assessed the heterogeneity by observing a forest plot and calculating I^2 -square (I^2) values (I^2 values of 0% to 40% might not be important; 30% to 60% may represent moderate heterogeneity; 50% to 90% may represent substantial heterogeneity; 75% to 100% may represent considerable heterogeneity).¹⁷ The reasons that heterogeneity was present ($I^2 > 50\%$) were assessed and a Cochrane χ^2 test (Q-test) was conducted, with $p < .10$ considered statistically significant.¹⁷ We planned to observe funnel plots and conduct Egger's test ($p < .05$) when we found more than 10 studies. [ClinicalTrials.gov](https://clinicaltrials.gov) and ICTRP were searched to identify finished but unpublished studies.

When heterogeneity was found in the results, a subgroup analysis was conducted to evaluate inconsistencies in primary outcomes using the following conditions: (1) mean age (a: 60 years or older, or b: younger than 60 years); (2) the number of BCT components (a: multiple components [more than two techniques], or b: single component); (3) control types (a: exercise regimen, b: usual care, or c: no active intervention, including waitlist); and (4) intervention duration (a: 6 months or longer, or b: less than 6 months). In addition, we conducted a sensitivity analysis to assess the treatment effect in primary outcomes, excluding studies with some concern or at high risk of bias in the

randomization process and those using imputed statistics.

Summary of findings

A summary of findings was created for physical function, QOL, the number of all adverse events, knee pain, exercise adherence, mobility, and self-efficacy following the Grading of Recommendations, Assessment, Development and Evaluation (GRADE) guidelines.²⁰ We used the GRADEpro GDT software. The comparison in the summary of findings included exercise regimen, usual care, or no active intervention. We reported outcome data for each outcome. The quality assessment of the evidence for each outcome was conducted based on five domains (limitations, inconsistency, indirectness, imprecision, and publication bias). The limitation domain was downgraded when trials had a high overall risk of bias and a high risk of bias in the randomization process. The inconsistency domain was downgraded considering heterogeneity (I^2 -value) and the direction of point estimates in each trial. The indirectness domain was downgraded when the included trials had characteristics different from our primary interest. The imprecision domain was downgraded when the 95% CI of effect measures was wide and the total sample size was less than 400. The publication bias domain was downgraded when asymmetrical funnel plots and statistically significant results of Egger's test were evident. It is recommended that the findings of systematic reviews be based on the effect size and the certainty of the evidence for better interpretability.²¹ The point estimate of the SMD or risk ratio was used as the magnitude of the effect, and 95% CI was used to judge the imprecision domain for the certainty of evidence. We presented results using a standardized expression.²¹

Differences between protocol and this review

A post hoc subgroup analysis was conducted based on the number of BCT components (multiple vs. single and four or more vs. three or less) for secondary outcomes that showed low to high certainty of evidence to explore the relevant implications between BCTs and outcomes.

RESULTS

We identified 8924 records from our initial search and screened 5470 records after duplicates were removed. We assessed 238 records for eligibility, and included 52 RCTs^{22–73} (55 records) for qualitative synthesis and

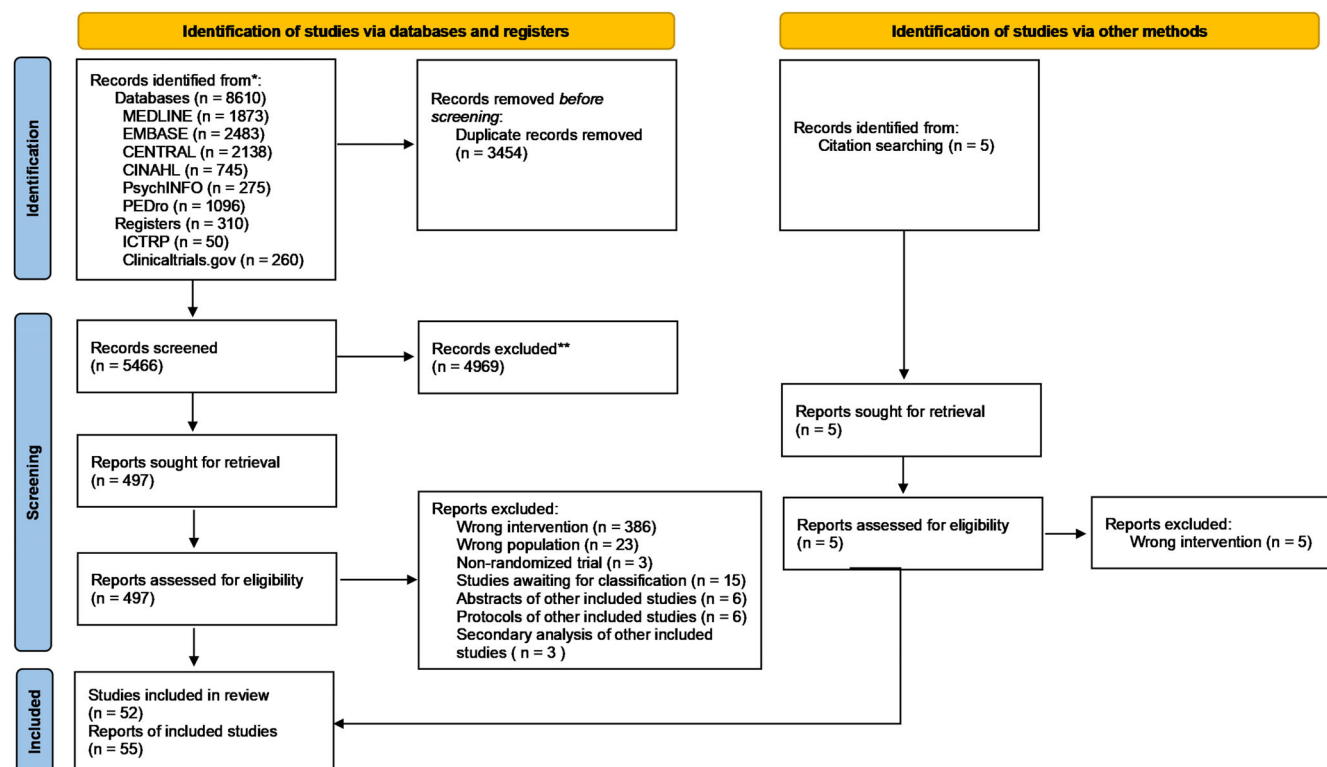


FIGURE 1 The Preferred Reporting Items for Systematic Reviews and Meta-Analyses (PRISMA) flow diagram.

21 RCTs^{24,26,27,30,32,36,42,43,45,46,54,55,57–59,61,66,68,69,71,72} with 1623 participants for the meta-analysis (Figure 1). Of the 52 included RCTs, 47 provided results and 5 were ongoing studies. The eligibility of 15 studies could not be judged due to insufficient information (studies awaiting classification), although the authors of those studies were contacted. Table S3 lists the studies excluded from this review and the reasons for their exclusion.

Characteristics of studies

Thirty-five studies (74.5%) had participants 60 years of age or older (Table 1). The disease conditions were assessed using the Kellgren-Lawrence grade and varied widely across the included studies (Table S4). Thirteen studies (27.7%) were from the United States. Thirty-seven included studies (78.7%) had an intervention duration of 3 months or less, and only three studies (6.4%) continued their intervention for more than 6 months. Through the BCT coding process, we identified 16 individual BCTs, and 20 studies (37.7%) used a single type of BCT. The most commonly used BCT was “adding objects to the environment,” which was integrated into 43 interventions (81.1%) among 53 interventions. The identification of the BCT used in the included studies is listed in Table S5. An exercise control group was used in only seven studies (14.9%), and usual care and no active intervention groups were used in

15 (31.9%) and 25 (53.2%) studies, respectively. All included studies had a randomized-controlled design. Three ongoing studies were identified (Table S6).

Risk of bias within studies

In this systematic review, 21 studies reporting 44 outcomes covered three primary and four secondary outcomes. The overall risk of bias was high in 17 studies and was of some concern in 4 studies (Tables S7 to S13). Nine of 21 studies (42.9%) were rated as high risk of bias in deviation from the intended interventions due to the lack of blinding participants and therapists to allocation, drop out from the intervention, or analysis other than ITT analysis. In 44 reported outcomes, 27 (61.4%) had high risk of bias in measurement of the outcome due to invalid measurement or lack of blinded assessors.

Primary outcomes

Five studies^{36,42,57,58,68} ($n = 288$) reported physical function outcomes measured using the WOMAC (physical function subscale), Late Life Function and Disability Index (basic lower limb function subscale), or Arthritis Impact Measurement Scales (physical activity subscale) 6 to 12 months after the intervention ended (Figure 2, Table 2). The types of control groups included exercise

TABLE 1 Characteristics of the included studies

Sample size	
Median (range)	50 (17–313)
Total (n)	3080
Mean age (n)	
>60 years	35
Kellgren-Lawrence grade (n)	
3	1
1 or 2	2
1–3	4
1–4	2
2 or 3	4
2–4	9
3 or 4	2
0–4	1
n.r.	22
Location (n) ^a	
USA	13
Australia	4
Brazil	4
Canada	4
China	4
Denmark	4
Finland	2
Netherlands	2
Nigeria	2
Other	9
Intervention duration (n)	
3 months or less	37
More than 3 to less than 6 month	7
6 month or longer	3
No. of BCTs used in the intervention (n)	
1	20
2	15
3	7
4	8
5	2
10	1
Types of BCTs (n)	
Adding objects to the environment	43
Instruction on how to perform the behavior	19
Self-monitoring of behavior	12
Social support (unspecified)	8
Feedback on behavior	8
Monitoring of behavior by others without feedback	8
Demonstration of the behavior	7
Graded tasks	4
Prompts cues	3
Review behavior goal(s)	2

(Continues)

TABLE 1 (Continued)

Behavioral practice/rehearsal	2
Problem solving	2
Information about health consequences	2
Action planning	1
Biofeedback	1
Goal setting (behavior)	1
Types of control group (n)	
No intervention	25
Usual care	15
Exercise	7

Note: n = 47; 53 interventions.

Abbreviations: BCTs, behavior control techniques; n.r.: not reported.

^aOne study was conducted in two countries (USA and Denmark).

(one study) and usual care (four studies). The evidence was very uncertain regarding the effect of exercise with BCT on physical function compared with the control group (SMD [95% confidence interval (CI)] 0.00 [−0.24, 0.24], $I^2 = 0$; very low certainty of evidence).

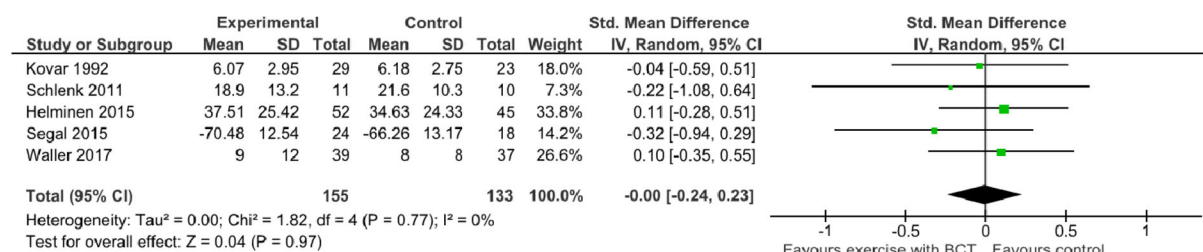
Two studies^{36,68} reported a QOL outcome as assessed by 15D (total score) and SF-36 (physical functioning subscale). The reported results evaluated different domains, and results could not be combined. Helminen et al.³⁶ reported no significant differences assessed with 15D 10.5 months after the end of the intervention compared with the usual care control group (−0.40 [95% CI −0.80, 0.00]). Waller et al.⁶⁸ reported no significant differences assessed with SF-36 at 12 months after intervention compared with the exercise control group (physical functioning subscale 0.00 [95% CI −7.37, 7.37]). Overall, the evidence of certainty was very low.

Eighteen studies^{24,26,27,30,32,36,42,43,45,46,54,55,58,59,61,66,69,71} (n = 1450) reported adverse events as assessed by questionnaires, reports from health care providers, or from a logbook or diary. The types of control groups were exercise (one study⁶⁹), usual care (eight studies^{30,32,36,42,43,46,54,58}), and no active intervention (nine studies^{24,26,27,45,55,59,61,66,71}). In nine studies,^{30,32,36,43,55,58,66,69,71} both the intervention and control groups reported no adverse events. One study²⁷ reported a reduction in the number of falls in the intervention group during the study, despite an increase in the no intervention control group. The evidence was very uncertain regarding the incidence of adverse events due to exercise with BCT compared with usual care or no active interventions (risk ratio 3.6 [95% CI 0.79, 16.45], $I^2 = 64\%$; very low certainty of evidence).

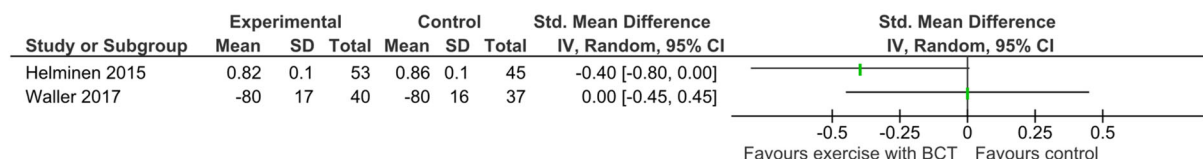
Secondary outcomes

Eight studies^{32,36,42,46,54,58,68,72} (n = 603) reported knee pain as assessed by the visual analog scale, the

(A) Physical function



(B) Quality of life



(C) Adverse events

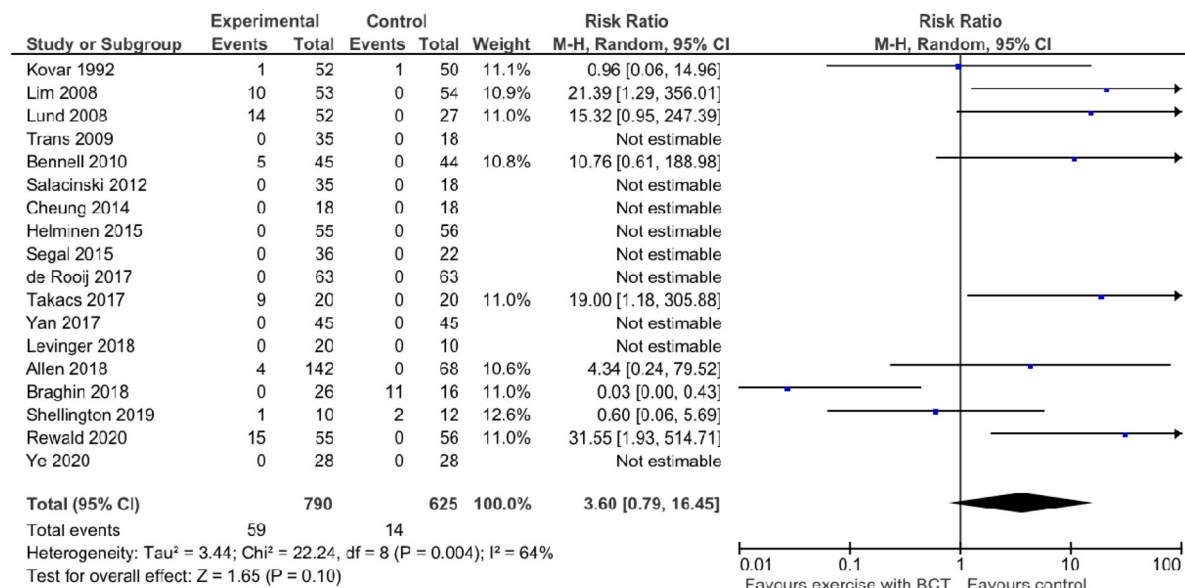


FIGURE 2 Forest plots of primary outcome.

WOMAC (pain subscale), the Knee injury and Osteoarthritis Outcome Score (pain subscale), or numerical pain rating scale 3 to 12 months after the end of the intervention (Figure 3, Table 2). The types of control groups were exercise (one study⁶⁸) and usual care (seven studies^{32,36,42,46,54,58,72}). Exercise with BCT likely reduces knee pain slightly (SMD -0.33 [95% CI -0.53 , -0.13], $I^2 = 31\%$; moderate certainty of evidence).

Two studies^{42,57} ($n = 61$) reported exercise adherence as assessed by self-reported walking distance or volume of exercise at 6 to 10 months after the end of the intervention compared with the usual care control group. The evidence of the effectiveness of exercise with BCTs between the groups for exercise adherence

was very uncertain (SMD 0.33 [95% CI -0.51 , 1.17], $I^2 = 59\%$; very low certainty of the evidence).

Four studies^{32,54,57,58} ($n = 231$) reported mobility outcomes as assessed by a 6 minute walking test (6MWT) or the Long-distance Corridor Walk Test, 3 to 9 months after the end of the intervention. The control group was usual care. Exercise with BCTs may improve mobility compared with the control group (SMD 0.21 [95% CI -0.05 , 0.47], $I^2 = 0$; low certainty of evidence).

Five studies^{36,42,54,57,72} ($n = 329$) reported on self-efficacy as assessed by the Arthritis Self-Efficacy Scale (pain subscale), Pain Self-Efficacy Questionnaire, or the Self-efficacy Scale 3 to 10.5 months after the end of

TABLE 2 Summary of findings in the comparison between exercise with behavior change techniques (BCTs) and exercise, usual care, or no active intervention.

Patient or population: knee osteoarthritis Setting: any Intervention: exercise with BCTs Comparison: exercise, usual care, or no active intervention					
Anticipated absolute effects ^a (95% CI)					
Outcomes	Risk with exercise, usual care, or no active intervention	Risk with exercise with BCT	Relative effect (95% CI)	No. of participants (studies)	Certainty of the evidence (grade)
Physical function WOMAC (physical function; Scale from 0 to 68), LLFDI (basic lower limb function; Scale from 0 to 100), AIMS (physical activity; Scale from 0 to 10) 6–12 months after the end of the intervention	—	SMD 0 (0.24 lower to 0.23 higher)	—	288 (5 RCTs)	⊕ ○ ○ ○ very low ^{b,c}
QOL Two different outcomes: 15D (Scale from 0 to 1) at 10.5 months after completion of the intervention; SF-36 (physical functioning; Scale from 0 to 100) at 12 months after completion of the intervention	—	There were no studies that found a difference between the intervention and control groups for QOL	—	Variable according to individual studies and outcome measures (2 RCTs)	⊕ ○ ○ ○ very low ^{c,d}
Adverse event Questionnaire or report from providers or participants, including logbook or diary	24 per 1000	87 per 1000 (19–397)	RR 3.60 (0.79–16.45)	1450 (18 RCTs)	⊕ ○ ○ ○ very low ^{e,f,g}
Knee pain VAS, WOMAC (pain), KOOS pain, NRS 3–12 months after the end of the intervention	—	SMD 0.33 lower (0.53 lower to 0.13 lower)	—	603 (8 RCTs)	⊕ ⊕ ○ ○ moderate ^h
Exercise adherence self-reported walking distance, volume of exercise (diary) 6–10 months after the end of the intervention	—	SMD 0.33 higher (0.51 lower to 1.17 higher)	—	61 (2 RCTs)	⊕ ○ ○ ○ very low ^{c,i}
Mobility walking speed, 6MWT, LDCWT 3–12 months after the end of the intervention	—	SMD 0.21 higher (0.05 lower to 0.47 higher)	—	231 (4 RCTs)	⊕ ⊕ ○ ○ low ^{j,k}
Self-efficacy ASES (pain), PSEQ, SES 3–10.5 months after the end of the intervention	—	SMD 0.04 higher (0.39 lower to 0.47 higher)	—	329 (5 RCTs)	⊕ ○ ○ ○ very low ^{c,l,m}

Note: GRADE Working Group grades of evidence. High certainty: we are very confident that the true effect lies close to that of the estimate of the effect. Moderate certainty: we are moderately confident in the effect estimate; the true effect is likely to be close to the estimate of the effect, but there is a possibility that it is substantially different. Low certainty: our confidence in the effect estimate is limited; the true effect may be substantially different from the estimate of the effect. Very low certainty: we have very little confidence in the effect estimate; the true effect is likely to be substantially different from the estimate of effect.

Abbreviations: AIMS, Arthritis Impact Measurement Scales; ASES, Arthritis Self-Efficacy Scale; BCTs, behavior change techniques; CI, confidence interval; KOOS, Knee Injury and Osteoarthritis Outcome Score; LDCWT, Long-distance Corridor walk test; LLFDI, Late Life Function and Disability Index; PSEQ, Pain Self-Efficacy Questionnaire; QOL, quality of life; RCTs, randomized controlled trials; RR, risk ratio; SMD, standardized mean difference; VAS, visual analogue scale; WOMAC, Western Ontario and McMaster Universities Osteoarthritis Index; 6MWT, 6 minute walking test.

^aThe risk in the intervention group (and its 95% confidence interval) is based on the assumed risk in the comparison group and the relative effect of the intervention (and its 95% CI).

^bDowngraded one level for serious risk of bias (four of five studies showed a high overall risk of bias, including two studies with a high risk of bias in the randomization process).

^cDowngraded two levels for very serious imprecision (small sample size [<400] and 95% CI includes 0.2 and -0.2).

^dDowngraded one level for serious risk of bias (15 of 18 studies showed high overall risk).

^eDowngraded one level for serious indirectness (for several studies we assumed that no adverse events occurred in the control group).

^fDowngraded one level for serious imprecision (sample size was lower than optimal information size and 95% CI includes the 1.0).

^gDowngraded one level for serious risk of bias (seven of eight studies showed high overall risk).

^hDowngraded one level for serious risk of bias (both studies showed a high overall risk of bias).

ⁱDowngraded one level for serious imprecision (small sample size [<400]).

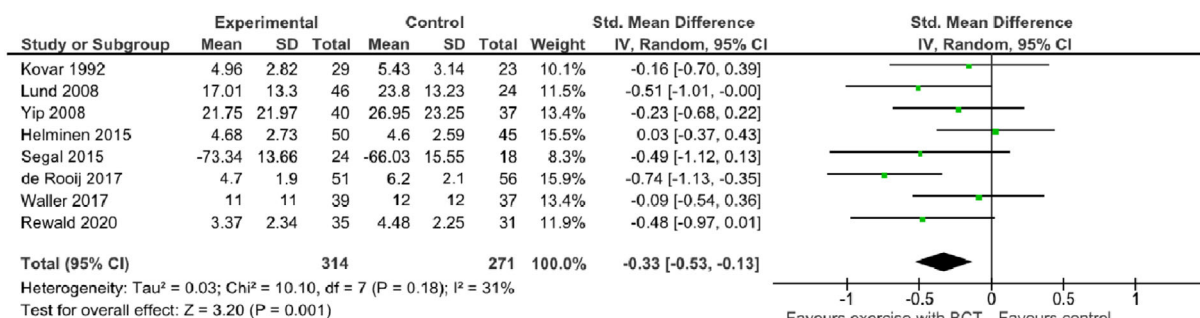
^jDowngraded one level for serious risk of bias (four of five studies showed a high overall risk of bias).

^kDowngraded one level for serious risk of bias (all studies showed a high overall risk of bias).

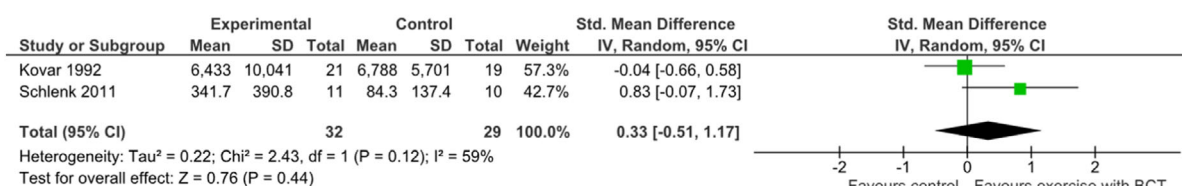
^lDowngraded one level for serious inconsistency (I^2 was 72% and point estimates vary widely among studies).

^m

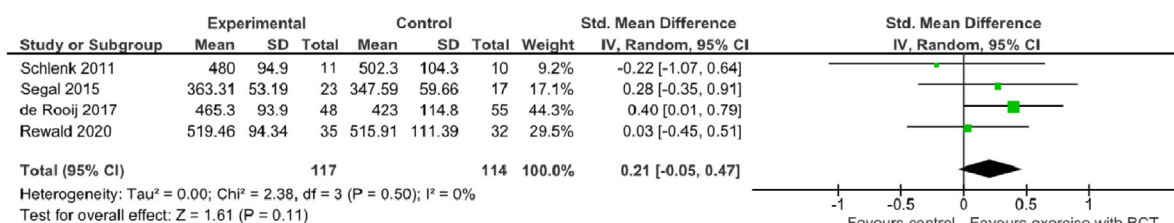
(A) Knee pain



(B) Exercise adherence



(C) Mobility



(D) Self-efficacy

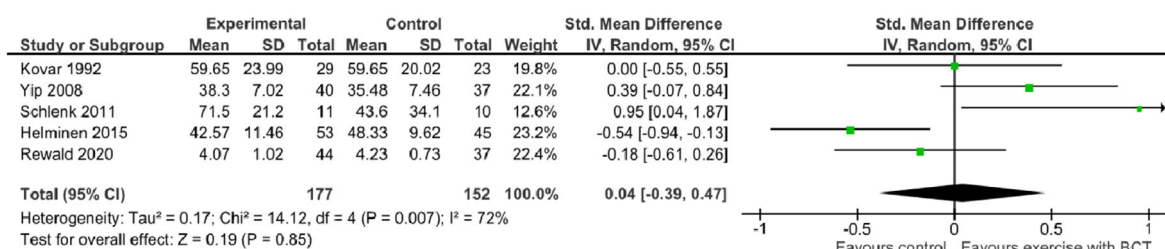


FIGURE 3 Forest plots of secondary outcome.

the intervention. The control group was usual care. The evidence is very uncertain regarding the effectiveness of exercise with BCT on self-efficacy compared with the usual care control group (SMD 0.04 [95% CI -0.39, 0.47], $I^2 = 72\%$; very low certainty of the evidence).

Additional analysis

We conducted a subgroup analysis for the primary outcome of adverse events, as we observed statistical

heterogeneity ($I^2 = 64\%$, $p = .04$) (Figures S1 and S2). The subgroup comparison was conducted in numbers of BCT, control intervention type, and intervention duration. Only type of control interventions showed significant differences ($I^2 = 66\%$, $p = .09$). Sensitivity analysis was also conducted for physical function and adverse events. Excluding studies with some concern of or at high risk of bias in the randomization process or studies that used imputed statistics did not result in any significant difference. We could not conduct observations of funnel plots and Egger's test due to an insufficient number of studies.

Post hoc analysis

We conducted post hoc subgroup analysis for knee pain and mobility outcomes dividing trials using multiple BCTs and single BCT (Figure S3). The SMD (95% CI) among trials using multiple BCTs for knee pain and mobility was -0.35 (-0.60 , 0.09) and 0.29 (-0.02 , 0.60), respectively. The SMD (95% CI) for those using single BCT for knee pain and mobility was -0.27 (-0.65 , 0.11) and 0.03 (-0.45 , 0.51), respectively. In addition, we conducted post hoc subgroup analysis of trials using four or more BCTs and those using three or fewer BCTs. The SMD (95% CI) among trials using four or more BCTs for knee pain and mobility was 0.03 (-0.37 , 0.43) and -0.22 (-1.07 , 0.64), respectively. The SMD (95% CI) for those using three or fewer BCTs for knee pain and mobility was -0.40 (-0.59 , -0.21) and 0.26 (-0.02 , 0.53), respectively.

DISCUSSION

This is the first systematic review with meta-analysis that examined the long-term effectiveness of exercise with BCT on core outcome sets in people with knee osteoarthritis, compared with exercise, usual care, or no active intervention. The certainty of evidence regarding clinically important outcomes such as physical function, QOL and adverse events was very low. These findings suggest that the BCTs used in the included trials might be suboptimal to enhance the exercise intervention.

Potential reasons for the very low certainty of evidence may be the lack of physical function and QOL outcomes measured at long-term time points and the risk of biases in each RCT. Only 5 and 2 of 52 RCTs reported physical function and QOL measured at long-term time points, respectively. The most common reason for downgrading the certainty of the evidence was the risk of bias in all outcomes of our review, followed by the imprecision domain in three outcomes, such as a small sample size. In the detail of risk of bias domains, deviation from intended interventions and measurement of outcome was consistently high risk among included trials. Thus future studies should consider the following four aspects. First, the authors of RCTs should investigate the effectiveness of exercise with BCTs on core outcome sets including physical function and QOL. Second, an ITT analysis should be used to improve the intervention effectiveness as allocated. Third, although blinding therapists and patients is difficult in non-pharmacological trials,⁷⁴ assessors should be blinded to decrease the risk of bias in measuring outcomes. Finally, RCTs with a larger sample size are needed to improve the precision of the estimates.

Our findings could not confirm whether integrating BCTs with exercise increased adverse events, which is

one of our primary outcomes, due to the very low certainty of evidence. Adverse events include non-serious adverse events such as pain, fatigue, or edema, and serious adverse events that result in death, hospitalization, or a deterioration in health.⁷⁵ Exercise therapy itself increases adverse events; however, these are mainly non-serious events including pain or fatigue.⁷⁵ The addition of BCTs into exercises may not significantly change this outcome. However, more than 70% of included trials in our review had a high risk of bias in the measurement of adverse events and 10 of 18 studies reported no description of adverse events, and it was uncertain if an adverse event was not produced or was not investigated appropriately. Future research should use the measure of adverse events with low risk of bias and should adhere to the use of a proper reporting format for clinical trials, which allows us to analyze the balance of risk and effectiveness comprehensively.

Regarding the effectiveness of exercises with BCTs on exercise adherence, our study revealed a very low certainty of evidence. In a previous review that reported slight improvement (SMD 0.2) in exercise adherence measured at 3 to 6 months after intervention by exercises with BCTs, knee osteoarthritis and several other chronic musculoskeletal conditions were included.⁶ For our review, we improved several methodological components (e.g., screening and data extraction conducted by two independent reviewers, excluding trials using BCTs in control groups, and comprehensive quality assessment of individual studies and evaluation of the certainty of evidence by GRADE approach) specifying the disease condition (knee osteoarthritis), compared to the previous study. Our findings indicate that further methodologically rigorous trials measuring exercise adherence, over the long-term, in the knee osteoarthritis population are needed. Furthermore, people with osteoarthritis may show clinically different responses to BCTs (calculated SMD 0.15), compared to other chronic musculoskeletal conditions such as rheumatoid arthritis (calculated SMD 0.31) or ankylosing spondylitis (calculated SMD 0.61),¹² according to a meta-analysis of six studies.¹²

Regarding knee pain and mobility, the SMD effect sizes for the improvement of knee pain and mobility were -0.33 (-0.53 , -0.13) and 0.21 (-0.05 , 0.47), respectively, and the intervention may have clinically important effects. However, Angst and colleague reported that the minimal clinically important difference (MCID) corresponded to an SMD of -0.38 for knee pain and SMD of 0.26 for mobility.⁷⁶ Therefore, the effectiveness on knee pain and mobility remains uncertain since these results cross MCID. There may be two reasons that the point estimates are below MCID. First, the number of BCTs used in several trials may be insufficient to improve the effectiveness. The post hoc subgroup analysis showed that exercise incorporating more than two BCTs tends to have higher SMD. For

mobility, SMD exceeds MCID in trials using more than two BCTs. In the current review, ~40% of the included trials used only a single BCT. A previous review showed that a greater number of BCTs had better exercise adherence.⁶ However, post hoc analysis also showed that exercise with four or more BCTs tends to be less effective for both knee pain and mobility outcomes. Therefore, increasing only the number of BCTs may not be appropriate for optimal intervention. Second, there may be a possibility that the BCTs used in the included trials may be inappropriate in terms of the quality to improve clinical outcomes for people with knee osteoarthritis. Another previous review showed the effectiveness of specific BCTs for people with lower limb osteoarthritis, namely, “behavioral contract,” “non-specific reward,” “goal setting” (behavior), “self-monitoring of behavior,” and “social support.”⁷⁷ The trials included in our meta-analysis used only “self-monitoring of behavior” (three trials^{57,70,72}), “social support” (two trials^{57,58}), “goal setting” (behavior) (one trial⁵⁷). Training needs are higher for optimal practice, particularly providing effective goal setting, since this technique requires the patient’s active involvement, thereby increasing their motivation and confidence.⁷⁸ Some BCTs may be easy to implement in daily clinical practice, but further consideration of the quantity and quality of BCTs is needed for appropriate use. Future studies using appropriate research methods such as a Delphi method⁷⁹ may be required to identify ideal combinations of BCTs for people with knee osteoarthritis. Then the combinations should be evaluated by observational studies and subsequent RCTs.

This review had a limitation. BCT coding was based on the description in the article and protocol, and BCTs performed without reporting may inevitably have been missed. In addition, Michie and colleagues reported that the behavior change interventions were inadequately described and inconsistent.⁸⁰ We addressed these points by using multiple reviewers who had training in BCT coding and classified the BCTs accordingly. We also contacted the authors to clarify ambiguities in their descriptions and to further determine eligibility to reduce the erroneous classification. However, we did not receive a response from 15 studies, and they could not be sufficiently evaluated. Researchers should report interventions in detail using the extensive taxonomy such as “BCT taxonomy v1.”⁹

CONCLUSION

Our review found that the certainty of the evidence regarding the effectiveness of exercise with BCTs on core outcome sets such as physical function, QOL, or adverse events was very low. Therefore, although BCTs are commonly used in clinical settings with recommendations from clinical practice guidelines, clinicians should critically appraise which BCTs to integrate

with exercise to improve the long-term clinical outcomes.

ACKNOWLEDGMENTS

We wish to thank Dr. Yuki Kataoka at Department of Internal Medicine, Kyoto Min-Iren Asukai Hospital for conceptual contributions; and Dr. Eeva-Eerika Helminen, MD, PhD, Psychiatry Department, Helsinki University Hospital; Dr. Neil Segal, MD, MS, Professor of Rehabilitation Medicine, University of Kansas Medical Center; Dr. Britt Elin Øiestad; Prof. Rajeshwar Nath Srivastava, Professor at the Department of Orthopedic Surgery, King George’s Medical University, Lucknow, India; and Dr. Sudeepti Ratan Srivastava, Research associate at the Indian Council of Medical Research, Department of Orthopedic Surgery, King George’s Medical University, Lucknow, India for information provision. We also wish to thank Ms. Rie Ichinose for her support in retrieving full-text articles and WORDVICE (wordvice.jp) for editing and reviewing this manuscript for English language.

DISCLOSURES

None.

DATA AVAILABILITY STATEMENT

The data sets are available from the corresponding author on reasonable request.

ORCID

Takashi Arie  <https://orcid.org/0000-0003-1457-3427>

REFERENCES

1. Cross M, Smith E, Hoy D, et al. The global burden of hip and knee osteoarthritis: estimates from the global burden of disease 2010 study. *Ann Rheum Dis*. 2014;73(7):1323-1330.
2. Puig-Junoy J, Ruiz ZA. Socio-economic costs of osteoarthritis: a systematic review of cost-of-illness studies. *Semin Arthritis Rheum*. 2015;44(5):531-541.
3. Mora JC, Przkora R, Cruz-Almeida Y. Knee osteoarthritis: pathophysiology and current treatment modalities. *J Pain Res*. 2018; 11:2189-2196.
4. Nicolson PJA, Hinman RS, Kasza J, Bennell KL. Trajectories of adherence to home-based exercise programs among people with knee osteoarthritis. *Osteoarthritis Cartilage*. 2018;26(4): 513-521.
5. Fransen M, McConnell S, Harmer AR, Van der Esch M, Simic M, Bennell KL. Exercise for osteoarthritis of the knee. *Cochrane Database Syst Rev*. 2015;1:CD004376.
6. Eisele A, Schagg D, Kramer LV, Bengel J, Gohner W. Behaviour change techniques applied in interventions to enhance physical activity adherence in patients with chronic musculoskeletal conditions: a systematic review and meta-analysis. *Patient Educ Couns*. 2019;102(1):25-36.
7. Nicolson PJA, Bennell KL, Dobson FL, Van Ginckel A, Holden MA, Hinman RS. Interventions to increase adherence to therapeutic exercise in older adults with low back pain and/or hip/knee osteoarthritis: a systematic review and meta-analysis. *Br J Sports Med*. 2017;51(10):791-799.
8. Pisters MF, Veenhof C, Schellevis FG, Twisk JW, Dekker J, De Bakker DH. Exercise adherence improving long-term patient

- outcome in patients with osteoarthritis of the hip and/or knee. *Arthritis Care Res (Hoboken)*. 2010;62(8):1087-1094.
9. Michie S, Richardson M, Johnston M, et al. The behavior change technique taxonomy (v1) of 93 hierarchically clustered techniques: building an international consensus for the reporting of behavior change interventions. *Ann Behav Med*. 2013;46(1):81-95.
10. Room J, Hannink E, Dawes H, Barker K. What interventions are used to improve exercise adherence in older people and what behavioural techniques are they based on? A systematic review. *BMJ Open*. 2017;7(12):e019221.
11. Osthoff AKR, Niedermann K, Braun J, et al. EULAR recommendations for physical activity in people with inflammatory arthritis and osteoarthritis. *Ann Rheum Dis*. 2018;77(9):1251-1260.
12. Osthoff AKR, Juhl CB, Knittle K, et al. Effects of exercise and physical activity promotion: meta-analysis informing the 2018 EULAR recommendations for physical activity in people with rheumatoid arthritis, spondyloarthritis and hip/knee osteoarthritis. *RMD Open*. 2018;4(2):e000713.
13. Smith TO, Hawker GA, Hunter DJ, et al. The OMERACT-OARSI core domain set for measurement in clinical trials of hip and/or knee osteoarthritis. *J Rheumatol*. 2019;46(8):981-989.
14. Page MJ, McKenzie JE, Bossuyt PM, et al. The PRISMA 2020 statement: an updated guideline for reporting systematic reviews. *BMJ*. 2021;372:n71.
15. Ariie T, Takasaki H, Okoba R, Taito S, Tsutsumi Y, Miki T, et al. The effectiveness of behavior change techniques with exercise for people with knee osteoarthritis: A systematic review and meta-analysis. PROSPERO 2020 CRD42020212904. https://www.crd.york.ac.uk/prospere/display_record.php?ID=CRD420202129042020. Accessed December 22, 2021.
16. Bannuru RR, Osani MC, Vaysbrot EE, et al. OARSI guidelines for the non-surgical management of knee, hip, and polyarticular osteoarthritis. *Osteoarthr Cartil*. 2019;27(11):1578-1589.
17. Higgins JPT, Thomas J, Chandler J, Cumpston M, Li T, Page MJ, Welch VA. Cochrane handbook for systematic reviews of interventions version 6.2 (updated February 2021). *Cochrane Database Syst Rev* 2021 <https://training.cochrane.org/handbook/current>. Accessed December 22, 2021.
18. Hochberg MC, Altman RD, April KT, et al. American College of Rheumatology 2012 recommendations for the use of nonpharmacologic and pharmacologic therapies in osteoarthritis of the hand, hip, and knee. *Arthritis Care Res (Hoboken)*. 2012;64(4):465-474.
19. Sterne JAC, Savovic J, Page MJ, et al. RoB 2: a revised tool for assessing risk of bias in randomised trials. *BMJ*. 2019;366:l4898.
20. Guyatt G, Oxman AD, Akl EA, et al. GRADE guidelines: 1. Introduction-GRADE evidence profiles and summary of findings tables. *J Clin Epidemiol*. 2011;64(4):383-394.
21. Santesso N, Glenton C, Dahm P, et al. GRADE guidelines 26: informative statements to communicate the findings of systematic reviews of interventions. *J Clin Epidemiol*. 2020;119:126-135.
22. Australian New Zealand Clinical Trials Registry. The Feldenkrais method in the Management of Pain, Function and Balance in People with Osteoarthritis of the Knee. Accessed December 22, 2021. <https://www.anzctr.org.au/Trial/Registration/TrialReview.aspx?id=374306>.
23. Ailly J, Castilho de Almeida A, da Silva RG, de Noronha M, Mattiello S. Is a periodized circuit training delivered by telerehabilitation effective for patients with knee osteoarthritis? A phase i randomized controlled trial. *Osteoarthr Cartil*. 2020;28:S468-S469.
24. Allen KD, Arbeeve L, Callahan LF, et al. Physical therapy vs internet-based exercise training for patients with knee osteoarthritis: results of a randomized controlled trial. *Osteoarthr Cartil*. 2018;26(3):383-396.
25. Aoki O, Tsumura N, Kimura A, Okuyama S, Takikawa S, Hirata S. Home stretching exercise is effective for improving knee range of motion and gait in patients with knee osteoarthritis. *J Phys Ther Sci*. 2009;21(2):113-119.
26. Bennell KL, Hunt MA, Wrigley TV, et al. Hip strengthening reduces symptoms but not knee load in people with medial knee osteoarthritis and varus malalignment: a randomised controlled trial. *Osteoarthr Cartil*. 2010;18(5):621-628.
27. Braghin RMB, Libardi EC, Junqueira C, Nogueira-Barbosa MH, de Abreu DCC. Exercise on balance and function for knee osteoarthritis: a randomized controlled trial. *J Bodyw Mov Ther*. 2018;22(1):76-82.
28. Bruce-Brand RA, Walls RJ, Ong JC, Emerson BS, O'Byrne JM, Moyna NM. Effects of home-based resistance training and neuromuscular electrical stimulation in knee osteoarthritis: a randomized controlled trial. *BMC Musculoskelet Disord*. 2012;13:118.
29. Cheing GL, Hui-Chan CW. Would the addition of TENS to exercise training produce better physical performance outcomes in people with knee osteoarthritis than either intervention alone? *Clin Rehabil*. 2004;18(5):487-497.
30. Cheung C, Wyman JF, Resnick B, Savik K. Yoga for managing knee osteoarthritis in older women: a pilot randomized controlled trial. *BMC Complement Altern Med*. 2014;14:160.
31. Colak TK, Kavlak B, Aydogdu O, et al. The effects of therapeutic exercises on pain, muscle strength, functional capacity, balance and hemodynamic parameters in knee osteoarthritis patients: a randomized controlled study of supervised versus home exercises. *Rheumatol Int*. 2017;37(3):399-407.
32. de Rooij M, van der Leeden M, Cheung J, et al. Efficacy of tailored exercise therapy on physical functioning in patients with knee osteoarthritis and comorbidity: a randomized controlled trial. *Arthritis Care Res*. 2017;69(6):807-816.
33. DeVita P, Aaboe J, Bartholdy C, Leonardis JM, Bliddal H, Henriksen M. Quadriceps-strengthening exercise and quadriceps and knee biomechanics during walking in knee osteoarthritis: a two-centre randomized controlled trial. *Clin Biomech*. 2018;59:199-206.
34. German Clinical Trials Register. Randomized controlled study in a wait-list control design to evaluate a 12-week app- and orthosis-supported training intervention in patients with moderate to severe knee osteoarthritis – AppExOA. https://www.drks.de/drks_web/setLocale_EN.do. Accessed December 22, 2021.
35. Fransen M, Crosbie J, Edmonds J. Physical therapy is effective for patients with osteoarthritis of the knee: a randomized controlled clinical trial. *J Rheumatol*. 2001;28(1):156-164.
36. Helminen EE, Sinikallio SH, Valjakka AL, Vaisanen-Rouvali RH, Arokoski JP. Effectiveness of a cognitive-behavioural group intervention for knee osteoarthritis pain: a randomized controlled trial. *Clin Rehabil*. 2015;29(9):868-881.
37. Henriksen M, Klokke L, Graven-Nielsen T, et al. Association of exercise therapy and reduction of pain sensitivity in patients with knee osteoarthritis: a randomized controlled trial. *Arthritis Care Res*. 2014;66(12):1836-1843.
38. Hunt MA, Keefe FJ, Bryant C, et al. A physiotherapist-delivered, combined exercise and pain coping skills training intervention for individuals with knee osteoarthritis: a pilot study. *Knee*. 2013;20(2):106-112.
39. Jan MH, Tang PF, Lin JJ, Tseng SC, Lin YF, Lin DH. Efficacy of a target-matching foot-stepping exercise on proprioception and function in patients with knee osteoarthritis. *J Orthop Sports Phys Ther*. 2008;38(1):19-25.
40. Keefe FJ, Blumenthal J, Baucom D, et al. Effects of spouse-assisted coping skills training and exercise training in patients

- with osteoarthritic knee pain: a randomized controlled study. *Pain*. 2004;110(3):539-549.
41. Kim JS, Kim CJ. Effect of a physical activity promoting program based on the IMB model on obese-metabolic health outcomes among obese older adults with knee osteoarthritis. *J Korean Acad Nurs*. 2020;50(2):271-285.
 42. Kovar PA, Allegrante JP, MacKenzie CR, Peterson MG, Gutin B, Charlson ME. Supervised fitness walking in patients with osteoarthritis of the knee. A randomized, controlled trial. *Ann Intern Med*. 1992;116(7):529-534.
 43. Levinger P, Dunn J, Nancy B, Michael B, George E, Hill K. Safety and feasibility of high speed resistance training with and without balance exercises for knee osteoarthritis: a pilot randomised controlled trial. *Phys Ther Sport*. 2018;34:154-163.
 44. Li L, Sayre EC, Grewal N, et al. Efficacy of a wearable-enabled physical activity counselling program for people with knee osteoarthritis. *Arthritis Rheumatol*. 2017;69(suppl 10). <https://acrabstracts.org/abstract/efficacy-of-a-wearable-enabled-physical-activity-counselling-program-for-people-with-knee-osteoarthritis/>. Accessed December 22, 2021.
 45. Lim BW, Hinman RS, Wrigley TV, Sharma L, Bennell KL. Does knee malalignment mediate the effects of quadriceps strengthening on knee adduction moment, pain, and function in medial knee osteoarthritis? *Arthritis Rheum*. 2008;59(7):943-951.
 46. Lund H, Weile U, Christensen R, et al. A randomized controlled trial of aquatic and land-based exercise in patients with knee osteoarthritis. *J Rehabil Med*. 2008;40(2):137-144.
 47. Mazloum V, Rabiei P, Rahnama N, Sabzehparvar E. The comparison of the effectiveness of conventional therapeutic exercises and pilates on pain and function in patients with knee osteoarthritis. *Complement Ther Clin Pract*. 2018;31:343-348.
 48. Rogers MW, Tamulevicius N, Semple SJ, Krkeljas Z. Efficacy of home-based kinesthesia, balance and agility exercise training among persons with symptomatic knee osteoarthritis. *J Sports Sci Med*. 2012;11(4):751-758.
 49. ClinicalTrials.gov. Efficacy of exercise on quality of life and physical function in patients with knee osteoarthritis. <https://clinicaltrials.gov/ct2/show/NCT01682980>. Accessed December 22, 2021.
 50. ClinicalTrials.gov. Knee biofeedback rehabilitation interface for game-based home therapy for patients with knee osteoarthritis (KneeBRIGHT). <https://clinicaltrials.gov/ct2/show/NCT04187092>. Accessed December 22, 2021.
 51. ClinicalTrials.gov. Exercise therapy for osteoarthritis pain: how does it work? (KOA-PAIN). <https://clinicaltrials.gov/ct2/show/NCT04362618>. Accessed December 22, 2021.
 52. Odole AC, Ojo OD. A telephone-based physiotherapy intervention for patients with osteoarthritis of the knee. *Int J Telerehabilitation*. 2013;5(2):11-20.
 53. Odole AC, Ojo OD. Is telephysiotherapy an option for improved quality of life in patients with osteoarthritis of the knee? *Int J Telerehabilitation*. 2014;2014:903816, 1-9.
 54. Rewald S, Lenssen AFT, Emans PJ, de Bie RA, van Breukelen G, Mesters I. Aquatic cycling improves knee pain and physical functioning in patients with knee osteoarthritis: a randomized controlled trial. *Arch Phys Med Rehabil*. 2020;101(8):1288-1295.
 55. Salacinski AJ, Krohn K, Lewis SF, Holland ML, Ireland K, Marchetti G. The effects of group cycling on gait and pain-related disability in individuals with mild-to-moderate knee osteoarthritis: a randomized controlled trial. *J Orthop Sports Phys Ther*. 2012;42(12):985-995.
 56. Schilke JM, Johnson GO, Housh TJ, O'Dell JR. Effects of muscle-strength training on the functional status of patients with osteoarthritis of the knee joint. *Nurs Res*. 1996;45(2):68-72.
 57. Schlenk EA, Lias JL, Sereika SM, Dunbar-Jacob J, Kwok CK. Improving physical activity and function in overweight and obese older adults with osteoarthritis of the knee: a feasibility study. *Rehabil Nurs*. 2011;36(1):32-42.
 58. Segal NA, Glass NA, Teran-Yengle P, Singh B, Wallace RB, Yack HJ. Intensive gait training for older adults with symptomatic knee osteoarthritis. *Am J Phys Med Rehabil*. 2015;94(10):848-858.
 59. Shellington EM, Gill DP, Shigematsu R, Petrella RJ. Innovative exercise as an intervention for older adults with knee osteoarthritis: a pilot feasibility study. *Can J Aging*. 2019;38(1):111-121.
 60. Simao AP, Avelar NC, Tossige-Gomes R, et al. Functional performance and inflammatory cytokines after squat exercises and whole-body vibration in elderly individuals with knee osteoarthritis. *Arch Phys Med Rehabil*. 2012;93(10):1692-1700.
 61. Takacs J, Krowchuk NM, Garland SJ, Carpenter MG, Hunt MA. Dynamic balance training improves physical function in individuals with knee osteoarthritis: a pilot randomized controlled trial. *Arch Phys Med Rehabil*. 2017;98(8):1586-1593.
 62. Thomas KS, Muir KR, Doherty M, Jones AC, O'Reilly SC, Bassey EJ. Home based exercise programme for knee pain and knee osteoarthritis: randomised controlled trial. *Br Med J*. 2002;325(7367):752.
 63. Thorstensson CA, Roos EM, Petersson IF, Ekdahl C. Six-week high-intensity exercise program for middle-aged patients with knee osteoarthritis: a randomized controlled trial [ISRCTN20244858]. *BMC Musculoskelet Disord*. 2005;6:27.
 64. Topp R, Pifer M. A preliminary study into the effect of 2 resistance training modes on proprioception of subjects with knee osteoarthritis. *J Public Health Res*. 2017;1(1):26-38.
 65. Topp R, Woolley S, Hornyak J 3rd, Khuder S, Kahaleh B. The effect of dynamic versus isometric resistance training on pain and functioning among adults with osteoarthritis of the knee. *Arch Phys Med Rehabil*. 2002;83(9):1187-1195.
 66. Trans T, Aaboe J, Henriksen M, Christensen R, Bliddal H, Lund H. Effect of whole body vibration exercise on muscle strength and proprioception in females with knee osteoarthritis. *Knee*. 2009;16(4):256-261.
 67. Vassao PG, de Souza MC, Silva BA, et al. Photobiomodulation via a cluster device associated with a physical exercise program in the level of pain and muscle strength in middle-aged and older women with knee osteoarthritis: a randomized placebo-controlled trial. *Lasers Med Sci*. 2020;35(1):139-148.
 68. Waller B, Munukka M, Rantalainen T, et al. Effects of high intensity resistance aquatic training on body composition and walking speed in women with mild knee osteoarthritis: a 4-month RCT with 12-month follow-up. *Osteoarthritis Cartil*. 2017;25(8):1238-1246.
 69. Yan A, Zhang K, Qin WK, et al. Clinical effects of rehabilitation exercise in the treatment of knee osteoarthritis based on the theory of "treating muscle for bone". *Zhongguo Gu Shang*. 2017;30(8):731-734.
 70. Ye J, Simpson MW, Liu Y, et al. The effects of Baduanjin qigong on postural stability, proprioception, and symptoms of patients with knee osteoarthritis: a randomized controlled trial. *Front Med*. 2020;6:1-10.
 71. Ye J, Zheng Q, Zou L, et al. Mindful exercise (Baduanjin) as an adjuvant treatment for older adults (60 years old and over) of knee osteoarthritis: a randomized controlled trial. *Evid Based Complement Alternat Med*. 2020;2020:9869161-9869169.
 72. Yip YB, Sit JW, Wong DY, Chong SY, Chung LH. A 1-year follow-up of an experimental study of a self-management arthritis programme with an added exercise component of clients with osteoarthritis of the knee. *Psychol Health Med*. 2008;13(4):402-414.
 73. Wortley M, Zhang S, Paquette M, et al. Effects of resistance and Tai Ji training on mobility and symptoms in knee osteoarthritis patients. *J Sport Health Sci*. 2013;2(4):209-214.
 74. Boutron I, Tubach F, Giraudeau B, Ravaud P. Blinding was judged more difficult to achieve and maintain in

- nonpharmacologic than pharmacologic trials. *J Clin Epidemiol*. 2004;57(6):543-550.
75. Niemeijer A, Lund H, Stafne SN, et al. Adverse events of exercise therapy in randomised controlled trials: a systematic review and meta-analysis. *Br J Sports Med*. 2020;54(18):1073-1080.
 76. Angst F, Benz T, Lehmann S, Aeschlimann A, Angst J. Multidimensional minimal clinically important differences in knee osteoarthritis after comprehensive rehabilitation: a prospective evaluation from the bad Zurzach osteoarthritis study. *RMD Open*. 2018;4(2):e000685.
 77. Willett M, Duda J, Fenton S, Gautrey C, Greig C, Rushton A. Effectiveness of behaviour change techniques in physiotherapy interventions to promote physical activity adherence in lower limb osteoarthritis patients: a systematic review. *PLoS One*. 2019;14(7):e0219482.
 78. Driver C, Kean B, Oprescu F, Lovell GP. Knowledge, behaviors, attitudes and beliefs of physiotherapists towards the use of psychological interventions in physiotherapy practice: a systematic review. *Disabil Rehabil*. 2017;39(22):2237-2249.
 79. Eubank BH, Mohtadi NG, Lafave MR, et al. Using the modified Delphi method to establish clinical consensus for the diagnosis and treatment of patients with rotator cuff pathology. *BMC Med Res Methodol*. 2016;16:56.
 80. Michie S, Fixsen D, Grimshaw JM, Eccles MP. Specifying and reporting complex behaviour change interventions: the need for a scientific method. *Implement Sci*. 2009;4:40.

SUPPORTING INFORMATION

Additional supporting information can be found online in the Supporting Information section at the end of this article.

How to cite this article: Ariie T, Takasaki H, Okoba R, et al. The effectiveness of exercise with behavior change techniques in people with knee osteoarthritis: A systematic review with meta-analysis. *PM&R*. 2023;15(8):1012-1025. doi:10.1002/pmrj.12898

CME Question

According to this systematic review with meta-analysis of patients with knee osteoarthritis, exercise with behavior change techniques (BCTs) demonstrated:

- a. Low certainty of evidence for knee pain reduction.
- b. High certainty of evidence for physical functioning.
- c. Low certainty of evidence for exercise adherence.
- d. High certainty of evidence for adverse events.

Answer online at <https://onlinelearning.aapmr.org/>

This journal-based CME activity is designated for 1.0 AMA PRA Category 1 Credit and can be completed online at <https://onlinelearning.aapmr.org/>. This activity is FREE to AAPM&R members and available to nonmembers for a nominal fee. CME is available for 3 years after publication date. For assistance with claiming CME for this activity, please contact (847) 737-6000.

All financial disclosures and CME information related to this article can be found on the Online Learning Portal (<https://onlinelearning.aapmr.org/>) prior to accessing the activity.

‘Hook’ Shape Lister Tubercle Is Associated with a Greater Incidence of Extensor Pollicis Longus Tendon Rupture after Distal Radius Fracture

Yosuke OGATA^{*,†}, Takeshi OGAWA[‡], Takumi HIRABAYASHI^{*,†}, Sho IWABUCHI^{*,†},
Yuichi YOSHII[§], Masashi YAMAZAKI^{*}

^{*}Department of Orthopaedic Surgery, Faculty of Medicine, University of Tsukuba, Japan

[†]Department of Orthopaedic Surgery and Sports Medicine, Mito Clinical Education and Training Centre,
University of Tsukuba Hospital, Mito Kyodo General Hospital, Japan

[‡]Department of Orthopaedic Surgery, National Hospital Organization Mito Medical Centre, Japan

[§]Department of Orthopaedic Surgery, Tokyo Medical University Ibaraki Medical Centre, Japan

Background: A rupture of the extensor pollicis longus (EPL) tendon located close to the Lister tubercle is an uncommon complication of distal radius fractures. This study aimed to determine whether the size and shape of Lister tubercle in patients with EPL rupture differs from a matched group of patients with distal radius fractures without EPL rupture.

Methods: We identified 15 patients with EPL rupture (3.5%) out of 426 with distal radius fractures treated conservatively at our hospital over 4 years. Out of the remaining 411 patients with distal radius fractures without EPL rupture, we selected patients using simple random sampling and pseudo-randomised them such that their age, sex and fracture type were matched with patients exhibiting EPL rupture. The size and shape of the Lister tubercle and the size of the EPL groove were measured in both groups using computed tomographic scans and compared.

Results: There was no difference in the size of the Lister tubercle or the EPL groove between both groups. A ‘hook’-shaped Lister tubercle was noted in 8 out of 15 patients with EPL rupture but in only 1 out of 15 matched patients without EPL rupture.

Conclusions: A ‘hook’-shaped Lister tubercle was seen more often in patients with EPL rupture following distal radius fracture.

Level of Evidence: Level III (Therapeutic)

Keywords: Lister tubercle, Extensor pollicis longus, Distal radius fracture, Hook shape deformation, Tendon rupture

INTRODUCTION

A rupture of the extensor pollicis longus (EPL) tendon is an uncommon complication of distal radius fractures.¹ Different mechanisms have been proposed to explain the rupture of the EPL tendon. Rivlin et al² suggested that the dorsal callus and osteophytes of patients who undergo distal radius osteotomies might contribute to the attritional rupture of the EPL tendon. Helal et al³ demonstrated that the EPL tendon is more likely to rupture in patients with undisplaced fractures due to the integrity of the extensor retinaculum. Engkvist and Lundborg⁴ demonstrated that increased pressure within the non-ruptured tendon sheath

Received: Dec. 20, 2021; Accepted: May 12, 2022

Published online: Sep. 28, 2022

Correspondence to: Takeshi Ogawa

280 Sakuranosato, Ibarakimachi

Ibaraki 311-3193, Japan

Tel: +81-29-240-7711, Fax: +81-29-240-7788

E-mail: ogawat@tsukuba-seikei.jp

jeopardises blood flow in the already poorly vascularised parts of the tendon that curves around the Lister tubercle, making it more prone to rupture.

Researchers have previously evaluated the size of the Lister tubercle in cadavers using callipers.⁵ In recent years, improvements in computed tomography (CT) imaging technology have been used to assess the relationship between different fracture types and the risk of tendon ruptures. Cha et al⁶ proposed that an island-shaped fracture of the Lister tubercle was associated with a higher risk of rupture because the callus narrowed the EPL groove. We hypothesised that there might be some characteristics, such as the size and/or shape of the Lister tubercle or the EPL groove, that contribute to a rupture of the EPL. This study aimed to determine whether the size and shape of the Lister tubercle in patients with EPL rupture differs from a matched group of patients with distal radius fractures without any EPL ruptures.

PATIENTS AND METHODS

This retrospective study was approved by the institutional review board of our hospital (H20-3), and written informed consent was obtained from the patients. We

looked at all patient records to identify those conservatively treated distal radius fractures that were presented at our hospital in the period between April 2015 and December 2020. The exclusion criteria were as follows: (i) patients <18 years of age, (ii) patients who underwent surgery, (iii) patients without CT scans during treatment and (iv) those with <8 weeks of follow-up. Data on age, sex, type of fracture (AO classification) and presence of EPL rupture were collected. The group of patients with the EPL rupture was labelled as the rupture group (RG). Out of the remaining patients without an EPL rupture, the same number of patients matched for age, sex and type of fracture among patients with EPL rupture were identified using random sampling. This group was labelled as the intact group (IG). A total of 426 patients with distal radius fractures treated conservatively presented at our hospital. Among them, 15 (3.5%) suffering from EPL rupture (1 male and 14 females; mean age: 63.1 [SD 15.6] years) were assigned to the RG. We selected 15 control patients (2 males and 13 females; mean age: 69.3 [SD 18.9] years) to match the intact EPL group (IG) (Fig. 1).

A 64-row CT scanner (Canon Aquilion, Toshiba) was used, and images were obtained with a 2-mm slice

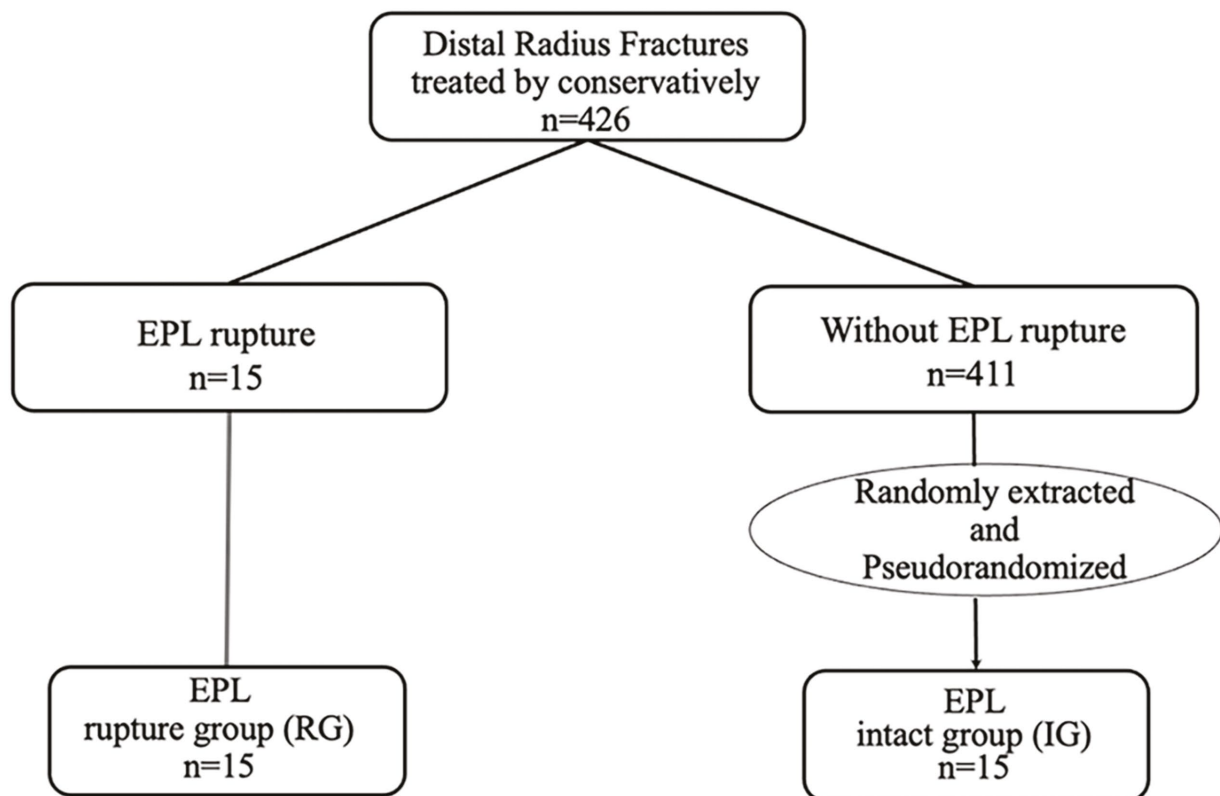


Fig. 1. Flowchart of the treatment and grouping of patients with distal radius fractures with and without extensor pollicis longus injury.

thickness. Axial CT images were analysed to determine the size and shape of the Lister tubercle and the size of the EPL groove. The axial CT was performed by reconstructing a slice perpendicular to the long axis of the radius. The slice that showed the Lister tubercle to appear the largest was used for measurement. The size of the Lister tubercle and the EPL groove was objectively measured using the method described by Chan and Chong.⁷ The radial and ulnar height of the Lister tubercle were measured using the transverse line, which acts as a reference line by connecting the inflexion points of the respective tubercles (Fig. 2). The depth and width of the EPL groove were also measured. The shape of the Lister tubercle was subjectively classified, namely the 'hook', 'dome' and 'spike' types, based on the shape and orientation of its peak. In a 'hook', the peak of Lister tubercle is pointing clearly, in a 'dome', the peak is flat and pointing dorsally, whereas, in a 'spike', the peak is sharp and pointing dorsally (Fig. 3). Two orthopaedic surgeons evaluated the images independently. A consensus was reached when different CT readings were observed between the two surgeons.

Statistical analysis: A propensity score analysis was performed to match patients' age, sex and treatment randomly. The size of the Lister tubercle was evaluated using

the Student *t*-test, and the morphometric findings⁷ were evaluated using the chi-square test. A *p* value of <0.05 was considered significant. The 'dome' and 'spike' types were combined into a 'non-hook' type, and the 'hook' and 'non-hook' types were compared using the chi-square test ($p < 0.05$). The Bell curve software for Excel was used for the above statistical analyses.

RESULTS

Fifteen patients were evaluated in each of the RG and IG. Table 1 shows the fracture types and the shape of the Lister tubercle in each group of patients. EPL ruptures occurred 7–90 days (average, 23.2 days) after sustaining a fracture. Fracture types at the time of injury were classified using the AO classification. In the RG, the most common fracture type was A2 ($n = 11$), followed by C2 ($n = 3$) and B2 ($n = 1$). In the IG, the most common fracture type was A2 ($n = 6$), followed by A3 ($n = 5$), B2, C1, C2 and C3 ($n = 1$).

Table 2 shows the results of CT measurements for RG and IG. The size of Lister tubercle did not differ significantly between the RG and IG with respect to the radial and ulnar tubercle heights or EPL groove depth

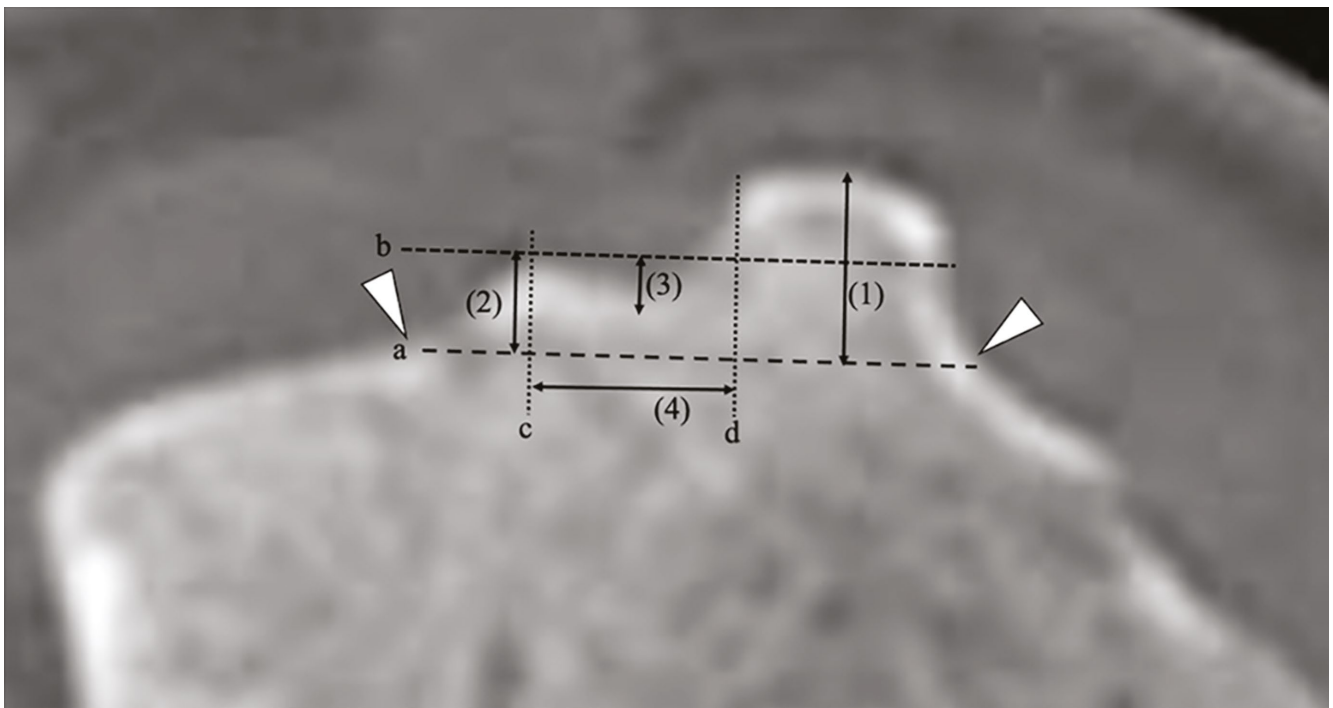


Fig. 2. Method of evaluating Lister tubercle size. Evaluating Lister tubercle size based on the: (1) radial height, (2) ulnar height, (3) depth of the extensor pollicis longus groove and (4) width of the extensor pollicis longus groove. Arrowheads: the inflexion points, where most change is noted in the slope of the respective tubercles. Line a: the reference line that connects the inflexion points. Line b: The bony landmark is the apex of the ulnar height. Line c: perpendicular to line a and passing through the vertex of the ulnar height. Line d: perpendicular to line a and passing through the ulnar side of the radial height.

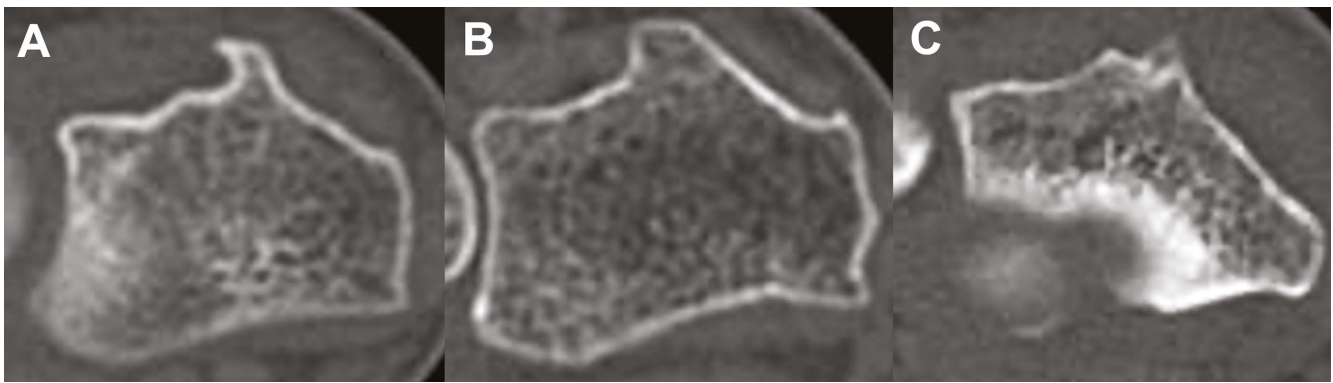


Fig. 3. Classification of the shape of Lister tubercle.

A. 'Hook' type.

B. 'Dome' type.

C. 'Spike' type.

Table 1. Clinical Data

EPL rupture group				EPL intact group			
Age (years)	Gender	AO classification	Lister tubercle type	Age (Years)	Gender	AO classification	Lister tubercle type
74	F	A2	Hook	83	M	A3	Spike
70	F	A2	Hook	72	F	A2	Dome
55	F	A2	Spike	76	F	A2	Dome
79	M	A2	Hook	76	F	C1	Dome
68	F	B2	Hook	88	F	C2	Dome
50	F	A2	Dome	76	F	A3	Spike
26	F	A2	Hook	41	F	B2	Dome
84	F	A2	Dome	67	F	A2	Dome
65	F	A2	Dome	65	F	A3	Hook
53	F	C2	Dome	83	F	C3	Dome
65	F	C2	Spike	58	F	A2	Dome
72	F	C2	Dome	43	M	A2	Dome
63	F	A2	Hook	67	F	A3	Dome
67	F	A2	Hook	72	F	A3	Dome
55	F	A2	Hook	73	F	A2	Spike

Table 2. Comparison of the Size of Lister Tubercle between the EPL Rupture Group and Intact Groups

	Rupture group	Intact group	P-value
Radial height (mm)	3.48	3.97	0.19
Ulnar height (mm)	1.83	1.86	0.94
Depth of EPL groove (mm)	1.16	1.49	0.22
Width of EPL groove (mm)	2.67	3.27	0.17

and width. Table 3 shows the distribution of the shapes of Lister tubercle. On analysis of the shape of Lister tubercle, the 'hook' shape was observed in 8 of 15 cases (53%) in the RG but only in 1 of 15 cases (6%) in the IG. Moreover, the distribution of the three Lister tubercle shapes, namely the 'hook', 'dome' and 'spike' types, differed significantly between the RG and IG ($p = 0.019$).

When 'dome' and 'spike' types were aggregated into a 'non-hook' type, the distribution of 'hook' and 'non-hook' types also differed significantly between the RG and IG ($p < 0.01$) (Table 4). Overall, two of the 15 patients with EPL rupture who did not have a 'hook' type deformation had a defect or irregularity of the EPL groove or floor by the fracture fragment (Fig. 4).

Table 3. The Distribution of the 'Hook', 'Dome' and 'Spike' Deformations of Lister Tubercle Across the EPL Rupture and Intact Groups

	Hook	Dome	Spike
Rupture group	8	5	2
Intact group	1	11	3
Total	9	16	5

Table 4. Distribution of the 'Hook' Type and 'Non-Hook' Type of Lister Tubercle in the EPL Rupture and Intact Groups

	Hook	Non-hook
Rupture group	8	7
Intact group	1	14
Total	9	21

DISCUSSION

In the present study, no significant differences were observed in the height of Lister tubercle and the depth and width of the EPL groove between the groups with and without EPL rupture. This indicates that the change in the size of Lister tubercle is only a few millimetres and that, consequently, the size may not contribute to a subsequent EPL rupture. Instead, we found that the Lister tubercle more frequently exhibited a 'hook' shape, with the point aimed towards the ulnar side in the EPL rupture group. This suggests that the 'hook' shape of the Lister tubercle may be associated with a tendon injury. Following a distal radius fracture, if the extensor retinaculum remains intact and the EPL tendon stays within the EPL groove, a hook-shaped Lister tubercle may predispose the EPL tendon to injury. If the 'hook-shaped' Lister tuberosity is found during the

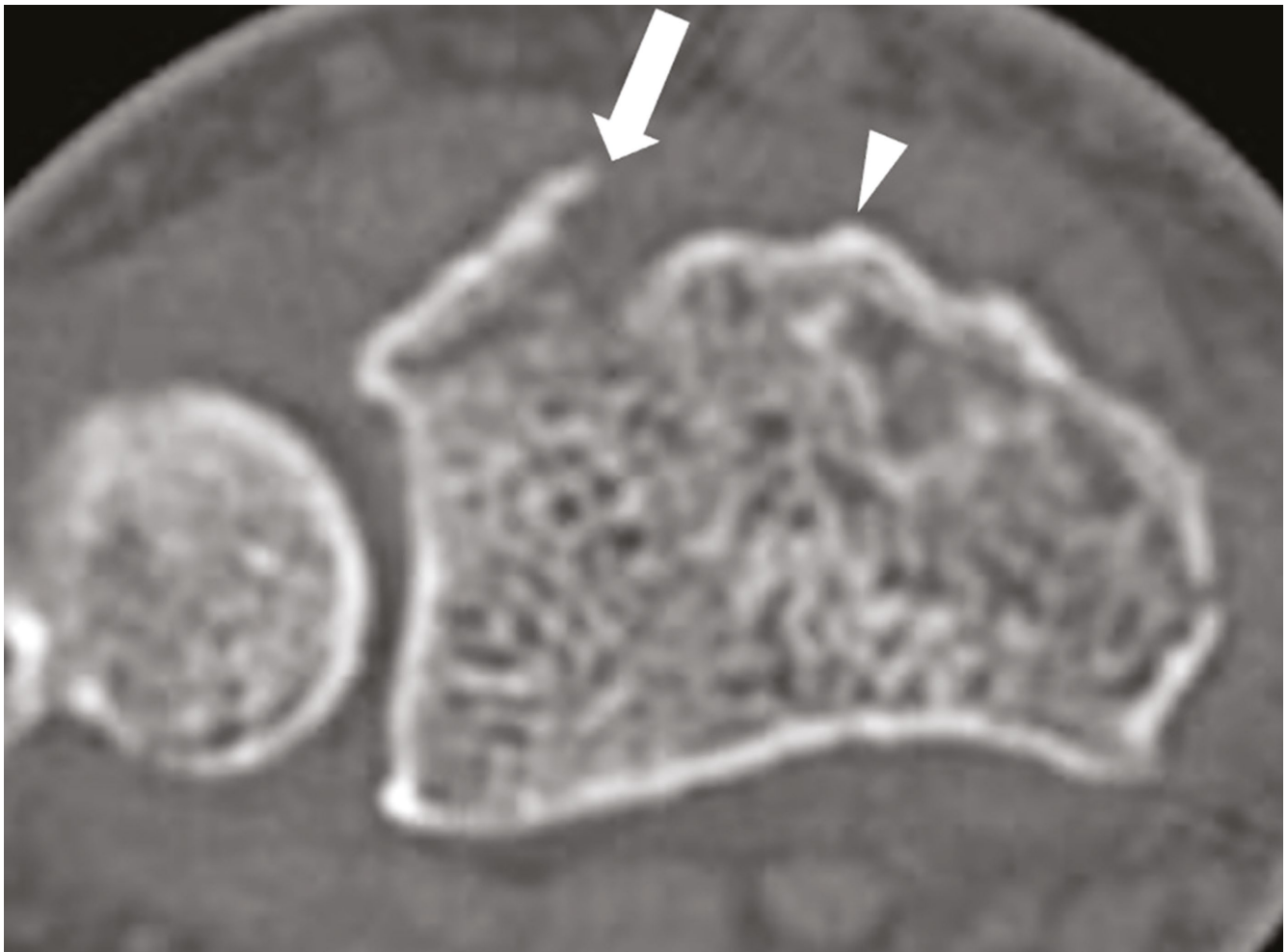


Fig. 4. The fracture fragment is sharpened towards the radial side. Arrowhead: Lister tubercle. Arrow: bone spicule by the fracture.

follow-up period of a distal radius fracture, it could suggest a greater EPL rupture risk. Therefore, early detection of EPL injury would be very useful for subsequent treatment. For example, if the pain and difficulty in movement persist after regular examinations, it may be an option to remove Lister tubercle surgically to achieve smooth tendon gliding.

Evaluation of distal radius fractures has mainly been performed using radiography, thus making it difficult to evaluate the configuration of the Lister tubercle in detail. Furthermore, EPL rupture was more likely to occur in undisplaced or minimally displaced fractures, occurring in a group of patients in whom CT is rarely performed. However, CT has become widely available across healthcare centres in recent years and has been used to evaluate fractures in greater detail. Cha et al⁶ used three-dimensional CT to identify the ‘island-shape’ of Lister tubercle as a risk factor for EPL injury. It was suggested that island-shaped fractures are associated with an increased risk of rupture because callus formation narrows the EPL groove. Our study focused on the shape and not the narrowing of the EPL groove. We believe that a ‘hook-shaped’ Lister tubercle protruding towards the EPL tendon has a greater propensity to injure the EPL tendon. However, we never perform CT only to visualise Hook deformity, but to evaluate comminuted fractures, to determine bone fusion or to detect when the unexpected occurs. In addition, it is sometimes difficult to determine whether the pain is due to fracture or EPL tear. We believe that CT is useful in such cases as well.

In our study, the two patients with EPL rupture did not have a ‘hook’ type Lister tubercle. In one patient, the dorsal fragment of radius pointed sharply towards the radial side from the ulnar side of the Lister tubercle (Fig. 4). In the other patient, there was an irregularity within the EPL groove. The mechanism of EPL rupture in these two patients is different from patients with the ‘hook-shaped’ Lister tubercle.

This study has some limitations. Firstly, CT was performed only after EPL rupture became evident; patients without EPL rupture often underwent imaging immediately after a fracture. As such, the shape of the Lister tubercle could change due to osteophytes and callus formation, depending on the timing of CT. Some EPL ruptures were observed in fractures with small bone irregularities. Consequently, more large-scale studies are warranted to validate our results.

In conclusion, there is no evidence supporting the hypothesis that the size of Lister tubercle affects EPL

tendon rupture. Instead, a ‘hook-shaped’ Lister tubercle may contribute to EPL tendon rupture. If the pain and difficulty in movement persist after regular examinations, CT should be performed. We believe that an increased risk of EPL rupture can be detected earlier if a ‘hook-shaped’ Lister tubercle is found during the follow-up period of the distal radius fracture. This might improve treatment subsequently, which includes EPL tendon release or excision of the Lister tubercle.

DECLARATIONS

Conflict of Interest: The authors do NOT have any potential conflicts of interest with respect to this manuscript.

Funding: The authors received NO financial support for the preparation, research, authorship and/or publication of this manuscript.

Ethical Approval: Ethical approval for this study was obtained from the institutional review board of Mito Kyodo General Hospital (NO 20-3) at 13 May 2020.

Informed Consent: Written informed consent was obtained from participants under treatment. The patients who completed the treatment were exempted from providing written consent by the institutional review board.

Acknowledgements: We would like to thank Editage for English language editing services.





REFERENCES

1. Seigerman D, Lutsky K, Fletcher D, et al. Complications in the management of distal radius fractures: How do we avoid them? *Curr Rev Musculoskelet Med.* 2019;12(2):204–212. <https://doi.org/10.1007/s12178-019-09544-8>.
2. Rivlin M, Fernández DL, Nagy L, Graña GL, Jupiter J. Extensor pollicis longus ruptures following distal radius osteotomy through a volar approach. *J Hand Surg Am.* 2016;41(3):395–398. <https://doi.org/10.1016/j.jhsa.2015.10.029>.
3. Helal B, Chen SC, Iwegbu G. Rupture of the extensor pollicis longus tendon in undisplaced Colles’ type of fracture. *Hand.* 1982;14(1):41–47. [https://doi.org/10.1016/s0072-968x\(82\)80038-7](https://doi.org/10.1016/s0072-968x(82)80038-7).
4. Engkvist O, Lundborg G. Rupture of the extensor pollicis longus tendon after fracture of the lower end of the radius – A clinical and microangiographic study. *Hand.*

- 1979;11(1):76–86. [https://doi.org/10.1016/s0072-968x\(79\)80015-7](https://doi.org/10.1016/s0072-968x(79)80015-7)
5. Clement H, Pichler W, Nelson D, Hausleitner L, Tesch NP, Grechenig W. Morphometric analysis of Lister tubercle and its consequences on volar plate fixation of distal radius fractures. *J Hand Surg Am.* 2008;33(10):1716–1719. <https://doi.org/10.1016/j.jhsa.2008.08.012>.
6. Cha SM, Shin HD, Lee SH. 'Island-shape' fracture of Lister tubercle have an increased risk of delayed extensor pollicis longus rupture in distal radial fractures after surgical treatment by volar locking plate. *Injury.* 2018;49(10):1816–1821. <https://doi.org/10.1016/j.injury.2018.08.019>.
7. Chan WY, Chong LR. Anatomical variants of Lister tubercle: A new morphological classification based on magnetic resonance imaging. *Korean J Radiol.* 2017;18(6):957–963. <https://doi.org/10.3348/kjr.2017.18.6.957>.
8. Roth KM, Blazar PE, Earp BE, Han R, Leung A. Incidence of extensor pollicis longus tendon rupture after nondisplaced distal radius fractures. *J Hand Surg Am.* 2012;37(5):942–947. <https://doi.org/10.1016/j.jhsa.2012.02.006>.
9. Naito K, Sugiyama Y, Dilokhuttakarn T, et al. A survey of extensor pollicis longus tendon injury at the time of distal radius fractures. *Injury.* 2017;48(4):925–929. <https://doi.org/10.1016/j.injury.2017.02.033>.
10. Hirasawa Y, Katsumi Y, Akiyoshi T, Tamai K, Tokioka T. Clinical and microangiographic studies on rupture of the E.P.L. tendon after distal radial fractures. *J Hand Surg Br.* 1990;15(1):51–57. [https://doi.org/10.1016/0266-7681\(90\)90048-9](https://doi.org/10.1016/0266-7681(90)90048-9).

Article

Use of a Small Car-Mounted Magnetic Resonance Imaging System for On-Field Screening for Osteochondritis Dissecans of the Humeral Capitellum

Kazuhiro Ikeda ^{1,2}, Yoshikazu Okamoto ³, Takeshi Ogawa ⁴, Yasuhiko Terada ⁵, Michiru Kajiwara ⁵, Tomoki Miyasaka ⁵, Ryuhei Michinobu ², Yuki Hara ⁶, Yuichi Yoshii ^{7,*}, Takahito Nakajima ³ and Masashi Yamazaki ²

¹ Department of Orthopedic Surgery, Kikkoman General Hospital, Noda 278-0005, Chiba, Japan

² Department of Orthopedic Surgery, Faculty of Medicine, University of Tsukuba, Tsukuba 305-8577, Ibaraki, Japan

³ Institute of Clinical Medicine, Department of Diagnostic and Interventional Radiology, University of Tsukuba, Tsukuba 305-8577, Ibaraki, Japan

⁴ Department of Orthopedic Surgery, Mito Medical Center, Ibaraki 311-3193, Ibaraki, Japan

⁵ Institute of Applied Physics, University of Tsukuba, Tsukuba 305-8577, Ibaraki, Japan

⁶ Department of Orthopedic Surgery, National Center of Neurology and Psychiatry, Kodaira 187-8551, Tokyo, Japan

⁷ Department of Orthopedic Surgery, Tokyo Medical University Ibaraki Medical Center, Ami 300-0395, Ibaraki, Japan

* Correspondence: yyoshii@tokyo-med.ac.jp; Tel.: +81-298871161



Citation: Ikeda, K.; Okamoto, Y.; Ogawa, T.; Terada, Y.; Kajiwara, M.; Miyasaka, T.; Michinobu, R.; Hara, Y.; Yoshii, Y.; Nakajima, T.; et al. Use of a Small Car-Mounted Magnetic Resonance Imaging System for On-Field Screening for Osteochondritis Dissecans of the Humeral Capitellum. *Diagnostics* **2022**, *12*, 2551. <https://doi.org/10.3390/diagnostics12102551>

Academic Editor: Rute Santos

Received: 21 September 2022

Accepted: 19 October 2022

Published: 20 October 2022

Publisher's Note: MDPI stays neutral with regard to jurisdictional claims in published maps and institutional affiliations.



Copyright: © 2022 by the authors. Licensee MDPI, Basel, Switzerland. This article is an open access article distributed under the terms and conditions of the Creative Commons Attribution (CC BY) license (<https://creativecommons.org/licenses/by/4.0/>).

Abstract: Mobile magnetic resonance imaging (MRI) using a car is a recent advancement in imaging technology. Specifically, a car-mounted mobile MRI system is expected to be used for medical check-ups; however, this is still in the research stage. This study demonstrated the practicality of a small car-mounted mobile MRI in on-field screening for osteochondritis dissecans (OCD) of the humeral capitellum. In the primary check-up, we screened the throwing elbows of 151 young baseball players using mobile MRI and ultrasonography. We definitively diagnosed OCD at the secondary check-up using X-ray photography and computed tomography or MRI. We investigated the sensitivity and specificity of mobile MRI and ultrasonography for OCD. Six patients were diagnosed with OCD. The sensitivity was 83.3% for mobile MRI and 66.7% for ultrasonography, with specificity of 99.3% vs. 100%, respectively. One patient was detected using ultrasonography but was missed by mobile MRI due to poor imaging quality at the first medical check-up. Following this false-negative case, we replaced a damaged radio frequency coil to improve the image quality, and the mobile MRI could detect all subsequent OCD cases. Two patients were diagnosed by mobile MRI only; ultrasonography missed cases lacking subchondral bone irregularity, such as a healing case, and an early-stage case. Mobile MRI could screen for OCD from the very early stages through the healing process and is therefore a practical tool for on-field screening.

Keywords: magnetic resonance imaging; mobile; portable; osteochondritis dissecans; OCD; baseball; medical check-up; screening; low-field MRI

1. Introduction

The use of mobile imaging tools is increasingly considered an effective way of utilizing limited medical resources [1–3]. Moreover, mobile imaging enables qualified medical personnel to practice remotely. It is currently widely applied for medical check-ups at workplaces or schools, and the time and cost reduction for examinees is expected to increase the examination rate [4].

In the bone and soft tissue field, mobile imaging tools play an important role in athletic medical check-ups [5–9]. Osteochondritis dissecans (OCD) of the humeral capitellum is a

bone and cartilage disorder for which athletic medical check-ups are useful. OCD occurs in young baseball players aged 9–12 years, with a prevalence of 2.1–3.4% [7,10]. Early detection is essential to prevent elbow dysfunction; 90% of patients with stage I OCD recover with conservative treatment, whereas 50% of patients with stage II OCD require surgery [11]. Since the early stage of OCD is often asymptomatic [12,13], a medical check-up is essential for early detection. Moreover, on-field screening is generally performed in Japan because it enables the examination of all players of the team. Currently, the gold standard imaging examination for on-field screening is ultrasonography (US) [7,10,12,13] due to its advantages, including portability, short examination time, no radiation exposure, and low cost. In addition, US detects the OCD lesion of subchondral bone irregularity from its early stage [7,10,12,13], making it an excellent qualitative examination tool for OCD detection.

Conversely, magnetic resonance imaging (MRI) is the gold standard for in-hospital diagnosis and evaluation of OCD lesions. MRI visualizes OCD lesions of the subchondral bone as low signal changes on T1-weighted images (T1WI) from the early stage, which cannot be detected by X-ray photography (X-p), computed tomography (CT) and US [14–16]. MRI detects qualitative changes in bone marrow edema, whereas X-p, CT, and US detect morphological changes and subchondral bone irregularities, as in other occult fractures [17]. MRI is therefore better suited to detect early cases than other imaging modalities. Although MRI has never been used for on-field OCD screening because it was not portable, introducing mobile MRI into OCD screening may help detect earlier cases.

However, the mobilization of MRI is still at the research stage, in contrast to X-p and US. As a result of prioritizing high resolution, current mobile MRI systems are equipped with 1.5 T magnets and require a 38-ton trailer [18,19]. Such a large mobile MRI truck is expensive, must be parked on a level area with reinforced pads, and requires a 480 V 3-phase power supply [3]; this mobile MRI truck has a high threshold for introduction and operation. Therefore, we proposed that a reduction in size and cost was essential for widespread use of mobile MRI, and a low-field MRI could realize this [20,21]. Using low-field MRI, we developed a small car-mounted mobile MRI system for human small joints [1]. This system, comprising a 0.2 T permanent magnet, enabled us to perform MRI anywhere using a 100 V external power supply. We have previously demonstrated excellent imaging using this mobile MRI system with healthy volunteers [1].

In this study, we introduced mobile MRI into OCD screening. This study aimed to examine the practicality and utility of this mobile MRI in on-field screening for OCD of the humerus (Figure 1).



Figure 1. Photograph of the mobile magnetic resonance imaging (MRI) system beside a baseball field. (Mercedes Benz, GH-639811, width 191 cm, height 193 cm, and length 476 cm). Mobile MRI enables players to practice while awaiting their turn for an MRI scan.

2. Materials and Methods

2.1. Study Design and Participants

This prospective, non-randomized observational study protocol conforms to the principles of the 1964 Declaration of Helsinki and its later amendments. The review board of our institution approved this study (IRB No: 30–144, approved 23 July 2019). Written informed consent was obtained from all participants. We evaluated 151 throwing-elbows of 151 young baseball players (149 boys and two girls; mean age 11.6 years; age range 8–15 years) who participated in our baseball medical check-up from October 2019 to May 2021. The median number of players per screening was 16 (8–19) among 10 teams.

2.2. The Mobile MRI system

The mobile MRI system consisted of a permanent magnet, gradient coils, a radio frequency (RF) probe with shielding cloths, and the MRI console (Figure 2). Since the RF probes are consumable, we replaced the damaged coil once during the study period; 32 cases were imaged with the first-generation RF probe, and 119 cases with the second-generation RF probe. The overall weight of the system was below the maximum authorized payload, and all the devices could be mounted in the vehicle. All the electronic devices were operated at 100 V AC, and the required current was 10 A. A power cable was connected from the vehicle to a wall outlet at the nearest building. Hence, we could perform MRI anywhere. Our mobile MRI system is comprehensively described in our previous paper [1].



Figure 2. The mobile MRI system. (a) Permanent magnet. The magnet is a 0.2 T permanent magnet (NEOMAX Engineering, Japan; 200 kg; 16 cm-gap; 44 cm × 50 cm × 36 cm). The magnet was screwed onto an aluminum stand that was anchored to the sheet rail of the vehicle; (b) an RF probe was placed inside the conductive shielding cloths (ESD EMI Engineering Corporation, Tokyo, Japan). The home-built RF probe consisted of a solenoid RF coil (12 turns, 130 mm long, 94 mm in diameter) and a rectangular shield box (200 mm (x) × 200 mm (y) × 132 mm (z)) made of 200- μ m-thick brass plates. The size of the RF coil was large enough to fit most of the junior baseball players; (c) MRI console: the MRI console consisted of a digital transceiver (DTRX6, MR Technology, Japan), a gradient driver (20 V, 10 A, DST Inc., Japan), a preamplifier (noise figure was 0.5 dB, gain was 30 dB; DST Inc., Asaka, Japan), an active transmit/receive switch, and a transmitter (9 MHz, 150 W; DST Inc.), which were installed on a 19-inch rack (56 cm × 77 cm × 60 cm, 80 kg). The MRI console was tightly fixed to the front seat with ropes.

2.3. OCD Screening

We conducted the primary medical check-up at the baseball field during the practice session of the target teams. In addition, we performed physical examinations, including the elbow range of motion (ROM), tenderness to palpation, and moving valgus test. Finally, we screened for OCD using the mobile MRI and US independently.

Once in the mobile MRI car, the participants sat on a legless chair and placed their forearm in the scanner, with the elbow joint in extension and the forearm supinated. The routine sequence images obtained were the sagittal elbow with T1WI and T2*-weighted imaging (T2*WI) and the coronal elbow with T2*WI (Figure 3 and Table 1). A musculoskeletal radiologist with 25 years' experience (Examiner A) read the images immediately and determined the presence of OCD.

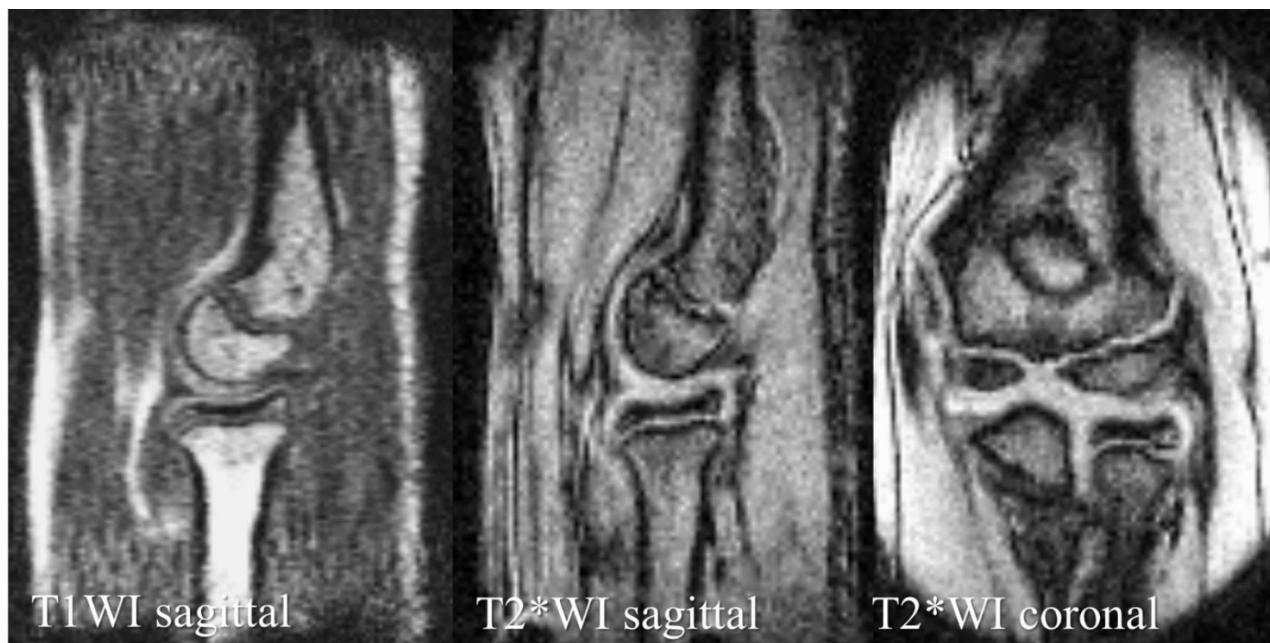


Figure 3. Mobile MRI of a healthy elbow of a 12-year-old boy.

Table 1. Imaging parameters.

Sequence Type	T1WI	T2*WI	T2*WI
Image plane	Sagittal	Sagittal	Coronal
FOV	$180 \times 120 \times 90 \text{ mm}^3$	$180 \times 180 \text{ mm}^2$	$180 \times 180 \text{ mm}^2$
Matrix size	$256 \times 128 \times 32$	256×192	256×192
Slice thickness, mm	-	3	3
TR, ms	40	500	500
TE, ms	4	16	16
Flip angel	60°	75°	75°
Scan time	1 min 22 s	1 min 38 s	1 min 38 s

T1WI, T1 weighted images; T2*WI, T2* weighted images; FOV, field of view; TR, repetition time; TE, echo time; ms: millisecond.

We can clearly identify bone morphology with T1WI sagittal images and articular cartilage morphology with T2*WI sagittal and coronal images.

We used a Viamo SV 7 scanner with a 3–10 MHz linear probe (Canon Medical Systems, Tochigi, Japan) for US examinations. The player sat on the chair and placed the arm on the table with the forearm supinated. We obtained a posterior longitudinal and short-axis view with the elbow fully flexed and an anterior longitudinal and short-axis view with the elbow fully extended [22–24]. Three orthopedic surgeons examined the US and determined the presence of OCD depending on the case: a hand surgeon with 23 years of experience (Examiner B) and two general orthopedic surgeons with 9 (Examiner C) and 8 (Examiner

D) years of experience, respectively. All three examiners had at least 3 years of OCD screening experience.

We referred OCD-positive patients diagnosed with either mobile MRI or US for a secondary check-up. Consequently, all the OCD-positive patients underwent X-p, with computed tomography (CT) or MRI as an additional imaging examination. Based on the obtained images, a hand surgeon with 23 years of experience (Examiner E), who did not participate in the primary check-up, made a definitive diagnosis of OCD. A flow diagram of our medical check-up is shown in Figure 4.

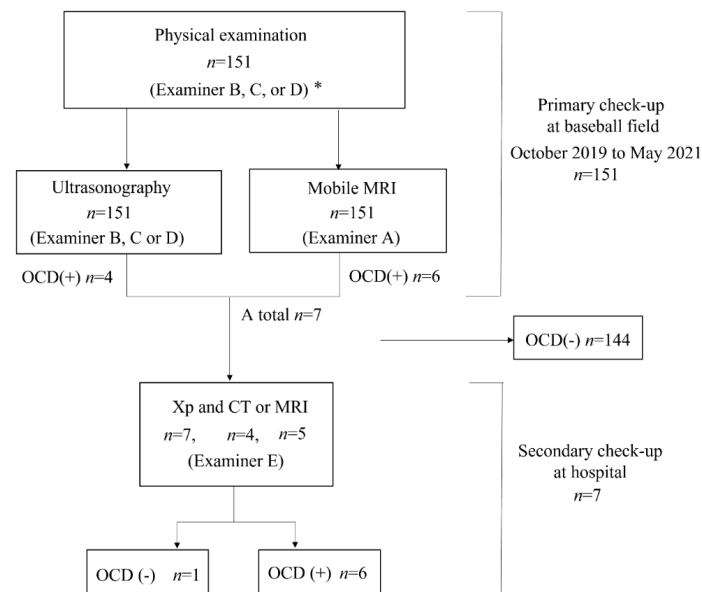


Figure 4. Flow diagram of our medical check-up. * Examiner A, a musculoskeletal radiologist with 25 years of experience; Examiner B, a hand surgeon with 23 years of experience; Examiner C, a general orthopedic surgeon with 9 years of experience; Examiner D, a general orthopedic surgeon with 8 years of experience; and Examiner E, a hand surgeon with 23 years of experience; OCD, osteochondritis dissecans of the humeral capitellum.

2.4. Evaluation Components

The evaluation components in this study were as follows. First, the sensitivity and specificity of the mobile MRI and US. In calculating sensitivity and specificity, we defined true positive cases as the patients with a definitive OCD diagnosis in the secondary check-up, and true negative cases as the other patients. Second, the details of the OCD-positive cases, i.e., physical examination findings, position, OCD stage and location, and the maximum diameter of the lesion were evaluated. Third, we evaluated the OCD stage [11] and its location with an anteroposterior X-p of the elbow at 45° of flexion (Xp–45°). We also measured the maximum diameter of the lesion with CT or MRI. In CT, we defined the lesion as a subchondral bone irregularity or sclerosis. In MRI, we detected signal changes in the subchondral bone.

3. Results

Of the 151 players, 6 (4.0%) were diagnosed with OCD through our medical check-ups (Table 2). Three patients with OCD had no elbow pain and positive physical examination findings for OCD. Out of the six OCD cases, five tested positive on mobile MRI and four on US; two were positive only on mobile MRI, and one was positive only on US. One patient was OCD-positive on mobile MRI but was diagnosed with a different disorder at the secondary check-up. Consequently, the sensitivity was 83.3% for mobile MRI and 66.7% in US, with specificities of 99.3% and 100%, with positive predictive value of 83.3% and 100%, respectively (Tables 2–4). Legends of the cases are shown in Figures 5–9.

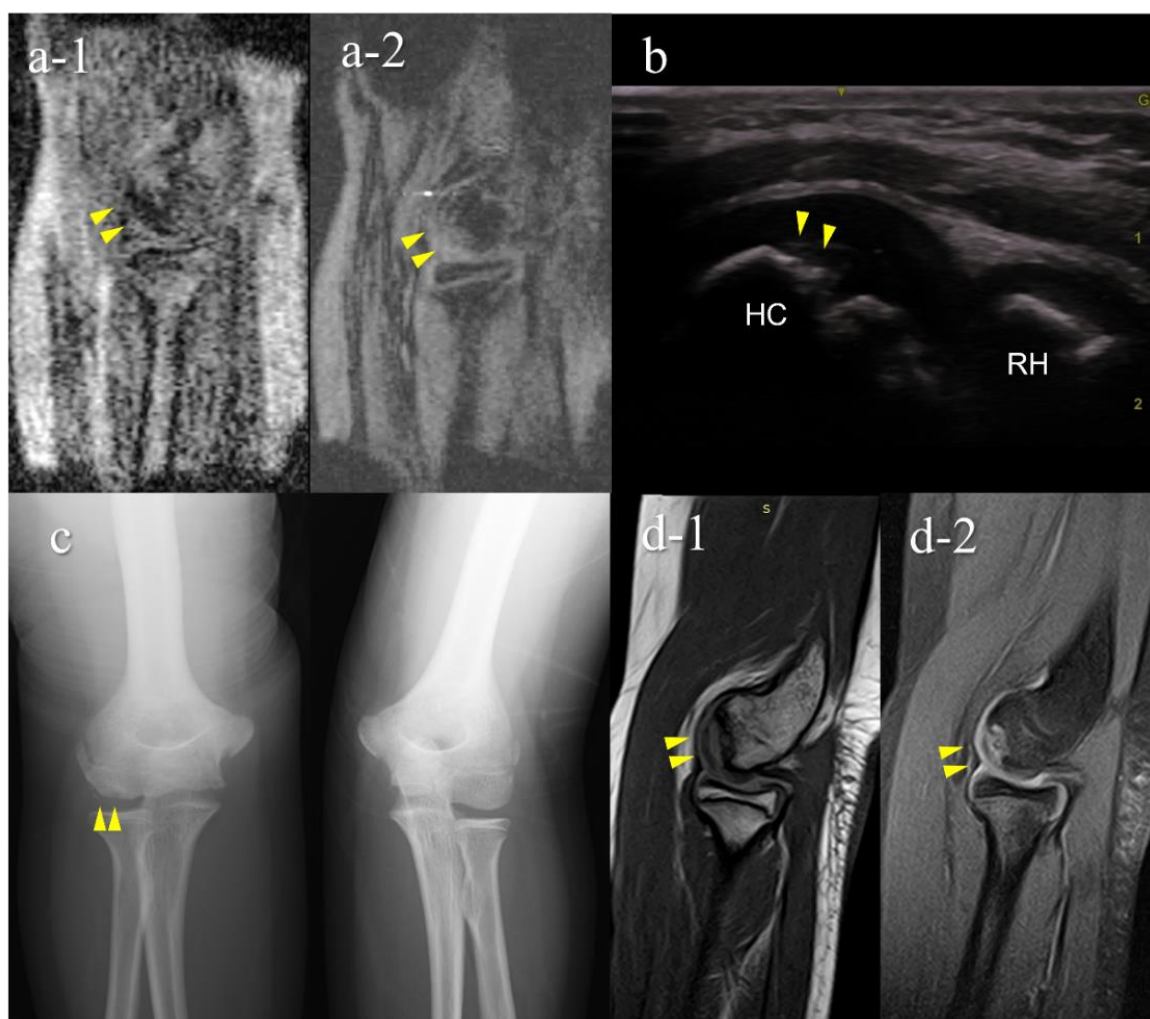


Figure 5. A false-negative OCD case with mobile MRI (Case 1): Mobile MRI (−), US (+). (a) Mobile MR (magnetic resonance) images: a-1, T1WI sagittal image; a-2, T2*WI sagittal image: Mobile MRI with poor imaging quality with low signal/noise ratio. Although the signal change was barely visible from the anterior to the humeral capitellum, we could not detect it; (b) US image of the posterior longitudinal view: US imaging revealed obvious subchondral bone irregularity; (c) X-p AP view with elbow 45° flexed: X-p 45° showing the lesion with fragmentation in the central capitellum, stage II OCD; (d) 3T MR images: d-1, proton density-weighted images (PDWI) sagittal image; d-2, PDWI-fat-suppressed (FS) sagittal image: 3T MRI easily detected the lesion. HC, humeral capitellum; RH, radial head; yellow arrowheads, lesions.

Table 2. Results of the medical check-up.

	OCD (−)	OCD (+)
Cases	145	6
Mean age (years)	11.6 ± 1.3	12.3 ± 1.2
Sex	Male: 143	Male: 6
	Female: 2	Female: 0
Medial elbow pain, n (%)	30 (20.7)	3 (50.0)
Lateral elbow pain, n (%)	6 (4.2)	3 (50.0)
No elbow pain, n (%)	113 (77.9)	3 (50.0)

Table 3. Diagnostic accuracy of OCD using mobile MRI.

		Definitive Diagnosis		
		OCD (+)	OCD (−)	
mobile MRI	OCD (+)	5	1	6
	OCD (−)	1	144	145
		6	145	151

Table 4. Diagnostic accuracy of OCD using US.

		Definitive Diagnosis		
		OCD (+)	OCD (−)	
US	OCD (+)	4	0	4
	OCD (−)	2	145	147
		6	145	151

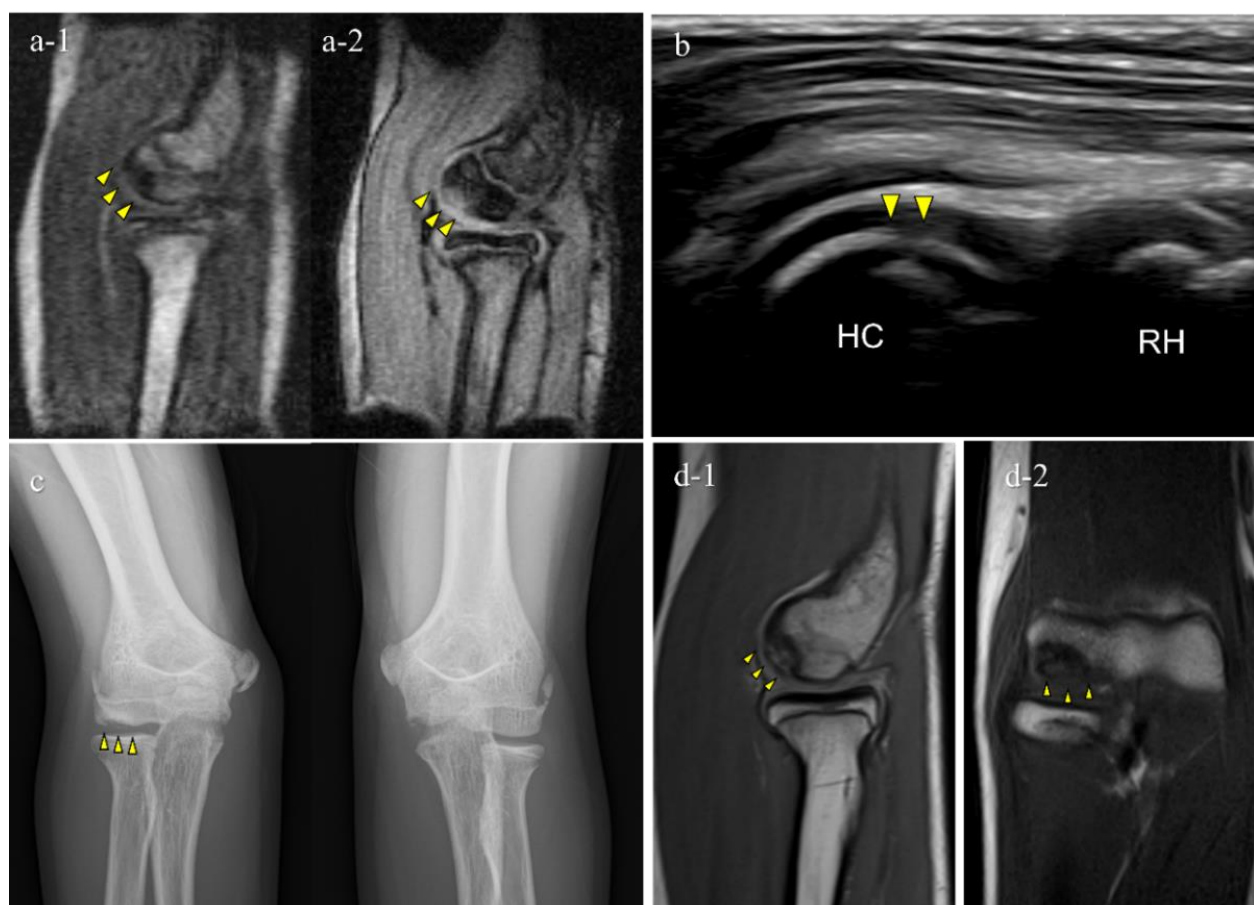


Figure 6. Typical OCD case (Case 3): Mobile MRI (+), US (+). (a) Mobile MR images; a-1, T1WI sagittal image; a-2, T2*WI sagittal image: Mobile MRI depicted the OCD lesion as a low-signal area in a T1WI sagittal image and a high-signal area in a T2* weighted image; (b) US image of the posterior longitudinal view: US showing subchondral bone irregularity; (c) X-p AP view with elbow 45° flexed: X-p 45° showing the lesion with fragmentation, stage II-OCD; (d) 3T MR images: d-1, PDWI sagittal image; d-2, coronal image: localization of the lesion was consistent with that of 3T MRI and mobile MRI.



Figure 7. An OCD case during the healing process (Case 5): Mobile MRI (+), US (-). (a) Mobile MR image of T1WI sagittal: Mobile MRI showing signal intensity changes reflecting bone marrow edema in the anterior humeral capitellum; (b) US image of the posterior longitudinal view: b-1, the central posterior; b-2, the lateral posterior: US images showing no significant findings in the central posterior longitudinal view. However, there was a subchondral bone discontinuity in the lateral posterior longitudinal view; (c) X-p AP view with elbow 45° flexed: X-p 45° showing delayed ossification in the lateral capitellum, observed in incomplete healing OCD cases [11]. In addition, there was a translucent area in the central capitellum, stage I-OCD; (d) CT images: d-1, sagittal image; d-2, coronal image; d-3, axial image: CT images showing the subchondral bone sclerosis, and the surface was almost repaired. White arrowheads: delayed ossification.

The results of the secondary check-up are presented in Table 5. There were three cases of stage I OCD, three cases of stage II OCD, and one case with a different disorder. The two cases that were diagnosed only using mobile MRI included an early OCD case and a healing case. The case that was diagnosed only with US was stage II OCD, which occurred at the first medical check-up using mobile MRI. Representative cases are described in Figures 4–8.

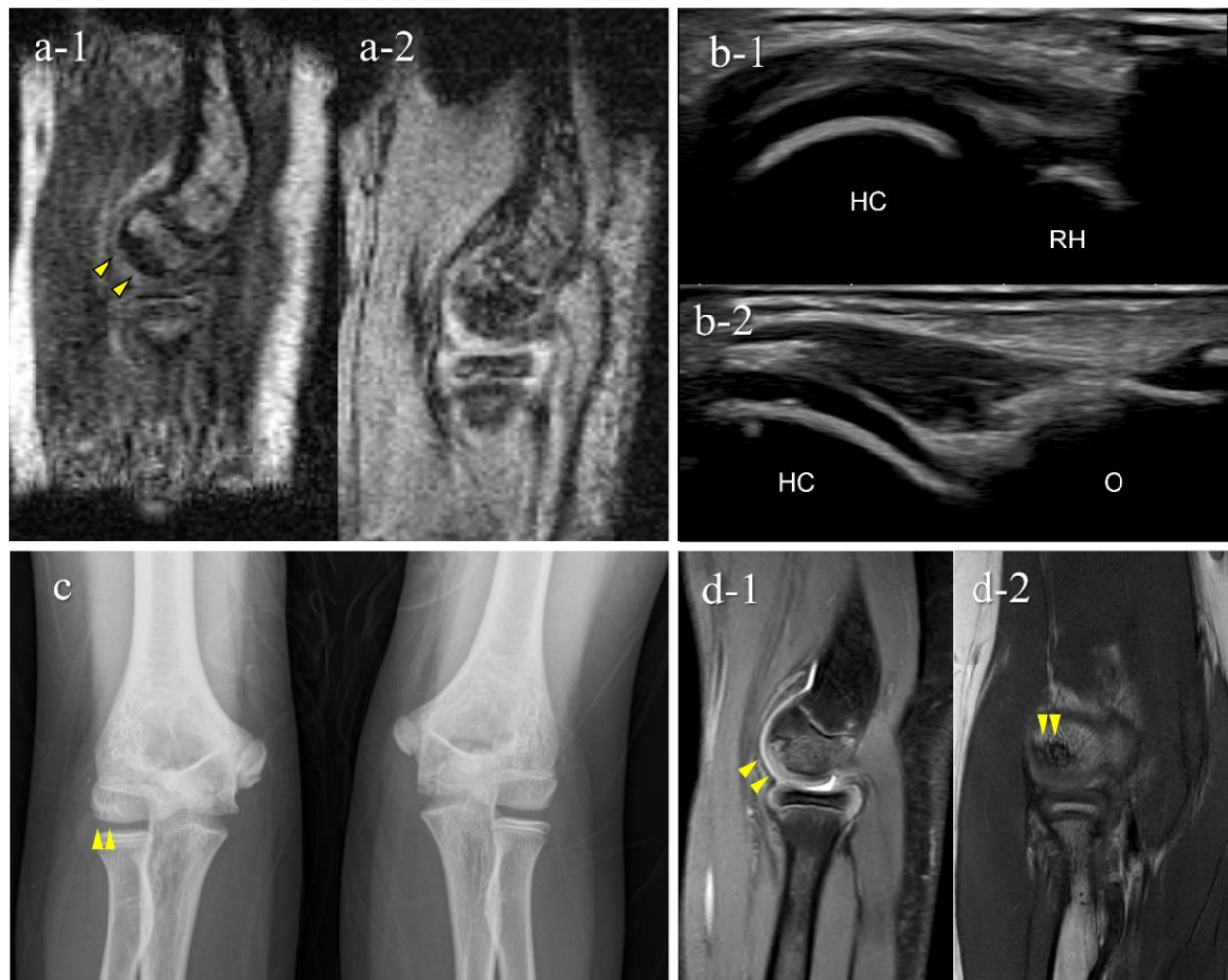


Figure 8. A very early stage of an OCD case (Case 7): Mobile MRI (+), US (−). (a) Mobile MR image of sagittal T1WI: Mobile MRI showing signal intensity changes reflecting bone marrow edema in the anterior humeral capitellum; (b) US image of the posterior longitudinal view: US did not show subchondral bone irregularity; (c) X-p AP view with elbow 45° flexed: X-p 45° showing a translucent area in the central capitellum, stage-I OCD; (d) 3T MR images: d-1, PDWI-FS sagittal image; d-2, PDWI coronal image: localization of the lesion was consistent with that of 3T MRI and mobile MRI.

Table 5. Characteristics of OCD-positive players.

Case	Age	Sex	Primary Check-Up			Secondary Check-Up			
			Elbow Symptom	Mobile MRI (RF Probe-Generation)	US (Examiner)	Diagnosis	Stage	Lesion Location	Lesion Diameter (mm)
1	12	M	-	− (1st)	+ (B)	OCD	II	lateral	15
2	11	M	+	+ (1st)	+ (B)	OCD	I	central	10
3	12	M	-	+ (2nd)	+ (B)	OCD	II	central	9
4	12	M	+	+ (2nd)	+ (B)	OCD	II	lateral	11
5	12	M	+	+ (2nd)	− (B)	OCD	I	central	3.5
6	15	F	-	+ (2nd)	− (C)	not OCD		posterior	3.5
7	12	M	-	+ (2nd)	− (D)	OCD	I	central	5.5

US, ultrasonography, M, male; F, female; RF probe, radio frequency probe.

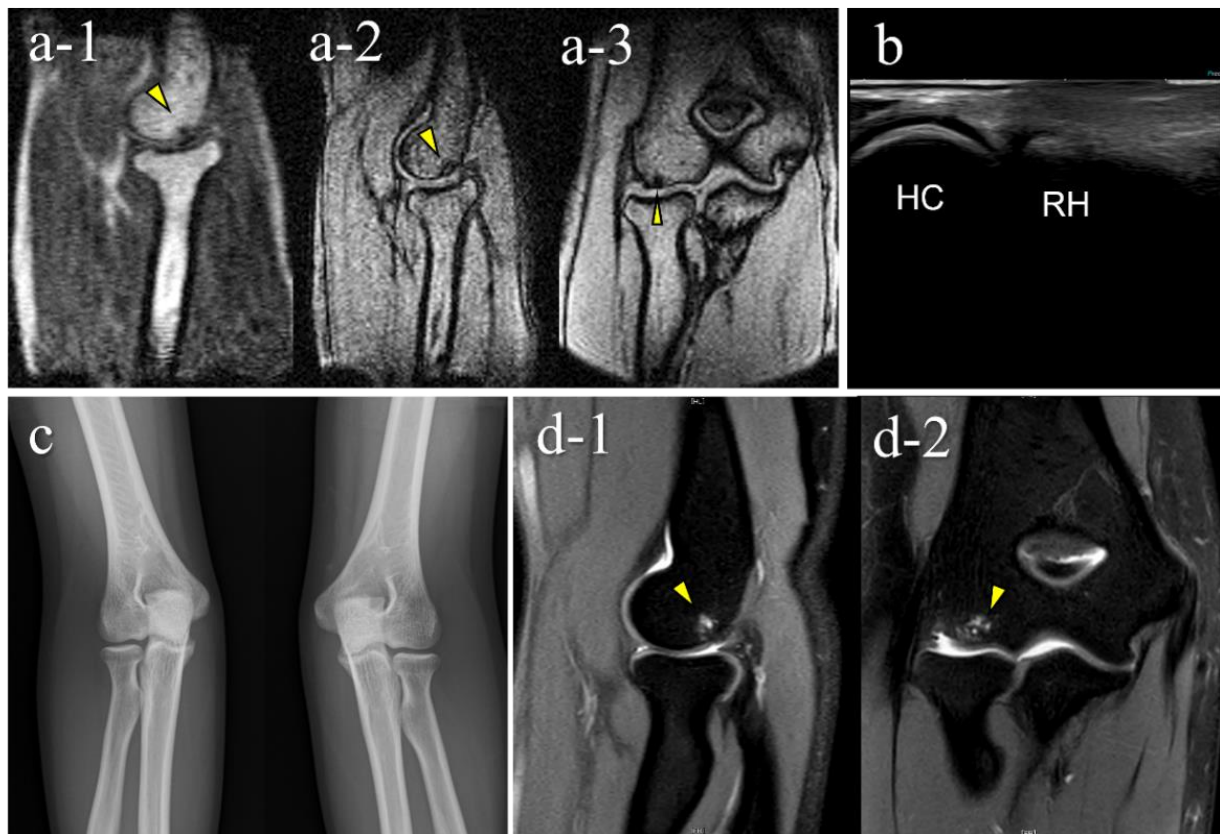


Figure 9. A false-positive case with mobile MRI (Case 6): Mobile MRI (+), US (-). (a) Mobile MR images: a-1, sagittal T1WI image; a-2, sagittal T2*WI image; a-3, coronal T2*WI image: mobile MR images showing a small subchondral bone-lesion in the posterior capitellum; (b) US images of the posterior longitudinal view: US did not reveal any remarkable findings; (c) X-p AP view with elbow 45° flexed: X-p 45° showed no significant findings; (d) 3T MR images: d-1, PDWI-FS sagittal image; d-2, PDWI-FS coronal image: 3-T MR image showing that the lesion was located in the posterior-central region of the capitellum and conflicted with the posterior synovial folds in the extended position. The pathogenesis differed from that of OCD caused by pitching according to the location of the lesion. Repeated hyperextension may have contributed to the pathology, as in Panner’s disease, based on the location of the lesion and the patient’s range of motion findings.

4. Discussion

This is the first report to show the clinical validity of a small car-mounted mobile MRI system. Our mobile MRI detected OCD cases from the very early stage through to the healing stage. Particularly in cases 5 and 7, mobile MRI detected OCD that was not detectable using US. One case was in the healing stage and the other was in the very early stage of OCD, without or with slight subchondral bone irregularity. Since US waves do not penetrate the subchondral bone, US cannot detect OCD without subchondral bone irregularity. In contrast, mobile MRI shows OCD-positive findings as distinct subchondral bone marrow edema. Mobile MRI has the potential to detect OCD cases without subchondral bone irregularities. Case 5 was in the healing process with a repaired subchondral bone surface. According to previous reports, shorter periods of conservative treatment tend to result in lower healing rates [11,24,25]. Thus, OCD in the healing stage is also a screening target. Case 7 was OCD at a very early stage. Although screening for early OCD before subchondral bone irregularities develop is ideal, this cannot be achieved using US. Therefore, from the perspective of early detection, mobile MRI is an excellent screening tool.

Meanwhile, there was a false negative case and false positive results with mobile MRI. The false negative case was due to poor imaging quality during the first medical check-up using the mobile MRI. The imaging quality of low-field MRI depends on various conditions,

including the quality of the RF probe, imaging parameters, the patient's motion, and the patient's positioning in the coil [26–29]. In particular, RF probes are consumables, and the image quality deteriorates over time. Based on our experience of this false-negative case, we replaced the RF probe to increase its sensitivity and reduce noise, and improved the legless chair to reduce motion artifacts. Subsequently, the imaging quality was improved, and the mobile MRI could detect all OCD cases. Although case 7 was a false positive case, mobile MRI detected a small imaging abnormality with excellent imaging quality.

Regarding the practicality of mobile MRI for on-field OCD screening, we overcame some disadvantages of conventional mobile MRI. Our mobile MRI went to an unpaved baseball field and obtained MRI images of sufficient quality for diagnosis using a household power source. As a result, the MRI scan time was relatively short (1.5 min per sequence), and we could screen all team members within one practice session. Our future aim is to further reduce the examination time for screening a large number of players. We have continued to improve our RF probes to achieve this. If the imaging quality is high enough to diagnose OCD with only T1WI sagittal imaging, we can save a considerable amount of examination time. We will continue our research to detect as many early OCD cases as possible.

This study had some limitations. First, it only demonstrated the clinical use of mobile MRI and did not include any statistical analysis. In the future, we will recruit more cases to compare the diagnostic ability of mobile MRI and US. Additionally, multiple examiners performed the US examinations for participants. Although all examiners had adequate experience with US, the quality of these examinations might have been inconsistent because US proficiency could have varied [30]. Finally, we only performed secondary check-up for patients shown to be positive in the primary check-up, which may affect the sensitivity and specificity results. However, US has been established as the gold standard for OCD-screening in Japan. Therefore, we considered our study design appropriate to determine the accuracy of the diagnosis using mobile MRI.

5. Conclusions

Mobile MRI was used for on-field screening for OCD for an entire youth baseball team of around 20 players during one practice session. Furthermore, the imaging quality was sufficient to diagnose OCD; mobile MRI could screen for OCD from the very early stages through to the healing process, including cases without subchondral bone irregularity, which could not be detected using US. Therefore, mobile MRI is a practical tool for on-field screening and has the potential to screen all stages of OCD.

Author Contributions: Conceptualization, Y.T. and Y.O.; methodology, Y.T.; software, Y.T.; formal analysis, K.I.; investigation, K.I., Y.O., T.O., Y.T., M.K., T.M., T.N., R.M. and Y.H.; resources, Y.T.; data curation, K.I. and Y.T.; writing—original draft preparation, K.I.; writing—review and editing, Y.O., T.O. and Y.T.; visualization, K.I.; supervision, T.O. and Y.Y.; project administration, Y.T. and M.Y. All authors have read and agreed to the published version of the manuscript.

Funding: This work was supported by JSPS KAKENHI Grant Number JP19K11435, and Orthopedic Network Tsukuba.

Institutional Review Board Statement: The study was conducted according to the guidelines of the Declaration of Helsinki and approved by the Institutional Review Board of the Tsukuba University (IRB No: 30–144, approved 23 July 2019).

Informed Consent Statement: Informed consent was obtained from all subjects involved in the study.

Data Availability Statement: Not applicable.

Conflicts of Interest: The authors declare no conflict of interest.

References

1. Nakagomi, M.; Kajiwar, M.; Matsuzaki, J.; Tanabe, K.; Hoshiai, S.; Okamoto, Y.; Terada, Y. Development of a small car-mounted magnetic resonance imaging system for human elbows using a 0.2-T permanent magnet. *J. Magn. Reson.* **2019**, *304*, 1–6. [\[CrossRef\]](#) [\[PubMed\]](#)
2. George, S.S.; Huang, M.C.; Ignjatovic, Z. Portable ultrasound imaging system with super-resolution capabilities. *Ultrasonics* **2019**, *94*, 391–400. [\[CrossRef\]](#) [\[PubMed\]](#)
3. Deoni, S.C.; Medeiros, P.; Deoni, A.; Burton, P.; Beauchemin, J.; D'Sa, V.; Boskamp, E.; By, S.; Nulty, C.M.; Mileski, W.; et al. Development of a mobile low-field MRI scanner. *Sci. Rep.* **2022**, *12*, e5690. [\[CrossRef\]](#)
4. Takahashi, Y.; Doi, M.; Yamada, T.; Tamanoi, T.; Murase, K.; Mochizuki, T. Present status and issues regarding X-ray medical checkup vehicles in preventive medicine: Usefulness of mass screening for lung cancer by an X-ray medical checkup vehicle. *Nihon Hoshasen Gijutsu Gakkai Zasshi* **2005**, *61*, 847–851. [\[CrossRef\]](#) [\[PubMed\]](#)
5. Okamoto, Y.; Maehara, K.; Kanahori, T.; Hiyama, T.; Kawamura, T.; Minami, M. Incidence of elbow injuries in adolescent baseball players: Screening by a low field magnetic resonance imaging system specialized for small joints. *Jpn. J. Radiol.* **2016**, *34*, 300–306. [\[CrossRef\]](#) [\[PubMed\]](#)
6. Kimura, M.; Kamada, H.; Tsukagoshi, Y.; Tomaru, Y.; Nakagawa, S.; Tanaka, K.; Mataka, Y.; Takeuchi, Y.; Ymazaki, M. Influence of commuting methods on low back pain and musculoskeletal function of the lower limbs in elementary school children: A cross-sectional study. *J. Orthop. Sci.* **2022**, *27*, 1120–1125. [\[CrossRef\]](#)
7. Matsuura, T.; Suzue, N.; Iwame, T.; Nishio, S.; Sairyo, K. Prevalence of osteochondritis dissecans of the capitellum in young baseball players: Results based on ultrasonographic findings. *Orthop. J. Sports. Med.* **2014**, *2*, e2325967114545298. [\[CrossRef\]](#)
8. Iwame, T.; Matsuura, T.; Suzue, N.; Kashiwaguchi, S.; Iwase, T.; Fukuta, S.; Hamada, D.; Goto, T.; Tsutsui, T.; Wada, K.; et al. Outcome of an elbow check-up system for child and adolescent baseball players. *J. Med. Invest.* **2016**, *63*, 171–174. [\[CrossRef\]](#)
9. Takagishi, K.; Matsuura, T.; Masatomi, T.; Chosa, E.; Takika, T.; Watanabe, M.; Iwame, T.; Otani, T.; Inagaki, K.; Ikegami, H.; et al. Shoulder and elbow pain in elementary school baseball players: The results from a nation-wide survey in Japan. *J. Orthop. Sci.* **2017**, *22*, 682–686. [\[CrossRef\]](#)
10. Kida, Y.; Morihara, T.; Kotoura, Y.; Hojo, T.; Tachiiri, H.; Sukenari, T.; Iwata, Y.; Furukawa, R.; Oda, R.; Arai, Y.; et al. Prevalence and clinical characteristics of osteochondritis dissecans of the humeral capitellum among adolescent baseball players. *Am. J. Sports. Med.* **2014**, *42*, 1963–1971. [\[CrossRef\]](#)
11. Matsuura, T.; Kashiwaguchi, S.; Iwase, T.; Takeda, Y.; Yasui, N. Conservative treatment for osteochondrosis of the humeral capitellum. *Am. J. Sports. Med.* **2008**, *36*, 868–872. [\[CrossRef\]](#) [\[PubMed\]](#)
12. Matsuura, T.; Iwame, T.; Iwase, J.; Sairyo, K. Osteochondritis dissecans of the capitellum: Review of the literature. *J. Med. Invest.* **2020**, *67*, 217–221. [\[CrossRef\]](#) [\[PubMed\]](#)
13. Matsuura, T.; Iwame, T.; Suzue, N.; Takao, S.; Nishio, S.; Arisawa, K.; Sairyo, K. Cumulative incidence of osteochondritis dissecans of the capitellum in preadolescent baseball players. *Arthroscopy* **2019**, *35*, 60–66. [\[CrossRef\]](#) [\[PubMed\]](#)
14. Kohyama, S.; Ogawa, T.; Mamizuka, N.; Hara, Y.; Yamazaki, M. A magnetic resonance imaging-based staging system for osteochondritis dissecans of the elbow: A validation study against the International Cartilage Repair Society Classification. *Orthop. J. Sports. Med.* **2018**, *6*, e2325967118794620. [\[CrossRef\]](#) [\[PubMed\]](#)
15. Kohyama, S.; Nishiura, Y.; Hara, Y.; Ogawa, T.; Ikumi, A.; Okano, E.; Totoki, Y.; Yoshii, Y.; Yamazaki, M. Preoperative evaluation and surgical simulation for osteochondritis dissecans of the elbow using three-dimensional MRI-CT image fusion images. *Diagnostics* **2021**, *11*, 2337. [\[CrossRef\]](#)
16. Takahara, M.; Shundo, M.; Kondo, M.; Suzuki, K.; Nambu, T.; Ogino, T. Early detection of osteochondritis dissecans of the capitellum in young baseball players. Report of three cases. *J. Bone. Joint. Surg. Am.* **1998**, *80*, 892–897. [\[CrossRef\]](#)
17. Carpenter, C.; Pines, J.M.; Schuur, J.D.; Muir, M.; Calfee, R.P.; Raja, A.S. Adult scaphoid fracture. *Acad. Emerg. Med.* **2014**, *21*, 101–121. [\[CrossRef\]](#)
18. Schutz, U.; Ehrhardt, M.; God, S.; Billich, C.; Beer, M.; Trattnig, S. A mobile MRI field study of the biochemical cartilage reaction of the knee joint during a 4,486 km transcontinental multistage ultramarathon using T2* mapping. *Sci. Rep.* **2020**, *10*, e8157. [\[CrossRef\]](#)
19. Schomoller, A.; Risch, L.; Kaplick, H.; Wochatz, M.; Engel, T.; Schraplau, A.; Sonnenburg, D.; Huppertz, A.; Mayer, F. Inter-rater and inter-session reliability of lumbar paraspinal muscle composition in a mobile MRI device. *Br. J. Radiol.* **2021**, *94*, e20210141. [\[CrossRef\]](#)
20. Mateen, F.J.; Cooley, C.Z.; Stockmann, J.; Rice, D.R.; Vogel, A.C.; Wald, L.L. Low-field portable brain MRI in CNS demyelinating Disease. *Mult. Scler. Relat. Disord.* **2021**, *51*, e102903. [\[CrossRef\]](#)
21. Deoni, S.C.L.; Bruchhage, M.M.K.; Beauchemin, J.; Volpe, A.; D'Sa, V.; Huentelman, M.; Williams, S.C.R. Accessible pediatric neuroimaging using a low field strength MRI scanner. *Neuroimage* **2021**, *238*, e118273. [\[CrossRef\]](#) [\[PubMed\]](#)
22. Harada, M.; Takahara, M.; Sasaki, J.; Mura, N.; Ito, T. Using sonography for the early detection of elbow injuries among young baseball players. *Am. J. Roentgenol.* **2006**, *187*, 1436–1441. [\[CrossRef\]](#) [\[PubMed\]](#)
23. Takahara, M.; Ogino, T.; Tsuchida, H.; Takagi, M.; Kashiwa, H.; Nambu, T. Sonographic assessment of osteochondritis Dissecans of the humeral capitellum. *Am. J. Roentgenol.* **2000**, *174*, 411–415. [\[CrossRef\]](#) [\[PubMed\]](#)
24. Niu, E.L.; Tepolt, F.A.; Bae, T.S.; Lebrun, D.G.; Kocher, M.S. Nonoperative management of stable pediatric osteochondritis dissecans of the capitellum: Predictors of treatment success. *J. Shoulder. Elbow. Surg.* **2018**, *27*, 2030–2037. [\[CrossRef\]](#) [\[PubMed\]](#)

25. Uno, T.; Takahara, M.; Maruyama, M.; Harada, M.; Satake, H.; Takagei, M. Qualitative and quantitative assessments of radiographic healing of osteochondritis dissecans of the humeral capitellum. *JSES Int.* **2021**, *5*, 554–560. [[CrossRef](#)]
26. Marques, J.P.; Simonis, F.F.J.; Webb, A.G. Low-field MRI: An MR physics perspective. *J. Magn. Reson. Imaging* **2019**, *49*, 1528–1542. [[CrossRef](#)]
27. Ghazinoor, S.; Crues, J.V., 3rd; Crowley, C. Low-field musculoskeletal MRI. *J. Magn. Reson. Imaging* **2007**, *25*, 234–244. [[CrossRef](#)]
28. Hori, M.; Hagiwara, A.; Goto, M.; Wada, A.; Aoki, S. Low-Field Magnetic Resonance Imaging: Its History and Renaissance. *Invest. Radiol.* **2022**, *56*, 669–679. [[CrossRef](#)]
29. Gach, H.M.; Curcuru, A.N.; Wittland, E.J.; Maraghechi, B.; Cai, B.; Mutic, S.; Green, O.L. MRI quality control for low-field MR-IGRT systems: Lessons learned. *J. Appl. Clin. Med. Phys.* **2019**, *20*, 53–66. [[CrossRef](#)]
30. Blehar, D.J.; Barton, B.; Gaspari, R.J. Learning curves in emergency ultrasound education. *Acad. Emerg. Med.* **2015**, *22*, 574–582. [[CrossRef](#)]



First manifestation of AQP4-IgG-positive neuromyelitis optica spectrum disorder following the COVID-19 mRNA vaccine BNT162b2

Shu Umezawa^{1,2,3} · Katsura Ioka⁴ · Satoshi Aizawa⁴ · Yuichi Tashiro⁴ · Kazuo Yoshizawa⁴

Received: 8 December 2021 / Accepted: 18 October 2022 / Published online: 27 October 2022
© Fondazione Società Italiana di Neurologia 2022

Abstract

BNT162b2 is one of the effective COVID-19 vaccines. However, some researchers have also reported some neurological adverse events after the vaccination. Here, we present a case of a 52-year-old female who developed aquaporin (AQP) 4-IgG-positive neuromyelitis optica spectrum disorder (NMOSD) 14 days after the first dose of BNT162b2. She experienced the neck pain, weakness of the left arm and leg, numbness of the left hand, and impaired temperature sensation of the right leg. MRI showed T2WI hyperintense lesions in the area postrema and cervical spinal cord ranging from C1 to C6 level and Gd-enhanced lesions from C3 to C5 level; especially left lateral column was predominantly enhanced. Cell-based assays showed anti-AQP4 antibody (AQP4Ab) was positive. We diagnosed AQP4-IgG-positive NMOSD. After high-dose glucocorticoid therapy, she is showing improved symptoms. The present case was characterized by the findings that a Gd-enhanced lesion in the cervical cord localized dominantly at the left lateral column, consistent with the side of the shoulder where the vaccine was injected. Many studies suggested that AQP4-IgG-positive NMOSD development has multistep mechanisms following the blood–brain barrier (BBB) breakdown. We suspected that immune responses following vaccination lead to BBB disruptions. Through the limitedly damaged BBB, the plasma cells producing AQP4Abs might be recruited to CNS, and AQP4Abs might bind to the cervical cord and the area postrema. A population-based study revealed that neurological events following COVID-19 vaccination were less likely to be observed than COVID-19 infectious symptoms. Considering rare adverse events, clinicians need to observe any changes in patient condition.

Keywords Neuromyelitis optica spectrum disorder · Myelitis · AQP4 · COVID-19 vaccine

Introduction

Severe acute respiratory syndrome coronavirus 2 (SARS-CoV-2), the pathogen that causes coronavirus disease (COVID-19), has been responsible for hospitalizations and deaths globally. COVID-19 presents with acute respiratory symptoms and also leads to long-term neurological ones. In

order to combat the COVID-19 pandemic, several vaccines have been developed and utilized worldwide.

BNT162b2 (Comirnaty®, BioNTech/Pfizer) is one of the effective COVID-19 vaccines. Many randomized trials and real-world studies have revealed that the vaccines are key to reducing COVID-19 infections, transmissions, hospitalizations, and death. However, some researchers have also reported that the vaccination leads to some neurological events. Here, we report a case of a patient who developed aquaporin (AQP) 4-IgG-positive neuromyelitis optica spectrum disorder (NMOSD) 2 weeks after vaccination with the first dose of BNT162b2.

Case presentation

A 52-year-old right-handed female experienced a first attack of NMOSD after vaccination with the first dose of BNT162b2. She had a mild fever the day after vaccination

✉ Shu Umezawa
shumez@med.tohoku.ac.jp; umezawa.shu@gmail.com

¹ Department of Education and Training, National Hospital Organization Mito Medical Center, Ibaraki, Japan

² Graduate Medical Education Center, Tohoku University Hospital, Miyagi, Japan

³ Department of Neurology, Tohoku University Hospital, Miyagi, Japan

⁴ Department of Neurology, National Hospital Organization Mito Medical Center, Ibaraki, Japan

but no other inflammation reactions, including local reactions in her left arm around the injection site for 13 days. Fourteen days after vaccination, she began to feel pain ranging from the neck to the left shoulder, weakness of the left arm, numbness of the left hand, and impaired temperature sensation of the right leg. Seventeen days after vaccination, she complained of weakness of the left leg.

Twenty-one days after vaccination, she was admitted to our department. On admission, she had no visual impairment. Ophthalmological checkups showed no remarkable findings suggesting optic neuritis. The other cranial nerves were intact. Distal-dominant moderate to severe weakness of the left upper extremity, mild weakness of the left lower extremity, and hypesthesia of the abdomen and the right thigh were found. Her left grasp power was 4.5 kg

compared with 19.0 kg for her right. Lhermitte sign was positive. Neither nausea nor hiccups were observed.

Magnetic resonance imaging (MRI) of the spinal cord showed that T2-weighted (T2WI) and fluid-attenuated inversion recovery (FLAIR) hyperintense lesions reached from the C1 to C6 level. Gadolinium (Gd)-enhancement lesion was located from the C3 to C5 level, and, especially, left lateral fasciculus was enhanced predominantly (Fig. 1). Cerebral MRI showed T2-weighted and double inversion recovery (DIR) hyperintense lesions in the area postrema and the obex of the medulla (Fig. 2). These lesions were not enhanced. No other remarkable signal changes were detected in the cortices or the optic nerves.

Routine blood tests detected no remarkable abnormal values. Cell-based assays showed that anti-AQP4 antibody (AQP4Ab) was positive. Other autoantibodies were absent.

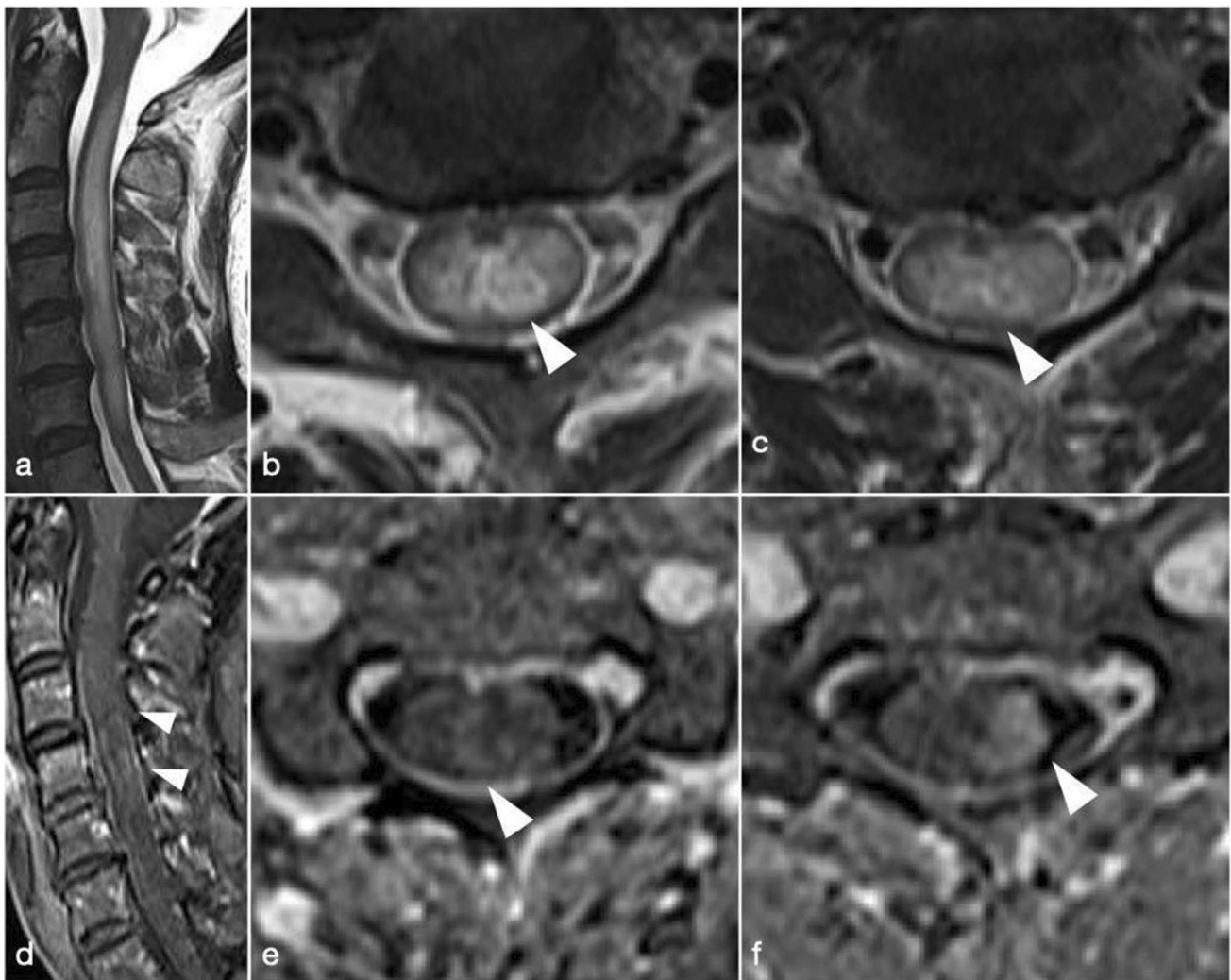
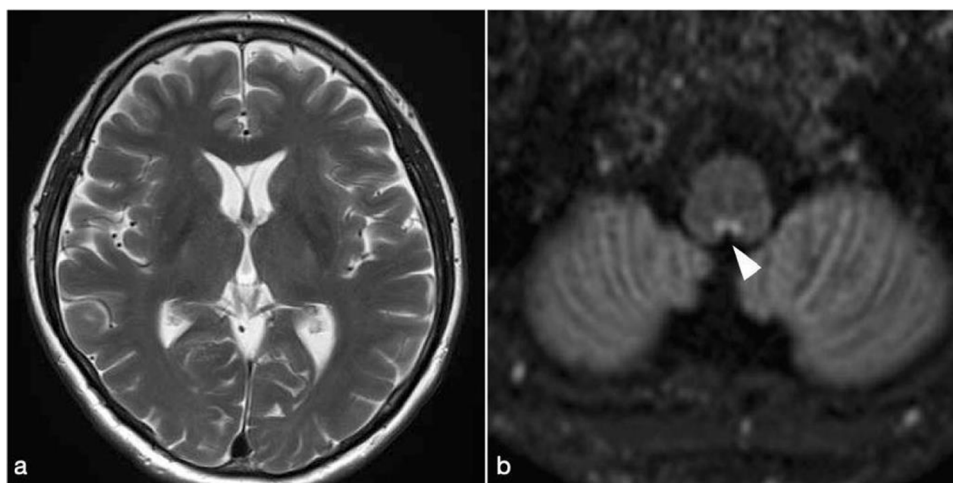


Fig. 1 Spinal MRI 21 days after vaccination. **a** T2WI showed hyperintense lesions from the C1 to C6 level. **b** C3 level. **c** C5 level. **d** Gd-enhancement image showed lesions from the C3 to C5 level. **e** C3

level. **f** C5 level. The left column predominantly enhanced at the C4 and C5 level

Fig. 2 Brain MRI 21 days after vaccination. **a** T2WI showed no signal changes in the cortex. **b** DIR image showed hyperintense lesions in the area postrema and the obex of medulla



On cerebrospinal fluid (CSF) analysis, mild pleocytosis (9 cells/ μ L), in which mononuclear cells dominated (7 cells/ μ L), mildly increased protein (49 mg/dL), and elevated myelin basic protein (MBP) (1550 pg/mL) were found. IgG index was normal (0.54), and oligoclonal bands were negative.

We ruled out SARS-CoV-2 infection by a negative polymerase chain reaction (PCR) test and the absence of antibodies against the SARS-CoV-2 N protein. In addition, she had no complaints of fever, cough, or other known COVID-19 symptoms before admission during the pandemic periods.

We ruled out SARS-CoV-2 infection by a negative polymerase chain reaction (PCR) test and the absence of antibodies against the SARS-CoV-2 N protein. In addition, she had no complaints of fever, cough, or other known COVID-19 symptoms before admission during the pandemic periods. The patient had a history of Guillain-Barré syndrome (GBS). At the age of 35, she developed weakness of the bilateral lower extremities. The onset was about a month after suffering a cervical sprain because of a car accident. These symptoms progressed for about a month until her admission to our department. On admission, a nerve conduction study (NCS) showed temporal dispersion findings and other demyelinating patterns at multiple nerves. MRI showed no remarkable signal changes in the spinal cord. We diagnosed GBS, and after intravenous immunoglobulin therapy, she fully recovered. She had experienced no similar symptoms until the present admission. The present MRI showed no enlargements of nerve roots or enhancement lesions in the cauda equina, and NCS showed no demyelinating patterns in the bilateral median nerves and no other findings suggesting peripheral neuropathy. The family history was negative for any neurologic disorders and autoimmune diseases.

After other differential diagnoses were excluded, following the 2015 International Consensus Diagnostic Criteria, we diagnosed AQP4-IgG-positive neuromyelitis optica spectrum disorder. We conducted two cycles of high-dose glucocorticoid therapy (each 1000 mg methylprednisolone i.v. for 3 days; the first cycle was initiated at 21 days after vaccination; the second cycle was at 28 days) and oral

administration of 40 mg prednisolone for 16 days and a tapering dose for about 2 weeks.

Twenty-eight days after vaccination, T2WI hyperintense lesions shrank to locate from the C3 to C5 level in the cervical spinal cord, and lateralization pattern at the left lateral column remained (Fig. 3). Currently, the patient is taking 25 mg of prednisolone orally and showing improved symptoms.

Discussion

To our knowledge, this is the first case of AQP4-IgG-positive NMOSD development following the initial dose of BNT162b2. The present case was noteworthy in terms of its temporal association with the vaccine, the type of vaccine, and AQP4-IgG status. Previously, there have been some reports of cases of NMOSD after COVID-19 vaccination, such as AQP4-IgG-positive NMOSD development 2 months after administration of inactivated vaccine [1], AQP4-IgG-positive after Gam-COVID-Vac [2], and AQP4-IgG-negative after mRNA-1273 [3]. In the present case, the duration from vaccination to development was 2 weeks. Considering myelitis and other neurological disorders following the vaccination occurred approximately at the tenth day, ranging from 1 to 2 weeks after vaccination in other previous reports, it is reasonable to assume that the present case followed the timecourse of the post-vaccine adverse events. Additionally, the available vaccines against COVID-19 include mRNA vaccines, BNT162b2 and mRNA-1273, and adenovirus vector vaccines, ChAdOx1nCoV and Gam-COVID-Vac. Recently, a large population-based study in the UK compared neurological events between BNT162b2 and ChAdOx1nCoV and showed that these have different risks of adverse events [4]. This study suggested that distinct mechanisms underlie adverse events following these two

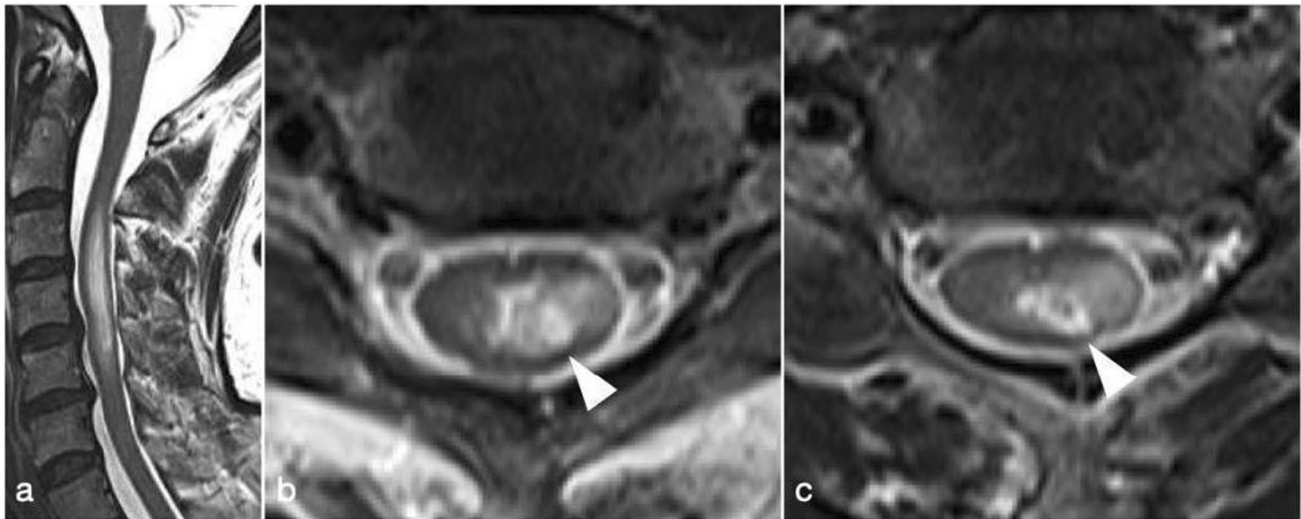


Fig. 3 Spinal MRI 28 days after vaccination. **a** T2WI showed hyperintense lesions from the C3 to C5 level in the cervical spinal cord. **b** C3 level. **c** C5 level. The lesions were lateralized to left lateral column from the C3 to C5 level

types of vaccine. Furthermore, AQP4Ab is a major disease-specific biomarker of NMOSD; simultaneously, AQP4Ab plays a direct role in astrocyte damage in NMOSD. The pathophysiology behind AQP4-IgG-positive NMOSD lies in astrocyte lysis, not demyelination, which is thought to underlie another subtype of NMOSD, namely MOG-IgG positive NMOSD. Clinically, AQP4-IgG serological status is incorporated into the International Diagnostic Criteria. In these regards, the present case is significant as the first manifestation of AQP4-IgG-positive NMOSD following BNT162b2.

The patient had a history of GBS in the present case. After intravenous immunoglobulin therapy, she recovered and had no experiences of similar symptoms for about 17 years. In addition, a month before GBS development, she suffered a cervical sprain because of a car accident. We are unsure whether this episode was related to the present NMOSD pathophysiology. At least, we assumed that the patient has a predisposition to humoral immunologic reactions triggered by exogenous factors.

Moreover, the present case was characterized by the finding that a Gd-enhancement lesion in the cervical spinal cord localized dominantly at the left lateral column, consistent with the side of the shoulder where the vaccine was injected. No local inflammation reactions occurred in her left arm. Although this feature may be only a coincidence, it does however need to be discussed in terms of pathophysiology. Many *in vivo* and *in vitro* studies showed that AQP4-IgG-positive NMOSD development has multistep mechanisms, including complement activations and astrocyte lysis following the blood–brain barrier (BBB) breakdown [5]. It is hypothesized that interleukin-6 (IL-6) signaling pathways

and humoral factors lead the BBB to increased permeability and decreased integrity with glial cells in the acute phase. Through damaged BBB, the plasma cells producing AQP4Abs and other inflammatory mediator cells are recruited to the central nervous system. AQP4Abs binding to AQP4 interact with complements, and astrocyte lysis follows by the classical complement cascade. It is also known that AQP4 is highly expressed in the area postrema, which was the lesion other than the cervical spinal cord in the present case. Taken together, we suspected that immune responses following vaccination lead to BBB disruptions. Through the limitedly damaged BBB, the plasma cells producing AQP4Abs or the other mediators might be recruited to the CNS, and AQP4Abs might bind to the cervical cord and the area postrema. One of the possible mechanisms underlying the present event could be the IL-6 signaling pathways. This concordance remains to be discussed, and further research is needed.

As mentioned above, there have been some reported cases of neurological events following COVID-19 vaccination as well as symptoms caused by infection. It has also been reported that some patients with NMOSD tended to be reluctant to receive vaccines. However, a large population-based study in the UK recently revealed that neurological events following COVID-19 vaccination including BNT162b2 and ChAdOx1nCoV-19 were less likely to be observed than ones caused by COVID-19 infection [4]. For example, there was an increased risk of encephalitis, meningitis, and myelitis 1–28 days after COVID-19 infection (incident rate ratio (IRR): 2.70) but not after vaccination (IRR: 1.14 (BNT162b2); 1.07 (ChAdOx1nCoV-19)). Therefore, weighing these two different risks, we recommend vaccination.

To encourage this, healthcare professionals have to provide more information about the risks of COVID-19-related neurological complications compared to those following COVID-19 vaccination. At the same time, considering rare adverse events reported, clinicians need to observe any changes in their condition after vaccination.

Data availability The datasets generated during and/or analyzed during the current study are available from the corresponding author on reasonable request.

Declarations

Ethics approval The study was performed in accordance with the Helsinki II Declaration and approved by the Institutional Review Board of our hospital.

Consent to participate All participants (or their legal representatives) gave written informed consent.

Consent for publication We thank the patient reported here for the consent given to describe and publish the case.

Conflict of interest The authors declare no competing interests.

References

1. Chen S, Fan XR, He S, Zhang JW, Li SJ (2021) Watch out for neuromyelitis optica spectrum disorder after inactivated virus vaccination for COVID-19. *Neurol Sci Off J Ital Neurol Soc Ital Soc Clin Neurophysiol* 42(9):3537–3539. <https://doi.org/10.1007/s10072-021-05427-4>
2. Badrawi N, Kumar N, Albastaki U (2021) Post COVID-19 vaccination neuromyelitis optica spectrum disorder: case report & MRI findings. *Radiol Case Rep* 16(12):3864–3867. <https://doi.org/10.1016/j.radcr.2021.09.033>
3. Fujikawa P, Shah FA, Braford M, Patel K, Madey J (2021) Neuromyelitis optica in a healthy female after severe acute respiratory syndrome coronavirus 2 mRNA-1273 vaccine. *Cureus* 13(9):e17961. <https://doi.org/10.7759/cureus.17961>
4. Patone M, Handunnetthi L, Saatci D, Pan J, Katikireddi SV, Razvi S, Hunt D, Mei XW, Dixon S, Zaccardi F, Khunti K, Watkinson P, Coupland C, Doidge J, Harrison DA, Ramanan R, Sheikh A, Robertson C, Hippisley-Cox J (2021) Neurological complications after first dose of COVID-19 vaccines and SARS-CoV-2 infection. *Nat Med*. <https://doi.org/10.1038/s41591-021-01556-7>
5. Takai Y, Misu T, Suzuki H, Takahashi T, Okada H, Tanaka S, Okita K, Sasou S, Watanabe M, Namatame C, Matsumoto Y, Ono H, Kaneko K, Nishiyama S, Kuroda H, Nakashima I, Lassmann H, Fujihara K, Itoyama Y, Aoki M (2021) Staging of astrocytopathy and complement activation in neuromyelitis optica spectrum disorders. *Brain J Neurol* 144(8):2401–2415. <https://doi.org/10.1093/brain/awab102>

Publisher's note Springer Nature remains neutral with regard to jurisdictional claims in published maps and institutional affiliations.



OPEN ACCESS

EDITED BY

Sree Bhushan Raju,
Nizam's Institute of Medical Sciences,
India

REVIEWED BY

Rahul Grover,
Max Super Speciality Hospital, India
Andrea Ranghino,
Azienda Ospedaliero Universitaria
Ospedali Riuniti, Italy
Sonu Manuel,
St Mary's Hospital, India

*CORRESPONDENCE

Kazuhiro Takahashi
kazu1123@md.tsukuba.ac.jp

†These authors have contributed
equally to this work

SPECIALTY SECTION

This article was submitted to
Nephrology,
a section of the journal
Frontiers in Medicine

RECEIVED 30 July 2022

ACCEPTED 10 October 2022

PUBLISHED 28 October 2022

CITATION

Takahashi K, Furuya K, Goshō M,
Usui J, Kimura T, Hoshi A,
Hashimoto S, Nishiyama H, Oda T,
Yuzawa K and Yamagata K (2022)
Prediction of early graft function after
living donor kidney transplantation by
quantifying the “nephron mass” using
CT-volumetric software.
Front. Med. 9:1007175.
doi: 10.3389/fmed.2022.1007175

COPYRIGHT

© 2022 Takahashi, Furuya, Goshō,
Usui, Kimura, Hoshi, Hashimoto,
Nishiyama, Oda, Yuzawa and
Yamagata. This is an open-access
article distributed under the terms of
the [Creative Commons Attribution
License \(CC BY\)](https://creativecommons.org/licenses/by/4.0/). The use, distribution
or reproduction in other forums is
permitted, provided the original
author(s) and the copyright owner(s)
are credited and that the original
publication in this journal is cited, in
accordance with accepted academic
practice. No use, distribution or
reproduction is permitted which does
not comply with these terms.

Prediction of early graft function after living donor kidney transplantation by quantifying the “nephron mass” using CT-volumetric software

Kazuhiro Takahashi^{1*†}, Kinji Furuya^{1†}, Masahiko Goshō^{2†},
Joichi Usui^{3†}, Tomokazu Kimura^{4†}, Akio Hoshi^{4†},
Shinji Hashimoto^{1†}, Hiroyuki Nishiyama^{4†}, Tatsuya Oda^{1†},
Kenji Yuzawa^{5†} and Kunihiro Yamagata^{3†}

¹Department of Gastrointestinal and Hepato-Biliary-Pancreatic Surgery, University of Tsukuba, Tsukuba, Japan, ²Department of Biostatistics, University of Tsukuba, Tsukuba, Japan, ³Department of Nephrology, University of Tsukuba, Tsukuba, Japan, ⁴Department of Urology, University of Tsukuba, Tsukuba, Japan, ⁵Department of Transplant Surgery, Mito Medical Center, Mito, Japan

Early renal function after living-donor kidney transplantation (LDKT) depends on the “nephron mass” in the renal graft. In this study, as a possible donor-recipient size mismatch parameter that directly reflects the “nephron mass,” the cortex to recipient weight ratio (CRWR) was calculated by CT-volumetric software, and its ability to predict early graft function was examined. One hundred patients who underwent LDKT were enrolled. Patients were classified into a developmental cohort ($n = 79$) and a validation cohort ($n = 21$). Using the developmental cohort, the correlation coefficients between size mismatch parameters, including CRWR, and the posttransplantation estimated glomerular filtration rate (eGFR) were calculated. Multiple regression analysis was conducted to define a formula to predict eGFR 1-month posttransplantation. Using the validation cohort, the validity of the formula was examined. The correlation coefficient was the highest for CRWR (1-month $r = 0.66$, $p < 0.001$). By multiple regression analysis, eGFR at 1-month was predicted using the linear model: $0.23 \times \text{donor preoperative eGFR} + 17.03 \times \text{CRWR} + 8.96 \times \text{preemptive transplantation} + 5.10$ (adjusted coefficient of determination = 0.54). In most patients in the validation cohort, the observed eGFR was within a 10 ml/min/1.73 m² margin of the predicted eGFR. CRWR was the strongest parameter to predict early graft function. Predicting renal function using this formula could be useful in clinical application to select proper donors and to avoid unnecessary postoperative medical interventions.

KEYWORDS

cortex weight recipient weight ratio, estimated glomerular filtration rate (eGFR), living-donor kidney transplantation (LDKT), multidetector raw CT (MDCT), weight ratio (WR)

Introduction

In most patients undergoing living-donor kidney transplantation (LDKT), immediate graft function (IGF), in which grafts show immediate urinary formation, is observed (1, 2). The serum creatinine level declines rapidly, and the level reaches nadir within a few weeks posttransplantation. The loss of nephrons owing to immunological and non-immunological factors reduces graft function on a yearly basis, and eventually, the function of the transplanted kidney is abolished (3–5). Early posttransplantation renal function affects subsequent renal function and long-term graft survival (6, 7). Therefore, maintaining the “nephron mass” of the renal grafts is essential for long-term graft survival. Owing to the progress in immunosuppressive therapy and the establishment of a highly accurate diagnostic and elaborate treatment strategy against immunological complications, the 5-year graft survival rate now reaches 90% in most countries (1, 8, 9).

Initial renal function after LDKT is affected by donor age, sex, donor preoperative estimated glomerular filtration rate (eGFR), donor-recipient size difference, etc., all of which reflect the “nephron mass” of the renal graft (10, 11). The donor-recipient size mismatch is manifested by the clearance capacity of the “nephron mass” in the donor graft, which is less than the recipient’s metabolite production. Because the “nephron mass” cannot be directly measured, alternative parameters that can be used as indicators of donor-recipient size mismatch include the donor to recipient weight ratio (WR), body mass index (BMI) ratio (BMIR), body surface area (BSA) index ratio (BSAR), actual graft weight (Graft-act) to recipient weight ratio (GRWR-act), and Graft-act to recipient BSA ratio, and the relationship between these parameters and posttransplantation renal function has been discussed in the previous literature (12–16). On the other hand, with the recent developments in medical technology, the “nephron mass” can be measured directly by quantifying the renal cortex using 3-dimensional (3D) CT-volumetry based on contrast-enhanced images obtained by multidetector raw CT (MDCT) (17).

The purpose of this study was to quantify the “nephron mass” of the renal graft using CT-volumetric software and examine whether our novel size mismatch parameter that directly reflects the “nephron mass,” the cortex to recipient weight ratio (CRWR), could determine early renal function after LDKT compared with other representative size mismatch parameters.

Abbreviations: BMI, body mass index; BMIR, body mass index ratio; BSA, body surface area; BSAR, body surface area index ratio; CRWR, cortex to recipient weight ratio; eGFR, estimated glomerular filtration rate; Graft-act, actual graft weight; GRWR-act, actual graft weight to recipient weight ratio; GRWR-sim, simulated graft weight to recipient weight ratio; GV, glomerular volume; IGF, immediate graft function; LDKT, living-donor kidney transplantation; MDCT, multidetector raw CT; WR, weight ratio; 3D, 3-dimensional.

Materials and methods

Study population

Between October 2013 and February 2022, 112 patients underwent ABO identical/compatible adult-to-adult LDKT at Tsukuba University Hospital ($n = 85$) and Mito Medical Center ($n = 27$). Patient records were identified by an administrative database. In both cohorts, all LDKTs were conducted with Asian pairs of donors and recipients, and none of the recipients demonstrated delayed graft function. Eight patients were excluded since the arterial phase of the contrast-enhanced CT was insufficient for reconstruction. Four patients were excluded since the patients demonstrated acute rejection within 12 months posttransplantation. Thus, a final population consisting of 100 pairs of LDKT was enrolled in our study. Patients who underwent transplantation at Tsukuba University Hospital ($n = 79$) were allocated as a developmental cohort to build a prediction model, and patients who underwent transplantation at Mito Medical Center ($n = 21$) were allocated as a validation cohort. All data for this study were collected in accordance with the Tsukuba University Hospital and Mito Medical Center Internal Review Boards.

Immunosuppression

In both centers, basiliximab (20 mg/body) was introduced on the day of surgery and 4 days after surgery. Maintenance immunosuppression was conducted with triple therapy comprising long-acting tacrolimus, mycophenolate mofetil, and steroids. The trough value of tacrolimus was maintained at 7–10 ng/mL 3 months after surgery and 5–8 ng/mL 4–12 months after transplantation.

CT-volumetric quantification

The Digital Imaging and Communications in Medicine data were obtained from MDCT with 1–2 mm slices (Brilliance 64 multidetector row CT scanner, Philips, Netherlands) and transferred to high-end simulation software (Synapse Vincent[®] ver. 6.1; Fujifilm Corporation, Tokyo, Japan), which semiautomatically calculates the volume of the kidney graft and its cortex (Supplementary Figure 1). The collecting system, vessels, cysts, and sinus were excluded from all parenchymal volume measurements. Graft-act was measured immediately after the back-table procedure. The simulated graft weight (Graft-sim) to recipient weight ratio (GRWR-sim), CRWR, and GRWR-act were defined as Graft-sim divided by

the recipient body weight (before LDKT), calculated cortex volume divided by the recipient body weight, and Graft-act divided by the recipient body weight, respectively. For the comparison between predicted kidney volume and actual kidney graft weight, we defined 1 g of kidney tissue as having a volume of 1 ml.

Assessment of renal function and urinary protein

Graft function was evaluated based on eGFR (ml/kg/1.73 m²), calculated using the conversion formula for Japanese individuals. Proteinuria was measured in 24-h urine samples. The donor eligibility criterion at both centers was renal function with an inulin clearance of at least 70 ml/min. In this study, since postoperative renal function was assessed by eGFR, eGFR was also used for preoperative renal function.

Glomerular morphometry of renal biopsy specimens

All protocol renal biopsy samples were obtained at 12 months posttransplantation using a percutaneous needle device. A 3 mm section of paraffin-embedded renal cortex specimen from the recipient was stained with hematoxylin-eosin. Glomerular area was measured by tracing the contour of the outer margins along the glomerular tufts using imaging software (BZ-X Analyzer, Keyence, Osaka, Japan) (Supplementary Figure 2). The volume of three glomeruli or more was measured from each slide, and the average value was used. The glomerular volume (GV)-ratio was calculated by dividing GV 12 months after transplantation by GV 1-h posttransplantation.

Statistical analysis

Categorical variables are presented as numbers and percentages, and groups were compared using the chi-square test. Continuous variables were expressed as median, minimum, and maximum values. Groups were compared using Student's *t*-test. Pearson's correlation coefficients (*r*) were calculated, and single and multiple regression analyses were performed. Analyses were conducted using SPSS 27.0 (SPSS Inc., Chicago, IL, USA) and SAS software V.9.4 (SAS Institute, Cary, NC, USA). All variables that had a *p* < 0.05 in a single regression model were included in a multiple regression model. A value of *p* < 0.05 was considered statistically significant.

Results

Demographic and clinical characteristics

Table 1 shows the demographic and clinical characteristics of the 100 patients. There were no significant differences in background factors, except for total ischemia time, between the developmental cohort and the validation cohort (113 min vs. 85.5 min, *p* < 0.001). The 1-year graft and patient survival rates were 100% in both cohorts.

Correlation between graft-sim and graft-act and between cortex to recipient weight ratio and simulated graft weight to recipient weight ratio and actual graft weight to recipient weight ratio

Graft-sim was positively correlated with Graft-act (*r* = 0.65, *p* < 0.001), and Graft-act tended to be heavier than Graft-sim (Figure 1A). CRWR and GRWR-sim and GRWR-act were positively correlated. CRWR was correlated more strongly with GRWR-sim than with GRWR-act (*r* = 0.98, *p* < 0.001 and *r* = 0.78, *p* < 0.001, respectively, Figures 1B,C).

Correlation between weight ratio, body mass index ratio, body surface area index ratio, actual graft weight to recipient weight ratio, simulated graft weight to recipient weight ratio, cortex to recipient weight ratio, and urinary protein and postoperative estimated glomerular filtration rate

Figure 2 demonstrates the correlations between WR, BMIR, BSAR, GRWR-act, GRWR-sim and CRWR and eGFR at 1, 6, and 12 months posttransplantation. WR and BSAR were correlated with postoperative renal function, but the correlation coefficients were low (WR, *r* = 0.34, *p* = 0.003; BSAR, *r* = 0.37, *p* < 0.001 for correlation with eGFR 1-month posttransplantation, respectively). BMIR did not show a significant correlation with postoperative renal function. Correlation coefficients between CRWR and posttransplantation eGFR were generally high compared with those with GRWR-sim and GRWR-act (CRWR *r* = 0.66, *p* < 0.001; GRWR-sim, *r* = 0.63, *p* < 0.001; GRWR-act, *r* = 0.36, *p* = 0.001 for correlation with eGFR 1-month posttransplantation, respectively).

TABLE 1 Demographic and clinical characteristics.

	Developmental cohort (<i>n</i> = 79)	Validation cohort (<i>n</i> = 21)	<i>p</i> -value
Recipient			
Age	45 (22–68)	51 (18–72)	0.20
Sex, male	55 (70%)	15 (71%)	0.87
BMI	22.9 (17.6–29.7)	22.1 (16.8–30.4)	0.24
Background disease			
Chronic glomerulonephritis	40 (51%)	11 (52%)	0.22
Diabetes mellitus	19 (24%)	2 (10%)	
Hypertension	7 (9%)	1 (5%)	
Others	13 (16%)	7 (33%)	
Donor			
Age	60 (32–78)	62 (42–73)	0.79
Sex, male	24 (30%)	10 (48%)	0.11
BMI, kg/m ²	23.7 (16.2–28.9)	23.2 (16.6–25.7)	0.56
Body side of the donated kidney, left	69 (87%)	21 (100%)	0.08
Diabetes mellitus, yes	7 (9%)	1 (5%)	0.69
Hypertension	22 (28%)	5 (24%)	0.87
eGFR, ml/min/1.73 m ²	81.2 (55.3–126.7)	75.8 (57.8–122.0)	0.09
Transplant			
ABO incompatible, yes	26 (33%)	8 (38%)	0.66
PEKT, yes	29 (37%)	4 (19%)	0.13
Relationship, parent	43 (54%)	7 (33%)	0.23
Spouse	31 (39%)	12 (57%)	
Sibling	5 (6%)	2 (10%)	
HLA mismatch	3 (0–6)	3 (1–5)	0.79
Warm ischemia time, min	3 (1–16)	4.5 (2–8)	0.06
Total ischemia time, min	113 (67–202)	85.5 (58–120)	<0.001
Bleeding amount, ml	208 (4–2760)	107 (3–871)	0.27

BMI, body mass index; PEKT, preemptive kidney transplant; eGFR, estimated glomerular filtration rate; HLA, human leucocyte antigen.

Correlation between cortex to recipient weight ratio and urinary protein and glomerular volume-ratio

Cortex to recipient weight ratio demonstrated a weak reverse correlation with urinary protein at 1 and 6 months posttransplantation ($r = -0.27$, $p = 0.02$ and $r = -0.34$, $p = 0.002$, respectively, [Figure 3A](#)), but not with urinary protein at 12 months posttransplantation ($r = -0.17$, $p = 0.16$).

The GV ratio showed a weak reverse correlation with CRWR ($n = 56$, $r = -0.35$, $p = 0.009$, [Figure 3B](#)). The GV ratio demonstrated a positive correlation with urinary protein at 1 and 6 months posttransplantation ($n = 55$, $r = 0.24$, $p = 0.07$ and $r = 0.38$, $p = 0.004$, [Figure 3C](#)). On the other hand, the GV ratio showed no correlation with urinary protein posttransplantation or glomerular sclerosis at 12 months posttransplantation ($n = 55$, $r = -0.08$, $p = 0.58$; $n = 53$, $r = -0.23$, $p = 0.10$, [Figure 3D](#)).

Multiple regression analysis using cortex to recipient weight ratio and estimated glomerular filtration rate at 1-month posttransplantation and validation

Single regression analysis showed that donor age ($\beta = -0.33$, $SE = 0.16$, $p = 0.04$), donor preoperative eGFR ($\beta = 0.37$, $SE = 0.11$, $p = 0.001$), CRWR ($\beta = 20.38$, $SE = 2.67$, $p < 0.001$), and preemptive kidney transplant (PEKT, $\beta = 14.34$, $SE = 3.43$, $p < 0.001$) were significantly correlated with recipient eGFR at 1-month posttransplantation. In multiple regression analysis, the donor preoperative eGFR ($\beta = 0.23$, $SE = 0.08$, $p = 0.006$), CRWR ($\beta = 17.03$, $SE = 2.49$, $p < 0.001$), and PEKT ($\beta = 8.96$, $SE = 2.64$, $p = 0.001$) became significantly associated with the recipient's eGFR at 1 month ([Table 2](#)). The formula for predicting eGFR at 1 month was expressed as

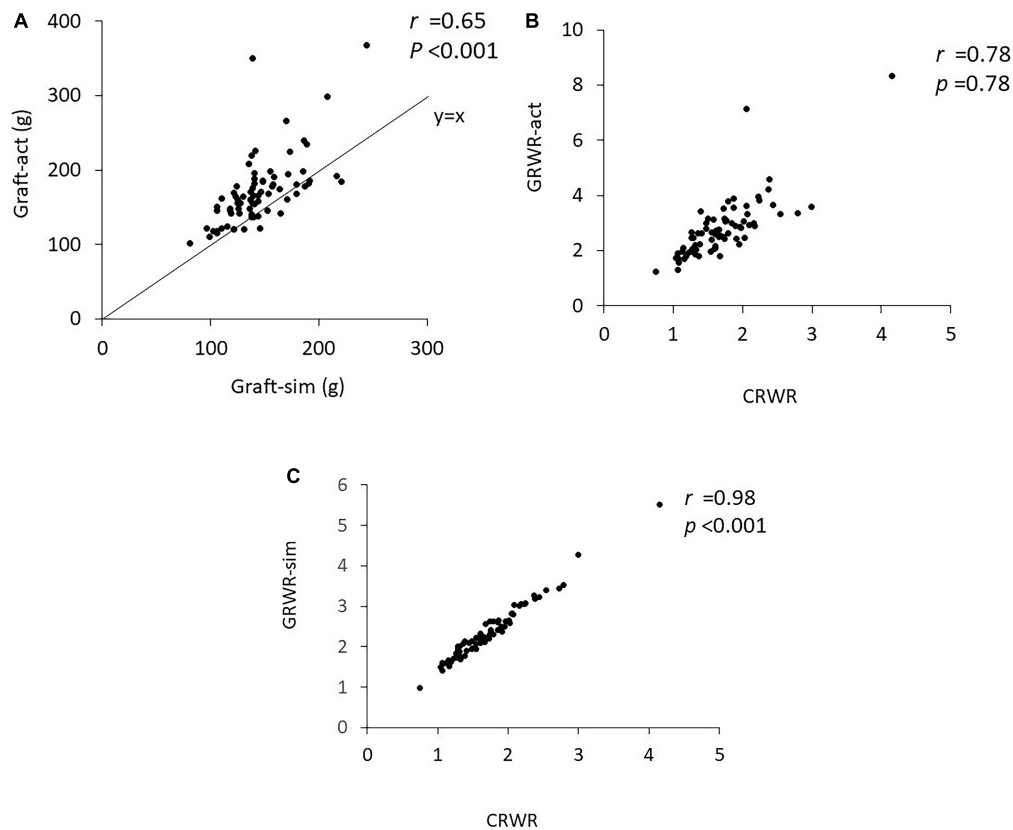


FIGURE 1

Correlation coefficient between Graft-sim and Graft-act and between CRWR and GRWR-act and GRWR-sim. (A) Correlation between Graft-sim and Graft-act. (B) Correlation between CRWR and GRWR-act. (C) Correlation between CRWR and GRWR-sim.

TABLE 2 Multiple regression analysis related to recipient's eGFR (ml/min/1.73 m²) at 1 month.

Variable	β	SE	P-value
Donor eGFR (ml/min/1.73 m ²)	0.23	0.08	0.006
CRWR	17.03	2.49	<0.001
Preemptive kidney transplant, yes	8.96	2.64	0.001

eGFR, estimated glomerular filtration rate; CRWR, cortex recipient weight ratio; β , regression coefficient; SE, standard error.

eGFR (ml/min/1.73 m²)

$$\begin{aligned}
 &= 0.23 \times \text{donor eGFR (ml/min/1.73 m}^2\text{)} \\
 &+ 17.03 \times \text{CRWR} + 8.96 \times \text{PEKT} \\
 &+ 5.10 \text{ (adjusted coefficient of determination} = 0.54\text{)}
 \end{aligned}$$

This formula is graphically illustrated in Figure 4A. In this graph, the donor eGFR is divided into approximately 50, 70, 90, and 110 ml/min/1.73 m², and it was possible to calculate the postoperative eGFR for each CRWR according to the presence or absence of PEKT. Furthermore, the formula was validated using the external cohort from the Mito Medical

Center ($n = 21$). In more than 80% of patients (17/21), the observed eGFR was within a 10 ml/min/1.73 m² margin of the predicted eGFR, showing that the performance of the formula was good (Figure 4B).

Discussion

The novelty of this study is that CRWR was a novel size mismatch parameter that directly reflected the “nephron mass” of the allograft and could be calculated from preoperative CT images using CT-volumetric software. CRWR demonstrated the strongest correlation with postoperative early renal function among the representative donor-recipient size mismatch parameters, and it enabled the prediction of early allograft function using a formula.

Factors that influence renal function after LDKT can be divided into immunologic and non-immunologic factors (5). In the 21st century, the introduction of immunosuppressive agents such as calcineurin inhibitors, mycophenolate mofetil, anti-CD25 monoclonal antibody, anti-human thymocyte rabbit immunoglobulin, and rituximab in blood group

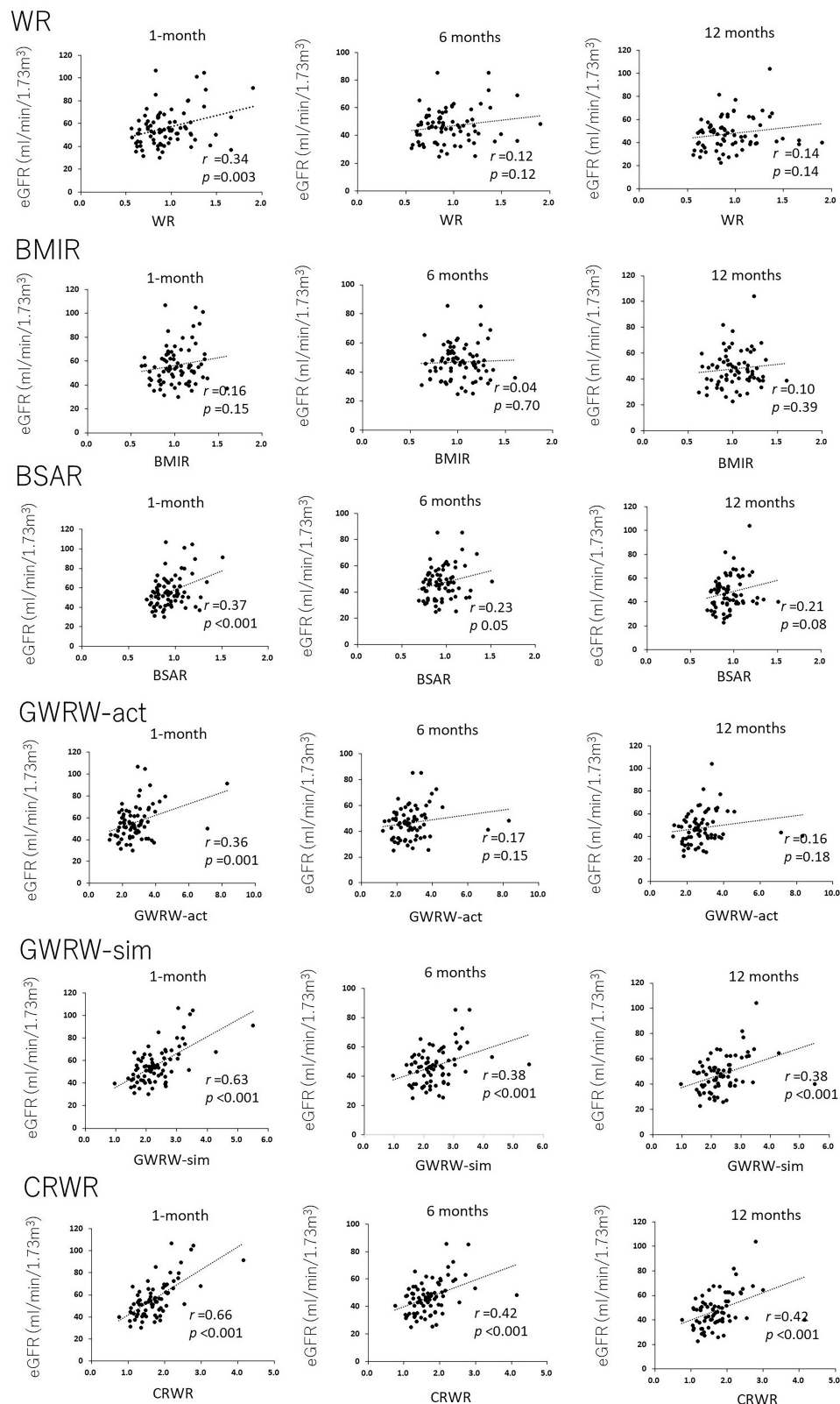


FIGURE 2

Correlation of donor-recipient size mismatch parameters (WR, BMIR, BSAR, GWRW-act, GWRW-sim, and CRWR) with renal function at 1, 6, and 12 months posttransplantation. The correlation coefficients for CRWR were the highest among the other size mismatch parameters.

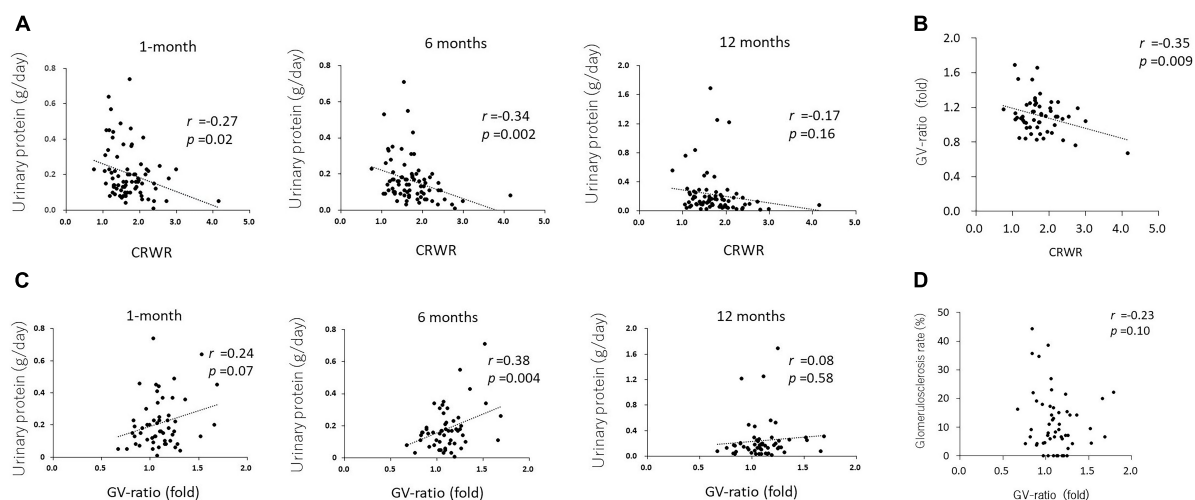


FIGURE 3
Correlation between CRWR and GV-ratio and urinary protein. **(A)** Correlation between CRWR and urinary protein at 1, 6, and 12 months posttransplantation. **(B)** Correlation between CRWR and GV-ratio. **(C)** Correlation between GV ratio and urinary protein at 1, 6, and 12 months posttransplantation. **(D)** Correlation between GV ratio and the percentage of glomerular sclerosis.

incompatible transplantation, as well as detailed elucidation of the pathogenesis of various immunologic rejective reactions, have enabled sustained control of immunological factors. Owing to these developments, the short- and mid-term outcomes over the last 20 years have improved dramatically. On the other hand, non-immunological factors, such as nephrotoxicity secondary to immunosuppressants, hypertension, obesity, diabetes, the recurrence of primary disease, donor-recipient size mismatch, and viral infection, affect not only the short-term but also the mid- and long-term outcomes. Controlling these non-immunologic factors to prolong graft survival has received attention from transplant physicians (4). After LDKT, most patients exhibit IGF, in which serum creatinine reaches its nadir within a few weeks posttransplantation. In this period, patients are usually under strong immunosuppression due to the use of anti-CD25 monoclonal antibodies and anti-human thymocyte rabbit immunoglobulin and high serum levels of maintenance calcineurin inhibitors. Thus, renal function in this early period is mostly defined by non-immunological factors, especially the “nephron mass” in the donor graft, reflected by donor age, donor preoperative eGFR, sex mismatch, and donor-recipient size mismatch, that accomplish subsequent baseline graft function (10, 11). In particular, the donor-recipient size mismatch is a direct reflection of the total throughput of the renal graft in the recipient. This can be understood on the basis of two facts: grafts from elderly donors demonstrate declined renal function because of the reduced “nephron mass” in the donor graft secondary to glomerulosclerosis due to aging, and grafts from sex mismatch transplantations, especially female to male transplantations, show worse posttransplantation renal function since female kidneys are smaller in size and have less

“nephron mass” in terms of absolute quantity than male kidneys (18, 19).

The correlation between postoperative renal function and parameters such as BMIR, BSAR, WR, and GRWR-act have previously been discussed as indicators of donor-recipient size mismatch (12–16). Several reports have demonstrated some degree of correlation, but none of these indices sufficiently reflect the quantity of the “nephron mass.” Although GRWR-act might be a closer indicator than other parameters, it does not always reflect the “nephron mass” because it includes the weight of perirenal fatty tissue, renal portal vessels, and the ureter. In fact, the results of our study showed that Graft-act (g) was generally heavier than Graft-sim (g), and the strength of the correlation between CRWR and GRWR-act was weaker than that between CRWR and GRWR-sim. Furthermore, GRWR-act was weakly correlated with early postoperative renal function than GRWR-sim and CRWR. Recently, some studies have reported the usefulness of the calculated renal graft volume, namely, the Graft-sim in our study, in which graft volume was measured by contrast-enhanced MDCT using 3D volumetry. Saxena et al. used MRI-based 3D volumetric software to quantify graft volume and reported that its weight ratio correlated with postoperative eGFR at 6 months and 1 year posttransplantation (16). Yanishi et al. used Synaps Vincent[®] to quantify graft volumes and reported that GRWR-sim was correlated with eGFR at 1-year postoperation (20). On the other hand, these reports did not compare GRWR-sim with other size mismatch parameters, and it was not clear how reliable GRWR-sim was compared with other parameters. Moreover, these researchers assessed postoperative renal function at the time when renal function can be modified by immunological factors

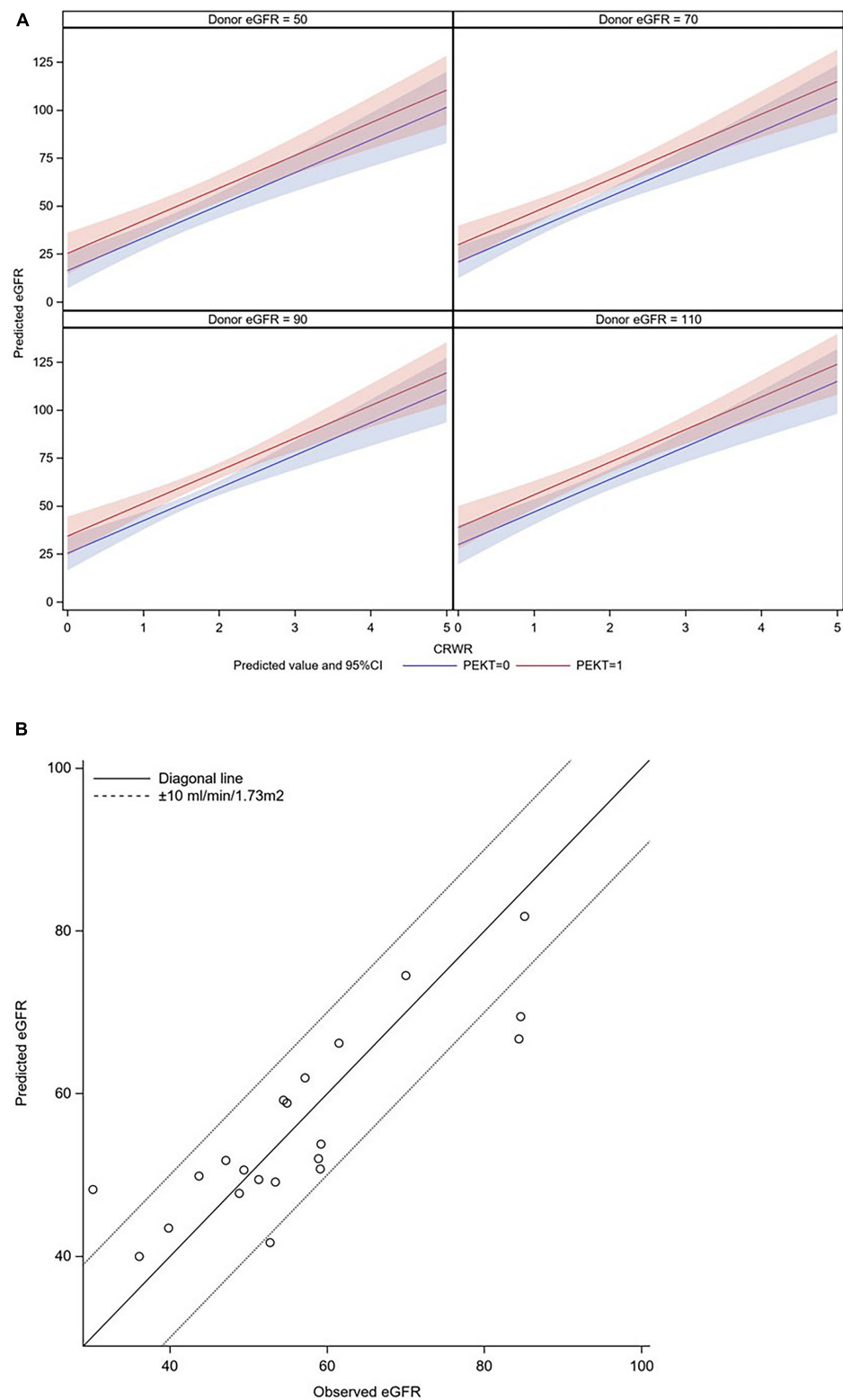


FIGURE 4

Graphic illustration of the formula for predicting eGFR at 1-month posttransplantation and its validation. **(A)** Graphic illustration of the formula. The donor eGFR is divided into approximately 50, 70, 90, and 110 ml/min/1.73 m². It was possible to calculate the postoperative eGFR for each CRWR according to the presence or absence of PEKT (red line; with PEKT, blue line; without PEKT). **(B)** Validation. In most patients (17/21), the observed eGFR was within a 10 ml/min/1.73 m² margin of the predicted eGFR.

and other non-immunological factors, such as diabetes, obesity, hypertension, and infection. CRWR, as we propose here, directly quantifies the renal cortex where functional glomeruli exist. Because donor non-functional glomeruli, i.e., nephrons with glomerulosclerosis secondary to aging, obesity, infarction, etc., are not contrasted by MDCT, these non-functional nephrons are not counted in CRWR (21). CRWR is more reliable as a surrogate of the “nephron mass” than the GRWR-sim, presented as the total graft volume. This is intuitively understandable from the fact that older donors or obese donors who have a thinning renal cortex on preoperative CT with a sufficient graft weight show worse postoperative renal function than expected. Indeed, in our study, CRWR correlated with early renal function more strongly than GRWR-sim at any time point postoperation.

In this study, eGFR at 1-month posttransplantation was expressed as a linear equation using donor preoperative eGFR, CRWR, and PEKT. This provides preoperative information on the degree to which renal function can be achieved postoperatively with any one donor in the case of multiple potential living donors. Therefore, this formula can be applied as a tool in donor selection. In addition, the ability to predict peak renal function avoids unnecessary fluid replacement or diuretic intervention when postoperative renal function has reached the predicted value, thereby avoiding prolonged hospitalization and wasteful use of medical resources. Conversely, if postoperative renal function is not the predicted value, the involvement of immunologic and other non-immunologic factors should be considered, providing a rationale for invasive interventions such as renal biopsy.

A decreased renal graft survival rate after LDKT has been reported in situations where a small donor kidney is transplanted to a large body size recipient (22–24). This is due to the increased hemodynamic load on a single glomerulus in the renal graft, resulting in a state of hyperfiltration. Chronic hyperfiltration associated with reduced functioning of the nephron mass damages the allograft, initiating a vicious cycle of further reduction in the nephron mass, which causes more significant hyperfiltration, leading to a progressive decline in the GFR, proteinuria, hypertension, and eventually graft failure. This was proposed as the “hyperfiltration theory” by Brenner et al. in who demonstrated the relationship between protein intake and the progression of glomerulosclerosis in small kidneys in animal experiments (25). These compensatory hemodynamic changes could also be a proinflammatory trigger leading to alloantigen-dependent kidney damage (22, 26). The results of our study demonstrated that CRWR was negatively correlated with glomerular enlargement. Namely, as the donor-recipient size mismatch increased, the glomerular size in the allograft increased, implying the pressure overload of each glomerulus. Furthermore, glomerular enlargement demonstrated a positive correlation with proteinuria in the

short-term after transplantation, implying glomerular damage. These results support the mechanisms of the “hyperfiltration theory” of donor-recipient size-mismatch transplantation. On the other hand, glomerular enlargement was not directly correlated with urinary protein or glomerular sclerosis at 12 months. The reason for these phenomena might be because in addition to hyperfiltration, glomerular damage and sclerosis at this time could be influenced by other factors, including immunologic and non-immunologic factors such as obesity, diabetes, and viral infection (27).

The limitations of this study are as follows. First, this is a retrospective study of patients at two institutions, and the sample size is small. Furthermore, since the study was conducted only in Asian, the size mismatches may not be as significant as those in other countries. Second, this study did not measure inulin clearance in the early postoperative period; thus, eGFR was used as an outcome measure. The eGFR is generally lower than the true GFR obtained from inulin clearance and therefore may not provide a precise evaluation of postoperative renal function. Third, GV should be evaluated by renal biopsies at each time point, but GV obtained from protocol biopsies at 12 months posttransplantation was used to evaluate postoperative GV altogether. Despite these limitations, given that we for the first time proposed CRWR as a surrogate parameter of the size mismatch that directly reflects the “nephron mass,” this study provides unique implications for the application of this novel indicator in clinical practice.

Data availability statement

The original contributions presented in the study are included in the article/**Supplementary material**, further inquiries can be directed to the corresponding author.

Ethics statement

The studies involving human participants were reviewed and approved by Tsukuba University Hospital and Mito Medical Center Internal Review Boards. Written informed consent for participation was not required for this study in accordance with the national legislation and the institutional requirements.

Author contributions

KT, KF, and TK collected the data. KT and MG analyzed the data. KT, KF, and MG wrote the manuscript. JU, AH, SH, HN, TO, KYu, and KYa did critical comments on the manuscript. All authors contributed to the article and approved the submitted version.

Conflict of interest

The authors declare that the research was conducted in the absence of any commercial or financial relationships that could be construed as a potential conflict of interest.

Publisher's note

All claims expressed in this article are solely those of the authors and do not necessarily represent those of their affiliated organizations, or those of the publisher, the editors and the reviewers. Any product that may be evaluated in this article, or

claim that may be made by its manufacturer, is not guaranteed or endorsed by the publisher.

Supplementary material

The Supplementary Material for this article can be found online at: <https://www.frontiersin.org/articles/10.3389/fmed.2022.1007175/full#supplementary-material>

SUPPLEMENTARY FIGURE 1

Measurement of the renal cortex by 3D CT volumetric software (Synaps Vincent®).

SUPPLEMENTARY FIGURE 2

The glomerular volume (GV)-ratio was calculated by dividing GV 1-year after transplantation by GV 1 h after transplantation.

References

- Lentine KL, Smith JM, Hart A, Miller J, Skeans MA, Larkin L, et al. OPTN/SRTR 2020 Annual data report: kidney. *Am J Transplant.* (2022) 22(Suppl. 2):21–136.
- Al Otaibi T, Ahmadpoor P, Allawi AA, Habhab WT, Khatami MR, Nafar M, et al. Delayed graft function in living-donor kidney transplant: a Middle Eastern perspective. *Exp Clin Transplant.* (2016) 14:1–11.
- Jevnikar AM, Mannon RB. Late kidney allograft loss: what we know about it, and what we can do about it. *Clin J Am Soc Nephrol.* (2008) 3(Suppl. 2):S56–67. doi: 10.2215/CJN.03040707
- Gaston RS, Fieberg A, Helgeson ES, Eversull J, Hunsicker L, Kasiske BL, et al. Late graft loss after kidney transplantation: is “death with function” really death with a functioning allograft? *Transplantation.* (2020) 104:1483–90.
- Gill JS, Abichandani R, Kausz AT, Pereira BJ. Mortality after kidney transplant failure: the impact of non-immunologic factors. *Kidney Int.* (2002) 62:1875–83.
- Hariharan S, McBride MA, Cherikh WS, Tolleris CB, Bresnahan BA, Johnson CP. Post-transplant renal function in the first year predicts long-term kidney transplant survival. *Kidney Int.* (2002) 62:311–8.
- Helleggering J, Visser J, Kloke HJ, D'Ancona FCH, Hoitsma AJ, van der Vliet JA, et al. Poor early graft function impairs long-term outcome in living donor kidney transplantation. *World J Urol.* (2013) 31:901–6.
- Transplant JSCR, Transplant JS. Annual progress report from the Japanese renal transplant registry: number of renal transplantations in 2020 and follow-up survey. *Ishoku.* (2022) 56:195–215.
- Boenink R, Astley ME, Huijben JA, Stel VS, Kerschbaum J, Ots-Rosenberg M, et al. The ERA registry annual report 2019: summary and age comparisons. *Clin Kidney J.* (2022) 15:452–72. doi: 10.1093/ckj/sfab273
- Dick AA, Mercer LD, Smith JM, McDonald RA, Young B, Healey PJ. Donor and recipient size mismatch in adolescents undergoing living-donor renal transplantation affect long-term graft survival. *Transplantation.* (2013) 96:555–9. doi: 10.1097/TP.0b013e31829d672c
- Zhao J, Song WL, Mo CB, Wang ZP, Fu YX, Feng G, et al. Factors of impact on graft function at 2 years after transplantation in living-donor kidney transplantation: a single-center study in China. *Transplant Proc.* (2011) 43:3690–3. doi: 10.1016/j.transproceed.2011.09.066
- Lee BM, Yoon SN, Oh CK, Kim JH, Kim SJ, Kim H, et al. Fractional creatinine clearance of the donated kidney using Cockcroft-Gault formula as a predictor of graft function after living donor transplantation. *Transplant Proc.* (2006) 38:1974–6. doi: 10.1016/j.transproceed.2006.06.024
- Yamakawa T, Kobayashi A, Yamamoto I, Nakada Y, Mafune A, Katsumata H, et al. Clinical and pathological features of donor/recipient body weight mismatch after kidney transplantation. *Nephrology (Carlton).* (2015) 20(Suppl. 2):36–9. doi: 10.1111/nep.12470
- McGee J, Magnus JH, Islam TM, Jaffe BM, Zhang R, Florman SS, et al. Donor-recipient gender and size mismatch affects graft success after kidney transplantation. *J Am Coll Surg.* (2010) 210:718–25.e1. doi: 10.1016/j.jamcollsurg.2009.12.032
- Ly J, Guga S, Huang H, Wang R, Zhang X, Shou Z, et al. The effect of donor-recipient body surface area ratio on donor age and donor glomerular filtration rate in Chinese patients undergoing a living-donor kidney transplant. *Exp Clin Transplant.* (2014) 12:515–21. doi: 10.6002/ect.2013.0258
- Saxena AB, Busque S, Arjane P, Myers BD, Tan JC. Preoperative renal volumes as a predictor of graft function in living donor transplantation. *Am J Kidney Dis.* (2004) 44:877–85.
- Torimoto I, Takebayashi S, Sekikawa Z, Teranishi J, Uchida K, Inoue T. Renal perfusional cortex volume for arterial input function measured by semiautomatic segmentation technique using MDCT angiographic data with 0.5-mm collimation. *Am J Roentgenol.* (2015) 204:98–104. doi: 10.2214/AJR.14.12778
- Luyckx VA, Shukha K, Brenner BM. Low nephron number and its clinical consequences. *Rambam Maimonides Med J.* (2011) 2:e0061.
- Denic A, Lieske JC, Chakkera HA, Poggio ED, Alexander MP, Singh P, et al. The substantial loss of nephrons in healthy human kidneys with aging. *J Am Soc Nephrol.* (2017) 28:313–20. doi: 10.1681/ASN.2016020154
- Yanishi M, Kinoshita H, Yoshida T, Takayasu K, Yoshida K, Mishima T, et al. Comparison of live donor pre-transplant and recipient post-transplant renal volumes. *Clin Transplant.* (2016) 30:613–8. doi: 10.1111/ctr.12727
- Nakazato T, Ikehira H, Imasawa T. An equation to estimate the renal cortex volume in chronic kidney disease patients. *Clin Exp Nephrol.* (2018) 22:603–12.
- el-Agroudy AE, Hassan NA, Bakr MA, Foda MA, Shokeir AA, Shehab el-Dein AB. Effect of donor/recipient body weight mismatch on patient and graft outcome in living-donor kidney transplantation. *Am J Nephrol.* (2003) 23:294–9.
- Miller AJ, Kiberd BA, Alwayn IP, Odutayo A, Tennankore KK. Donor-recipient weight and sex mismatch and the risk of graft loss in renal transplantation. *Clin J Am Soc Nephrol.* (2017) 12:669–76.
- Vianello A, Calconi G, Amici G, Chiara G, Pignata G, Maresca MC. Importance of donor/recipient body weight ratio as a cause of kidney graft loss in the short to medium term. *Nephron.* (1996) 72:205–11. doi: 10.1159/000188843
- Brenner BM, Meyer TW, Hostetter TH. Dietary protein intake and the progressive nature of kidney disease: the role of hemodynamically mediated glomerular injury in the pathogenesis of progressive glomerular sclerosis in aging, renal ablation, and intrinsic renal disease. *N Engl J Med.* (1982) 307:652–9. doi: 10.1056/NEJM198209093071104
- Sanchez-Fructuoso AI, Prats D, Marques M, Pérez-Contín MJ, Fernández-Pérez C, Contreras E, et al. Does renal mass exert an independent effect on the determinants of antigen-dependent injury? *Transplantation.* (2001) 71:381–6. doi: 10.1097/00007890-200102150-00007
- Naik AS, Sakhuja A, Cibrik DM, Ojo AO, Samaniego-Picota MD, Lentine KL. The impact of obesity on allograft failure after kidney transplantation: a competing risks analysis. *Transplantation.* (2016) 100:1963–9. doi: 10.1097/TP.0000000000000983

Article

Clinical Relevance of Ultrasonographic and Electrophysiological Findings of the Median Nerve in Unilateral Carpal Tunnel Syndrome Patients

Takamasa Kudo ¹, Yuichi Yoshii ^{1,*} , Yuki Hara ², Takeshi Ogawa ³  and Tomoo Ishii ¹

¹ Department of Orthopedic Surgery, Tokyo Medical University Ibaraki Medical Center, Ami 300-0395, Ibaraki, Japan

² Department of Orthopedic Surgery, University of Tsukuba Hospital, Tsukuba 305-8577, Ibaraki, Japan

³ Department of Orthopaedic Surgery, Mito Medical Center, Mito 311-3193, Ibaraki, Japan

* Correspondence: yyoshii@tokyo-med.ac.jp; Tel.: +81-29-887-1161

Abstract: Few studies have compared the unaffected and affected sides in the same carpal tunnel syndrome (CTS) patients using ultrasonography and electrophysiological tests. We focused on unilateral idiopathic CTS patients to investigate whether clinical test results differ between the unaffected and affected sides. The bilateral wrist joints of 61 unilateral idiopathic CTS patients were evaluated. The median nerve cross-sectional area of ultrasound image, and latencies of the compound muscle action potential (CMAP) and sensory nerve action potential (SNAP) were measured. The values obtained were compared between the affected and unaffected sides. The diagnostic accuracies of each parameter were assessed, and cut-off values were defined. Significant differences were observed in all parameters between the affected and unaffected sides ($p < 0.01$). Area under the curve (AUC) values were 0.74, 0.88, and 0.73 for the cross-sectional area, CMAP distal latency, and SNAP distal latency, respectively. Cut-off values were 11.9 mm², 5.1 ms, and 3.1 ms for the cross-sectional area, CMAP distal latency, and SNAP distal latency, respectively. The most reliable parameter that reflected clinical symptoms was the distal latency of CMAP. Cut-off values for each parameter are considered to be an index for the onset of the clinical symptoms of CTS.

Keywords: carpal tunnel syndrome; nerve conduction study; ultrasound; median nerve



Citation: Kudo, T.; Yoshii, Y.; Hara, Y.; Ogawa, T.; Ishii, T. Clinical Relevance of Ultrasonographic and Electrophysiological Findings of the Median Nerve in Unilateral Carpal Tunnel Syndrome Patients. *Diagnostics* **2022**, *12*, 2799. <https://doi.org/10.3390/diagnostics12112799>

Academic Editor: Antonio Barile

Received: 19 October 2022

Accepted: 14 November 2022

Published: 15 November 2022

Publisher's Note: MDPI stays neutral with regard to jurisdictional claims in published maps and institutional affiliations.



Copyright: © 2022 by the authors. Licensee MDPI, Basel, Switzerland. This article is an open access article distributed under the terms and conditions of the Creative Commons Attribution (CC BY) license (<https://creativecommons.org/licenses/by/4.0/>).

1. Introduction

Carpal tunnel syndrome (CTS) is defined as a compression neuropathy of the median nerve at the wrist joint. As clinical findings, night pain has been identified as a sensitive symptom predictor (96%), and the useful signs for the diagnosis are sensory impairment in the median nerve area of the hand (76%) and Tinel's sign (71%) [1]. However, clinical findings are subjective as they are based on self-reported symptoms by patients. In addition, symptoms may occur outside of the median nerve control area [2]. Therefore, difficulties are associated with reliably diagnosing CTS based solely on clinical findings. CTS is commonly diagnosed by a comprehensive assessment of clinical signs, electrophysiology, and imaging. Many studies have reported the utility of electrophysiological tests and ultrasonography for comparing CTS patients with normal subjects [3,4]. However, few studies have compared the unaffected and affected sides in the same CTS patients because many patients have bilateral symptoms. Therefore, we herein focused on unilateral idiopathic CTS patients and investigated whether clinical test results differed between the unaffected and affected sides. The aim of the present study was to characterize the findings of ultrasonography and nerve conduction studies on the symptomatic and asymptomatic sides of unilateral CTS patients and to indicate the cutoff values for the symptom expression. This study attempted to identify the clinical parameters in which patients perceive their symptoms by comparing the results of clinical examinations of symptomatic and asymptomatic

hands. We hypothesized that morphology and nerve conduction of the median nerve differ between the symptomatic and asymptomatic sides in the CTS patients with unilateral symptom.

2. Materials and Methods

The protocol for the present study was reviewed and approved by our Institutional Review Board (approved number T2020-0061). The bilateral wrist joints of 61 unilateral idiopathic CTS patients (122 wrists, 22 males, 39 females, 30–89 years, mean 65.3 years) were evaluated. Patients with chronic kidney disease, thyroid disease, and rheumatoid arthritis were excluded. Patients with a history of upper limb surgery were also excluded. CTS was diagnosed based on clinical symptoms and the results of motor and sensory nerve conduction studies as well as ultrasonography. Patients were asked to complete the JSSH version of the CTS instrument [5]. Clinical evaluation included the presence of typical sensory symptoms, Phalen's test and Tinel's sign, sensory testing by two-point discrimination on the middle finger, muscle testing, and examination for thenar atrophy. Informed consent was obtained from all patients for inclusion in the present study. In this study, we defined unilateral CTS as patients with characteristic symptoms on one side of the hand and no symptoms on the other side. The diagnosis of CTS was confirmed based on the clinical symptoms of pain, numbness, tingling in the median nerve distribution of the hand, and the presence of at least one positive provocative test result, in addition to meeting the criteria of nerve conduction study findings in the American Association of Electrodiagnostic Medicine (AAEM) guidelines [6]. For the asymptomatic side, the patients were also asked about the clinical symptoms of pain, numbness, and muscle weakness. Then, the strength of APB muscle and positivity of provocation tests were evaluated. It was defined as asymptomatic if none of the above clinical symptoms and evaluations were observed. A single hand surgeon discriminated between the asymptomatic and symptomatic sides based on interview and clinical findings. All patients underwent a nerve conduction study and ultrasound imaging.

The cross-sectional area of the median nerve was measured by following method. Ultrasound imaging was routinely performed in patients with suspected CTS to differentiate abnormalities around the carpal tunnel. During the diagnostic process, the cross-sectional area of the median nerve was measured at the wrist crease level (proximal carpal tunnel) (Figure 1). Each patient was asked to sit and place their forearm on the table with the palmar side up. An ultrasound scanner (Hi Vision Avius; Hitachi Aloka Medical, Ltd., Tokyo, Japan) equipped with a linear array transducer was set to a depth of 20 mm. The frequency of the transducer was 15 MHz. Cross-sectional ultrasonographic images of the carpal tunnel were analyzed using ImageJ Software (National Institutes of Health, Bethesda, MD, USA). The median nerve was outlined, and its area was calculated. All ultrasound studies were performed by a hand surgery specialist. The hand surgeon has been certified as a specialist and an instructor by the Japanese Society of Surgery of the Hand.

The nerve conduction study was performed on all patients using a standard electromyography system (Neuropack MEB-2208, Nihon Kohden Co., Tokyo, Japan). All studies were performed by a clinical technician who was blinded to clinical symptoms. At the time of the nerve conduction study, room temperature was maintained at 27 °C. Among patients with cold hands, the hands were warmed to bring the skin temperature closer to room temperature. In the motor conduction study, the compound muscle action potential (CMAP) of the abductor pollicis brevis muscle was recorded. CMAP was induced by a stimulation 7 cm proximal to the recording electrode. In the sensory conduction study, a stimulating electrode was placed at the index finger, and a recording electrode was placed at 14 cm proximal to the stimulating electrode. The sensory nerve action potential (SNAP) was recorded. The latencies of CMAP and SNAP were measured (Figure 2). Results were excluded from the analysis if there was no action potential in some cases.

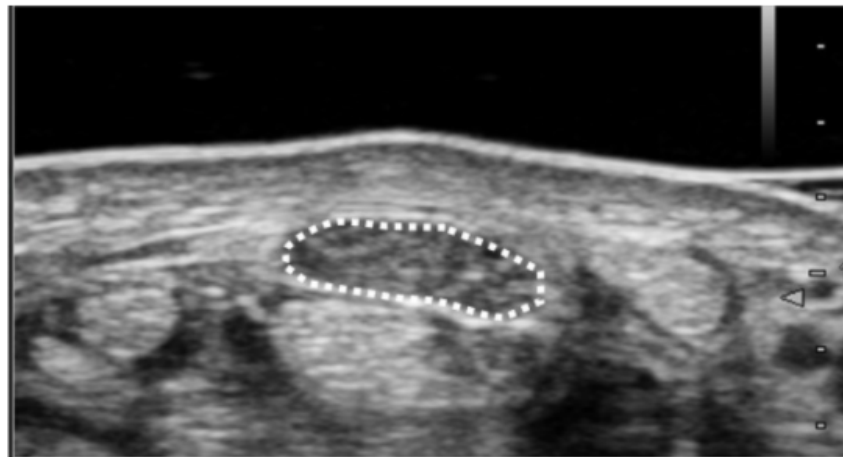


Figure 1. Ultrasound measurement of median nerve cross-sectional area. Cross-sectional area was measured as the only parameter for the image analysis. Measurement of the median nerve cross-sectional area was performed at the wrist crease level. The median nerve was outlined, and its area was calculated.

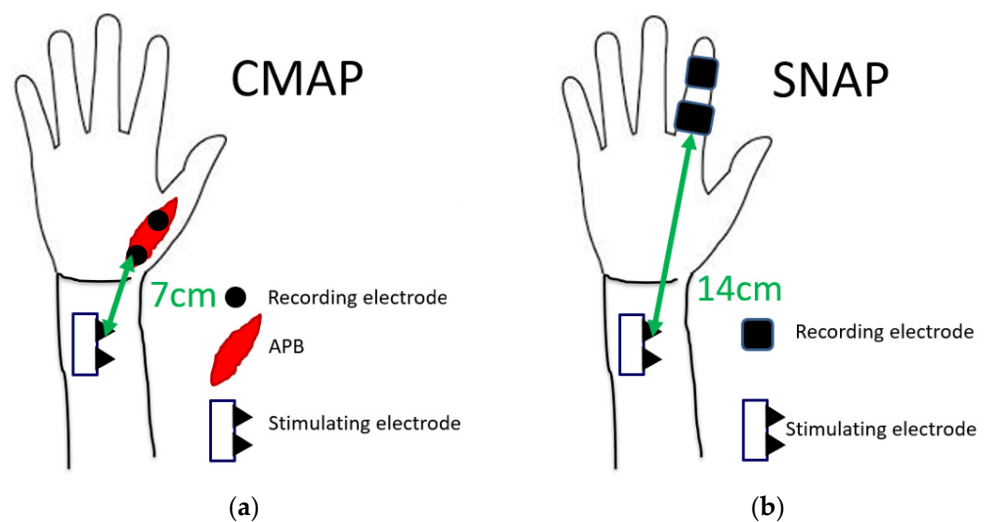


Figure 2. Measurement conditions of latencies of (a) CMAP and (b) SNAP.

Statistical analysis was evaluated by the method described here. Results are expressed as the mean \pm standard deviation. Measured values were compared between the affected and unaffected sides using the χ^2 test. A receiver operating characteristic (ROC) curve was created using a logistic analysis. Diagnostic accuracy was evaluated by the area under the curve (AUC value) based on the ROC curve analysis. Cut-off values and sensitivity/specificity were assessed using the Youden Index method. All analyses were performed using Bellcurve for Excel (version 2.14).

3. Results

Table 1 shows the patient demographics. Table 2 shows the results obtained for each parameter. Figure 3 shows the ROC curves for each parameter. The cross-sectional areas of the median nerve in six cases were larger on the unaffected side than on the affected side. In the motor nerve conduction study, CMAP was not derived on the affected side in 12 cases. In the sensory nerve conduction study, SNAP was not derived on the affected side in 16 cases. CMAP and SNAP waveforms were derived on the unaffected side in all cases. Significant differences were observed in all parameters between the affected and unaffected sides ($p < 0.01$). AUC values were 0.74, 0.88, and 0.73 for the cross-sectional

area, CMAP distal latency, and SNAP distal latency, respectively. Cut-off values were 11.9 mm², 5.1 ms, and 3.1 ms for the cross-sectional area, CMAP distal latency, and SNAP distal latency, respectively.

Table 1. Patient demographics.

Gender	Male	22
	Female	39
Age	Ave (SD)	65.3 ± 11.2
	Min	30
	Max	89
Height (cm)	Ave (SD)	157.6 ± 8.6
Weight (kg)	Ave (SD)	61.3 ± 11.9
BMI	Ave (SD)	24.6 ± 3.8
Work Status (%)	Manual work	44.8
	Desk work	13.8
	Unemployed	41.4
Disease period (%)	Less than 3 months	38.6
	3 months to 1 year	33.3
	More than 1 year	28.1
APB strength (MMT, %)	0~1	19.3
	2~3	40.4
	4~5	40.4

Table 2. Results obtained for each parameter.

	Affected Side	Unaffected Side	AUC	Cut-Off Values
Cross-sectional area (mm ²)	14.2 ± 4.0	11.3 ± 2.7	0.74	11.9
Distal Latency for CMAP (ms)	6.6 ± 1.8	4.4 ± 0.9	0.88	5.1
Distal Latency for SNAP (ms)	3.5 ± 0.8	2.8 ± 0.4	0.73	3.1

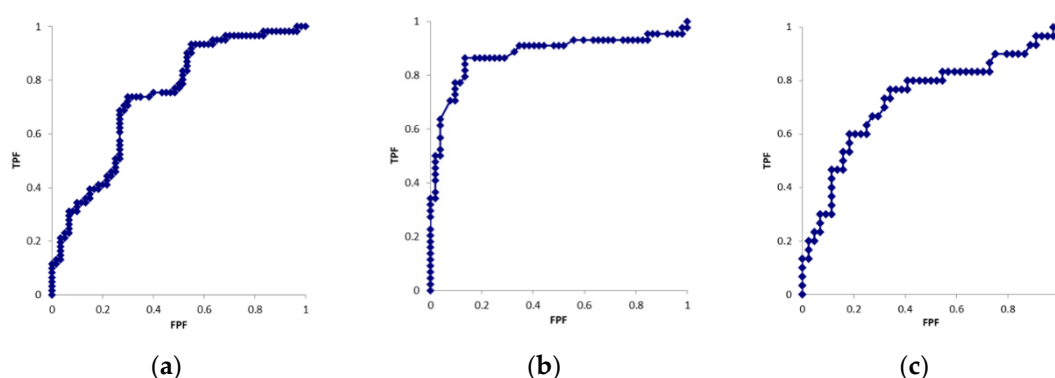


Figure 3. ROC curves of the (a) cross-sectional area, (b) CMAP latency (c) SNAP latency.

4. Discussion

In the present study, the cut-off values were defined in the cross-sectional areas and nerve conduction study distinguished CTS as symptomatic and asymptomatic. An important point in this study was that it could characterize asymptomatic conditions despite positive ultrasound and electrophysiological findings. This could be characterized by examining unilateral CTS patients. The most accurate diagnostic parameter in this study was the distal latency of CMAP. It has been known that most of CTS patients have bilateral symptoms. The asymptomatic side may develop symptoms in the future. By characterizing a unilateral asymptomatic situation in this study, it may allow early therapeutic intervention to prevent progression of neuropathy.

The diagnostic accuracy of ultrasonography was previously reported to be similar to that of the nerve conduction study [7]. Although ultrasonography alone has sufficient diagnostic accuracy, it has been pointed out that combining ultrasonography and nerve conduction study improves diagnostic accuracy [8]. Ultrasonography is less stressful on the patient and can identify neuromas or space-occupying lesions within the carpal tunnel, which could not be evaluated electrophysiologically. It can also identify a well-developed median artery and the compression of the median nerve associated with that arterial thrombus. In Nakamichi's studies, space-occupying lesions were found only in the unilateral group (7/20 = 35%), and it is said that careful examination of unilateral carpal tunnel syndrome on suspicion of local pathology, especially space-occupying lesion, is important [9]. Prior confirmation of these findings is useful in selecting a treatment. However, device/examiner dependency on the visualization of peripheral nerves is a limitation of this technique [10,11]. Furthermore, swelling of the median nerve is difficult to detect in patients older than 80 years, regardless of their severity of CTS [12]. In addition, diabetic conditions are known to affect the size of the median nerve [13,14]. These factors should be considered when assessing median nerve size.

The present study also showed that the cross-sectional area of the median nerve was significantly higher on the affected side than on the unaffected side. In the present study, the cut-off value for the cross-sectional area was 11.9 mm² and the AUC value was 0.74 (sensitivity: 72%, specificity: 68%). Cut-off values in previous studies varied between 6.5 and 15 mm² [15–17]. Only three studies defined a cut-off value of 11.9 mm² or higher. It has been pointed out that the cutoff value of cross-sectional area changes as conditions change [18], but in this study, differences within patients are compared, so the conditions are considered to be relatively homogeneous. Similar to the nerve conduction study, cut-off values were higher in the present study than that in a study comparing CTS patients with normal subjects. In addition, the asymptomatic hands of 62–85% of cases met the general diagnostic criteria (cross-sectional area 8.5–10 mm² or higher) [19]. When considered in the context of the Japanese people, Sugimoto's studies have shown that the average of Japanese median nerve cross-sectional area (carpal tunnel inlet at the pisiform bone level) was 8.5 ± 1.7 mm², which is a study of healthy subjects [20]. It has been suggested that the physical characteristics such as sex, dominant hand, age, height, weight, body mass index (BMI) and wrist circumference are associated with nerve size [20]. Compared to Sugimoto's study, the present case is older, shorter in height and BMI (the average ages of the subject were 35 and 65 years, heights were 164 cm and 157 cm, and BMI were 22.3 and 24, in the Sugimoto's and the present studies, respectively). In that study, age and BMI were positively, and height was negatively correlated with cross-sectional area. Although it is pointed out that these factors may cause the cross-sectional area in this case to be larger, we think that the value of cross-sectional area was larger even taking these factors into account. These findings suggest that even patients with unilateral symptoms have morphological changes in the median nerve of the asymptomatic hand.

Additionally, in the previous study, the mean median nerve cross-sectional area for carpal tunnel inlet seems to be similar for middle east (8.77 mm²), Oceania (8.71 mm²), Europe (8.90 mm²) and Asia (8.68 mm²) studies [21]. Although these were not directly compared, it shows that there is no racial difference in the cross-sectional area of median nerve. Despite the lack of significant differences between ethnic groups, the cutoff values for the present cases are larger compared to the general values, which based on values from previous literature [19]. One reason is that, as mentioned above, morphological changes in the median nerve is seen because the subjects of this study are unilateral symptoms. However, Nakamichi's study compared the Japanese with normal subjects, and even then, the cutoff value for cross-sectional area was set at 12 mm² (sensitivity 67%, specificity 97%), which is a higher value compared to the results of other countries [22]. This suggests that the cutoff value may be larger in the Japanese. From this finding, Japanese may be less likely to complain about physical symptoms than the patients in other country even when the swelling of the median nerve is present.

Because ultrasound can easily observe changes over time, it may help to predict symptom onset or determine the therapeutic effect. For more accurate diagnosis, we are thinking to use the wrist to forearm ratio for the ultrasound parameter [23]. Ultrasound can also detect increased intraneural blood flow of the median nerve with using Doppler sonography. It has been pointed out that it may be an indicator of early diagnosis and severity [24]. Nerve compression caused by elevated pressure in the carpal tunnel is believed to provoke a three-stage process that is initiated with venous congestion of the median nerve followed by nerve edema and then by impairment of the venous and arterial blood supplies. Comparison of findings of sonography and nerve conduction studies showed that nerve hypervascularization and nerve swelling yielded the best detectability of carpal tunnel syndrome [25]. Because there were several methods to identify median nerve pathological changes, it is clear that cross-sectional area measurement alone is not sufficient for a comprehensive ultrasound evaluation of peripheral nerves [26]. It may be possible to improve the accuracy of diagnosis by combining several parameters.

The nerve conduction study is one of a clinical test that is used to diagnose CTS [6]. It also helps to distinguish CTS from other clinical disorders. Additionally, it has been pointed out that the severity of CTS can be evaluated. Furthermore, the effects of surgery may be objectively evaluated by performing the study before and after the surgery [27]. On the other hand, the nerve conduction study is affected by age, height, finger circumference, sex, and skin temperature [28–32]. Therefore, previous studies adjusted for backgrounds, such as age/sex and finger usage, to eliminate selection bias in comparisons of healthy subjects and CTS patients. In the present study, it was possible to define cut-off values for clinical tests in patients with CTS symptoms by comparing the symptomatic and asymptomatic sides in the same patients. We considered two reasons why the distal latency of CMAP was found to be the most accurate. First, it has been pointed out that, Japanese may be less likely to complain about physical symptoms than the patients in other country even when neurological abnormalities are present [33]. The average latency of CMAP in asymptomatic hands in this study was 4.4 ± 0.9 ms, suggesting that the condition progresses to some extent insidiously according to previous grading [34]. Generally, sensory nerves are damaged first, and the onset of CTS is confirmed by a decrease in the sensory conduction velocity. In the case of Japanese patients, it is thought that the first hospital visit is often made after the symptoms have progressed to the extent that CMAP is impaired. Second, SNAP is affected by the factors such as body surface and room temperatures, and often becomes unrecordable when the CTS symptoms become more severe [35]. Because of these factors, the distal latency of CMAP was found to be the most accurate in the present study.

Individuals with certain occupations, such as postal staff, healthcare professionals, builders, and assembly workers, are more susceptible to CTS [36]. Evaluations of electrophysiological tests revealed the following prevalence of carpal tunnel syndrome: 20% for forest workers using vibration tools, 23% for staff working in general merchandise stores, 53% for meat workers, 17.8% for furniture makers, and 30% for dentists [37–40]. A common factor in these occupations is repetitive compression of the median nerve. Abnormal nerve conduction has been detected in some clinically asymptomatic nerves and has been defined as subclinical CTS [41]. MCV decreases with age, even in healthy subjects [42,43]. Therefore, the asymptomatic side in unilateral CTS patients is considered to be in a state of subclinical CTS. A previous study reported that the rate of subclinical CTS was approximately 18% [33]. Cut-off values were higher in the present study than in a previous study that compared normal subjects and CTS patients. This difference was attributed to the values measured being higher in the asymptomatic hands of unilateral CTS patients than in normal subjects. Among asymptomatic hands, there were cases in which 34% of sensory nerve conduction study and 50% of motor nerve conduction study met the diagnostic criteria of carpal tunnel syndrome [7]. To improve diagnostic accuracy, it may be necessary to devise diagnostic criteria that combine ultrasonography and nerve conduction studies [17].

Since symptoms such as numbness and pain are subjective, they are difficult to quantify and adapt to all patients. Furthermore, these symptoms may be hidden by patients. This

study compared values in symptomatic and asymptomatic hands in Japanese patients. Therefore, the cut-off values obtained are close to the values at which symptoms reach a level that interferes with daily activity. A previous study reported that approximately 30% of CTS patients showed significant improvements in their natural course [44]. Based on the values measured in the present study, patients with values near the cut-off values may be able to improve with conservative treatment. In addition, these values may be used as reference values for the selection of surgical treatment for patients.

There were several limitations that need to be addressed. First, sex, dominant hand, age, height, weight, BMI and wrist circumference were not evaluated in this study. There have been no reports of differences in nerve size between Japanese and other ethnic groups. In the present study, the cutoff value for symptom onset may be higher in Japanese, and thus, we think additional studies are needed. Second, the cross-sectional area was measured at wrist crease level without bony landmark. Nakamichi et al. reported the ultrasound measurements at three levels, and described that reliable data were obtained [20]. One of the levels was based on wrist crease, and reliable data were obtained even without bony landmarks. On the other hand, many papers measured with bony landmarks (at the level of pisiform). We may need to consider the differences of nerve size in the different levels of median nerve. In addition, automatic image analysis procedures have been reported recently [11]. The results of our manual measurement may need to compare the results with automatic analyzing procedure. Third, the characteristics of patients in which SNAP or CMAP was not derived were not evaluated. Lastly, cut-off values were not confirmed when symptoms appeared on the asymptomatic side. These limitations should be considered in the future study.

5. Conclusions

In conclusions, the ultrasonographic and electrophysiological features of unilateral idiopathic CTS patients were evaluated. It was found that the most reliable parameter that reflected clinical symptoms was the distal latency of CMAP. The cut-off values of each parameter are considered to be an index for the onset of the clinical symptoms of CTS.

Author Contributions: T.K.: acquisition and analysis of data and writing the manuscript, Y.Y.: research design, acquisition and analysis of data and writing the manuscript, Y.H.: acquisition and analysis of data and writing the manuscript, T.O.: acquisition and analysis of data and writing the manuscript, T.I.: acquisition and analysis of data and writing the manuscript. All authors have read and agreed to the published version of the manuscript.

Funding: This research received no external funding.

Institutional Review Board Statement: This study protocol was approved by our Institutional Review Board (T2020-0061).

Informed Consent Statement: Written consent was obtained from all study participants.

Data Availability Statement: The datasets analyzed during the present study are available from the corresponding author upon reasonable request.

Conflicts of Interest: The authors declare no conflict of interest.

References

1. Robert, M.S.; Robert, R.S.; Thomas, B.F.; Donna, B.S.; Wahida, K.S. The Value of Diagnostic Testing in Carpal Tunnel Syndrome. *J. Hand Surg.* **1999**, *24*, 704–714. [[CrossRef](#)]
2. Stevens, J.C.; Smith, B.E.; Weaver, A.L.; Bosch, E.P.; Deen Jr, H.G.; Wilkens, J.A. Symptoms of 100 patients with electromyographically verified carpal tunnel syndrome. *Muscle Nerve* **1999**, *22*, 1448–1456. [[CrossRef](#)]
3. Padua, L.; Lo, M.M.; Valente, E.M.; Tonali, P.A. A useful electrophysiologic parameter for diagnosis of carpal tunnel syndrome. *Muscle Nerve* **1996**, *19*, 48–53. [[CrossRef](#)]
4. Pinilla, I.; Martin-Hervas, C.; Sordo, G.; Santiago, S. The usefulness of ultrasonography in the diagnosis of carpal tunnel syndrome. *J. Hand Surg. Eur. Vol.* **2008**, *33*, 435–439. [[CrossRef](#)] [[PubMed](#)]
5. Imaeda, T.; Toh, S.; Nakao, Y.; Nishida, J.; Hirata, H.; Ijichi, M.; Kohri, C.; Nagano, A. Validation of the Japanese Society for Surgery of the Hand version of the Carpal Tunnel Syndrome Instrument. *J. Orthop. Sci.* **2007**, *12*, 14–21. [[CrossRef](#)]

6. Jablecki, C.K.; Andary, M.T.; Floeter, M.K.; Miller, R.G.; Quartly, C.A.; Vennix, M.J.; Wilson, J.R. Practice parameter: Electrodiagnostic studies in carpal tunnel syndrome. Report of the American Association of Electrodiagnostic Medicine, American Academy of Neurology, and the American Academy of Physical Medicine and Rehabilitation. *Neurology* **2002**, *58*, 1589–1592. [\[CrossRef\]](#)
7. Fowler, J.R.; Cipolli, W.; Hanson, T. A comparison of three diagnostic tests for carpal tunnel syndrome using latent class analysis. *J. Bone Jt. Surg. Am.* **2015**, *97*, 1958–1961. [\[CrossRef\]](#)
8. Ooi, C.C.; Wong, S.K.; Tan, A.B.H.; Chin, A.Y.H.; Bakar, R.A.; Goh, S.Y.; Mohan, P.C.; Yap, R.T.J.; Png, M.A. Diagnostic criteria of carpal tunnel syndrome using high-resolution ultrasonography: Correlation with nerve conduction studies. *Skelet. Radiol* **2014**, *43*, 1387–1394. [\[CrossRef\]](#)
9. Nakamichi, K.; Tachibana, S. Unilateral carpal tunnel syndrome and space-occupying lesions. *J. Hand Surg. Br.* **1993**, *18*, 748–749. [\[CrossRef\]](#)
10. Nakamichi, K. Ultrasonography for the management of carpal tunnel syndrome. *Clin. Neurol.* **2013**, *23*, 1217–1219. [\[CrossRef\]](#)
11. Obuchowicz, R.; Kruszynska, J.; Strzelecki, M. Classifying median nerves in carpal tunnel syndrome: Ultrasound image analysis. *Biocybern. Biomed. Eng.* **2021**, *41*, 335–351. [\[CrossRef\]](#)
12. Miwa, T.; Miwa, H. Ultrasonography of carpal tunnel syndrome: Clinical significance and limitations in elderly patients. *Intern. Med.* **2011**, *50*, 2157–2161. [\[CrossRef\]](#) [\[PubMed\]](#)
13. Chen, I.J.; Chang, K.V.; Lou, Y.M.; Wu, W.T.; Özçakar, L. Can ultrasound imaging be used for the diagnosis of carpal tunnel syndrome in diabetic patients? A systemic review and network meta-analysis. *J. Neurol.* **2020**, *267*, 1887–1895. [\[CrossRef\]](#) [\[PubMed\]](#)
14. Byra, M.; Hentzen, E.; Du, J.; Andre, M.; Chang, E.Y.; Shah, S. Assessing the performance of morphologic and echogenic features in median nerve ultrasound for carpal tunnel syndrome diagnosis. *J. Ultrasound Med.* **2020**, *39*, 1165–1174. [\[CrossRef\]](#)
15. Fowler, J.R.; Gaughan, J.P.; Ilyas, A.M. The sensitivity and specificity of ultrasound for the diagnosis of carpal tunnel syndrome: A meta-analysis. *Clin. Orthop. Relat. Res.* **2011**, *469*, 1089–1094. [\[CrossRef\]](#)
16. Ozsoy-Unubol, T.; Bahar-Ozdemir, Y.; Yagci, I. Diagnosis and grading of carpal tunnel syndrome with quantitative ultrasound: Is it possible? *J. Clin. Neurosci.* **2020**, *75*, 25–29. [\[CrossRef\]](#)
17. Fujimoto, K.; Kanchiku, T.; Kido, K.; Imajo, Y.; Funaba, M.; Taguchi, T. Diagnosis of severe carpal tunnel syndrome using nerve conduction study and ultrasonography. *Ultrasound Med. Biol.* **2015**, *41*, 2575–25780. [\[CrossRef\]](#)
18. Padua, L.; Coraci, D.; Erra, C.; Pazzaglia, C.; Paolasso, I.; Loreti, C.; Caliandro, P.; Hosbon-Webb, L.D. Carpal tunnel syndrome: Clinical features, diagnosis, and management. *Lancet Neurol.* **2016**, *15*, 1273–1284. [\[CrossRef\]](#)
19. Cartwright, M.S.; Hobson-Webb, L.D.; Boon, A.J.; Alter, K.E.; Hunt, C.H.; Flores, V.H.; Werner, R.A.; Shook, S.J.; Thomas, T.D.; Primack, S.J.; et al. Evidence-based guideline: Neuromuscular ultrasound for the diagnosis of carpal tunnel syndrome. *Muscle Nerve* **2012**, *46*, 287–293. [\[CrossRef\]](#)
20. Nakamichi, K.; Tachibana, S. Enlarged median nerve in idiopathic carpal tunnel syndrome. *Muscle Nerve* **2000**, *23*, 1713–1718. [\[CrossRef\]](#)
21. Audrey, J.T.N.; Ramya, C.; Prakash, A.; Mogali, S.R. A systematic review: Normative reference values of the median nerve cross-sectional area using ultrasonography in healthy individuals. *Sci. Rep.* **2022**, *12*, 9217. [\[CrossRef\]](#)
22. Nakamichi, K.; Tachibana, S. Ultrasonographic measurement of median nerve cross-sectional area in idiopathic carpal tunnel syndrome: Diagnostic accuracy. *Muscle Nerve* **2002**, *26*, 798–803. [\[CrossRef\]](#) [\[PubMed\]](#)
23. Hobson-Webb, L.D.; Massey, J.M.; Juel, V.C.; Sandres, D.B. The ultrasonographic wrist-to-forearm median nerve area ratio in carpal tunnel syndrome. *Clin. Neurophysiol.* **2008**, *119*, 1353–1357. [\[CrossRef\]](#) [\[PubMed\]](#)
24. Venderschuere, G.A.; Meys, V.E.; Beekman, R. Doppler sonography for the diagnosis of carpal tunnel syndrome: A critical review. *Muscle Nerve* **2014**, *50*, 159–163. [\[CrossRef\]](#)
25. Mallouhi, A.; Pülzl, P.; Trieb, T.; Piza, H.; Bodner, G. Predictors of carpal tunnel syndrome: Accuracy of gray-scale and color Doppler sonography. *AJR Am. J. Roentgenol.* **2006**, *186*, 1240–1245. [\[CrossRef\]](#)
26. Tagliafico, A.S. Peripheral nerve imaging: Not only crosssectional area. *World J. Radiol.* **2016**, *8*, 726–728. [\[CrossRef\]](#)
27. El-Hajj, T.; Tohme, R.; Sawaya, R. Changes in electrophysiological parameters after surgery for the carpal tunnel syndrome. *J. Clin. Neurophysiol.* **2010**, *27*, 224–226. [\[CrossRef\]](#)
28. Rivner, M.H.; Swift, T.R.; Malik, K. Influence of age and height on nerve conduction. *Muscle Nerve* **2001**, *24*, 1134–1141. [\[CrossRef\]](#)
29. Stetson, D.S.; Albers, J.W.; Silverstein, B.A.; Wolfe, R.A. Effects of age, sex, and anthropometric factors on nerve conduction measures. *Muscle Nerve* **1992**, *15*, 1095–1104. [\[CrossRef\]](#)
30. Huang, C.R.; Chang, W.N.; Chang, H.W.; Tsai, N.W.; Lu, C.H. Effects of age, gender, height, and weight on late responses and nerve conduction study parameters. *Acta Neurol. Taiwan* **2009**, *18*, 242–249.
31. Ludin, H.P.; Bayeler, F. Temperature dependence of normal sensory nerve action potentials. *J. Neurol.* **1977**, *216*, 173–180. [\[CrossRef\]](#) [\[PubMed\]](#)
32. Werner, R.A.; Andary, M. Carpal tunnel syndrome: Pathophysiology and clinical neurophysiology. *Clin. Neurophysiol.* **2002**, *113*, 1373–1381. [\[CrossRef\]](#)
33. Nathan, P.A.; Takigawa, K.; Keniston, R.C.; Meadows, K.D.; Lockwood, R.S. Slowing of sensory conduction of the median nerve and carpal tunnel syndrome in Japanese and American industrial workers. *J. Hand Surg. Br.* **1994**, *19*, 30–34. [\[CrossRef\]](#)
34. Hirani, S. A study to further develop and refine carpal tunnel syndrome (CTS) nerve conduction grading tool. *BMC Musculoskelet. Disord.* **2019**, *20*, 581. [\[CrossRef\]](#)

35. Sonoo, M.; Menkes, D.L.; Bland, J.D.P.; Burke, D. Nerve conduction studies and EMG in carpal tunnel syndrome: Do they add value? *Clin. Neurophysiol.* **2018**, *3*, 78–88. [[CrossRef](#)] [[PubMed](#)]
36. Tanaka, S.; Wild, D.K.; Seligman, P.J.; Halperin, W.E.; Behrens, V.J.; Putz-Anderson, V. Prevalence and work-relatedness of self-reported carpal tunnel syndrome among U.S. workers: Analysis of the Occupational Health Supplement data of 1988 National Health Interview Survey. *Am. J. Ind. Med.* **1995**, *27*, 451–470. [[CrossRef](#)] [[PubMed](#)]
37. Koskimies, K.; Färkkilä, M.; Pyykkö, I.; Jäntti, V.; Aatola, S.; Starck, J.; Inaba, R. Carpal tunnel syndrome in vibration disease. *Br. J. Ind. Med.* **1990**, *47*, 411–416. [[CrossRef](#)]
38. Osorio, A.M.; Ames, R.G.; Jones, J.; Castorina, J.; Rempel, D.; Estrin, W.; Thompson, D. Carpal tunnel syndrome among grocery store workers. *Am. J. Ind. Med.* **1994**, *25*, 229–245. [[CrossRef](#)]
39. Isolani, L.; Bonfiglioli, R.; Raffi, G.B.; Violante, F.S. Different case definitions to describe the prevalence of occupational carpal tunnel syndrome in meat industry workers. *Int. Arch. Occup. Environ. Health* **2002**, *75*, 229–234. [[CrossRef](#)]
40. Hamann, C.; Werner, R.A.; Franzblau, A.; Rodgers, P.A.; Siew, C.; Gruinger, S. Prevalence of carpal tunnel syndrome and median mononeuropathy among dentists. *J. Am. Dent. Assoc.* **2001**, *132*, 163–170. [[CrossRef](#)]
41. Neary, D.; Ochoa, J.; Gilliatt, R.W. Sub-clinical entrapment neuropathy in man. *J. Neurol. Sci.* **1975**, *24*, 283–298. [[CrossRef](#)]
42. Bouche, P.; Cattelin, F.; Saint-Jean, O.; Léger, J.M.; Queslati, S.; Guez, D.; Moulonguet, A.; Brault, Y.; Aquino, J.P.; Simunek, P. Clinical and electrophysiological study on the peripheral nerves system in the elderly. *J. Neurol.* **1993**, *240*, 263–268. [[CrossRef](#)] [[PubMed](#)]
43. Verdú, E.; Ceballos, D.; Vilches, J.J.; Navarro, X. Influence of aging on peripheral nerve function and regeneration. *J. Peripher. Nerv. Syst.* **2000**, *5*, 191–208. [[CrossRef](#)]
44. Futami, T.; Kobayashi, A.; Ukita, T.; Endoh, T.; Fujita, T. Carpal tunnel syndrome; Its natural history. *Hand Surg.* **1997**, *2*, 129–130. [[CrossRef](#)]

Article

Clinical Significance of Maximum Intensity Projection Method for Diagnostic Imaging of Thoracic Outlet Syndrome

Takeshi Ogawa ^{1,2} , Shinzo Onishi ^{2,3}, Naotaka Mamizuka ⁴, Yuichi Yoshii ^{5,*} , Kazuhiro Ikeda ⁶, Takeo Mammoto ² and Masashi Yamazaki ³

¹ Department of Orthopedic Surgery, National Hospital Organization Mito Medical Center, 280 Sakuranosato, Ibarakimachi 311-3193, Japan

² Department of Orthopedic Surgery and Sports Medicine, Mito Clinical Education and Training Center, University of Tsukuba Hospital, Mito Kyodo General Hospital, 3-2-7 Miya-Machi, Mito 310-0015, Japan

³ Department of Orthopedic Surgery, Faculty of Medicine, University of Tsukuba, Tsukuba 305-8577, Japan

⁴ Baseball and Sports Clinic, 2-228-1 Kosugi, Park City Musashikosugi the Garden Towers West 1st Floor W4, Nakahara-Ward, Kawasaki 211-0063, Japan

⁵ Department of Orthopedic Surgery, Tokyo Medical University Ibaraki Medical Center, Ami 300-0395, Japan

⁶ Department of Orthopedic Surgery, Kikkoman General Hospital, Noda 278-0005, Japan

* Correspondence: yyoshii@tokyo-med.ac.jp; Tel.: +81-298871161

Abstract: The aim of this study was to use the magnetic resonance imaging maximum-intensity projection (MRI-MIP) method for diagnostic imaging of thoracic outlet syndrome (TOS) and to investigate the stricture ratios of the subclavian artery (SCA), subclavian vein (SCV), and brachial plexus bundle (BP). A total of 113 patients with clinically suspected TOS were evaluated. MRI was performed in a position similar to the Wright test. The stricture was classified into four grades. Then, the stricture ratios of the SCA, SCV, and BP in the sagittal view were calculated by dividing the minimum diameter by the maximum diameter of each structure. Patients were divided into two groups: surgical ($n = 22$) and conservative ($n = 91$). Statistical analysis was performed using the Mann–Whitney U test. The stricture level and ratio in the SCV were significantly higher in the surgical group, while the stricture level and the ratio of SCA to BP did not show significant differences between the two groups. The MRI-MIP method may be helpful for both subsidiary and severe diagnoses of TOS.

Keywords: maximum intensity projection; subclavian vein; thoracic outlet syndrome



Citation: Ogawa, T.; Onishi, S.; Mamizuka, N.; Yoshii, Y.; Ikeda, K.; Mammoto, T.; Yamazaki, M. Clinical Significance of Maximum Intensity Projection Method for Diagnostic Imaging of Thoracic Outlet Syndrome. *Diagnostics* **2023**, *13*, 319. <https://doi.org/10.3390/diagnostics13020319>

Academic Editor: Riemer H.J.A. Slart

Received: 15 December 2022

Revised: 4 January 2023

Accepted: 12 January 2023

Published: 15 January 2023



Copyright: © 2023 by the authors. Licensee MDPI, Basel, Switzerland. This article is an open access article distributed under the terms and conditions of the Creative Commons Attribution (CC BY) license (<https://creativecommons.org/licenses/by/4.0/>).

1. Introduction

Thoracic outlet syndrome (TOS) is probably more common than is believed, especially among young people. Diagnosing TOS is difficult because no reliable mechanical examination has been shown [1–7]. However, TOS has a wide variety of symptoms, and its pathogenesis is still debated. The diagnosis of TOS is also dependent on various evoked tests, and a classification of disputed neurogenic TOS has been proposed [8–12]. Patients with no abnormal findings on electrophysiological examination but with a variety of subjective symptoms are difficult to diagnose, and cases suspected to have TOS may actually be diagnosed with hysterical paralysis. One possible method, although not very reliable, to diagnose disputed neurogenic TOS is a medial antebrachial cutaneous nerve conduction study [13,14]. Imaging tests such as 3D-CT angiography, 3D-MR angiography, brachial plexus angiography, and angiography are used to visualize stenotic areas in blood vessels and nerves [15–20]; however, these cause problems related to radiation exposure and the use of contrast media. In this study, we report the application of the maximum intensity projection (MIP) method in MRI, which is well known for the depiction of the cerebral vasculature, and its use in the diagnosis of TOS. MIP is used to represent the highest intensity values along one axis of a three-dimensional volume in a two-dimensional (2D) image,

allowing rapid interpretation of the entire volume based on this 2D projection (Figure 1A,B). The objective of this study was to evaluate the diagnostic significance of the MIP method for TOS. We also classified the degree of stenosis in the subclavian artery (SCA), subclavian vein (SCV), and brachial plexus and calculated the stricture rate to evaluate the usefulness of MRI-MIP images in the diagnosis of TOS.

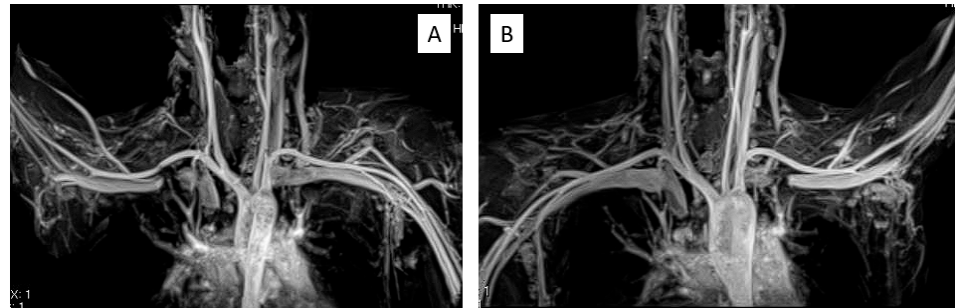


Figure 1. MRI-MIP display from the chest to the upper arm. (A) Raised right arm. (B) Raised left arm. MRI-MIP, magnetic resonance imaging maximum-intensity projection.

2. Materials and Methods

This study included 113 patients (60 men and 53 women) with clinically suspected TOS who underwent MRI-MIP at our hospital from May 2014 to March 2021, consecutively. The patients had an average age of 32.5 (14–67) yr. The institutional review board of the University of Tsukuba Hospital approved this study (Study Number: NO 22-44). Subjective symptoms varied from pain, numbness, and lethargy in the upper limbs and fingers to tenderness in the oblique interosseous muscle, intercostal space, or pectoralis minor tendon area. Patients with positive Roos test, Wright test, Adson test, or Eden test results were included in this study.

MRI was performed using a clinical 3 Tesla machine (Magnetom Skyra 3T, Siemens, Berlin, Germany). The patients were placed in a supine position with the upper limb raised further than that in the Wright test position (Figure 2A). Imaging was performed with the upper limb and trunk firmly fixed with a whole-body coil and bandages (Figure 2B). The imaging conditions were as follows: 3D-STIR with a slice thickness of 1.3 mm; FOV, 380 mm; TR/TE, 387/50; matrix, 320 × 256; and flip angle, 120°. A special pulse monitor was attached to the healthy index finger to synchronize imaging with the heartbeat. The subclavian arteries (SCA) and subclavian veins (SCV) were reconstructed using MIP and evaluated in the intercostal space.

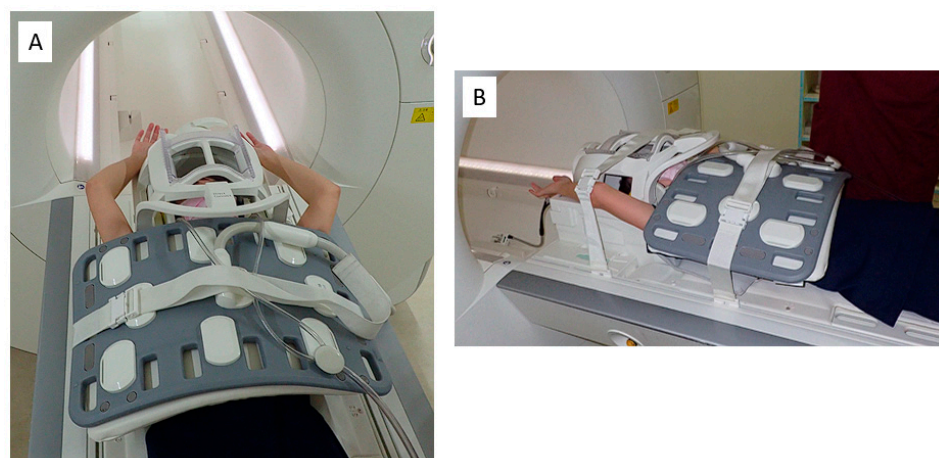


Figure 2. MRI imaging limb position. (A) The patient is placed in a supine position with the upper limb further elevated than in the Wright test position. (B) The upper extremities from the trunk are secured. MRI, magnetic resonance imaging.

The degree of SCA and SCV stenosis in MRI-MIP images were classified into four grades: grade 0 = no stenosis; grade 1 = stenosis < 50% of the maximum diameter of the SCA or SCV; grade 2 = stenosis > 50% of the maximum diameter of the SCA or SCV; and grade 3 = stenosis to the point of interruption (Figure 3). On the second evaluation, we used proton-density-weighted (PDW) sagittal images to quantitatively evaluate the stricture rate of the SCA, SCV, and nerve bundle at the costovertebral gap. The stricture rate was calculated by dividing the minimum diameter (a) of each SCA, SCV, and nerve bundle in the PDW sagittal image by the maximum diameter (b) as follows: $(1 - a/b) \times 100$ (Figure 4). A slice in which the first rib was the longest in a plate-like shape was used as the reference position. The maximum and minimum diameters were measured in the area where the first rib was located. The stricture grade and rate of SCA, SCV, and nerve bundle were statistically compared.

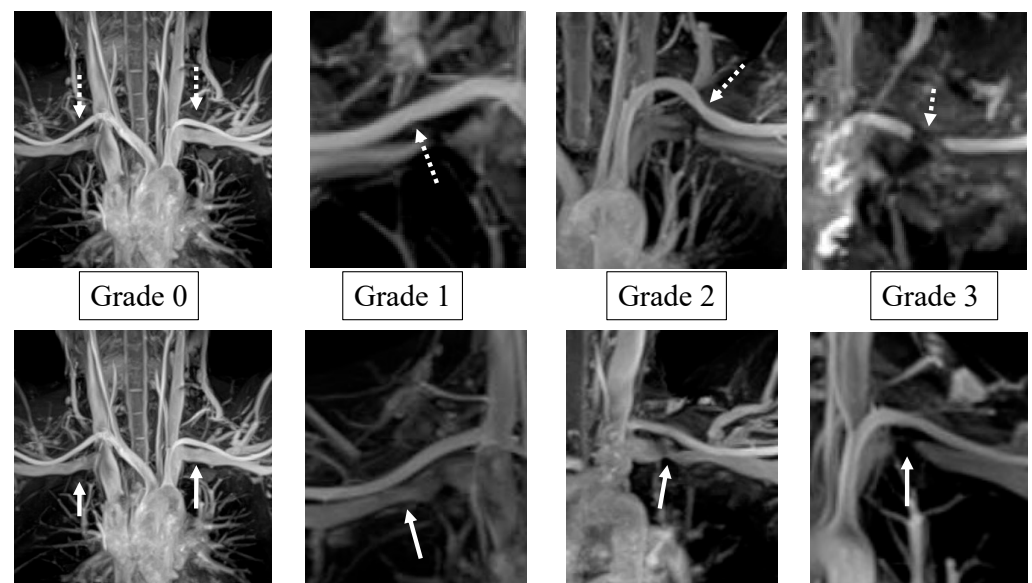


Figure 3. The degree of stenosis of SCA and SCV is classified into 4 levels. Upper row (dotted arrow), a stenosis part of SCA. Lower row (solid line arrow), a stenosis part of SCV. Grade 0; no stenosis. Grade 1; mild stenosis, less than 50%. Grade 2; moderate stenosis, more than 50%. Grade 3; severe stenosis to the point of discontinuity. SCA, subclavian artery; SCV, subclavian vein.

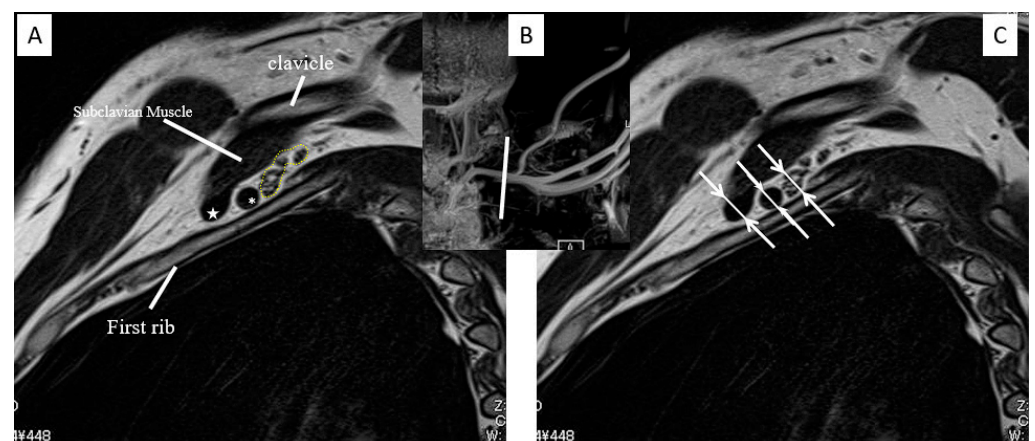


Figure 4. Left sagittal view. (A) The SCV (star), SCA (asterisk), and nerve bundle (dot line) are shown. (B) Scout view of MRI-MIP image. (C) SCA, SCV, and nerve bundle diameter measurements (arrows). MRI-MIP, magnetic resonance imaging maximum-intensity projection; SCA, subclavian artery; SCV, subclavian vein.

A total of 22 patients underwent surgery (first rib resection), and 91 successfully underwent conservative treatment. The Mann–Whitney U test was used for statistical analysis, and a p -value of less than 0.05 was considered significant. Indications for surgery were defined as patients who were clinically diagnosed with TOS, refractory to conservative treatment such as oral medication and rehabilitation, or who requested surgery. In addition, only some cases from both groups were compared in terms of the stenosis rate between the affected and normal sides. None of the patients had symptoms on the healthy side, and only those cases for which data were available were included in this study.

3. Results

A total of 22 patients (13 men and 9 women) belonged to the surgical group, with a mean age of 34.8 yr (14–56 yr), and 91 patients (47 men and 44 women) in the conservative group, with a mean age of 33.0 yr (15–67 yr). No significant differences were reported in the demographic profile between the two groups. The main indications for surgery were sports such as baseball in six cases, numbness and pain in the upper limbs that persisted for many years in twelve cases, and a strong cold sensation in addition to numbness in the hands in four cases. The background characteristics of the patients in the surgical group are shown in Table 1. The average duration of illness was 4.6 yr (2–15 yr). A total of three cases were arterial TOS, while the other cases involved neurogenic TOS. Patient satisfaction after surgery at the final follow-up was excellent in seven cases, good in thirteen cases, fair in two cases, and no case was classified as unsatisfactory.

Table 1. Background of patients in the surgery group.

	Age at Surgery	Affected Side	Cause or Occupation	Symptom	Duration of Illness (Years)	Classification of TOS	Co-Morbid Disease or Symptom	Satisfaction after Surgery
1	37	L	Baseball	Numbness after throwing	2	Disputed neurogenic		Good
2	15	R	Baseball	Numbness after throwing	2	Disputed neurogenic		Good
3	41	R	Baseball	Numbness after throwing	4	Disputed neurogenic		Good
4	17	R	Baseball	Numbness after throwing	2	Disputed neurogenic	UCL injury of same side elbow	Excellent
5	20	R	Baseball	Numbness after throwing	2	Disputed neurogenic		Good
6	19	R	Baseball	Numbness after throwing	3	Disputed neurogenic		Good
7	14	R	Tennis	Numbness and pain	2	Disputed neurogenic		Excellent
8	40	R	Researcher	Cold sensation and numbness	5	Arterial	Skin lesion of fingers, upper limb weakness	Excellent
9	43	L	Office worker	Cold sensation and numbness	3	Arterial	Numbness after jogging	Excellent
10	15	R	Malformation of first rib	Cold sensation and numbness	2	Arterial	Malformation of first rib	Excellent
11	56	L	Service industry	Cold sensation and numbness	6	Disputed neurogenic	Post operation of cervical stenosis	Good
12	32	L	Traffic accident	Numbness and pain	2	Disputed neurogenic		Fair
13	48	R	Service industry	Numbness and pain	6	Disputed neurogenic		Excellent
14	47	R	Nurse	Numbness and pain	5	Disputed neurogenic		Good
15	22	L	Office worker	Numbness and pain	3	Disputed neurogenic		Good

Table 1. Cont.

	Age at Surgery	Affected Side	Cause or Occupation	Symptom	Duration of Illness (Years)	Classification of TOS	Co-Morbid Disease or Symptom	Satisfaction after Surgery
16	51	L	Care worker	Numbness and pain	15	Disputed neurogenic	Post operation of same side cubital tunnel syndrome	Good
17	26	L	Service industry	Numbness and pain	4	Disputed neurogenic		Good
18	24	R	Service industry	Numbness and pain	4	Disputed neurogenic		Excellent
19	55	L	Construction industry	Numbness and pain	4	Disputed neurogenic		Fair
20	53	L	Forestry industry	Numbness and pain	5	Disputed neurogenic		Good
21	44	L/R	Unemployed	Numbness and pain	10	Disputed neurogenic	Post operation of cervical stenosis	Good

TOS, thoracic outlet syndrome.

Table 2 shows the breakdown of SCA and SCV stricture grades in MRI-MIP images. The SCV showed a significantly stronger stricture in the surgery group ($p < 0.01$), whereas the SCA showed more grade 0 patients without stricture in both groups, showing no difference between the two groups ($p = 0.33$).

Table 2. Breakdown of SCV and SCA stenosis grade in MRI-MIP images.

		Grade 0	Grade 1	Grade 2	Grade 3	<i>p</i> -Value
SCV	Surgery ($n = 22$)	0	3	4	15	0.0113
	Conservative ($n = 91$)	5	35	20	31	
SCA	Surgery ($n = 22$)	11	7	2	2	0.33
	Conservative ($n = 91$)	59	22	8	2	

MRI-MIP, magnetic resonance imaging maximum-intensity protection; SCA, subclavian artery; SCV, subclavian vein.

The mean stricture rates of SCA, SCV, and nerve bundle were 34.6%, 76.7%, and 34.5% in the surgical group, and 28%, 67.7%, and 34.5% in the conservative group. There was a significantly higher stricture rate in the surgery group for SCV ($p = 0.036$). In contrast, the SCA ($p = 0.21$) and nerve bundle stenosis rates ($p = 0.53$) did not differ between the two groups (Table 3).

Table 3. Stenosis rates of SCV, SCA, and nerve bundle.

	Surgery (%) $n = 22$	Conservative (%) $n = 91$	<i>p</i> -Value
SCV	76.7	67.7	0.036
SCA	34.6	28	0.21
Nerve bundle	34.5	34.5	0.53

SCA, subclavian artery; SCV, subclavian vein.

In a comparative study of the affected and normal sides, there were seven and 24 cases in the surgical and conservative groups, respectively (Table 4). A trend was reported towards greater strictures on the affected side of the SCA in the surgery group ($p = 0.064$).

However, no significant differences were found in other endpoints between the affected and normal sides.

Table 4. Stricture rate of SCV, SCA, and nerve bundle on surgery and conservative group. There was a trend toward greater stenosis on the affected side of the SCA in the surgery group.

	Surgery (<i>n</i> = 7) Conservative (<i>n</i> = 24)	Affected Side	Normal Side	<i>p</i> -Value
SCV	Surgery	66.7	74.4	0.20
	Conservative	67.1	66.9	0.47
SCA	Surgery	47.4	28.5	0.064
	Conservative	29.3	32.5	0.28
Nerve bundle	Surgery	46.0	40.3	0.24
	Conservative	74.8	71.2	0.36

SCA, subclavian artery; SCV, subclavian vein.

Representative Case

A 40-year-old man presented with weakness in the right upper limb. He has been experiencing lethargy of the right upper limb for five years, which was aggravated by running. He worked as a researcher, and his symptoms worsened three months ago, making it difficult for him to handle a pipette. He was diagnosed with right TOS by his local doctor and referred to our hospital. He had numbness in the right fingertips, epidermal avulsion of the fingertips, and nail deformity (Figure 5A). The Roos and Wright test results were positive. He was limited to 20 s in the Roos test due to numbness and sluggishness in his right arm, and his hand turned pale. Radiography showed no cervical ribs, while MRI-MIP image and 3D-CT angiography showed stenosis of the SCA (grade 1) and SCV (grade 3) in the intercostal space (Figure 6A,B,D). The patient opted to undergo surgery; hence, first rib resection using the transaxial approach [7] was performed. Postoperatively, numbness in the right upper extremity decreased, and skin lesions on the tips of the fingers improved after three months (Figure 5B). Limping of the upper extremities during running also disappeared. One year after surgery, the MRI-MIP images showed no stenosis of the SCA (grade 0), and the sagittal section showed that the anterior scalene muscle, which was in contact with the SCA before surgery, had disappeared (Figure 6C,E).

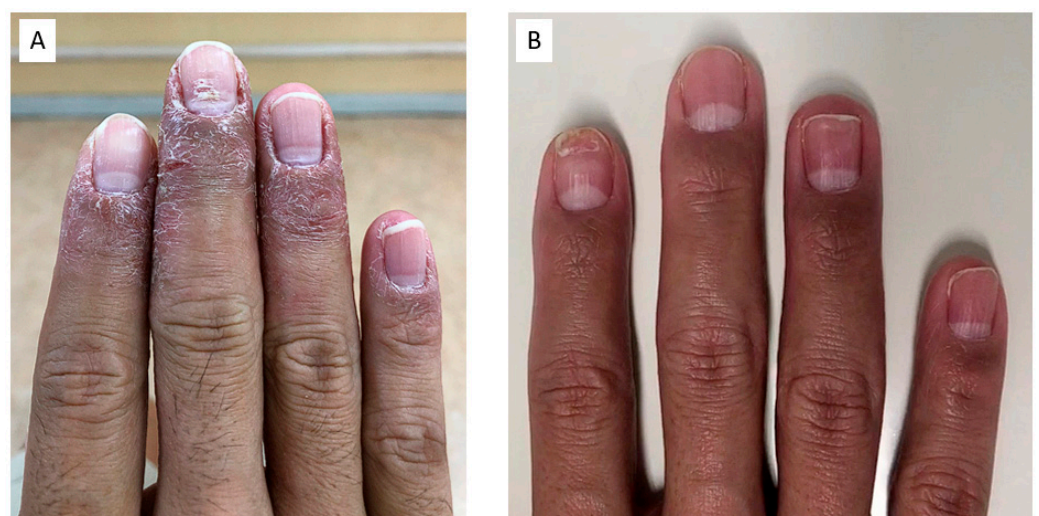


Figure 5. Skin manifestations of the right fingers: (A) preoperative finding; (B) postoperative finding.

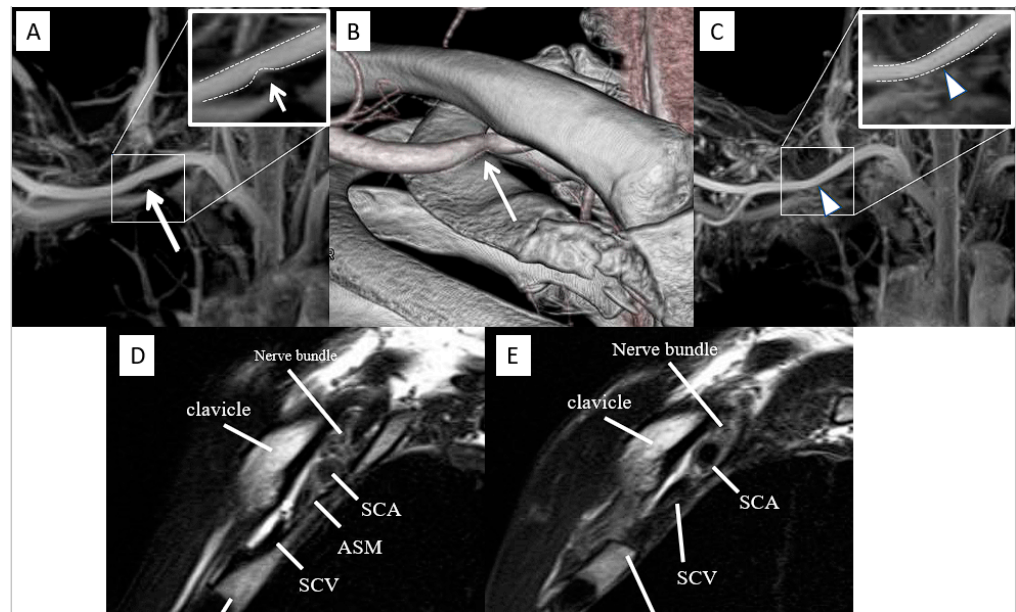


Figure 6. Preoperative and postoperative images. (A) Preoperative MRI-MIP image showing grade 1 stenosis of the SCA (arrow). (B) Preoperative 3D-CT angiography showing stenosis from below at the site where the SCA meets the clavicle (arrow). (C) Postoperative MRI-MIP image revealing stenosis of SCA disappeared and identified as grade 0 (arrowhead). (D) Preoperative sagittal view shows that the anterior scalene muscle is in contact with the SCA, and the SCV is disrupted. (E) Postoperative sagittal view shows that the first rib was resected, and the anterior scalene muscle, which was in contact with the SCA, was absent. Stenosis of the SCV remained. MRI-MIP, magnetic resonance imaging maximum-intensity projection; SCA, subclavian artery; SCV, subclavian vein.

4. Discussion

In this study, MRI-MIP imaging showed that the stricture rate of the SCV reflected the severity of TOS, whereas the stricture of the SCA and nerve bundles was independent of severity, despite the absence of venous TOS. The application of MRI-MIP imaging in the diagnosis of TOS has been reported in only one case by Esposito et al. [21]. Zhang et al. described the usefulness of contrast-enhanced magnetic resonance angiography for the diagnosis of TOS in 27 cases [22]. Hardy et al. investigated the accuracy of MRI diagnosis in 48 TOS cases and reported its usefulness [23]. This study evaluated 113 MRI-MIP images, making it the largest survey conducted to date.

With the increasing resolution of MRI, it has become possible to evaluate the pathophysiology of TOS in a minimally invasive, non-contrast-enhanced method, which was previously considered difficult. On the other hand, Furushima et al. reported that the maximum systolic blood flow velocity and the distance between the bases of the oblique muscle triangles on the first rib on ultrasonography reflected the severity of the disease [7]. Ultrasound is less invasive, but there are still problems in terms of procedural reproducibility and accuracy [24]. There are also cases of TOS with no obvious upper extremity or back pain, and they may not develop characteristic clinical symptoms [3,14].

A comprehensive diagnosis of TOS, which is a complex disease, requires a detailed medical history, assessment of clinical symptoms, and neurological examination. Hence, the presence of SCV disconnection on MRI-MIP images does not necessarily lead to the diagnosis of venous TOS, and there have been cases in which SCA stenosis was not observed on MRI-MIP images despite the presence of symptoms of SCA stenosis. The cases included in this study did not include “True TOS” [10,14], which is difficult to diagnose using MRI alone. However, disputed neurogenic TOS may be effective in excluding false positives. Apart from cases clearly attributable to sports, the absence of any vascular stenosis on MRI-MIP images in cases of suspected cervical spine origin or psychological cases is unlikely to

indicate severe TOS requiring surgery. MRI-MIP images are useful in daily practice because they can be visually explained to the patients themselves. Moreover, when combined with sagittal and axial images taken simultaneously, as in Figure 4, it is possible to pick up the bone and soft tissue abnormalities and inflammation of the brachial plexus. However, if only MIP is used, only blood vessels can be detected.

In surgery, 3D-CT angiography is more useful than MRI because of its short imaging time to determine the position of the blood vessels in relation to the clavicle and ribs. However, it is difficult to perform this procedure in all patients with suspected TOS considering the use of contrast media and exposure to radiation. In this study, SCVs in surgical cases that were considered more severely stenosed showed a higher stenosis rate. Therefore, it is recommended that 3D-CT angiography be performed only in cases in which surgery is clinically indicated to avoid the unnecessary use of contrast media and exposure to radiation.

As to the cause of stenosis, the SCA, SCV, and nerve bundles are often stenosed even in the normal position, depending on the imaging position, as shown in previous studies in comparison to the normal side. In reviewing our surgical cases, most of the stenoses were caused by fibrous bands of the anterior scalene muscle and other anatomical factors [18,19]. In comparison with the healthy side, only the SCA in the surgery group tended to show strong stenosis, suggesting that anatomical factors of the anterior scalene muscle may be considered in cases in which there is a difference between the normal and affected sides of the SCA, which is less affected by posture. Moreover, the comparison with normal cases is warranted.

This study has two major limitations, which include the imaging of limb position and diagnosis of severity. The MRI imaging position was supine, and although the patient was in the Wright test position, there is a high likelihood that the SCA was not adequately compressed owing to high intravascular pressure and strong elasticity. The SCV also had a non-physiological compression and was not considered to fully reflect stenosis in the actual examination technique. Another problem with this method is that the patient must be in a symptomatic position for at least 20 min during imaging. Regarding TOS severity, in this study, surgical cases were compared with conservative treatment cases as severe. However, because surgery was decided solely based on the patient's subjective assertion, it may not reflect severe organic stenosis, which may have caused variation in the data. Since the TOS itself lacks a clear quantitative index, further studies are needed to accumulate more cases in the future. In addition, other factors need to be considered for future study, which include cost-effectiveness, utility, indications for use, homogenization of sample size, and the ability to rule out other diagnoses.

5. Conclusions

On MRI-MIP images, the degree of stenosis of the SCV and SCA was classified into four grades, and the SCV was significantly more severely stenosed in the operated cases. Sagittal section images of the SCV, SCA, and nerve bundle showed significantly greater stenosis of the SCV in the operated cases but no significant difference in the SCA or nerve bundle between the operated and conservative treatment cases. MRI-MIP may be a useful adjunctive diagnostic method for understanding the stenosis status of vascular nerve bundles.

Author Contributions: Conceptualization, T.O. and N.M.; methodology, T.O.; software, T.O.; formal analysis, T.O.; investigation, T.O., S.O., N.M., T.M. and K.I.; resources, T.O., S.O. and N.M.; data curation, T.O.; writing—original draft preparation, T.O.; writing—review and editing, Y.Y.; visualization, T.O. and S.O.; supervision, N.M. and Y.Y.; project administration, Y.Y. and M.Y. All authors have read and agreed to the published version of the manuscript.

Funding: This research received no external funding.

Institutional Review Board Statement: This study was approved by the Institutional Review Board of the Mito Clinical Education and Training Center, University of Tsukuba Hospital, Mito Kyodo General Hospital (IRB No:22–44, approved 6 December 2022).

Informed Consent Statement: Informed consent was obtained from all the subjects involved in this study.

Data Availability Statement: Not applicable.

Acknowledgments: The authors thank Katsuhiko Kobayashi and Takuya Hirochi, a radiology technician, and other members of the radiology department at Mito Kyodo General Hospital for their cooperation in MRI imaging.

Conflicts of Interest: The authors declare no conflict of interest.

References

1. Ruopasa, N.; Ristolainen, L.; Vastamäki, M.; Vastamäki, H. Neurogenic Thoracic Outlet Syndrome with Supraclavicular Release: Long-Term Outcome without Rib Resection. *Diagnostics* **2021**, *11*, 450. [\[CrossRef\]](#) [\[PubMed\]](#)
2. Povlsen, S.; Povlsen, B. Diagnosing Thoracic Outlet Syndrome: Current Approaches and Future Directions. *Diagnostics* **2018**, *8*, 21. [\[CrossRef\]](#) [\[PubMed\]](#)
3. Kuhn, J.E.; Lebus, G.F.; Bible, J.E. Thoracic Outlet Syndrome. *J. Am. Acad. Orthop. Surg.* **2015**, *23*, 222–232. [\[CrossRef\]](#) [\[PubMed\]](#)
4. Peek, J.; Vos, C.G.; Ünlü, Ç.; van de Pavoordt, H.D.W.M.; van den Akker, P.J.; de Vries, J.-P.P. Outcome of Surgical Treatment for Thoracic Outlet Syndrome: Systematic Review and Meta-Analysis. *Ann. Vasc. Surg.* **2017**, *40*, 303–326. [\[CrossRef\]](#)
5. Beteck, B.; Shutze, W.; Richardson, B.; Shutze, R.; Tran, K.; Dao, A.; Ogola, G.O.; Pearl, G. Comparison of Athletes and Nonathletes Undergoing Thoracic Outlet Decompression for Neurogenic Thoracic Outlet Syndrome. *Ann. Vasc. Surg.* **2018**, *54*, 269–275. [\[CrossRef\]](#)
6. Burks, S.S.; Wolfe, E.M.; Yoon, J.W.; Levi, A.D. Supraclavicular Resection of a Cervical Rib Causing Thoracic Outlet Syndrome: 2-Dimensional Operative Video. *Oper. Neurosurg.* **2020**, *19*, E520. [\[CrossRef\]](#)
7. Furushima, K.; Funakoshi, T.; Kusano, H.; Miyamoto, A.; Takahashi, T.; Horiuchi, Y.; Itoh, Y. Endoscopic-Assisted Transaxillary Approach for First Rib Resection in Thoracic Outlet Syndrome. *Arthrosc. Sport. Med. Rehabil.* **2021**, *3*, e155–e162. [\[CrossRef\]](#)
8. Ransom, E.F.; Minton, H.L.; Young, B.L.; He, J.K.; Ponce, B.A.; McGwin, G.; Meyer, R.D.; Brabston, I.E.W. Intermediate and Long-Term Outcomes Following Surgical Decompression of Neurogenic Thoracic Outlet Syndrome in an Adolescent Patient Population. *Hand* **2020**, *17*, 43–49. [\[CrossRef\]](#)
9. Perchoc, A.; Andro, C.; Letissier, H.; Schiele, P.; Le Nen, D. Long-term functional outcomes after surgical treatment of nonspecific thoracic outlet syndrome: Retrospective study of 70 cases at a mean of 8 years' follow-up. *Hand Surg. Rehabil.* **2019**, *38*, 195–201. [\[CrossRef\]](#) [\[PubMed\]](#)
10. Wilbourn, A.J. Thoracic outlet syndrome is over diagnosed. *Muscle Nerve* **1999**, *22*, 130–136. [\[CrossRef\]](#)
11. Ferrante, M.A.; Ferrante, N.D. The thoracic outlet syndromes: Part 2. The arterial, venous, neurovascular, and disputed thoracic outlet syndromes. *Muscle Nerve* **2017**, *56*, 663–673. [\[CrossRef\]](#) [\[PubMed\]](#)
12. Masocatto, N.O.; Da-Matta, T.; Prozzo, T.G.; Couto, W.J.; Porfirio, G. Thoracic outlet syndrome: A narrative review. *Rev. Col. Bras. Cir.* **2019**, *46*, e20192243. [\[CrossRef\]](#)
13. Seror, P. Medial antebrachial cutaneous nerve conduction study, a new tool to demonstrate mild lower brachial plexus lesions. A report of 16 cases. *Clin. Neurophysiol.* **2004**, *115*, 2316–2322. [\[CrossRef\]](#) [\[PubMed\]](#)
14. Sonoo, M. Thoracic outlet syndrome. *Brain Nerve* **2014**, *66*, 1429–1439. (In Japanese) [\[CrossRef\]](#)
15. Remy-Jardin, M.; Remy, J.; Masson, P.; Bonnel, F.; Debatselier, P.; Vinckier, L.; Duhamel, A. Helical CT Angiography of Thoracic Outlet Syndrome. *Am. J. Roentgenol.* **2000**, *174*, 1667–1674. [\[CrossRef\]](#) [\[PubMed\]](#)
16. Demondion, X.; Herbinet, P.; Van Sint Jan, S.; Boutry, N.; Chantelot, C.; Cotten, A. Imaging Assessment of Thoracic Outlet Syndrome. *Radiographics* **2006**, *26*, 1735–1750. [\[CrossRef\]](#)
17. Likes, K.; Rochlin, D.H.; Call, D.; Freischlag, J.A. Coexistence of Arterial Compression in Patients With Neurogenic Thoracic Outlet Syndrome. *JAMA Surg.* **2014**, *149*, 1240–1243. [\[CrossRef\]](#)
18. Sanders, R.J.; Annest, S.J. Thoracic outlet and pectoralis minor syndromes. *Semin. Vasc. Surg.* **2014**, *27*, 86–117. [\[CrossRef\]](#)
19. Raptis, C.A.; Sridhar, S.; Thompson, R.W.; Fowler, K.; Bhalla, S. Imaging of the Patient with Thoracic Outlet Syndrome. *Radiographics* **2016**, *36*, 984–1000. [\[CrossRef\]](#)
20. Ersoy, H.; Steigner, M.L.; Coyner, K.B.; Gerhard-Herman, M.D.; Rybicki, F.J.; Bueno, R.; Nguyen, L.L. Vascular Thoracic Outlet Syndrome: Protocol Design and Diagnostic Value of Contrast-Enhanced 3D MR Angiography and Equilibrium Phase Imaging on 1.5- and 3-T MRI Scanners. *Am. J. Roentgenol.* **2012**, *198*, 1180–1187. [\[CrossRef\]](#)
21. Esposito, M.D.; Arrington, J.A.; Blackshear, M.N.; Murtagh, F.R.; Silbiger, M.L. Thoracic outlet syndrome in a throwing athlete diagnosed with MRI and MRA. *J. Magn. Reson. Imaging* **1997**, *7*, 598–599. [\[CrossRef\]](#) [\[PubMed\]](#)
22. Zhang, T.; Xu, Z.; Chen, J.; Liu, Z.; Wang, T.; Hu, Y.; Shen, L.; Xue, F. A Novel Approach for Imaging of Thoracic Outlet Syndrome Using Contrast-Enhanced Magnetic Resonance Angiography (CE-MRA), Short Inversion Time Inversion Recovery Sampling Perfection with Application-Optimized Contrasts Using Different Flip Angle Evolutions (T2-STIR-SPACE), and Volumetric Interpolated Breath-Hold Examination (VIBE). *Med. Sci. Monit.* **2019**, *25*, 7617–7623. [\[CrossRef\]](#) [\[PubMed\]](#)

23. Hardy, A.; Pougès, C.; Wavreille, G.; Behal, H.; Demondion, X.; Lefebvre, G. Thoracic Outlet Syndrome: Diagnostic Accuracy of MRI. *Orthop. Traumatol. Surg. Res.* **2019**, *105*, 1563–1569. [[CrossRef](#)] [[PubMed](#)]
24. Brownie, E.R.; Abuirqeba, A.A.; Ohman, J.W.; Rubin, B.G.; Thompson, R.W. False-negative upper extremity ultrasound in the initial evaluation of patients with suspected subclavian vein thrombosis due to thoracic outlet syndrome (Paget-Schroetter syndrome). *J. Vasc. Surg. Venous Lymphat. Disord.* **2020**, *8*, 118–126. [[CrossRef](#)] [[PubMed](#)]

Disclaimer/Publisher’s Note: The statements, opinions and data contained in all publications are solely those of the individual author(s) and contributor(s) and not of MDPI and/or the editor(s). MDPI and/or the editor(s) disclaim responsibility for any injury to people or property resulting from any ideas, methods, instructions or products referred to in the content.



Importance of TKI treatment duration in treatment-free remission of chronic myeloid leukemia: results of the D-FREE study

Chikashi Yoshida¹ · Hiroki Yamaguchi² · Noriko Doki³ · Kazunori Murai⁴ · Masaki Iino⁵ · Yoshihiro Hatta⁶ · Makoto Onizuka⁷ · Norio Yokose⁸ · Katsumichi Fujimaki⁹ · Masao Hagihara¹⁰ · Gaku Oshikawa¹¹ · Kayoko Murayama¹² · Takashi Kumagai¹³ · Shinya Kimura¹⁴ · Yuho Najima³ · Noriyoshi Iriyama⁶ · Ikuyo Tsutsumi¹ · Koji Oba¹⁵ · Hiroshi Kojima¹⁶ · Hisashi Sakamaki³ · Koiti Inokuchi² on behalf of the Kanto CML Study Group

Received: 10 October 2022 / Revised: 21 January 2023 / Accepted: 22 January 2023
© The Author(s) 2023

Abstract

Treatment-free remission (TFR) is a new goal for patients with chronic myeloid leukemia in chronic phase (CML-CP) with a sustained deep molecular response (DMR) to treatment with tyrosine kinase inhibitors (TKIs). However, optimal conditions for successful TFR in patients treated with second-generation (2G)-TKIs are not fully defined. In this D-FREE study, treatment discontinuation was attempted in newly diagnosed CML-CP patients treated with the 2G-TKI dasatinib who achieved BCR-ABL1 levels of $\leq 0.0032\%$ (MR4.5) on the international scale (*BCR-ABL1*^{IS}) and maintained these levels for exactly 1 year. Of the 173 patients who received dasatinib induction therapy for up to 2 years, 123 completed and 60 (48.8%) reached MR 4.5. Among the first 21 patients who maintained MR4.5 for 1 year and discontinued dasatinib, 17 experienced molecular relapse defined as loss of major molecular response (*BCR-ABL1*^{IS} > 0.1%) confirmed once, or loss of MR4 (*BCR-ABL1*^{IS} > 0.01%) confirmed on 2 consecutive assessments. The estimated molecular relapse-free survival rate was 16.7% at 12 months. This study was prematurely terminated according to the protocol's safety monitoring criteria. The conclusion was that sustained DMR for just 1 year is insufficient for TFR in CML-CP patients receiving dasatinib for less than a total of 3 years of treatment.

Keywords Chronic myeloid leukemia · Dasatinib · Treatment-free remission

✉ Chikashi Yoshida
c.yoshida@mitomedical.org

¹ Department of Hematology, National Hospital Organization Mito Medical Center, 280 Sakuranosato, Ibarakimachi, Higashiibarakigun, Ibaraki 311-3193, Japan

² Department of Hematology, Nippon Medical School, Tokyo, Japan

³ Hematology Division, Tokyo Metropolitan Cancer and Infectious Diseases Center, Komagome Hospital, Tokyo, Japan

⁴ Department of Hematology, Iwate Prefectural Central Hospital, Morioka, Japan

⁵ Department of Medical Oncology, Yamanashi Prefectural Central Hospital, Kofu, Japan

⁶ Division of Hematology and Rheumatology, Nihon University School of Medicine, Tokyo, Japan

⁷ Department of Hematology and Oncology, Tokai University School of Medicine, Isehara, Japan

⁸ Department of Hematology, Nippon Medical School Chiba Hokusoh Hospital, Inzai, Japan

⁹ Department of Hematology, Fujisawa City Hospital, Fujisawa, Japan

¹⁰ Department of Hematology, EIJU General Hospital, Taito-Ku, Japan

¹¹ Japanese Red Cross Musashino Hospital, Musashino, Japan

¹² Division of Hematology, Gunma Prefectural Cancer Center, Ohta, Japan

¹³ Department of Hematology, Ome Municipal General Hospital, Ome-Shi, Tokyo, Japan

¹⁴ Division of Hematology, Respiratory Medicine and Oncology, Department of Internal Medicine, Faculty of Medicine, Saga University, Saga, Japan

¹⁵ Department of Biostatistics, The University of Tokyo, Tokyo, Japan

¹⁶ Ibaraki Clinical Education and Training Center, University of Tsukuba Hospital, Kasama, Japan

Introduction

Prognosis of chronic myeloid leukemia in chronic phase (CML-CP) has improved dramatically since the approval of imatinib mesylate, the first-generation tyrosine kinase inhibitor (TKI), in 2001 [1]. In addition, second-generation TKIs (2G-TKIs) were developed for patients who are resistant and/or intolerant to imatinib and later approved for newly diagnosed patients [2–4]. With the development of these TKIs, the life expectancy of patients with CML-CP has become almost the same as that of age-matched healthy individuals [5]. However, long-term treatment with TKIs has raised new concerns, such as adverse events including cardiovascular side effects, avoidance of pregnancy by women due to possible teratogenicity, and increased health care costs [6–8]. Thus, discontinuation of TKI therapy has been attempted in patients with a sustained deep molecular response (DMR), and it has been reported that about half of them can maintain a treatment-free remission (TFR), which has become a new goal [9]. However, it is still difficult to predict in advance the chance of relapse for each patient. Although several guidelines have proposed clinical factors for successful TFR, they are primarily based on evidence with imatinib [10–12]. Since 2G-TKIs induce a molecular response faster than imatinib [2–4], it is possible that they lead to TFR in a larger number of patients and after a shorter treatment period, potentially minimizing the problems caused by TKI therapy. The multicenter phase II study D-FREE was conducted to clarify optimal conditions for TFR in newly diagnosed patients with CML-CP treated with the 2G-TKI dasatinib. We attempted discontinuation of dasatinib treatment for patients who achieved DMR and sustained it for exactly 1 year.

Materials and methods

Patients

Eligible patients were adults (≥ 18 years) with confirmed newly diagnosed CML-CP who had received no prior anti-leukemia treatment (except ≤ 1 months of hydroxyurea), Eastern Cooperative Oncology Group (ECOG) performance status groups of 0 to 2, and with adequate functions of major organs (liver, kidney, and lung). Patients whose *BCR-ABL1* mRNA levels could not be assessed by real-time quantitative polymerase chain reaction (RQ-PCR) based on an international scale (*BCR-ABL1*^{IS}) were excluded. Patients were excluded if they had active multiple cancers, were pregnant, lactating, with a history or

complications of myocardial infarction within the previous 6 months, with a history of angina pectoris, or gastrointestinal hemorrhage, or congestive cardiac failure within the previous 3 months, plural effusion, electrocardiogram QTc interval exceeding 450 ms prolongation, or present/past history of pulmonary hypertension. Similarly, patients with a history or complications of diseases judged by the investigators as inappropriate for study implementation were not eligible. This study was conducted in accordance with the Ethical Guidelines for Medical and Health Research Involving Human Subjects, the Clinical Trials Act in Japan, and the Declaration of Helsinki. All patients provided written informed consent. The study protocol was reviewed by the institutional review board for each center at the start of study, then reviewed again by the Certified Review Board, Institutional Review Board of Nippon Medical School Foundation, after the enforcement of the Clinical Trials Act established in 2018. The trial was registered at the University Hospital Medical Information Network (UMIN000022254) and Japan Registry of Clinical Trials (jRCTs031180332).

Study design and treatment

D-FREE was an open-label, multicenter, phase II study. Its design is shown in Fig. 1. In the induction phase, newly diagnosed CML-CP patients were treated with dasatinib at 100 mg once daily. The maximum daily dose was 140 mg, and the dose could be adjusted or temporarily stopped at the discretion of investigators as needed. Molecular response was assessed by measuring *BCR-ABL1* mRNA levels in peripheral blood every 3 months by RQ-PCR standardized on an international scale in one of three commercial laboratories (BML, Inc., SRL, and LSI Medience Corporation) using an RT-qPCR kit, ODK-1201 (Otsuka Pharmaceutical Co. Ltd) validated by SA Pathology, Adelaide, Australia, a recognized reference laboratory [13]. When patients achieved MR4.5 (*BCR-ABL1*^{IS} $\leq 0.0032\%$) during the induction phase for up to two years, they were immediately entered into the consolidation phase, where dasatinib was administered for 12 months. Sustained MR4.5 in this phase was defined as confirmation of this level of molecular response on 5 consecutive RQ-PCR tests three months apart. Patients who did not achieve MR4.5 during the induction phase or did not sustain it during the consolidation phase were removed from the study and its follow-up. Patients who sustained MR4.5 throughout the consolidation phase were eligible to enter the stop phase and discontinue dasatinib treatment. During the stop phase, molecular response was assessed every month in the first year and every three months thereafter. Molecular relapse was defined as loss of major molecular response (MMR) (*BCR-ABL1*^{IS} $> 0.1\%$) confirmed once, or loss of MR4 (*BCR-ABL1*^{IS} $> 0.01\%$)

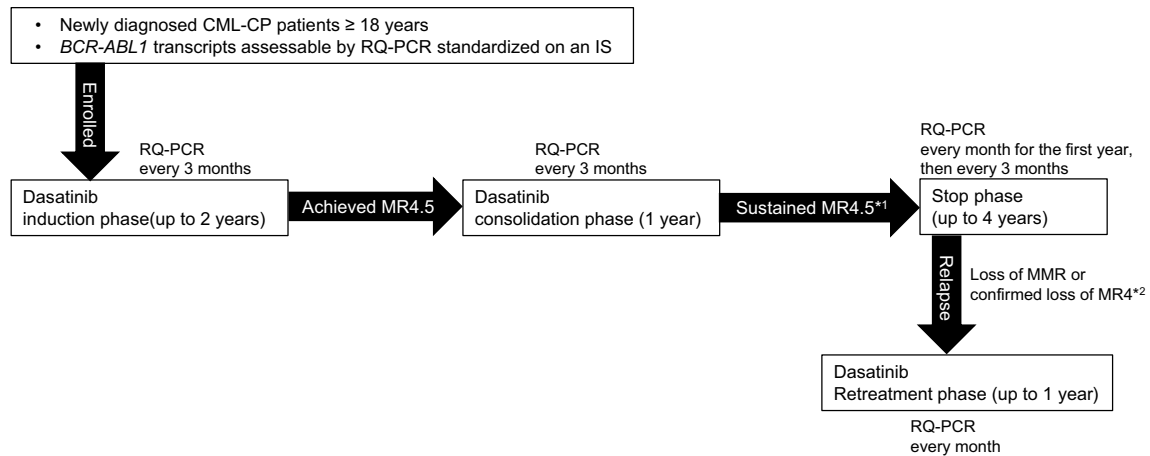


Fig. 1 D-FREE study design. *CML-CP* chronic myeloid leukemia in chronic phase, *RQ-PCR* real-time quantitative polymerase chain reaction, *IS* international scale, *MR4.5* *BCR-ABL1* mRNA levels assessed by RQ-PCR based on an IS ($BCR-ABL1^{IS} \leq 0.0032\%$), *MMR* major

molecular response. *¹ Defined as maintaining MR 4.5 with 5 RQ-PCR assessments every 3 months. *² Defined as $BCR-ABL1^{IS} > 0.01\%$ on two consecutive assessments

confirmed on 2 consecutive assessments. Currently, most recent trials consider molecular relapse as loss of MMR [9, 14], but since this D-FREE was a study in which dasatinib was discontinued after a shorter DMR period, the loss of MR4 confirmed on 2 consecutive assessments was also considered as molecular relapse for safety reasons. In the case of molecular relapse during the stop phase, patients were immediately retreated with dasatinib at the consolidation phase final dose. Molecular response was assessed every month by RQ-PCR until patients regained MR4 ($BCR-ABL1^{IS} \leq 0.01\%$), and every three months thereafter, for up to one year. Adverse events were graded according to the National Cancer Institute Common Terminology Criteria for Adverse Events (CTCAE) version 4.0. In this study, hematologic adverse events with grade 4 and non-hematological adverse events with grade 3 or higher were reported.

Study endpoints and assessments

The primary endpoint was the proportion of patients in TFR who showed no molecular relapse and did not need to resume dasatinib 12 months after treatment discontinuation. Secondary endpoints included the proportion of patients in TFR 24, 36, and 48 months after discontinuation of dasatinib treatment, molecular relapse-free survival (MRFS) 12 months after discontinuation of dasatinib treatment, overall survival (OS) including all causes of death 12, 24, 36, and 48 months after discontinuation of dasatinib treatment, dasatinib doses and time to MR4.5, event-free survival (EFS) during the dasatinib treatment period, and frequency and degree of TKI withdrawal syndrome after discontinuation of dasatinib treatment. Exploratory endpoints included analysis of factors related to achievement of MR4.5 and

sustained TFR for risk scores (EUTOS Score, Sokal Score, Hasford Score), gender, molecular response 3 and 6 months after start of dasatinib treatment, dasatinib treatment period, and time to MMR, MR4.0, and MR4.5. MRFS was defined as duration of survival from the date of dasatinib discontinuation in the stop phase to molecular relapse or death. EFS was defined as the duration from the date of registration to disease progress or death. If patients died without disease progress, they were regarded as having progress at the date of death. If patients received dasatinib and did not have disease progression or death, the study was discontinued at the date when hematologic, cytogenetic, or molecular evaluation was finally done during dasatinib treatment. If patients did not receive dasatinib and did not have disease progression or death, the study was discontinued at the date of registration. Disease progression was defined as loss of complete hematologic response, loss of major cytogenetic response or complete cytogenetic response, loss of molecular response, progression to accelerated or blastic phase, or death during dasatinib treatment.

Statistical analyses

The threshold value of TFR rate and expected value at 12 months after discontinuation of dasatinib treatment were hypothesized to be 41% and 55%, respectively, based on historical data [15, 16]. Based on the above hypothesis, the required number of patients eligible for treatment discontinuation (Stop phase) was calculated to be 83 with a power of 80% and a one-sided alpha of 5%. Considering about 20% dropouts due to MR4.5 loss during the 12-month consolidation phase and consent withdrawal, etc., and the historical data of a 35% MR4.5 achievement rate after 24 months [17],

the planned number of registered patients with first-onset CML-CP was calculated as 300, including 5% ineligible patients.

Two safety monitoring criteria were included in D-FREE to assess the appropriateness of continuing the study. Thus, the trial should be suspended if (1) more than 15% of the patients who lost MMR in the Stop phase did not reach MMR by 12 months of dasatinib retreatment and (2) the TFR rate was less than or equal to 25% when 20 patients reached the primary endpoint. On the 6th November 2019, 15 patients out of 20 patients after discontinuation of dasatinib treatment relapsed during the stop phase. Data and safety monitoring board recommended stopping the study on the basis of the efficacy concerns. When the study was stopped on the 3rd December 2019, 17 out of 21 patients in the stop phase relapsed. Thereafter, all participant patients were recommended to receive standard treatment based on consultation with their physicians. Baseline characteristics, efficacy, and safety results are reported for patients who entered the induction phase. MRFS was depicted using the Kaplan–Meier method. Other time-to-event data were also analyzed by the Kaplan–Meier method. An assessment of prognostic factors for achieving MR4.5 within 24 months of dasatinib treatment in the induction phase was conducted using univariate and multivariable logistic regression analyses. The frequencies of AEs, laboratory abnormalities, and predefined groupings of AE types of special interest were summarized for the induction and consolidation phases. The data presented herein are based on a cutoff date of September 30th, 2021, at which time all patients had finished the safety follow-up after the termination of study treatment. The significance level of the two-sided *p* values was 0.05 for all statistical tests. Analyses were done with SAS Release 9.4 (SAS Institute, Cary, NC).

Results

Characteristics of patients

Between July 2016 and May 2019, a total of 181 patients with newly diagnosed CML-CP were enrolled in 41 centers in Japan. Patients' disposition is shown in Fig. 2. Four patients were excluded after screening, and no further information was available for 4 patients. Overall, 173 patients received treatment according to the study protocol. Demographics and baseline disease characteristics are listed in Table 1. The median patient age was 54 years (18–83 years). The rates of Sokal low-, intermediate-, high-risk groups, and unknown were 45.7, 38.2, 15.6, and 0.6%, respectively. The rates of Hasford low-, intermediate-, high-risk groups, and unknown were 39.9, 50.9, 8.7, and 0.6%, respectively. The

rates of EUTOS low- and high-risk groups were 89.6 and 10.4%, respectively.

Treatment responses

Of the 123 patients who completed the induction phase, 60 (48.8%) achieved MR4.5 for up to 2 years. The median duration of dasatinib for achieving MR4.5 was 7.7 months (range 3.0–21.1 months). We evaluated the relationship between cumulative dose and MR4.5 attainment rate and calculated the cumulative dose corresponding to MR4.5 attainment rate of 50% (for one subject there was no dose information). The total dasatinib dose corresponding to 50% MR4.5 by the Kaplan–Meier method was 63,600 mg (95% confidence interval 43,500 to N.A.), but the 95% confidence interval was wide due to the small number of patients who reached MR4.5, and the upper limit of the 95% confidence interval could not be estimated (data not shown). Single and multivariate analyses showed that the achievement of MMR at 3 months, but not gender, Sokal risk score, Hasford risk score, EUTOS risk score, or age (< 60 vs. ≥ 60), was predictive of the achievement of MR4.5 within 2 years (Table 2).

Patients who achieved MR 4.5 in the induction phase immediately entered the consolidation phase and received dasatinib treatment for one year. Fifteen patients could not sustain MR4.5 and finished study treatment during the consolidation phase. EFS for patients treated with dasatinib during the induction and consolidation phases was estimated to be 94.9% for 1 year and 63.5% for 2 years. A large number of patients were censored due to early discontinuation of the study, as described above.

Discontinuation of dasatinib in the stop phase

Among the first 20 patients who could sustain MR4.5 for 12 months in the consolidation phase and discontinued dasatinib treatment in the stop phase, 15 experienced molecular relapse within 12 months and required retreatment with dasatinib as of November 6, 2019. The study was terminated prematurely on December 3, 2019, in accordance with the data and safety monitoring board's recommendation, based on the pre-specified interim analysis criterion that it would be stopped if the TFR rate was less than or equal to 25% in the first 20 patients of the stop phase. At that point in time, 17 out of 21 patients in the stop phase had molecular relapse within 12 months and were being retreated with dasatinib (Table 3). Molecular relapse was determined by the loss of MMR in 11 patients and two consecutive losses of MR4 in 6 patients. The estimated MRFS was 16.7% at 12 months (Fig. 3). As a result, the proportion of patients in TFR who showed no molecular relapse and did not need to resume dasatinib 12 months after treatment discontinuation was not estimated, because only one subject was confirmed to have

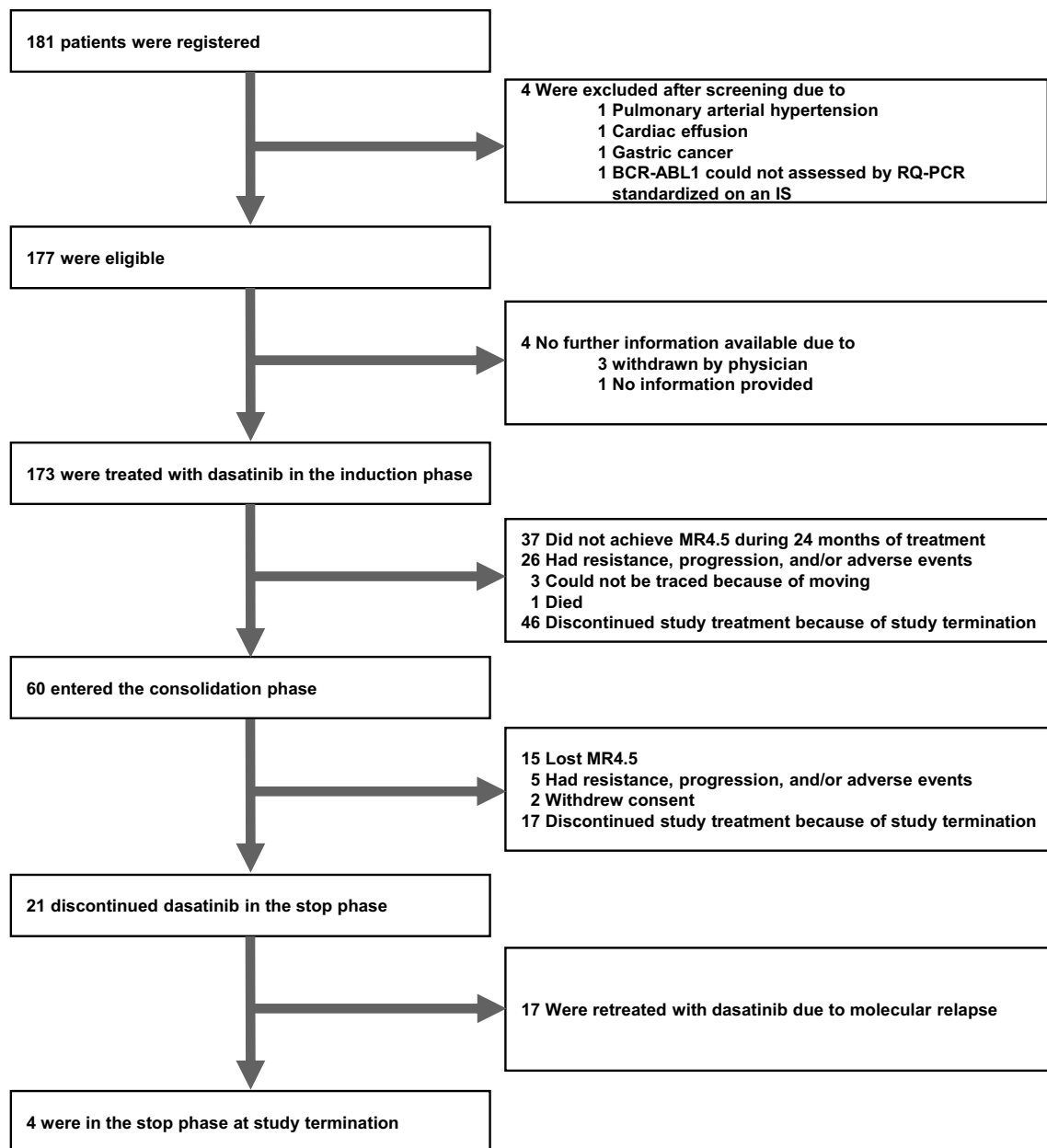


Fig. 2 Patient disposition. *RQ-PCR* real-time quantitative polymerase chain reaction, *IS* international scale, *MR4.5* *BCR-ABL1* mRNA levels assessed by RQ-PCR based on an $IS \leq 0.0032\%$)

TFR at 12 months after discontinuation of dasatinib. The median time of molecular relapse after the cessation was 3.5 months (range 2.0–6.4). In those patients, the median duration of dasatinib treatment, including the induction and the consolidation phases, was 18.9 months (range 14.9–25.5) before the cessation of dasatinib. At termination, 46 patients were in the induction, 17 were in the consolidation, and 4 were in the stop phase. Of note, one patient (no. 7) remained in TFR for 17.8 months after receiving dasatinib treatment for only 18.6 months during the induction and consolidation phases (Table 3). All 17 patients who entered the dasatinib

retreatment phase due to molecular relapse regained MR4 (Table 3 and Fig. 4). The median duration of dasatinib retreatment until MR4 re-achievement was 2.3 months (range 1.0–5.1).

Safety

No patients progressed to the accelerated/blastic phase or died due to CML during the study treatment. Grade 4 hematologic and grade 3/4 non-hematologic AEs were reported in this study. Among patients who were treated with dasatinib

Table 1 Baseline characteristics at study entry

Characteristic	Total population (<i>n</i> = 173)
Age, median (range) (years)	54 (18–83)
Males, <i>n</i> (%)	100 (57.8)
Sokal risk score, <i>n</i> (%)	
Low	79 (45.7)
Intermediate	66 (38.2)
High	27 (15.6)
NR	1 (0.6)
Hasford risk score, <i>n</i> (%)	
Low	69 (39.9)
Intermediate	88 (50.9)
High	15 (8.7)
NR	1 (0.6)
EUTOS risk score, <i>n</i> (%)	
Low	155 (89.6)
High	18 (10.4)
Prior hydroxyurea treatment, <i>n</i> (%)	
No	124 (71.7)
Yes	49 (28.3)

NR not reported

in the induction phase, grade 4 neutropenia, anemia, and thrombocytopenia were reported in 2.3% (*n* = 4), 0.6% (*n* = 1), and 1.2% (*n* = 2), respectively. There were no grade 4

hematologic AEs reported in consolidation, stop, and dasatinib retreatment phases. Grade 3/4 non-hematologic AEs were reported as a total of 8.1% (*n* = 14) in the combined induction, consolidation, and retreatment phases. Among them, death in one patient (unknown cause; family refused to report) and hospitalization due to gallstones, both occurring in the induction phase, were reported as grade 4 AEs. Cardiovascular events were reported in 2 patients (1.2%), one with grade 3 ischemic syndrome during the consolidation phase and the other with grade 3 ischemic cerebrovascular disease during the dasatinib retreatment phase. Among the 21 patients who entered the stop phase, TKI withdrawal syndrome was observed in 2 (no. 1 and no. 20, Table 3). Two patients (9.5%) had arthralgia grade 1 and one (4.8%) had myalgia grade 1, both of whom recovered. The two patients who developed TKI withdrawal syndrome both had molecular relapse at 2.6 and 6.3 months.

Discussion

Discontinuation of treatment in newly diagnosed CML-CP patients after up to 2 years of induction therapy with dasatinib followed by 1 year of MR4.5 did not show TFR rates comparable to previous TKI discontinuation studies, which have reported rates of approximately 50% [18–21]. This indicates that dasatinib treatment for 3 years or less,

Table 2 Prognostic factors for achieving MR4.5 within 24 months of dasatinib treatment in the induction phase

	Univariate			Adjusted		
	Odds ratio	95% CI	<i>p</i>	Odds ratio	95% CI	<i>p</i>
Gender						
Male	0.853	0.458–1.589	0.853	0.768	0.370–1.596	0.4797
Female	1			1		
Sokal risk score						
High	1.133	0.456–2.812	0.7879	1.466	0.451–4.767	0.5253
Intermediate	1.419	0.723–2.785	0.3088	1.002	0.404–2.484	0.9966
Low	1			1		
Hasford risk score						
High	1.25	0.398–3.931	0.7026			
Intermediate	1.238	0.644–2.381	0.5219			
Low	1					
EUTOS score						
High	0.814	0.290–2.284	0.6952	0.604	0.153–2.384	0.4715
Low	1					
Age, years						
60 ≥	1.55	0.830–2.893	0.1687	1.531	0.668–3.512	0.3144
60 <	1			1		
MMR at 3 months						
Yes	9.412	4.058–21.831	<0.0001	11.192	4.583–27.334	<0.0001
No	1			1		

Table 3 Details of patients in the stop phase

Pt no.	Age, y	Gender	Sokal risk score	Hasford risk score	EUTOS score	Duration of induction phase, mo	Duration of DAS treatment, mo	Duration of stop phase, mo	Relapse after DAS discontinuation	Achievement of MR4 after DAS retreatment, mo
1	77	F	H	H	L	3.1	15.7	6.3	Yes	1.9
2	72	F	H	H	H	3.4	14.9	3.2	Yes	3.7
3	68	M	H	I	H	13.3	25.5	2.5	Yes	2.8 ^{‡4}
4	62	M	I	I	L	6.0	18.9	2.4	Yes	3.1
5	64	F	I	I	L	8.9	22.0	3.4	Yes	1.0
6	38	M	L	L	L	6.4	18.9	4.8	Yes	5.1
7	53	F	H	I	L	5.8	18.6	17.8	No	—
8	72	F	I	I	L	6.5	19.4	2.5	Yes	2.1
9	77	F	I	I	L	6.3	18.3	5.0	Yes	1.0
10	49	F	I	L	L	12.2	24.8	3.9	Yes	3.0
11	57	M	L	I	H	8.7	21.7	3.8	Yes	2.1
12	29	F	I	L	L	6.0	18.6	4.4	Yes	3.0
13	63	F	I	I	L	3.5	16.2	2.3	Yes	1.8
14	68	F	I	I	L	6.3	19.2	9.2	No	—
15	64	F	I	I	L	8.8	21.6	4.8	Yes	2.3
16	38	F	L	L	L	5.7	18.8	5.3	Yes	1.1
17	69	F	I	I	L	6.0	18.9	7.1	No	—
18	54	M	L	I	L	6.0	18.7	4.6	Yes	1.9
19	27	M	L	L	L	5.8	17.8	4.1	Yes	4.6
20	70	M	I	L	L	6.2	18.6	4.4	No	—
21	46	M	L	L	H	6.9	18.9	2.6	Yes	3.1

Pt patient, no. number, y. years, F female, M male, L low risk, I intermediate risk, H high risk, mo. Months, DAS dasatinib, —, not applicable

^{‡4}Reached MR4 after 2.8 months of DAS retreatment phase and simultaneously discontinued study treatment due to adverse events

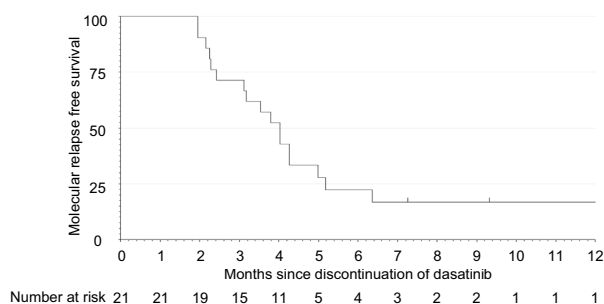


Fig. 3 Kaplan–Meier estimate of molecular relapse-free survival after discontinuation of dasatinib in the first 21 patients who entered the stop phase

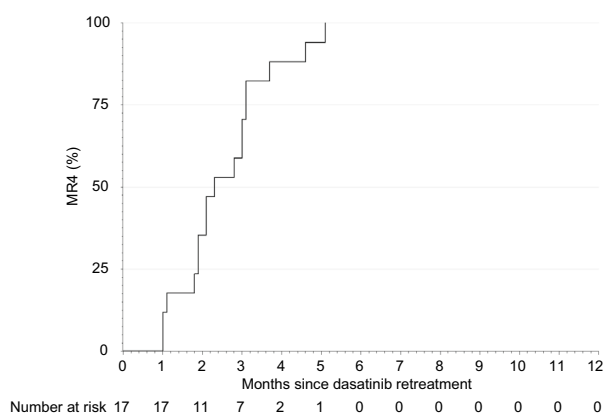


Fig. 4 Cumulative incidence of MR4 in patients who entered the dasatinib retreatment phase due to molecular relapse. MR4 *BCR-ABL1* mRNA levels assessed by RQ-PCR based on an international scale $\leq 0.01\%$

including just 1 year of MR4.5 maintenance, is not sufficient for successful TFR in untreated patients with CML-CP.

2G-TKIs, including dasatinib and nilotinib, are stronger inhibitors of ABL kinase activity than imatinib and have been the subject of several clinical trials because of their potential to improve TFR rates. Comparisons of TKI discontinuation trials in patients who received 2G-TKI as first-line treatment, including D-FREE study, are summarized in Table 4. The ENESTfreedom study enrolled patients who were treated with nilotinib ≥ 2 years and reached MR4.5 [20]. Those patients were treated with nilotinib for an additional 52 weeks and stopped the treatment. A total of 51.6% of patients remained in MMR without treatment reinitiation after 48 weeks of nilotinib cessation. The median duration of nilotinib therapy was 43.5 (32.9–88.9) months in that study. Kimura et al. reported the results of the first-line DADI trial where treatment was stopped for patients who had received first-line dasatinib for at least 36 months with a sustained DMR (defined as $\leq 0.0069\%$) for at least one year [21].

The TFR at 6 months was 55.2%. The duration of dasatinib treatment and of DMR was 40.4 months (38.1–51.1) and 23.3 months (15.7–29.4), respectively. Although these trials could not demonstrate a clear improvement in TFR rates compared to the discontinuation trials with imatinib [14, 19], they suggested that a shorter treatment period could result in similar TFR rates if 2G-TKIs were used for at least 3 years, and DMR was maintained for at least 1 year. However, the optimal duration of treatment with a 2G-TKI and maintenance of DMR for successful TFR was not clear. This is because the duration of TKI treatment and DMR maintenance in those trials was “at least” and not a fixed duration. Shorter treatment periods for TFR would minimize the problems associated with TKI therapy. We therefore conducted two TKI discontinuation studies in patients with newly diagnosed CML-CP, imposing a fixed DMR duration before cessation of TKI. In the earlier D-News trial, patients with newly diagnosed CML-CP were enrolled and treated with dasatinib for up to 2 years during the induction phase to achieve DMR (defined as 0.0069% or less), then stopped dasatinib treatment after just 2 years of sustained DMR [22]. The median duration of dasatinib treatment before the cessation was 995 days (33.1 months). The 12-month MRFS was 38.5%. In contrast, the estimated MRFS was even lower, at 16.7% at 12 months, in the present D-FREE study. Compared to the D-NewS trial, the duration of the induction phase with dasatinib in the D-FREE study was the same, with a maximum of 2 years, but the duration of DMR was shorter, exactly 1 year. Considering the more stringent definition of DMR (MR4.5) in D-FREE, the decrease in the MRFS rate is presumably due to the shorter duration of TKI treatment, in addition to the shorter DMR duration, although direct comparison between different trials is not possible.

The European LeukemiaNet (ELN) published a recommendation of requirements for TKI discontinuation, of which the optimal condition was the duration of TKI therapy > 5 years and of DMR > 2 years if MR4.5 [10]. The National Comprehensive Cancer Network (NCCN) guidelines describe criteria for TKI discontinuation as being the duration of approved TKI therapy for at least 3 years and stable MR4 for ≥ 2 years [12], which is less strict than the ELN recommendations. Etienne et al. published the results of their evaluation of the rate of patients eligible for TKI discontinuation and MRFS after stopping according to several recommendations/guidelines, including the ELN and the NCCN [23]. They found that the MRFS of patients who fulfilled the selection criteria proposed by the ELN was significantly different from that of those who did not, whereas no difference in MRFS was observed regarding the criteria proposed by the NCCN. In addition, meeting the selection criteria suggested by the ELN recommendations and front-line 2G-TKIs led to the highest MRFS, reaching 80%, suggesting that TKI therapy for at least 5 years

Table 4 Published TKI discontinuation clinical trials using second-generation TKIs as first-line treatment

Trial	Number of patients discontinuing TKI	TKI	Study criteria		TFR eligibility	Definition of relapse for reinitiating TKI	Total TKI treatment duration, median (months)	DMR duration before TKI discontinuation (months)	TFR/MRFS rate (%); time after discontinuation	References
			Duration of TKI treatment before consolidation phase	Duration of consolidation with sustained DMR						
ENEST free-dom	190	nilotinib	At least 2 years	1 year (52 weeks)	MR4.5 for ≥ 1 year (52 weeks)	Loss of MMR	43.5	30.3 ^{*1}	51.6%; 48 weeks	[20]
First-line DADI	58	dasatinib	At least 2 years	1 year	DMR ($BCR\text{-}ABL/^{IS} \leq 0.0069\%$) for ≥ 1 year	Loss of DMR at two consecutive timepoints or loss of MMR at a single timepoint	40.4	23.3 (median)	55.2%; 6 months	[21]
D-NewS	26	dasatinib	Up to 2 years	2 years	DMR ($BCR\text{-}ABL/^{IS} \leq 0.0069\%$) for 2 years	Loss of DMR at two consecutive timepoints or loss of MMR at a single timepoint	33.1	24 ^{*2}	38.5%; 1 year	[22]
D-FREE	21	dasatinib	Up to 2 years	1 year	MR4.5 for 1 year	Loss of MR4 at two consecutive timepoints or loss of MMR at a single timepoint	18.9	12.7 (median)	16.7%; 1 year	–

TKI, tyrosine kinase inhibitor; DMR, deep molecular response; TFR, treatment-free remission; MRFS, molecular relapse-free survival; Ref., references; $BCR\text{-}ABL/^{IS}$, $BCR\text{-}ABL/^{IS}$ levels on an international scale; MR4.5, $BCR\text{-}ABL/^{IS} \leq 0.0032\%$; MR4, $BCR\text{-}ABL/^{IS} \leq 0.01\%$; MMR, major molecular response ($BCR\text{-}ABL/^{IS} \leq 0.1\%$); –, not applicable

^{*1}Calculated from the median time from first achievement of MR4.5 to study entry (18.3 months) and the duration of consolidation phase (52 weeks) specified in the study protocol

^{*2}Duration as specified in the study protocol

as recommended by the ELN, which is longer than that recommended by the NCCN, may improve TFR. Rea et al. reported on the TFR after two different durations of nilotinib consolidation in patients previously treated with imatinib [24]. They registered the patients who did not achieve MR4.0 after ≥ 24 months of imatinib treatment and treated them with nilotinib. After 1 year of induction, the patients who achieved MR4.0 were randomized to 1 or 2 years of consolidation with nilotinib followed by discontinuation of treatment. The treatment-free survival rate of one and two years of consolidation was 34.5% and 42.5%, respectively, and was not significantly different, suggesting that there is no significant benefit for successful TFR from an additional year of consolidation treatment with nilotinib for patients who achieved sustained DMR after 2 years on nilotinib following a switch from imatinib. It suggests that the duration of DMR may not be the most important factor for the success of TFR. Indeed, the final analysis of the EURO-SKI trial evaluating 755 patients mostly treated with imatinib was recently reported: the prognostic factor for MMR loss after 6 months of TKI discontinuation was the duration of TKI treatment but not the duration of DMR [25]. Although most molecular relapses occurred within 6 months of dasatinib discontinuation in the D-FREE study, the duration of TKI treatment may be important for improving TFR even in patients treated with 2G-TKIs, which are more potent than imatinib. However, there is overlap between the TKI treatment and the DMR periods, making it difficult to analyze which one is more important. The incidence of TKI withdrawal syndrome in this study (2 of 21 patients) was lower than in previous TFR trials (23–30%) [26–28]. This may be related to the short duration of treatment, as a previous study has shown that longer treatment duration predisposes to TKI withdrawal syndrome [28].

It is not known by which mechanism the duration of TKI treatment affects the success of TFR. Previous reports showed that the patients with successful discontinuation had larger and more functional NK cells than the failed patients [29, 30]. Although not examined in our study, it is possible that anti-tumor NK cells may not be able to be maintained by short-term TKI administration. It is also possible that a short TKI treatment period may not reduce CML stem cells to a sufficient level to prevent relapse after treatment cessation. However, the relationship between CML stem cells and TFR is still controversial, as there is a report that CML stem cells can be detected in the peripheral blood of patients during successful TKI discontinuation [31].

Interestingly, one patient maintained TFR for 17.8 months after 18.6 months of dasatinib treatment in our study. It is difficult to detect the difference in patient's background between successful and unsuccessful TFR in our patients because of its limited number. However, it is very important to find the prognostic factors of successful TFR, so that it

may prove possible to shorten duration of TKI treatment in a good prognosis group, thus minimizing AEs, avoiding restriction of pregnancy in women, and reducing the financial challenge of TKI treatment.

This D-FREE study is the largest prospective clinical trial to register newly diagnosed CML-CP patients treated with dasatinib in Japan. In this study, a high MR4.5 attainment rate of 48.8% within 2 years was observed. Although not directly comparable, this rate was higher than that of other trials previously reported worldwide [2, 32, 33]. A similar trend was reported in the Japanese cohort analysis of the DASISION trial [17]. This may be due to the inclusion of a large number of low-risk patients in Japan, where health checkups are well developed and blood cell abnormalities are easily detected at an early stage. Although the study did not focus on collecting safety information during dasatinib treatment, no new serious adverse events were reported. The incidence of cardiovascular events grade 3 or higher during the study period was 1.2%.

In conclusion, DMR for just one year is not enough for successful TFR in CML-CP patients treated with 2G-TKIs for less than three years. A yet unknown sufficient duration of treatment before discontinuation of TKIs is important for improving the TFR treatment goal.

Acknowledgements This study was supported by the Ibaraki Hematology, Oncology & Palliation Expert Meeting (IB-HOPE). This research was conducted as an Investigator Sponsored Research with financial support by Bristol-Myers Squibb Co., Ltd (BMS). The authors thank Kazuteru Ohashi (Tokyo Metropolitan Cancer and Infectious Diseases Center, Komagome Hospital), Hideharu Muto (Tokyo Metropolitan Ohtsuka Hospital), Kensuke Usuki (NTT Medical Center Tokyo), Kenji Yokoyama (Tokai University Hachioji Hospital), Koh Yamamoto (Yokohama City Minato Red Cross Hospital), Nobuyuki Aotsuka (Japanese Red Cross Narita Hospital), Kenichi Ishizawa (Yamagata University Hospital), Naoki Takezako (Nerima Hikarigaoka Hospital), Takuto Miyagishima (Kushiro Rosai Hospital), Tadao Ishida (Japanese Red Cross Medical Center), Atsushi Shinagawa (Hitachi General Hospital), Kentaro Wakasa (Obihiro-Kosei General Hospital), Tsuyoshi Nakamaki (Showa University School of Medicine), Naoto Tomita (St. Marianna University School of Medicine), Katsutoshi Ozaki (Nippon Medical School Tama Nagayama Hospital), Takayoshi Itoh (JA Toride Medical Center), Shugo Kowata (Iwate Medical University School of Medicine), Kenji Tajika (Yokohamaminami-Kyousai Hospital), Takayuki Fujio (Ibaraki Prefectural Central Hospital), Masahiro Onozawa (Hokkaido University Faculty of Medicine), Masahide Yamamoto (Tokyo Medical and Dental University), and Takeshi Kondo (Aiiku Hospital) for participating in this study. They thank Akiko Yamana, Hitomi Miyata, and Yumi Terakado at IB-HOPE. They are grateful to Prof. Junia V. Melo (University of Adelaide, Australia) for language editorial assistance.

Data availability The data that support the findings of this study are available from the corresponding author, CY, upon reasonable request.

Declarations

Conflict of interest CY received research funding from BMS and honoraria from BMS, Novartis, Pfizer, Janssen, Chugai, Ono, Otsuka, AbbVie, Nippon Shinyaku, and Takeda and from advisory board of

Novartis and AbbVie. HY received research funding from BMS and Otsuka; consulting fee from Novartis; and honoraria from Novartis, Otsuka, and Pfizer. ND received honoraria from Novartis and Janssen. KM received honoraria from BMS, Otsuka, Chugai, Ono, Novartis, Pfizer, and Takeda. YH received honoraria from BMS. MO received honoraria from Novartis, Pfizer, Otsuka, Jansen, and Nihon Shinyaku. NY received research funding from Chugai, Kyowa Kirin, and Takeda and honoraria from BMS. KF received honoraria from BMS, Novartis, Pfizer, Nippon Shinyaku, Meiji Seika, CSL Behring, Otsuka, AbbVie, Jansen, Chugai, and Takeda. GO received honoraria from BMS, Novartis, Pfizer, Nippon Shinyaku, Kyowa Kirin, Celgene, SymBio, Sanofi, Ono, Meiji, Nippon Kayaku, Alexion, Otsuka, AbbVie, Jansen, Chugai, Astellas, Sumitomo Dainippon, Takeda, Eisai, MSD, Mundipharma, and AstraZeneca. TK received honoraria from BMS, Novartis, Chugai, Ono, and Pfizer. SK received research funding from BMS and Pfizer and honoraria from BMS, Novartis, Pfizer, and Otsuka. NI received honoraria from BMS, Novartis, Pfizer, and Otsuka. IT received research funding from National Hospital Organization and honoraria from Life Science Publications and Medical View. KO received honoraria from Chugai and Daiichi Sankyo and payment from Takeda and from data safety monitoring/advisory board of Ono, Eisai, and Janssen. HK received honoraria from Taiho, AbbVie, AstraZeneca, and Chugai. KI received research funding from BMS and honoraria from BMS, Otsuka, and Novartis. MI, MH, KM, YN, and HS have nothing to disclose.

Open Access This article is licensed under a Creative Commons Attribution 4.0 International License, which permits use, sharing, adaptation, distribution and reproduction in any medium or format, as long as you give appropriate credit to the original author(s) and the source, provide a link to the Creative Commons licence, and indicate if changes were made. The images or other third party material in this article are included in the article's Creative Commons licence, unless indicated otherwise in a credit line to the material. If material is not included in the article's Creative Commons licence and your intended use is not permitted by statutory regulation or exceeds the permitted use, you will need to obtain permission directly from the copyright holder. To view a copy of this licence, visit <http://creativecommons.org/licenses/by/4.0/>.

References

- Hochhaus A, Larson RA, Guilhot F, Radich JP, Branford S, Hughes TP, et al. Long-term outcomes of imatinib treatment for chronic myeloid leukemia. *N Engl J Med*. 2017;376:917–27.
- Cortes JE, Saglio G, Kantarjian HM, Baccarani M, Mayer J, Boqué C, et al. Final 5-year study results of DASISION: the dasatinib versus imatinib study in treatment-naïve chronic myeloid leukemia patients trial. *J Clin Oncol*. 2016;34:2333–40.
- Kantarjian HM, Hughes TP, Larson RA, Kim DW, Issaragrisil S, le Coutre P, et al. Long-term outcomes with frontline nilotinib versus imatinib in newly diagnosed chronic myeloid leukemia in chronic phase: ENESTnd 10-year analysis. *Leukemia*. 2021;35:440–53.
- Cortes JE, Gambacorti-Passerini C, Deininger MW, Mauro MJ, Chuah C, Kim DW, et al. Bosutinib versus imatinib for newly diagnosed chronic myeloid leukemia: results from the randomized BFORE trial. *J Clin Oncol*. 2018;36:231–7.
- Bower H, Bjorkholm M, Dickman PW, Högglund M, Lambert PC, Andersson TM. Life expectancy of patients with chronic myeloid leukemia approaches the life expectancy of the general population. *J Clin Oncol*. 2016;34:2851–7.
- Aghel N, Delgado DH, Lipton JH. Cardiovascular toxicities of BCR-ABL tyrosine kinase inhibitors in chronic myeloid leukemia: preventive strategies and cardiovascular surveillance. *Vasc Health Risk Manag*. 2017;13:293–303.
- Berman E, Druker BJ, Burwick R. Chronic myelogenous leukemia: pregnancy in the era of stopping tyrosine kinase inhibitor therapy. *J Clin Oncol*. 2018;36:1250–6.
- Yamamoto C, Nakashima H, Ikeda T, Kawaguchi SI, Toda Y, Ito S, et al. Analysis of the cost-effectiveness of treatment strategies for CML with incorporation of treatment discontinuation. *Blood Adv*. 2019;3:3266–77.
- Cortes J, Rea D, Lipton JH. Treatment-free remission with first- and second-generation tyrosine kinase inhibitors. *Am J Hematol*. 2019;94:346–57.
- Hochhaus A, Baccarani M, Silver RT, Schiffer C, Apperley JF, Cervantes F, et al. European LeukemiaNet 2020 recommendations for treating chronic myeloid leukemia. *Leukemia*. 2020;34:966–84.
- Rea D, Ame S, Berger M, Cayuela JM, Charbonnier A, Coiteux V, et al. Discontinuation of tyrosine kinase inhibitors in chronic myeloid leukemia: recommendations for clinical practice from the French Chronic Myeloid Leukemia Study Group. *Cancer*. 2018;124:2956–63.
- Deininger MW, Shah NP, Altman JK, Berman E, Bhatia R, Bhatnagar B, et al. Chronic myeloid leukemia, version 2.2021, NCCN clinical practice guidelines in oncology. *J Natl Compr Canc Netw*. 2020;18:1385–415.
- Yoshida C, Nakamae H, Fletcher L, Koga D, Sogabe T, Matsuura I, et al. Validation of a rapid one-step high sensitivity real-time quantitative PCR system for detecting major BCR-ABL1 mRNA on an International Scale. *Springerplus*. 2016;5:569.
- Rousselot P, Charbonnier A, Cony-Makhoul P, Agape P, Nicolini FE, Varet B, et al. Loss of major molecular response as a trigger for restarting tyrosine kinase inhibitor therapy in patients with chronic-phase chronic myelogenous leukemia who have stopped imatinib after durable undetectable disease. *J Clin Oncol*. 2014;32:424–30.
- Mahon FX, Rea D, Guilhot J, Guilhot F, Huguet F, Nicolini F, et al. Discontinuation of imatinib in patients with chronic myeloid leukaemia who have maintained complete molecular remission for at least 2 years: the prospective, multicentre Stop Imatinib (STIM) trial. *Lancet Oncol*. 2010;11:1029–35.
- Rea D, Nicolini FE, Tulliez M, Rousselot P, Guilhot F, Gardembas M, et al. Dasatinib or Nilotinib discontinuation in chronic phase (CP)-chronic myeloid leukemia (CML) patients (pts) with durably undetectable BCR-ABL transcripts: Interim Analysis of the STOP 2G-TKI Study with a Minimum Follow-up of 12 Months – on Behalf of the French CML Group Filmc. *Blood*. 2014;124:811.
- Fujisawa S, Nakamae H, Ogura M, Ishizawa K-I, Taniwaki M, Utsunomiya A, et al. Efficacy and safety of dasatinib versus imatinib in Japanese patients with newly diagnosed chronic-phase chronic myeloid leukemia (CML-CP): subset analysis of the DASISION trial with 2-year follow-up. *Int J Hematol*. 2014;99:141–53.
- Saussele S, Richter J, Guilhot J, Gruber FX, Hjorth-Hansen H, Almeida A, et al. Discontinuation of tyrosine kinase inhibitor therapy in chronic myeloid leukaemia (EURO-SKI): a prespecified interim analysis of a prospective, multicentre, non-randomised, trial. *Lancet Oncol*. 2018;19:747–57.
- Takahashi N, Tauchi T, Kitamura K, Miyamura K, Saburi Y, Hatta Y, et al. Deeper molecular response is a predictive factor for treatment-free remission after imatinib discontinuation in patients with chronic phase chronic myeloid leukemia: the JALSG-STIM213 study. *Int J Hematol*. 2018;107:185–93.
- Hochhaus A, Masszi T, Giles FJ, Radich JP, Ross DM, Gomez Casares MT, et al. Treatment-free remission following frontline nilotinib in patients with chronic myeloid leukemia in chronic

- phase: results from the ENEST freedom study. *Leukemia*. 2017;31:1525–31.
21. Kimura S, Imagawa J, Murai K, Hino M, Kitawaki T, Okada M, et al. Treatment-free remission after first-line dasatinib discontinuation in patients with chronic myeloid leukaemia (first-line DADI trial): a single-arm, multicentre, phase 2 trial. *Lancet Haematol*. 2020;7:e218–25.
 22. Yamaguchi H, Takezako N, Ohashi K, Oba K, Kumagai T, Kozai Y, et al. Treatment-free remission after first-line dasatinib treatment in patients with chronic myeloid leukemia in the chronic phase: the D-NewS Study of the Kanto CML Study Group. *Int J Hematol*. 2020;111:401–8.
 23. Etienne G, Faberes C, Bauduer F, Adiko D, Lifermann F, Dagada C, et al. Relevance of treatment-free remission recommendations in chronic phase chronic leukemia patients treated with frontline tyrosine kinase inhibitors. *Cancer Med*. 2021;10:3635–45.
 24. Rea D, Kyrz-Krzemien S, Sportoletti P, Mayer J, Illes A, Angona A, et al. Treatment-Free Remission (TFR) after two different durations of nilotinib consolidation in patients with chronic myeloid leukemia (CML) previously treated with imatinib: Enestpath study results. *Blood*. 2021;138:635.
 25. Mahon F-X, Richter J, Hochhaus A, Panayiotidis P, Medina de Almeida A, Mayer J, et al. FINAL analysis of a PAN European STOP tyrosine kinase inhibitor trial in chronic myeloid leukemia: the EURO-SKI study. *Blood*. 2021;138:633.
 26. Richter J, Söderlund S, Lübking A, Dreimane A, Lotfi K, Mark- evärn B, et al. Musculoskeletal pain in patients with chronic myeloid leukemia after discontinuation of imatinib: a tyrosine kinase inhibitor withdrawal syndrome? *J Clin Oncol*. 2014;32:2821–3.
 27. Lee SE, Choi SY, Song HY, Kim SH, Choi MY, Park JS, et al. Imatinib withdrawal syndrome and longer duration of imatinib have a close association with a lower molecular relapse after treatment discontinuation: the KID study. *Haematologica*. 2016;101:717–23.
 28. Berger MG, Pereira B, Rousselot P, Cony-Makhoul P, Gardembas M, Legros L, et al. Longer treatment duration and history of osteoarticular symptoms predispose to tyrosine kinase inhibitor withdrawal syndrome. *Br J Haematol*. 2019;187:337–46.
 29. Imagawa J, Tanaka H, Okada M, Nakamae H, Hino M, Murai K, et al. Discontinuation of dasatinib in patients with chronic myeloid leukaemia who have maintained deep molecular response for longer than 1 year (DADI trial): a multicentre phase 2 trial. *Lancet Haematol*. 2015;2:e528–35.
 30. Ilander M, Olsson-Stromberg U, Schlums H, Guilhot J, Bruck O, Lahteenmaki H, et al. Increased proportion of mature NK cells is associated with successful imatinib discontinuation in chronic myeloid leukemia. *Leukemia*. 2017;31:1108–16.
 31. Bocchia M, Sicuranza A, Abruzzese E, Iurlo A, Sirianni S, Gozzini A, et al. Residual peripheral blood CD26(+) leukemic stem cells in chronic myeloid leukemia patients during TKI therapy and during treatment-free remission. *Front Oncol*. 2018;8:194.
 32. Marin D, Hedgley C, Clark RE, Apperley J, Foroni L, Milojkovic D, et al. Predictive value of early molecular response in patients with chronic myeloid leukemia treated with first-line dasatinib. *Blood*. 2012;120:291–4.
 33. Breccia M, Stagno F, Luciano L, Abruzzese E, Annunziata M, D'Adda M, et al. Dasatinib first-line: multicentric Italian experience outside clinical trials. *Leuk Res*. 2016;40:24–9.

Publisher's Note Springer Nature remains neutral with regard to jurisdictional claims in published maps and institutional affiliations.

Case Reports

Sustained Lumen Area by Paclitaxel-Coated Balloon Following Rotational Atherectomy for Napkin-Ring Left Main Trunk Ostial Lesion

Takumi Osawa, MD; Tomomi Koizumi, MD, PhD; Yuta Ito, MD

Department of Cardiovascular Medicine, National Hospital Organization Mito Medical Center, Ibaraki, Japan

Abstract

Late lumen enlargement after percutaneous coronary intervention (PCI) with drug-coated balloon has contributed to good clinical results. However, late lumen enlargement with drug-coated balloon following rotational atherectomy has not been well reported. This report describes a case of calcified napkin-ring ostial lesion at the left main trunk that showed a sustained lumen area after PCI with drug-coated balloon following rotational atherectomy. An 85-year-old female patient was admitted to the hospital with dyspnea. Echocardiography showed hypokinesis in the anteroseptal and inferior walls. Electrocardiograph-gated cardiac computed tomography showed a calcified ostial lesion in the left main trunk. Invasive angiography of the coronary artery showed severe stenosis in the left main trunk ostium. Percutaneous coronary intervention was performed with a drug-coated balloon after rotational atherectomy. The minimal lumen area measured by intravascular ultrasound grew mildly from 4.09 to 4.17 mm² immediately after PCI. Follow-up angiography and intravascular ultrasound performed after 6 months showed that the minimal lumen area in the left main trunk ostium was further enlarged from 4.17 to 4.69 mm². The presence of sustained lumen area after PCI with drug-coated balloon following rotational atherectomy for a napkin-ring left main trunk ostial lesion was confirmed. This case demonstrates sustained lumen area after drug-coated balloon following rotational atherectomy in the left main trunk ostium, improving the patient's chest symptom. Hence, drug-coated balloon after rotational atherectomy may be an option for complex stent sites, such as the left main trunk ostium in geriatric patients and sites with highly calcified lesions.

Keywords: Atherectomy; coronary artery disease; percutaneous coronary intervention

Introduction

Rotational atherectomy is a recently established procedure for calcified plaque debulking. Most calcified lesions are treated by stenting following rotational atherectomy. However, percutaneous coronary intervention (PCI) with a drug (paclitaxel)-coated balloon (DCB) is a well-established stentless strategy for in-stent restenosis and small vessel disease. The use of DCB could cause an increase in the late lumen area in the chronic phase without extensive dissection and recoil.¹ Late lumen enlargement (LLE) after PCI with DCB has contributed to good clinical outcomes.^{1,2} Although these 2 strategies (rotational atherectomy and DCB) each have advantages, LLE with DCB following rotational atherectomy for severely calcified lesions has not been well reported.

This report describes a case of napkin-ring calcified ostial lesion at the left main trunk (LMT) that showed sustained lumen area confirmed by intravascular ultrasound (IVUS) after PCI with rotational atherectomy and DCB.

Citation: Osawa T, Koizumi T, Ito Y. Sustained lumen area by paclitaxel-coated balloon following rotational atherectomy for napkin-ring left main trunk ostial lesion. *Tex Heart Inst J*. 2023;50(2):e227883. doi:10.14503/THIJ-22-7883

Corresponding author: Takumi Osawa, MD, Department of Cardiovascular Medicine, National Hospital Organization Mito Medical Center, Sakuranosato, 280, Ibaraki-machi, Higashi-Ibarakigun, Ibaraki, Japan (tosawa49710@gmail.com)

© 2023 by The Texas Heart® Institute, Houston

Case Report

An 85-year-old female patient was admitted to the hospital because of dyspnea on exertion in March 2020. The patient reported no medical history except rheumatoid arthritis and glaucoma. She had no cardiovascular risk factors. On initial physical examination, her blood pressure was 116/64 mm Hg, heart rate was 81 beats per minute, respiratory rate was 12 breaths per minute, pulse oximetric oxygen saturation was 98% on room air, and body temperature was 36.6 °C. The patient's height and weight were 140.0 cm and 34.8 kg, respectively. Examination of her cardiovascular system revealed no abnormal murmurs, and lung sounds were clear. Her jugular venous pressure was not elevated, and she did not exhibit heart failure symptoms, such as shortness of breath or leg edema.

An electrocardiogram showed atrial fibrillation at 75 beats per minute, horizontal ST depression, and negative T wave in the V_4 , V_5 , and V_6 leads. Transthoracic echocardiography revealed hypokinesis in the antero-septal and inferior walls with an ejection fraction of 54%. Electrocardiograph-gated cardiac computed tomography revealed a stenotic calcified ostial lesion at the LMT (Fig. 1A and 1B). Hence, invasive coronary angiography (CAG) was performed (Fig. 2A), revealing severe stenosis of the LMT ostium, wherein a 5F diagnostic catheter could be wedged into the LMT ostium.

Abbreviations and Acronyms

CAG	coronary angiography
DCB	drug-coated balloon
LLE	late lumen enlargement
LMT	left main trunk
MLA	minimal lumen area
PCI	percutaneous coronary intervention

Ischemic functional evaluations, including single-photon emission computed tomography or fractional flow reserve, were not performed. The electrocardiogram showed no abnormal Q waves, and the myocardium appeared to be viable.

Percutaneous coronary intervention was planned for the LMT ostial lesion, considering the patient's Synergy Between Percutaneous Coronary Intervention With TAXUS and Cardiac Surgery (SYNTAX) score of 20, advanced age, and frailty. Intra-aortic balloon pump insertion was performed before PCI. A 7F Glidesheath Slender (Terumo) was inserted into the right radial artery. Percutaneous coronary intervention was then performed using a 7F JL 3.5 guide catheter. The LMT and left anterior descending artery were crossed with the guide wire (ASAHI SION blue; ASAHI Intecc). Intravascular ultrasound (OptiCross Imaging Catheter; Boston Scientific) examination was performed from the left anterior descending artery to LMT ostium, which showed a highly calcified lesion with a calcium

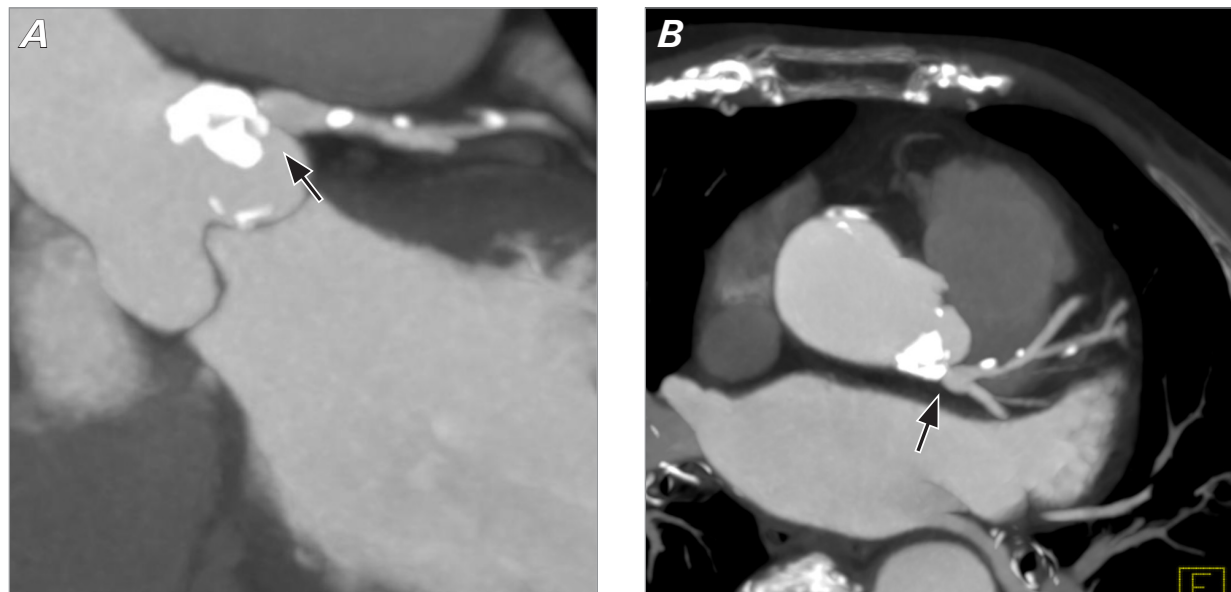


Fig. 1 Electrocardiograph-gated cardiac computed tomogram reveals severe stenosis in the calcified ostial lesion at the left main trunk (arrows) in **A)** coronal and **B)** axial views.

arc of 360°, that is, “napkin ring” (Fig. 2B). Therefore, rotational atherectomy (Rotalink Plus, 1.5-mm and 2.0-mm burrs; Boston Scientific) was performed and a cutting balloon (Wolverine Cutting Balloon, 3.0/10 mm; Boston Scientific) was inflated. Thrombolysis in Myocardial Infarction flow grade 3 and the absence of a flow-limiting dissection were confirmed. Hence, a DCB (SeQuent Please, 3.5/15 mm; B. Braun) was inflated in the LMT ostium owing to the possibility of aortic dissection by pressure expanding metallic stent or stent edge exiting into the aorta. The minimal lumen area (MLA) was mildly enlarged from 4.09 to 4.17 mm² after PCI, and the 7F guide catheter was no longer wedged into the LMT ostium (Fig. 3A and 3B). A staged PCI was scheduled with a rotational atherectomy and drug-eluting stent, using a larger burr size (≥ 2.15 mm) with PCI, if necessary, at follow-up CAG.

In October 2020, follow-up CAG showed no restenosis in the LMT ostium (Fig. 4A). Intravascular ultrasound examination confirmed sustained lumen area of the LMT ostial lesion. The MLA in the LMT ostium was enlarged to 4.69 mm², compared with 4.17 mm² after the previous PCI (Fig. 4B). Although other factors, including differences in catheter position for each

procedure, might be related, the sustained left main result (LLE, based on the numerical value) after PCI with DCB following rotational atherectomy for a napkin-ring LMT ostial lesion was verified. This MLA is acceptable for a smaller Asian woman, such as the patient in the present case (height of 140 cm and weight of 34.8 kg), according to the 2018 European Society of Cardiology/European Association for Cardio-Thoracic Surgery Guidelines on myocardial revascularization.³ Therefore, the choice was made to defer further PCI with additional rotational atherectomy. The patient has remained free of chest pain for 10 months from the procedure.

Discussion

Late lumen enlargement with DCB following rotational atherectomy for severe calcified ostial lesions has not been well reported. This article reports a case of sustained lumen area confirmed by IVUS after PCI with rotational atherectomy and DCB for a napkin-ring LMT ostial lesion.

A growing body of evidence suggests that the efficacy of DCB for the treatment of in-stent restenosis or small vessel disease has been established.^{4,7} However, there are

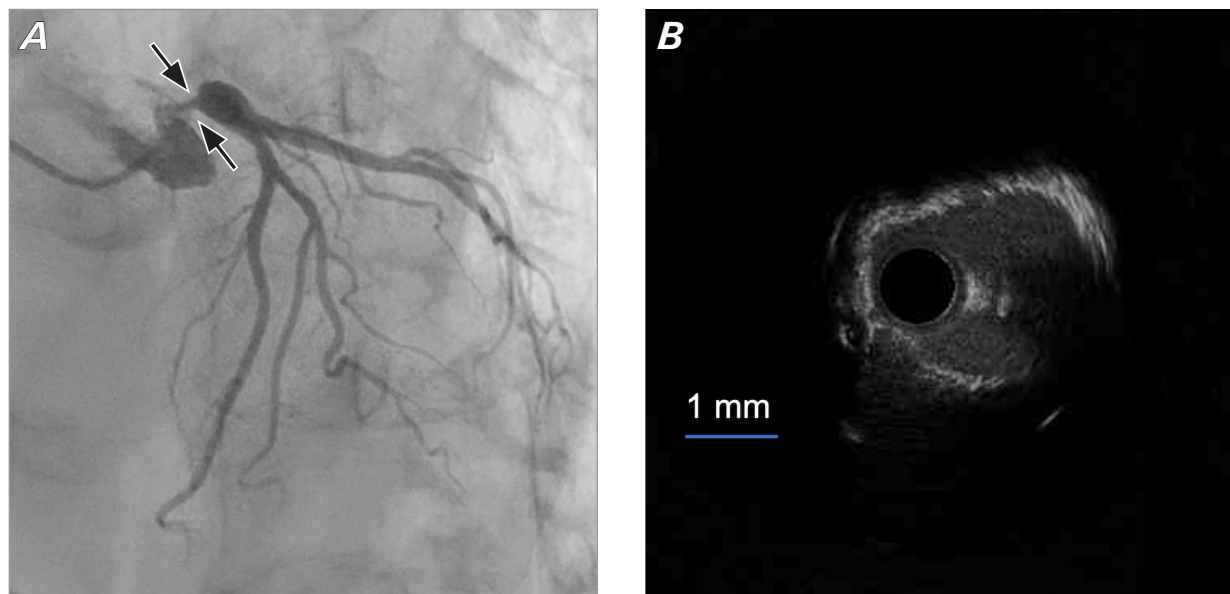


Fig. 2 Angiogram of the coronary artery and intravascular ultrasound before the procedure. **A)** Pre-PCI angiogram (left cranial view) demonstrates severe stenosis of the LMT ostium (arrows). The supplemental motion image also shows severe stenosis lesion at the LMT. **B)** Pre-PCI intravascular ultrasound at the LMT ostium shows a minimal lumen area of 4.09 mm².

Supplemental motion image is available for [Figure 2](#).

LMT, left main trunk; PCI, percutaneous coronary intervention.

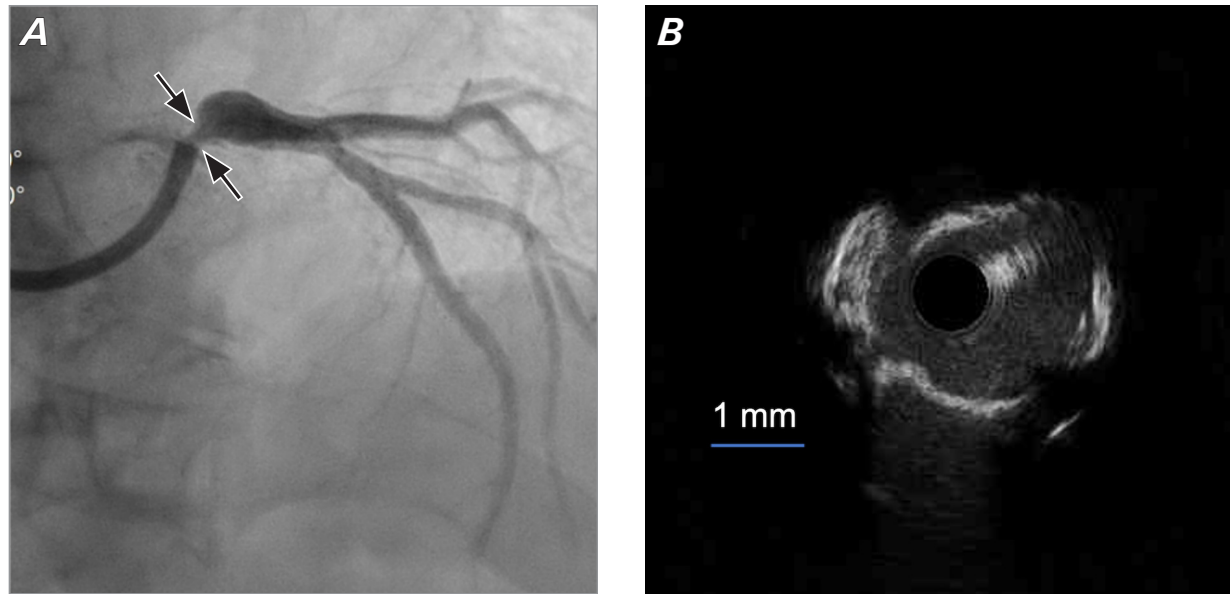


Fig. 3 Angiogram of the coronary artery and intravascular ultrasound immediately after the procedure. **A)** Post-PCI angiogram (left cranial view) indicates a mildly enlarged lesion at the LMT (arrows). There was a coronary dissection (National Heart, Lung, and Blood Institute coronary dissection criteria type A) at the LMT without flow limit. The supplemental motion image also shows the lesion following the procedure. **B)** Post-PCI intravascular ultrasound at the LMT ostium shows a minimal lumen area of 4.17 mm².

Supplemental motion image is available for [Figure 3](#).

LMT, left main trunk; PCI, percutaneous coronary intervention.

limited data regarding its efficacy for calcified lesions. A previous trial that used DCB for the treatment of calcified lesions showed comparable late lumen loss and restenosis rates between calcified and noncalcified lesions.⁸ Rissanen et al⁹ reported outcomes of 65 patients with calcified lesions treated with DCB following rotational atherectomy, who showed low rates of major adverse cardiovascular events and target-lesion revascularization. In a study by Nagai et al,¹⁰ approximately 39% of lesions showed LLE after PCI with rotational atherectomy and DCB. There were no cardiac deaths, and the target lesion revascularization rate was 16.4% during the midterm follow-up. Drug-coated balloon after rotational atherectomy seems to be a feasible and safe procedure.

In this case, rotational atherectomy and cutting balloon modified the napkin-ring calcified lesion, and paclitaxel might have penetrated easily. Although little is known about how paclitaxel works on calcium to modify calcified lesions, there are several reports of paclitaxel action on vascular calcification. Shimizu et al¹¹ reported vascular calcification closely related to morphogenic protein signaling and gene regulators of osteogenesis, such as the *Mx2* gene and osteoprotegerin. Also, apoptosis

of smooth muscular cells and release of matrix vesicles are important factors in coronary artery calcification.¹² Paclitaxel attenuates differentiation of vascular smooth muscle cells into osteoblast, that is, vascular calcification by downregulation of osteogenic signal and inhibiting matrix vesicle release.¹³

Stent implantation in severely calcified lesions is associated with worse outcomes owing to defective stent expansion and strut apposition.¹⁴⁻¹⁶ A previous randomized trial found that postprocedural stent asymmetry was associated with 1-year ischemic events.¹⁷ In this case, the disadvantages of stent implantation at calcified LMT ostial lesion included the possibility of inadequate dilation, the risk of aortic dissection by pressure expanding the metallic stent, the possibility of stent edge exiting into the aorta, and the inability to perform a second PCI with rotational atherectomy. Although the mechanism of LLE in severe calcified lesion by paclitaxel is not fully understood, further study should be undertaken to confirm the utility of a paclitaxel-eluting balloon for very severe calcified coronary artery lesions instead of deploying stents.

The 2018 European Society of Cardiology/European Association for Cardio-Thoracic Surgery Guidelines

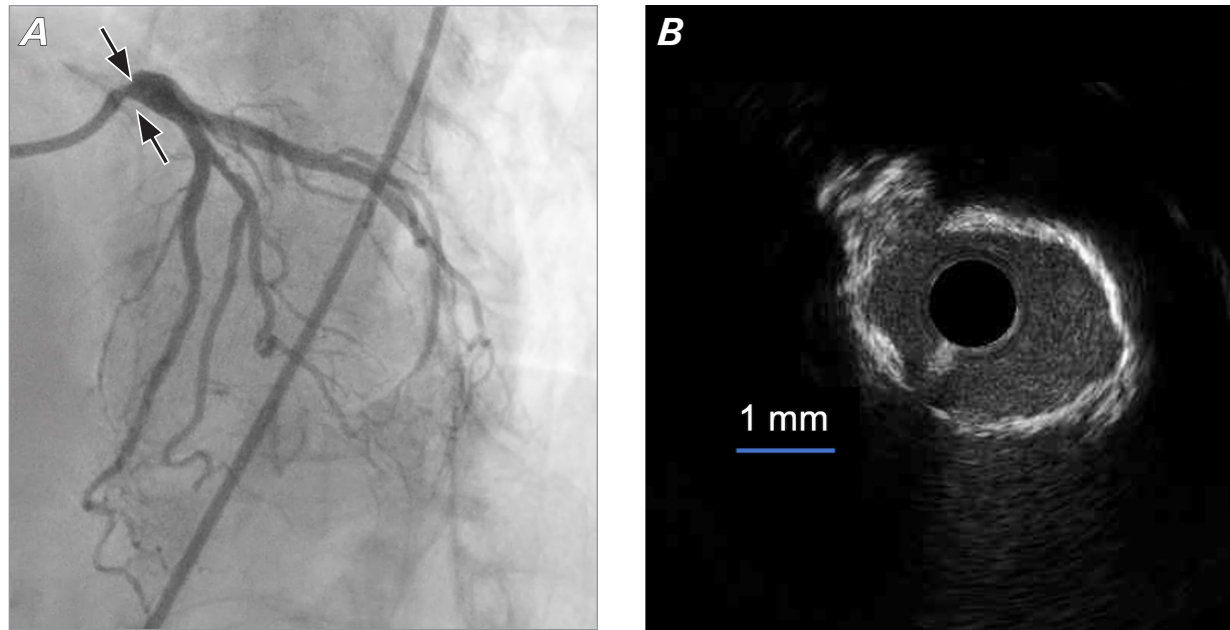


Fig. 4 Follow-up angiogram of the coronary artery and intravascular ultrasound. **A)** Follow-up angiogram shows no restenosis in the LMT ostium (arrows). The supplemental motion image also shows the follow-up angiography of the lesion. **B)** Follow-up intravascular ultrasound at the LMT ostium shows a minimal lumen area of 4.69 mm².

Supplemental motion image is available for [Figure 4](#).

LMT, left main trunk.

on myocardial revascularization state that “in Asian patients with generally smaller heart sizes, studies have suggested that an IVUS MLA of 4.5-4.8 mm² may be the most appropriate.”³ Therefore, the MLA of 4.69 mm² in this case is within the recommended range.

Conclusion

In this patient, paclitaxel-coated balloon after rotational atherectomy for napkin-ring calcified ostial lesion resulted in a sustained lumen area in the chronic phase. This treatment option might be considered for lesions that are not suitable for stent implantation, such as severe calcified LMT ostium.

A small advantage of LLE was seen after local delivery of paclitaxel in a calcified lesion in the present case. Future investigation is needed to clarify the mechanism of paclitaxel on calcified lesions, which may provide a treatment option for severe calcified coronary artery disease.

Acknowledgments

The authors appreciate expert review of this report by Heidi N. Bonneau, RN, MS, CCA.

Published: 23 March 2023

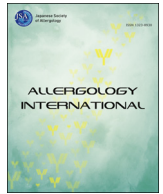
Conflict of Interest Disclosures: The authors have no relevant financial relationships to disclose.

Funding/Support: The authors report no specific funding related to this article.

References

1. Kleber FX, Schulz A, Waliszewski M, et al. Local paclitaxel induces late lumen enlargement in coronary arteries after balloon angioplasty. *Clin Res Cardiol.* 2015;104(3):217-225. doi:10.1007/s00392-014-0775-2
2. Scheller B, Fischer D, Clever YP, et al. Treatment of a coronary bifurcation lesion with drug-coated balloons: lumen enlargement and plaque modification after 6 months. *Clin Res Cardiol.* 2013;102(6):469-472. doi:10.1007/s00392-013-0556-3
3. Neumann F-J, Sousa-Uva M, Ahlsson A, et al. 2018 ESC/EACTS guidelines on myocardial revascularization. *Eur Heart J.* 2018;40(2):87-165. doi:10.1093/eurheartj/ehy394

4. Scheller B, Hehrlein C, Bocks W, et al. Treatment of coronary in-stent restenosis with a paclitaxel-coated balloon catheter. *N Engl J Med*. 2006;355(20):2113-2124. doi:10.1056/NEJMoa061254
5. Unverdorben M, Vallbracht C, Cremers B, et al. Paclitaxel-coated balloon catheter versus paclitaxel-coated stent for the treatment of coronary in-stent restenosis. *Circulation*. 2009;119(23):2986-2994. doi:10.1161/CIRCULATIONAHA.108.839282
6. Nestelberger T, Jeger R. Drug-coated balloons for small coronary vessel interventions: a literature review. *Interv Cardiol*. 2019;14(3):131-136. doi:10.15420/icr.2019.06.R3
7. Jeger RV, Farah A, Ohlow MA, et al. Drug-coated balloons for small coronary artery disease (BASKET-SMALL 2): an open-label randomised non-inferiority trial. *Lancet*. 2018;392(10150):849-856. doi:10.1016/S0140-6736(18)31719-7
8. Ito R, Ueno K, Yoshida T, et al. Outcomes after drug-coated balloon treatment for patients with calcified coronary lesions. *J Interv Cardiol*. 2018;31(4):436-441. doi:10.1111/joic.12484
9. Rissanen TT, Uskela S, Siljander A, et al. Percutaneous coronary intervention of complex calcified lesions with drug-coated balloon after rotational atherectomy. *J Interv Cardiol*. 2017;30(2):139-146. doi:10.1111/joic.12366
10. Nagai T, Mizobuchi M, Funatsu A, Kobayashi T, Nakamura S. Acute and mid-term outcomes of drug-coated balloon following rotational atherectomy. *Cardiovasc Interv Ther*. 2020;35(3):242-249. doi:10.1007/s12928-019-00611-y
11. Shimizu T, Tanaka T, Iso T, et al. Notch signaling induces osteogenic differentiation and mineralization of vascular smooth muscle cells: role of *Mx2* gene induction via Notch-RBP-Jk signaling. *Arterioscler Thromb Vasc Biol*. 2009;29(7):1104-1111. doi:10.1161/ATVBAHA.109.187856
12. Otsuka F, Sakakura K, Yahagi K, Joner M, Virmani R. Has our understanding of calcification in human coronary atherosclerosis progressed? *Arterioscler Thromb Vasc Biol*. 2014;34(4):724-736. doi:10.1161/ATVBAHA.113.302642
13. Lee K, Kim H, Jeong D. Microtubule stabilization attenuates vascular calcification through the inhibition of osteogenic signaling and matrix vesicle release. *Biochem Biophys Res Commun*. 2014;451(3):436-441. doi:10.1016/j.bbrc.2014.08.007
14. Guedeney P, Claessen BE, Mehran R, et al. Coronary calcification and long-term outcomes according to drug-eluting stent generation. *JACC Cardiovasc Interv*. 2020;13(12):1417-1428. doi:10.1016/j.jcin.2020.03.053
15. Hemetsberger R, Abdelghani M, Toelg R, et al. Impact of coronary calcification on clinical outcomes after implantation of newer-generation drug-eluting stents. *J Am Heart Assoc*. 2021;10(12):e019815. doi:10.1161/JAHA.120.019815
16. G  n  reux P, Madhavan MV, Mintz GS, et al. Ischemic outcomes after coronary intervention of calcified vessels in acute coronary syndromes. Pooled analysis from the HORIZONS-AMI (Harmonizing Outcomes With Revascularization and Stents in Acute Myocardial Infarction) and ACUITY (Acute Catheterization and Urgent Intervention Triage Strategy) trials. *J Am Coll Cardiol*. 2014;63(18):1845-1854. doi:10.1016/j.jacc.2014.01.034
17. Suwannasom P, Sotomi Y, Ishibashi Y, et al. The impact of post-procedural asymmetry, expansion, and eccentricity of bioresorbable everolimus-eluting scaffold and metallic everolimus-eluting stent on clinical outcomes in the ABSORB II trial. *JACC Cardiovasc Interv*. 2016;9(12):1231-1242. doi:10.1016/j.jcin.2016.03.027



Original Article

Classifications of moderate to severe asthma phenotypes in Japan and analysis of serum biomarkers: A Nationwide Cohort Study in Japan (NHOM Asthma Study)

Maho Suzukawa ^{a, **}, Ken Ohta ^{a, b, *}, Yuma Fukutomi ^c, Hiroya Hashimoto ^{d, e}, Takeo Endo ^f, Masahiro Abe ^g, Yosuke Kamide ^c, Makoto Yoshida ^h, Yoshihiro Kikuchi ⁱ, Toshiyuki Kita ^j, Kenji Chibana ^k, Yasushi Tanimoto ^l, Kentaro Hyodo ^m, Shohei Takata ⁿ, Toshiya Inui ^o, Masahide Yasui ^p, Yoshinori Harada ^q, Toshio Sato ^r, Yumi Sakakibara ^s, Yoshiaki Minakata ^t, Yoshikazu Inoue ^u, Shinji Tamaki ^v, Tsutomu Shinohara ^w, Kazutaka Takami ^x, Motofumi Tsubakihara ^y, Masahide Oki ^z, Kentaro Wakamatsu ^{aa}, Masahide Horiba ^{bb}, Gen Ideura ^{cc}, Koko Hidaka ^{dd}, Akiko M. Saito ^d, Nobuyuki Kobayashi ^{a, ee}, Masami Taniguchi ^{c, ff}

^a Clinical Research Center, National Hospital Organization Tokyo National Hospital, Tokyo, Japan

^b Japan Anti-Tuberculosis Association, JATA Fukujiji Hospital, Tokyo, Japan

^c Clinical Research Center, National Hospital Organization Sagami National Hospital, Kanagawa, Japan

^d Clinical Research Center, National Hospital Organization Nagoya Medical Center, Nagoya, Japan

^e Core Laboratory, Nagoya City University Graduate School of Medical Sciences, Nagoya, Japan

^f National Hospital Organization Mito Medical Center, Ibaraki, Japan

^g National Hospital Organization Ehime Medical Center, Ehime, Japan

^h National Hospital Organization Fukuoka National Hospital, Fukuoka, Japan

ⁱ National Hospital Organization Morioka Medical Center, Iwate, Japan

^j National Hospital Organization Kanazawa Medical Center, Ishikawa, Japan

^k National Hospital Organization Okinawa National Hospital, Okinawa, Japan

^l National Hospital Organization Minami-Okayama Medical Center, Okayama, Japan

^m National Hospital Organization Ibaraki Higashi National Hospital, Ibaraki, Japan

ⁿ National Hospital Organization Fukuoka Higashi Medical Center, Fukuoka, Japan

^o National Hospital Organization Disaster Medical Center, Tokyo, Japan

^p National Hospital Organization Nanao National Hospital, Ishikawa, Japan

^q Department of Rheumatology & Allergy, National Hospital Organization Osaka Minami Medical Center, Osaka, Japan

^r National Hospital Organization Okayama Medical Center, Okayama, Japan

^s Federation of National Public Service Personnel Mutual Aid Associations Hiratsuka Kyosai Hospital, Kanagawa, Japan

^t National Hospital Organization Wakayama Hospital, Wakayama, Japan

^u National Hospital Organization Kinki-Chuo Chest Medical Center, Osaka, Japan

^v National Hospital Organization Nara Medical Center, Nara, Japan

^w National Hospital Organization Kochi National Hospital, Kochi, Japan

^x Kanto Central Hospital of the Mutual Aid Association of Public School Teachers, Tokyo, Japan

^y National Hospital Organization Yokohama Medical Center, Kanagawa, Japan

^z Department of Respiratory Medicine, National Hospital Organization Nagoya Medical Center, Aichi, Japan

^{aa} National Hospital Organization Omuta National Hospital, Fukuoka, Japan

^{bb} Division of Respiratory Medicine, National Hospital Organization Higashisaitama National Hospital, Saitama, Japan

^{cc} National Hospital Organization Shinshu Ueda Medical Center, Nagano, Japan

^{dd} National Hospital Organization Kokura Medical Center, Fukuoka, Japan

^{ee} Fureai Machida Hospital, Tokyo, Japan

^{ff} Shonan Kamakura General Hospital, Kanagawa, Japan

* Corresponding author. Japan Anti-Tuberculosis Association, JATA Fukujiji Hospital, 3-1-24 Matsuyama, Kiyose-City, Tokyo 204-8522, Japan.

** Corresponding author. Clinical Research Center, National Hospital Organization Tokyo National Hospital, 3-1-1 Takeoka, Kiyose-City, Tokyo 204-8585, Japan.

E-mail addresses: fueta-tyk@umin.ac.jp (M. Suzukawa), kenohta3@gmail.com (K. Ohta).

Peer review under responsibility of Japanese Society of Allergy.

ARTICLE INFO

Article history:

Received 18 January 2022

Received in revised form

17 May 2022

Accepted 25 May 2022

Available online 2 July 2022

Keywords:

Asthma

Biomarkers

Cluster analysis

Phenotype

Tree analysis

Abbreviations:

ACQ, Asthma control questionnaire;

AERD, Aspirin-exacerbated respiratory

disease; FeNO, Fractional exhaled nitric

oxide; GERD, Gastroesophageal reflux

disease; GINA, Global initiative for asthma;

ICS, Inhaled corticosteroid; OCS, Oral

corticosteroid; SA, Severe asthma;

SAS, Sleep apnea syndrome

ABSTRACT

Background: Asthma is a heterogeneous disease, and phenotyping can facilitate understanding of disease pathogenesis and direct appropriate asthma treatment. This nationwide cohort study aimed to phenotype asthma patients in Japan and identify potential biomarkers to classify the phenotypes.

Methods: Adult asthma patients ($n = 1925$) from 27 national hospitals in Japan were enrolled and divided into Global Initiative for Asthma (GINA) steps 4 or 5 (GINA 4, 5) and GINA Steps 1, 2, or 3 (GINA 1–3) for therapy. Clinical data and questionnaires were collected. Biomarker levels among GINA 4, 5 patients were measured. Ward's minimum variance hierarchical clustering method and tree analysis were performed for phenotyping. Analysis of variance, the Kruskal–Wallis, and chi-square tests were used to compare cluster differences.

Results: The following five clusters were identified: 1) late-onset, old, less-atopic; 2) late-onset, old, eosinophilic, low FEV₁; 3) early-onset, long-duration, atopic, poorly controlled; 4) early-onset, young, female-dominant, atopic; and 5) female-dominant, T1/T2-mixed, most severe. Age of onset, disease duration, blood eosinophils and neutrophils, asthma control questionnaire Sum 6, number of controllers, FEV₁, body mass index (BMI), and hypertension were the phenotype-classifying variables determined by tree analysis that assigned 79.5% to the appropriate cluster. Among the cytokines measured, IL-1RA, YKL40/CHI3L1, IP-10/CXCL10, RANTES/CCL5, and TIMP-1 were useful biomarkers for classifying GINA 4, 5 phenotypes.

Conclusions: Five distinct phenotypes were identified for moderate to severe asthma and may be classified using clinical and molecular variables (Registered in UMIN-CTR; UMIN000027776.)

© 2022 Japanese Society of Allergology. Published by Elsevier B.V. This is an open access article under the CC BY-NC-ND license (<http://creativecommons.org/licenses/by-nc-nd/4.0/>).

Introduction

Asthma is a global health problem that affects around 300 million patients of all ages.¹ Evidence on the diversity and heterogeneity of the pathogenesis, symptoms, triggers, severity, response to treatment, and prognosis of asthma has been established. Among patients with asthma, 5%–10% have severe asthma (SA), which is clinically characterized by poor control and treatment refractoriness.² Even SA patients receiving Global Initiative for Asthma (GINA) Step 4 or 5 treatment (GINA 4, 5), with proper adherence and correct inhaler technique, may have poor asthma control.^{2,3}

In an attempt to understand the disease background, mechanisms, and clinical characteristics of asthma, cluster analyses of large numbers of asthma patients have been employed to determine clinical phenotypes in many different regions in the world.^{4,5} The different phenotypes were identified to define different clinical characteristics and were believed to have different underlying pathophysiologic mechanisms associated with various biomarkers.^{4,6–12} In addition to the need to identify phenotypes in asthma, the determination of biomarkers remains an important task. Biomarkers of type 2 inflammation include elevated serum periostin, blood and sputum eosinophil counts, fractional exhaled nitric oxide (FeNO), and antigen-specific IgE. These biomarkers have been widely accepted and are now increasingly used to predict response and help in selecting patients for biological drug treatment.^{13–17} However, in real-world clinical settings, the use of these biomarkers to identify asthma phenotypes has not been established.

In Japan, the population is unique in terms of having a long life expectancy and a relatively uniform racial background. Moreover, all Japanese residents have mandatory health insurance. Therefore, a nationwide prospective survey would be necessary to identify the components and distribution of asthma phenotypes, which may be different in Japan compared to other countries. Therefore, we aimed to elucidate the distribution of asthma phenotypes in Japan using cluster analysis and characterize the phenotypes and underlying pathogenesis by measuring various serum and urine biomarkers.

Methods

Study design

This study (NHOM Asthma Study) was a multicenter, prospective, observational cohort conducted from July 2017 to September 2018 at 27 participating national hospitals (mainly belonging to the National Hospital Organization, NHO) across Japan (Supplementary Fig. 1). The study protocol was approved by the ethics committee of the National Hospital Organization, and written informed consent was obtained from all participants. The study was conducted in accordance with the Ethical Guidelines for Medical and Health Research Involving Human Subjects (the Ministry of Education, Culture, Sports, Science and Technology and the Ministry of Health, Labor and Welfare, Japan) and complied with the ethical principles consistent with the Declaration of Helsinki. This study was registered in the University Hospital Medical Information Network Clinical Trials Registry (UMIN-CTR; UMIN000027776).

Patients

Adult patients (aged ≥ 18 years) diagnosed and treated for asthma for more than one year and managed by pulmonary or allergy specialists in the participating hospitals were recruited. In the cohort, patients on medium- or high-dose inhaled corticosteroids (ICS) in combination with more than one asthma controller, i.e., long-acting β_2 agonist; leukotriene receptor antagonist; sustained-release theophylline; tiotropium bromide hydrate, which is a long-acting anticholinergic; omalizumab; mepolizumab; and systemic corticosteroid, were defined as GINA Step 4 or 5 (GINA 4, 5). Other patients were defined as GINA Step 1, 2, or 3 (GINA 1–3). Patients were treated based on their physicians' standard practices in a real-world clinical setting.

Data collection and outcome measures

The physician in charge collected the following clinical data from the medical records using an electronic data capture system:

age, sex, height, weight, asthma treatment status, and laboratory variables, including lung function, peripheral white blood cell (WBC) and differential count, total and specific IgE, forced oscillation technique, and FeNO. For biologics, only omalizumab and mepolizumab were available in Japan during the study period.

Patients were requested to complete and send by mail a basic questionnaire, which included demographic data, such as age, sex, family history, smoking history, medical history, allergy status, pet breeding, and presence of comorbidities; the asthma control questionnaire (ACQ) 6; the asthma quality of life questionnaire; the self-assessment of allergic rhinitis and asthma questionnaire; and the adherence starts with knowledge 20. For patients in GINA 4, 5, and who were able to follow-up for one year, asthma control was assessed by the physicians based on unscheduled visits, hospital admission, asthma exacerbation that required systemic corticosteroids, intensive care unit admission, and emergency room visits. Serum and urine samples were collected and frozen at the participating hospitals before being sent to the central laboratory to measure the biomarkers.

The primary endpoint was the identification of the phenotypes of GINA 4, 5 in the study population. The secondary outcomes included the characteristics of the GINA 4, 5, compared with GINA 1–3; the distribution of the molecular biomarkers in GINA 4, 5 phenotypes; and identification of the determinants of each GINA 4, 5 phenotype.

Biomarker measurements

The serum samples from GINA 4, 5 were stored frozen at -20°C at the Tokyo National Hospital for as long as one year and were subsequently analyzed for biomarker levels using R&D Systems Luminex Assay (R&D Systems, Minneapolis, MN, USA) and MAGPIX System (Luminex, Austin, TX, USA), according to the manufacturers' instructions. The biomarkers analyzed were eotaxin 1/CCL11, IFN- γ , interleukin (IL)-1 RA, IL-2, IL-4, IL-5, IL-6, IL-7, IL-8/CXCL8, IL-12p70, IL-13, IL-18, IL-25, IL-33, leptin, MCP-1/CCL2, MIP-1 α /CCL3, MIP-1 β /CCL4, MMP1, MMP2, MMP3, MMP8, MMP12, IP-10/CXCL10, periostin, PDGF-BB, RANTES/CCL5, ST2/IL-1R4, TARC/CCL17, TIMP-1, TNF- α , and YKL40/CHI3L1. Before performing the respective assays, the serum samples were diluted $10 \times$ for IL-1RA, leptin, MMP1, MMP3, periostin, and YKL40/CHI3L1 and $30 \times$ for MMP2, PDGF-BB, RANTES, and TIMP-1. Standard curves were generated using serial dilutions of the assay standards for quantification. The xPONENT 4.2 Software for MAGPIX was used for bead acquisition and analysis of median fluorescence intensity. For TGF- β analysis, the serum samples were diluted $70 \times$ before analysis using an ELISA kit (ThermoFisher Scientific, Waltham, MA, USA).

Urine LTE4 measurement

The LTE4 concentration in spot urine was measured, as previously described¹⁸ and was expressed as pg/mL of creatinine.

Statistical analysis

Ward's minimum variance hierarchical clustering method was performed. Dendrograms were used to determine the number of clusters. Variables with a high number of missing values were excluded from the cluster analysis; if the correlation between variables was high, cluster analysis was limited to one variable from a clinical perspective. Finally, 26 variables from the patient's background, asthma history, comorbidities, laboratory examinations, asthma treatment, and asthma control were chosen for the analysis (Supplementary Table 1). For continuous variables, z-

scores were used, whereas for categorical variables, the designations 0 and 1 were used. Stepwise discriminant analysis was performed to select the variables that have a significant impact on clustering among the variables used in the cluster analysis. The selected variables were then used to create a decision tree to evaluate patient classification. To avoid overfitting, the decision tree was cost-complexity pruned. To compare differences among the clusters, analysis of variance, Kruskal–Wallis, and chi-square tests were used for parametric continuous, nonparametric continuous, and categorical variables, respectively. The cytokine and urine LTE4 measurements were summarized using the geometric mean and standard deviation, and the log-transformed values were used for statistical tests.

All statistical analyses were conducted using SAS version 9.4 (SAS Institute Inc., Cary, NC, USA) and R version 3.6.2 (R Core Team 2019, R Foundation for Statistical Computing, Vienna, Austria). A p-value of <0.05 was considered statistically significant. The tests for the biomarkers were evaluated with Bonferroni's correction at a significance level of 0.00147 ($\approx 0.05/34$).

Results

Comparison of baseline characteristics between GINA 4, 5, and GINA 1–3 in Japan

Of the 1925 patients enrolled in the study, 738 (38.3%) were classified as having GINA 4, 5. Among the enrolled patients, one had missing baseline data, and 152 did not meet the eligibility criteria. A total of 1772 patients were analyzed to compare GINA 4, 5, and GINA 1–3. Further, 498 patients in GINA 4, 5 with the full analysis set were subjected for cluster analysis (Fig. 1).

As shown in Table 1, compared with patients with GINA 1–3, those with GINA 4, 5 were significantly older, had longer disease duration, a more frequent family history of asthma, and a higher proportion of patients with a smoking history. The comorbidities of sinusitis, pollinosis, drug allergy, chronic obstructive pulmonary disease (COPD), gastroesophageal reflux disease (GERD), sleep apnea syndrome (SAS), hypertension, and aspirin-exacerbated respiratory disease (AERD) were more frequent in patients with GINA 4, 5 than in those with GINA 1–3.

Compared with patients with GINA 1–3, those with GINA 4, 5 had a significantly lower lung function, including lower FEV1, % FEV1, and FEV1%. Both FeNO and WBC counts were significantly higher in GINA 4, 5 than in GINA 1–3, but there was no significant difference in the eosinophil count and total IgE. Alternatively, compared with the GINA 1–3 group, the GINA 4, 5 group had a significantly higher proportion of patients who had atopy and positivity for specific IgE against molds and pollens.

For asthma therapy, the ICS doses were higher, and there was more frequent use of asthma controllers in the GINA 4, 5 group than in the GINA 1–3 group. Compared with the GINA 1–3 group, the GINA 4, 5 group had a more frequent intake of oral corticosteroid (OCS) (12.9% vs. 2.3%, $p < 0.001$) and biologics (11.6% vs. 0.3%, $p < 0.001$) for asthma control. Based on the significantly higher ACQ 6 and more frequent unscheduled visits and hospital admissions, asthma control was worse among patients with GINA 4, 5 than in those with GINA 1–3.

Cluster analysis of patients with GINA 4, 5

For cluster analysis of patients with GINA 4, 5 using Ward's method, only those with a full dataset of the variables shown in Supplementary Table 1 were selected. In any of the variables, there were no significant differences between the overall GINA 4, 5

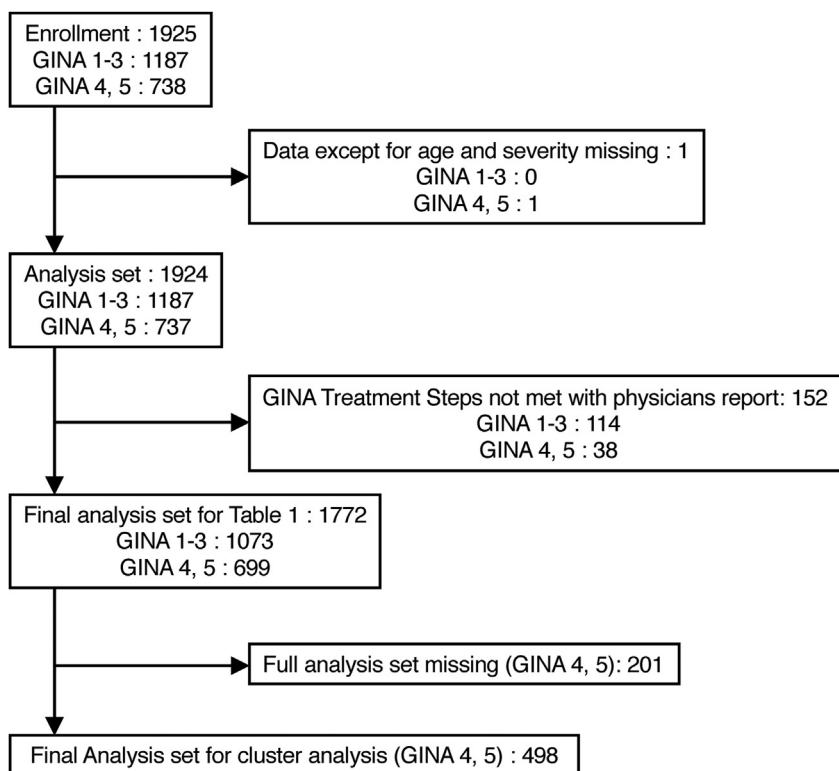


Fig. 1. Patient flow diagram.

population and the population used for the cluster analysis (data not shown). A total of 498 patients were classified into five clusters by the dendrogram (Fig. 2, Table 2). The characteristics of these five clusters are given below.

Cluster 1: late-onset, old, less-atopic

A total of 119 patients (23.9%) were grouped in this cluster, including a relatively old population with equal sex distribution. All cases in cluster 1 were adult-onset asthma, with the shortest asthma duration among the clusters. This cluster comprised the largest proportion of ex-smokers had a high percentage of patients with COPD, and comprised the smallest percentage of patients with atopy. Interestingly, FEV₁ was preserved in this cluster, with patients who used the least ICS dose and the smallest number of controllers and had the least frequent OCS and biologics used. The ACQ 6 and the number of unscheduled visits, acute exacerbations, and admissions for asthma were the lowest in this cluster.

Cluster 2: late-onset, old, eosinophilic, low FEV₁

Cluster 2 included 116 subjects (23.3%) and comprised the oldest age at enrollment, the least female proportion, and the second oldest asthma onset. This cluster included more ex-smokers and had the most frequent comorbidity of Asthma-COPD overlap, defined as patients with a smoking history of more than 10 pack-years and FEV₁/FVC <70%, self-reported COPD, and the lowest FEV₁, FEV₁%, and %FEV₁. Additionally, cluster 2 cases accounted for the highest FeNO, blood eosinophils, and total IgE, and the second-highest proportion of positive cases for the specific IgE against molds. The ICS dose was lower for asthma treatment, but the number of controllers was higher in cluster 2 than in the other clusters. The frequency of OCS and biologics use was the second

highest following cluster 5. For asthma control, cluster 2 had the highest ACQ Sum 6 and relatively frequent unscheduled visits, acute exacerbation, and admission.

Cluster 3: early-onset, long-duration, atopic, poorly controlled

Cluster 3 included the most number of patients (n = 127, 25.5%). Subjects in cluster 3 had the youngest disease onset, the longest duration of asthma, and the highest body mass index (BMI). The proportion of adult-onset asthma cases was the lowest, and a family history of asthma was the highest in cluster 3. There was no characteristic comorbidity, except for a high rate of allergic conjunctivitis. However, pulmonary function, as assessed by FEV₁, FEV₁%, and %FEV₁, was the second-lowest in cluster 3. The percentage of patients with atopy was the highest in cluster 3, with the second-highest total IgE. For asthma controller therapy, the proportion of patients on high-dose ICS was the second largest among the clusters. Although the ACQ Sum 6 was not high, the number of unscheduled visits and acute exacerbations were high in cluster 3.

Cluster 4: early-onset, young, female-dominant, atopic

Cluster 4 included 104 subjects (20.9%), was female-dominant and comprised the youngest patients with early disease onset. The proportion of never smokers was the largest in this cluster. Moreover, the patients in cluster 4 had frequent comorbidities of other allergic diseases, such as allergic rhinitis, atopic dermatitis, pollinosis, and AERD. The FEV₁ in this cluster was the best among the clusters. The prevalence of atopy was high, and specific IgEs against dust mites, pets, and pollen were frequently detected in cluster 4. Asthma controller therapy was relatively not intense in this cluster, and the asthma control status was good, based on the number of unscheduled visits, acute exacerbations, and admissions.

Table 1

Baseline characteristics of GINA 4, 5 and GINA 1–3.

Variables	GINA 1–3 (n = 1073)	GINA 4, 5 (n = 699)	Total (n = 1772)	P value
Age at enrolment, years	61.7 (15.2) [†]	63.5 (14.9)	62.4 (15.1)	0.011
Sex, % female	61.9	59.4	60.9	0.290
BMI, kg/m ²	23.8 (4.3)	24.1 (4.4)	23.9 (4.4)	0.159
Age of asthma onset, years	44.1 (21.5)	42.9 (21.2)	43.6 (21.4)	0.295
Asthma duration, years	15.1 (14.8)	17.8 (14.8)	16.1 (14.9)	<0.001
Course of asthma, %				0.840
Carried over from childhood asthma	5.7	5.3	5.6	
Recurred from childhood asthma	10.0	10.8	10.3	
Adult onset	84.3	83.9	84.1	
Family history of asthma, %	25.7	30.3	27.5	0.034
Smoking status, %				0.037
Current smoker	4.9	4.9	4.9	
Ex-smoker	35.6	41.7	38.0	
Never smoker	59.5	53.4	57.1	
Smoking history, pack-years	9.2 (18.3)	11.9 (24.1)	10.3 (20.8)	0.008
Comorbidities, %				
Sinusitis	36.3	43.2	39.1	0.004
Allergic rhinitis	27.9	27.5	27.7	0.878
Allergic conjunctivitis	8.4	10.5	9.2	0.155
Atopic dermatitis	8.8	9.1	8.9	0.819
Pollinosis	31.5	37.7	33.9	0.008
Food allergy	7.6	8.2	7.8	0.600
Drug allergy	9.2	12.4	10.5	0.036
Anaphylaxis	5.9	5.9	5.9	0.990
Urticaria	11.5	11.0	11.3	0.762
COPD	5.1	10.2	7.1	<0.001
GERD	15.5	20.3	17.4	0.010
SAS	6.1	9.0	7.2	0.024
Hypertension	27.1	32.5	29.3	0.015
Otitis media	14.6	15.3	14.9	0.691
AERD	3.8	8.2	5.5	<0.001
Mental disorder	9.7	12.7	10.9	0.058
FEV ₁ , mL	2192 (742)	2045 (798)	2131 (769)	<0.001
FEV ₁ % pred, %	97 (21)	88 (29)	94 (24)	0.004
FEV ₁ /FVC, %	73 (12)	70 (14)	72 (13)	<0.001
FeNO, ppb	33.9 (31.7)	38.7 (38.8)	35.8 (34.8)	0.015
WBC count, /μL	6050 (1676)	6623 (1966)	6293 (1827)	<0.001
Blood eosinophils, /μL	279 (297)	256 (290)	269 (294)	0.123
Total IgE, IU/mL	489.4 (1236.7)	457.1 (909.2)	474.5 (1097.5)	0.575
Atopy [†] , %	51.3	57.8	53.8	0.007
Specific IgE (dust mites), %	38.8	38.6	38.7	0.952
Specific IgE (molds), %	17.2	27.5	21.3	<0.001
Specific IgE (cats/dogs), %	12.3	15.3	13.5	0.070
Specific IgE (pollen), %	45.8	52.8	48.5	0.004
Specific IgE (insects), %	20.8	22.5	21.4	0.400
Treatment				
ICS dose, %				
Low	61.6	13.6	52.0	<0.001
Medium	36.7	49.2	39.2	
High	1.7	37.3	8.8	
Number of controllers	1.3 (0.9)	2.8 (1.1)	1.9 (1.2)	<0.001
OCS use, %	2.3	12.9	6.5	<0.001
OCS, PSL mg	0.1 (0.9)	0.9 (3.0)	0.4 (2.0)	<0.001
Use of biologics, %	0.3	11.6	4.7	<0.001
ACQ Sum 6	0.6 (0.7)	1.0 (0.9)	0.7 (0.8)	<0.001
Asthma control				
Unscheduled visits, %				
0	79.4	62.2	72.6	<0.001
1	9.7	14.3	11.5	
2	3.6%	7.8	5.3	
3	1.7	4.8	2.9	
4	2.0	2.6	2.3	
5–9	2.8	5.9	4.0	
≥10	0.8	2.4	1.4	
Admission, %				
0	92.2	77.6	86.4	<0.001
1	5.2	12.9	8.3	
2	1.4	4.2	2.5	

(continued on next page)

Table 1 (continued)

Variables	GINA 1–3 (n = 1073)	GINA 4, 5 (n = 699)	Total (n = 1772)	P value
3	0.7	2.4	1.4	
4	0.3	1.1	0.6	
5–9	0.2	1.3	0.6	
≥10	0.0	0.5	0.2	

ACQ, asthma control questionnaire; AERD, aspirin-exacerbated respiratory disease; FeNO, fractional exhaled nitric oxide; GERD, gastroesophageal reflux disease; ICS, inhaled corticosteroid; OCS, oral corticosteroid; SAS, sleep apnea syndrome.
† Numeric data are expressed as mean (SD).
‡ Specific IgE responsiveness to common inhaled allergens.

Cluster 5: female-dominant, T1/T2-mixed, most severe

Cluster 5 was the smallest cluster with 32 subjects (6.4%) and comprised a female-dominant population with the highest BMI and, mainly, adult-onset asthma. The proportion of current smokers was the largest in cluster 5 and had the most frequent comorbidities of anaphylaxis and otitis media. Cluster 5 had a better %FEV₁ than clusters 2 and 3. Although eosinophil counts of cluster 5 were low, FeNO was the second highest. Notably, the WBC and neutrophil counts were the highest in cluster 5. The proportions of patients who used high-dose ICS, OCS, and biologics were the highest in cluster 5 among all clusters. The ACQ Sum 6 and the number of unscheduled visits, asthma exacerbations, and admissions were high.

Biomarkers

Table 3 shows a comparison of serum biomarkers and urine LTE4 levels among the clusters. P-values between the two

respectively clusters analyzed by Tukey–Kramer methods are shown in Supplemental Table 2. Cluster 5 had the highest levels of IL-1RA, MMP3, MMP8, and ST2/IL-1R4 and tended to have the highest levels of IFN- γ , IL-6, IL-7, MCP-1/CCL2, MMP12, and TGF- β . Among them, IL-1RA and MMP8 were significantly higher than any other cluster. Serum leptin was significantly higher than clusters 2 and 4, and MMP3 was significantly higher than clusters 1, 3, and 4. Cluster 4, which included the youngest cases with atopy, showed significantly lower serum IL-1RA, ST2/IL-1R4, and YKL-40/CHI3L1 compared to all the other clusters. Cluster 4 also had significantly higher IL-12p70 and IL-33 than clusters 1, 2, and 3. Cluster 2, which showed eosinophilia, had significantly higher serum IL-5 and urine LTE4 compared to clusters 1 and 3. Serum MMP-3 and TIMP1 in cluster 2 was significantly higher than clusters 1 and 4. In cluster 2, MMP-1 was significantly higher than cluster 1, and MMP-2 was significantly higher than clusters 3 and 4. The older cases in clusters 1 and 2 had high levels of periostin and YKL40/CHI3L1. Overweight patients in clusters 3 and 5 had significantly high levels of leptin.

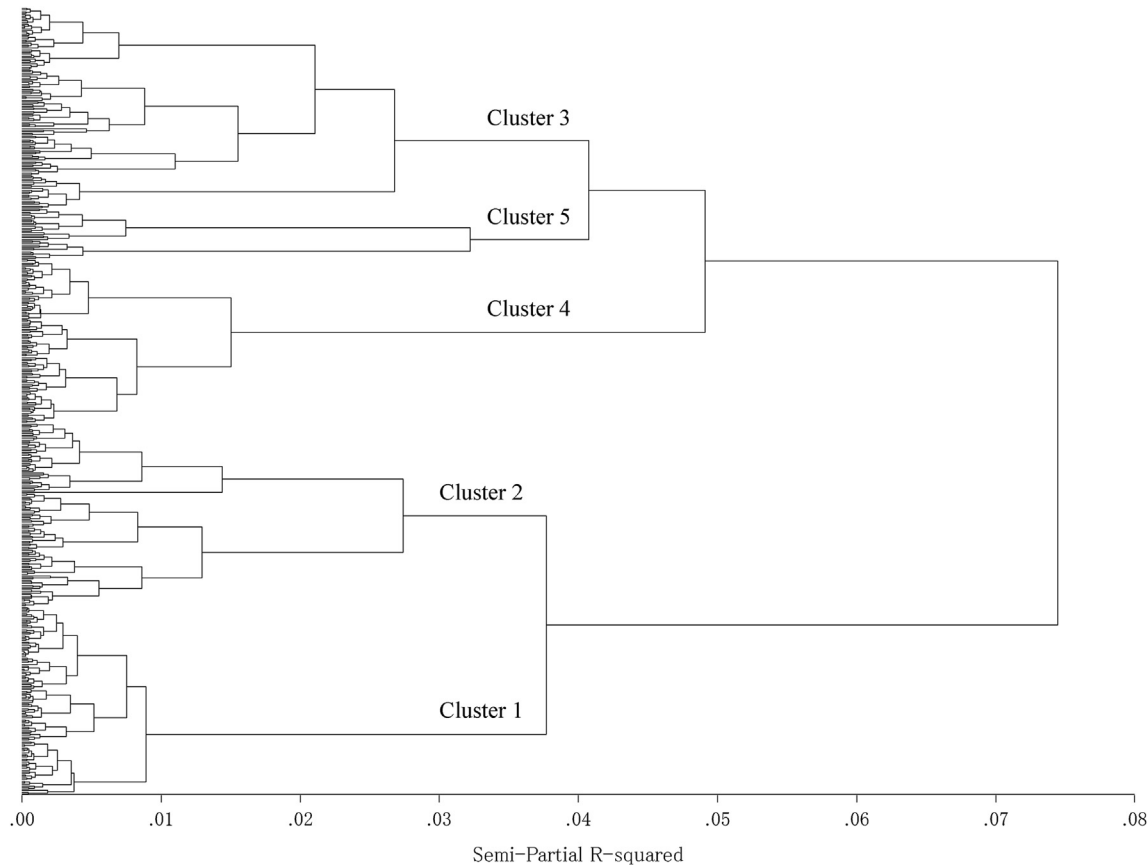


Fig. 2. Dendrogram.

Table 2
Cluster analysis of GINA 4, 5.

Summary	Cluster 1 (n = 119) Late onset, Old, Less-atopic	Cluster 2 (n = 116) Late onset, Old, Eosinophilic, Low FEV1	Cluster 3 (n = 127) Early onset, Long duration, Atopic, Poorly controlled	Cluster 4 (n = 104) Early onset, Young, Female-dominant, Atopic	Cluster 5 (n = 32) Female-dominant, T1/T2 mixed, Most severe	Significance (P value)*
Age at enrolment, years	69.6 (9.9) [†]	71.6 (9.4)	63.2 (13.7)	47.8 (11.7)	61.8 (12.5)	<0.001
Sex, % female	56.3	47.4	59.8	75.0	75.0	<0.001
BMI, kg/m ²	24.3 (3.2)	24.2 (3.8)	25.5 (5.7)	21.5 (3.3)	25.5 (3.5)	<0.001
Age of asthma onset, years	61.3 (11.2)	55.1 (12.5)	26.3 (16.5)	29.4 (15.6)	43.5 (20.3)	<0.001
Asthma duration, years	8.3 (7.0)	16.6 (11.2)	30.6 (15.6)	12.5 (9.1)	14.7 (11.8)	<0.001
Course of asthma, %						<0.001
Carried over from childhood asthma	0.0	0.0	11.8	3.8	3.1	
Recurred from childhood asthma	0.0	0.0	22.8	19.2	9.4	
Adult onset	100.0	100.0	65.4	76.9	87.5	
Family history of asthma, %	24.4	31.0	40.9	24.0	31.3	0.030
Smoking status, %						<0.001
Current smoker	1.7	3.4	8.7	2.9	9.4	
Ex-smoker	55.5	50.0	35.4	26.9	43.8	
Never smoker	42.9	46.6	55.9	70.2	46.9	
Smoking history, pack-years	15.0 (28.3)	15.4 (23.8)	9.0 (15.3)	3.1 (8.8)	16.5 (48.6)	<0.001
Asthma-COPD overlap, [‡] %	11.8	31.9	17.3	1.0	18.8	<0.001
Comorbidities (self-reported), %						
Sinusitis	46.2	47.4	46.5	46.2	37.5	0.904
Allergic rhinitis	21.0	19.8	29.9	47.1	31.3	<0.001
Allergic conjunctivitis	5.0	5.2	17.3	14.4	15.6	0.004
Atopic dermatitis	3.4	4.3	13.4	17.3	12.5	<0.001
Pollinosis	34.5	31.9	29.9	66.3	46.9	<0.001
Food allergy	3.4	6.0	11.0	11.5	15.6	0.052
Drug allergy	10.1	11.2	12.6	21.2	9.4	0.108
Anaphylaxis	0.8	6.9	10.2	5.8	12.5	0.023
Urticaria	9.2	8.6	18.1	9.6	9.4	0.111
COPD	12.3	18.9	5.0	0.0	6.5	<0.001
GERD	20.2	24.1	22.8	11.5	25.0	0.139
SAS	10.1	8.6	9.4	8.7	12.5	0.966
Hypertension	41.2	47.4	31.5	5.8	43.8	<0.001
Otitis media	7.6	19.8	15.0	18.3	37.5	<0.001
AERD	1.8	7.3	11.6	15.8	6.5	0.005
Mental disorder	11.2	8.2	15.4	20.0	16.1	0.123
FEV ₁ , mL	2108 (640)	1624 (643)	1918 (704)	2670 (791)	2023 (796)	<0.001
FEV ₁ % pred, %	101 (21)	77 (27)	86 (25)	102 (17)	93 (27)	<0.001
FEV ₁ /FVC, %	73 (10)	63 (14)	68 (13)	79 (10)	70 (16)	<0.001
FeNO, ppb	30.5 (24.4)	59.3 (51.7)	33.0 (30.2)	34.4 (37.5)	41.2 (46.7)	<0.001
WBC count, /μL	5940 (1295)	6968 (1813)	6772 (1810)	5673 (1359)	10,081 (3059)	<0.001
Blood eosinophils, /μL	178 (151)	464 (454)	216 (212)	205 (174)	131 (134)	<0.001
Blood neutrophils, /μL	3393 (1064)	4059 (1347)	4046 (1560)	3308 (1066)	7538 (2881)	<0.001
Total IgE, IU/mL	321.2 (562.4)	709.7 (1586.7)	540.9 (820.8)	245.6 (362.6)	350.9 (568.2)	0.002
Atopy [§] , %	49.6	60.3	70.1	67.3	53.1	0.009
Specific IgE (dust mites) %	23.5	33.6	56.7	51.0	37.5	<0.001
Specific IgE (molds), %	17.6	35.3	39.4	21.2	21.9	<0.001
Specific IgE (cats/dogs), %	7.6	11.2	18.9	23.1	15.6	0.010
Specific IgE (pollen), %	46.2	59.5	61.4	70.2	43.8	0.002
Specific IgE (insects), %	16.0	28.4	25.2	26.0	18.8	0.178
Treatment						
ICS dose, %						
~ Medium	60.5	58.7	38.6	50.0	34.4	0.006
High	39.5	41.4	61.4	50.0	65.6	
Number of controllers, %	2.2 (0.8)	3.2 (1.0)	2.9 (1.1)	3.0 (1.1)	3.3 (0.9)	<0.001
OCS use, %	1.7	19.0	16.5	15.4	31.3	<0.001
OCS, PSL mg	0.1 (0.6)	1.3 (3.8)	0.9 (2.1)	0.8 (2.1)	3.3 (6.7)	<0.001
Use of biologics, %	5.0	17.2	15.0	12.5	28.1	0.005
ACQ Sum 6	0.6 (0.6)	1.4 (1.0)	1.0 (1.0)	0.7 (0.7)	1.3 (0.9)	<0.001
Asthma control						
Unscheduled visits, %						
0	84.9	83.6	76.4	83.7	46.9	<0.001
1	13.4	10.3	11.0	9.6	15.6	
2	0.8	1.7	2.4	5.8	15.6	
3	0.8	2.6	3.9	1.0	3.1	
4	0.0	0.9	2.4	0.0	6.3	
5–9	0.0	0.9	3.9	0.0	9.4	
≥10	0.0	0.0	0.0	0.0	3.1	
Acute exacerbation, %						
0	81.5	59.5	55.9	76.9	25.0	<0.001
1	16.8	25.0	15.0	14.4	12.5	
2	0.8	6.9	7.9	6.7	9.4	

(continued on next page)

Table 2 (continued)

Summary	Cluster 1 (n = 119) Late onset, Old, Less-atopic	Cluster 2 (n = 116) Late onset, Old, Eosinophilic, Low FEV1	Cluster 3 (n = 127) Early onset, Long duration, Atopic, Poorly controlled	Cluster 4 (n = 104) Early onset, Young, Female-dominant, Atopic	Cluster 5 (n = 32) Female-dominant, T1/T2 mixed, Most severe	Significance (P value) [*]
3	0.8	6.0	5.5	0.0	3.1	
4	0.0	0.9	5.5	1.0	0.0	
5–9	0.0	1.7	9.4	1.0	15.6	
≥10	0.0	0.0	0.8	0.0	34.4	
Admission, %						
0	95.8	92.2	94.5	95.2	81.3	0.033
1	4.2	5.2	3.1	3.8	9.4	
2	0.0	1.7	2.4	1.0	3.1	
3	0.0	0.9	0.0	0.0	0.0	
5–9	0.0	0.0	0.0	0.0	6.3	

ACQ, asthma control questionnaire; AERD, aspirin-exacerbated respiratory disease; FeNO, fractional exhaled nitric oxide; GERD, gastroesophageal reflux disease; ICS, inhaled corticosteroid; OCS, oral corticosteroid; SAS, sleep apnea syndrome.

^{*} Using analysis of variance for continuous variables and Chi square test for proportions.

[†] Numeric data are expressed as mean (SD).

[‡] Asthma-COPD overlap patients were defined as patients with a smoking history of more than 10 pack-years and FEV₁/FVC <70%.

[§] Specific IgE responsiveness to common inhaled allergens.

Tree diagram

Figure 3 shows the tree analysis of the variables used for cluster analysis to classify patients with GINA 4, 5. The variables chosen for the tree analysis were the age of onset, disease duration, eosinophils, neutrophils, ACQ Sum 6, number of controllers, FEV₁, BMI, and hypertension; these were deemed to be important in determining the GINA 4, 5 phenotypes. Using this tree analysis, 79.5% of all subjects were assigned to the appropriate cluster. When the biomarkers shown in Table 3 were added as variables, only the level of IL-1RA was selected for inclusion in the tree analysis; however, the accuracy slightly went down to 78.7%, compared with the accuracy of the tree analysis that included only the clinical variables.

The characteristics of the patients who were not correctly assigned by the tree analysis are shown in Supplementary Table 3. Incorrect assignment of patients tended to be more frequent in clusters 2, 4, and 5 than in the others. In particular, cluster 5 cases of poorly controlled asthma with intense treatment tended to be incorrectly assigned. Among these incorrectly assigned patients, use of the IL-1RA, YKL40/CHI3L1, IP-10/CXCL10, RANTES/CCL5, and TIMP-1 biomarkers to classify patients with SA resulted in 62.4% accuracy (Supplementary Fig. 2).

Discussion

This nationwide asthma cohort study in Japan revealed that patients with GINA 4, 5, as defined by receipt of GINA 2016 treatment steps 4 or 5, were older and had longer disease duration, more family history of asthma, and more smoking history, than those who had GINA 1–3. Moreover, patients with GINA 4, 5 had relatively frequent sinusitis, pollinosis, drug allergy, COPD, GERD, SAS, hypertension, and AERD; had lower lung function; were on relatively intense asthma therapy, and had relatively poor asthma control. Among patients with GINA 4, 5, five distinct phenotypes were identified. These phenotypes differed in patient demographics; disease onset and duration; and disease expressions, such as atopy or nonatopy, lung function, asthma symptoms, medication use, and health care utilization. In addition, the different distributions of multiple serum biomarkers implied different pathophysiologic mechanisms among the five clinical phenotypes. The decision tree model that we used in this study differentiated the patients into five phenotypes with an accuracy of 79.5%.

This study may be one of the largest nationwide cohort studies on patients with asthma in Japan. The study population comprised well-characterized patients who visited core national hospitals that had advanced medical equipment. The clinical data are presumed to be reliable because specialists in pulmonary medicine and/or allergy were the ones who managed the patients. In addition to the clinical information from precise questionnaires, comprehensive biomarker levels were analyzed among patients with GINA 4, 5. Most of the characteristics in this present cohort were similar to the previously reported baseline characteristics (i.e., age, disease duration, and smoking history) of GINA 4, 5 cases, including a recent study in Japan,^{6,19–21} except for older age, which is likely due to Japan's high-age society. Moreover, similar to the previously reported cohorts, this present cohort had relatively frequent comorbidities, such as sinusitis, other allergic diseases, COPD, GERD, SAS, hypertension, and aspirin sensitivity, which may partly be explained by the older age of GINA 4, 5 cases. Interestingly, similar to a previous report,¹⁹ neutrophil count was high in GINA 4, 5; this may have partly resulted from the frequent use of systemic corticosteroids.

However, there were some differences between the present and previous studies. A recent report on GINA 4, 5 based on a health insurance database in Japan showed a lower percentage of patients with GINA 4, 5 (7.8%),²² than that in this study. Moreover, compared with this study, previous studies included GINA 4, 5 cases with lower FEV₁ and showed more frequent atopy in GINA 1–3 cases than in GINA 4, 5 cases.^{6,19–21} These differences may have resulted from the broader definition of GINA 4, 5 (i.e., less severe) in this study than in previous reports. Notably, the public health insurance system is applicable to all residents in Japan. In certain areas, the medical expenses for asthma caused by air pollution are subsidized; this intensified asthma treatment may have increased the apparent disease severity among patients in Japan. Another feature of the present cohort is that there is a high smoking history, which is a result of the enrollment setting of this study, where smokers and COPD patients were not excluded. However, this study represents the real-world clinical practice of asthma in Japan.

Asthma is characterized by variability in pathogenesis, presenting symptoms, disease severity, response to treatment, and prognosis. With the increasing treatment options for GINA 4, 5, considering the phenotypes in the decision making would be better and had been attempted by several clinical studies.^{4,6–10,23–27} In

Table 3

Biomarker levels among the GINA 4, 5 clusters.

Summary	Cluster 1 (n = 119) Late onset, Old, Less-atopic	Cluster 2 (n = 116) Late onset, Old, Eosinophilic, Low FEV ₁	Cluster 3 (n = 127) Early onset, Long duration, Atopic, Poorly controlled	Cluster 4 (n = 104) Early onset, Young, Female-dominant, Atopic	Cluster 5 (n = 32) Female-dominant, T1/T2 mixed, Most severe	Significance (P value)*
Eotaxin 1/CCL11 [pg/mL]	143.03 (1.76) [†]	161.43 (2.04)	137.95 (1.81)	138.37 (2.00)	148.21 (2.31)	0.348
IFN- γ [pg/mL]	25.29 (2.30)	27.22 (2.79)	29.18 (2.38)	36.10 (3.10)	36.60 (2.73)	0.043
IL-1RA [ng/mL]	1.16 (1.35)	1.31 (1.39)	1.27 (1.43)	1.01 (1.39)	1.71 (1.45)	<0.001
IL-2 [pg/mL]	36.88 (3.67)	32.51 (4.06)	32.30 (3.63)	48.68 (5.02)	47.40 (3.87)	0.128
IL-4 [pg/mL]	19.50 (3.38)	20.05 (3.12)	22.43 (3.17)	25.24 (3.76)	23.14 (3.36)	0.520
IL-5 [pg/mL]	2.28 (1.51)	2.79 (1.90)	2.20 (1.43)	2.45 (1.65)	2.28 (1.50)	0.002
IL-6 [pg/mL]	2.38 (1.45)	2.69 (1.67)	2.58 (1.60)	2.24 (1.37)	2.89 (1.76)	0.005
IL-7 [pg/mL]	14.07 (1.57)	13.96 (1.58)	14.59 (1.73)	16.48 (1.65)	16.77 (1.43)	0.037
IL-8/CXCL8 [pg/mL]	10.50 (1.98)	10.92 (1.87)	9.52 (2.07)	9.21 (2.09)	9.79 (1.89)	0.334
IL-12p70 [pg/mL]	75.07 (2.77)	68.55 (2.42)	74.86 (2.40)	110.01 (3.47)	88.00 (2.66)	0.007
IL-13 [pg/mL]	170.69 (1.72)	176.15 (1.72)	167.22 (1.69)	194.98 (2.08)	185.41 (1.69)	0.316
IL-18 [pg/mL]	162.60 (1.70)	172.63 (1.94)	162.32 (1.76)	147.01 (1.82)	198.08 (1.58)	0.096
IL-25 [pg/mL]	98.46 (1.43)	95.56 (1.26)	94.85 (1.30)	106.85 (1.72)	95.54 (1.18)	0.089
IL-33 [pg/mL]	8.21 (2.46)	8.32 (2.83)	8.94 (2.48)	13.10 (3.14)	11.86 (2.74)	0.002
Leptin [ng/mL]	22.84 (2.13)	20.75 (2.15)	24.78 (2.23)	16.46 (1.97)	31.59 (2.21)	<0.001
MCP-1/CCL2 [pg/mL]	367.74 (1.43)	368.93 (1.62)	364.95 (1.42)	301.59 (1.65)	379.58 (1.95)	0.002
MIP-1 α /CCL3 [pg/mL]	66.51 (1.84)	65.21 (1.89)	71.33 (1.89)	72.73 (2.17)	74.26 (2.03)	0.640
MIP-1 β /CCL4 [pg/mL]	203.13 (1.81)	190.30 (1.67)	201.42 (1.75)	193.53 (1.76)	220.48 (1.58)	0.675
MMP1 [ng/mL]	3.63 (1.72)	4.56 (1.86)	4.06 (1.83)	4.00 (1.81)	4.17 (1.73)	0.061
MMP2 [ng/mL]	258.27 (1.31)	275.94 (1.30)	250.29 (1.27)	247.30 (1.32)	247.90 (1.30)	0.014
MMP3 [ng/mL]	19.05 (1.64)	24.76 (1.83)	22.13 (1.89)	18.96 (1.84)	34.23 (2.14)	<0.001
MMP8 [ng/mL]	0.95 (2.18)	1.21 (1.97)	1.14 (2.04)	0.91 (1.94)	1.99 (1.74)	<0.001
MMP12 [pg/mL]	22.07 (2.29)	23.94 (2.58)	22.40 (2.29)	30.24 (2.89)	30.69 (2.61)	0.039
IP-10/CXCL10 [pg/mL]	16.98 (1.43)	18.36 (1.57)	17.45 (1.57)	13.38 (1.43)	16.13 (1.58)	<0.001
Periostin [ng/mL]	365.41 (1.59)	378.08 (1.61)	324.00 (1.56)	303.02 (1.46)	304.71 (1.64)	<0.001
PDGF-BB [ng/mL]	6.63 (1.54)	7.09 (1.63)	7.38 (1.59)	7.81 (1.44)	7.70 (1.55)	0.062
RANTES/CCL5 [ng/mL]	29.28 (1.64)	29.78 (1.67)	29.19 (1.68)	30.82 (1.55)	27.16 (1.71)	0.770
ST2/IL1R4 [ng/mL]	7.93 (1.56)	7.99 (1.66)	7.50 (1.58)	6.22 (1.66)	9.00 (1.67)	<0.001
TARC/CCL17 [pg/mL]	609.43 (1.97)	774.24 (2.02)	612.09 (2.08)	514.35 (1.87)	604.09 (2.04)	<0.001
TIMP-1 [ng/mL]	132.14 (1.22)	142.26 (1.22)	137.29 (1.23)	124.33 (1.20)	155.76 (1.21)	<0.001
TGF- β [ng/mL]	16.86 (1.36)	17.08 (1.41)	17.60 (1.50)	19.13 (1.31)	20.03 (1.32)	0.009
TNF- α [pg/mL]	3.66 (1.76)	3.93 (1.85)	3.71 (1.62)	4.70 (2.40)	3.73 (1.58)	0.028
YKL40/CHI3L1 [ng/mL]	68.92 (2.35)	68.78 (2.25)	52.80 (2.40)	24.74 (1.94)	52.81 (2.33)	<0.001
Urine LTE4 [pg/mg creatinine]	89.91 (1.90)	137.90 (2.45)	102.45 (2.11)	105.84 (2.16)	99.23 (2.48)	<0.001

[†] Numeric data expressed as geometric mean (geometric SD).

* Significance level was set at 0.00147 by Bonferroni's correction.

this study, an unsupervised modeling approach of cluster analysis was employed for phenotyping GINA 4, 5 in Japan to identify five phenotypes. Consistent with previous reports,^{4,6,8,9} this study identified phenotypes that were mainly differentiated by the onset, allergic/non-allergic pathophysiology, and symptom severity. Therefore, the characteristics that identify GINA 4, 5 phenotypes may be universally applicable. Most of the old patients who had relatively late disease onset were classified in clusters 1 and 2, which had different disease severities and degree of eosinophilia. Cluster 1 had a milder disease and had the best asthma control status, whereas cluster 2 had the highest percentage of Asthma-COPD overlap, declined pulmonary function, higher ACQ Sum 6, and more evident eosinophilia. Cluster 2 may be a mixed phenotype of both severe eosinophilic asthma with fixed airway obstruction^{6,19–21} and Asthma-COPD overlap as eosinophilic COPD with elevated IgE has been reported to constitute a phenotype in COPD.^{6,19–21} Previous report by Konno *et al.* clearly demonstrated that there are two distinct smoking asthma phenotypes, one of which presented high blood eosinophils and serum IgE with elevated sinus scores.²⁸ In the present study, cluster 2 may include both smoking phenotypes identified by Konno *et al.* The high proportion of smokers in the present cohort may have influenced the cluster analysis, where an independent study may be necessary for patients with asthma who smoked. Notably, doses of ICS and OCS and use of biologics were not the highest in cluster 2; this may be due to the more frequent comorbidities and older age of cluster 2

than in the other clusters. Patients with early-onset asthma with frequent family history of asthma, high rate of atopy, and other allergic diseases were classified in clusters 3 and 4. In cluster 3, observations, such as long asthma duration, the highest BMI, and the high percentage of current smokers, may have resulted in airflow limitation and poor asthma control, as seen in the high rate of unscheduled visits and acute exacerbations. Conversely, asthma control was fair in cluster 4, which comprised the youngest patients. Finally, the most severe cases with female dominance and obesity were classified as cluster 5. Notably, the use of asthma controllers and medications was intense, and the asthma control status was the worst in cluster 5. Therefore, cluster 5 may be the target for exploring the underlying pathogenesis and developing new therapeutic strategies.

In addition to the identification of clinical phenotypes, analysis of biomarker distribution was of special interest. One compelling finding was that the most severe cluster 5 showed the highest levels of multiple inflammatory mediators, growth factors, and chemokines (i.e., IL-1RA, MMP3, and MMP8) indicative of underlying systemic inflammation in cluster 5. Previous reports supported the concept of low-grade systemic inflammation in GINA 4, 5, such as elevated serum and tissue IL-6 and TNF- α in bronchoalveolar lavage fluid in asthmatic patients.^{29–32} It was noteworthy that chemokines for many of the inflammatory cells as well as mediators, which may be involved in airway remodeling, i.e., MMPs, were significantly elevated in cluster 5 suggestive of

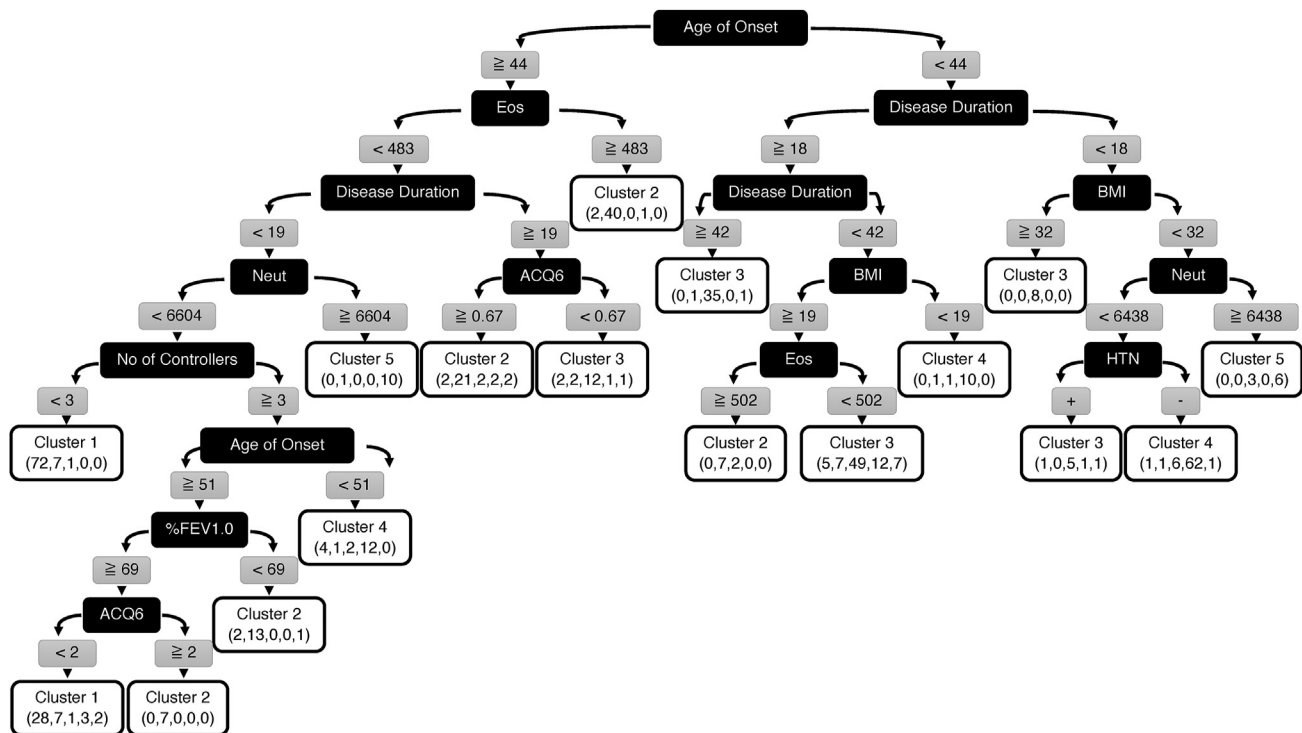


Fig. 3. Tree analysis. Using variables from the cluster analysis, a tree analysis was performed to assign GINA 4, 5 to five clusters. Numbers in parenthesis under each cluster indicate the number of patients belonging to each cluster (Clusters 1, 2, 3, 4, and 5).

promoted airway remodeling in this cluster, which would make the disease unresponsive to treatment.^{33–35} However, it is noteworthy that cluster 5 had the highest rate of OCS and biologics use, which may influence the level of serum biomarkers. Indeed, blood eosinophils were low and blood neutrophils were high, which may have been influenced by OCS use in cluster 5.

Aside from the elevated biomarkers in cluster 5, some biomarkers showed trends that correlated with clinical characteristics. The high serum IL-5, TARC/CCL17 and urine LTE4 levels in cluster 2, characterized by eosinophilia, suggested the potential treatment indications of eosinophil activating mediators for this cluster. The high levels of TIMP-1 and MMPs 1–3 in cluster 2 may have been related to smoking or COPD.^{36–38} In the overweight phenotypes clusters 3 and 5, results suggested the pathophysiologic role of the adipokine leptin. Furthermore, age may have influenced the cytokine levels, as demonstrated by the high levels of periostin and YKL40/CHI3L1 in the older phenotypes clusters 1 and 2.^{39,40} Interestingly, the tree analysis in this study revealed that the cytokine that was useful in assigning clusters was IL-1RA, which was high among the more severe clusters 2, 3, and 5. Although the relationships of IL-1RA with asthma and airway inflammation have been reported,^{41–43} the precise role of IL-1RA need to be further evaluated.

One of the purposes of this study was to improve our understanding of the basis for GINA 4 and 5 and to develop an asthma classification algorithm using comprehensive phenotyping approaches that reflect pathophysiology and disease heterogeneity. The most important variables for assigning the phenotypes were related to the age of onset and disease duration; type of inflammation based on the eosinophil or neutrophil count; %FEV₁; physical stature and comorbidities; medication use; and asthma control based on symptoms. Previous studies have similarly

identified age of asthma onset and current disease activity as the key features in discriminating the phenotypes.⁴⁴ Because the algorithm that we used in the present study was successful in classifying about 80% of GINA 4, 5 cases into clusters. It may be utilized to assign GINA 4, 5 to phenotypes for personalized asthma management.

The present study had several limitations. First, the definition of GINA 4, 5 was based on GINA treatment steps 4 or 5. However, the standard definition of SA includes a requirement for treatment with high-dose ICS plus a second controller and/or systemic corticosteroids for asthma control.² Therefore, a simple comparison of our results with previously reported data may not be accurate. Second, because the patients in the present cohort were recruited from national hospitals in Japan, their disease may have been more complex with more comorbidities, compared with those in previous cohorts. Third, the information on comorbidities in the present study was based on patients' questionnaires; hence, it may have been underestimated. Comorbidity with COPD is particularly important as previous studies have clearly demonstrated the asthma phenotype with COPD.^{6,19–21} Therefore, further studies on asthma phenotypes based on accurate medical examination of comorbidities would be valuable in the future. Fourth, this study did not have enough population to perform validation; therefore, it may be used for generating hypothesis until appropriate validation of phenotypes found in this study is completed. Lastly, because cluster analysis is a descriptive method, the clusters may have been defined without an underlying definite structure. Moreover, the variables used for cluster analysis might have conditioned the characteristics of the identified clusters.

In conclusion, the present cohort study on asthma revealed the characteristics and five distinct phenotypes of GINA 4, 5 in Japan. Well-defined differential molecular biomarkers within the clusters

may be useful for asthma phenotyping and may lead to new drugs for GINA 4, 5.

Acknowledgments

The authors thank all the patients and employees of the participating hospitals, Mr. Isao Asari and Mr. Masaaki Minegishi and Ms. Sayaka Igarashi, for their skilled technical assistance, and Ms. Taeko Kawabe and Ms. Mariko Yoshizawa for their excellent secretarial work. We are very grateful to Dr. Hiroyuki Nagase, M.D., Ph. D., from Teikyo University, for fruitful discussions. This project was supported by Grant-in-Aid for Clinical Research from the National Hospital Organization in Japan.

Appendix A. Supplementary data

Supplementary data to this article can be found online at <https://doi.org/10.1016/j.alit.2022.06.002>.

Conflict of interest

MS received Grants from Astellas, AstraZeneca, GlaxoSmithKline, Kyorin, MSD, Sanofi, and Shionogi, honoraria for lectures from AstraZeneca, Novartis Pharma, and Sanofi. YF received Grants from GlaxoSmithKline and Novartis Pharma, honoraria for lectures from Kyorin, Mylan, Novartis Pharma, Sanofi, ThermoFisher Diagnostics, and Torii Pharmaceutical. ST received honoraria for lectures from AstraZeneca, Boehringer Ingelheim Japan, Bristol-Meyers Squibb, GlaxoSmithKline, Kyorin, Novartis Pharma, Sanofi, and Teijin Pharma. MTa received Grants from GlaxoSmithKline, Novartis Pharma, and Sanofi. The rest of the authors have no conflict of interest.

Authors' contributions

MS, KO, YF, NK, and MTa designed the study and wrote the manuscript. TE, MA, YKa, MYo, YKi, TK, KC, YT, KHy, ST, TI, MYa, YH, TSa, YS, YM, YI, ST, TSh, KT, MTs, MO, KW, MH, GI, and KHi contributed to data collection. HH performed the statistical analysis and interpretation of the results. AMS contributed to data management and curation. All authors have read and approved the final manuscript. KO was a primary investigator for the grant submission.

References

- Bousquet J, Mantzouranis E, Cruz AA, Aït-Khaled N, Baena-Cagnani CE, Bleecker ER, et al. Uniform definition of asthma severity, control, and exacerbations: document presented for the World Health Organization Consultation on Severe Asthma. *J Allergy Clin Immunol* 2010;**126**:926–38.
- Chung KF, Wenzel SE, Brozek JL, Bush A, Castro M, Sterk PJ, et al. International ERS/ATS guidelines on definition, evaluation and treatment of severe asthma. *Eur Respir J* 2014;**43**:343–73.
- Hermosa JL, Sanchez CB, Rubio MC, Minguez MM, Walther JL. Factors associated with the control of severe asthma. *J Asthma* 2010;**47**:124–30.
- Halder P, Pavord ID, Shaw DE, Berry MA, Thomas M, Brightling CE, et al. Cluster analysis and clinical asthma phenotypes. *Am J Respir Crit Care Med* 2008;**178**:218–24.
- Moore WC, Meyers DA, Wenzel SE, Teague WG, Li H, Li X, et al. Identification of asthma phenotypes using cluster analysis in the severe asthma research program. *Am J Respir Crit Care Med* 2010;**181**:315–23.
- Moore WC, Bleecker ER, Curran-Everett D, Erzurum SC, Ameredes BT, Bacharier L, et al. Characterization of the severe asthma phenotype by the national heart, lung, and blood institute's severe asthma research program. *J Allergy Clin Immunol* 2007;**119**:405–13.
- Schatz M, Hsu JW, Zeiger RS, Chen W, Dorenbaum A, Chipps BE, et al. Phenotypes determined by cluster analysis in severe or difficult-to-treat asthma. *J Allergy Clin Immunol* 2014;**133**:1549–56.
- Wu W, Bleecker E, Moore W, Busse WW, Castro M, Chung KF, et al. Unsupervised phenotyping of Severe Asthma Research Program participants using expanded lung data. *J Allergy Clin Immunol* 2014;**133**:1280–8.
- Siroux V, Basagana X, Boudier A, Pin I, Garcia-Aymerich J, Vesin A, et al. Identifying adult asthma phenotypes using a clustering approach. *Eur Respir J* 2011;**38**:310–7.
- Leflaudeux D, De Meulder B, Loza MJ, Peffer N, Rowe A, Baribaud F, et al. U-BIOPRED clinical adult asthma clusters linked to a subset of sputum omics. *J Allergy Clin Immunol* 2017;**139**:1797–807.
- Pavlidis S, Takahashi K, Ng Kee Kwong F, Xie J, Hoda U, Sun K, et al. "T2-high" in severe asthma related to blood eosinophil, exhaled nitric oxide and serum periostin. *Eur Respir J* 2019;**53**:1800938.
- Kuo CS, Pavlidis S, Loza M, Baribaud F, Rowe A, Pandis I, et al. T-helper cell type 2 (Th2) and non-Th2 molecular phenotypes of asthma using sputum transcriptomics in U-BIOPRED. *Eur Respir J* 2017;**49**:1602135.
- Castro-Rodriguez JA, Holberg CJ, Wright AL, Martinez FD. A clinical index to define risk of asthma in young children with recurrent wheezing. *Am J Respir Crit Care Med* 2000;**162**:1403–6.
- Ortega H, Li H, Suruki R, Albers F, Gordon D, Yancey S. Cluster analysis and characterization of response to mepolizumab. A step closer to personalized medicine for patients with severe asthma. *Ann Am Thorac Soc* 2014;**11**:1011–7.
- Corren J, Lemanske RF, Hanania NA, Korenblat PE, Parsey MV, Arron JR, et al. Lebrikizumab treatment in adults with asthma. *N Engl J Med* 2011;**365**:1088–98.
- Djukanovic R, Wilson SJ, Kraft M, Jarjour NN, Steel M, Chung KF, et al. Effects of treatment with anti-immunoglobulin E antibody omalizumab on airway inflammation in allergic asthma. *Am J Respir Crit Care Med* 2004;**170**:583–93.
- Hanania NA, Wenzel S, Rosen K, Hsieh HJ, Mosesova S, Choy DF, et al. Exploring the effects of omalizumab in allergic asthma: an analysis of biomarkers in the EXTRA study. *Am J Respir Crit Care Med* 2013;**187**:804–11.
- Kawagishi Y, Mita H, Taniguchi M, Maruyama M, Oosaki R, Higashi N, et al. Leukotriene C4 synthase promoter polymorphism in Japanese patients with aspirin-induced asthma. *J Allergy Clin Immunol* 2002;**109**:936–42.
- The ENFUMOSA cross-sectional European multicentre study of the clinical phenotype of chronic severe asthma. European Network for Understanding Mechanisms of Severe Asthma. *Eur Respir J* 2003;**22**:470–7.
- Shaw DE, Sousa AR, Fowler SJ, Fleming LJ, Roberts G, Corfield J, et al. Clinical and inflammatory characteristics of the European U-BIOPRED adult severe asthma cohort. *Eur Respir J* 2015;**46**:1308–21.
- Wang E, Wechsler ME, Tran TN, Heaney LG, Jones RC, Menzies-Gow AN, et al. Characterization of severe asthma worldwide: data from the international severe asthma Registry. *Chest* 2020;**157**:790–804.
- Nagase H, Adachi M, Matsunaga K, Yoshida A, Okoba T, Hayashi N, et al. Prevalence, disease burden, and treatment reality of patients with severe, uncontrolled asthma in Japan. *Allergol Int* 2020;**69**:53–60.
- Kaneko Y, Masuko H, Sakamoto T, Iijima H, Naito T, Yatagai Y, et al. Asthma phenotypes in Japanese adults - their associations with the CCL5 ADRB2 genotypes. *Allergol Int* 2013;**62**:113–21.
- Gupta S, Hartley R, Khan UT, Singapur A, Hargadon B, Monteiro W, et al. Quantitative computed tomography-derived clusters: redefining airway remodeling in asthmatic patients. *J Allergy Clin Immunol* 2014;**133**:729–38. e718.
- Moore WC, Hastie AT, Li X, Li H, Busse WW, Jarjour NN, et al. Sputum neutrophil counts are associated with more severe asthma phenotypes using cluster analysis. *J Allergy Clin Immunol* 2014;**133**:1557–63. e1555.
- Baines KJ, Simpson JL, Wood LC, Scott RJ, Gibson PG. Transcriptional phenotypes of asthma defined by gene expression profiling of induced sputum samples. *J Allergy Clin Immunol* 2011;**127**:153–60. 160.e1–9.
- Yan X, Chu JH, Gomez J, Koenigs M, Holm C, He X, et al. Noninvasive analysis of the sputum transcriptome discriminates clinical phenotypes of asthma. *Am J Respir Crit Care Med* 2015;**191**:1116–25.
- Konno S, Taniguchi N, Makita H, Nakamaru Y, Shimizu K, Shijubo N, et al. Distinct phenotypes of smokers with fixed airflow limitation identified by cluster analysis of severe asthma. *Ann Am Thorac Soc* 2018;**15**:33–41.
- Yokoyama A, Kohno N, Fujino S, Hamada H, Inoue Y, Fujioka S, et al. Circulating interleukin-6 levels in patients with bronchial asthma. *Am J Respir Crit Care Med* 1995;**151**:1354–8.
- Bradding P, Roberts JA, Britten KM, Montefort S, Djukanovic R, Mueller R, et al. Interleukin-4, -5, and -6 and tumor necrosis factor- α in normal and asthmatic airways: evidence for the human mast cell as a source of these cytokines. *Am J Respir Cell Mol Biol* 1994;**10**:471–80.
- Higashimoto Y, Yamagata Y, Taya S, Iwata T, Okada M, Ishiguchi T, et al. Systemic inflammation in chronic obstructive pulmonary disease and asthma: similarities and differences. *Respirology* 2008;**13**:128–33.
- Howarth PH, Babu KS, Arshad HS, Lau L, Buckley M, McConnell W, et al. Tumour necrosis factor (TNF α) as a novel therapeutic target in symptomatic corticosteroid dependent asthma. *Thorax* 2005;**60**:1012–8.
- Dahlen B, Shute J, Howarth P. Immunohistochemical localisation of the matrix metalloproteinases MMP-3 and MMP-9 within the airways in asthma. *Thorax* 1999;**54**:590–6.
- Prikk K, Maisi P, Pirilä E, Reintam MA, Salo T, Sorsa T, et al. Airway obstruction correlates with collagenase-2 (MMP-8) expression and activation in bronchial asthma. *Lab Invest* 2002;**82**:1535–45.
- Lavigne MC, Thakker P, Gunn J, Wong A, Miyashiro JS, Wasserman AM, et al. Human bronchial epithelial cells express and secrete MMP-12. *Biochem Biophys Res Commun* 2004;**324**:534–46.
- Ostridge K, Williams N, Kim V, Bennett M, Harden S, Welch L, et al. Relationship between pulmonary matrix metalloproteinases and quantitative CT markers of small airways disease and emphysema in COPD. *Thorax* 2016;**71**:126–32.
- Segura-Valdez L, Pardo A, Gaxiola M, Uhal BD, Becerril C, Selman M. Upregulation of gelatinases A and B, collagenases 1 and 2, and increased parenchymal cell death in COPD. *Chest* 2000;**117**:684–94.

38. Culpitt SV, Rogers DF, Traves SL, Barnes PJ, Donnelly LE. Sputum matrix metalloproteinases: comparison between chronic obstructive pulmonary disease and asthma. *Respir Med* 2005;**99**:703–10.
39. Johansen JS, Pedersen AN, Schroll M, Jørgensen T, Pedersen BK, Bruunsgaard H. High serum YKL-40 level in a cohort of octogenarians is associated with increased risk of all-cause mortality. *Clin Exp Immunol* 2008;**151**:260–6.
40. Sakazaki Y, Hoshino T, Takei S, Sawada M, Oda H, Takenaka S, et al. Overexpression of chitinase 3-like 1/YKL-40 in lung-specific IL-18-transgenic mice, smokers and COPD. *PLoS One* 2011;**6**:e24177.
41. Mao XQ, Kawai M, Yamashita T, Enomoto T, Dake Y, Sasaki S, et al. Imbalance production between interleukin-1beta (IL-1beta) and IL-1 receptor antagonist (IL-1Ra) in bronchial asthma. *Biochem Biophys Res Commun* 2000;**276**:607–12.
42. Sousa AR, Lane SJ, Nakhosteen JA, Lee TH, Poston RN. Expression of interleukin-1 beta (IL-1beta) and interleukin-1 receptor antagonist (IL-1ra) on asthmatic bronchial epithelium. *Am J Respir Crit Care Med* 1996;**154**:1061–6.
43. Hernandez ML, Mills K, Almond M, Todoric K, Aleman MM, Zhang H, et al. IL-1 receptor antagonist reduces endotoxin-induced airway inflammation in healthy volunteers. *J Allergy Clin Immunol* 2015;**135**:379–85.
44. Wenzel SE. Asthma phenotypes: the evolution from clinical to molecular approaches. *Nat Med* 2012;**18**:716–25.